LBL-13840

LBL--13840

DE83 004059

DISCLAIMER

This report was prepared as an account of work sponsored by an agency of the United States Government. Neither the United States Government nor any agency thereof, nor any of their employees, makes any warranty, express or implied, or assumes any legal liability or responsibility for the accuracy, completeness, or usefulness of any information, apparatus, product, or process disclosed, or represents that its use would not infringe privately owned rights. Reference herein to any specific commercial product, process, or service by trade name, trademark, manufacturer, or otherwise, does not necessarily constitute or imply its endorsement, recommendation, or favoring by the United States Government or any agency thereof. The views and opinions of authors expressed herein do not necessarily state or reflect those of the United States Government or any agency thereof.

MATERIALS AND MOLECULAR RESEARCH DIVISION

Annual Report 1981

August 1982

Alan W. Searcy, Division Head
Rolf H. Muller, Asst. Division Head for Research
Conway V. Peterson, Asst. Division Head for Administration

NOTICE

PORTIONS OF THIS REPORT ARE ILLEGIBLE. It has been reproduced from the best available copy to permit the broadest possible availability.

Lawrence Berkeley Laboratory
University of California
Berkeley, California 94720

DISTRIBUTION OF THIS DOCUMENT IS UNLIMITED

Contents

GENERAL INTRODUCTION 1
Alan W. Searcy

I. MATERIALS SCIENCES
A. Metallurgy and Ceramics
1. Structure of Materials

a. Structure and Properties of Transformation Interfaces
Ronald Gronsky, Investigator

1. Segregation and Pre-Precipitation Phenomena at Grain Boundaries 5
2. *Atomistics of Grain Boundary Precipitation* 5
3. Work in Progress 6

1981 Publications and Reports 6

b. Microstructure, Properties, and Alloy Design: Inorganic Materials
Gareth Thomas, Investigator

A. Alloy Design: Medium Carbon Steels, "Qua-Tough Alloys"

1. In-Situ Studies of Fracture of 0.3C Steels 8
2. Tempered Martensite Embrittlement in Fe/Cr/Mn/C Alloys 8
3. Fundamental Studies of Wear in Ferrous Materials 9
4. Two-Body, Dry Abrasive Wear of Fe/Cr/C Experimental Alloys 9
5. Mechanical Properties and Microstructure of Lower Bainitic Fe/C/Cr Alloys 10
6. Work in Progress 11

B. Low Carbon *Dual-Phase Steels*

1. Dual-Phase (Duplex) Steel for Pipelines 11
2. Microstructure-Properties of Controlled Rolled Microalloyed Low Carbon Steel 11
3. Work in Progress 12

C. Magnetic Materials

1. Precipitation Hardening Sm-Co Base Permanent Magnets 12
2. Annealing of High Permeability $(MnZn)Fe_2O_4$ 14
3. Work in Progress 14

1981 Publications and Reports 14

c. Solid State Phase Transformation Mechanisms
Kenneth H. Westmacott, Investigator

1. *Crystallographic Theory of Precipitation* 17
2. Precipitation Reactions in Austenitic Stainless Steels 18
3. Work in Progress 18

1981 Publications and Reports 19

d. National Center for Electron Microscopy
Gareth Thomas, Ronald Gronsky,
and Kenneth H. Westmacott, Investigators

1. 1.5 MeV High Voltage Electron Microscope 20
2. Atomic Resolution Microscope 23
3. *Image Simulation and Analysis* 23

e. In-Situ Investigations of Gas Solid Reactions by Electron Microscopy
James W. Evans and Kenneth H. Westmacott, Investigators

1. The Microstructure and Reactivity of Nickel Oxide 24
2. Work in Progress 24

f. Local Atomic Configurations in Solid Solutions
Didier de Fontaine, Investigator

1. Cluster Thermodynamics 25
2. Ionic and Magnetic Ordering 26
3. Thermodynamics and Kinetics of Clustering 26

1981 Publications and Reports 27

2. Mechanical Properties

a. Theoretical Problems in Alloy Design
J. W. Morris, Jr., Investigator

1. The Linear Elastic Theory of Structural Transformations in Solids 28
2. The Precipitate Habit and Internal Strain of Nitride Precipitates in Steel 28
3. The Precipitate Morphology and Coarsening Characteristics of Nitride Precipitates in Steel 28
4. Accumulation of Charge in the Strain Field of a Dislocation in a Metal 29
5. The Thickness Distortion of ^{57}Fe Backscatter Mössbauer Spectrum 29
6. A Mössbauer Study of Microstructural and Chemical Change in Fe-9Ni 29
7. Observations on the Differences Reported in Region 1 for the Superplastic Zn-22%Al Eutectoid 29
8. Stereological Characterization of Fracture Surfaces in Fe-6Ni Cryogenic Steel 30
9. Inherent Intergranular Fracture in Fe-12Mn Broken at Low Temperature 30
10. The Properties of Microconstituents in Fe-6Ni Cryogenic Steel 30
11. The Consequences of Rapid Thermal Cycling in Fe-9Ni Steel 30
12. Welding of Iron-Based Superalloys 31
13. The Crystallographic Orientation of A15 V_3Ga and Nb_3Al Precipitates in BCC Matrices 31
14. Microstructural Characterization and Modification in Multifilamentary Nb_3Sn 31
15. Research on Powder Processed Nb_3Al Superconducting Wire 31

1981 Publications and Reports 32

b. Structure-Property Relationships in Semiconductor Materials
Jack Washburn, Investigator

1. Effect of Oxygen on Cr-Structural Defect Interaction in Ion-Implanted GaAs 33
2. High Resolution Observations of Copper Vacancy Ordering in Chalcocite (Cu_2S) and the Transformation to Djurleite ($Cu_{1.97-1.94}S$) 33
3. The Effect of Recoiled Oxygen on Damage Annealing In As-Implanted SiO_2/Si 34
4. The Mechanism of the Crystal to Amorphous Transformation in Si 35
5. The Effect of Impurity Atoms on the Kinetics of the Amorphous to Crystal Transformation in Silicon 36
6. Zinc Diphosphide as a New Photovoltaic Material 36
7. MeV He^+ Dechanneling From Secondary Defects in Si 36
8. Progress on the Fabrication of Pulsed Electron Beam Annealer 37

1981 Publications and Reports 38

c. Mechanical Properties of Ceramics
A. G. Evans, Investigator

High Temperature Failure

1. High Temperature Failure in Ceramics 39
2. Effects of Inhomogeneities on Creep Rupture 39
3. The Response of Cracks to Creep in Ceramic Polycrystals 40
4. High Temperature Failure Initiation in Liquid Phase Sintered Ceramics 41

Final Stage Sintering

1. Pore, Grain Boundary Separation Mechanisms 42
2. Coarsening During Final Stage Sintering 42
3. Experimental Studies of Final Stage Sintering 42
4. Work in Progress 44

1981 Publications and Reports 44

d. Environmentally Affected Crack Growth in Engineering Materials
R. O. Ritchie, Investigator

1. Influences of Gaseous Environment on Low Growth-Rate Fatigue Crack Propagation in Steels 46

1981 Publications and Reports 47

3. Physical Properties

a. Interfaces and Ceramic Microstructures
Joseph A. Pask, Investigator

1. Wetting Behavior in the Iron-Silver System 49
2. Some Aspects of Liquid Phase Sintering of Alumina 49

1981 Publications and Reports 49

b. High Temperature Reactions
Alan W. Searcy, Investigator

1. Formation of a Highly CO_2-Deficient Calcite 51
2. The Effects of Solid Catalysts and of Sample Size on $MgSO_4$ Decomposition 51
3. Development of Bimodal Pore Size Distribution In CaO From Calcite Decomposition 52
4. A Microsintering Study by Adsorption Methods: CaO in CO_2 53
5. Surface Diffusion of High-Temperature Vapors Through Porous Alumina 53

1981 Publications and Reports 54

c. Chemical Properties of Ceramic Alloys
Lutgard C. De Jonghe, Investigator

1. The Reaction Interface in Reduction 55

1981 Publications and Reports 56

d. Structure and Electrical Properties of Composite Materials
Robert H. Bragg, Investigator

1. Electrical Properties of Glassy Carbon 57
2. Work in Progress 57

1981 Publications and Reports 58

e. High Temperature Oxidation and Corrosion of Materials
David P. Whittle, Investigator

1. Growth Mechanism of Cr_2O_3 Scale and Its Breakdown in $CO/CO_2/SO_2$ Atmospheres 59
2. High Temperature Corrosion of Iron in Sulfur Containing Atmospheres 59
3. Thermodynamics of Na_2SO_4-Induced Hot Corrosion 60
4. Internal Oxidation and Sulfidation of Iron-Based Binary Alloys 60
5. Peg Formation by Short Circuit Diffusion in Al_2O_3 Scales Containing Oxide Dispersions 60
6. Fracture Aspects of Oxide Scales Subjected to Microindentation 61
7. Enhanced Diffusion of Oxygen During Internal Oxidation 63
8. Growth Mechanism of Internal Al_2O_3 Precipitates in Dilute Ni-Al Alloys and the Role of Reactive Elements 63
9. Interdiffusion in the Fe-Al System 64

1981 Publications and Reports 64

f. Refractories Project Processing
Lutgard C. De Jonghe, Investigator

1981 Publications and Reports 67

g. Erosion of Brittle Solids
A. G. Evans, Investigator

1. Work in Progress 68

h. Chemical Degradation of Refractories
David P. Whittle, Investigator

1. High Temperature Degradation of Refractories in Mixed Gas Environments 69

i. Ceramic Interfaces
Andreas M. Glaeser, Investigator

1. Technique for Measuring Grain Boundary Mobility and Its Application to Mg-Doped Al_2O_3 70

1981 Publications and Reports 71

4. Engineering Materials

a. Abrasive, Erosive, and Sliding Wear of Materials
Iain Finnie, Investigator

1. Simulation of Sliding Wear by Plastic Deformation Under Combined Stress 72
2. Abrasive Wear 72
3. Work in Progress 73

1981 Publications and Reports 73

b. Erosion-Corrosion Wear Program
Alan V. Levy, Investigator

1. The Effect of Heat Treatment of Steel on Erosion Behavior 74
2. Erosion of Hard Metals 75
3. Effect of Particle Variables on Erosion of Ductile Metals 76
4. Analytical Model of Erosion Behavior of Ductile Metals 76
5. Prediction of Particle Laden Liquid Two Phase Flow 76
6. Boundary Layer Control by Means of Strong Injection 77
7. Oxidation Behavior of Surface Doped 304SS With Modified Composition 77

Work in Progress

1. Elevated Temperature Erosion of Aluminum and Steel Alloys 78
2. Laser Doppler Velocimetry Measurements of Gas/Particle Flows in a 90° Curved Duct 79

1981 Publications and Reports 79

B. Solid-State Physics
1. Experimental Solid-State Physics

a. Far-Infrared Spectroscopy
Paul L. Richards, Investigator

1. Infrared Spectroscopy of Quasi-One-Dimensional Conductors 80
2. Characterization of Ge:Ga Photoconductive Detectors 80
3. Improved Fabrication Techniques for Infrared Bolometers 81
4. Work in Progress 81

1981 Publications and Reports 82

b. Experimental Solid-State Physics and Quantum Electronics
Y. Ron Shen, Investigator

1. Detection of Molecular Monolayers by Optical Second Harmonic Generation 83
2. Studies of Molecular Adsorption on Silver in an Electrolytic Solution 83
3. Effect of Extended Surface Plasmons on Surface-Enhanced Raman Scattering 84
4. Anharmonicity, Phonon Localization, Two-Phonon Bound States, and Vibrational Spectra 84
5. Laser Interaction with Molecular Beams 84

1981 Publications and Reports 84

c. Excited Quantum Fluids in Solids
Carson D. Jeffries, Investigator

1. Correlation in the Electron-Hole Liquid in Ge 87
2. Bifurcation and Chaotic Behavior in Nonlinear Semiconductor Phenomena 87
3. Electric Detection of Spin Resonance of Electrons at Dislocations in Ge 88

1981 Publications and Reports 88

d. Time-Resolved Spectroscopies in Solids
Peter Y. Yu, Investigator

1. Non-Thermalized Photoluminescence in Cu_2O 90
2. Work in Progress 90

1981 Puhlications and Reports 90

e. Superconductivity, Superconducting Devices, and 1/f Noise
John Clarke, Investigator

1. Quantum Noise in Josephson Junctions and DC Squids 92
2. Phonon-Induced Gap Enhancement in Superconducting Aluminum 92
3. Chaos in Josephson Junctions 93

1981 Publications and Reports 94

2. Theoretical Solid-State Physics

a. Theoretical Studies of the Electronic Properties of Solid Surfaces
L. M. Falicov, Investigator

1. Theoretical Studies of the Electronic, Chemical and Magnetic Properties of Transition- and Noble-Metal Overlayers on Transition- and Noble-Metal Substrates 96
2. Theoretical Study of Lithium Intercalation in Transition-Metal Dichalcogenides 96
3. Work in Progress 96

1981 Publications and Reports 97

b. Theoretical Solid-State Physics
Marvin L. Cohen, Investigator

1. Total Energy Calculations 98
2. Surfaces and Interfaces 98
3. Electronic Structure 98
4. Work in Progress 99

1981 Publications and Reports 99

C. Materials Chemistry
1. Chemical Structure

a. Low Temperature Properties of Materials
Norman E. Phillips, Investigator

1. Comparison of an NBS "Fixed Point Device" with Cerium Magnesium Nitrate and Nuclear Orientation Thermometers 101
2. Pressure and Field Dependence of the Low-Temperature Heat Capacity of α-Cerium 101
3. Pressure Dependence of the Low-Temperature Heat Capacity of Teflon 102
4. Work in Progress 102

1981 Publications and Reports 103

b. Electrochemical Processes
Charles W. Tobias, Investigator

1. Effects of Suspended Particles on the Rate of Mass Transfer to a Rotating Disk Electrode 104
2. Electrochemical Machining of Cemented Titanium Carbide 105
3. A Study of Electropolishing of Ferrous Alloys Using Rotating Disk Electrodes 106

1981 Publications and Reports 106

2. High Temperature and Surface Chemistry

a. High Temperature Thermodynamics
Leo Brewer, Investigator

1. Use of Gaseous Equilibration to Characterize Stability of Strongly Interacting Intermetallic Phases 108
2. Gradient Furnace Use for Determination of the Hexagonal Phase Stability in the Cobalt-Molybdenum System 109
3. Work in Progress 109

1981 Publications and Reports 109

b. Chemistry and Materials Problems in Energy Production Technologies
Donald R. Olander, Investigator

1. Water and Brine Movement in Salt Containing Nuclear Wastes 111
2. Thermochemistry of Fission Products in Reactor Fuel Rods 111
3. Fission Product Behavior in Reactor Fuel Rods Under Accident Conditions 111
4. Extrapolation of Low Temperature Vapor Pressure Data of Uranium Carbide to the Liquid Region 112
5. The Zirconium-Iodine Reaction by Modulated Molecular Beam Mass Spectrometry 112
6. The Kinetics of Laser Pulse Vaporization of Uranium Dioxide by Mass Spectrometry 113

1981 Publications and Reports 114

c. Plasma Enhanced Deposition of Thin Films
Dennis W. Hess, Investigator

1. Plasma-Deposited Titanium Oxide Photoanodes 116
2. Structure and Magnetic Properties of Plasma Deposited Iron Oxide Films 116

1981 Publications and Reports 117

d. Electrochemical Phase Boundaries
Rolf H. Muller, Investigator

1. Spectroscopic Ellipsometry of Model Inhibitor Systems 118
2. Nucleation and Growth of Anodic Silver Oxide Films: Light Scattering and Ellipsometry 119
3. Noncircular Collision Cross-Sections of Induced Electric Dipoles 119
4. Electrochemical Properties of Metal Clusters 120
5. Work in Progress 120

1981 Publications and Reports 120

e. Solid-State and Surface Reactions
Gabor A. Somorjai, Investigator

Surface Structure and Chemisorption by Low Energy Electron Diffraction

1. The Structure of Epitaxially Grown Metal Layers on Single Crystal Surfaces of Other Metals: Gold on Pt(100) and Platinum on Au(100) 121
2. The Surface Reconstructions of the (100) Crystal Faces of Iridium, Platinum and Gold: I. Experimental Observations and Possible Structural Models. II. Structural Determination by Leed Intensity Analysis 121
3. A Surface Crystallography Study by Dynamical Leed of the ($\sqrt{3} \times \sqrt{3}$)R30° CO Structure on the Rh(111) Crystal Surface 122
4. Pulse Counting Low Energy Electron Diffraction Instrument 122
5. Potassium and Potassium Oxide Monolayers on the Platinum (111) and Stepped (755) Crystal Surfaces. A Leed, AES, and TDS Study 122
6. Surface Debye Temperatures of Rh(100) and (111) Surfaces 122
7. The Structure and Stability of Surface Platinum Oxide and of Oxides of Other Noble Metals 122
8. Adsorption and Bonding of Butane and Pentane on the Pt(111) Crystal Surfaces: Effects of Oxygen Treatments and Deuterium Preadsorption 122
9. Dynamical and Approximate LEED Theories Applied to Layers of Large Molecules 123
10. The Desorption, Decomposition, and Deuterium Exchange Reactions of Unsaturated Hydrocarbons (Ethylene, Acetylene, Propylene, and Butenes) on the Pt(111) Crystal Face 123
11. The Growth and Chemisorption Properties of Ag and Au Monolayers on Platinum Single Crystal Surfaces: An AES, TDS, and LEED Study 123
12. The Structures of Small Hydrocarbon Molecules on Rh(111) Studied by Low Energy Electron Diffraction: Acetylene, Ethylene, Methylacetylene, and Propylene 123
13. Arrangement of CO Molecules Adsorbed on Low Index Metal Surfaces: A Comparison Between LEED and HREELS or IRS 124

Electron Spectroscopy Studies of Solid Surfaces and Adsorbates

1. The Strong Influence of Potassium on the Adsorption of CO on Platinum Surfaces: A TDS and HREELS Study. 124
2. Electron Spectroscopy Studies on the Clean Thorium and Uranium Surfaces: The Chemisorption and Initial Stages of Reaction with O_2, CO and CO_2 124
3. Design and Construction of a High Stability, Low Noise, Power Supply for Use with High Resolution Electron Energy Loss Spectrometers. 124

Molecular Beam-Surface Interactions

1. Detection of Rotational Energy Transfer in NO by Laser Ionization During Molecular Beam-Surface Scattering. 125
2. Iron Single Crystals as Ammonia Synthesis Catalysts: Effect of Surface Structure on Catalyst Activity. 125
3. High Pressure Studies of the Au-Pt System: The Effect of Gold on Hydrocarbon Conversion Reactions. 125
4. Work in Progress. 126

1981 Publications and Reports 126

f. Nuclear Magnetic Resonance
A. Pines, Investigator

1. Anisotropic Diffusion in Liquid Crystals 130
2. Double Quantum Coherence of Spin 1 in Liquids 130
3. Molecular Conformation in Liquid Crystals 130
4. Selective Excitation of High n-Quantum Transitions. 131
5. Noise in Two Dimensional Spectroscopy 131
6. High Resolution NMR in Inhomogeneous Fields 132

II. CHEMICAL SCIENCES
A. Fundamental Interactions
1. Photochemical and Radiation Studies

a. Photon-Assisted Surface Reactions, Materials, and Mechanisms
Gabor A. Somorjai, Investigator

1. Photodissociation of Water on Iron-Based Oxide Surfaces. 137
2. The Composition and Structure of Oxide Films Grown on the (110) Crystal Face of Iron 137
3. Work in Progress. 137

1981 Publications and Reports 137

b. Photochemistry of Materials in the Stratosphere
Harold S. Johnston, Investigator

1. Nitrogen Oxides and the SST Controversy Ten Years Later: A Case Study in the Use of Science for Decision Making. 139
2. High-Resolution Absorption Spectrum of the Nitrate Free Radical 139
3. Primary Products in the Photolysis of Chlorine Nitrate 140
4. Integrated Absorption Coefficients for Several Vibration-Rotation Transitions of the Gas-Phase Hydroxyl Radical Using a Tunable Diode Laser. 140
5. Rate Constant for the Resonant Energy Transfer Between Electronically Excited Oxygen, $O_2(^1\Delta_g)$, and the HOO Free Radical. 141
6. The Rate of Reaction of Hydroxyl Radicals with Nitric Acid as a Function of Temperature. 141

1981 Publications and Reports 141

2. Chemical Physics

a. Energy Transfer and Structural Studies of Molecules on Surfaces
Charles B. Harris, Investigator

1. Energy Transfer Studies Between Adsorbed Molecules and Ag Surfaces in Ultrahigh Vacuum 143
2. Role of Surface Plasmons in Energy Transfer to Metal Surfaces Through Near Field Dipole Components 143
3. The Modification of Surface Optical Response Through Chemisorption 144
4. Laser Raman Studies of Adsorbates on Ag(110) and Ag(111) Surfaces. 145
5. Separation of the Repulsive and Attractive Intermolecular Potentials in Liquids from the Temperature Dependence of Picosecond Coherent Stokes Scattering 145
6. A High Power Picosecond Laser System Optimized for Coherent Stimulated Stokes Scattering Experiments in Liquids 146
7. Picosecond Pulse Compression Using Kodak Heptamethine Pyrilium Dye No. 5 as a Saturable Absorber 146

1981 Publications and Reports 147

b. Molecular Beam Spectroscopy
John S. Winn, Investigator

1. Mechanisms of Metal Carbonyl Dissociations. 149
2. Molecular Beam Electric Resonance Spectroscopy 149

1981 Publications and Reports 150

c. Selective Photochemistry
C. Bradley Moore, Investigator

1. Kinetics of Transient Species of Importance in Combustion Chemistry. 151
2. High Overtone Spectroscopy. 151
3. Dissociative Ionization of Water Induced by Single-Photon Vibrational Excitation. 152

1981 Publications and Reports 152

d. Physical Chemistry with Emphasis on Thermodynamic Properties
Kenneth S. Pitzer, Investigator

1. Ab Initio Effective Core Potentials Including Relativistic Effects: A Procedure for the Inclusion of Spin-Orbit Coupling in Molecular Wavefunctions. 154
2. Improved Ab Initio Effective Potentials for Ar, Kr, and Xe With Applications to Their Homonuclear Dimers 154
3. Reliable Static Electric Dipole Polarizabilities for Heavy Elements. 155
4. Some Recent Applications of Group Theory to Chemical Physics. 155
5. Work in Progress. 155

1981 Publications and Reports 155

e. Molecular Interactions
William A. Lester, Jr., Investigator

1. Work in Progress

1981 Publications and Reports 157

f. Chemical Dynamics Studies
Bruce H. Mahan, Yuan T. Lee, and John S. Winn, Investigators

1. Electron Impact Production of CH^+ from Methane. 159
2. Charge Transfer From N_2 and Ar to N_2^+ 159

g. Theory of Atomic and Molecular Collision Processes
William H. Miller, Investigator

1. Reaction Path Model for Polyatomic Reaction Dynamics. 161
2. Mode-Specificity in Unimolecular Reaction Dynamics. 161
3. Classical Models for Electronically Non-Adiabatic Collision Processes 162

1981 Publications and Reports 162

h. Photoelectron Spectroscopy
David A. Shirley, Investigator

1. Shape Resonances in K-Shell and Auger Photoelectron Distributions from CO, CO_2, and N_2. 163
2. Electron Spectroscopy Study of Inner-Shell Photoexcitation Ionization of Xe 164

3. Autoionizing Resonance Profiles in the Photoelectron Spectra of Atomic Cadmium 164
4. Rotationally-Resolved Photoelectron Spectroscopy of n-H_2, p-H_2, HD, and D_2 165
5. Photoelectron Angular Distributions from H_2 and D_2 166
6. Photoionization Cross Sections and Photoelectron Asymmetries of the Valence Orbitals of NO 166
7. Multiphoton Ionization Photoelectron Spectroscopy of CCl_2F_2 and CCl_3F 167
8. A Double-Crystal Monochromator for the Energy Region 550-5000 eV 168
9. Normal Photoelectron Diffraction Studies of Selenium and Sulfur Overlayers on Ni(011) and Ni(111) 169
10. Off-Normal Photoelectron Diffraction Study of the c(2x2) Selenium Overlayer on Ni(001). 169
11. Angle-Resolved Photoemission Study of the Valence Bands of W(011) in the Energy Range 1000-1250 eV 170
12. Angle-Resolved Photoemission Studies of the Valence Band Structure of Stepped Crystal Surfaces: Cu(S)-[3(111)x(100)] 171
13. Valence Band Structure of Antiferromagnetic Cr Along Δ and 172
14. Work in Progress. 173

1981 Publications and Reports 173

i. Crossed Molecular Beams
Yuan T. Lee, Investigator

1. $O(^3P) + C_2H_3Br$: Reactive Scattering. 175
2. $O(^3P) + 1,1\text{-}C_2H_2Cl_2$: Reactive Scattering 175
3. $O(^3P)$ + Propene: Reactive Scattering 176
4. Reaction Dynamics of the $H_2^+ + N_2$, CO, and O_2 Systems 177
5. The Lifetime of Metastable $(a^4\pi_u)O_2^+$ 177
6. Rare Gas-Halogen Atom Interaction Potentials from Molecular Beam Studies: $I(^2P_{3/2}) + Kr, Xe\ (^1S_0)$ 178

1981 Publications and Reports 178

j. Potential Energy Surface for Chemical Reactions
Henry F. Schaefer III, Investigator

1. Hydroxycarbene (HCOH) and Protonated Formaldehyde: Two Potentially Observable Interstellar Molecules 181
2. Bis(Cyclobutadiene)Nickel: Geometrical and Electronic Structure 182
3. A Unimolecular Reaction ABC → A + B + C Involving Three Product Molecules and A Single Transition State: Photodissociation of Glyoxal 182
4. Theoretical Studies of the 1,2 Hydrogen Shift: The Controversial Barrier Height Between Silaethylene and Methylsilylene 183
5. Isomeric Structures of CH_2LiF, The Prototype Carbenoid 183

1981 Publications and Reports 184

3. Atomic Physics

a. Atomic Physics
R. Marrus, Investigator

1. Electron Capture by Ne^{10+} Trapped at Very Low Energies 186
2. Parity Violation in Atomic Thallium 187
3. Charge Changing Cross-Section for Fe Ions 187

1981 Publications and Reports 188

B. Processes and Techniques
1. *Chemical Energy*

a. Formation of Oxyacids of Sulfur from SO_2
Robert E. Connick, Investigator

1981 Publications and Reports 189

b. Catalytic Hydrogenation of CO: Catalysis on Well-Characterized Surfaces
Gabor A. Somorjai, Investigator
and
Catalysis by Supported Metals
Alexis T. Bell, Investigator

1. *The Formation of Oxygen Containing Organic Molecules* by the Hydrogenation of CO Using Lanthanum Rhodate Catalysts 190
2. Effects of Dispersion on the Activity and Selectivity of Alumina-Supported Ruthenium Catalysts for Carbon Monoxide Hydrogenation 190
3. Studies of Carbon Monoxide Hydrogenation Over Ruthenium Using Transient-Response Techniques 191
4. Reactive Scavenging of Surface Species Formed During Hydrogenation of Carbon Monoxide Over Ruthenium 191
5. Work in Progress. 191

1981 Publications and Reports 192

c. *Organometallic Chemistry of Coal Conversion*
K. Peter C. Vollhardt, Investigator

1. Biscarbyne Clusters as Homogeneous Analogs of Fischer-Tropsch Intermediates on Surfaces 194
2. Hydrocarbon Formation on Polymer-Supported $_n^5$-Cyclopentadienyl Cobalt 194
3. The Extrusion of Sulfur Monoxide from Small Molecules 195
4. The Mechanism of the Reppe Cyclooctatetraene Synthesis from Ethyne 195
5. Work in Progress. 195

1981 Publications and Reports 195

d. Synthetic and Physical Chemistry
William L. Jolly, Investigator

1. The Study of Molecular Electron Distribution by X-Ray Photoelectron Spectroscopy 197
2. The Use of Core Electron Binding Energies for the Quantification of the Bonding and Antibonding Character of Molecular Orbitals 197
3. X-Ray Photoelectron Spectroscopic Study of Organometallic Nitrosyl Compounds of Chromium, Molybdenum, and Tungsten 198
4. An XPS Study of Thiocarbonyl and Thionitrosyl Complexes 198
5. Work in Progress. 198

1981 Publications and Reports 198

e. Chemistry and Morphology of Coal Liquefaction
Heinz Heinemann, Investigator, with Alexis T. Bell,
R. G. Bergman, James W. Evans, Richard H. Fish,
E. E. Petersen, A. V. Levy, G. A. Somorjai, and
K. Peter C. Vollhardt, Investigators

[See Fossil Energy Section]

f. Electrochemical Systems
John Newman, Investigator

1. Mathematical Modeling of the Liquid-Junction Photovoltaic Cell 200
2. Work in Progress. 201

1981 Publications and Reports 201

g. Surface Chemistry--Application of Coordination Principles
Earl L. Muetterties, Investigator

1981 Publications and Reports 202

h. High-Energy Oxidizers and Delocalized-Electron Solids
Neil Bartlett, Investigator

1. Graphite Intercalation by Fluorine and Hydrogen Fluoride 204
2. X-Ray Diffraction and Vibrational Studies of
$(GeF_5)_n^{n-}$ Salts 204
3. Fluoride-Ion Affinities and Electron Affinities of
High-Oxidation-State Fluorides 206

1981 Publications and Reports 206

i. Transition Metal Catalyzed Conversion of CO, NO, H_2,
and Organic Molecules to Fuels and Petrochemicals
Robert G. Bergman, Investigator

1. Acyl- and Aldehyde-Forming Reactions of
Metal Alkyl Complexes: Evidence for Solvent Coordination in
the Migratory CO Insertion Step 208
2. C-H Activation in Completely Saturated Hydrocarbons:
Direct Observation of M + R-H → R-M-H 210
3. Work in Progress

1981 Publications and Reports 211

2. Chemical Energy

a. Analysis of Transplutonium Elements in Dilute Solution
Steven D. Brown, Investigator

1. Resolution of Overlapped Electrochemical Peaks with the Use
of the Kalman Filter 213
2. Peak Resolution by Semiderivative Voltammetry 213
3. Speciation of Metal Complex Systems Using the Kalman Filter 213

1981 Publications and Reports 213

3. Chemical Engineering Sciences

a. High-Pressure Phase Equilibria in Hydrocarbon-Water (Brine) Systems
John M. Prausnitz, Investigator

1. Experimental High-Pressure Vapor-Liquid-Equilibrium Measurements. 215
2. Pure-Component Equations of State 215
3. Local-Composition Mixing Rules for Equations of State 216

1981 Publications and Reports 216

III. NUCLEAR SCIENCES
A. Low-Energy Nuclear Sciences
1. Heavy Element Chemistry

a. Acinide Chemistry
Norman M. Edelstein, Richard A. Andersen, Neil Bartlett, John G. Conway, Kenneth N. Raymond, Glenn T. Seaborg, Andrew Streitwieser, Jr., David H. Templeton, and Alan Zalkin, Investigators

Specific Sequestering Agents for the Actinides

1. Synthetic Enterobactin Analogues: Carboxamide-2,3-Dihydroxy Terephthalate Conjugates of Spermine and Spermidine 221
2. Siderophilin Metal Coordination 223
3. Synthetic and Structural Chemistry of Tetrakis(Dialkylhydroxamate)-Thorium(IV) Complexes 223
4. Tricatecholamide Analogs of Enterobactin as Gallium- and Indium-Binding Radiopharmaceuticals 225

Synthetic and Structural Studies of Actinides and Other Compounds

1. *Tertiary Phosphine Derivatives of the f-Block Metals;* Preparation of $X_4MMe_2PCH_2CH_2PMe_2)_2$ Where X is Halide, Methyl, and Phenoxo and M is Thorium or Uranium. Crystal Structure of Tetra (Phenoxo)Bis[bis(1,2-Dimethylphosphino) Ethane] Uranium(IV) 225
2. Crystal Structure of Bis(Pentamethylcyclopentadienyl) Bis(Pyridine) Ytterbium(II) 225
3. Bis(Pentamethylcyclopentadienyl)Carboxylato and Dithiocarbamato Derivatives of Neodymium(III) and Ytterbium(III). Crystal Structure of Bis(Pentamethylcyclopentadienyl)Diethyldithio Carbamato Ytterbium 226
4. Preparation and Crystal Structure of Bis(Pentamethylcyclopentadienyl) Ytterbium(III) Tetracarbonyl Cobaltate(Tetrahydrofuran); An Ytterbium Isocarbonyl(Yb-OC-Co) Bond 227
5. *Concerning the Reaction of Metallocene Dichlorides of* Titanium(IV) and Zirconium(IV) with Lithium Bis(Trimethylsilyl)Amide . 227
6. Syntheses and Characterization of $(\eta^5-C_5H_5)_2U(NR_2)_2$ Compounds 227
7. Synthesis and Structure of Dicyclopentenouranocene, $U[C_8H_6(CH_2)_3]_2$ 228
8. Synthesis and Structure of a Uranyl Complex with a Disulfide Ligand . . . 229
9. The Structure of Nickel Uranyl Acetate Hexahydrate 230
10. The Synthesis and Characterization of $(UCp_3)_2$(Pyrazine) and $[U(MeCp)_3]_2$(Pyrazine): π-Bridged Dimers of U^{3+} 231
11. Synthesis and Crystal Structure of $UCp_3(C_3H_3N_2)$ A New Mode of Pyrazolate Bonding 231
12. Crystal and Molecular Structure of $[Nd(tren)_2(CH_3CN)](ClO_4)_3$ 231

Physical and Spectroscopic Properties

1. Electronic Structure of UCl_5: A Reexamination 232
2. Optical Spectra and Zeeman Effect for Pr^{3+} and Nd^{3+} in $LuPO_4$ and YPO_4 232
3. The Syntheses and Electronic Structures of Decamethylmetallocenes 233
4. Spectrum and Energy Levels of Nb^{4+} 233

1981 Publications and Reports 234

IV. FOSSIL ENERGY

a. Electrode Surface Chemistry
Phillip N. Ross, Investigator

1. Surface Properties of Pt-Zr and Pt-Ti Alloys 241
2. Interaction of Oxygen with Pt Surfaces at Elevated Temperature 242
3. Oxygen Reduction on Pt In Perfluoroalkylsulfonic Acid 242

1981 Publications and Reports 243

b. Deuterium Analysis of Coal by NMR
A. Pines, Investigator

1. High Resolution NMR of Deuterium in Organic Solids 244
2. Resolved ^{27}Al NMR in Zeolites 244
3. Carbon-13 NMR of Whole and Processed Coals 245
4. *High Resolution Proton NMR of Dilute Spins in Solids* 246
5. Cylindrical Sample Turbine for Magic Angle NMR 246
6. Synthesis of Labeled Model Compounds and Crystals 246

1981 Publications and Reports 246

c. Coal Liquefaction Alloy Test Program
Alan V. Levy, Investigator

1. Erosion Behavior of Alloys in Coal Slurries 248
2. The Erosion Mechanism of Steels in Coal-Kerosene Slurries 249

1981 Publications and Reports 249

d. Utilization of Metals in Oil Shale Retort Components
Alan V. Levy, Investigator

1. High Temperature Corrosion
2. Low Temperature Corrosion

1981 Publications and Reports 252

e. Chemistry and Morphology of Coal Liquefaction
Heinz Heinemann, Investigator, with Alexis T. Bell,
R. G. Bergman, James W. Evans, Richard H. Fish,
E. E. Petersen, A. V. Levy, G. A. Somorjai, and
K. Peter C. Vollhardt, Investigators

Introduction 254

Task 1: Selective Synthesis of Gasoline Range Components from Synthesis Gas
A. T. Bell, Investigator, with R. Dictor and J. Canella 255

Task 2: Electron Microscope Studies of Coal During Hydrogenation
J. W. Evans, Investigator, with D. Coates and M. L. Perez 255

Task 3: Catalyzed Low Temperature Hydrogenation of Coal
G. A. Somorjai, Investigator, with H. Heinemann and A. Cabrera. 256

Task 4: Selective Hydrogenation, Hydrogenolysis, and Alkylation of Coal and Coal Related Liquids by Organometallic Systems
K. P. C. Vollhardt, Investigator. 256

1. The Reaction of Benzene with Aluminum Trichloride 256
2. On the Reversibility of η^4-Cyclobutadiene Metal Formation from Complexed Alkynes 257
3. Preparative Separation of Organometallic Compounds by High Performance Liquid Chromatography 258
4. Work in Progress
5. Laser-Powered Homogeneous Dissociation of Tetralin 258
6. Homogeneous Catalytic Hydrogenation of Polynuclear Aromatic and Heteroaromatic Nitrogen Compounds with Transition Metal Carbonyls . . . 259

1981 Publications and Reports 260

f. Solution Thermodynamics of Sulfites and Sulfite Oxidation Mechanisms
Leo Brewer and Robert Connick, Investigators

1. The Rate and Mechanism of the Oxidation of Bisulfite Ion by Oxygen 262
2. Solid-Gas Equilibria and Kinetics of the $CaSO_3$-H_2O System 262
3. Thermodynamic Data for Flue-Gas Desulfurization Processes 263

VIII. NUCLEAR WASTE MANAGEMENT

a. Thermodynamic Properties of Chemical Species in Nuclear Waste
Norman M. Edelstein, Investigator

1. Studies on Trivalent and Tetravalent Neptunium and Plutonium with Computer Controlled Voltammetry 307
2. Application of Convolutive Voltammetric Curve Fitting Techniques to Non-Reversible Electrochemical Systems 308

1981 Publications and Reports 309

IX. WORK FOR OTHERS

a. Phase Equilibria for Fixed Bed Gasification Products, Byproducts, and Water
John M. Prausnitz, Investigator

1. Measurement of Phase Equilibria 313
2. Theoretical Methods for Correlation of Phase Equilibria 313
3. Characterization 314

1981 Publications and Reports 314

b. Improved Beta-Alumina Electrolytes for Advanced Storage Batteries
Lutgard C. De Jonghe, Investigator

1. Chemical Coloration 316
2. Transport in an Inhomogeneous Electrolyte 316
3. Mode I Failure: Electro-Mechanical Fracture 317
4. Mode II Degradation: Internal Sodium Deposition 317

1981 Publications and Reports 318

X. APPENDICES

Appendix A. Materials and Molecular Research Division Personnel

Scientific Staff. 321
Support Staff 331

Appendix B. MMRD Committees. 332

Appendix C. List of Seminars 333

Appendix D. Index of Investigators 339

General Introduction

This slimmed-down report of Materials and Molecular Research Division (MMRD) activities in calendar 1981 reflects a change in the report format, and a report-cost savings, not a drop-off in research activities. Investigators have been asked to provide more succinct summaries of their completed research, with references to publications and LBL reports in which those studies are reported in detail.

At the end of 1981 there were affiliated with MMRD 8 staff senior scientists, 52 University of California, Berkeley (UCB) faculty investigators, 12 staff scientists, 170 postdoctorals and other temporary scientific personnel, 386 graduate students, and 80 technical, administrative, and clerical support staff--for a total of 708. During the calendar year 378 journal articles and LBL reports were published by members of MMRD. Students associated with MMRD were awarded 41 Ph.D. and 5 M.S. degrees.

Among awards and honors received by MMRD personnel in 1981 were the following:

- Six investigators, Marvin L. Cohen, William H. Miller, C. Bradley Moore, Earl L. Muetterties, Henry F. Schaefer, III, and David A. Shirley were among the 1000 most-cited authors in all fields of science in the period 1965-78.

- Five investigators, Harold S. Johnston, Bruce H. Mahan, C. Bradley Moore, Norman E. Phillips, and Alan W. Searcy were elected Fellows of the American Association for the Advancement of Science.

- Neil Bartlett was awarded an Honorary Doctor of Science degree, University of Newcastle-upon-Tyne, England. He was also the Brotherton Visiting Research Professor in the Department of Inorganic and Structural Chemistry, University of Leeds.

- Alexis T. Bell received the Curtis W. McGraw Research Award given by the American Society of Engineering Education.

- Robert G. Bergman was awarded a Miller Foundation Professorship at the University of California, Berkeley for the 1982-83 academic year.

- Leo Brewer was the Frontiers in Chemical Research Lecturer at Texas A&M University.

- Marvin L. Cohen's research on theoretical prediction of properties of carbon-family solids was judged the outstanding scientific accomplishment in solid state physics in the U.S. Department of Energy 1981 Materials Sciences Research Competition. Professor Cohen also received the Kendall Award in Materials Chemistry, given by the American Chemical Society.

- Lutgard C. De Jonghe was chairman of the 1981 Gordon Conference on The Science of Ceramic Processing.

- Anthony G. Evans presented the Sosman Memorial Lecture sponsored by the Basic Science Division of the American Ceramic Society.

- Charles B. Harris was given the Alexander von Humboldt (U.S. Senior Scientist) Award. He also was Distinguished Lecturer, Department of Chemistry, University of Texas.

- Kee C. Kim won the Student Best Paper Award from the Materials Science and Technology Division of the American Nuclear Society, for a paper co-authored with his thesis director, Donald R. Olander.

- Yuan T. Lee was Lester P. Kuhn Memorial Lecturer, Chemistry Department, Johns Hopkins University.

- C. Beat Meyer was awarded the Gold Medal of the German Cellular Polymer Division of the International Society of the Plastics Industry.

- Earl L. Muetterties was elected Honorary Fellow of the Royal Society of Chemistry. He was also recipient of the Edgar Fahs Smith Award, sponsored by the Philadelphia Section of the American Chemical Society.

- Joseph A. Pask received the Outstanding Educator in Ceramic Engineering Award of the American Ceramic Society.

- Alexander Pines was Robert W. Vaughan Lecturer, California Institute of Technology, and was recipient of the American Chemical Society Award in Graduate Education; he was also Guy Allen Lecturer at Yale University.

- Nack J. Kim was given the John E. Dorn Achievement Award, American Society for Materials.

- John M. Prausnitz was elected 1981 Faculty Research Lecturer, University of California, Berkeley.

- Paul L. Richards received the Alexander von Humboldt Senior Scientist Award.

- Henry F. Schaefer, III, was Chemistry Department Colloquium Committee Distinguished Lecturer, Purdue University.

- Y. Ron Shen was awarded a Miller Research Professorship at the University of California, Berkeley for 1981-82.

- David A. Shirley gave the 22nd Annual Gilbert Newton Lewis Memorial Lecture, University of California; his topic was "Photoelectron Spectroscopy: The Electron's View of Matter."

- Gabor A. Somorjai received the American Chemical Society 1981 Award in Colloid or Surface Chemistry, as well as the award for Outstanding Sustained Research in Materials

Chemistry ("The Building of New Metal Catalysts - The Structure and Reactivity of Metal Monolayers on the Surfaces of Other Metals") in the 1981 Materials Sciences Research Competition, U.S. Department of Energy. He also was chosen to present the Mack Lectures at Ohio State University.

- Andrew Streitwieser, Jr., was chosen to receive the 1982 James Flack Norris Award in Physical Organic Chemistry, sponsored by the Northeastern Section, American Chemical Society.

- Charles W. Tobias was selected Diamond-Shamrock Lecturer, Case Western University.

- James C. Weisshaar as the recipient of the American Chemical Society Nobel Laureate Signature Award for a Graduate Student in Chemistry.

Three achievements of MMRD investigators and their associates were cited in the first issue of Technology as among 100 notable contributions to technology in the past twelve months. These citations were for the remote-reference method of magnetotellurics by John Clarke (MMRD), Thomas Gamble (Ensco), and Wolfgang M. Goubau (Earth Sciences Division, LBL); the production of welds which are ductile at cryogenic temperatures by John W. Morris, Jr. (MMRD), and his associates; and the development of a nontoxic chelate for Pu by Frederick Weitl and Kenneth Raymond, both MMRD.

Conferences and meetings hosted by MMRD during 1981 included Actinides '81, an international conference exploring new developments in the physics and chemistry of actinide elements, chaired by Norman M. Edelstein. Professor Werner Muller of the European Institute for Transuranium Elements (Karlsruhe, West Germany) was Chairman of the International Program Advisory Committee of the Conference.

Another international meeting at MMRD/UCB during the year was a workshop on State Specific Photodissociation: Formaldehyde, co-chaired by William H. Miller, C. Bradley Moore, and Henry F. Schaefer III.

Three new investigators joined MMRD during 1981: William A. Lester, Jr., who had served ably as LBL Associate Director and Head of the National Resource for Computation in Chemistry, and has now joined the UCB faculty as Professor of Chemistry; Robert O. Ritchie, a newly appointed Associate Professor of Metallurgy in the Department of Materials Science and Mineral Engineering at UCB; and Andreas M. Glaeser, a newly appointed Assistant Professor of Ceramic Engineering in the same UCB department.

The Annual Review of our 1981 programs was held on 8-9 February 1982. Dr. Samuel Liu, of Oak Ridge National Laboratory, served as Chairman. Other members were Dr. Richard Bernstein, Senior Vice President of Occidental Research Corporation; Professor Michel Boudart, Department of Chemical Engineering, Stanford University; Professor Richard Bradt, Chairman, Department of Materials Science, Pennsylvania State University; Dr. George Parshall, E. I. duPont de Nemours & Co.; and Dr. Harold Paxton, Vice President of Research, U.S. Steel Corporation.

Alan W. Searcy
Division Head

I Materials Sciences

A. Metallurgy and Ceramics

1. Structure of Materials

a. Structure and Properties of Transformation Interfaces*

Ronald Gronsky, Investigator

Introduction. The useful applications of a material are intimately related to those solid state transformations which either produce a desirable atomic structure at the outset (e.g., precipitation hardening) or modify the original atomic structure due to in-service conditions (e.g., oxidation). One approach to controlling these transformations and thereby extending the usefulness of materials is to examine in detail the interface between transformed and untransformed regions, paying close attention to the changes in atomic arrangement which occur across such a boundary. By relating the atomic structure of a transformation interface to its various properties (mobility, diffusivity, reactivity, conductivity, strength, ductility), a better understanding of the transformation process and its effect on material performance can be achieved. This is the goal of the present research program.

In order to conduct this study, specimens are carefully prepared to isolate the interfaces of interest, then subjected to both structural and chemical analyses at high spatial resolution in the transmission electron microscope. Comparisons are made with theoretical transition lattice models for interfacial structure and pertinent measured properties.

During the past year, effort has been devoted to both metallic alloys, summarized below, and semiconductor materials, a collaborative effort with J. Washburn described under Mechanical Properties, in the section "Structure-Property Relationships in Semiconductor Materials."

1. SEGREGATION AND PRE-PRECIPITATION PHENOMENA AT GRAIN BOUNDARIES†

Jose Briceno-Valero and Ronald Gronsky

The segregation of solute species to grain boundaries is known to affect both the mechanical properties of alloys, through its effect on cohesion, and the transformation properties of alloys, through its effect on kinetic phenomena.[1] In the present study the relationship between the segregation of Zn solute to grain boundaries in Al and the grain boundary precipitation of Zn in Al is sought. Both phenomena are correlated to grain boundary structure in order to better understand the atomistics of these processes, in particular the site specificity for solute clustering and nucleation at grain boundaries.

Specimens for this study were prepared by controlled doping of Zn in Al bicrystals followed by a short diffusion anneal. The boundary regions were subsequently analyzed by high resolution TEM and energy dispersive x-ray spectroscopy (EDS). Segregation profiles were obtained over regions ~ 10 nm in diameter both across and along the boundary plane.

An anisotropic distribution of Zn atoms is found along even the same grain boundary plane, where in fact a periodic distribution of segregation events was often observed. This arrangement of solute has been associated with regions of boundary structural defects corresponding to relaxation of the O-lattice, as well as extrinsic defects (Fig. 1) where a drastic accumulation of Zn was observed. The transition from this type of clustering event to an identifiable nucleus of the Zn-rich phase is shown to be straightforward in that all thermodynamic conditions for nucleation are favored by the formation of such clusters.

* * *

†Condensed version of LBL-13820 and LBL-13626.

1. E. D. Hondros and D. McLean, in Grain Boundary Structure and Properties, G. A. Chadwick and D. A. Smith (eds.), Academic Press, New York, 1976, p. 201.

2. ATOMISTICS OF GRAIN BOUNDARY PRECIPITATION†

Jean-Michel Penisson and Ronald Gronsky

The causal distinction between active and passive sites for formation of a new phase at a grain boundary is not only difficult to detect, but also nearly impossible to predict. This difficulty in understanding grain boundary precipitation has persisted in part due to a lack of spatial resolution in experimental studies. In this research program, an application is made of the highest resolution imaging methods currently available to characterize and understand the atomistics of grain boundary precipitation in an Al-Zn binary alloy.

A specimen of an Al 10 at% Zn alloy was aged at 150°C for 15 minutes, thinned by jet electropolishing, and viewed in a JEOL JEM 200 CX electron microscope equipped with a top-entry ultrahigh resolution goniometer stage and a high brightness LaB_6 gun. Micrographs were recorded in the

*This work was supported by the Director, Office of Energy Research, Office of Basic Energy Sciences, Materials Science Division of the U.S. Department of Energy under Contract No. DE-AC03-76SF00098.

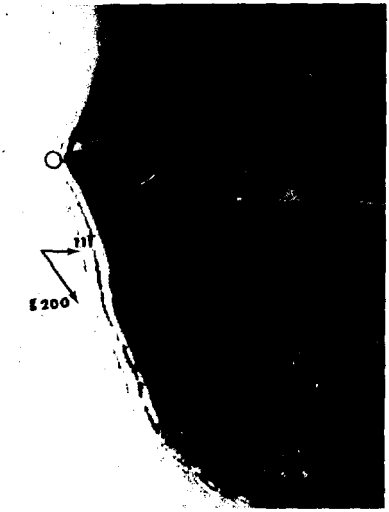

Fig. 1. Weak beam image and corresponding EDS trace of a grain boundary segment showing an enhancement of Zn concentration at the arrowed boundary cusp (dotted profile) over the surrounding boundary vicinity (solid profile). (XBB 810-9962)

270,000 x to 850,000 x magnification range, and all were accompanied by their corresponding electron diffraction patterns.

The resulting images were interpreted in terms of atomic structure, as shown for example in Fig. 1. This micrograph clearly shows that the growth front of the grain-boundary-nucleated Zn-rich phase (lower portion of the image) consists of extended planar portions of close-packed atomic planes during the growth into the upper grain. This microledge structure is the result of a dominant crystallographic influence on interface formation and/or propagation, which originates at the earliest appearance of the boundary-nucleated phase.

* * *

†Condensed version of LBL-13821.

3. WORK IN PROGRESS

The interface between crystalline and amorphous silicon is currently under investigation at high spatial resolution to clarify the mechanisms of amorphization, e.g., during ion-implantation.

Fig. 1. High resolution image of the interface between a grain boundary nucleated precipitate (bottom) and matrix grain (top). The dashed line marks the location of planar facets at the interface which assume a parallel orientation consistent with the crystallography of the close-packed planes. A defect is present within the arrowed portion. (XBB 817-6571)

Grain boundary segregation of phosphorous in LPCVD polycrystalline silicon is also under study to reveal the extent of segregation, its microdistribution with respect to boundary type and its effect on electronic properties.

Research continues on the mechanisms of deformation accommodation at grain boundaries as an experimental study of the interaction between crystal slip dislocations and secondary grain boundary dislocations.

A new program on the atomic mechanisms of precipitate plate growth has also been initiated (collaborative effort with Dr. H. I. Aaronson, R. F. Mehl Professor, Carnegie-Mellon University).

1981 PUBLICATIONS AND REPORTS

Refereed Journals

1. R. Gronsky and P. Furrer, "Grain Boundary Precipitation in Aluminum Alloys: Effect of Boundary Structure," Met. Trans. 12A, 121 (1981); LBL-9737.

2. D. J. H. Cockayne and R. Gronsky, "Lattice Imaging of Modulated Structures," Phil. Mag. A44, 159 (1981); LBL-10158.

3. C. B. Carter, J. Rose, and D. G. Ast, "TEM Study of Tilt Boundary in Hot-Pressed Silicon," in Proc. 39th Annual Meeting Elec. Mic. Soc. Amer., G. W. Bailey (ed.), Claitor's, Baton Rouge, 1981, p. 160.

LBL Reports

1. J. A. Little and R. Gronsky, "The Microstructure of High Rank Coals at Lattice Resolution," LBL-11612 Revised.

2. J. Briceno-Valero and R. Gronsky, "Pre-Precipitation Phenomena at Grain Boundaries," LBL-13820.

3. J. M. Penisson and R. Gronsky, "Experimental Studies on the Atomistics of Grain Boundary Precipitation," LBL-13821.

4. T. O. Sands, "The Effects of Oxygen on the Microstructure of $Cu_{2-x}S$ Thin Films," (M.S. thesis), LBL-13659.

5. J. Briceno-Valero, "On the Morphology of Grain Boundary Segregation: Effect of Grain Boundary Structure in Al-Zn Alloys," (Ph.D. thesis), LBL-13626.

6. J. M. Penisson and R. Gronsky, "A High Resolution Study of a Σ41 Tilt Boundary in Molybdenum," LBL-13822.

7. T. O. Sands, J. Washburn and R. Gronsky, "High Resolution Observations of Copper Vacancy Ordering in Chalcocite (Cu_2S) and the Transformation to Djurleite $(Cu_{1.97-1.83}S)^2$," LBL-13746.

Other Publications

1. G. Thomas, R. Gronsky, O. L. Krivanek, and R. K. Mishra, "Physical and Chemical Characterization of Interfaces by Electron Optical Methods," in Surfaces and Interfaces in Ceramic and Ceramic-Metal Systems, J. Pask and A. G. Evans (eds.), Plenum Press, 1981, p. 35; LBL-11413.

Invited Talks

1. R. Gronsky, "Grain Boundary Precipitation: Effect of Boundary Structure," Rockwell International Science Center, Thousand Oaks, CA, January 28, 1981.

2. R. Gronsky, "Atomic Resolution in Transmission Electron Microscopy," Sandia National Laboratory, Livermore, CA, April 29, 1981.

3. R. Gronsky, "Microscopic Determination of Grain Boundary Structure and Segregation," BES/RRT Working Meeting on Radiation-Induced Solute Flows and Their Effects on Mechanical Properties of Alloys, Argonne National Laboratory, Argonne, IL, May 11-12, 1981.

4. P. Furrer and R. Gronsky, "Precipitation on Grain Boundaries," 7th. International Light Metals Congress, Loeben, Vienna, June 21-23, 1981.

5. J. M. Penisson and R. Gronsky, "High Resolution Imaging of Grain Boundaries," TMS/AIME and BSD/ACS Fall Meeting, Louisville, KY, October 11-15, 1981.

b. Microstructure, Properties, and Alloy Design: Inorganic Materials*

Gareth Thomas, Investigator

Introduction. Current projects endeavor to understand the relations between microstructure, both metallic and ceramic, at a fundamental level. This is necessary not only to design and utilize new technological materials, but to conserve both the materials and energy necessary to make them. Thus, the experimental programs involve characterization of materials using the most modern and sophisticated methods available today, notably, high resolution and analytical electron microscopy.

Main areas of research include A) alloy design of medium carbon steels ("qua-tough" alloys), B) low carbon dual-phase steels, and C) magnetic materials. A brief description of each category follows.

A. Alloy Design: Medium Carbon Steels, "Qua-Tough Alloys." This continuing program on controlling combinations of high strength and good toughness has concentrated on optimizing the dislocated lath and stable interlath austenite duplex microstructures by controlling composition, heat treatment and melting practice. Because of considerable interest from the mining and agricultural industries, the wear and corrosion aspects of these steels are now under investigation. It seems that stable retained austenite is also a significant factor in these properties.

New programs being developed include surface treatments such as laser glazing, to control surface microstructures and properties (e.g., for improved wear).

B. Low Carbon Dual-Phase Steels. This program is concerned with the effects of composition and heat treatment on the strength, fracture, and corrosion resistance of simple low carbon steels. Although the initial motivation for this program came from the need to improve strong steels with high formability for automobile manufacture, to attain fuel savings (and which has been successful, e.g., the patented Fe/Si/C steels), the potential for dual-phase steels in structural applications is very broad indeed. New programs to improve pipeline steels and high tensile wires are in progress, and a new project on welding of these steels will be initiated in the Spring of 1982.

C. Magnetic Materials. Hard (Sm-Co type, Mn-Al-C, Fe-Cr-Co) and soft (ferrites, glasses, garnets) magnetic materials are investigated to establish the mechanisms of magnetization; in particular, the influence of defects, precipitates and processing variables are being studied. Magnets are key elements in power generation and transformer equipment, hence the technical objectives are directed towards improving magnetic properties through control of composition and microstructure.

A. Alloy Design: Medium Carbon Steels, "Qua-Tough Alloys"

1. IN-SITU STUDIES OF FRACTURE OF 0.3C STEELS†‡

G. Thomas

Thin foils of quenched, and quenched and tempered Fe/Cr/0.3C with Mn or Ni have been examined to fracture in a high voltage electron microscope equipped with a tensile stage. The fractures always occur within the martensite laths which have been shown to be depleted with respect to carbon, whilst the surrounding retained austenite is enriched in carbon. This austenite decomposes to interlath carbide on tempering. In the tough condition, fracture is preceded by localized dislocation slip, work hardening, thinning down (necking) and hole formation. Packets of laths unfavorably oriented do not participate in fracture initiation. In the tempered condition, slip and failure depends on carbide morphology. Some retained austenite may transform to thinned martensite, but the main benefit of the austenite to improved toughness appears to be indirect. It is suggested that the fracture process depends primarily on the plastic deformation characteristics of the martensite (or bainite) laths which in turn are affected by the microstructure.

* * *

†The A. von Humboldt Foundation generously provided a Senior Science Award which allowed the in-situ experiments to be performed at the Max-Planck-Institute, Stuttgart, Germany. The support of Dr. Manfred Ruhle and his staff is gratefully acknowledged.

‡Conference on Modern Developments in Physical Metallurgy of Steel, Liverpool, England, The Metals Society, in press.

2. TEMPERED MARTENSITE EMBRITTLEMENT IN Fe/Cr/Mn/C ALLOYS

Ashok Jhingan†

In order to achieve combinations of high strength and high toughness, a microstructure consisting of dislocated lath martensite and continuous retained austenite films at interlath boundaries, is desirable. Films of retained austenite decompose upon tempering in the temperature range of 200-400°C.[1] Concomitant with this microstructural change, a sharp drop in impact toughness is observed. Therefore, an understanding of the kinetics and mechanism of decomposition of retained austenite is required to understand temper martensite embrittlement.

---

*This work was supported by the Director, Office of Energy Research, Office of Basic Energy Sciences, Materials Sciences Division of the U.S. Department of Energy under Contract No. DE-AC03-76SF00098.

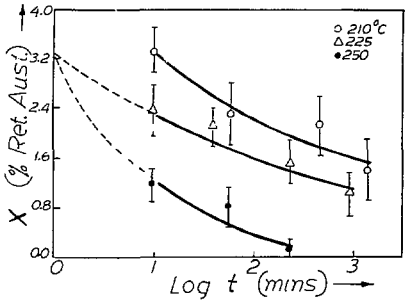

Fig. 1. Percent austenite decomposition with tempering as measured by X-ray analysis. (XBL 8110-11731)

X-ray diffraction studies were carried out to determine the amount of retained austenite. Samples were tempered for different times in the temperature range of 210-250°C. Some results are shown in Fig. 1. The activation energy for the decomposition of retained austenite is approximately 74 kcal/mole. This shows that the retained austenite is highly stable, although the austenite stabilization mechanism(s) is not uniquely known. It is established that segregation of carbon and chromium occurs to the austenite/martenite interfaces which would decrease their mobility, but more detailed study requires field ion atom probe analyses of austenite interfaces and austenite.

* * *

†Ph.D. thesis research: in progress

1. G. Thomas, Met. Trans., 9A, 439 (1978).

3. FUNDAMENTAL STUDIES OF WEAR IN FERROUS MATERIALS†‡

W. J. Salesky§

In an effort to more fully understand the events and processes that lead to wear, this program examines deformed surface regions developed during wear in several ferrous materials, and attempts to characterize the structures developed during sliding and abrasive wear, subsequently relating them to the wear debris that forms.

Results to date indicate the formation of a steep strain gradient decreasing with distance from the surface. Recent high voltage electron microscopy studies performed on worn pure iron reveal that fine dislocation cell structures are formed on the order of 0.1 μm diameter at 1-2 μm from the surface, to > 1 μm at a distance of more than 15 μm from the surface (see Fig. 1). Comparison to similar structures formed during wire drawing of the same material suggests true strains on the order of magnitude of 5-6% are experienced

Fig. 1. An example of the dislocation-cell size gradient on worn pure iron. The figure is from a region 4 microns from the interface (to the left of the figure). The sliding direction is indicated by the arrow. (XBB 8112-11945)

at and near the surface, falling off rapidly to less than 1 at a distance of ~ 15 μm. The structures are typical of those from high strain-rate deformation.

Recognition of these dislocation interactions as being significant to wear, is important to the methodology employed to reduce it. Presence of ultra-fine, hard, carbides in a tough ductile matrix (dispersion strengthening) or a matrix with ultra-fine grain size (as formed through laser treatment) would greatly inhibit the motion of dislocations.

* * *

†We acknowledge the interaction of Dr. R. M. Fisher and the use of equipment at U.S. Steel Research Labs., Monroeville, PA.

§Ph.D. thesis research: in progress.

‡Proceedings of International Conference on Wear, San Francisco, CA, March 30-April 4, 1981.

4. TWO-BODY, DRY ABRASIVE WEAR OF Fe/Cr/C EXPERIMENTAL ALLOYS

Chi Kong Kwok†

Wear is a form of mechanical failure that is very general, but poorly understood. Maintenance and replacement of machinery represents a significant cost to industry. In the United States alone, an estimated $16 billion per year can be saved if proper wear prevention is implemented.[1]

A systematic study of abrasive wear resistance of Fe/Cr/Mn/C based alloys has been carried out using a two-body, pin-on-disc wear machine. Abrasives used were silicon carbide, alumina and quartz.

The goal of this study was to develop information so as to improve wear resistance of these experimental alloys by means of thermal treatments. Results showed that bulk hardness and tensile strength (Fig. 1) are both very important factors in abrasive wear. The experimental alloy, which has superior tensile and toughness properties, has better wear resistance than most of the commercial alloys tested. Grain refinement by double heat treatment improved the toughness but appeared to have little effect on the abrasive wear resistance. Future research will concentrate on the mechanism of wear, and the enhancement of wear resistance by means of selective microstructural changes and surface treatments.

* * *

†M.S. thesis, Fall 1981, LBL-13393

1. M. P. Jost, Mechanical Engineering, 97, 26 (1975).

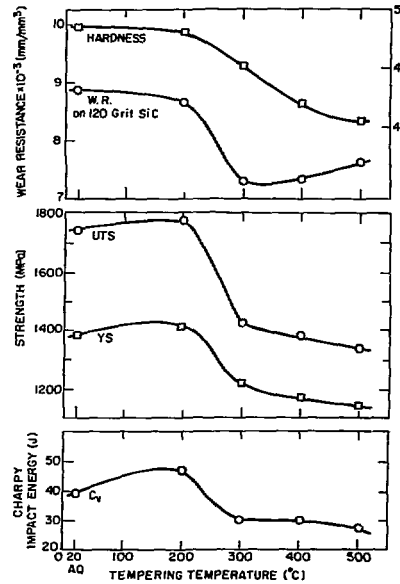

Fig. 1. Relationship between wear resistance and other mechanical properties of the experimental alloy at different temperatures. (XBL 819-6555)

5. MECHANICAL PROPERTIES AND MICROSTRUCTURE OF LOWER BAINITIC Fe/C/Cr ALLOYS

Hiroyuki Tokushige†

In thick section components, it is difficult to obtain fully martensitic structures, so mechanical and microstructural features have been studied in lower bainitic Fe/C/Cr base alloys.[1]

Lower bainite was produced by isothermal transformation at 30°C above the M_S temperature.

An example of the lower bainitic structure is shown in Fig. 1. The structure is bainitic ferrite laths and intralath carbides. However, the morphology and configuration of the retained austenite have not yet been determined. In spite of its lower strengths the lower bainite shows substan-

Fig. 1. Transmission electron micrographs of the lower bainite in a 0.3%C-3%Cr-2%Mn steel (isothermally transformed for 18 min. at 360°C). a) BF b)DF taken from the reflections encircled in c and c) SAD showing [100]f, [111]f, [110]a, and unidentified carbide diffraction patterns. (XBB 8112-11732)

tially lower Charpy impact values than the martensite. Although more intensive work is needed on microscopy and fractography, from a practical point of view, the lower bainite in these steels does not appear to provide comparable mechanical properties to the martensite.

* * *

†Ph.D. thesis research: in progress.
1. B. V. N. Rao and G. Thomas, Met. Trans., 11A, 441 (1980).

6. WORK IN PROGRESS

The main emphasis of current research is to obtain a more fundamental understanding of wear mechanisms and optimization of surface treatments for improving wear properties. Laser and other rapid surface heating and cooling methods are under investigation (J. Rayment). Further research on fatigue behavior will be done jointly with Professor R. O. Ritchie. A new alloy design project is to achieve improved abrasion resistance in higher tensile strength steels (0.4%C) by dispersing fine carbides in dislocated laths without forming embrittling interlath carbide films. Further work is being done also on bainitic structures.

B. Low Carbon Dual-Phase Steels

1. DUAL-PHASE (DUPLEX) STEEL FOR PIPELINES†‡

N. J. Kim and G. Thomas

The need for pipeline transportation in arctic regions has resulted in more demanding quality requirements for pipeline steels, viz., higher strength and toughness at lower temperatures. Pipelines are large-tonnage, low-cost items. Thus, a simple dual-phase steel, i.e., ferrite and either martensite or bainite, has been developed in order to achieve the desired properties.

The alloy used in this investigation was air-melted Fe/1.5Mn/.06C. The dual-phase structure was obtained by hot rolling with subsequent water quenching. Slabs were soaked at 1100°C for 45 minutes and hot rolled 35% at 1000°C and then finish rolled 50% in the temperature range of 750°C to 950°C. The microstructure of the steel thus treated is roughly 70% ferrite and 30% upper bainite. By lowering the finish rolling temperature, the strength increases with no appreciable change in elongation, and the ductile-brittle transition temperature (DBTT) decreases to -120°C (Fig. 1). These changes are due to the refinement of ferrite grain size.

The advantage of this as-hot-rolled ferrite-bainite steel is its continuous yielding behavior and high initial work-hardening rate. There is an additional increase in yield strength during the pipe fabrication, whereas fabrication reduces the strength of conventional ferrite-pearlite structures.

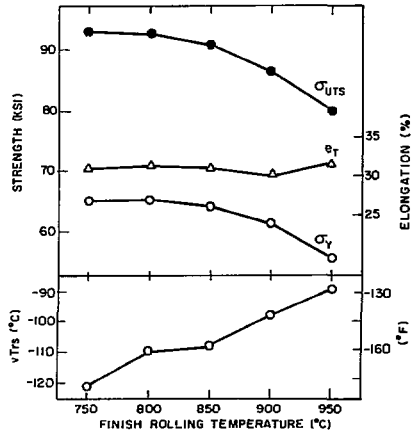

Fig. 1. Variation of mechanical properties of the ferrite-bainite structure with finish rolling temperature. (XBL 813-5376)

* * *

†Brief version of LBL-12661, November, 1981.
‡International Conference of Steels for Line Pipe & Pipeline Fittings, Grosvenor House, London, England, October 21-23, 1981; LBL-13543.

2. MICROSTRUCTURE-PROPERTIES OF CONTROLLED ROLLED MICROALLOYED LOW CARBON STEEL†

A. J. Yang,‡ N. J. Kim, and G. Thomas

As part of a continuing program aimed at improving the low temperature toughness of dual-phase steels for pipeline application, the effect of Nb on the hot rolling characteristics and resulting microstructure and mechanical properties of base Fe/Mn/C steel has been investigated.

Addition of Nb has been shown to retard the recrystallization of austenite, thus giving rise to finer and more elongated austenite grains. The resulting microstructure consists of small islands of martensite and bainite in a matrix of highly dislocated acicular ferrite.

This structure shows higher yield strength and lower work-hardening rate than ferritic-martensitic and/or ferritic-bainitic dual-phase structures. This steel has high strength (σ_{UTS} = 95 ksi) and good impact toughness (DBTT ~ -110°C). A wide range of finish rolling temperatures can be used without appreciable effect on the microstructure and resulting mechanical properties. The above properties are desirable in the manufacture of pipelines, especially in very cold regions.

* * *

†Met. Trans. (in press)

‡Present address: Shanghai Jiao Tong University, 1954 Hua Shan Road, Shanghai 200030, Peoples Republic of China.

3. WORK IN PROGRESS

a. Continued alloy design applications are in progress, e.g., optimizing the thermal-mechanical treatments for improved low-temperature toughness. An understanding of the effects of carbide precipitation in ferrite is being sought to improve flexibility in heat treatment. It is anticipated that design targets for high tensile strength wire will be achieved.

b. Tensile and fatigue crack growth properties of AISI 1018 Fe/2Si/0.1C DFM steels with different martensite morphologies are being examined (J. Wasynczuk).

c. A detailed microstructural examination of Fe/1.0Al/0.1C steel has been carried out by X. F. Wu† and G. Thomas. The tensile strength and impact ductility were determined after different heat treatments of both air and vacuum melted alloys. In both cases, it was found that the tensile strength and the work hardening do not increase linearly with the martensite volume fraction. Fine plate precipitates were found to be homogeneously distributed in the ferrite phase and oriented on or near {100} planes. These plates are about 30 Å thick with a diameter of 100-250 Å. The density of these precipitates varies with martensite volume fraction, and they produce dispersion strengthening of the ferrite.

d. A new program on welding of dual-phase steels will start in Spring 1982.

* * *

†Visiting Scientist from Beijing University of Iron and Steel Technology, Beijing, Peoples Republic of China.

C. Magnetic Materials

1. PRECIPITATION HARDENING Sm-Co BASE PERMANENT MAGNETS†‡

Lew Rabenberg§

Samarium-cobalt based permanent magnets with energy products in excess of 30 MGOe are now available.[1] Typically, these magnets have overall compositions between those of the $SmCo_5$ and Sm_2Co_{17} intermetallic compounds, modified by additions of Fe, Cu, and small amounts of Zr. These pentenary alloys are sintered and subsequently step-aged to produce high intrinsic coercivity and high energy products. Their microstructures generally have a two-phase cellular morphology where the 2:17 phase forms the cell interiors and the 1:5 phase forms the cell walls.[2] The high coercivity is attributed to pinning of the magnetic domain walls by the cellular structure. The chemical differentiation between the two phases is thought to be crucial in determining the domain wall pinning strength and the resultant coercivity.

Transmission electron microscopy and microanalysis techniques are being used to determine the structure-property relationships and solid-state phase transformation mechanisms for this class of magnets. This information will be useful for the design of higher coercivity magnets through microstructural manipulation.

The best currently available magnets have the cellular structure of 8 nm thick hexagonal $SmCo_5$ walls and 50 nm twinned rhombohedral Sm_2Co_{17} interiors. Superimposed on this structure are thin (< 5 nm) plates, lying perpendicular to the crystallographic c-axis, of a Zr-enriched phase isomorphic with the $SmCo_3$ binary phase. These features are visible in Fig. 1. Development of this structure during 800°C anneals is followed by step-aging to 400°C which produces the required partitioning of Fe and Cu between the 2:17 and 1:5 phases. The Zr serves to drive this process toward completion; it also stabilizes the 1:3 phase plates which serve as enhanced diffusion paths for the Co, Fe, and Cu.

* * *

†Specimens and magnetic measurements supplied by T. Ojima and TDK Research & Development Laboratories, Chiba, Japan are gratefully acknowledged.

‡L. Rabenberg, R. K. Mishra, and G. Thomas, 27th Annual Magnetism and Magnetic Materials Meeting, Atlanta, GA, November 10-13, 1981.

§Ph.D. thesis research: in progress.

1. T. Ojima, S. Tomizawa, T. Yoneyama, and T. Hori, IEEE Trans. Mag. MAG-13, 1317 (1977).
2. J. D. Livingston and D. L. Martin, J. Appl. Phys. 48, 1350 (1977).

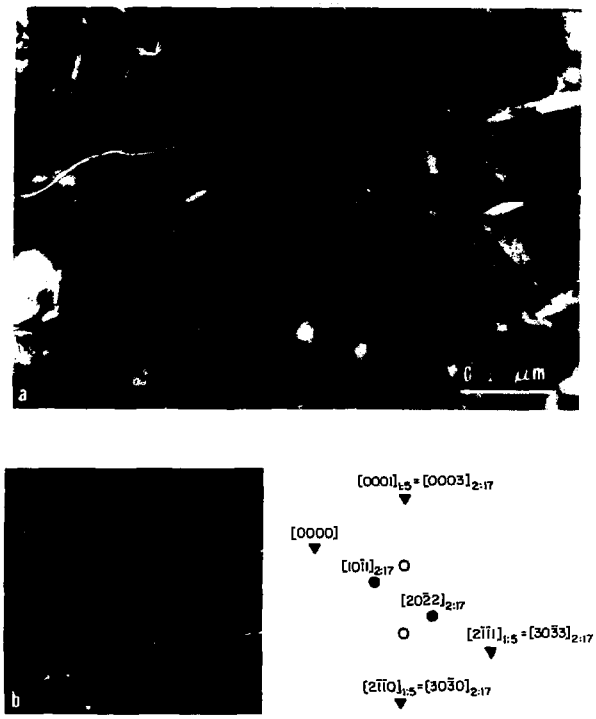

Fig. 1. a) Transmission electron micrograph (symmetric [01$\bar{1}$0] orientation) showing the microstructure of a 3% Zr alloy near peak aging. The c-axis is in the plane of the paper in the direction indicated. b) Selected area diffraction pattern and indexing showing hexagonal 1:5 and rhombohedral 2:17 spots. Solid triangles correspond to spots common to all phases; solid circles are from one 2:17 variant, open circles from the other. (XBB 810-9499)

2. ANNEALING OF HIGH PERMEABILITY $(MnZn)Fe_2O_4$

I-Nan Lin†

MnZn-ferrite is mainly used in telecommunication and entertainment electronics. In this application, high electrical resistivity is necessary in order to minimize eddy current loss, and attain high initial permeability. Conventionally, CaO is added to MnZn-ferrite to obtain high electrical resistivity by forming an insulating layer along grain boundaries. However, CaO additions lower the permeability whether they are segregated at grain boundaries or dissolved in the matrix. Moreover, the advantage of forming an insulating layer is completely lost at high operating frequency.

In the present research, electrical resistivity of high initial permeability materials has been increased as much as two orders of magnitude by controlled atmosphere annealing (Fig. 1). In the heat treatment, the specimen is kept at 1000-1100°C for 24 hours under a controlled atmosphere to ensure the completeness of reaction. The atmosphere is controlled by regulating the ratio of the flow rate of N_2 and O_2 gases. The oxygen partial pressure of the mixture is measured by an oxygen monitor and it is controlled between 0.012 and 1.2%.

Presumably, the Fe^{2+} ions are oxidized to

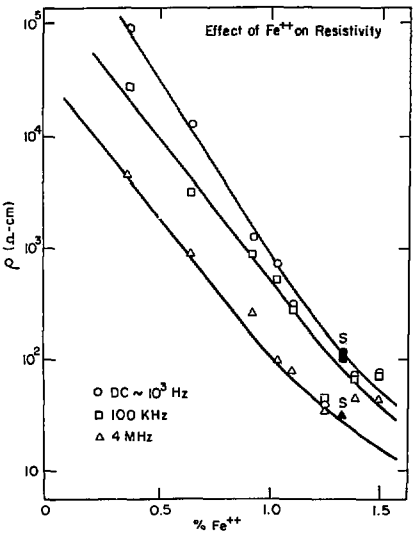

Fig. 1. The effect of controlled atmosphere annealing on resistivity of MnZn-ferrite; resistivity increases as Fe^{++} ion content decreases due to annealing. (XBL 8112-13184)

Fe^{3+} ions during heat treatment. The hopping of electrons between Fe^{2+} ions and Fe^{3+} ions, which is the proposed conducting mechanism of MnZn-ferrite, is thus suppressed. The electrical resistivity increases exponentially as Fe^{2+} ion content decreases. The result of the heat treatment on improving electrical resistivity is shown in Fig. 1.

* * *

†Ph.D. thesis research: in progress.

3. WORK IN PROGRESS

R. K. Mishra, J. S. Gau, and K. Krishnan

a) Mn-Al-C Magnets. The metastable MnAl "T" phase is the only known potential permanent magnet material that does not contain Co, and is, therefore, of considerable technological interest. The purpose of this work is the development of useful permanent magnetic materials in the Mn-Al-C system by microstructural characterization and thermomechanical and thermomagnetic processing.

b) Magnetic Anisotropy in Garnets. Crystallographic studies by electron diffraction are in progress to establish possible crystallographic anisotropies in relation to magnetic properties.

c) Crystal Structure Analysis of CGGG. $Ca_3Ga_2Ge_3O_{12}$ garnet (space group: Ia3d) is suitable substrate for ferrimagnetic garnets for bubble memory devices. The CGGG is characterized by microsegregated defects. Computer simulation of the structure image is currently underway to reveal the atomic configurations at various orientations. This work will provide the necessary experimental operating conditions for high resolution electron microscopy (HREM) studies.

1981 PUBLICATIONS AND REPORTS

Refereed Journals

1. T. F. Roth, R. K. Mishra, and G. Thomas, "Segregation of Czochralski Grown Calcium Gallium Germanium Garnet Single Crystals," J. Appl. Phys., 52(1), 219-26 (1981); LBL-10832.

2. Y. Belli, R. K. Mishra, K. Kubarych, and M. Okada, "The Effect of V and V + Ti on the Magnetic and Mechanical Properties of Fe/Cr/Co Hard Magnets," Materials Science and Engineering, 47, 69-75 (1981); LBL-8384.

3. N. J. Kim and G. Thomas, "Effects of Morphology on the Mechanical Behavior of Dual-Phase Fe/Si/C Steels," Met. Trans. 12A, 483-89 (1981); LBL-10457.

4. R. K. Mishra and G. Thomas, "Microstructure Properties of Step-Aged Rare Earth Alloy Magnets," J. Appl. Phys., 52(3), 2517-19 (1981); LBL-11680.

5. E. K. Goo, R. K. Mishra, and G. Thomas, "Electron Microscopy Study of Ferroelectric Domain

& Domain Wall Structure in $PbZr_{.52}Ti_{.48}O_3$," J. Appl. Phys., 52, 2940 (1981); LBL-11256.

6. U. Dahmen, K. H. Westmacott, and G. Thomas, "A Study of Precipitation in Interstitial Alloys-I. Precipitation Sequence in Ta-C Alloys," Acta Met., 29, 627-35 (1981); LBL-11244.

7. S. J. Barnard, G. D. W. Smith, M. Sarikaya, and G. Thomas, "Carbon Atom Distribution in a Dual-Phase Steel: Atom Probe Study," Scripta Met., 15, 387 (1981); LBL-12267.

8. G. Thomas and Y. L. Chen, "Structure and Mechanical Properties of Fe-Cr-Mo-C Alloys with and without Boron," Met. Trans., 12A, 933-50 (1981); LBL-8310.

9. R. H. Hoel and G. Thomas, "Ferrite Structure and Mechanical Properties of Low Alloy Duplex Steels," Scripta Met., 15, 867-72 (1981); LBL-11101.

10. E. K. Goo, R. K. Mishra, and G. Thomas, "Transmission Electron Microscopy of $Pb(Zr_{.52}Ti_{.48})O_3$," J. Am. Cer. Soc., 64, 517 (1981); LBL-11369.

11. J. J. Rayment and B. Cantor, "The As-Quenched Microstructure & Tempering Behavior of Rapidly Solidified Tungsten Steels," Met. Trans., 12A, 1557 (1981); LBL-12121.

12. A. Nakagawa, J. Y. Koo, and G. Thomas, "Effect of Vanadium on Structure-Property Relations of Dual-Phase Fe/Mn/Si/0.1 Steels," Met. Trans., 12A, 1965-72 (1981); LBL-11929.

13. R. K. Mishra and G. Thomas, "Recent Progress in Studies of Microstructure of Ferrites," Proceedings of the Third International Conference on Ferrites, Kyoto, Japan, September 30 - October 2, 1981, Invited Key-Note Speaker, pp. 257-264; LBL-11571.

14. G. Thomas, R. Gronsky, O. Krivanek, and R. Mishra, "Physical and Chemical Characterization of Interfaces by Electron Optical Methods," Proceedings of the Conference on Surfaces & Interfaces in Ceramic & Ceramic-Metal Systems, July 28 - August 1, 1981, Berkeley, CA, pp. 35-49; LBL-11413.

LBL Reports

1. C. Ahn, "Microstructure & Grain Boundary Chemistry of Hot-Pressed Silicon Nitride," M.S. thesis, LBL-12836.

2. A. Nakagawa, "Effect of Vanadium on Dual-Phase Fe/Mn/Si/0.1C Steels," M.S. thesis, LBL-12843.

3. J. Gau, "Microstructure and Mechanical Properties of 0.1C Steel with Nb," M.S. thesis, LBL-12058.

4. S. Kwok, "Two-Body Dry Abrasive Wear of Fe-Cr-C Experimental Alloys-Relationship Between Microstructure & Mechanical & Wear Properties," M.S. thesis, LBL-13393.

5. N. Kim, "Design of Dual-Phase Fe/Mn/C Steel for Low Temperature Application," Ph.D. thesis, LBL-12661.

6. C. Kung, "Fatigue Properties of Qua-Tough Steel Fe-4Cr-XMn-0.25C," LBL-13465.

7. R. K. Mishra and G. Thomas, "Amorphous Grain Boundary Phases in Ferrimagnetic $(MnZn)Fe_2O_4$ & Ferroelectric PZT Ceramics," Proceedings of the Conference on Surfaces & Interfaces in Ceramic and Ceramic-Metal Systems, July 28 - August 1, Berkeley, CA, pp. 199-206 (1981), LBL-11511.

8. U. Dahmen, K. Westmacott, and G. Thomas, "An Electron Microscopy Analysis of a Simple Metal-Ceramic Interface," Proceedings of the Conference on Surfaces & Interfaces in Ceramic and Ceramic-Metal Systems, July 28 - August 1, Berkeley, CA, pp. 391-99 (1981), LBL-11405.

9. M. Sarikaya, "Determination of Exact Orientation Relationships Between Martensite and Austenite in Steels in Microdiffraction," Proceedings of the 39th Annual EMSA Meeting, Atlanta, Georgia, August 10-14, pp. 364-5 (1981), LBL-12289.

10. W. J. Salesky, "Design of Medium Carbon Steel for Wear Applications," Proceedings of the International Conference on Wear of Materials, San Francisco, CA, March 30 - April 1, pp. 298-305 (1981), LBL-12447.

11. N. Kim and G. Thomas, "Dual-Phase Steels for Pipelines," LBL Patent Applied for in 1981, LBL-13543.

12. J. Gau, J. Koo, A. Nakagawa, and G. Thomas, "Microstructure and Properties of Dual-Phase Steels Containing Fine Precipitates" in Fundamentals of Dual-Phase Steels, R. A. Kot, and B. L. Bramfitt, eds., AIME, New York, NY, LBL-12177.

Other Publications

1. "Microstructure & Magnetic Domain Wall Motion in $(MnZn)Fe_2O_4$." I-Nan Lin and G. Thomas, Proceedings of the 39th Annual EMSA Meeting, Atlanta, GA, August 10-14, G. W. Bailey, ed., p. 324 (1981).

2. "Computer Control of STEM for X-Ray and Energy Loss Imaging," P. Rez and C. Ahn, Proceedings of the 39th Annual EMSA Meeting, Atlanta, GA, August 10-14, 1981, pp. 262-265.

Invited Talks

1. J. Rayment, O. Ashiru, and B. Cantor, "The As-Quenched Microstructures of Rapidly Solidified Fe-25 wt% Ni," International Conference on Solid-Solid Phase Transformation Proceedings, Pittsburgh, PA, August 10-14, 1981, H. I. Aaronson, ed.; LBL-13272.

2. G. Thomas and M. Sarikaya, "Lath Martensites in Carbon Steels - Are They Bainitic?," International Conference on Solid-Solid Phase Transformations Proceedings, Pittsburgh, PA, August 10-14, 1981, H. I. Aaronson, ed.; LBL-13098.

3. M. Sarikaya, G. Thomas, J. W. Steeds, S. Barnard, and G. D. W. Smith, "Solute Element Partitioning and Austenite Stabilization in Steels," International Conference on Solid-Solid Phase Transformation Proceedings, Pittsburgh, PA, August 10-14, 1981, H. I. Aaronson, ed.; LBL-13099.

4. G. Thomas, M. Sarikaya, G. D. W. Smith, and S. Barnard, "Microstructure, Retained Austenite and Mechanical Properties of Experimental 0.3 % C Steels," Conference on Advances in Physical Metallurgy and Applications of Steels, Proceedings of the Metal Society, Liverpool, England, September, 1981; LBL-13048.

c. Solid State Phase Transformation Mechanisms*

Kenneth H. Westmacott, Investigator

Introduction. Crystal lattice defects are known to play a role in solid state phase transformations but the real nature of their involvement is not well understood. In the present research evidence has been found that in a variety of alloy systems, substitutional and interstitial, face-centered-cubic and body-centered-cubic, vacancies and dislocations are structurally indispensable in the precipitation processes observed. The new links thus established have led to the recognition of a fundamental connection between the martensite, O-lattice and elastic inclusion theories of phase transformations not previously appreciated, and to the development of a unifying theory.

1. CRYSTALLOGRAPHIC THEORY OF PRECIPITATION†

U. Dahmen and K. H. Westmacott

Further developments of the basic concepts of martensite and O-lattice theory have resulted in a crystallographic theory of precipitation. Two basic postulates of this theory are that 1) precipitate needles follow invariant line directions and thus lie on the cones of unextended lines, and 2) minimization of the necessary shape accommodation dictates that precipitate growth and loss of coherency will occur only for those precipitates favorably oriented for shear loop nucleation.

Precise experimental results on Cu-Cr alloys are available[1] for comparison with the theory. Figure 1 shows the typical morphology of Cr needles (bcc structure) in a Cu matrix (fcc structure). The needle directions in this system, which appear almost random in Fig. 1, were analyzed[1] and are

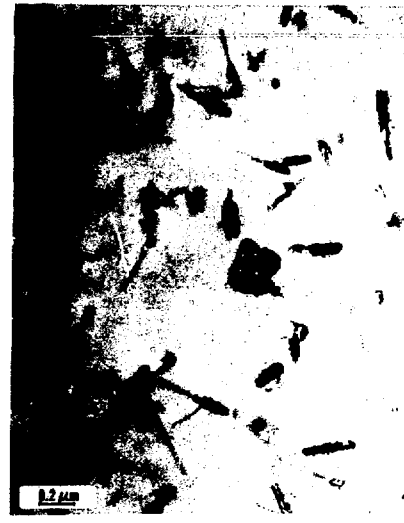

Fig. 1. Micrograph of precipitate needles in quench-aged Cu-Cr illustrating apparently random distribution. (XBB 821-190)

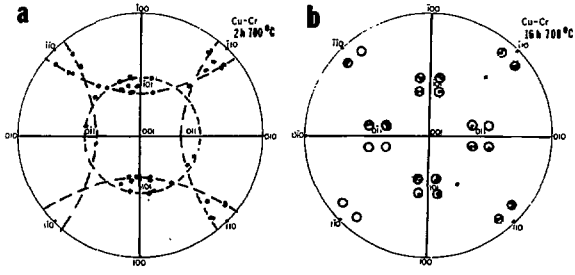

Fig. 2. Stereograms showing the excellent agreement between the predicted and experimentally observed data for Cu-Cr: (a) shows coherent needles lie on cones of unextended lines; (b) shows loss of coherency leads to clustering in <6.3, 5.3, 1>. (XBL 817-10887B)

*This work was supported by the Director, Office of Energy Research, Office of Basic Energy Science, Materials Sciences Division of the U. S. Department of Energy under Contract No. DE-AC03-76SF00098.

plotted on stereograms in Fig. 2. It is seen in (a) that indeed all observed coherent needle directions (after a short aging time) were on or near the calculated cones of unextended lines.

After longer aging times the precipitates lose coherency and grow. Theory predicts that only those needles lying along <6.3, 5.2, 1> directions are favorably oriented to do so. Again, comparison between the predicted poles and experimentally observed needle axes, Fig. 2(b), shows excellent agreement. Furthermore, theoretically predicted and experimentally observed orientation relationships are also in excellent accord.

Continued precipitate growth occurs with the same orientation relationship and should lead to a characteristic morphology which differs from that resulting from heterogeneous nucleation. This aspect is now being studied.

* * *

†Short version of LBL-13336.

1. K. H. Westmacott, U. Dahmen, A. Pelton, and M. J. Witcomb, "Solid State Phase Transformation Mechanisms," LBL-13336 (1981).

2. PRECIPITATION REACTIONS IN AUSTENITIC STAINLESS STEELS

A. R. Pelton and K. H. Westmacott

Although the crystallographic theory is being tested primarily against simple alloy systems it is also applicable to more complex alloys of practical importance.

Interstitial phase precipitation reactions in an austenitic stainless steel were studied, and the connection between the precipitate structure and quenched-in vacancies was established. However, because of the fine scale of the precipitates and small volume fraction, changes in the matrix lattice parameter were used to monitor the progress of the phase decomposition. The necessary precision was achieved by recording Convergent Beam Electron Diffraction patterns and measuring the shifts in the relative positions of higher order Laue zone lines in the zero order disc (see Fig. 1). Relative to the as-quenched sample, where all the solute atoms are in solution, aging at 500°C for 10h or 600°C for 1 hour decreased the lattice parameter by 2 parts in 10^4. Aging at 500°C for 100h decreased it by 4 in 10^4. The magnitude of these changes was related to the size, density, and nature of phosphide and carbide precipitates.

* * *

†Short version of LBL-13336.

3. WORK IN PROGRESS

J-M. Lang, U. Dahmen and K. H. Westmacott

From earlier work it is predicted that in the Mo-C system small platelets of Mo_2C will precipitate on the {310} matrix planes after quench-aging. Moreover, the orientation relationship between the carbide and matrix should be near that proposed by Burgers. Figure 1 shows a high resolution lattice image of an interface between Mo_2C and Mo. A slight misorientation between the (0001) planes of

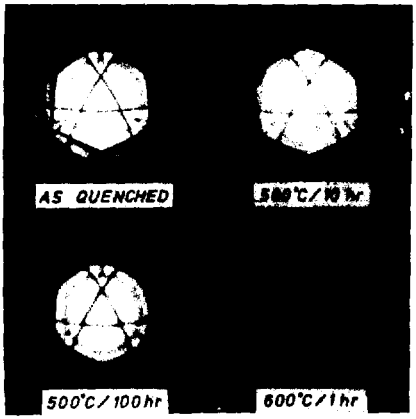

Fig. 1. Convergent beam electron diffraction patterns showing the triangle of high order Laue zone lines used for precision lattice parameter measurements after various heat treatments. (XBB 818-7267)

Fig. 1. High resolution lattice image of the carbide/matrix interface structure in a quench-aged Mo-C alloy. (XBB 821-179)

the carbide and the (110) planes of the matrix is readily apparent. The arrows mark missing fringes in the matrix, which indicate the presence of regularly-spaced dislocations.

1981 PUBLICATIONS AND REPORTS

Refereed Journals

1. U. Dahmen, G. Thomas and K. H. Westmacott, "A Study of Precipitation in Interstitial Alloys, I. Precipitation Sequence in TaC Alloys," Acta. Metallurgica, 29, 627, 1980; LBL-11244.

2. U. Dahmen, "The Role of the Invariant Line in the Search for an Optimum Boundary by O-lattice Theory," Scripta Metallurgica, 15, 77, 1981; LBL-11804.

3. U. Dahmen, "Further Discussion of Orientation Relationships, Surface Reliefs and FCC-BCC Transformations in Steels," Scripta Metallurgica, 15, 465, 1981; LBL-11803.

4. M. J. Witcomb, U. Dahmen and K. H. Westmacott, "An Analysis of Thin Plate-Shaped Precipitates by Convergent Beam Microdiffraction," Proceedings of the Electron Microscopy Society of Southern Africa, Volume 11, (1981) p. 45.

5. U. Dahmen, "Answer to the Preceding Note on BCC-BCC Orientation Relationships, Surface Relief and Displacive Transformations in Steels," Scripta Metallurgica, 15, 963 (1981).

6. A. Pelton, "Vacancy-Assisted Precipitation in a 18 w/o Cr - 10 w/o Ni - 0/3 w/o P Steel," 39th Annual Proceedings Electron Microscopy Society America, Atlanta, Georgia, G. W. Bailey, ed. (1981) p. 324.

7. U. Dahmen, "Orientation Relationships in Precipitation Systems," Acta Metallurgica, 30, 63, (1982).

LBL Reports

1. K. H. Westmacott, U. Dahmen, A. Pelton and M. J. Witcomb, "Solid State Phase Transformation Mechanisms," LBL-13336.

Invited Talks

1. K. H. Westmacott, "The Structural Role of Vacancies in Precipitation Processes," Sandia Labs, Livermore, CA, April 3, 1981.

d. National Center for Electron Microscopy*

Gareth Thomas, Ronald Gronsky, and Kenneth H. Westmacott, Investigators

Introduction. The National Center for Electron Microscopy (NCEM) has now been formally established within MMRD. This culminates over nine years of preparation and planning,[1] with considerable input from Professors John Cowley (ASU) and Robert Sinclair (Stanford).

The National Center (the first of its kind in the United States) aims to provide unique facilities for electron microscopy characterization of materials. The very high cost of modern instruments dictates time sharing centers where facilities, support, and staff are all available. The present facilities consist of an installed 650-kV Hitachi (1969) and a new 1.5-MeV Kratos microscope, largely for in-situ work, a 1-MeV atomic resolution microscope (ARM), which is expected to be delivered in September 1982, and two back-up commercial microscopes (JEOL 200 CX, Siemens 102). One of the principles of the facility is that while a microscope is normally dedicated to a single purpose, certain projects will involve use of many if not all of these microscopes. Hence considerable outlay is needed for equipment and staffing.

The Center will be guided by a Steering Committee whose present non-LBL members are Drs. M. Simnad (Chairman), W. L. Bell, D. A. Howitt, J. J. Hren, J. C. H. Spence, and A. Taylor.

* * *

1. See LBL Pub-106.

1. 1.5 MeV HIGH VOLTAGE ELECTRON MICROSCOPE†

K. H. Westmacott

By years end, installation of the new Kratos 1.5 MeV HVEM had been essentially completed[1] and calibrations were being done in preparation for opening the facility for outside use.

All of the original instrument specifications have now been met and initial results indicate that performance will exceed expectations in many areas.

The vibration isolation and seismic-restraint system is also functioning within specifications, and external vibrations are not expected to limit the resolution attainable on this instrument.

Initial Applications

D. Ackland, U. Dahmen and K. H. Westmacott

Preliminary Work. During the testing phase of this instrument it was possible to perform preliminary work on a number of projects. A few illustrations of the instrument capabilities follow.

Critical Voltage Measurements. The ability to vary the microscope voltage over the full range of accelerating voltage from 150-1500 kV is an important asset in the measurement of critical voltage (V_c) which is the voltage at which particular reflections are minimized in intensity. A number of important physical and metallurgical parameters, such as atomic scattering factors, lattice potentials, degree of order, bond energy etc., may be obtained from the V_c. However, in many materials of practical interest some of these voltages lie in the range of 1200-1500 kV and have thus far been inaccessible on instruments in the United States.

A series of micrographs that bracket V_c for copper is shown in Fig. 1.

Precipitate in Pt-C. In many applications the additional transparency at high voltages may be used to advantage to obtain better statistical analysis of, for example, crystallographic data or defect or precipitate densities.

Figure 2 shows the apparent variation in the density of carbide precipitates in Pt in a wedged-foil. By using the thicker regions of the foil precipitate count statistics are better. Furthermore, it has been found that during in-situ annealing, coarsening behavior typical of bulk material is observed.

In-Situ Kinetic Studies. The kinetics of precipitate growth or dissolution, as well as secondary defect annealing, may be studied in-situ in the HVEM using the side entry hot stage. An example of this type of experiment, which shows the shrinkage of cavities in aluminum during isothermal annealing at 210°C, is shown in Fig. 3.

Radiation-Induced Amorphitization

R. Sinclair,‡ K. H. Westmacott and G. Thomas

The HVEM has been used to confirm an important new result obtained initially on the Osaka University 3-MeV instrument[2] that certain metallic alloys may be rendered amorphous by irradiation with high energy electrons.

The alloys being studied are Ni-Ti shape-memory alloys with compositions in the range 50-51.5 at% Ni. Specimens were annealed at 1000°C in vacuum, and quenched to 0°C before electropolishing.

A series of micrographs illustrating the progressive changes in the microstructure of an austenitic (ordered B2 structure) region of the foil is shown in Fig. 4. The gradual change in structure from the crystalline to amorphous states

*This work was supported by the Director, Office of Energy Research, Office of Basic Energy Sciences, Materials Science Division of the U.S. Department of Energy under Contract No. DE-AC03-76SF00098.

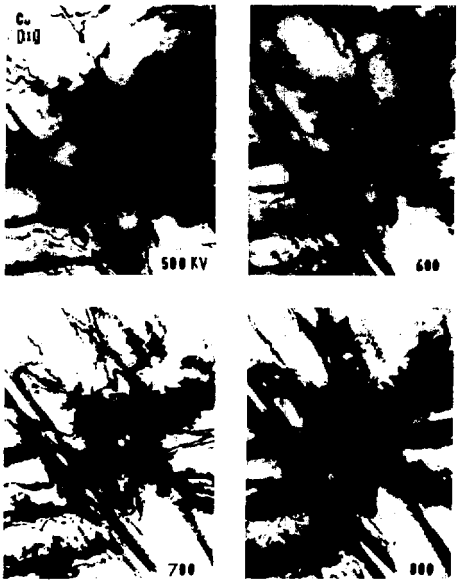

Fig. 1. Series of micrographs showing the variation in bend-contour patterns in a copper foil with changes in electron accelerating voltage. At the critical voltage (~ 600 kV for Cu) a distinctive pattern is observed. (XBB 821-191)

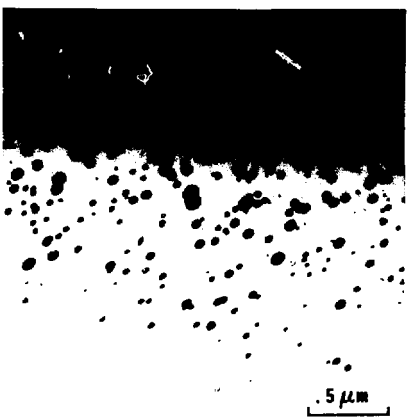

is manifested in both the micrographs and the diffraction patterns. As the extinction bend contours disappear, Fig. 4(A-D), diffuse rings associated with the amorphous structure develop and the crystalline diffraction spots disappear, Fig. 4(E,F). This transformation was effected by fully condensing the 1.5 MeV electron beam on the sample (current density ~ 30A/cm^2) for a few minutes.

The effect appears to be a displacement rather than an ionization damage phenomenon.

Fig. 2. Apparent variation of precipitate density in a wedge-shaped foil of Pt-C. During in-situ annealing precipitate shrinkage occurs in the thinner regions of the foil and precipitate coarsening in the thick parts. (XBB 821-224)

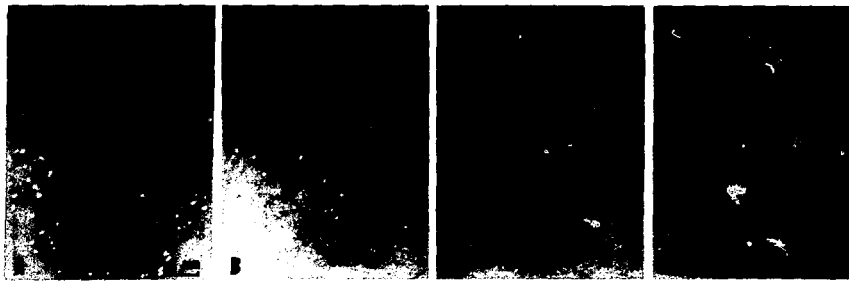

Fig. 3. Sequence of micrographs illustrating the shrinkage of cavities in aluminum during in-situ annealing at 210°C. (A) t = 0, (B) t = 5 min, (C) t = 10 min, (D) t = 30 min. (XBB 821-189)

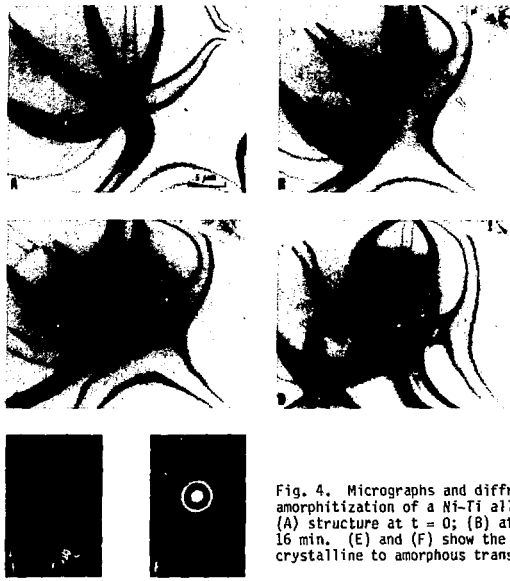

Fig. 4. Micrographs and diffraction patterns showing the progressive amorphitization of a Ni-Ti alloy during electron irradiation at 1.5 MeV. (A) structure at t = 0; (B) at t = 4 min, (C) at t = 8 min, (D) at t = 16 min. (E) and (F) show the diffraction patterns before and after the crystalline to amorphous transition has occurred.

(XBB 821-188)

* * *

†Stanford University

1. It is a pleasure to acknowledge the contributions and dedication of the Plant Engineering staff and others who helped to bring this project to fruition.

2. G. Thomas, H. Mori, H. Fujita and R. Sinclair, Scripta Met 1982 in press.

2. ATOMIC RESOLUTION MICROSCOPE

R. Gronsky

Progress on the Atomic Resolution Microscope (ARM) project has been steady, with the construction of the instrument (see Fig. 1) one month ahead of schedule at mid-December, 1981. The manufacturer (JEOL, Tokyo) has also completed the prototype version of the goniometer stage, judged to be the most crucial design effort in this undertaking. Initial results at the factory were within specifications, and up-scaling for installation in the ARM has begun.

Construction of the ARM building is also on schedule and due to be ready for the arrival of the instrument during August of 1982. The vibration isolation system and seismic restraints have already been delivered to LBL and are currently in storage until actually needed.

Construction of the Atomic Resolution Microscope Support Laboratory (ASL) addition to LBL Building 72 should start in March of 1982 with planned completion by January 1983. This addition will house the feeder microscopes, instrument development lab, image simulation and analysis hardware, specimen preparation labs and photographic darkrooms needed for the operation of the ARM on a shareable basis.

Fig. 1. Manufacturers' photograph of the ARM under construction at JEOL Akishima Works, Japan. The single tank Cockroft-Walton accelerator is visible on the upper platform with the electron-optical column below. (XBB 821-194)

3. IMAGE SIMULATION AND ANALYSIS

R. Kilaas and R. Gronsky

In order to provide the necessary theoretical support for image interpretation at high voltage and high resolution operation, the computational capacity of the NCEM is being expanded. Currently in file storage with interactive access through LBL's mainframe are a full range of dynamical scattering, multislice, and Bloch wave programs for direct simulation of images obtained in present and future NCEM microscopes.

These programs have also been modified to enable the simulation of crystalline defects through the use of a periodic extension model, and an example output is shown in Fig. 1. This is a successful simulation of a difficult atomic configuration, which shows excellent agreement with experimental images.

Fig. 1. Computer-simulated atomic resolution image of a Mo bicrystal (grain boundary vertical) of 15nm thickness as it would appear when images in a JEM 200 CX microscope at 200kV, - 145nm under-focus, and a beam convergence angle of 0.3mrad. (XBB 811-11946)

e. In-Situ Investigations of Gas Solid Reactions by Electron Microscopy*

James W. Evans and Kenneth H. Westmacott,
Investigators

Introduction. There is considerable evidence in the literature that there is a link between the defect structure of a solid and the kinetics of reaction of the solid with a liquid or gas. However, there has been little examination of the nature of this link, presumably because of the difficulty of simultaneously reacting the solid and characterizing its microstructure. Such simultaneous measurements are necessary in view of the propensity for a microstructure to change between the time of its characterization and any reaction experiments that are subsequent, rather than simultaneous. This difficulty has recently been overcome with the use of an "environmental cell" in a high voltage transmission electron microscope, which permits observation of the microstructure while the solid simultaneously reacts.

1. THE MICROSTRUCTURE AND REACTIVITY OF NICKEL OXIDE†

J. W. Evans, D. J. Coates, and K. H. Westmacott

Since early in this century there was indirect evidence that the defect structure of NiO affects its reactivity. It has been observed that mechanical deformation or proton irradiation increases the reactivity (say in hydrogen reduction to nickel) while annealing reduces the reactivity. A plausible explanation is that the kinetics are controlled by the nucleation of the new solid phase (nickel) and such nucleation occurs preferentially on one of the crystal defects in the oxide.

This hypothesis may be tested using the environmental cell in the transmission microscope, where the microstructure and the nucleation of the nickel during reduction with hydrogen are visible in-situ.

The most likely candidates for nucleating defects in NiO single crystals are dislocations; however, experiments in the environmental cell have so far failed to reveal any preferred nucleation of nickel on dislocations. The evidence is still not complete, but it appears that the intersection of the boundaries of the antiferromagnetic domains with the NiO surfaces are the preferential sites for nucleation. Much effort has been spent on examining such boundaries. Figure 1 is an electron micrograph of a group of these boundaries in a single crystal NiO specimen. The antiferromagnetic nature of NiO produces a rhombohedral structure. Domains are established having slightly different orientations, their boundaries lying on {100} and {110} NiO planes. The boundaries intersect the surfaces of the NiO producing linear discontinuities in the surface which may provide nucleation sites for nickel during reduction.

Fig. 1. Antiferromagnetic domain boundaries in nickel oxide. (XBB 810-11372)

* * *

†Brief version of LBL-13704.

2. WORK IN PROGRESS

Studies of the reduction of NiO using the environmental cell are continuing. An auxiliary experiment has been started in which the gas leaving the cell is analyzed in a mass spectrometer which should permit quantitative analysis of the reaction products.

*This work was supported by the Director, Office of Energy Research, Office of Basic Energy Sciences, Materials Science Division of the U.S. Department of Energy under Contract No. DE-AC03-76SF00098.

f. Local Atomic Configuration in Solid Solutions*

Didier de Fontaine, Investigator

1. CLUSTER THERMODYNAMICS

Pierre De Roo and Didier de Fontaine

It is often necessary to obtain a rough picture of actual local atomic arrangements in a crystalline solution when some of its microscopic properties are known, such as pair probabilities obtained from x-ray or neutron diffuse intensity measurements. One method of obtaining such information was developed years ago by J. B. Cohen and coworkers: it consists in performing rather time-consuming Monte-Carlo simulation. In the present study, we have investigated a new method, the so-called crystal growth method (CGM), originally devised by Welberry and Galbraith, and recently modified by Kikuchi.

Calculations were carried out for a two-dimensional square lattice with nearest-neighbor (n.n.) pair interactions ϵ ($\epsilon > 0$: ordering, $\epsilon < 0$: clustering), with two types of atoms (or magnetic spins). Theoretical probabilities of atomic configurations on n.n. square clusters were first calculated by a statistical thermodynamical method known as the cluster variation method (CVM). The n.n. square cluster probabilities were then used as input for the CGM program which fills up the lattice row by row with, say, A and B atoms. The computer code allows the atomic configurations to be printed out at any required temperature, and pair probabilities to be given for arbitrary pair separations.

Values of resulting Warren-Cowley short-range order parameters (SRO) are plotted at various temperatures for $\epsilon < 0$ (Fig. 1a) and $\epsilon < 0$ (Fig. 1b). As expected, the magnitude of short-range order increases as the transition temperature is approached from above. Different runs with different random number sequences gave slightly different values, hence the error bars in Fig. 1. It is interesting to note, however, that the spread in the results is much less than the values of the SRO parameters, even for fifth neighbor pairs, although the input to the CGM involves only n.n. square probabilities. It is planned to pursue

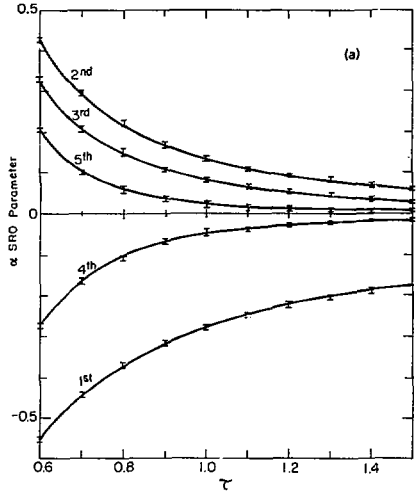

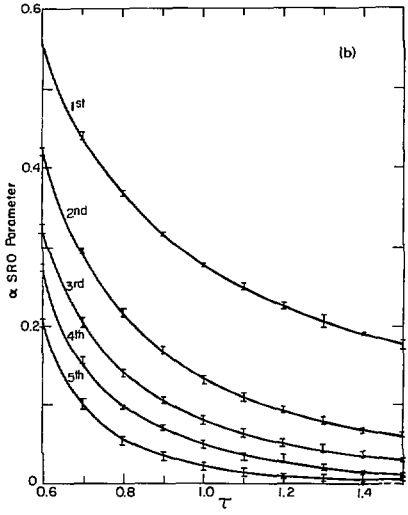

Fig. 1. Warren-Cowley SRO parameters for 1st, 2nd ... 5th neighbor pairs vs. reduced temperature (K_BT/ϵ) for a binary two-dimensional square lattice, (a) ordering case ($\epsilon < 0$ or antiferromagnetism), (b) clustering case ($\epsilon < 0$ or ferromagnetism).

(XBL 8111-6998 and 6999)

*This work was supported by the Director, Office of Energy Research, Office of Basic Energy Sciences, Materials Science Division of the U.S. Department of Energy under Contract No. DE-AC03-76SF00098.

this analysis by performing appropriate Fourier transforms to compare to recently derived theoretical formulas of SRO intensity. The ultimate aim will be to deduce local atomic arrangements from experimentally determined diffraction intensities.

2. IONIC AND MAGNETIC ORDERING

Kannan Krishnan and Didier de Fontaine

The influence of magnetic interactions on the phase stability of binary alloys and, conversely, the influence of chemical interactions on the magnetic transition temperatures have not been completely analyzed as yet. Theoretical analysis traditionally has been either restricted to the study of only one of the two effects or for systems with only one magnetic component. Some studies of simultaneous atomic and magnetic ordering for binary b.c.c. systems have been carried out recently but the mean field approximation used (Bragg-Williams) was too crude to have real predictive value. The purpose of the present work is to perform a similar calculation for an f.c.c. binary system with both magnetic and chemical interactions employing the more sophisticated CVM, in the n.n. tetrahedron approximation.

The CVM involves two basic steps: (1) the calculation of the configurational entropy, i.e., calculation of an approximate expression for the number of configurations Ω of a crystal lattice with a definite cluster distribution, and (2) minimization of the free energy $F = E - TS$ (where E is the energy of the configuration and S is the entropy of the system) to obtain the equilibrium cluster distribution. The critical temperature is then determined by that temperature at which the matrix (F) of second derivatives of the free energy with respect to the r-body correlation functions becomes singular, i.e., det(F) = 0. Finally, the nature of the transition, i.e., magnetic or chemical, can be determined from the orientation of the eigenvectors of F at or around the critical temperature.

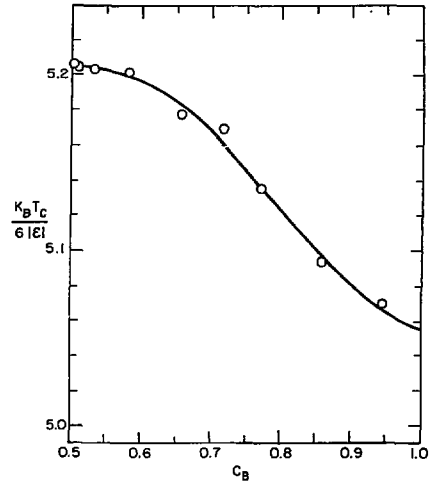

Fig. 1. Variation of the magnetic transition temperature with concentration. The values of the coupling constants were $\frac{J}{|\varepsilon|} = -3$, $\frac{\varepsilon}{|\varepsilon|} = -1$, i.e., an antiferromagnetic-clustering system.
(XBL 8111-12833)

Initial CVM calculations have been carried out for the variation of the magnetic transition temperature with concentration for a hypothetical antiferromagnetic (magnetic coupling constant, $J < 0$) and "compositional" clustering (chemical coupling constant, $\varepsilon < 0$) system. The variation of the magnetic transition temperature T_m with the chemical concentration for the particular case of $J/\varepsilon = 3$ is shown in Fig. 1. This variation, although small, is significant. A more interesting case is one in which the chemical and magnetic transition temperatures are more closely coupled. Similar calculations to determine the temperature and nature of the transition over the entire range of compositions for such a system are in progress. The ultimate practical object of the proposed calculations is to attempt to determine how to modify the composition of a ferromagnet in such a way as to obtain a magnetic transition at a predetermined temperature.

3. THERMODYNAMICS AND KINETICS OF CLUSTERING

Didier de Fontaine and Osamu Dairiki

Empirically determined time-temperature-transition (TTT) diagrams are essential for understanding and optimizing the heat treatment of industrial alloys, in particular, of steels. Although the literature on relevant phase transformations is abundant, there has been little recent work on the problem of explaining, or at least rationalizing the general features of TTT diagrams from general principles. In particular, there appears to be no theoretical explanation of why the "C" curves of low carbon steels tend to evolve into "S"-shaped curves upon alloying with substitutional elements.

Obviously, possible explanations will be based on nucleation theory, but multicomponent nucleation treatments (required to treat alloy steel problems) are hard to come by in metallurgical publications. In a recent review paper,[1] the senior author extended formalisms borrowed from the physics literature and showed how, in principle, one might develop a very crude theory for TTT diagrams.

Since the publication of the aforementioned review, it has become clear that further progress can be made by combining multicomponent nucleation theory and multicomponent free energy diagrams. The relative positions of free energy minima will

then yield different driving forces for nucleation depending on the requirements of solute partitioning. Simple calculations based on these ideas will presently be carried out. Available data on solute partitioning will be reviewed and, in the future some analytical STEM experiments will be carried out on simple Fe-C systems with one substitutional solute.

* * *

1. See LBL-12865, June 1981.

1981 PUBLICATIONS AND REPORTS

Publications

1. D. de Fontaine, "Thermodynamics and Kinetics of Phase Separation" in Treatises in Metallurgy, J. Elliott and J. K. Tien, eds., ASM/TSM-AIME, 1981, LBL-12865.

Invited Talks

1. D. de Fontaine, "Thermodynamics and Kinetics of Phase Separation" First China-USA Bilateral Metallurgical Conference, Beijing, People's Republic of China, November 1981 (based on LBL-12865).

2. Mechanical Properties

a. Theoretical Problems in Alloy Design*

J. W. Morris, Jr., Investigator

Introduction. The purpose of this research project is to advance the science of the development of new materials through appropriate fundamental research and through the accomplishment of demonstration projects in the development of new materials having exceptional engineering properties. The materials development projects currently fall in three areas: new structural steels, particularly those intended for applications at cryogenic temperatures, weld filler metals and welding procedures for high strength structural steels, and high field super-conducting wire. The supporting fundamental research involves theoretical studies of microstructure, processing, and mechanical properties of materials, and experimental research in materials characterization and analysis.

1. THE LINEAR ELASTIC THEORY OF STRUCTURAL TRANSFORMATIONS IN SOLIDS†

J. W. Morris, Jr., Sheree H. Wen,‡ and A. G. Khachaturyan§

Phase transformations in real solids usually involve the formation or reconfiguration of elements which differ in size or shape from the typical structural component of the parent phase. The phase transformation has the effect of introducing volumetric defects into the parent that are internally distorted themselves and cause distortions in the matrix in which they lie. The associated elastic strain influences the energetics of the phase transformation, the morphology of the product, and sometimes even the crystal structure and composition of the product phase. It has been known for some time that many of the consequences of volumetric distortion can be understood or predicted from a linear elastic model in which both the defects and the matrix are taken to be linear elastic bodies. The linear elastic theory has been developed along two lines: as a microscopic model that treats the properties of solid solutions and the nature of decomposition reactions, and as a microscopic model that treats the nature, shapes, and habits of precipitates within the parent phase. The research completed in this task draws on earlier theoretical work by Khachaturyan and obtains both the microscopic and macroscopic formulations of the theory from a single starting point: the strong harmonic model of a solid solution. It is shown that the resulting theory contains virtually all relevant features of the elastic theory of phase transformations, and that these can be extracted in a straightforward way. New extensions of the model are identified.

* * *

†Brief version of LBL-9800.
‡Present address: Thos. J. Watson Research Lab., Yorktown Heights, NY.
§Present address: Inst. of Crystallography, Academy of Sciences, Moscow, Russia.

2. THE PRECIPITATE HABIT AND INTERNAL STRAIN OF NITRIDE PRECIPITATES IN STEEL†

M. Hong,‡ D. E. Wedge,§ and J. W. Morris, Jr.

The linear elastic theory of precipitates in the solid state shows that these should, in the limit of large particle size, approach a thin plate morphology with a definite crystal habit and should be internally strained by an amount which is predictable from the crystal structure mismatch between the matrix and the precipitate in the precipitate habit. The α" nitride precipitate in steel is an interesting case because its commonly observed habit differs from that predicted by the theory in the large particle limit. It is also known that nitride precipitates gradually develop into a thin-plate morphology from a more blocky initial state. Theoretical calculations of the habit of α" which considered the consequences of its gradual change in aspect ratio have been shown to predict a change in precipitated habit during growth. The small particle, or initial habit, is that which is observed experimentally. Given the habit, one can predict the lattice parameters of the precipitate in its constrained state. The results are in excellent agreement with experiment and appear to explain a consistent discrepancy between experimental observations reported by previous workers.

* * *

†Brief version of LBL-12973.
‡Present address: Bell Laboratories, Murray Hill, NJ.
§Present address: Varian Associates, 2800 Mitchell Dr., Walnut Creek, CA.

3. THE PRECIPITATE MORPHOLOGY AND COARSENING CHARACTERISTICS OF NITRIDE PRECIPITATES IN STEEL†

D. E. Wedge‡ and J. W. Morris, Jr.

For purposes of theoretical calculation, precipitate phases in solids have usually been assumed to have the shape of discs or ellipsoids embedded in an isotropic matrix. The Khachaturyan formula-

*This work was supported by the Director, Office of Energy Research, Office of Basic Energy Sciences, Materials Sciences Division of the U.S. Department of Energy under Contract No. DE-AC03-76SF00098.

tion of the elastic theory permits the straightforward computation of the elastic energy of arbitrary precipitate shapes in an anisotropic matrix. The theory has been used to show that the α" nitride precipitate in ferritic steel, in fact, prefers a lens-like shape to that of either a disc or an ellipsoid. The lens-like shape is, in fact, much closer to the somewhat complex precipitate morphology observed experimentally. The results of the calculation are then used to compute the change in precipitate aspect ratio during coarsening. The results can be fitted to experimental coarsening data to estimate an isotropic surface energy for the precipitate. The results are physically plausible.

* * *

†Brief version of LBL-10630.
‡Present address: Varian Associates, 2700 Mitchell Dr., Walnut Creek, CA.

4. ACCUMULATION OF CHARGE IN THE STRAIN FIELD OF A DISLOCATION IN A METAL

T. Mohri and J. W. Morris, Jr.

An important practical problem in the mechanical behavior of structural materials in superconducting magnets concerns the possible influence of the magnetic field on the yield and flow strength. One possible source of such an influence would be the Lorentz force on a moving dislocation which carried a charge. The strain of dislocations in metals should accumulate charge, and the present work was done to see if this charge might be of sufficient magnitude to couple strongly to the magnetic field. The charge accumulation in the strain field of an edge dislocation was computed in the free electron model. The charge accumulation appears to be small, suggesting that moving dislocations do not interact strongly with the imposed magnetic field.

5. THE THICKNESS DISTORTION OF ^{57}Fe BACKSCATTER MÖSSBAUER SPECTRUM†

B. Fultz and J. W. Morris, Jr.

In many important applications of Mössbauer spectroscopy in materials science, including specifically the analysis of fracture surfaces, the Mössbauer spectrum must be taken in the backscatter mode rather than in the more conventional transmission mode. To extract quantitative information from backscatter Mössbauer spectroscopy, one must be able to correct for the thickness distortion of the spectrum due to the fact that the incident gamma rays are absorbed over a range of depths near the surface. While the thickness distortion is well known for the transmission geometry, it has not been previously computed in the backscatter mode. In this research the thickness distortion was computed. It was also shown to be possible to cast the thickness distortion into a simple approximate form which permits its straightforward use for Mössbauer spectra.

* * *

†Brief version of LBL-11022.

6. A MÖSSBAUER STUDY OF MICROSTRUCTURAL AND CHEMICAL CHANGE IN Fe-9Ni

B. Fultz and J. W. Morris, Jr.

The analysis of changes that occur during tempering of steel make it very useful to have analytic techniques which can both monitor structural changes and changes in chemical distribution during heat treatment. In this research Mössbauer spectroscopy was used to monitor those changes, and was found to be a useful technique. Hyperfine field effects in Fe-Ni alloys were systematically analyzed and shown to give quantitative information concerning the temper-induced chemical composition changes. The kinetics of segregation of alloying elements from the martensite into the fresh austenite precipitate during tempering could be determined simultaneously with the amount of austenite which formed. The results give valuable new information on the progress of temoering in Fe-9Ni cryogenic steel.

7. OBSERVATIONS ON THE DIFFERENCES REPORTED IN REGION 1 FOR THE SUPERPLASTIC Zn-22%Al EUTECTOID

D. Grivas,† J. W. Morris, Jr., and T. G. Langdon‡

The Zn-22%Al eutectoid alloy is a superplastic material which has been used in many fundamental investigations into the phenomena of superplasticity and also has commercial applications in superplastic forming. Despite extensive investigation, however, both the phenomenology and mechanism of the creep behavior that bounds superplastic behavior at the low stress end remain controversial. The principal controversy centers around the appropriate value of the exponent in the power law creep relation that governs deformation at stresses below that needed to achieve superplastic deformation. The value of this exponent has been variously determined as 1.0 and 0.3. A re-analysis of both published and unpublished data upon low stress superplastic creep taken at LBL and elsewhere appears to establish that the proper value of the stress exponent is 0.3. Experiments suggesting an exponent of 1.0 are concluded to be unreliable. The result has important implications for the mechanisms of superplasticity, since the phenomenology of the behavior strongly suggests that the mechanism leading to the low stress creep is a distinct creep mechanism which is in series with the mechanism leading to superplastic deformation.

* * *

†Present address: Dept. of Administrative Technology of Greece, Athens, Greece.
‡Present address: Dept. of Materials Science, U.S.C., Los Angeles, CA.

8. STEREOLOGICAL CHARACTERIZATION OF FRACTURE SURFACES IN Fe-6Ni CRYOGENIC STEEL

G. Fior and J. W. Morris, Jr.

It is well known that the ductile-to-brittle transition in typical structural steels is associated with a change in the fracture mode from ductile rupture to a brittle mode which may represent transgranular cleavage or intergranular separation. To gain insight into this transition stereographic techniques have been used to characterize the features appearing on fracture surfaces of quenched Fe-6Ni steels tested over a range of temperatures passing through the ductile-to-brittle transition temperature. The results clearly show intrusion of a transgranular cleavage fracture mode as the ductile-to-brittle transition is encountered. Analysis of the geometry of the features shows that the ductile portion of the fracture surface is relatively constant in its geometry, suggesting that the ductile-fracture mechanism is unchanged. The geometry of the cleavage portion of the surface does change with temperature, which suggests that two independent cleavage modes are operating. Further work is concentrated on the distinction between these different cleavage modes.

9. INHERENT INTERGRANULAR FRACTURE IN Fe-12Mn BROKEN AT LOW TEMPERATURE†

H. J. Lee and J. W. Morris, Jr.

Ferritic Fe-12Mn alloys generally fracture in an intergranular brittle mode below the ductile-to-brittle transition which involves a separation along the prior austenite grain boundaries. A temper embrittlement of the steel facilitates the intergranular mode and substantially raises the ductile-to-brittle transition. To set firm guidelines for the design of tough ferritic Fe-Mn alloys, it is essential to understand the mechanism of the intergranular fracture. Detailed Auger spectroscopic analysis of intergranular fracture in Fe-12Mn in the as-quenched state has demonstrated that this fracture mode occurs without any necessary consistent accumulation of grain boundary embrittling species. These results reinforce our earlier conclusions that the intergranular fracture mode below the ductile-brittle transition is inherent to the alloy, and represents a microstructurally driven rather than a chemically-induced behavior. During temper embrittlement even relatively pure alloys exhibit a clear segregation of manganese to the prior austenite grain boundaries. The manganese segregation appears to promote intergranular fracture. Long time tempering causes nucleation of the austenite phase along the prior austenite grain boundaries, which mitigates, and can even remove, the tendency toward intergranular fracture.

* * *

†Brief version of LBL-12898.

10. THE PROPERTIES OF MICROCONSTITUENTS IN Fe-6Ni CRYOGENIC STEEL†

H. J. Kim,‡ J. I. Kim,§ and J. W. Morris, Jr.

The control of the ductile-to-brittle transition in commercial Fe-Ni cryogenic steels is based on the use of an appropriate tempering treatment to introduce a fine distribution of stable austenite phase into the ferrite matrix. The development of clear alloy design criteria for improved Fe-Ni cryogenic steels requires that the function of this austenite be clearly understood. Previous work suggest that a primary function of this austenite is to break up the crystallographic alignment within the original martensite phase, hence reducing the mean-free path of propagating cleavage fractures and making cleavage more difficult. It is, however, possible that the mechanical properties of the tempered martensite and austenite phases themselves also play a role. To clarify this issue, samples of both martensite and austenite were melted that have the compositions of the two phases in tempered 6Ni steel, as determined by STEM analysis. Tests on these constituent alloys show that both phases are very brittle at low temperature even after the heat treatment normally given 6Ni steel. This result supports the conclusion that the good low temperature properties of 6Ni steel are a consequence of the microstructural configuration of the two phases rather than their inherent properties. The thermal stability of the austenite phase is virtually identical to that of the austenite precipitate within the 6Ni steel, which suggests that the stability of the precipitated austenite is principally controlled by composition rather than by its configuration or state of strain within the tempered martensite matrix.

* * *

†Brief version of LBL-12903.

‡Present address: Korean Military Academy Donbong-Ku, Seoul, Korea.

§Present address: Thos. J. Watson Research Lab., IBM, Yorktown Heights, NY.

11. THE CONSEQUENCES OF RAPID THERMAL CYCLING IN Fe-9Ni STEEL

H. J. Kim, H. Shin, and J. W. Morris, Jr.

It is known from previous welding research in Japan, supplemented by work here at LBL, that ferritic Fe-Ni cryogenic steels can be successfully welded with ferritic filler metals for low temperature service if the welding is done in a multipass gas tungsten arc process. The GTA process establishes a chemically clean weldment. Multipasses establish a good microstructure, almost certainly because subsequent weld passes heat treat the material previously laid down, and preserve good microstructure within the weld heat-affected zone. The properties of ferritic welded 9Ni steel are, however, puzzling, since the welding process

largely destroys the precipitated austenite content within the weld heat-affected zone, which is believed to be the source of the good low temperature properties of this alloy. To clarify the processes occurring during multi-pass welding, and to establish alloy design criteria for improved weld development, research has been conducted on the response of the alloy to rapid cycling treatments. The results have shown that appropriate rapid thermal cycling treatments will establish good cryogenic properties within the steel even in the absence of precipitated austenite. Initial metallographic results suggest that rapid thermal cycling leads to the breakup of crystallographically aligned packets within the 9Ni steel through the intrusion of new martensite variants. The details of this process are not yet understood and are under continuing investigation.

12. WELDING OF IRON-BASED SUPERALLOYS

L. Summers, M. Strum, and J. W. Morris, Jr.

There are a number of engineering applications, including in particular the forced-cooled conductor case for high field superconducting magnets, in which it is desirable to weld iron-based superalloys so that after subsequent heat treatment, the mechanical properties of the weldment and the base plate will be homogeneous. The desired homogeneity in properties is, however, difficult to achieve because of the difference in aging characteristics between the weld metal and the alloy base plate. The present research was conducted to gain insight into the source of this difference in aging characteristics and provide guidelines for alloy development research to overcome it. Two sources of different aging characteristics have been identified: local chemical segregation in the freshly solidified weld metal, and effective grain size differences between the weld metal and the base plate. Characterizations of the resulting aging curves show that it is possible to achieve matching weld metal-base plate properties, but at some sacrifice in the optimal properties of the base plate. To overcome this problem it will be necessary to improve both the kinetics of aging in the weld metal and the attainable peak strength. Metallographic studies are now under way to specify the microscopic sources of the difference in weld aging properties so that appropriate weld processes and treatments can be designed.

13. THE CRYSTALLOGRAPHIC ORIENTATION OF A15 V_3Ga AND Nb_3Al PRECIPITATES IN BCC MATRICES†

I. W. Wu, M. Hong,‡ and J. W. Morris, Jr.

To control the nature and morphology of A15 phases developed through solid state reaction within high field superconductors, it is essential to understand the fundamental nature of the precipitation process. The present work was undertaken to determine the crystallographic orientation of the typical A15 phases of V_3Ga and NB_3Al in BCC matrices. Convergent beam transmission electron diffraction was used to find the crystallographic orientation of submicron size particles of the two A15 compounds. In each case the crystallographic orientation was (to within an uncertainty of ± 5°): $[001]_{A15} \| [111]_{BCC}$; $(100)_{A15} \| (1\bar{1}0)_{BCC}$. This lattice correspondence is intuitively plausible, since it ensures that the closest-packed planes and directions of the precipitate parallel those of the matrix.

* * *

†Brief version of LBL-12222.
‡Present address: Bell Laboratories, Murray Hill, NJ.

14. MICROSTRUCTURAL CHARACTERIZATION AND MODIFICATION IN MULTIFILAMENTARY Nb_3Sn†

I. W. Wu, M. Hong,‡ and J. W. Morris, Jr.

The critical current characteristic of multifilamentary Nb_3Sn made by the bronze process is determined by the configuration of the multifilamentary composite, the niobium to bronze ratio, the tin content of the bronze, and the reaction heat treatment. In the case of multifilamentary wire the first three parameters are set by the manufacturing process. The present project was intended to identify improved heat treatments leading to an increase in critical current. To accomplish this detailed microstructural characterization, studies were done on the reacted Nb_3Sn layer at the niobium-bronze interface. Microstructurally, the layer proved to be divisible into three distinguishable components: a columnar grain structure at the niobium interface, a fine-grained structure at the center of the reacted layer, and a coarse-grained structure along the periphery of the filament. The composition of the reacted layer was found to vary from tin-rich composition at the bronze interface to a tin-poor composition at the niobium interface. The microstructural state of the wire improved as the reaction temperature was lowered. The chemical distribution within the wire improved as the reaction temperature was raised. The former characteristic is particularly important to the critical current at low fields; the latter characteristic largely determines the critical current at high fields. It was found that two-step heat treatments combining a low temperature initial treatment followed by a high temperature, brief final treatment yields good mix of microstructure and composition and improves the critical current over the full range of operating fields.

* * *

†Brief version of LBL-13015.
‡Present address: Bell Laboratories, Murray Hill, NJ.

15. RESEARCH ON POWDER PROCESSED Nb_3Al SUPERCONDUCTING WIRE†

M. H. Hong, J. Holthuis, and J. W. Morris, Jr.

Several of the most promising A15 superconducting phases cannot, for thermodynamic reasons, be made into wires by the bronze process. A promising alternative process for these materials is the

direct powder process, in which powders of the primary constituents are mixed, drawn into a wire, and reacted at high temperature to form A15 superconducting phase. In this project the powder process was used to make high field superconducting wires from Nb and Al powders reacted to form the Nb_3Al compound. Detailed materials characterization studies were carried out to determine the progress of the reaction at the Nb-Al interface. The reaction proves to yield a complex mixture of fine grains of the A15 and σ phases. Promising critical currents were obtained, and were found to increase with the aluminium content in the wire, up to 4 wt.% aluminium, and with the extent of deformation in the wire prior to reaction. Appropriate double-aging heat treatments were also found to be beneficial.

* * *

†Brief version of LBL-13013.

1981 PUBLICATIONS AND REPORTS

Refereed Journals

1. S. H. Wen, E. Kostlan, M. Hong, A. G. Khachaturyan, and J. W. Morris, Jr., "The Habit of a Tetragonal Precipitate in a Cubic Matrix," Acta Met., 29, 1247 (1981); LBL-10262.

2. Sheree Chen, A. G. Khachaturyan, and J. W. Morris, Jr., "Computer Simulation of a 'Tweed-Transformation' in an Idealized Elastic Crystal," Met. Trans. 12A, 581 (1981); LBL-11238.

3. M. Hong, D. R. Dietderich, I. W. Wu, and J. W. Morris, Jr., "Microstructure and Properties of A15 Superconductors Formed by Direct Precipitation," IEEE Trans. on Magnetics vol. MAG-17:1 (1981); LBL-11605.

4. B. Fultz and J. W. Morris, Jr., "The Thickness Distortion of Fe^{57} Backscatter Mössbauer Spectra," Nucl. Inst. & Methods, 188, 197 (1981); LBL-11022.

5. I. W. Wu, M. Hong, and J. W. Morris, Jr., "The Crystallographic Orientation of A15 V_3Ga and Nb_3Al Precipitates in BCC Matrices," Appl. Phys. Lett., 39, 110 (1981); LBL-12222.

6. D. Grivas, J. W. Morris, Jr., and T. G. Langdon, "Observations on the Differences Reported in Region I for the Superplastic Zn-22% Al Eutectoid," Scripta Met., 15, 229 (1981); LBL-12225.

Other Publications

1. J. I. Kim, C. K. Syn and J. W. Morris, Jr., "Advances in the Heat Treatment of Steels," in Advances in Metal Processing, eds., Burke, Mehrabion and Weiss, Plenum Press (1981).

LBL Reports

1. M. A. Green et al., "Ground Plane Insulation Failure in the First TPC Superconducting Coil," LBL-12326.

2. M. Hong, D. E. Wedge, and J. W. Morris, Jr., "The Preferred Habit of a Coherent, Thick-Plate Precipitate: $Fe_{16}N_2$," LBL-12973.

3. D. E. Williams and J. W. Morris, Jr., "Weldability of Grain Refined Fe-12Ni-0.25Ti Steel for Cryogenic Applications," LBL-11777.

4. H. J. Kim, "The Role of the Microstructural Components in a 3-step Heat Cycled, Low Carbon Fe-6Ni Alloy," LBL-12903.

5. J. M. Hong, J. Holthuis, I. W. Wu, and J. W. Morris, Jr., "Developmental Studies on Powder Processed Nb_3Al Superconducting Wire," LBL-13013.

6. M. Hong, I. W. Wu and J. W. Morris, Jr., "An Investigation on the Enhancement of the Critical Current Densities in Bronze-Processed Nb_3Sn," LBL-13015.

7. H. J. Kim, C. K. Syn, and J. W. Morris, Jr., "Ferritic Weldment of Ferritic Ni Steels for Liquid Helium Temperature," LBL-13017.

8. D. E. Wedge, "Study of Precipitate Morphology by Consideration of Elastic Strain Energy," LBL-10639.

Invited Talks

1. J. W. Morris, Jr., "Development of High-Field Superconducting Wires," Metal Physics Institute, Kiev, Russia, March 17, 1981.

2. J. W. Morris, Jr., "Microstructural Determinations of the Ductile-Brittle Transition in Steels," Physical Technical Institute for Low Temperatures, Kharkov, Russia, March 19, 1981.

3. J. W. Morris, Jr., "Elastic Effects of Martensitic Transformations," International Workshop on Transformation Toughening, Munich, West Germany, June 17-19, 1981.

4. J. W. Morris, Jr., "The Linear Elastic Theory of Bolumetric Defects in Solids," Phase Transformation Conference, Pittsburg, PA, August 10, 1981.

5. J. W. Morris, Jr., "Science of Alloy Design," EXXON Colloquia in Metallurgy, Linden, NJ, September 4, 1981.

6. J. W. Morris, Jr., "Chromium in Fe- and Ni-based Alloys—Alloy Design View," Workshop on Critical Materials, Chicago, IL, September 23-24, 1981.

7. J. W. Morris, Jr., "Theory of Alloy Design," U.S. Steel Corp. seminar, Pittsburg, PA, December 2, 1981.

b. Structure-Property Relationships in Semiconductor Materials*

Jack Washburn, Investigator

1. EFFECT OF OXYGEN ON Cr-STRUCTURAL DEFECT INTERACTION IN ION-IMPLANTED GaAs†

D. K. Sadana, J. Washburn, T. Zee, and R. G. Wilson‡

The redistribution of Cr in ion-implanted and subsequently furnace-annealed GaAs has been studied. Although gettering of Cr at structural defects has been suggested, none of the published work has been able to fully explain the anomalous redistribution of Cr in the implanted region. Understanding this phenomenon is important because the electrical properties of the implanted region change where Cr segregation occurs. In the present work, direct depth correlations between Cr and structural defects were obtained for the first time and the anomalous redistribution of Cr is explained by considering a combined Cr-structural defect-oxidation interaction during the annealing.

Cr doped semi-insulating (100) GaAs samples were self-implanted (i.e., with Ga and As ions) at RT. The secondary ion mass spectroscopy (SIMS) results showed that the Cr distribution was flat in the implanted but unannealed sample and corresponded to the bulk level. After a low-temperature annealing ($\leq$ 600°C), there was a remarkable change in the Cr distribution in the implanted region; Cr started to out-diffuse from the bulk to occupy sites at the dislocation cores. There was a one to one depth correlation between the presence of Cr peaks and the occurrence of high dislocation density regions. At 840°C, Cr peaks still occurred in the regions containing dislocations but there was also a peak where no defects were visible. It was hypothesized that at temperatures $\leq$ 600°C, oxygen from the ambient migrated via pipe diffusion into the implanted region containing a high density of dislocations. Because of the presence of O, Cr-O complexes formed and remained in this region even after the dislocations had annealed out.

More direct evidence of O involvement in the Cr redistribution process was obtained when O was implanted into already self implanted GaAs samples and the samples were subsequently annealed at 600-840°C. Figure 1 shows that there is similarity between the shapes and depth distribution (Fig. 1b) of the Cr and O profiles. The highest Cr peak in this case occurred at a depth beyond the implanted region. These results directly demonstrate the influence of O on the Cr redistribution in GaAs. The Cr in the self plus O implanted case also starts to out-diffuse from the bulk in a similar manner as in the simple self implanted case. However, because of the abundance of O, Cr-O complexes now form even near the tail of the implanted O profile. The detection of a Cr peak at the surface in almost all the annealed GaAs samples in this study as well as in the earlier reported work is also consistent with the formation of stable Cr-oxygen complexes at the external surface.

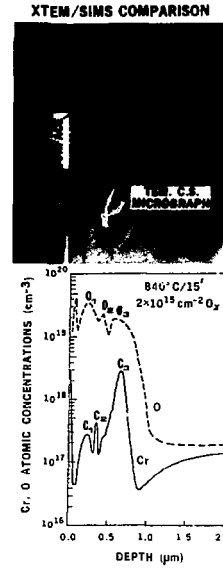

Fig. 1. (a) TEM cross-section view micrograph showing the defects distribution in 840°C/15' annealed sample containing O; (b) Cr and O atoms distributions from the same sample as in (a). (XBB 819-8826)

* * *

†Extended abstract of LBL-13527, also presented at the Intern. Conf. on GaAs and Related Compounds, Oiso (Japan), September 20-23, 1981. LBL-13527

‡Hughes Research Laboratories, Malibu, CA 90265.

*This work was supported by the Director, Office of Energy Research, Office of Basic Energy Sciences, Materials Sciences Division of the U.S. Department of Energy, under Contract No. DE-AC03-76SF00098.

2. HIGH RESOLUTION OBSERVATIONS OF COPPER VACANCY ORDERING IN CHALCOCITE (Cu_2S) AND THE TRANSFORMATION TO DJURLEITE ($Cu_{1.97-1.94}S$)†

Timothy D. Sands, Jack Washburn, and Ronald Gronsky

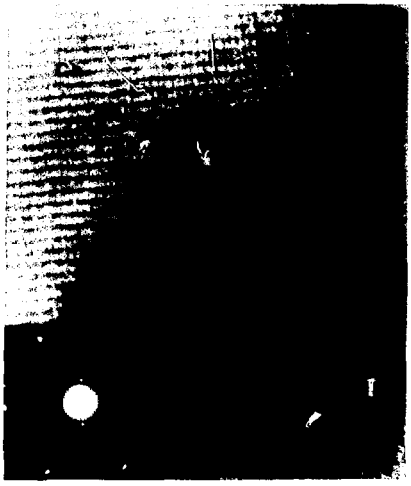

Fig. 1. High resolution TEM image of chalcocite/Djurleite interface. (XBB 819-9275A)

Thin film p-$Cu_{2-x}S$/n-(Cd,Zn)S solar cells can be mass produced by inexpensive and well known techniques. The efficiency of these devices has been increased to current levels of between 8 and 10%. Unfortunately, the device lifetime and reproducibility are limited by the compositional proximity of the desirable chalcocite phase (Cu_2S) and the undesirable djureleite phase ($Cu_{1.97-1.94}S$). Furthermore, the lack of understanding of the chalcocite-djurleite transformation mechanism has inhibited the design of a stable and reproducible copper sulfide layer. It is the objective of this study to determine the structural relationships between these two phases so that the low temperature ($T < 100°C$) transformation mechanism may be determined.

The technique of high resolution transmission electron microscopy has permitted the first real space observations of the ordering of copper in the sulfur sublattices of chalcocite and djurleite, TEM images show that copper sulfide thin films formed by the ion exchange process from CdS single crystals are composed of small domains of the two phases (ten to several hundred nanometers in diameter) separated by abrupt, coherent interfaces. Strain calculations for these interfaces agree qualitatively with experimental observations. In addition, the chalcocite in the vicinity of chalcocite/djurleite interfaces contains a high density of 1/4[010] faults (see arrows in Fig. 1). Structural considerations show that these faults may be formed by clustering of copper vacancies. The role of these faults in the chalcocite-djurleite transformation is currently being investigated.

* * *

†Extended abstract of LBL-13746 submitted to Physica Status Solidi.

3. THE EFFECT OF RECOILED OXYGEN ON DAMAGE ANNEALING IN As-IMPLANTED SiO_2/Si†

D. K. Sadana, J. Washburn, N. R. Wu and M. C. Current‡

The direct implantation of dopant atoms into Si through a screen oxide of thickness ranging from a few hundred to several thousand angstroms has become a common practice in metal-oxide-semiconductor (MOS) device technology. However, the disadvantage of the thorough-oxide-implant is the drive-in of oxygen knock-on atoms into Si due to collisions between the incoming atoms and oxygen in the SiO_2 screen layer. A detailed account of oxygen recoil related structural and electrical effects in As-implanted SiO_2 (775 Å)/(100) Si has been reported. Figure 1 shows the TEM, RBS, SIMS and electrical results from such a sample after being annealed at 1000°C for 1/2-hr. in dry N_2. The implantation temperature, energy and dose were RT, 120 keV and $7.5 \times 10^{15} cm^{-2}$, respectively.

Comparison of the TEM results from bare Si and through-oxide implanted Si shows that the annealing-out of the defects is considerably retarded in the latter case. The persistence of irregularly shaped dislocation loops at high temperature ($\geq 1000°C$) indicated that the dislocation loops were pinned. Also a peak in the O distribution occurred at a depth (900 Å) identical to that of the dislocation loops. This suggests that oxygen complexes are likely to be responsible for the pinning of the loops. Oxide complexes or precipitates large enough to be seen by TEM, are formed near the surface. Only 30% of the total As present in the implanted region was electrically active. Moreover, channeling measurements indicated that about 50% of the As was non-substitutional. Non-substitutional As is known to be electrically inactive. The channeling results also showed that the non-substitutional As distribution peaks at a depth of 1000 Å below the surface, i.e., in the same region where the dislocation loops are located and the O peak is found. This suggests that complex interactions between As, O and the damage exist in the implanted region.

* * *

†Extended abstract of LBL-14004, also presented at the Symposium on the Electron Microscopy of Semiconductors, Oxford (England) April 1981; Proc. Inst. Phys. (London) 60 453 (1981).

‡Signetics Corporation, Sunnyvale, CA

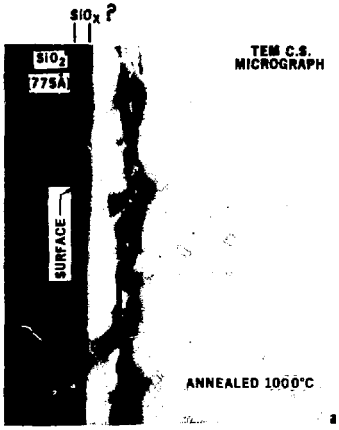

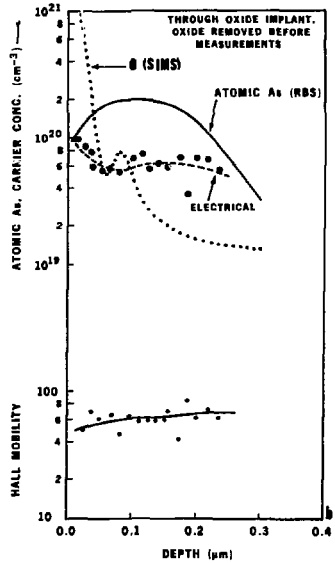

Fig. 1. (a) TEM cross-section micrograph. (b) As, O, carrier concentration and mobility profiles from the same sample as in (a).

(XBB 813-2737A)

4. THE MECHANISM OF THE CRYSTAL TO AMORPHOUS TRANSFORMATION IN Si†

J. Washburn, C. S. Murty, D. K. Sadana, P. Byrne,‡ and N. Cheung‡

The effect of roughness of the amorphous/single crystal (a/C) interface on regrowth of amorphous Si has been studied in ion implanted Si. Cross-sectional TEM (XTEM) was used to obtain direct views of the a/C interface.

An 11-MeV As^+ implant was carried out into (100) Si at LN_2 temperature to a dose of $10^{15}cm^{-2}$. The resulting damage, as observed by XTEM was a buried amorphous layer of thickness 4.45 μm (Fig. 1a). The XTEM micrograph also revealed that the upper a/C interface was irregular with extensive interpenetration of amorphous and crystalline regions while the lower a/C interface was quite sharp. The difference in the roughness of the two interfaces is believed to be due to difference in the gradient of total displacement damage and to dynamic regrowth of small amorphous zones during the As irradiation. The deeper a/C interface is at a position of steep damage gradient. Subsequent two step annealing of this sample at 550°C for 20 hours and 950°C for 15 minutes resulted in a buried layer of entangled dislocations and a layer of

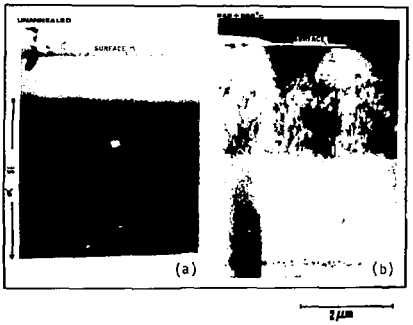

Fig. 1. 11 MeV As^+ implantation into (100) Si (a) XTEM corresponding to the as-implanted specimen (b) XTEM corresponding to the 545° + 950°C annealed specimen. Note the difference in the sharpness of the upper and lower a/c interfaces in (a).

(XBB 8110-9336A)

small dislocation loops, the latter layer being beyond the mean projected range (Rp). Comparison of results from the unannealed and annealed samples showed that defect-free solid phase epitaxial growth occurred from the deeper α/C interface that was sharp, while a high density of dislocations were nucleated from the upper α/C interface that was fuzzy. Figure 1 also shows that the two oppositely moving interfaces met each other in the middle at a depth of 2.4 μm where the dislocations terminated.

These results clearly demonstrate that there is a correlation between the nucleation of dislocations and the roughness of the α/C interface. It is likely that poor electrical properties of high temperature implanted Si, where a rough α/C interface commonly occurs is associated with this high dislocation density.

* * *

†Extended abstract of LBL-14005, to be submitted to App. Phys. Lett.

‡Electrical Engineering and Computer Science Department, University of California, Berkeley.

5. THE EFFECT OF IMPURITY ATOMS ON THE KINETICS OF THE AMORPHOUS TO CRYSTAL TRANSFORMATION IN SILICON†

P. Ling and J. Washburn

Ion implantation can be used to obtain amorphous layers on single-crystal substrates. The regrowth process that these layers undergo during low temperature annealing is known to be sensitive to the implanted ion concentration and the identity of the implanted ions.[1,2] Csepregi et al.[3] have shown that B, P, and As increase the regrowth rate, but C, O and Ar decrease it.[4] The experimental program reported here is designed to test the hypotheses a) that all impurities accelerate the regrowth rate when present at concentrations below their solid solubility limit in crystalline silicon and b) that all impurities decrease regrowth rate when present in concentration above the solid solubility limit.

When the impurity concentration exceeds its maximum solubility in the crystal then regrowth requires redistribution by diffusion in the amorphous phase, resulting in a retarded growth rate. Higher concentrations of an impurity can cause further complications. If the growth rate is slow enough, the impurity may precipitate during the regrowth process. The impurity may precipitate in the amorphous phase homogeneously, providing nuclei for crystalline silicon and causing regrowth as polycrystals.

For B, P, and As the solubility is large. Regrowth rates have only been measured in the region below their maximum solubilities, and these elements have always been observed to increase the regrowth rate. For C, O, and Ar the solubility is very small; the effects of these elements on regrowth rate have been measured only in the region above the solubility limit.

* * *

†Extended abstract of LBL-14006.

1. R. M. Drosd, Ph.D. thesis. University of California, Berkeley, 1979. LBL-9990.
2. S. S. Lau, J. Vac. Sci. Tech. 15, 1656 (1978).
3. L. Csepregi et al., J. Appl. Phys. 48, 4234 (1977).
4. E. F. Kennedy et al., J. Appl. Phys. 48, 4241 (1977).

6. ZINC DIPHOSPHIDE AS A NEW PHOTOVOLTAIC MATERIAL†

T. Mowles and J. Washburn

This research was conducted to evaluate zinc diphosphide as a possible material for use in terrestrial photovoltaic devices.

It has been shown that zinc diphosphide can be grown from the elemental vapors at sub-atmospheric partial pressures. While undoped crystals were invariably p-type, indium doping from the vapor can produce n-type conduction.

A model for the vapor growth and doping has been constructed from thermodynamic data. Optical property measurements have verified that zinc diphosphide is a direct gap semiconductor with a 1.53 eV room temperature bandgap. This is near-optimum for high efficiency solar cells. Experiments on the thermochemical stability showed that zinc diphosphide is unstable toward oxidation at room temperature resulting in long-term microscopic surface decomposition. The presence of water facilitates the degradation. The products of the decomposition change as the temperature is raised. The phosphates produced are unstable thermochemically with respect to the loss of phosphorus oxide. Oxidation at a temperature sufficient for acceptable growth rate yields a two-phase deposit unsuitable for subsequent photolithography.

Zinc diphosphide is a possible new photovoltaic material but it would require encapsulation for terrestrial use.

* * *

†Extended abstract of LBL-14007; T. Mowles, Ph.D. thesis, University of California, Berkeley, 1981.

7. MeV He^+ DECHANNELING FROM SECONDARY DEFECTS IN Si†

D. K. Sadana and J. Washburn

This work was aimed at improving the interpretation of channeled RBS for various kinds of defects and their depth distribution by comparing the channeling results with transmission electron microscopy observations on the same specimens. Comparison studies on defect structures involving single and multiple amorphous layers in ion implanted Si have been reported previously.[1] For this study, P^+ implanted (111) Si samples containing dislocation networks, dislocation loops,

a

b

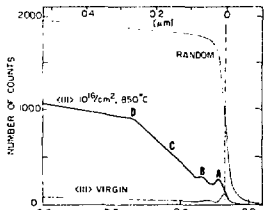

c

Fig. 1. Weak-beam TEM micrograph using a (111)-type reflection (a) before stripping the surface layer and (b) after stripping the surface layer (c) 1.6 MeV He^+ channeling spectrum. (XBB 8112-11936)

point-defect clusters, or a combination of these were chosen for comparison.

Figure 1 shows results from a sample that was implanted with P at 400°C to a dose of $10^{16}cm^{-2}$ and subsequently furnace annealed at 850°C for 20 min. The TEM weak-beam plan-view micrograph from this sample revealed a high density of fine point-defect cluster damage (≤ 20 Å across) near the surface together with a dislocation network and loops (Fig. 1a). In order to find the depth distribution of the fine damage, a surface layer of a few hundred angstrom thickness was removed by ion-beam milling. The weak-beam micrograph after the surface-layer removal showed mainly faulted dislocation loops and rods and some long dislocations but no fine point-defect cluster damage (Fig. 1b). The corresponding cross-sectional TEM micrograph showed a 250 Å-wide dense band of fine defect clusters at the surface. Below this band was present a three-dimensional dislocation network that extended to a depth of 2300 Å. A band of dislocation loops was also present at 1700 to 3000 Å; a part of this band overlapped with the dislocation network. The mean diameters and the density of the loops were 600 Å and $10^{11}cm^{-2}$, respectively. The 1.6 MeV He^+ channeling spectrum (Fig. 1c) from the same sample indicated the following: a damaged surface (peak A), a lightly disordered region at a mean depth of 550 Å (peak B), and an increasing disorder in the depth range 650 to 2500 Å (note the steep dechanneling slope C beyond peak B).

In order to separate out the effect of dechanneling due to the presence of the loops and fine clusters from that due to dislocations, samples containing either only the dislocation loops or the point-defect clusters were analyzed. The results show that dechanneling caused by three-dimensional dislocation networks can be distinguished from that resulting from small dislocation loops and smaller point-defect clusters. Small dislocation loops were found to be the least effective in producing dechanneling.

* * *

†Extended abstract LBL-12953; Phys. Rev. B. 24 3626 (1981).

1. D. K. Sadana et al., J. App. Phys. 51, 5718 (1980).

8. PROGRESS ON THE FABRICATION OF PULSED ELECTRON BEAM ANNEALER†

M. Strathman,‡ D. K. Sadana, R. True,§ W. Chupp‖ and G. Stoker¶

The fabrication of a high power pulsed electron beam annealer (PEBA) was undertaken nearly two years ago to establish an in-house facility to study surface-modification related phenomena in semiconductors (especially Si and GaAs) and metals. The equipment completed is shown in Fig. 1. The annealer will produce 100-ns pulses of an electron beam with a power of 1.5 J cm^{-2} which will be enough to melt surface layers of ≥ 1 μm of the above materials. The voltage of the beam at the target will be in the order of 20 kV. Debugging should be completed by early 1982.

* * *

†M. Strathman, D. K. Sadana and R. True, DOE Invention case No. RL 7981 (S-54, 209).

‡Instrumentation Technologies Division, Lawrence Berkeley Laboratory.

§Litton Industries, San Carlos, CA.

‖Advanced Accelerator Development Group, Lawrence Berkeley Laboratory.

¶Special Projects Division, Electronic Engineering Division, Lawrence Berkeley Laboratory.

Fig. 1. High power linear pulsed electron beam annealer designed and fabricated at Lawrence Berkeley Laboratory. The annealer is capable of delivering 100ns pulses at a power of 1.5 J cm^{-2} at 20 kV and will be used for surface modification studies of semiconductors and metals.
(XBB 810-11404)

1981 PUBLICATIONS AND REPORTS

Refereed Journals

1. J. Washburn, "Formation and Effects of Secondary Defects in Ion Implanted Silicon," Defects in Semiconductors (Materials Research Society Symposium) 2, 209-223 (1981).

2. R. Drosd and J. Washburn, "Some Observations on the Amorphous to Crystalline Transformation in Si," J. App. Phys. 53 (1982); LBL-13526.

3. D. K. Sadana and J. Washburn, "MeV He^+ Dechanneling from Secondary Defects in Si," Phys. Rev. (B) 24, 3626-29 (1981); LBL-12953.

4. D. K. Sadana, J. Washburn, M. Strathman, M. Current, and M. Maenpaa, "Arsenic Implants through SiO_2/Si: A TEM, RBS and MOS Device Characteristics Study." Proc. Ins. Phys. (London) 60, 453-458 (1981).

5. M. G. Grimaldi, B. M. Paine, M. Maenpaa, M. A. Nicolet, and D. K. Sadana, "Epitaxial Regrowth of Thin Amorphous GaAs Layers," App. Phys. Lett. 39, 70-72 (1981).

6. M. Maenpaa, T. F. Kuech, M. A. Nicolet, S. S. Lau, and D. K. Sadana, "The Heteroepitaxy of Ge on Si: A Comparison of Chemical Vapor and Vacuum Deposited Layers," J. App. Phys. 53, 1076-1083 (1982).

7. M. G. Grimaldi, B. M. Paine, M. A. Nicolet, and D. K. Sadana, "Ion Implantation and Low Temperature Epitaxial Growth of GaAs," J. App. Phys. 52, 4038-4046 (1981).

8. M. Hockly, D. K. Sadana, G. R. Booker, N. J. Barrett, and B. J. Sealy, "TEM Studies of GaAs Implanted with Zn or Si and Laser or Furnace Annealed," Proc. Inst. Phys. (London) 60, 113-120 (1981).

9. D. K. Sadana, J. Washburn, M. D. Strathman, G. R. Booker, and M. H. Badawi, "Effects of Damage-Impurity Interaction on Electrical Properties of Se^+ Implanted GaAs," Defects in Semiconductors (Materials Research Society Symposium) 2, 515-519 (1981).

Other Publications

1. T. Mowles, Ph.D. Thesis, University of California, Berkeley; LBL-14007.

2. D. K. Sadana, J. Washburn, T. Zee, and R. G. Wilson, "Direct Evidence of Cr-Structural Defects—Oxygen Interaction in Ion Implanted GaAs," presented at the Intern. Symp. on GaAs and Related Compounds, Oiso (Japan), Sept. 20-23, 1981; LBL-13527.

3. L. S. Hung, B. Y. Tsaur, J. W. Mayer, S. S. Lau, W. F. Tsang, and D. K. Sadana, "Crystallization Investigation of $NiSi_2$ Thin Films," J. Electronic Mat. 11, 289-301 (1982).

4. M. Current, D. K. Sadana and M. Strathman, "As Implants through Screen Oxides: An RBS/TEM Study," 159th ECS Mtg., Minneapolis, MN, May 10-15, 1981.

Invited Talks

D. K. Sadana, "Structural-Electrical Correlations in Ion Implanted and Subsequently Laser or Furnace Annealed Si and GaAs," presented at Centre Electronique Horloger, S.A., Neuchatel (Switzerland), April 15, 1981; and at Thomas Watson Research Center (IBM), York Town Heights, NY, April 2, 1981.

c. Mechanical Properties of Ceramics*

A. G. Evans, Investigator

Introduction. The current research activity is devoted to studies of both high temperature deformation and failure, and microstructure development during sintering. High temperature deformation and failure addresses the response of refractory materials to stress. Research in this area is devoted to the generation of a self-consistent scientific comprehension of the mechanisms of deformation and failure, using both experimental and theoretical techniques. The ultimate objective of the study if the development of a scheme for predicting high temperature mechanical failure.

The development of microstructure during sintering has a direct influence upon the defect structure in the material and hence, upon the mechanical strength. Much of the microstructure evolution occurs during the final stage of sintering. A study of microstructural changes occurring during this stage, using a combination of theory and experiment, has been embarked upon in order to identify and quantify the critical issues. Particular emphasis is devoted both to the pore/grain boundary separation phenomenon, and to the concomitant coarsening and pore shrinkage processes.

High Temperature Failure

1. HIGH TEMPERATURE FAILURE IN CERAMICS†

A. G. Evans and W. Blumenthal

High temperature failure generally proceeds by the sequential nucleation and propagation of cracks. The former typically prevails at low stresses and high temperatures, while the latter is more critical at stresses and temperatures approaching those typically associated with brittle failure. Analysis of crack nucleation by the localized diffusive nucleation, growth and coalescence of cavities indicates that the nucleation times exhibit temperature and stress dependencies dominated by a product of the nucleation time with either the steady-state creep rate of the material (Monkman-Grant behavior) or the rate of growth of the individual cavities (Orr-Sherby-Dorn behavior). The former dominates when the local strains induced by the inhomogeneous cavitation can not be accommodated by the elasticity of the material: notably at very high temperatures or very low stresses.

* * *

†Short version of LBL-12772.

2. EFFECTS OF INHOMOGENEITIES ON CREEP RUPTURE†

S. M. Johnson, W. Blumenthal, and A. G. Evans

The inhomogeneous nature of the high temperature failure process results in a wide statistical distribution of failure times. The specific influence of microstructural inhomogeneities on the probabilistics of high temperature failure thus constitutes an important aspect of high temperature structural design.

Experimental observations performed on Al_2O_3 have indicated that two of the dominant sources of accelerated failure involve either grain boundaries with atypically low values of the dihedral angle (the ratio of the surface to the grain boundary energy) or large grained regions. The failure propensities associated with each of these inhomogeneities have been compared for single phase ceramic polycrystals. The analysis indicates that large or small grained zones can be sources both of stress concentration and of differing cavitation susceptibilities, resulting in failure times up to an order of magnitude shorter than the failure times in microstructurally homogeneous material (Fig. 1). This range compares with a factor of 2 to 3 range for failure times attributed to a typical spectrum of dihedral angles.

The major microstructural variable that dictates the small extreme of the premature failures is the cavity spacing within atypically grained regions. The magnitudes of the cavity spacing, although experimentally accessible, are not predictably related to microstructural features. It thus remains to identify the cavity nuclei and to determine the influence of the local grain size on the density of cavity nucleation sites.

* * *

†Short version of LBL-13582.

*This work was supported by the Director, Office of Energy Research, Office of Basic Energy Sciences, Materials Science Division of the U.S. Department of Energy under Contract No. DE-AC03-76SF00098.

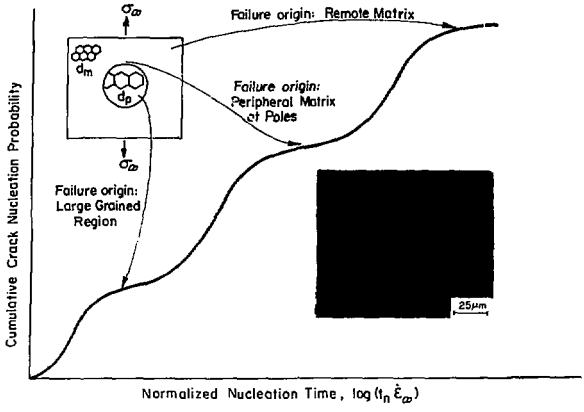

Fig. 1. A schematic indicating cumulative failure probabilities for high temperature fracture in the presence of microstructural inhomogeneity. (XBB 810-11[illegible]3)

3. THE RESPONSE OF CRACKS TO CREEP IN CERAMIC POLYCRYSTALS†

W. Blumenthal and A. G. Evans

Crack propagation controlled failure in ceramic polycrystals is accompanied by crack blunting, concurrent with the formation of a creep damage zone (Fig. 1). The counteracting blunting and damaging processes result in an apparent threshold stress intensity, K_{th}, for crack growth. At stress intensities > K_{th}, the damage rate exceeds the blunting rate and crack advance leads to eventual failure; while at stress intensities < K_{th}, failure from pre-existent cracks appears to be excluded (but may occur from remote cavitation prone microstructural regions, by nucleation controlled mechanisms). The magnitude of K_{th} thus becomes an important material parameter.

Studies of the crack blunting and damage rates have focused on the characteristics of the crack field displacements and the morphology of the damage zone in fine grained Al_2O_3. The crack opening and out-of-plane displacements are found to conform closely with those expected for a linearly viscous material, thereby permitting the crack tip stress (strain) field to be readily expressed in terms of the external loading. Further scrutiny indicates that the intense damage is not coplanar with the crack, but extends along a contour of constant out-of-plane displacement. This observation identifies the importance of the out-of-plane stresses to the damage process and hence, to the crack advance mechanism. Further studies of the damage process will emphasize the out-of-plane features of the crack tip stress field.

* * *

†Short version of LBL-13685.

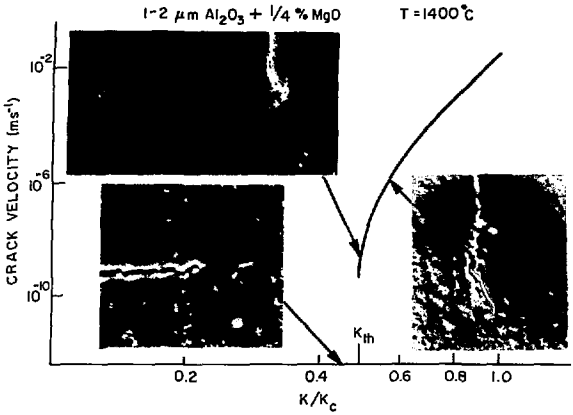

Fig. 1. A schematic indicating the crack tip deformation processes that occur above and below the creep crack growth threshold in Al_2O_3.
(XBB 810-11495)

4. HIGH TEMPERATURE FAILURE INITIATION IN LIQUID PHASE SINTERED CERAMICS†

J. Marion and A. G. Evans

The high temperature failure of ceramics made by liquid phase sintering is known to be dominated by the viscous properties of the second phase (often, an amorphous phase). However, the specific characteristics of the second phase that determine the failure time remain to be elucidated. This problem has been addressed by studying the failure evolution process in Si_3N_4.

The study has identified the central significance of the critical stress for viscous hole nucleation at the two grain channel (Fig. 1): as dictated by the surface energy, viscosity and (especially) the thickness of the second phase. Local stresses in excess of this critical stress result in profuse hole nucleation and rapid failure.

Failure at stresses below the critical stress occurs by hole nucleation at three grain channels (a relatively easy process), followed by liquid depletion (to form a triple junction cavity) and subsequent cavity enlargement by solution/reprecipitation. Analysis of the cavitation sequence under these conditions indicates that the latter process generally occupies the major portion of the time needed to create a full-facet cavity, consistent with the frequent observation of triple junction cavities.

Finally, it is noted that failure is prohibited at stresses below the critical stress required for hole nucleation at three grain channels. This critical stress thus constitutes a natural failure threshold and the attainment of microstructures that exclude three grain channels represents an eventual microstructural design objective.

* * *

†Short version of LBL-13684.

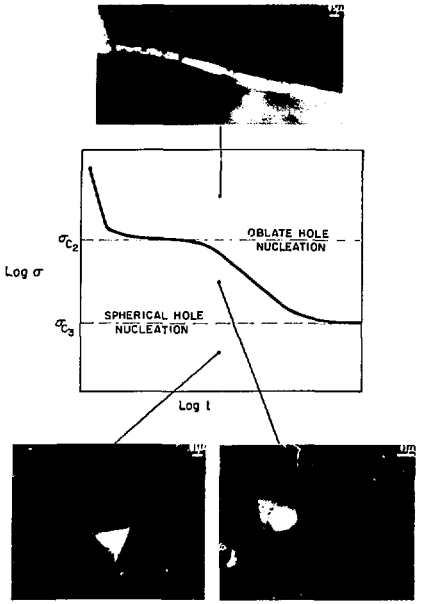

Fig. 1. A schematic indicating the various failure initiation processes that can occur in liquid phase sintered ceramics, and their dependence on the local stress. (XBB 822-968)

Final Stage Sintering

1. *PORE, GRAIN BOUNDARY SEPARATION MECHANISMS*†

C. H. Hsueh and A. G. Evans

The separation of pores from two grain interfaces represents a deleterious event during final stage sintering, because pore isolation essentially prohibits complete densification and may also initiate exaggerated grain growth. An analytic study of pore motion by surface diffusion has established the existence of a critical pore size, a_c. Pores smaller than a_c are invariably capable of moving at the same rate as the attached grain boundary and thus resist separation; while pores > a_c are unstable at high velocities and thus highly susceptible to breakaway. The analysis also revealed that pore and grain boundary distortion are a necessary adjunct to pore motion and breakaway.

The analytically predicted critical pore size depends on the surface diffusivity D_s, the dihedral angle Ψ, and the grain boundary mobility M_b. Small values of M_b and Ψ and large values of D_s encourage attachment. The strong influence of solutes on M_b and smaller, but significant, effects on D_s and Ψ provide one of the bases for comprehending the important influence of additives on microstructure development during final stage sintering.

* * *

†Short version of LBL-13397.

2. COARSENING DURING FINAL STAGE SINTERING†

M. A. Spears and A. G. Evans

The identification of a critical pore size for pore, boundary separation (Hsueh and Evans) establishes the existence of a pore coarsening limit for the attainment of full density during final stage sintering. The pore coarsening and shrinkage associated with microstructure evolution during the final stage involves the concurrent motion of pores at three grain edges (by surface diffusion or evaporation/condensation)--as motivated by the grain coarsening process--and pore shrinkage by grain boundary and lattice diffusion. The presence of pores at the three grain edges moderates the grain growth process and can sufficiently impede grain coarsening that pore shrinkage may be completed prior to the onset of significant grain growth. In this circumstance, the peak pore size can be maintained below the critical breakaway size; thereby permitting the attainment of fine grained, fully dense microstructures.

Explicit comparison of the peak pore size with the critical breakaway size indicates that breakaway is typically assisted by small values of the ratio of the surface to boundary diffusivity and small values of the grain boundary mobility. The former is consistent with the basic requirements for densification during initial stage sintering, although the existence of different quantitative limits on the permissible magnitude of the diffusivity ratio suggests that the optimum sintering temperatures may be different during the initial and final stages.

* * *

†Short version of LBL-12619.

3. EXPERIMENTAL STUDIES OF FINAL STAGE SINTERING†

M. Sakarkan and A. G. Evans

The motion of pores at grain boundaries during final stage sintering has been studied in poly-

Fig. 1. A micrographic sequence obtained on MgO indicating the pore and grain boundary distortions that occur during the pore, boundary separation process. (XBB 810-10702)

crystalline MgO. Inspection of final stage microstructures (developed by hot pressing and subsequent annealing) have identified the presence of pore, grain boundary configurations (Fig. 1) similar to those anticipated by the accompanying theoretical studies (Hsueh, Spears, Evans). Detailed analysis of pore and grain boundary shapes has revealed the existence of steady state pore motion (both pore surfaces moving at the same velocity) in slowly moving pores, and of nonsteady-state motion in highly distorted pores (i.e., in imminent breakaway configurations); thereby confirming that the onset of nonsteady state provides the impetus for breakaway.

A concomitant investigation of the size distribution of intragranular pores and of the grain growth rates in dense polycrystals has provided a self-consistent correlation with the predicted critical pore size, by permitting independent estimates of the grain boundary mobility and surface diffusivity. The results conform quite well with independent measurements performed in prior studies.

* * *

†Short version of LBL-13686.

4. WORK IN PROGRESS

Several unresolved aspects of high temperature failure are under current investigation. The quantitative validity of the recently developed crack nucleation controlled failure models are subject to experimental scrutiny by means of systematic rupture time measurements on Al_2O_3 (single phase) and Si_3N_4 (two phase) materials. A probabilistic treatment of the results, expressed in terms of microstructural variables (grain size, solute content, etc.), will provide the basis for correlations with the existing theory.

The deficient comprehension of crack propagation controlled high temperature failure is being addressed by studies of crack blunting and crack tip damage rates in Al_2O_3, glass, and Si_3N_4. High resolution scanning electron microscopy, surface relief measurements, and stress analysis of regions adjacent to the tip of blunting cracks are being used to identify the microstructural entities that respectively permit blunting and induce damage.

The completed final stage sintering studies, coupled with prior studies of initial stage sintering, have identified the critical influence of the ratio of the surface to the grain boundary diffusivity on the attainment of fully dense, fine grained microstructures. Yet the paucity of measurements of the diffusivity ratio (on a size scale pertinent to sintering), and its dependence on temperature, solute content, etc., prohibits the systematic prediction of optimum sintering conditions. A technique for measuring the diffusivity ratio on the appropriate size scale has accordingly been devised. The technique involves simultaneous measurements of the growth rate and the surface profile of necks formed between spheres subject to an external compressive load. These measurements, coupled with finite difference computations of the neck growth process, permit the direct determination of the diffusivity ratio.

1981 PUBLICATIONS AND REPORTS

Refereed Journals

1. A. G. Evans, "Fatigue in Ceramics," Jnl. of Fracture 16, 485, (1980); LBL-9529.

2. A. G. Evans, D. B. Marshall and N. H. Burlingame, "Transformation Toughening in Ceramics," Advances in Ceramics 3, 202 (1981); LBL-11598.

3. J. R. Porter, W. Blumenthal and A. G. Evans, "Creep Fracture in Ceramic Polycrystals - I. Creep Cavitation Effects in Polycrystalline Alumina," Acta Met. 29, 1899 (1981); LBL-11560 1/2.

4. C. H. Hsueh and A. G. Evans, "Creep Fracture in Ceramic Polycrystals - II. Effects of Inhomogeneity on Creep Rupture," Acta Met. 29, 1907 (1981); LBL-11560 2/2.

Other Publications

1. A. G. Evans and C. H. Hsueh, "Creep Fracture in Ceramic Polycrystals," in Deformation and Failure of Engineering Materials and Structures, eds. B. Wilshire and D. Owen, Pineridge, March 1981, p. 409.

LBL Reports

1. M. Spears, C. H. Hsueh and A. G. Evans, "Port Breakaway in Final Stage Sintering," LBL-11954.

2. A. G. Evans, "The Structural Reliability of Ceramics: A Processing Dependent Phenomenon," LBL-12208.

3. W. Blumenthal and A. G. Evans, "High Temperature Failure in Ceramics," LBL-12772.

4. C. H. Hsueh, A. G. Evans, and M. Spears, "Microstructure Development During Final Stage Sintering: I. Pore/Grain Boundary Separation," LBL-12619 1/2.

5. M. Spears and A. G. Evans, "Microstructure Development During Final Stage Sintering: II. Grain and Pore Coarsening," LBL-12619 2/2.

6. J. Marion, A. G. Evans, and M. O. Drory, "Mechanisms of High Temperature Failure in Liquid Phase Sintered Materials," LBL-13389.

7. C. H. Hsueh, "Void Behavior During Creep and Sintering at High Temperatures," Ph.D. thesis, LBL-13397.

8. S. M. Johnson, W. R. Blumenthal and A. G. Evans, "High Temperature Failure Origins in Ceramics," LBL-13582.

Invited Talks

1. A. G. Evans, Structural Reliability of Ceramics: A Processing Dependent Phenomenon, Sosman Lecture, American Ceramic Society, Washington, DC, May 1981.

2. A. G. Evans, Creep Fracture in Ceramics, International Conference on The Creep and Failure of Engineering Materials and Structures, Swansea, U.K., March 1981.

3. A. G. Evans and W. Blumenthal, High Temperature Failure in Ceramics, Conference on the Fracture Mechanics of Ceramics, Penn. State Univ., July 1981.

4. A. G. Evans, Toughening Mechanisms in Ceramics, Sandia Labs, Sept. 1981.

5. C. H. Hsueh and A. G. Evans, A Study of Pore-Grain Boundary Separation in Final Stage Sintering, 34th Pacific Coast Regional Meeting, American Ceramic Society, Newport Beach, CA, October 1981.

6. J. Marion and A. G. Evans, A Time to Failure Model for Creep Cavitation in Two Phase Ceramics, 34th Pacific Coast Regional Meeting, American Ceramic Society, Newport Beach, CA, October 1981.

7. S. M. Johnson, W. Blumenthal and A. G. Evans, Creep Rupture in Ceramics, American Ceramic Society, Washington, DC, May 1981.

8. S. M. Johnson and A. G. Evans, The Effects of Inhomogeneities in Creep Rupture in Ceramics, 34th Pacific Coast Regional Meeting, American Ceramic Society, Newport Beach, CA, October 1981.

9. M. Sakarkan and A. G. Evans, Experimental Analyses of Pore Breakaway in MgO, 34th Pacific Coast Regional Meeting, American Ceramic Society, Newport Beach, CA, October 1981.

10. M. A. Spears and A. G. Evans, Coarsening During Final Stage Densification, 34th Pacific Coast Regional Meeting, American Ceramic Society, Newport Beach, CA, October 1981.

11. W. Blumenthal and A. G. Evans, The Growth of Cracks During Creep in Fine-Grain Al_2O_3, 34th Pacific Coast Regional Meeting, American Ceramic Society, Newport Beach, CA, October 1981.

d. Environmentally Affected Crack Growth in Engineering Materials*

R. O. Ritchie, Investigator

Introduction. The objective of this work is to examine mechanical and microstructural factors involved in the micromechanisms of environmentally-influenced subcritical crack propagation in engineering materials. The current emphasis is on the role of dry and moist environments, specifically gaseous hydrogen and moist air, in influencing crack growth in fatigue at very low crack velocities (below 10^{-6} mm/cycle) approaching the so-called threshold stress intensity ΔK_0 below which cracks remain dormant or grow at experimentally undetectable rates. At such very low crack velocities, where crack tip opening displacements are at the micron and sub-micron level, the comparable size-scales of the fracture surface morphology and corrosion deposits can lead to premature closure of the crack which can markedly influence subsequent crack growth behavior. Based on these concepts, we have developed models for environmentally-affected near-threshold crack growth behavior involving enhanced crack closure at low stress intensities, which provide a novel yet accurate description of the effects of microstructure and environments at very low cyclic growth rates.

This work, described in the following section, was previously supported at M.I.T. by the DOE Office of Basic Energy Sciences under Contract No. DE-AC02-79ER10389. A000.

1. INFLUENCES OF GASEOUS ENVIRONMENT ON LOW GROWTH-RATE FATIGUE CRACK PROPAGATION IN STEELS†

R. O. Ritchie, S. Suresh and J. Toplosky‡

Lower strength steels, of yield strength below 800 MPa, have traditionally been considered to be relatively immune to embrittlement in the presence of hydrogen gas. In this program, it is demonstrated that, contrary to conventional wisdom, there are two regimes of fatigue crack growth where propagation rates in hydrogen gas are significantly faster than corresponding rates in moist air. Environmental influences in these two regions are shown to be dominated by entirely different mechanisms.

In particular, in the near-threshold region (growth rates smaller than ~ 10^{-6} mm/cycle), it is seen that, with reference to moist air environments, near-threshold growth rates are faster in dry hydrogen and dry helium gases, marginally slower in distilled water and unaffected in wet hydrogen. Unlike behavior dominated by hydrogen embrittlement mechanisms at higher growth rates, such surprising results are interpreted in terms of a new approach, termed "oxide-induced crack closure," based on the role of crack flank corrosion debris in "wedging-closed" the crack at positive loads. Evidence in support of the wedging action of the corrosion deposits has been obtained indirectly using Auger and ESCA analysis of fracture surface oxide deposits and directly with the aid of ultrasonics techniques to measure closure loads. Simple continuum mechanics calculations on the effect of such deposits are found to be in agreement with closure measurements. Furthermore, concepts of crack closure are shown to provide an accurate description on the effects of load ratio, environment, microstructure and variable amplitude loading on near-threshold fatigue behavior in steels (Fig. 1).

Current and future work in this program is centered around the role of oil environments on crack growth, where hydrodynamic wedge effects can result, and in developing guidelines for the alloy design of materials with improved resistance to near-threshold fatigue crack propagation based on promoting crack closure by irregular fracture morphologies.

* * *

†Brief version of L8L-13421, September 1981, and Met. Trans. 12A, 1435 (1981).

‡Present address: M.I.T., Cambridge, MA 02139.

*This work was supported by the Director, Office of Energy Research, Office of Basic Energy Sciences, Materials Sciences Division of the U.S. Department of Energy under Contract No. DE-AC03-76SF00098.

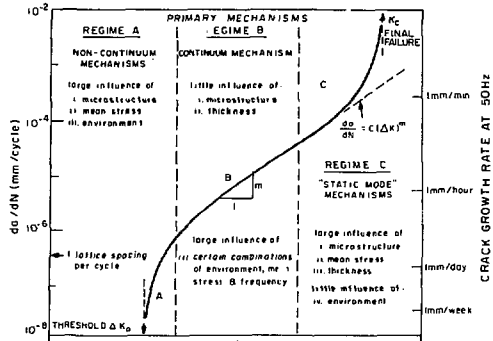

REGIME	NEAR - THRESHOLD	MID - GROWTH RATE	HIGH - GROWTH RATE
TERMINOLOGY	Stage I	Stage II	–
MECHANISM	Single Shear	Alternating or Simultaneous Shear on Two Slip Systems (Striation Growth)	Additional Static Modes
CRACK TIP DISPLACEMENTS	Modes II + I	Mode I	Mode I
NATURE OF FRACTURE SURFACES	Serrated or Faceted	Planar (Striations)	Additional Cleavage, Intergranular or Microvoid Coalescence
CLOSURE LEVELS	High $\left(\frac{K_{cl}}{K_{max}} \gtrsim 0.5\right)$	Low $\left(\frac{K_{cl}}{K_{max}} \lesssim 0.2\right)$	–
OCCURRENCE	Plastic Zone Size $\lesssim$ Grain Size	Plastic Zone Size $\gtrsim$ Grain Size	Plastic Zone Size $\gg$ Grain Size

Fig. 1. Schematic representation of the characteristics of fatigue crack propagation behavior at different growth rates showing regimes principally affected by crack closure. (XBL 8112-12994)

1981 PUBLICATIONS AND REPORTS

Refereed Journals

†1. S. Suresh, G. F. Zamiski, and R. O. Ritchie, "Oxide-Induced Crack Closure: An Explanation for Near-Threshold Corrosion Fatigue Crack Growth Behavior," Met. Trans. A, 12A, 1435 (1981).

†2. J. Toplosky and R. O. Ritchie, "On the Influence of Gaseous Hydrogen in Decelerating Fatigue Crack Grown Rates in Ultrahigh Strength Steels," Scripta Met., 15, 905 (1981).

‡3. M. A. Ritter and R. D. Ritchie, "On the Calibration, Optimization and Use of D.C. Electrical Potential Methods for Monitoring Mode III Crack Growth in Torsionally-Loaded Samples," Fat. of Eng. Matls. & Struct., 4, 306 (1981).

LBL Reports

†1. S. Suresh and R. O. Ritchie, "On the Influence of Fatigue Underloads on Cyclic Crack Growth in Steels," LBL-13353.

2. R. O. Ritchie, "Why Ductile Fracture Mechanics?" LBL-13359.

†3. R. O. Ritchie, S. Suresh and J. Toplosky, "Influences of Gaseous Environment on Low Growth-Rate Fatigue Crack Propagation in Steels," LBL-13421.

§4. J. F. McCarver and R. O. Ritchie, "Fatigue Crack Propagation Thresholds for Long and Short Cracks in Rene 95 Nickel-Base Superalloy," LBL-13453.

5. S. Suresh and R. O. Ritchie, "Mechanistic Dissimilarities Between Environmentally-Influenced Fatigue Crack Propagation at Near-Threshold and Higher Growth Rates in Lower Strength Steels," LBL-13585.

Other Publications

†1. R. O. Ritchie, "The Application of Fracture Mechanics to Fatigue, Corrosion Fatigue and Hydrogen Embrittlement," in Analytical and Experimental Fracture Mechanics, G. C. Sih and M. Mirabile, eds., p. 81, Sijthoff and Noordhoff, Holland, 1981.

‡2. F. A. McClintock and R. O. Ritchie, "Modelling Low Cycle Torsional Fatigue Crack Growth under Variable Amplitude Loading," in Mechanics of Fatigue, T. Mura, ed., AMD-Vol. 47, p. 1, ASME, NY, 1981.

†3. R. O. Ritchie, "Environmental Effects on Near-Threshold Fatigue Crack Propagation in Steels: A Re-Assessment," in Fatigue Thresholds, J. Bäcklund, A. Blom and C. J. Beevers, eds., EMAS Ltd., Warley 1981.

†4. S. Suresh, D. M. Parks and R. O. Ritchie, "Crack Tip Oxide Formation and its Influence on Fatigue Thresholds," in Fatigue Thresholds, J. Bäcklund, A. Blom, and C. J. Beevers, eds., EMAS Ltd., Warley, 1981.

†5. E. K. Tschegg, R. O. Ritchie and S. E. Stanzl, "Ultrasonic Methods for Determination of Near-Threshold Fatigue Crack Growth Rates," in Fatigue Thresholds, J. Bäcklund, A. Blom, and C. J. Beevers, eds., EMAS Ltd., Warley 1981.

†6. S. Suresh and R. O. Ritchie, "Mechanisms of Environmentally-Assisted Fatigue Crack Growth in Low Strength Steels," in Advances in Fracture Research, Proceedings of Fifth International Conf. on Fracture, Cannes, D. Francois, et al., eds., p. 1873, Pergamon Press, NY, 1981.

Invited Talks

1. R. O. Ritchie, "Fatigue Crack Propagation Based on Elastic-Plastic Fracture Mechanics," Technology Today, Golden Gate Metals and Welding Conf., San Francisco, CA, January 1981.

2. R. O. Ritchie, "Oxide-Induced Crack Closure - A New Mechanism for Corrosion Fatigue Crack Propagation," Department of Materials Science and Engineering, Laboratory for Research on the Structure of Matter, University of Pennsylvania, Philadelphia, PA, February 1981.

3. R. O. Ritchie, "Analysis of Corrosion Fatigue," 1981 Gordon Research Conference on Physical Metallurgy, Andover, NH, July 1981.

4. R. O. Ritchie, "A General Review of Near-Threshold Fatigue Crack Growth Rate Testing," Battelle Pacific N.W. Laboratories, Richland, WA, August 1981.

5. R. O. Ritchie, "Environmentally-Influence Fracture," 18th Annual Meeting of the Society for Engineering Science, Brown University, Providence, RI, September 1981.

6. R. O. Ritchie, "The Future Trend of Fatigue Crack Growth and Small Crack Studies," Westinghouse Research and Development Center, Pittsburgh, PA, September 1981.

7. R. O. Ritchie, "New Directions in the Role of Environment in Influencing Fatigue Behavior of Long and Short Cracks," Rockwell International Science Center, Thousand Oaks, CA, September 1981.

8. R. O. Ritchie, "The Mechanical and Metallurgical Factors Associated with Corrosion Fatigue Crack Growth," Joint ASM and SESA Santa Clara Valley Chapter Meeting, October 1981.

9. R. O. Ritchie, "New Models for Corrosion Fatigue in Steels," Department of Materials Science and Mineral Engineering, University of California, Berkeley, CA, October 1981, Department of Materials Science and Engineering, Stanford University, CA, October 1981, and Stanford Research Institute, Menlo Park, CA, December 1981.

10. R. O. Ritchie, "Near-Threshold Corrosion Fatigue Crack Growth at Conventional Frequencies," Engineering Foundation Conference on Fatigue and Corrosion Fatigue up to Ultrasonic Frequencies, Seven Springs Resort, PA, October 1981.

11. S. Suresh, "Recent Advances in Fatigue," Indian Institute of Technology, Madras, India, January 1981.

12. S. Suresh, "Oxidation Effects in Fatigue," Lockheed Palo Alto Research Laboratory, Palo Alto, CA, June 1981.

* * *

†Work supported in part at M.I.T. by Office of Basic Energy Sciences and the Office of Fossil Energy Research, of the U.S. Department of Energy, under Contract Nos. DE-AC02-79ER10389. AO00 and EX-76-A-01-2295, TO 40.

‡Work supported at M.I.T. by the Division of Energy Conservation, U.S. Department of Energy, under Contract No. EX-76-A-01-2295, TO 51.

§Work supported in part by National Science Foundation through the Center for Materials Science and Engineering, M.I.T. under Contract No. DMR-78-24185.

3. Physical Properties

a. Interfaces and Ceramic Microstructures*

Joseph A. Pask, Investigator

Introduction. The purpose of this work is to advance basic understanding of the nature of interfaces primarily between dissimilar materials, e.g., metals and ceramics, particularly in terms of bonding and adherence. This understanding is critical in the development of composites, protective coatings, glass/ceramic to metal seals, and in the reduction of corrosion at interfaces. The work involves studies of thermodynamics and kinetics of reactions at interfaces and of wetting and spreading of liquids.

Another objective in this work is to advance the understanding of the factors that play roles in the development of desired microstructures in ceramic materials, with and without a liquid phase. This understanding depends on a knowledge of the interfacial phenomena from a thermodynamics point of view.

1. WETTING BEHAVIOR IN THE IRON-SILVER SYSTEM†

Antoni P. Tomsia, Zhang Feipeng, and Joseph A. Pask

Sessile drops of molten Ag on Fe at 1000°C, under O_2 partial pressures of 10^{-5} and 10^{-15} Pa, show acute contact angles that vary with experimental conditions. Surface energies of Fe, and correspondingly contact angles, are sensitive to the degree of saturation of the Fe with Fe oxide and to the degree of adsorptivity of oxygen, which is dependent on the activity of oxide in Fe and the $p(O_2)$ in the atmosphere. Obtuse angles form when the surface energy of solid is sufficiently decreased by formation of oxide layer on the Fe surface without affecting the surface energy of the molten Ag drops and the solid/liquid interfacial energy. Adherence of the chemical bonding type occurs when thermodynamic stable phase equilibrium is attained and maintained at the interface, represented by saturation of each phase by the other, which is the case for the Fe-Ag system in the absence of a discrete oxide phase.

* * *

†Brief version of LBL-13390.

*This work was supported by the Director, Office of Energy Research, Office of Basic Energy Sciences, Materials Science Division of the U.S. Department of Energy under Contract No. DE-AC03-76SF00098.

2. SOME ASPECTS OF LIQUID PHASE SINTERING OF ALUMINA†

Philip L. Flaitz and Joseph A. Pask

Microstructure development in liquid/crystal systems is dependent on the nature of the distribution of the liquid phase. Sessile drop experiments of $CaO-Al_2O_3-SiO_2$ glasses on sapphire to determine wetting behavior and on polycrystalline alumina to determine the penetration behavior of the liquid into the compact were made in the range of 1500 to 1600°C. Wetting, but no spreading, occurred on sapphire in all cases, including the case of a starting liquid undersaturated in alumina. Studies of penetration of liquid into a number of polycrystalline aluminas indicated the criticality of the nature of the grain boundaries. Most rapid and complete penetration (with isolation of grains in the presence of sufficient liquid) was exhibited with alumina hot-pressed in graphite dies. Subsequent annealing, and/or additions of MgO sintered at 1750°C reduced the rate but not degree of penetration. A commercial alumina with an MgO addition but fired at 1900°C (Lucalox) showed penetration only along three-grain junctions. It is presumed that these variations are associated with variations in the grain boundary energy (γ_{SS}) and that the driving force for penetrations is represented by $(\gamma_{SS} - 2\gamma_{Sl})$, the crystal/liquid interfacial energy being γ_{Sl}. Complete penetration occurs when $(\gamma_{SS} > 2\gamma_{Sl})$, which corresponds to a zero dihedral angle. Spreading of a liquid on the solid, which occurs when $[(\gamma_{SV} - \gamma_{Sl}) > \gamma_{lV}]$, thus is not necessary for liquid phase sintering.

* * *

†Brief version of LBL-13849.

1981 PUBLICATIONS AND REPORTS

Refereed Journals

1. P. R. Sharps, A. P. Tomsia, and J. A. Pask, "Wetting and Spreading in the Cu-Ag System," Acta Metallurgica, 29, 855-865 (1981); LBL-11119.

2. B. Wong and J. A. Pask, "A Thermodynamic Derivation of the Dihedral Angle Equation for a Two Phase System," J. Materials Science, 16 - Letters, 261-262 (1981); LBL-9670.

3. S. S. Chiang, M. Nishioka, R. M. Fulrath, and J. A. Pask, "Effects of Processing on Microstructure and Properties of PZT Ceramics," Bull. Am. Ceram. Soc., 60, 484-489 (1981); LBL-8868.

4. S. S. Chandratreya, R. M. Fulrath, and J. A. Pask, "Reaction Mechanisms in the Formation of PZT

Solid Solutions," J. Am. Ceram. Soc., 64, 422-425, (1981); LBL-8867.

5. M. Nishioka, S. S. Chiang, R. M. Fulrath, and J. A. Pask, "Influence of Mixing Medium on Sintering and Coupling Coefficient of PZT Ceramics," Ceramics International, 7(3), 87-89 (1981); LBL-8869.

6. A. P. Tomsia and J. A. Pask, "Kinetics of Iron-Sodium Disilicate Reactions and Wetting," J. Am. Ceram. Soc., 64, 523-528 (1981); LBL-10443.

7. S. S. Chiang, R. M. Fulrath, and J. A. Pask, "Influence of Microcracking and Slow Crack Growth on the Planar Coupling Coefficient in PZT," Commun. Am. Ceram. Soc., 64, c141-c143 (1981); LBL-9205.

LBL Reports

1. Y. Nurishi and J. A. Pask, "Sintering of α-Al_2O_3-Amorphous Silica Compacts," LBL-12457.

2. A. P. S. Rana, O. Aiko and J. A. Pask, "Sintering of α-Al_2O_3 Quartz and α-Al_2O_3 Cristobalite Compacts," LBL-12458.

3. S. Tso and J. A. Pask, "Reaction of Glasses with Hydrofluoric Acid Solution," LBL-12880.

4. S. Tso and J. A. Pask, "Reaction of Fused Silica with Hydrogen Gas," LBL-12881.

5. S. Tso and J. A. Pask, "Reactions of Silicate Glasses and Mullite with Hydrogen Gas," LBL-12882.

6. S. Johnson and J. A. Pask, "Formation of Mullite in Kaolinite and Al_2O_3 Mixtures," LBL-13062.

Other Publications

1. J. A. Pask and A. G. Evans, eds., Surfaces and Interfaces in Ceramic and Ceramic-Metal Systems, Materials Science Research, V. 14, Plenum Press, New York and London.

2. J. S. Moya, W. M. Kriven, and J. A. Pask, "Influence of Grain Boundary Silica Impurity on Alumina Toughness," in Surfaces and Interfaces in Ceramic and Ceramic-Metal Systems, Plenum Press, New York and London (LBL-12190).

3. J. A. Pask and A. P. Tomsia, "Wetting, Spreading and Reactions at Liquid/Solid Interfaces," in Surfaces and Interfaces in Ceramic and Ceramic-Metal Systems, Plenum Press, New York and London (LBL-11335).

b. High Temperature Reactions*

Alan W. Searcy, Investigator

Introduction. Current research is focused on the kinetics and thermodynamics of decomposition reactions, on the characterization of their solid products, and on surface diffusion by high-temperature vapors. Each of these areas continues to prove fruitful of novel or unexpected findings. The reports abstracted below include a presentation of TEM evidence that in vacuum small volume elements of calcite lose a significant fraction of their CO_2 content before a second-phase, normal CaO is formed. Another report illustrates how weight-loss data for decomposition of $MgSO_4$ powder can be tested for the establishment of equilibrium or of irreversible decomposition. Conventional methods of analysis have not distinguished between these fundamentally different modes of powder decomposition. The same report presents experimental evidence that surface diffusion through a porous MgO product layer keeps the effectiveness of the catalyst high throughout ~ 90% of the decomposition of an $MgSO_4$ powder. Another report describes the first quantitative measurement of surface diffusion of salts on an oxide surface. Two others report the use of adsorption isotherm measurements 1) to prove that when large crystals of calcite decompose, the ~ 0.01-μm cross section CaO particles undergo a rearrangement to repack in a duplex structure with some pores of < 0.1 μm cross section and others of ~ 1 μm cross section, and 2) to measure surface area and volume changes in these porous CaO aggregates as a function of sintering time in CO_2 atmospheres.

1. FORMATION OF A HIGHLY CO_2-DEFICIENT CALCITE†

Tien Tien Dai and Alan W. Searcy

Shukla, Meschi, and Searcy[1] have shown that at 500-600°C calcite becomes thermodynamically unstable relative to the reaction $CaCO_3(s) \rightarrow CaO(s) + CO_2(g)$ when the CO_2 content decreases below that in the parent crystals by less than 0.1%. We find transmission electron microscope (TEM) evidence that when calcite is heated in the same temperature range in vacuum, small volume elements of the calcite phase lose more than one-fourth of their CO_2 content before transforming rapidly to the CaO phase.

Sequential single-crystal electron diffraction patterns from thin sections of calcite were observed during heating at ~ 500-600°C. Spacings of the five strongest crystal reflections in successive patterns decreased by 3.9 ± 0.1%, 4.9 ± 0.1%, and 5.9 ± 0.2%. The last pattern showed weak new spots oriented along the c-axis of the $CaCO_3$ hexagonal unit cell. The powder pattern of normal, NaCl-type, CaO appeared in the next film and the distorted calcite pattern was absent.

These observations suggest that the calcite unit cell undergoes a decrease in volume of ~ 17% before a sudden transformation to CaO. The superlattice spots probably reflect partial substitution of O^{2-} for CO_3^{2-} ions in alternate planes along the calcite c-axis. If the calcite defect phase just before transformation is assumed to be an ideal solution of CaO in $CaCO_3$, the composition $Ca(CO_3)_{0.73}(O)_{0.27}$ is calculated. Probably many other decomposition reactions in vacuum go through a similar evolution of highly metastable defect structures. TEM studies of such reactions can open an interesting new range of solids for study.

* * *

†From LBL-13602.

1. R. K. Shukla (Ph.D. thesis), LBL-9885.

2. THE EFFECTS OF SOLID CATALYSTS AND OF SAMPLE SIZE ON $MgSO_4$ DECOMPOSITION†

Susan Roche and Alan W. Searcy

This study concentrates attention on two neglected but important aspects of decomposition reactions: 1) whether (and if so, how) a solid catalyst can influence the rate of decomposition after the catalyst is separated from the reactant surface by a growing layer of porous solid reaction product, and 2) whether an equilibrium or far-from-equilibrium product gas pressure is approached in a powder bed when the powder is decomposed in vacuum.

Magnesium sulfate, which at equilibrium yields SO_2 gas, O_2 gas, and much lower pressures of SO_3 gas, was decomposed in Knudsen effusion cells with and without intimately mixed Fe_2O_3 and Pt. powder and in open crucibles. The latter were loaded to three different depths with powder of 28% packing density. Weight losses were measured as functions of temperature and of time at constant temperature. The gaseous products were identified by mass spectrometry and the solids were examined before and after decomposition by x-ray diffraction, scanning electron microscopy, and BET measurements of the surface areas. Auger spectroscopy was used, with negative results, to seek evidence of penetration of the catalysts through the porous MgO reaction product, but catalyst penetration at concentrations below the detection limit could account for the effects observed.

Catalysis of $MgSO_4$ decomposition is here found to be less effective in open crucibles than in Knudsen cells. This fact implies that the catalytic step probably involves two adsorbed SO_3 molecules or an adsorbed SO_3 molecule and a gas-

*This work was supported by the Director, Office of Energy Research, Office of Basic Energy Sciences, Materials Sciences Division of the U.S. Department of Energy under Contract No. DE-AC03-76SF00098.

eous SO_3 molecule. Meschi and Searcy[1] have shown that a catalyst cannot raise the SO_2 and O_2 pressures to > 10^2 times the SO_3 pressure, as reported in earlier studies,[2] if the catalyst acted only on the SO_3 gas decomposition reaction; the catalyst *must influence the rate of a surface or condensed* phase step. In Knudsen cells, either Fe_2O_3 or Pt is here found to increase measured rates of SO_2 generation throughout the first 90% of reaction. This result means that either the catalyst or the adsorbed SO_3 must diffuse over the MgO surface to maintain the observed catalytic effect. It seems probable that surface diffusion is a more important factor in heterogeneous catalyses than has generally been recognized.

The fact that at the highest temperature studied the decomposition rate is unchanged by increasing the sample mass (Fig. 1) shows that a metastable equilibrium is established in the powder bed when the SO_3 gas pressure in the bed is 10^{-1} times the equilibrium pressure measured in Knudsen cells. At the lowest temperatures and smallest sample loadings, the flux approaches a rate characteristic of the slowest step per unit area of total $MgSO_4$ *surface. That rate is only 10^{-5} times the maximum* possible rate of reaction. Conventional methods of analysis of decomposition reaction kinetics would not reveal the fact that these data were measured in a transition range between two distinctly different regimes.

* * *

†From LBL-13381.

1. D. J. Meschi and A. W. Searcy, paper in preparation.
2. H. H. Lau, D. Cubicciotti, and D. L. Hildebrand, J. Chem. Phys. 66, 4532 (1977).

3. DEVELOPMENT OF BIMODAL PORE SIZE DISTRIBUTION IN CaO FROM CALCITE DECOMPOSITION†

Dario Beruto, Luigi Barco, and Alan W. Searcy

Previous studies by us and coworkers have shown that when large crystals of calcite are partially decomposed in vacuum, cross sections show two layers of products and that both layers are normal NaCl-type CaO. Powell and Searcy[1] recently suggested that the outer layer, which is the only product formed when decomposition is complete, is formed from the intermediate layer by a cooperative (diffusionless) rearrangement of the particles of the highly porous CaO to produce a duplex pore distribution. We have tested their suggestion that the pore size distribution is bimodal by measuring the volume of pores smaller than ~ 0.2 μm cross section for comparison with the total porosity. We have tested their suggestion that the transformation is diffusionless by measuring the surface areas and submicron pore volumes as functions of the extent of reaction.

Calcite crystals were partially decomposed at 686°C in vacuum in successive steps, each of which drove off ~ 10% of the initial CO_2 content. A dual furnace permitted measurement of N_2 adsorption isotherms to be made at 78 K without exposing the easily hydrated CaO to air. A tare in the

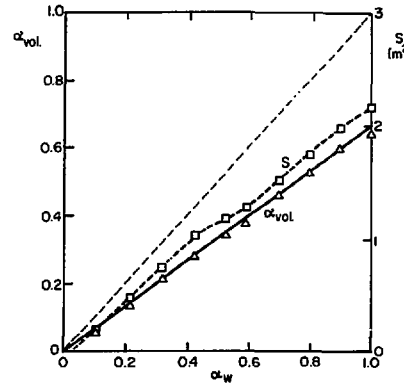

Fig. 1. Fraction of total porosity that is made up of pores < 0.2 μm, α_{vol}, and surface area, S, as functions of fraction of CO_2 removed from a $CaCO_2$ crystal. (XBL 818-6277)

second furnace chamber made possible the correction of weight changes for buoyancy.

Surface areas were obtained by the BET method, and the volume of pores ≤ 0.2 μm diameter was obtained from the weight of N_2 adsorbed when the pressure of N_2 approached saturation. The total porosity was obtained by measuring the exterior dimensions of the CaO aggregate of known mass after the total decomposition of the calcite single crystal. Total porosity was 54% (compared to 56% if no change had occurred from the dimensions of the initial calcite).

About 36% by volume of the final sample was composed of small (< 0.2 μm) pores, with their pore cross sections clustered at 3 to 6 nm. The 18% difference between 54% total porosity and 36% must be accounted for by closed pores (unlikely) and/or by pores too large for significant capillary condensation. If diffusional processes were responsible for growth of the final CaO layer from the initial CaO layer, the rates of generation of surface areas and of volume would be expected to decrease as reaction proceeds (as they do when CO_2 causes sintering; see next report). Both the surface area and the volume of the 3 to 6 nm pores were quasilinear functions of the fraction of calcite decomposed (Fig. 1). The duplex pore structure must form by a cooperative diffusionless process, as suggested by Powell and Searcy.

* * *

†From LBL-13882. Work performed at the University of Geneva by Beruto and Barco, and at MMRD by Beruto and Searcy.

1. E. K. Powell and A. W. Searcy, J. Am. Ceram. Soc., in press (LBL-11207).

4. A MICROSINTERING STUDY BY ADSORPTION METHODS: CaO in CO_2†

Dario Beruto, Luigi Barco, and Alan W. Searcy

Sintering studies are usually carried out with particles of > 1 μm cross section and have seldom been made with particles of < 0.1 μm cross sections. In this study the dual furnace apparatus that was described in the previous report was used to study the sintering of CaO particles that were initially ~ 0.01 μm in cross section.

The CaO was prepared by decomposing $CaCO_3$ single crystals of carefully measured dimensions in the apparatus. Surface areas and the volume of small (< 0.2 μm) pores were measured before and after the CaO was sintered in a series of heatings of each sample in fixed CO_2 pressures a little below the calcite decomposition pressure. Changes in sample weight caused by changes in CO_2 absorption by the sample were measured as a function of time during each period of sintering, and exterior dimensions of the sample at the end of a series of heatings were measured to obtain the net densification. Figure 1 shows the decreases in surface area and in the volume of those pores ≤ 0.2 μm in cross section as a function of the time of sintering, and Fig. 2 shows the corresponding change in pore size distribution that is calculated on the assumption that pores are all slit-shaped. (The qualitative trend in these data would be independent of the assumed geometry.)

The CO_2 content of the sample decreases in direct proportion to the decrease in surface area, showing that within small limits of error almost all of the CO_2 is on the surface; enough CO_2 is present to convert about half the surface O^{2-} ions to CO_3^{2-} ions. The series of sintering steps with 1.3×10^3 Pa pressure results in a 9.5% decrease in total pore volume; the surface area is reduced from 120 m^2/g to 30 m^2/g, and the volume of > 1 μm pores increases from 12% to 40% as the volume of pores of < 0.2 μm cross section decreases to 10% of the sample volume.

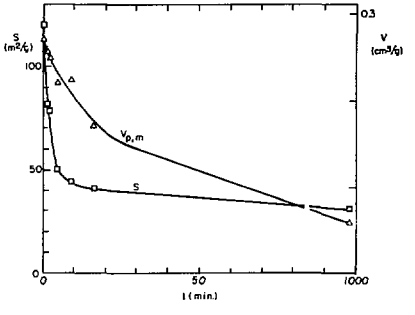

Fig. 1. Variation of surface area S (m^2/g) and of volume V of pores < 0.2 μm in cross section with time of sintering in CO_2. (XBL 818-6280)

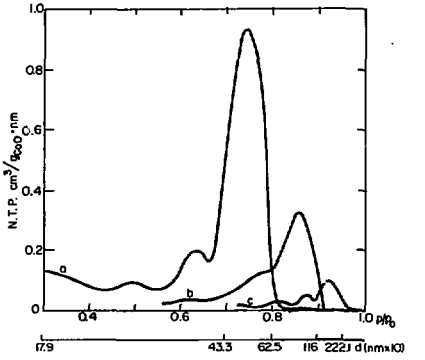

Fig. 2. Initial pore size distribution (curve a), distribution after 5 minutes sintering in CO_2 (curve b), and after 10 minutes (curve c). (XBL 818-6279)

* * *

†Brief version of LBL-13630. This research was performed at the University of Geneva by Beruto and Barco, and at MMRD by Beruto and Searcy.

5. SURFACE DIFFUSION OF HIGH-TEMPERATURE VAPORS THROUGH POROUS ALUMINA†

Nathan S. Jacobson and Alan W. Searcy

Surface diffusion is known or suspected to play a significant role in a variety of important processes such as sintering, heterogeneous catalysis, and the escape of vapors from Knudsen cells that are used for the study of vapor pressures. But quantitative data for high-temperature surface diffusion is sparse. Measurements of the transmission of equilibrium vapors through a porous barrier is here shown to be a useful technique for obtaining such data. In alumina which is traversed with 1-μm pores, surface transport proves to be at least as important as vapor transport for three alkali halides, and the temperature dependence of transport proves to be different from what might have been expected from measurements of surface diffusion of gases.[1]

The pores and porosities of alumina disks, 1 mm thick, were characterized by Hg poresimetry, by BET adsorption, and by direct scanning electron microscope observation. The probability that those molecules of He or of seven other gases that strike one face of the barrier will emerge at the other face is found at room temperature to average $(6.5 \pm 1) \times 10^{-4}$. At high temperatures, the probability of transmission of Zn is $(8.1 \pm 1.5) \times 10^{-4}$. For NaCl, NaF, and LiF the probabilities are respectively $(1.7 \pm 0.2) \times 10^{-3}$, $(3.9 \pm 0.4) \times 10^{-3}$, and $(7.9 \pm 0.7) \times 10^{3}$.

These measurements show that surface diffusion is unimportant for Zn vapor through alumina pores of ~ 1 μm or greater cross sections, but is important for the alkali halides. Because the ratio of transport by surface diffusion to vapor phase transport is proportional to the inverse of the pore diameters, that surface diffusion should not significantly influence vapor pressures measured for these salts in alumina Knudsen effusion cells, which have orifice diameters of > 0.2 mm (though LiF penetration along alumina grain boundaries is significant). The temperature dependence of transport by surface diffusion for the alkali halide vapors below their melting points is indistinguishable from that for vapor transport (Fig. 1). The

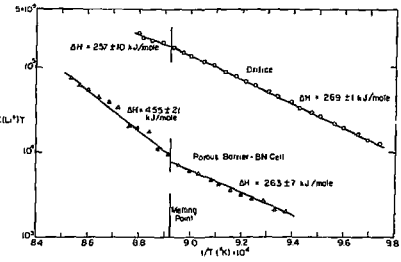

Fig. 1. Variation of intensity of major mass spectrometer peak from LiF(g) with temperature measured through an orifice and through a porous Al_2O_3 barrier. (XBL 816-6304A)

transition state complexes for transport in this range must be alkali halide molecules that have very weak bonds to the surface. Transport above the melting point is generally significantly higher, but evidently is a sensitive function of temperature gradients in the barrier. Probably if the temperature decreases through the barrier in the direction of transport, a monolayer film of alkali halide penetrates part way through the barrier and a much lower concentration of alkalic halide, like that present below the melting point, covers the remainder of the alumina surface.

* * *

†From LBL-13227.

1. R. Ash, R. M. Barrer, J. H. Clint, R. J. Dolphin, and C. L. Murray, Royal Soc. (London) Phil. Trans. 275, 255 (1953).

1981 PUBLICATIONS AND REPORTS

Refereed Journals

1. D. Beruto, L. Barco, G. Belleri, and A. W. Searcy, "Vapor-phase hydration of submicrometer CaO particles," J. Am. Ceram. Soc. 64(2), 74-80 (1981).

2. T. Darroudi and A. W. Searcy, "The effect of CO_2 on the rate of decomposition of calcite," J. Phys. Chem. 85, 3971-4 (1981).

LBL Reports

1. E. K. Powell and A. W. Searcy, "Surface areas and morphologies of CaO produced by decomposition of large $CaCO_3$ crystals in vacuum," June 1981, LBL-11207. Accepted by J. Am. Ceram. Soc.

2. A. W. Searcy and D. J. Meschi, "Electronic ceramics in high temperature environments," January 1981, LBL-11821. Accepted by J. Am. Ceram. Soc.

3. G. F. Knutsen, A. W. Searcy, and D. Beruto, "Effect of LiCl on the rate of calcite decomposition," October 1981, LBL-12043. Accepted by J. Am. Ceram. Soc.

4. N. S. Jacobson, "The diffusion of gases in capillaries" (Ph.D. thesis) August 1981, LBL-13227.

5. T. T. Dai, "Decomposition of Group II carbonates: An investigation by transmission electron microscopy" (Ph.D. thesis) November 1981, LBL-13602.

6. D. Beruto, L. Barco, and A. W. Searcy, "A microsintering study by adsorption methods: CaO in CO_2," November 1981, LBL-13630. To be submitted to J. Am. Ceram. Soc.

Invited Talks

1. T. A. Reis, D. J. Meschi, and A. W. Searcy, "Thermodynamic metastable state in solid MgO," Pacific Coast Regional Meeting, American Ceramic Society, October 27, 1981.

2. S. L. Roche and A. W. Searcy, "Thermal decomposition of magnesium sulfate," Pacific Coast Regional Meeting, American Ceramic Society, October 27, 1981.

3. J. Farnsworth and A. W. Searcy, "Vapor transport through porous barriers," Pacific Coast Regional Meeting, American Ceramic Society, October 27, 1981.

* * *

†Supported in part by the Division of Materials Sciences, Office of Basic Energy Sciences, U.S. Department of Energy; and in part by the Italy-U.S. Exchange Program of CNR (Italy) and NSF.

c. Chemical Properties of Ceramic Alloys*

Lutgard C. De Jonghe, Investigator

When an oxide such as cobalt ferrite is reacted with hydrogen, a porous metal scale will form topochemically from its surface. The pores in the metal scale permit the reducing gas to reach the reaction interface directly. At the pore bottoms, the parent oxide is then destroyed by the reduction process, the oxygen is removed in the form of water vapor, and the cations that are produced at the pore bottoms are transported to the adjacent metal phase. Gaseous reduction of oxides can be considered to occur in three steps: 1) external mass transfer, 2) gas transport through the porous product scale, and 3) chemical reaction at the interface. Under conditions of sufficient gas flow at the specimen, the mass transfer step may be ignored. For reduction of a semi-infinite flat slab by pure hydrogen, the reduction kinetics for a simple topochemical reaction in which there is a phase sequence of unreduced oxide/porous metal scale, a simple kinetic equation prevails[1]

$$J = C^o_{H_2}\left(\frac{\xi}{D_{eff}} + \frac{1}{k_r}\right)^{-1} \qquad (1)$$

where J = the rate of reduction; $C^o_{H_2}$ = the hydrogen concentration at the specimen surface; R = the gas constant; T = the absolute temperature; D_{eff} = effective gas diffusivity in the porous product scale; k_r = interface reaction parameter. From an analysis of thermogravimetric data of oxide reduction it is then possible to determine D_{eff} and k_r from the slope and intercept of a J^{-1} versus ξ plot, provided Eq. (1) is valid. Porter and De Jonghe established the validity of Eq. (1) for cobalt ferrite[1] below 650°C.

* * *

1. J. R. Porter and L. C. De Jonghe, Met. Trans., 12B, 299 (1981).

1. THE REACTION INTERFACE IN REDUCTION†

An analysis was performed to obtain k_r as a function of $p^o_{H_2}$ and T, for cobalt ferrite reduced by hydrogen in the temperature range 560 to 620°C and in $p^o_{H_2}$ range 50 to 250 torr. This analysis yielded information on the nature of the reactions occuring at the oxide/scale interface. The reduction kinetics of cobalt ferrite by hydrogen were determined thermogravimetrically. The details of the method have been described previously. The oxide was 99% dense, with a grain size of about 10 microns. The hydrogen gas had a controlled H_2O content of 100 ppm. Gas flow rates were such that the external mass transfer resistance could be neglected. It was found that the reaction occurring at the oxide/metal interface, described by the parameter k_r, followed Langmuir-Hinshelwood kinetics. Thus, k_r may be written as:

$$k^{-1} = A_1 + A_2\, C^o_{H_2} \qquad (2)$$

where A_1 and A_2 are rate parameters, and $C^o_{H_2} = p^o_{H_2}/RT$. k_r relates the reaction rate J and the hydrogen concentration at the interface. The hydrogen concentration at the interface $C^i_{H_2}$ equals $C^o_{H_2}$ when the layer thickness ξ = o. Thus, $J^o = k_r\, C^o_{H_2}$. The values of A_1 and A_2 were obtained from the data by finding k_r as a function of $p^b_{H_2}$ from Eq. (1); they have been plotted in Fig. 1, and their activation enthalpies have been indicated. The values of A_1 and A_2 can give an indication of the nature of the reaction interface processes. A solid state diffusion process

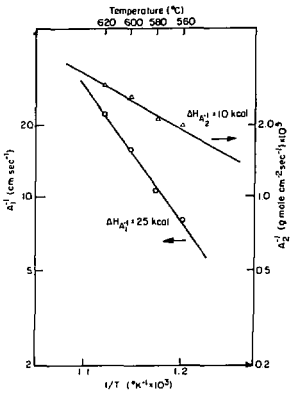

Fig. 1. Arrhenius plot for the rate constants A_1^{-1} and A_2^{-1} of Eq. 2. The activation enthalpies are indicated. (XBL-805-5236)

*This work was supported by the Director, Office of Energy Research, Office of Basic Energy Sciences, Materials Science Division of the U. S. Department of Energy under Contract No. DE-AC03-76SF00098.

must occur at the reaction interface to permit the continued development of the reaction product scale. This solid state diffusion step could involve interface diffusion or volume diffusion. From the values of the activation energies of A_1 and A_2 and from the structural information of the reaction interface, it could be concluded that the interface reaction is controlled by a gas-oxide reaction at the pore bottom, coupled with interface diffusion of the generated excess cations to the metal phase and of the oxygen to the pore bottoms.

Continued research is planned to examine CO/CO_2 reduction of these oxides. With these gases, whiskers rather than simple porous scales develop, accompanied by a large volume increase. This implies that the gas chemistry has a significant effect on the interface reaction process.

* * *

†Short version of M. Chang and L. C. De Jonghe, "Surfaces and Interfaces in Ceramics and Ceramic-Metal Systems," J. Pask and A. G. Evans, Eds. Plenum Press, 1981, Pgs. 137-145.

1981 PUBLICATIONS AND REPORTS

Refereed Journals

1. J. R. Porter and L. C. De Jonghe, "Hydrogen Reduction of Cobalt Ferrite," Met. Trans. 12B, 299 (1981); LBL-9801.

2. J. S. Allender and L. C. De Jonghe, "Gaseous Reduction of an Alloy Oxide," J. Mat. Sci., 16, 2717 (1981); LBL-11125.

Other Publications

1. Mei Chang and L. C. De Jonghe, "The Reaction Interface Reduction," in "Surfaces and Interfaces in Ceramics and Ceramic-Metal Systems," J. Pask and A. G. Evans, Eds, Plenum Press, 1981, pg. 137-145.

d. Structure and Electrical Properties of Composite Materials*

Robert H. Bragg, Investigator

Introduction. The purpose of this work is to understand how the properties of the two broad classes of carbon materials are related to their structure. Soft carbons, typified by pyrolytic graphite (PG) become physically soft when heated above about 2000°C, whereas hard carbons such as glassy carbon (GC) are little affected by heat to 3000°C, or by most corrosive chemicals. While PG is fairly well understood, our knowledge concerning GC is still rudimentary. The latter, a hard brittle substance which fractures conchoidally, is used as a model material because it is obtained as a chemically pure (i.e., elemental carbon) monolithic solid suitable for a wide variety of measurements of physical properties. X-ray diffraction, small angle x-ray scattering, transmission and scanning electron microscopy, and other techniques are used to characterize the structure of GC; and structural changes are induced by heat treatments in inert atmospheres to 2750°C. Electrical properties are measured at temperatures T down to 2.8 K in magnetic fields H up to 5 tesla. Previous studies have shown that glassy carbon is a highly disordered, porous material composed of interwound laths or ribbons of tubostratic carbon.

1. ELECTRICAL PROPERTIES OF GLASSY CARBON†

Dennis F. Baker and Robert H. Bragg

The quasi-amorphous structure of GC is evident in earlier results on the electrical properties, where it was reported that the electrical conductivity σ was characteristic of variable range hopping between localized states. The magnetoresistance $\Delta\rho/\rho$, however, was found to be negative. This behaviour is an anomalous phenomenon except for magnetic scattering; in GC, it could arise from localized spins and therefore should be a function of H/T, and saturate for large H/T. These hypotheses form the basis of the major unresolved questions that the current work addresses.

Samples were heat-treated for three hours at temperatures from 1200 to 2700°C. Measurements of σ, the Hall coefficient R_H, and $\Delta\rho/\rho$ were made using a four-probe-bar specimen and low-frequency excitation current. The major change from previous work was that the lowest measurement temperature was extended from 10 down to 2.8K, and extensive measurements of R_H were made.

Recent results show that R_H is nearly independent of T, positive $\Delta\rho/\rho$ is observed for samples heat treated below 1600°C and less than 20 K, and except for a small positive component, $|\Delta\rho/\rho|$ (Fig. 1) arises from scattering of conduction electrons by electrons in localized states (Curie paramagnetism) and electrons in extended states (Pauli paramagnetism). The overall picture of GC that is well-established now is that of an amorphous semiconductor characterized by variable range hopping between localized states but which at the lowest temperatures seems to conduct like a thin film of a poorly conducting metal.

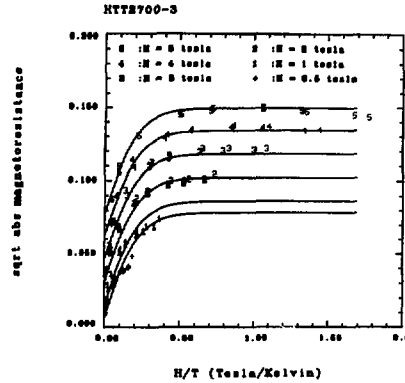

Fig. 1. Negative magnetoresistance in high-temperature heat-treated glassy carbon.
(XBL 822-7819)

* * *

†Brief version of LBL-13652, "The Magnetoresistance, Electrical Conductivity, and Hall Effect in Glassy Carbon," Ph.D. thesis of D. Baker in preparation.

2. WORK IN PROGRESS

Measurements of wide range (> 10° 2θ) x-ray diffraction and small angle x-ray scattering are in progress on a series of GC samples heated in the range 1000-2750°C in order to obtain better values for the activation energies of graphitization and pore coarsening. More closely controlled heat treatments afforded by our specially designed drop quench furnace mechanism, and improved x-ray line profile analysis procedures,[1] are expected to remove a possible 10% discrepancy between values of activation energies obtained for soft and hard carbons. If no discrepancy is found in this work, the Ph.D. dissertation of Leo G. Henry will strongly support our contention that the annealing mechanisms are the same in all carbons. The possibil-

*This work was supported by the Director, Office of Energy Research, Office of Basic Energy Sciences, Materials Sciences Division of the U.S. Department of Energy under Contract No. DE-AC03-76SF00098.

ity of using the radius of gyration in kinetic analyses of pore coarsening is being investigated by J. Hoyt. This could afford an identification of an annealing mechanism in GC, a major achievement in this field. A. Pearson is doing work to determine how removing the small-angle x-ray scattering from wide range diffraction patterns affects the radial distribution function. It is hoped that details associated with interlayer spacing and layer stacking order can be identified and thereby enable a choice to be made among proposed mechanisms of graphitization. Loss of residual hydrogen, typically about 1%, is felt to be the most likely cause.

Work to test the hypothesis that the large volume increase (i.e., density decrease), which occurs when GC is heat treated above about 1000°C, has been completed by B. Mehrotra. He is redirecting the work on preparation of graphite intercalation compounds from gaseous infiltration to ion implantation.

* * *

1. LBL-13628, December 1981.

1981 PUBLICATIONS AND REPORTS

Refereed Journals

1. D. F. Baker and R. H. Bragg, "The Thermal Expansion of the Directionally Solidified Al-$CuAl_2$ Eutectic," Met. Trans. A 12, 95 (1981).

2. S. Bose and R. H. Bragg, "Kinetics of Pore Coarsening in Glassy Carbons," Carbon 19, 289 (1981).

LBL Reports

1. L. G. Henry and R. H. Bragg, "Procedure for Analyzing the X-Ray Line Profiles of Disordered Carbons," LBL-13698.

2. J. Hoyt and R. H. Bragg, "Pore Size and Growth Kinetics using Small Angle X-Ray Scattering," LBL-13784.

Invited Talks

1. D. F. Baker and R. H. Bragg, "The Hall Effect, Magnetoresistance and Electrical Conductivity of Glassy Carbon," 15th Bienniel Conference on Carbon, Philadelphia, PA, June 21-26, 1981, p. 8.

2. L. G. Henry and R. H. Bragg, "Experimental Determination of Compton Scattering from Pyrolytic Graphite and Glassy Carbon," 15th Biennial Conference on Carbon, Philadelphia, PA, June 21-26, 1981, p. 478.

3. B. Mehrotra and R. H. Bragg, "The Mechanism of Density Decrease in Glassy Carbon," 15th Biennial Conference on Carbon, Philadelphia, PA, June 21-26, 1981, p. 530.

4. D. F. Baker and R. H. Bragg, "Paramagnetism and Negative Magnetoresistance in Glassy Carbon," 34th Pacific Coast Regional Meeting, American Ceramic Society, Newport Beach, CA, October 25-28, 1981.

5. L. G. Henry and R. H. Bragg, "Correction of X-Ray Diffraction Line Profiles of Glassy Carbon," 34th Pacific Coast Regional Meeting, American Ceramic Society, Newport Beach, CA, October 25-28, 1981.

6. B. N. Mehrotra and R. H. Bragg, "Nonkinetic Factors in the Thermal Expansion of Glassy Carbon," 34th Pacific Coast Regional Meeting, American Ceramic Society, Newport Beach, CA, October 25-28, 1981.

7. A. Pearson and R. H. Bragg, "Radial Distribution Function of Heat Treated Glassy Carbon," 34th Pacific Coast Regional Meeting, American Ceramic Society, Newport Beach, CA, October 25-28, 1981.

8. J. Hoyt and R. H. Bragg, "Pore Shape and Growth Kinetics in Glassy Carbon," 34th Pacific Coast Regional Meeting, American Ceramic Society, Newport Beach, CA, October 25-28, 1981.

e. High Temperature Oxidation and Corrosion of Materials*

David P. Whittle, Investigator

Introduction. This program aims at advancing the understanding of materials behavior, particularly in response to the unique environments associated with the conversion or combustion of fossil fuels. A number of aspects are covered, and the first four reports deal with the role of sulfur in gaseous form or as a sulfate deposit in influencing scale formation. One of the methods of achieving adequate protection lies in forming and maintaining protective oxide scales, especially Al_2O_3. The scale is far more adherent when its interface with the substrate is highly convoluted, and a way of achieving this is reported in article 5: this result has important ramifications in the design of coatings. Article 6 presents a new method for studying scale/alloy adhesion. Dissolution and diffusion of oxygen in the substrate alloy is also potentially important in understanding oxide formation and studies of internal oxidation are summarized in articles 7 and 8. Finally, measurements of metallic interdiffusion coefficients in Al-containing systems are summarized in article 9.

1. GROWTH MECHANISM OF Cr_2O_3 SCALE AND ITS BREAKDOWN IN $CO/CO_2/SO_2$ ATMOSPHERES

Haroun Hindam and David P. Whittle

The mechanism of sulfur-induced attack of Cr_2O_3-forming alloys in $H_2/H_2O/H_2S$ gas mixtures, simulating coal processing environments, was identified in a previous publication.[1] As a continuation of this project and in order to elucidate the growth mechanism of Cr_2O_3 and the effect of sulfur on its transport properties, the reactions of Cr and Co-25Cr in CO/CO_2 as well as mixtures containing SO_2 were investigated at 1000°C. The oxygen and sulfur potentials were varied from 10^{-13} to 10^{-8} atm and 10^{-10} to 10^{-2} atm, respectively, which are typical of fuel combustion atmospheres.

Typical reaction kinetics are shown in Fig. 1. In the sulfur-free gas, a fine grained convoluted Cr_2O_3 scale grew on Cr conforming nearly to parabolic kinetics at a slightly decreasing rate with the oxygen fugacity, consistent with Cr interstitials as predominant point defects. The slower reaction rate of Co-25Cr alloy was independent of pO_2. 'Breakaway' kinetics, associated with the development of CrS beneath the Cr_2O_3 film, were observed in the sulfur-containing atmospheres. The reaction rate prior to the onset of the accelerated attack was directly dependent on pS_2. Diffusion models, involving lattice or

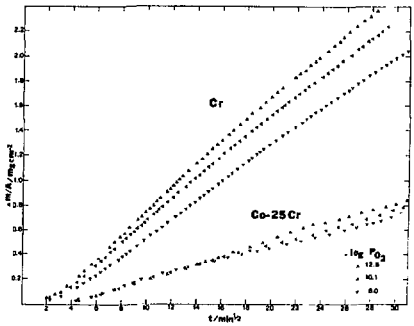

Fig. 1. Parabolic plots for the growth of Cr_2O_3 on Cr and Co-25 Cr alloy in Co/CO_2 mixtures at 1000°C. (XBL 8112-13011)

short-circuit transport through structural defects in the scale, were advanced to account for these observations.

* * *

1. H. Hindam and D. P. Whittle, LBL-12052.

2. HIGH TEMPERATURE CORROSION OF IRON IN SULFUR CONTAINING ATMOSPHERES†

Frank Yang and David P. Whittle

The presence of SO_2 in an oxidizing environment invariably causes accelerated rates of alloy oxidation. Even though the sulfur potential is apparently very low, formation of sulfides within the oxide scale is commonly observed. This leads to the obvious conclusion that sulfur can penetrate growing oxide layers; the mechanism is, however, in some doubt.

Iron samples have been exposed to SO_2-CO_2 and SO_2-O_2 atmospheres of controlled sulfur and oxygen fugacities, and although thermodynamic calculations predict only oxide formation, a complex scale comprising both oxides and sulfides is formed. Detailed kinetic, morphological and analytical studies have indicated that the existence of sulfide within the scale is due to a depletion of oxygen contiguous to scale/gas interface, shifting the thermodynamic equilibrium to a region where sulfide is stable. Rapid growth of the sulfide phase produces a highly irregular scale surface which exacerbates the problem. In addition, the scale is porous, allowing continued inward transport of the sulfur-containing species through

*This work was supported by the Director, Office of Energy Research, Office of Basic Energy Sciences, Materials Sciences Division of the U.S. Department of Energy under Contract No. DE-AC03-76SF00098.

the scale. The porosity results from a contribution of anion transport to the scale growth, which is induced by the presence of the sulfide.

* * *

†Brief version of LBL-12851.

3. THERMODYNAMICS OF Na_2SO_4-INDUCED HOT CORROSION†

Ajaya Misra, David P. Whittle, and Wayne L. Worrell‡

Formation of a molten sulfate is a necessary precursor to the accelerated rates of oxidation or hot corrosion observed on first stage blades and vanes of gas turbines operated at intermediate temperatures (600-850°C) in marine and industrial applications. Solid sulfate deposits are relatively innocuous. The low melting point sulfate is formed by the interaction of the alloy oxidation products, NiO and/or CoO (Co_3O_4), SO_3 in the environment and Na_2SO_4 as a surface deposit. The thermodynamics of the liquid sulfate melts in the Na_2SO_4-$CoSO_4$ and Na_2SO_4-$NiSO_4$ systems have been determined using a gas equilibration technique.

Oxide-Na_2SO_4 mixtures were equilibrated with argon-SO_2-SO_3-air mixtures of different compositions at 1000 to 1173 K, the extent of sulfate formation being determined thermogravimetrically and by analysis of the melt. The data are consistent with a regular solution model for the liquid sulfate solution (Temkin mixing) with an interaction parameter of - 5.21 kcal/mole. The Gibb's free energy of formation of $NiSO_4(\ell)$ is (-40695+36.95T) cals.

Based on these measurements, the minimum P_{SO_3} for liquid sulfate formation in Co-base systems is almost an order of magnitude lower than in corresponding Ni-base systems (10^{-4}atm compared to 8×10^{-4} at 1000 K), making Co-base alloys more susceptible to this low temperature hot corrosion: as indeed observed in practice.

* * *

†Brief version of LBL-13561, submitted to J. Electrochem. Soc.

‡Department of Material Science, University of Philadelphia, PA.

4. INTERNAL OXIDATION AND SULFIDATION OF IRON-BASED BINARY ALLOYS†

Peter J. Risse and David P. Whittle

A significant feature of corrosion in mixed gas environments is the formation of internal oxides and sulfides behind the surface scale. This formation occurs by partial dissociation of the surface scale at the scale/alloy interface, dissolution of the oxygen or sulfur in the alloy, and diffusion inwards where the non-metal reacts with the dissolved Cr or Al to form internal precipitates. The solubility times diffusivity (permeability) product of the oxidant is the important parameter.

Using different gas mixtures of $H_2S/H_2/H_2O$/argon, the activities of the oxidants (sulfur and oxygen) have been confined to the region where Fe, in Fe-based binary alloys (1 or 5% Al and 1 and 5% Cr), acts as a noble metal, the rates of internal penetration have been determined. Permeability products at 1200 K were 3.3×10^{-12} and 5.4×10^{-12} cm^2/sec for oxygen and sulfur respectively in Fe-Al alloys, and 1.1×10^{-11} cm^2/sec for oxygen and sulfur combined. Sulfur permeabilities in the Fe-Cr system were in the range $2.7-2.9 \times 10^{-12}$ cm^2/sec.

The morphologies exhibited by the internal precipitates, sulfides and oxides, were a complex function of alloy content, temperature and gas composition. In Al-containing systems the sulfide precipitates adopted a strongly oriented acicular shape, whilst in Cr-containing systems, the precipitates were approximately spherical. Growth morphologies were analyzed in terms of existing theories relating to the fluxes of solute and oxidant at the precipitation front.

* * *

†Brief version of LBL-12785.

5. PEG FORMATION BY SHORT CIRCUIT DIFFUSION IN Al_2O_3 SCALES CONTAINING OXIDE DISPERSIONS†

Haroun Hindam and David P. Whittle

The formation of inwardly growing protrusions (pegs) of Al_2O_3, which mechanically key the scale to the substrate, are mainly responsible for the improved scale ahesion in Al_2O_3-forming alloys and coatings containing Hf, Y, Ce, other active elements, or oxide dispersions. Our earlier interpretations of peg formation in Hf-containing alloys have implicitly suggested that Al_2O_3 grow inward in the alloy encapsulating the internal HfO_2 particles via preferential oxygen diffusion along the precipitate/alloy interface.

More recent observations reveal that the HfO_2 particles included in the scale themselves act as short circuit paths for inward oxygen transport, leading to localized scale thickening in the neighbourhood of these particles. Figure 1 demonstrates that the scale thickness measured parallel to the local growth direction at random positions, as shown in the inset, increases linearly with increasing thickness of the HfO_2 precipitates.

The model implies that differences in transport rates through the oxide of the active element and the host scale should be critical. Accordingly, the following generalizations can be made. Al_2O_3 grows very slowly and almost any addition might be expected to increase its local growth rate. This is not the case for Cr_2O_3 scales, which may well explain why active element additions to Cr_2O_3-forming alloys do not generally lead to appreciable oxide peg development although some improvement in adhesion is usually observed.

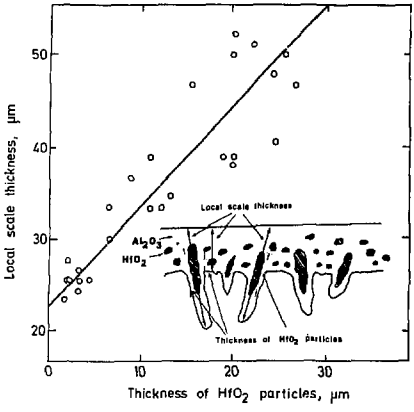

* * *

†Brief version of LBL-13640, submitted to J. Electrochem. Soc.

Fig. 1. Local Al_2O_3 scale thickness as a function of the thickness of HfO_2 particles: Fe-10 Al-1Hf oxidized at 1200°C for 300 hr.

(XBL 8111-12347)

---

6. FRACTURE ASPECTS OF OXIDE SCALES SUBJECTED TO MICROINDENTATION†

Haroun Hindam and David P. Whittle

In the previous report, a short-circuit diffusion model was evoked to account for the formation of inwardly growing pegs that were purported to improve the adhesion between surface scale and substrate. A similar effect can be achieved by internal oxidation, in which the oxide of the addition element precipitated within the alloy constitutes the peg. This report is concerned with the application of a micro-indentation technique to assess quantitatively the adhesion strength imported by such additions and the microstructural aspects of scale fracture.

Two systems were considered: FeAlHf, and NiHf alloys oxidized in air at 1200°C. Unlike FeAlHf oxidation, oxidation of Ni-2 wt% Hf alloy gives rise to internal rod-like, continuous precipitates, which have a composition (Hf_3NiO) different from the outer scale (NiO). Figure 1 is a typical example depicting the development of cracks in the vicinity of indentations formed at successively larger loads in the scale and at the scale/alloy interface. The pegs are not discernible in this conventionally prepared sample, but are readily revealed by deep etching.

The salient fracture characteristics that are revealed by this technique are: flaw initation and propagation at a much smaller load within the scale that at the tortuous interface due to the blocking effect of the Hf-depleted alloy phase adjoining the pegs in this location; anisotropic crack propagation in a direction approximately parallel to the interface, inferring asymetrical stress distribution, and crack deflection at small loads by matrix discontinuities, e.g., grain boundaries and second phase particles.

* * *

†Brief version of paper presented at the 34th Pacific Coast Regional Meeting of the American Ceramic Society, Newport Beach, CA, October 1981.

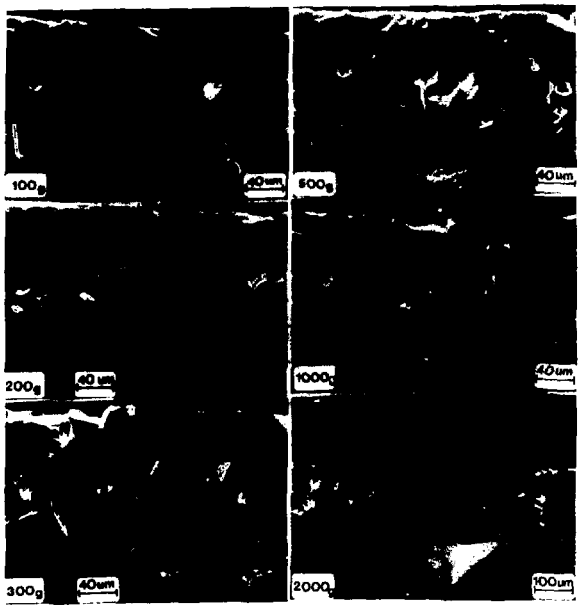

Fig. 1. Microhardness identations at increasing loads in the oxide scale formed on Ni-2Hf alloy. (XBB 810-9981)

7. ENHANCED DIFFUSION OF OXYGEN DURING INTERNAL OXIDATION†‡

David P. Whittle, Yoishi Shida,§ Graham C. Wood,‖ F. Howard Stott‖ and Brian D. Bastow¶

The classical model of internal oxidation has generally been successful in describing the internal oxidation behavior of a wide range of dilute alloys, in which the solute metal forms a more stable oxide than the solvent metal, and in which oxygen has appreciable solubility and diffusivity. However, in contradiction to the model, the rate of internal oxidation of dilute Ni-Cr and Ni-Al at temperatures in the range 800 to 1100°C was found to be virtually independent of solute content, and this has now been interpreted in terms of a model for enhanced oxygen diffusion.

The basic thesis of the model is that oxygen diffusion within the internal oxidation zone is enhanced along the incoherent interfaces between oxide particles and matrix. Unlike at high temperatures, there is no contribution by Al diffusion. As a result, the ratio of "apparent" oxygen permeability to that in pure Ni is a linear function of mole fraction

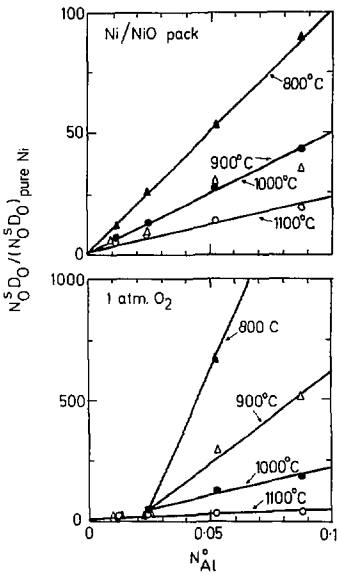

Fig. 1. Apparent permeability product for Ni-Al alloys oxidized in Ni/NiO packs and 1 atm. O_2 as a function of alloy Al content.

(XBL 8110-11838)

$$\frac{(N_O D_O)_{app}}{(N_O D_O)_{N_i}} = 1 + \left\{ \frac{D_{O,i}\,\delta_i}{D_{O,\ell}} \frac{2}{d} - 1 \right\} \frac{V_{ox}}{V_{all}} N_{BO_v}$$

of internal oxide (identical, under these conditions to the solute atomic fraction in the original alloy). This is shown in Fig. 1 for Ni-Al samples oxidized either in Ni/NiO packs (no external scale formation) or in 1 atm O_2. Ratios of interface ($\delta_i \approx 10$Å) to lattice diffusion coefficients of dissolved oxygen decrease from ~ 10^4 at 800°C to ~ 10^2 at 1100°C. Similar results are obtained for dilute Ni-Cr alloys.

* * *

†Brief version of LBL-13521, submitted to Philosophical Magazine A.

‡This work was carried out at the Corrosion and Protection Center, University of Manchester Institute of Science and Technology, and the authors are grateful to Sumito Metals Industry, Japan for support.

§Central Research Laboratories, Sumito Metals Industries Ltd, Amagaski, Japan.

‖Corrosion and Protection Center, U.M.I.S.T., Manchester, England.

¶British Nuclear Fuels, Seascale, Cumbria, England.

8. GROWTH MECHANISM OF INTERNAL Al_2O_3 PRECIPITATES IN DILUTE Ni-Al ALLOYS AND THE ROLE OF REACTIVE ELEMENTS†

Haroun Hindam and David P. Whittle

The preceding study has indicated that the growth of Al_2O_3 internal precipitates in dilute NiAl alloys is controlled by oxygen diffusion and that the relative contribution of boundary diffusion diminishes rapidly as the temperature is raised from 800 to 1100°C. In order to corroborate the validity of this finding at higher temperature and its possible effect on the reaction mechanism, a detailed examination of the microstructure and distribution of the precipitates formed at 1200°C was undertaken using a deep-etching sample preparation technique. Variation in the alloy composition (up to 4 wt% Al), and addition of small amounts of reactive elements (Ta and Hf) were both effective in controlling precipitate morphology.

The advance of the precipitation zone in the pure alloys followed parabolic relationships at a decreasing rate with Al alloy content. The presence of reactive elements added to a ~2 wt% Al alloy did not affect the growth rate significantly.

The structure and density of the precipitates varied markedly in all alloys as shown in Fig. 1. Al_2O_3 grew as polyhedral crystallites in preponderance to a plate like structure in a Ni-0.5 Al alloy; while Al_2O_3 extended as continuous rods in Ni-2 and Ni-4 Al alloys. Distinct rectangular

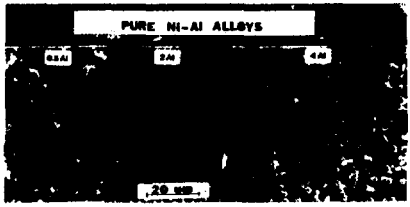

Fig. 1. Deep-etched, transverse sections of internally oxidized Ni-Al alloys.

(X88 810-9928)

platelets were observed in the reactive element containing alloys.

Al depletion in the alloy ahead of the precipitation front and an equivalent enrichment in the reaction zone suggested that at this temperature the growth of the precipitates is controlled by simultaneous outward Al and inward oxygen diffusion. Accordingly, the oxygen permeability product can be calculated, 1.1×10^{10} cm^2/sec; it is independent of alloy composition or the presence of reactive elements. This finding coupled with the conspicuous difference in the distribution of the precipitates, and hence the interfacial boundaries, confirms that these interfaces are ineffective for oxygen transport above about 1100°C.

* * *

†Brief version of paper presented at the 34th Pacific Coast Regional Meeting of the American Ceramic Society, October 1981.

9. INTERDIFFUSION IN THE Fe-Al SYSTEM†

Hilary C. Akuezue and David P. Whittle

Previous studies have shown a strong dependence of the interdiffusion coefficient on composition in binary Fe-Al alloys. This study has been undertaken to examine this dependency and to provide a basis for later studies of diffusion in multicomponent Fe-base systems containing Al.

Al was diffused into pure Fe samples from an aluminizing pack of Al_2O_3, Fe-50% Al and NH_4Cl(activator) powder mixtures. Values of $\tilde{D}$ which were obtained from the measured concentration profiles, were varied by about an order of magnitude over the composition range 0-50 at Al. The activation energy for D decreased to a minimum at about 23 at% Al and attained local maxima at about 31 and 38 at% Al. Two other minima occur at about 35 and 43 at% Al.

Now that the baseline for Al diffusion in the binary alloy system has been established, work is in progress to determine the diffusion coefficients in appropriate ternary Al-containing systems.

* * *

†Brief version of LBL-13548, submitted to Metal Science Journal.

1981 PUBLICATIONS AND REPORTS

Refereed Journals

1. D. P. Whittle, F. Gesmundo, B. D. Bastow, and G. C. Wood, "Formation of Subscales of Varying Composition," Phil. Mag. A44, 43-62 (1981); LBL-10067.

2. O. T. Goncel, D. P. Whittle, and J. Stringer, "The Oxidation Behavior of Fe-Cr Alloys Containing HfO_2-dispersed Phase," Oxidation of Metals 15, 287-296 (1981).

3. D. P. Whittle, F. Gesmundo, and F. Viani, "Parabolic Growth of Solid Solution Scales; Semi-empirical Approach," Oxidation of Metals 16, 81-98 (1981); LBL-11735.

4. D. P. Whittle, F. Gesmundo, B. D. Bastow, and G. C. Wood, "Formation of Solid Solution Oxides During Internal Oxidation," Oxidation of Metals 16, 159-174 (1981); LBL-11496.

5. G. W. Roper and D. P. Whittle, "Interdiffusion in Two-phase Ternary Solid Solutions," Met. Sci. J. (April 1981) 148-153; LBL-11689.

6. Y. Shida, G. C. Wood, F. H. Stott, D. P. Whittle, and B. D. Bastow, "Intergranular Oxidation and Internal Void Formation in Ni-40% Cr Alloys," Corrosion Science 21, 581-597 (1981).

7. F. H. Stott, G. C. Wood, Y. Shida, D. P. Whittle, and B. D. Bastow, "Development of Internal and Intergranular Oxides in Ni-Cr-Al Alloys at High Temperature, " Corrosion Science 21, 599-624 (1981).

8. B. D. Bastow, D. P. Whittle, and G. C. Wood, "Morphologies of Uniform Adherent Scales on Binary Alloys," Oxidation of Metals 16, 1-28 (1981); LBL-13364.

9. R. A. Rapp, J. H. Devan, D. L. Douglass, P. C. Nordine, F. S. Pettit and D. P. Whittle, "High Temperature Corrosion in Energy Systems," J. Mat. Engng. 50, 1-17 (1981).

Other Publications

1. D. P. Whittle, M. E. El Dahshan, and A. V. Levy, "Corrosion of Materials in In-situ Oil Shale Retorting Environments," Proc. 8th Int. Congress on Metallic Corrosion VI. II, Frankfurt, 1981, publ. by DECHMA (1981) p. 1863.

2. J. Stringer, D. P. Whittle, I. G. Wright, V. Nagarajan and M. E. El Dahshan, "A Novel Method for Designing SiO_2-Forming Alloys," Proc. 8th Int. Congress on Metallic Corrosion, Frankfurt, 1981, publ. by DECHEMA (1981) pp. 655-661.

3. D. P. Whittle and D. H. Boone, "Oxidation Characteristics of CoCrAl Type Protective

Coatings," Proc. 8th Int. Congress on Metallic Corrosion, Vol. I, Frankfurt, 1981; publ. by DECHEMA (1981) pp. 718-723.

4. D. P. Whittle and D. H. Boone, "Alumina Scale Adherence to CoCrAl Alloys and Coatings," Proc. Int. Ceramics Conf. on Surfaces and Interfaces in Ceramic and Ceramic-Metal Systems, Berkeley, Calif. (1980); ed. J. Pask and A. G. Evans, Plenum Press (1981) 487-502; LBL-12421.

LBL Reports

1. H. Hindam and D. P. Whittle, "Corrosion Behavior of Cr_2O_3-Former Alloys in H_2-H_2S-H_2O Atmospheres," LBL-12052.

2. D. P. Whittle, "Oxidation Mechanisms for Alloys in Single Oxidant Gases," LBL-12614.

3. P. J. Risse, "Internal Oxidation and Sulfidation of Iron Based Binary Alloys," (M. S. thesis) LBL-12785.

4. A. V. Malik and D. P. Whittle, "Oxidation of Fe-C Alloys in the Temperature Range 600-850°C," LBL-12804.

5. F. Yang, "High Temperature Corrosion of Iron in Sulfur Containing Atmospheres," (M. S. thesis) LBL-12851.

6. D. P. Whittle and D. H. Boone, "Interactions between Coatings and Substrates at Elevated Temperatures," LBL-13350.

7. D. P. Whittle, Y. Shida, G. C. Wood, F. H. Stott, and B. D. Bastow, "Enhanced Diffusion of Oxygen During Internal Oxidation of Nickel-Base Alloys," LBL-13521.

8. H. C. Akuezue and D. P. Whittle, "Interdiffusion in the Fe-Al System: Aluminizing," LBL-13548.

9. A. K. Misra, D. P. Whittle and W. L. Worrell, "Thermodynamics of Na_2SO_4-Induced Hot Corrosion," LBL-13561.

10. H. Hindam and D. P. Whittle, "Peg Formation by Short Circuit Diffusion in AL_2O_3 Scales Containing Oxide Dispersions," LBL-13640.

Invited Talks

1. D. P. Whittle, D. H. Boone, and S. Shaffer, "Oxidation Properties of CoCrAl-Based Coatings," Annual Meeting of AIME, Chicago, Illinois, February 1981.

2. D. H. Boone, D. P. Whittle and D. A. Crane, "The Surface Structure of Superalloy Aluminide Coatings," Annual Meeting of AIME, Chicago, Illinois, February 1981.

3. D. P. Whittle, "Oxidation Mechanisms for Alloys in Single Oxidant Gases," (Plenary Lecture) International Conference on High Temperature Corrosion, NACE, San Diego, CA, March 1981.

4. D. H. Boone, D. A. Crane, and D. P. Whittle, "Oxide Structure on Aluminide Coatings," International Conference on Metallurgical Coatings, San Francisco, CA, April 1981.

5. D. H. Boone, D. A. Crane, and D. P. Whittle, "The Structure and Interdiffusional Degradation of Aluminide Coatings on Oxide Dispersion Strengthened Alloys," International Conference on Metallurgical Coatings, San Francisco, CA, April 1981.

6. D. P. Whittle, S. Shaffer, and D. H. Boone, "Relationships Between Oxide Morphology and Coating Structure," International Conference on Metallurgical Coatings, San Francisco, CA, April 1981.

7. D. P. Whittle, I. G. Wright, and J. W. Fairbanks, "Needs in High Temperature Coatings Research and Education," International Conference on Metallurgical Coatings, San Francisco, CA, April 1981.

8. J. Maasberg, D. H. Boone, D. P. Whittle, and A. V. Levy, "Erosion Resistance of CoCrAl-Coatings Containing Active Element Additions," International Conference on Metallurgical Coatings, San Francisco, CA, April 1981.

9. D. P. Whittle, "Parabolic Growth of Oxides Solid Solutions," Bay Area High Temperature Science and Technology Meeting, U. C. Davis, April 1981.

10. D. P. Whittle and H. Hindam, "Corrosion Behavior of Cr_2O_3 Forming Alloys in H_2-H_2O-H_2S Atmospheres," Corrosion '81 NACE, Toronto, Canada, April 1981.

11. D. P. Whittle, "Quantitative Understanding of Growth of Solid Solutions Scales and Alloys," Gordon Research Conference on Corrosion, New London, NH, July 1981.

12. D. P. Whittle and D. H. Boone, "Interactions Between Coatings and Substrates at Elevated Temperatures," Second Conference on Advanced Materials for Alternative Fuel Capable Heat Engines, Monterey, CA, August 1981.

13. D. P. Whittle and D. H. Boone, "Oxidation Characteristics CoCrAl-Type Protective Coatings," 8th International Congress on Metallic Corrosion, Mainz, West Germany, September 1981.

14. J. Stringer, D. P. Whittle, I. G. Wright, V. Nagarajan, and M. E. El Dahshan, "A Noble Method for Designing SiO_2-Forming Alloys," 8th International Congress on Metallic Corrosion, Mainz, West Germany, September 1981.

15. D. P. Whittle, M. E. El Dahshan, and A. V. Levy, "Corrosion of Materials in In-Situ Oil Shale Environments," 8th International Congress on Metallic Corrosion, Mainz, West Germany, September 1981.

16. D. P. Whittle, "Al_2O_3 and Cr_2O_3 Scale Formation Adherence on Alloys and Coatings," (Keynote Lecture) 22nd Corrosion Science Symposium, Newcastle, England, September 1981.

17. H. Hindam and D. P. Whittle, "Growth Mechanism of Internal Al_2O_3 Precipitates In Dilute Nickel Aluminum Alloys and the Role of Reactive Elements," 34th Pacific Coast Regional Meeting of the American Ceramic Society, Newport Beach, CA, October 1981.

18. D. P. Whittle, H. Hindam, and S. Shaffer, "Modifications of the Al_2O_3 Substrate Interface to Improve Oxide Scale Adherence," 34th Pacific Coast Regional Meeting of the American Ceramic Society, Newport Beach, CA, October 1981.

f. Refractories Project: Processing*

Lutgard C. De Jonghe, Investigator

PRE-EUTECTIC DENSIFICATIONS IN REACTIVE POWDERS

Refractories are typically prepared by reactive sintering of a number of component oxides. In such materials, it is desirable to control microstructure, porosity, phase distribution, and phase composition to within specified requirements. During the fabrication of such ceramics [illegible] or reactive liquid phases usually are [illegible] and play an important role in the final pore and phase distribution. These pore and phase distributions, as well as the microstructural aspects of the dense parts of the ceramic, will largely determine the high temperature chemical stability and mechanical properties. The first step in the understanding of the sintering of chemically reactive powders is the study of the pre-eutectic densification processes. Such pre-eutectic densification processes were studied on the model system magnesium fluoride-calcium fluoride. This system has a eutectic at 980°C and its components have limited mutual solubility. Dilatometric studies can therefore be conducted below 1,000°C. Of particular significance were the pre-eutectic densification rates, as well as the associated grain growth phenomena that occurred during this densification.

Powder mixtures of magnesium fluoride with small additions of calcium fluoride were prepared and pressed to a standard 55% of the theoretical density. The specimens were sintered by three different methods: (1) arrested zone sintering, (2) constant heating rate sintering, and (3) constant temperature sintering. The arrested zone sintering was developed by De Jonghe and Goo.[1] The microstructural evolution and local shrinkage could be examined for long samples that were partially fed into the hot zone of a furnace kept at some fixed temperature. Shrinkage rates were determined as a function of time and temperature in the constant heating rate and constant temperature sintering experiments. The grain sizes were determined from etched and polished sections of samples. An example of some of the dilatometric data on the constant heating rate densification of four different powders is shown in Fig. 1, together with the observed grain sizes that were found for samples quickly withdrawn from the furnace at the indicated temperature. The heating rate in these experiments was 4.5°C/min.

As Fig. 1 demonstrates, enhanced densification below the eutectic temperature is observed for the magnesium fluoride containing the eutectic additive calcium fluoride. Enhanced densification begins as much as 200°C below the eutectic temperature. The effect appears to saturate at 1 wt% of calcium fluoride. Interestingly, the grain size still

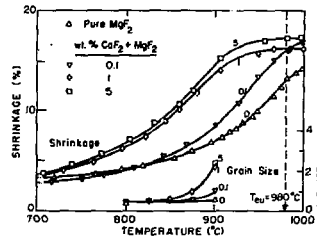

Fig. 1. Shrinkage and grain size vs. temperature for MgF_2 with 0, 0.1, 1 and 5 wt% CaF_2 eutectic forming additive. The heating rates were constant at 4.5°C/min. in these experiments.

(XBL 814-5598)

remains fairly low although there is a significant increase in the densification rates. For the 1 and the 5 weight % calcium fluoride containing powders, the maximum densification rate was about 100°C below the eutectic temperature. Calculations of the densification rates, based on interdiffusion data obtained from a calcium fluoride-magnesium fluoride interdiffusion experiment, showed that the enhanced pre-eutectic densification had to be due to a significantly enhanced grain boundary transport. Scanning auger microscopy of intergranularly fractured samples also showed significantly enhanced calcium concentrations at the grain boundaries. The experiments thus demonstrated the significance of grain boundary processes in pre-eutectic densification of chemically reactive powders. Future research is concerned with the calcium oxide-aluminum oxide system which is the basis for a large class of practical refractories.

* * *

1. L. C. De Jonghe and E. Goo, Processing of Crystalline Ceramics, Eds. H. Palmour III, R. F. Davis and T. Hare, Eds., Plenum Press, 1978, p. 433.

1981 PUBLICATIONS AND REPORTS

1. S. C. Hu, "Pre Eutectic Densification in MgF_2-CaF_2, MS thesis, LBL 12849, May, 1981.

*This work was supported by the Director, Office of Energy Research, Office of Basic Energy Sciences, Materials Science Division of the U. S. Department of Energy under Contract No. DE-AC03-76SF00098.

g. Erosion of Brittle Solids*

A. G. Evans, Investigator

Introduction. This erosion program was initiated in 1981. The intent of the program is to develop a fundamental comprehension of the erosion and coupled erosion/corrosion of brittle surfaces, with emphasis on high temperature material removal. The study will involve the observation and analysis of the impact damage and erosion mechanisms pertinent to homogeneous ceramics and glasses and to oxide films on metallic and ceramic alloys. The relatively comprehensive understanding of material removal by lateral cracking--used to predict the dependence of the ambient temperature erosion of brittle materials on the fracture toughness, hardness and elastic modulus--will provide an established background for the proposed study.

Studies of the analogous processes of the machining and wear of brittle surfaces will be used to provide additional insights, as required. Complementary studies of the adhesion of thin films, using indentation techniques, will also provide a more informed basis for the analysis of the erosion process.

Previous studies of surface damage in ceramics have identified a fracture threshold that dictates a transition from a modest to a rapid material removal rate. The dependence of this fracture threshold on material properties has yet to be adequately elucidated. Threshold studies will constitute a major theme of the current program.

1. WORK IN PROGRESS

Recent studies of matching rates in brittle solids have suggested the existence of a subsurface damage zone that dictates the machining forces. The damage zone probably depends on the fracture toughness, hardness and modulus of the material, as well as specific microstructural characteristics, such as the grain size. Methods for studying this damage zone, using scanning and transmission electron microscopy, are being devised. The results of this study will assist in the comprehension of the machining process and will establish the basis for examining the important details of high temperature erosion. Information concerning the fracture threshold will also emerge from these studies.

An apparatus for studying high temperature damage mechanisms induced by the impact of single, angular projectiles is being constructed. This apparatus will permit the in-situ development of oxide layers on ceramic and metal alloys, prior to projectile impact (over a range of velocities). Sectioning methods will then be used to characterize the damage and hence, to define the mechanisms of high temperature material removal.

*This work was supported by the Director, Office of Energy Research, Office of Basic Energy Sciences, Materials Sciences Division of the U.S. Department of Energy under Contract No. DE-AC03-76SF00098.

h. Chemical Degradation of Refractories*

David P. Whittle, Investigator

Introduction. The extremely aggressive environments that exist within the reaction chambers of most coal conversion processes and the requirement to keep heat losses to a minimum, demand that the vessels be refractory-lined. The result is that the ceramic materials are exposed to the combined action of gaseous or liquid phase attack at temperatures as high as 1500°C. The objective of this project is to establish the scientific principles of chemical interactions under conditions relevant to advanced coal technology systems. Of particular significance is the role of the intergranular phases and the presence of substantial porosity.

Two aspects of corrosive attack are being investigated. The first concerns degradation induced by gaseous environments of low oxygen potential but containing sulfur impurities. The second aspect is related to the influence of liquid slags, which originate from coal ash, on the corrosion process. The program only started in August 1981, and is thus in the early stages of development.

1. HIGH TEMPERATURE DEGRADATION OF REFRACTORIES IN MIXED GAS ENVIRONMENTS

Stephen Smith and David P. Whittle

A refractory system that is showing great promise is the aluminum oxide - calcium oxide system. Its use may take many forms, from dense Al_2O_3, where CaO appears as an impurity to highly porous calcium aluminate bonded alumina refractories. In all cases, calcium aluminate phases are present intergranularly. Initially, this work is concentrating on the behavior of Al_2O_3 containing up to 10% CaO and samples showing varying degrees of porosity have been prepared by hot pressing. The samples will be exposed to H_2-H_2O-H_2S mixtures of controlled sulfur and oxygen fugacities at temperatures in the range 1000-1400°C. The construction of the high temperature exposure facility is now completed; metered flows of H_2 and H_2S are mixed and saturated with the required amount of H_2O by passing through a water bath maintained at the appropriate constant temperature.

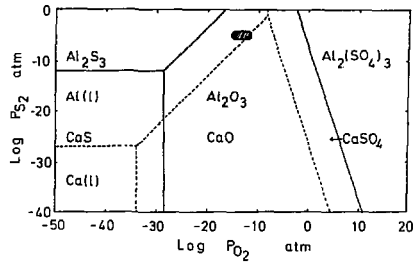

Fig. 1. Phase stability diagrams for the Al-S-O and Ca-S-O systems at 1200°C; the shaded area shows the range of experimental gas composition. (XBL 822-7788)

Figure 1 indicates the ranges of sulfur and oxygen fugacities to be used. These are superimposed on the Al-O-S and Ca-O-S phase stability diagrams at 1200°C, which have been calculated from available thermodynamic data. The diagram was constructed assuming unit activities of all condensed phases, and thus, can only be considered as approximate. The program predicts that the probable reactions between the refractories and the mixed gas environment will involve the calcium containing phases. Therefore, of particular interest will be the behavior of the grain boundary and intergranular phases, in which the formation of sulfides seems likely. Equally important is the presence of porosity since localized variations in gas composition in stagnant pockets of gas may occur, resulting in behavioral patterns not immediately apparent from the stability diagrams. Similar changes in gas composition are observed during metallic corrosion in these environments, and programs have been devised to compute the change in the gaseous activities due to the removal of one or other of the components.

*This work was supported by the Director, Office of Energy Research, Office of Basic Energy Sciences, Materials Sciences Division of the U.S. Department of Energy under Contract No. DE-AC03-76SF00098.

I. Ceramic Interfaces*

Andreas M. Glaeser, Investigator

Introduction. Numerous properties of ceramics are strongly dependent upon the nature of the microstructure. Consequently successful fabrication of ceramics that meet design requirements necessitates that the characteristics of the microstructure (grain size, pore size, etc.) that develop during processing and/or high temperature applications be controlled. The grain size and other microstructural characteristics are directly or indirectly affected by the rate of grain boundary motion. Thus control of microstructural development requires that the rate of grain boundary migration be controlled. The focus of this program is to investigate and further our understanding of the factors that influence or control the nature of the boundary migration process.

Values of the grain boundary mobility (defined as the boundary velocity per unit driving force) extracted from several grain growth studies of a particular ceramic material, Al_2O_3 being just one example, often differ by orders of magnitude at a particular temperature. These mobility differences have been attributed to differences in the extent to which interactions between the grain boundary and solutes, pores, precipitates, etc., influence the boundary migration rate. However, an experimental technique, easily applicable to high temperature oxides, that would permit the drag forces due to these interactions or the effect of a particular variable (driving force, solute content, etc.) on the migration rate to be isolated and systematically investigated was lacking. Consequently, the nature of these interactions and their effects on microstructure development are poorly understood. An experimental technique permitting these interactions to be studied was developed, and an investigation of the migration behavior of individual grain boundaries in Mg-doped Al_2O_3 is in progress.

1. TECHNIQUE FOR MEASURING GRAIN BOUNDARY MOBILITY AND ITS APPLICATION TO Mg-DOPED Al_2O_3†

Andreas M. Glaeser and Jiin-Chau Chen

When a sufficiently large grain develops in a fine-grained matrix, abnormal grain growth occurs. The large grain grows at a substantially higher rate than the matrix grains, and thus consumes the approximately constant size fine-grained matrix. Monitoring the growth rate of the large grain is an ideal means of investigating grain boundary migration, since by systematically varying one of the characteristics of the matrix at a time, such as the grain size, solute content, or volume fraction porosity, the effect of driving force, solutes, or pores on boundary migration rates can be isolated and studied. The difficulty in the past has been the inability to introduce large grains into a fine-grained matrix in a simple and controlled manner.

In the present work, a small region of a pore-free find-grained Al_2O_3 sample has been melted by using a laser as a heat source. During solidification, a coarse-grained region bounded by (unmelted) fine-grained matrix is produced. Thus, the technique permits large grains to be introduced into a fine-grained matrix and abnormal grain growth to be "seeded." The characteristics of the matrix can be adjusted by changes in the processing procedures and appropriate heat treatment prior to the laser melting. In principle, the technique is applicable to a wide variety of materials.

Growth rates of laser-introduced abnormal grains, naturally occurring abnormal grains, and the fine grained matrix grains at 1600°C in Mg-doped Al_2O_3, were measured and grain boundary mobilities for each type of grain determined (Table 1). The growth rates of both types of ab-

Table 1. Grain boundary mobility ($M^3/N\text{-}s$) at 1600°C

Abnormal grains	Laser nucleated 7×10^{-13} (max)	Naturally nucleated 4×10^{-13} (max.)
Normal grains	Fine grained matrix 2×10^{-13} (average)	

*This work was supported by the Director, Office of Energy Research, Office of Basic Energy Sciences, Materials Sciences Division of the U.S. Department of Energy under Contract No. DE-AC03-76SF00098.

normal grains were spatially nonuniform; minimum growth rates and hence minimum boundary mobilities could not be measured. However, the maximum mobilities and other aspects of the migration behavior of the two types of abnormal grains are similar, suggesting little if any effect of the laser melting on the subsequent behavior. Further, the maximum mobilities of the abnormal grains are comparable in magnitude to the "average" mobility of the matrix grains (estimated from the matrix grain growth rate). Measurements of the temperature dependence of the grain boundary mobility are in progress.

* * *

†Brief version of LBL-13800.

1981 PUBLICATIONS AND REPORTS

Invited Talks

1. A. M. Glaeser, "Grain Growth in Ceramics," Pacific Coast Regional Meeting of the American Ceramic Society, Newport Beach, CA, October 25-28, 1981.

4. Engineering Materials

a. Abrasive, Erosive, and Sliding Wear of Materials*

Iain Finnie, Investigator

Introduction. Traditionally, wear has been studied by empirical tests designed to simulate the behavior of specific components. Unfortunately, the information gained in this manner is of limited value in understanding the basic mechanisms of wear or in predicting the wear to be expected in new applications. Because of the enormous economic importance of wear, the purpose of the present work is to obtain a more detailed understanding of wear mechanisms. In the period covered by this report, attention has been focused on sliding wear of dissimilar metals and abrasive wear.

The traditional approach to explaining sliding wear was based on adhesion. This has become questioned in recent years. After reviewing recent work in this field we have concluded that the accumulation of plastic deformation below the surface followed by crack propagation and final separation is the principal source of sliding wear. Based on this review, a mechanical test to simulate sliding wear has been developed and some encouraging correlations have been obtained.

Our work on wear of metals by hard abrasive particles has shown that present knowledge can predict wear rates, at best, within an order of magnitude. Work is underway to study the reasons for this discrepancy. We have also conducted high temperature abrasive wear tests for the first time and have found that the usual correlation of resistance to abrasive wear against indentation hardness is not applicable.

1. SIMULATION OF SLIDING WEAR BY PLASTIC DEFORMATION UNDER COMBINED STRESS†

Iain Finnie, Susan Chavez, and Remy Glardon‡

Research over the past decade has led to a better understanding of sliding wear mechanisms. It is now fairly well established that the cyclic accumulation of plastic deformation in the subsurface and the nucleation and propagation of cracks in this highly deformed layer play an essential role in the generation of wear debris. However, despite this improved understanding at a phenomenological level, the quantitative relation between wear behavior and mechanical properties is still unclear.

One of the main reasons for this lack of correlation between wear and conventional mechanical tests is that microstructural features are developed during wear that are completely different from those produced in conventional mechanical tests. In our program a test fixture has been developed to simulate sliding wear by testing specimens under combined cyclic compression and shear loading. Accompanying these tests, the wear rate and microstructural features of a number of Cu-Zu alloys have been studied.

Based on the cyclic deformation tests, it appears that three material parameters are needed to describe sliding wear resistance. One of these was predicted to determine the depth of the highly deformed layer in wear tests. Experiments show an encouraging agreement with this hypothesis.

* * *

† (a) A Review of the Recent Literature on Unlubricated Sliding Wear of Dissimilar Metals, J. Eng. Materials and Technology, 103, 333, 1981.
(b) The Simulation of Sliding Wear by Cyclic Plastic Deformation Under Combined Stress, LBL-14052.

‡Present address: Mettler Instrumente A.G. 8605 Greifensee, Switzerland.

2. ABRASIVE WEAR

Iain Finnie and S. Soemantri

Abrasive wear has been estimated to include about 50% of the wear problems in industry. Considerable attention has been devoted to the type of abrasive wear in which the abrading grains are fixed as in abrasive paper (two-body wear). Much less attention has been given to the problem of loose abrasive grains (three-body wear) which occurs more often in practice.

In previous work supported by DOE contracts on campus a special tester for three-body wear was designed. A large amount of testing was carried out and was summarized in a survey article.[1] In recent work we have taken two approaches. One is to attempt to apply current knowledge for wear prediction at ambient temperature, the other is to carry out a high temperature three-body wear test to simulate the conditions which may arise in existing and new industrial processes.

Existing predictive methods were found to be very limited. Even with a great deal of information available on the abrasive material and test conditions, wear predictions within an order of magnitude are the best that can be expected. Work is continuing to improve this prediction. The

*This work was partially supported, since October 1, 1981, by the Director, Office of Energy Research, Office of Basic Energy Sciences, Materials Science Division of the U.S. Department of Energy under Contract No. DE-AC03-76SF00098.

high temperature abrasive wear behavior observed with titanium, aluminum and copper showed no correlation with existing explanations of abrasive wear. We are attempting to use these results to guide the development of improved analysis.

* * *

1. A Review of the Abrasive Wear of Metals, to be published in J. Eng. Materials and Technology.

3. WORK IN PROGRESS

We will study the microstructure of the mechanical test specimens and make comparisons with the deformed layer in sliding wear. Our testing has been confined to Cu-Zu alloys, nickel and bronze. It needs to be shown that the correlations developed apply to a wider range of alloys.

Attempts to develop a better model for the mechanisms of material removal in abrasive wear of ductile metals are continuing. Throughout this work we are attempting to relate abrasive and erosive wear so that one type of wear test may be used to rank materials for their resistance to other types of wear.

1981 PUBLICATIONS AND REPORTS

Refereed Journals

1. I. Finnie and A. Misra, "On the Size Effect in Abrasive and Erosive Wear," Wear 65, 359-373 (1981).

2. I. Finnie and A. Misra, "Correlations Between Two-Body and Three-Body Abrasion and Erosion of Metals," Wear 68, 33-39 (1981).

3. I. Finnie, "Some Observations on Two-Body Abrasive Wear," Wear 68, 41-56 (1981).

4. I. Finnie and A. Misra, "An Experimental Study of Three-Body Abrasive Wear," Wear of Materials 1981, (edited by S. K. Rhee et al.), ASME, New York, 1981.

5. I. Finnie and R. E. Glardon, "Some Observations on the Wear of Single Point Diamond Tools Used for Machining Glass," J. Mat. Sci., 16, 1776-1784 (1981).

6. I. Finnie and R. E. Glardon, "A Review of the Recent Literature on Unlubricated Sliding Wear of Dissimilar Metals," J. Eng. Mat. & Technology, 103, 333-340 (1981).

Invited Talks

1. Seminar, "The Mechanisms of Erosive Wear" delivered at American Society of Metals, Monterey, CA, annual seminar April 25, 1981. Also gave this seminar at California Institute of Technology May 5, 1981, and at SRI-International, Palo Alto, CA, May 18, 1981.

2. Seminar, "An Overview of Wear Mechanisms," IBM Research Lab., San Jose, CA, May 12, 1981.

b. Erosion-Corrosion Wear Program*

Alan V. Levy, Investigator

Introduction. The degradation of materials subjected to streams of gases containing small solid particles, $\leq$ 600 μm, moving at velocities $\leq$ 90 m/s is being studied. The conversion of coal to clean, combustible gas and the direct combustion of pulverized coal in fluidized bed combustors subjects the materials containing these reactions to erosive forces. The mechanism of the erosion must be understood in order to prevent unacceptable degradation of the containment wall surfaces.

In 1981 several aspects of the erosive behavior of metals were investigated. The effect of the eroding particle characteristics on the erosion mechanism in ductile alloys was determined. The erosive behavior of hard metals was studied as was the effect of various strengthening heat treatments in low alloy steels. Erosion rates at elevated temperatures were determined for aluminum and steel alloys. An initial model of erosion embodying a mechanism of forging-extrusion of metal platelets was developed.

The corrosion of stainless steels whose surfaces were modified by doping with aqueous nitrate salts of active elements applied to the surface was determined. Modification of the reactivity of turbulent gases in curved pipes by injection of water vapor in the unstable boundary layer was studied.

1. THE EFFECT OF HEAT TREATMENT OF STEEL ON EROSION BEHAVIOR†

Tom Foley and Alan Levy

The use of heat treatments to tailor the engineering performance of alloys for various service environments is common. The effects of such heat treatments on the erosion of structural materials must be determined in order to design long life components for coal conversion and combustion systems. In earlier work, it was determined that plastic deformation of metals had a direct relationship to erosion resistance. The effects of various heat treatments on the nature of the flow of alloys and, hence, their erosion resistance was determined.

Plain carbon 1020 steel was tested in its pearlitic and spherodizied microstructures above and below its ductile brittle transition temperature; low alloy 4340 steel was tested in the as-quenched, 200°C and 500°C temper conditions and spheroidized annealed and 304 stainless steel was tested in the as-rolled and fully annealed conditions. The alloys were eroded by a stream of Al_2O_3 particles, 140 μm diam. average size at 30, 60, 90 m/s velocity at impingement angles of 30° and 90° in air at 25°C.

The erosion rates decreased with increasing elongation and increased with increasing hardness, further verifying earlier work in this project. The observed mechanism of erosion in all of the steels tested was the formation and removal of small platelets of metal by a forging-extrusion mechanism. The four 4340 steel heat treatments all showed approximately the same erosion rate. They had similar tensile elongations, but major differences in tensile strength and hardness indicating that these properties had little effect on erosion behavior. All of the alloys reached steady state erosion in 60 to 200 grams of impacting particles, indicating that erosion rates of steels can be determined in relatively short time tests.

The 304SS with the higher strain hardening coefficient (0.45) reached steady state erosion after 30 grams of particles while the 1020 steel with the lower strain hardening coefficient (0.15) reached steady state erosion after 100 grams of particles. This behavior supports the mechanism of erosion developed earlier - that a cold-worked region develops beneath the eroding surface that enhances the erosiveness of the impacting particles, behaving as an anvil in the forging-extrusion of platelets. Figure 1 shows this effect.

* * *

†Brief version of LBL-13745.

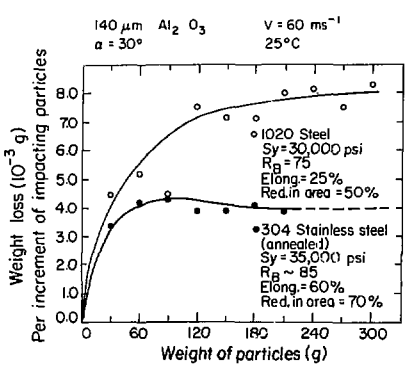

Fig. 1. Effect of strain hardening coefficient of 1020 steel and 304SS on onset of steady state erosion. (XBL 8110-1395)

*This work was supported by the Director, Office of Energy Research, Office of Basic Energy Sciences, Materials Sciences Division of the U.S. Department of Energy under Contract No. DE-AC03-76SF00098.

2. EROSION OF HARD METALS†

Tom Bakker and Alan Levy

The use of protective coatings on structural metals to enhance their wear and/or corrosion resistance has increased considerably in recent years. Many new coating systems and insert materials for critical areas of coal conversion valves, pumps and other components are now becoming available whose resistance to erosion by solid particles must be determined.

In this project several materials were tested that used the hard metals SiC, WC and Si_3N_4 with various binders and the oxide Cr_2O_3. The materials were fabricated into thin coatings by chemical vapor deposition (CVD), detonation gun spraying and plasma spraying on steel and graphite substrates or by hot pressing into solid bodies suitable for valve inserts. The materials were eroded by SiC particles, 200 μm diam, in an air stream at 30 m/s at 25°C. Impingement angles of 30°, 60° and 90° were used. Erosion rates and mechanisms of erosion were determined and related to the composition and microstructure of the hard metals.

The materials tested were basically hard metal particles bonded with either cobalt or silicon. They all eroded in a brittle manner, i.e., the erosion rate was greater at an impingement angle of 90° than at 30°. The rates of erosion of the materials varied over a wide range (Fig. 1). Comparative steady state erosion rates for steel alloys range from 0.5 to 2.0 g/g. The most erosion resistant material was CVD deposited CNTD silicon carbide bonded with silicon that had an extremely fine grain size, ~ 1000 Å diam. The grain size was so fine that the angle of impingement effect observed on all of the other materials tested and, generally, on all brittle materials was not in evidence.

The mechanism of erosion for all of the materials tested was microscopically observed to be cracking and chipping of micron size pieces of material. Hardness did not directly relate to erosion resistance, although the hardest material was CNTD SiC which had a DPH of 3266. The results support the conclusion from earlier work that a fine grain size and low level of porosity enhance erosion resistance of brittle materials. The rates of erosion of the materials reached steady state values after only a few grams of erodent at most had impacted them, also conforming to earlier studies of the erosion of brittle materials. The erosion rates of the hard metals in most cases exceeded those of low alloy and austenitic stainless steels.

* * *

†Brief version of LBL-13801.

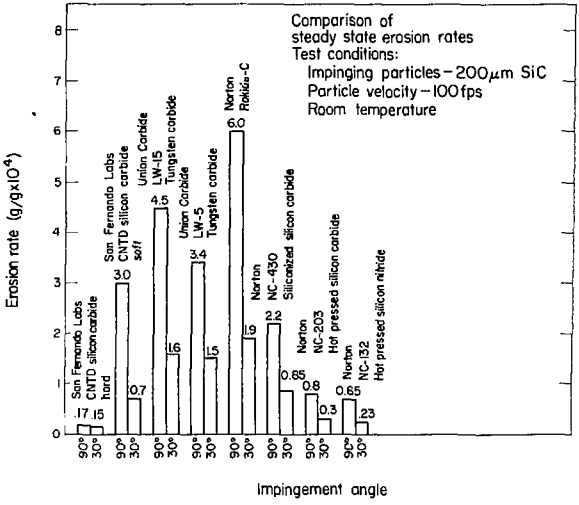

Fig. 1 Comparison of steady state erosion rates of hard metals.
(XBL 818-11438)

3. EFFECT OF PARTICLE VARIABLES ON EROSION OF DUCTILE METALS†

Pauline Chik and Alan Levy

The erosion of materials is dependent upon their erosion resistance and the erosion conditions. The effect of variations in the impacting particles on the erosion of ductile metals was investigated to determine how sensitive erosion was to this major variable. In actual service involving solid particle impact erosion, the particles are generally of mixed composition, size, shape and properties. Erosion testing in the laboratory usually uses single composition particles of a comparatively narrow range of sizes and shapes. Whether discrepancy should be of concern was determined in this project.

Five different minerals were obtained of an average particle size of 200 μm diam. They ranged in hardness from a VHN of 115 for calcite and 300 for apatite to 700 for SiO_2, 1900 for Al_2O_3 and 3000 for SiC. Steel shot of 200 μm diam, in both angular and spherical shapes was also used. All tests were made at 75 m/s and impingement angles of 30° and 90° at 25°C. Steady state erosion rates were determined and the mechanism of erosion was studied microscopically for a 1020 plain carbon steel target material.

Angular shaped particles above a minimum hardness of approximately VHN = 700 had the same erosivity on 1020 steel (Fig. 1). This is an important finding in that the test particles need not specifically duplicate particles in real environments, but only need be in their general hardness range if below VHN = 700 and can be at any hardness level if above VHN = 700. Thus, the highly reproducible SiC or Al_2O_3 particles will give usable erosion rates for actual service particles of hardness ranging from that of sand upward.

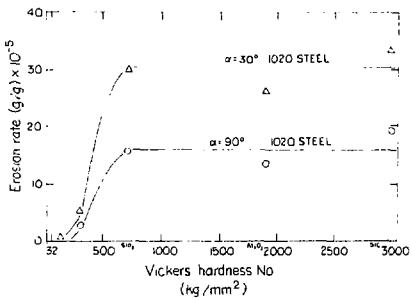

Fig. 1. Effect of eroding particle hardness/integrity on erosion behavior of 1020 steel. (XBL 8110-7180)

It was also determined that it was not the hardness, per se, that determined the erosivity of the particles, but rather their physical integrity. The softer minerals, calcite and apatite, fractured on impact and could not carry sufficient kinetic energy to the target surface to cause erosion at the higher rates of the stronger minerals. The angular steel shot eroded the 1020 steel at almost four times the rate of the spherical steel shot of nominally the same particle size.

* * *

†Brief version of LBL-13802.

4. ANALYTICAL MODEL OF EROSION BEHAVIOR OF DUCTILE METALS†

Jolen Flores and Alan Levy

Mounting evidence to support the concept of the erosion of ductile metals by a forging-extrusion mechanism has prompted the development of an analytical model based on that concept to predict erosion of structural alloys. The properties of a material that affect its plastic deformation and surface heating as the result of adiabatic shear deformation and friction must be incorporated into expressions that describe the generation of small platelets of target material. A statistical treatment is also required to account for the average number of impacts necessary to have platelets reach their fracture strain.

Forging equations were utilized and balanced with the energy available to the target material for plastic deformation and that which is used to generate local heating of the near-surface region. Additional kinetic energy for impacting particles is assigned to the subsurface cold working of the target material. The surface temperature during erosion is arrived at by balancing the heat generated by plastic deformation and friction with the heat loss due to convection between subsequent particle impacts. An impact angle of 90° was used.

An erosion model based on forging equations was developed and coupled with basic heat transfer equations. These were in turn coupled with a simple statistical analysis. The predicted erosion rates exhibit the same general profile when plotted against the number of eroding particles as observed experimentally. The temperatures developed on the surface fall within the range of the recrystallization temperature, as postulated from microscopic observation of the eroded surface.

* * *

†Brief verison of LBL-13803.

5. PREDICTION OF PARTICLE LADEN LIQUID TWO PHASE FLOW†

Farzad Pouramahdi and Joseph Humphrey

In order to fully understand the erosion of metals exposed to liquid-solid particle slurry streams, it is necessary to determine the fluid

mechanics of the two-phase flows. In addition to conducting experiments to determine the velocities and positions of the particles in turbulent flow through curved ducts it is important to develop a numerical calculation scheme for predicting such flows. The purpose of this investigation was to develop the model and, subsequently, to use it to predict two-phase flow in laser doppler velocimeter (LDV) monitored flow experiments.

A numerical calculation code, SPLATS (Solid Particles, Liquid and Turbulence Solver) has been developed for predicting turbulent two phase, solid particle-liquid flows in straight and curved two-dimensional channels. Predictions of the solid particle-liquid slurry flow characteristics of various documented cases in the literature show good agreement with the reported experimental results.

* * *

†Brief version of LBL-13808.

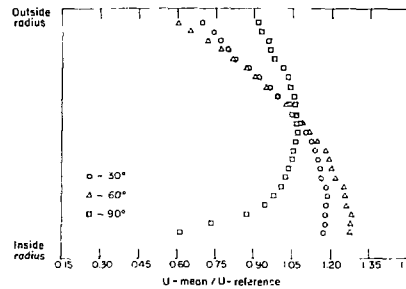

Fig. 1. Streamwise velocity profiles at various stations in a 90° bend. (XBL 8201-4404)

6. BOUNDARY LAYER CONTROL BY MEANS OF STRONG INJECTION†

Ruey-Jen Yang and Maurice Holt

The gas mixture produced by a coal gasifier contains components that have serious corrosive effects on the boundaries of the pipe flow system. Injection of a protective gas into the turbulent boundary layer of the coal gas products in a direction parallel to the wall markedly reduces the corrosivity of the inviscid gas stream. The interaction between the injected gas and the product gas pipe flow is investigated analytically; it is an example of the so-called wall jet problem.

The model adopted is that of a two-dimensional incompressible, turbulent free-mixing layer. The corrosive gas, H_2S, forms the upper fast moving stream. The injected protective H_2O vapor in the lower stream is bounded by the solid wall of the pipe. The flow geometry and the development of the mean velocity, U_1, and concentration profiles of the H_2S, Mi, are shown in Fig. 1. The wall jet flow can be divided into three distinct regions. In the first region, farthest upstream, the upper main stream interacts with the lower injected stream in a free mixing process with a boundary δ_f away from extension of the splitter plate. A turbulent boundary layer develops along the pipe wall bounding the lower stream at a distance δ_w from the wall. In the second region the lower half of the free mixing layer interacts with the wall turbulent boundary layer. In the third region stream mixing has been completed and all diffusion takes place in a thickened turbulent boundary layer. The H_2S initially reaches the pipe wall at this point.

The calculated ratio of the distance from the H_2O injection point to where the mass concentration of H_2S diffuses to the wall surface to the slot height of injection is of the order of 100 slot heights for a given velocity ratio of two free streams in the mixing layer. Additional distance down the tube wall is required before the partial pressures of oxygen and sulfur reach sulfidizing conditions. This additional distance is estimated to be another ~ 100 slot heights. Thus, injection of water vapor through a 1-cm slot will provide protection against oxidation of the pipe for up to two meters from the point of injection. This distance could make boundary layer gas injection a practical method for protecting surfaces against sulfidation in coal conversion systems.

* * *

†Brief version of LBL-13807.

7. OXIDATION BEHAVIOR OF SURFACE DOPED 304SS WITH MODIFIED COMPOSITION†

Ed Yaniv, Richard Gray, Don Boone, Alan Levy

The purpose of this study was to determine what effect the minor alloying elements manganese and silicon in surface doped stainless steels have on corrosion resistance. This knowledge should be helpful in understanding why the surface application of yttrium to 304SS so improves its high temperature oxidation resistance.

Specimens of 18Cr-8Ni steels were prepared with and without Mn or Si additions and were doped by applying yttrium nitrate in a water solution to polished specimens that had been heated to 500°C in air for 5 minutes. The doped specimens were next heated for 30 minutes at 500°C in air, cooled, and exposed to cyclic oxidation tests for 20 hr/cycle at 1000°C.

Only the 18Cr-8Ni steels that contained silicon had their elevated temperature oxidation resistance enhanced by surface doping with yttrium. The commercial 304SS and the alloy containing only silicon were improved while the 18Cr-8Ni steel with neither Mn nor Si, and the one with only Mn, had their

scales spall on the first thermal cycle, as did the undoped 304SS.

* * *

†Brief version of L8L-13810.

Work in Progress

1. ELEVATED TEMPERATURE EROSION OF ALUMINUM AND STEEL ALLOYS

Jennifer Paterson and Alan Levy

The erosion of materials by particles in coal conversion and utilization systems occurs at elevated temperatures. Testing of these materials at service temperatures in order to determine rates and mechanisms of erosion requires close control of temperature, flow rates, and corrosion conditions. Tests on a newly constructed elevated temperature test device of the required precision have been initiated.

Specimens were exposed to 240 μm diam SiC particles at a velocity of 30 m/s at temperatures up to 900°C. The erosion weight loss of both the 1100-0 aluminum and 310SS were similar functions of the test temperature. Both alloys are FCC single phase metals but they have great differences in strength, modulus of elasticity and other properties. As the temperature was increased to a homologous temperature of approximately 0.15, the erosion rate decreased. At a homologous temperature of 0.3, the highest erosion rate was measured for both alloys, being considerably greater than the room-temperature rate and probably due to changes in the plastic deformation characteristics of the alloys and the actual surface deformation temperature. At a still higher homologous temperature of 0.5 for both alloys, the erosion rates had decreased to the lowest levels in the test series.

At the highest test temperature, considerable amounts of SiC were detected embedded in the surface of the specimens. This SiC could account for the low weight loss measured. Microscopic cross sections and surface observations both showed that the erosion of ductile metals had occured by the characteristic mechanism of platelet formation.

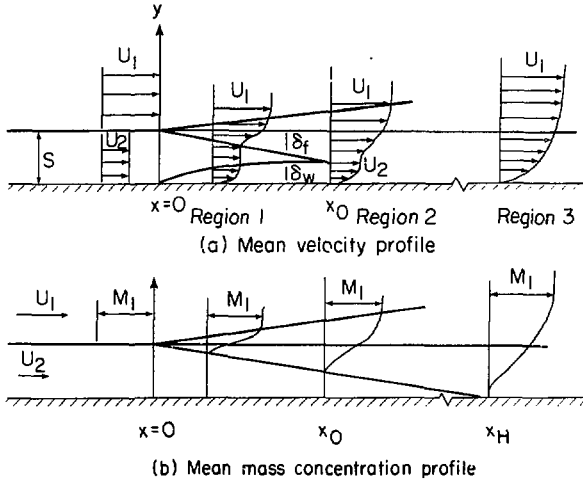

Fig. 1. Behavior of a protective gas boundary layer in a reactive gas flow passage (see next page). (XBL 8201-4403)

2. LASER DOPPLER VELOCIMETRY MEASUREMENTS OF GAS/PARTICLE FLOWS IN A 90° CURVED DUCT

Peter Turi and Jolen Flores

The apparatus designed for the investigation of particle laden air flow in conduits using laser doppler velocimetry (LDV) is now operational and is being used to acquire data relevant to erosion/corrosion during coal gasification. The purpose of this work is to test recently developed analytical models that predict flow of this type in curved ducts.

Velocity measurements were made in the streamwise and radial directions using atomized mineral oil for particles. Figure 1 shows the profiles at various centerline stations in the 90° bend. The bend causes a gradual transition from a uniform flow (up-stream) to one resembling a potential vortex. This tendency, evident in the 30° and 60° profile, was predicted in earlier, analytical modeling work in this program. The 90° profile shows the influence of the secondary flow. Measurements in the radial direccion have quantified this phenomenon. These data agree with the predictions made earlier. A radially inward flow on the walls and a radially outward flow at the centerline have been observed.

1981 PUBLICATIONS AND REPORTS

Refereed Journals

1. A. Levy, "The Solid Particle Erosion Behavior of Steel as a Function of Microstructure," Wear 68-3, 269-288 (May 1981).

2. G. Zambelli and A. Levy, "Particulate Erosion of NiO Scales," Wear 68-3, 305-332 (May 1981).

3. R. Bellman, Jr., and A. Levy, "Erosion Mechanism in Ductile Metals, Wear 70-1, 1-28 (July, 1981).

4. I. Hutchings, "A Model for the Erosion of Metals by Spherical Particles at Normal Incidence," Wear 70-3, 269-282 (August 1981).

5. J. Maasberg and A. Levy, "Erosion of Elevated Temperature Corrosion Scales on Metals," Wear 73-2, 371-386 (December 1981).

6. S. W. Yeung, R. J. Yang, "Application of the Method of Integral Relations to the Calculation of Two-Dimensional, Incompressible, Turbulent Boundary Layer," J. Applied Mechanics (December 1981).

7. J. Laitone (Deceased), "A Numerical Solution for Gas-Particle Flows at High Reynolds Number," J. Applied Mechanics 48, 465-471 (September 1981).

Other Publications

1. T. Foerster and A. Levy, "Corrosion of Metals in Coal Char Environments," Proc. International Conference on High Temperature Corrosion, NACE, San Diego, CA, (March 2-6, 1981).

2. R. Bellman, Jr. and A. Levy, "Platelet Mechanism of Erosion of Ductile Metals," Proc. 3rd International Conference on Wear of Materials, ASME, San Francisco, CA, (March 30 - April 2, 1981).

3. A. Levy and T. Bakker, "Erosion Behavior of Hard Surface Coatings/Inserts on Ductile Metals," Proc. International Conference on the Science of Hard Materials, NSF, Moran, WY, (August 23 - 28, 1981).

LBL Reports

1. A. Levy, and T. Bakker, "Erosion Behavior of Hard Surface Coatings/Inserts," LBL-13801.

2. A Levy and P. Chik, "Effect of Particle Variations on the Erosion of Ductile Metals," LBL-13802.

3. J. Flores and A. Levy, "Analytical Model of Erosion of Ductile Metals," LBL-13803.

4. T. Foley and A. Levy, "The Effect of Heat Treatment on the Erosion Behavior of Steels," LBL-13745.

5. R. Yang (Ph.D. thesis), "Boundary Layer Control by Means of Strong Injection," LBL-13807.

6. F. Pouramahdi (Ph.D. thesis), "Turbulence Modelling of Single and Two Phase Curved Channel Flows," LBL-13808.

7. E Yaniv, R. Gray, D. Boone, and A. Levy, "Oxidation Behavior of Surface Doped 304SS with Modified Composition," LBL-13810.

Presentations

1. A. Levy, "Erosion Behavior in Gasification and Liquefaction Piping and Vessel Environments," ASM Regional Conference, Oak Ridge, TN, May 12, 1981.

2. M. Landkof, D. Boone, D. Whittle, A. Levy, "The Effect of Surface Doping on the Oxidation of Chromia Former Alloys," Gordon Research Conference, New London, NH, July 20, 1981.

3. A Levy and P. Chik, "Effect of Particle Variations on the Erosion of Ductile Metals," AIME-TMS Meeting, Louisville, KY, October 15, 1981.

4. T. Foley, "The Effect of Heat Treatment on the Erosion of Alloy Steels," AIME-TMS Meeting, Louisville, KY, October 15, 1981.

5. A. Levy, "Gas and Liquid-Solid Particle Erosion," Exxon Corporate Research Lab seminar, Linden, NJ, October 9, 1981.

6. A. Levy, "Erosion Behavior of Hard Metals," Union Carbide Corp. Coatings Service Department Research Lab seminar, Indianapolis, IN, October 15, 1981.

7. A. Levy, "Erosion Behavior of Materials," DOE-EMAC seminar, Germantown, MD, October 16, 1981.

8. A. Levy, "Erosion Behavior of Materials," Combustion Engineering Corp. Metallurgy Research Lab seminar, Chattanooga, TN, October 19, 1981.

B. Solid-State Physics

1. Experimental Solid-State Physics

a. Far-Infrared Spectroscopy*

Paul L. Richards, Investigator

Introduction. The objective of our research is to use the infrared and near-millimeter wavelength range of the electromagnetic spectrum as a probe to do experiments which are selected for their technical novelty and potential for revealing new physics.

We are developing new measurement techniques, including sensitive infrared detectors for use in experiments in which the background photon level is low. The Ge:Ga photoconductors, the composite bolometers, and the superconducting diode photon detectors developed by our group are now the most sensitive existing infrared and near-millimeter detectors over the wavelength range from 30μm to 8 mm. The superconducting diode devices are also the most sensitive available heterodyne receivers at mm wavelengths.

We are now using sensitive infrared technology to measure the spectra of one dimensional conductors, of molecules chemisorbed on metal surfaces, of dust clouds in our galaxy and of the 3K *blackbody radiation that fills the universe.*

1. INFRARED SPECTROSCOPY OF QUASI-ONE-DIMENSIONAL CONDUCTORS†

William A. Challener, Pierre Monceau,‡ and Paul L. Richards

Quasi-one-dimensional conductors have been the subject of intense study for the past decade. Among the most important discoveries in this field are the existence of a new nonlinear mechanism for collective charge transport, and the existence of organic superconductivity. Collective charge transport via sliding charge density waves (CDW's) was first discovered in $NbSe_3$. We have extensively investigated the far infrared properties of $NbSe_3$ to obtain information about carrier concentrations and relaxation times, CDW energy gap formation at the Fermi surface, and coupling between the CDW and optical phonons.

We have made polarized far infrared absorption and reflection measurements on aligned crystals of $NbSe_3$ over the frequency range from 3 to 700 cm^{-1} and the temperature range from 2 to 90K.

The number of strong phonon modes in the spectra are found to be in good agreement with the 24 modes expected (from our group theoretical analysis) to couple strongly to the CDW. Variations in linewidths of phonon absorptions provide indirect evidence for an energy gap above 120cm^{-1} A far-infrared reflectance edge is seen which resembles the effects of the plasma frequency in a free electron gas. This edge appears at lower frequencies for light polarized parallel to the fiber axis. Fitting the IR reflectance at 2K to a simple Drude model gives a zero-crossing of $Re(\varepsilon)$ at 135cm^{-1}, which is significantly below the expected plasma frequency of the free carriers in $NbSe_3$. The measured reflectivity above the edge can be interpreted in terms of a background dielectric constant of order 50-100.

* * *

†LBL-13760 and LBL-13762, Abstracts.
‡CRTBT, CNRS Grenoble, France.

2. *CHARACTERIZATION OF Ge:Ga PHOTOCONDUCTIVE* DETECTORS†

Eugene E. Haller,‡ Mark R. Hueschen and Paul L. Richards

Gallium-doped germanium photoconductive infrared detectors are the most sensitive detectors of infrared radiation over the wavelength range from 30 to 230 μm. The sensitivity should approach the limit set by the fluctuations inherent in the stream of background photons, even for photon rates as low as 10^8/sec. Other investigators have reported excess noise in such detectors at relatively high photon rates. We have produced photoconductive detectors from conventional Ge:Ga, and also from low compensation Ge:Ga made from ultrapure starting material. We have carried out detailed characterization measurements to understand these detectors and to improve their performance.

Measurements have been made of the responsivity and noise of these detectors over a wide range of photon backgrounds, optical modulation frequencies, and applied bias voltages. DC responsivity, which is proportional to the product of the lifetime and the mobility of the carriers, has been measured as a function of photon background, applied bias voltage, and temperature. The effects due to lifetime and mobility have been separated by the use of Hall effect measurements made in the difficult ultrahigh impedance regime which occurs at low temperatures and low photon backgrounds.

The measured performances of our detectors were within a factor of 2 of the ideal background photon noise limit for a range of more than three orders-of-magnitude in background level (Fig.1).

*This work was supported by the Director, Office of Energy Research, Office of Basic Energy Sciences, Materials Sciences Division of the U.S. Department of Energy under Contract No. DE-AC03-76SF00098.

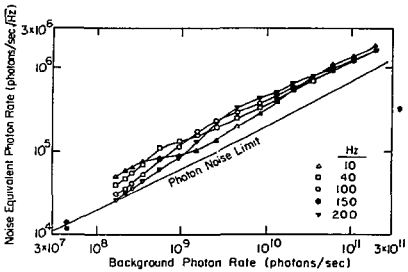

Fig. 1. Measured detector noise as a function of the rate of arrival of background infrared photons for several modulation frequencies. The noise expected from the fluctuations in the background photons is shown as a straight line. These results show that a wide variety of far infrared experiments need not be detector noise limited.
(XBL 8112-12877)

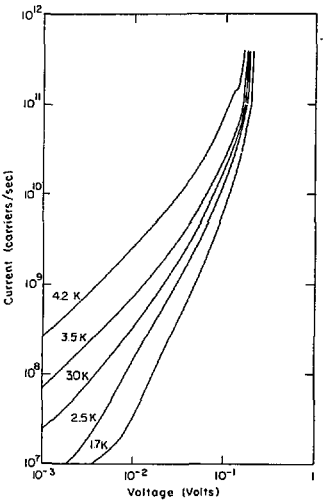

Fig. 2. Measured detector response current as a function of bias voltage for several detector temperatures. Hall effect measurements show that the observed nonlinearities result from the voltage and temperature dependence of the carrier lifetime.
(XBL 8112-12876)

A small degradation in performance was observed at high backgrounds which is not yet understood. The detector responsivity was found to be a very nonlinear function of the applied voltage, and very dependent on temperature (Fig.2). The Hall effect measurements show that these variations are due to the dependence of the carrier lifetime on temperature and electric field. By contrast, the carrier mobility changes only slightly with temperature and electric field.

* * *

†Work supported in part by NASA. Short version of LBL-13761.
‡Department of Instrument Techniques, LBL.

3. IMPROVED FABRICATION TECHNIQUES FOR INFRARED BOLOMETERS†

Eugene E. Haller,‡ Ernst Kreysa, Andrew E. Lange, Stephen E. McBride and Paul L. Richards

The infrared bolometer is the most sensitive direct detector at submillimeter wavelengths. The composite bolometer with metal film absorber that was developed by our group is used where large detector areas are required. Users in the infrared community have reported various problems with these bolometers. We have introduced new fabrication techniques which eliminate these problems and done characterization tests which demonstrate near-ideal performance of composite bolometers.

We have developed an ion implantation and metallization procedure for making electrical contact to the doped Ge thermometric element of the bolometer. These contacts essentially eliminate the current dependent inverse frequency noise which limits the performance of most infrared bolometers. The metallized contact allows the thermometer to be soldered to the bolometer substrate. Tests show that the thermal contact is thereby improved by one order of magnitude over the epoxy joint used in most bolometers. The use of an evaporated NiCr alloy in place of Bi has eliminated the problem of degradation of the absorber film. Tests have shown that He exchange gas must be rigorously excluded from the space around the bolometer before good performance is obtained. A low temperature blackbody has been built as a source for absolute bolometer calibrations.

Our composite bolometers are reliable, their noise is caused by unavoidable thermodynamic fluctuations, and they have an optical efficiency of 43 ± 3%.

* * *

†Brief version of LBL-13832.
‡Department of Instrument Techniques, LBL.

4. WORK IN PROGRESS

A new experiment is being prepared to measure the spectrum of the cosmic microwave back-

ground radiation. It will be different in most respects from our previous experiment. It is designed to test the apparent deviations from a blackbody spectrum.

A balloon experiment designed to survey the sky at far-infrared wavelengths was flown in 1979. The results were seriously limited by the performance of the composite bolometer detectors. The bolometer developments described above should permit a successful flight.

Infrared emission and absorption experiments are being developed to measure the vibrational spectra of molecules chemisorbed on metal surfaces. Both experiments have shown sufficient sensitivity to observe a fraction of one monolayer.

Work on one-dimensional compounds has been extended to the organic superconductor $(TMTSF)_2 ClO_4$. We expect to measure the conventional superconducting energy gap and to search for reported effects of superconducting fluctuations.

1981 PUBLICATIONS AND REPORTS

Refereed Journals

1. R. B. Bailey, T. Iri and P. L. Richards, "Infrared Spectra of Carbon Monoxide on Evaporated Nickel Films: A Low Temperature Thermal Detection Technique," Surface Science 100, 626 (1980), LBL-10159.

2. D. K. Lambert and P. L. Richards, "Far Infrared and Capacitance Measurements of Electrons on Liquid Helium," Phys. Rev. B23, 3282 (1981), LBL-11420.

3. D. P. Woody and P. L. Richards, "Near-Millimeter Spectrum of the Microwave Background," Astrophys. Jr. 248, 18 (1981), LBL-10343.

†4. T. Timusk and P. L. Richards, "Near-Millimeter Wave Band-Pass Filters," Applied Optics 20, 1355 (1981), LBL-11931.

‡5. D. Britt and P. L. Richards, "An Adiabatic Demagnetization Refrigerator for Infrared Bolometers," Int'l. Journal of Infrared and Millimeter Waves 2, 1083 (1981).

§6. W. R. McGrath, P. L. Richards, A. D. Smith, H. van Kempen, R. A. Batchelor, D. Prober and P. Santhanam, "Large Gain, Negative Resistance and Oscillations in Superconducting Quasiparticle Heterodyne Mixers," Appl. Phys. Lett. 39, 655 (1981).

‖7. A. D. Smith, W. R. McGrath, P. L. Richards, H. van Kempen, D. Prober and P. Santhanam, "Negative Resistance and Conversion Gain in SIS Mixers," Physica 108 B+C, 1367 (1981).

‖8. T-M Shen "Conversion Gain in Millimeter Wave Quasi-Particle Heterodyne Mixers," IEEE Journal of Quantum Electronics QE-17, 1151 (1981).

‖9. T-M Shen and P. L. Richards, "Computer Simulations of the Performance of Quasiparticle Heterodyne Mixers," IEEE MAG-17, 677 (1981).

LBL Reports

1. W. R. McGrath and P. L. Richards, "A Convenient Low Temperature Heat Sink for Electrical Leads," LBL-13764. Paper submitted to the Review of Scientific Instruments.

Other Publications

‖1. P. L. Richards, "Superconducting Detectors and Mixers for Near-Millimeter Wavelengths," McGraw-Hill Yearbook of Science and Technology.

‖2. P. L. Richards, "Superconducting Devices for Detection, Mixing and Amplification at Millimeter Wavelengths, Physics News in 1980, P. F. Schewe, ed. (A.I.P., New York, 1980), pp 31-32.

‖3. W. R. McGrath, P. L. Richards, A. D. Smith, H. van Kempen, D. Prober and P. Santhanam, "SIS Quasiparticle Tunnel Junctions as Microwave Mixers," Bull. Am. Phys. Soc. 26, 307 (1981).

4. M. R. Hueschen, P. L. Richards and E. E. Haller, Gallium-Doped Germanium Far Infrared Photoconductors," Bull. Am. Phys. Soc. 26, 446 (1981), LBL-11997.

5. W. A. Challener and P. L. Richards, "Far Infrared Optical Properties of $NbSe_3$," Bull. Am. Phys. Soc. 26, 449 (1981), LBL-11998.

Invited Talks

1. P. L. Richards, "Superconducting Devices for Detection and Mixing at Near-MM Wavelengths," Twentieth General Assembly of the Int'l. Union of Radio Science, Washington, D.C. August 10-18, 1981.

Also, at the New Orleans Meeting of the APS, 23-25 November 1981.

2. P. L. Richards, "Detectors for Near-MM Wavelengths," 1981 Conference of CalSpace Institute, U.C.L.A., March 24-25, 1981.

3. A. D. Smith, "Large Gain With Low Noise in SIS Quasiparticle Heterodyne Mixers," Twentieth General Assembly of the Int'l. Union of Radio Science, Washington, D.C. August 10-15, 1981.

4. P. L. Richards, "Superconducting Microwave Devices Reach Fundamental Quantum Limits," 1981 IEEE Int'l. Conference on Infrared and Millimeter Waves, Miami Beach, December 7-12, 1981.

Also, at seminar at U.C. Irvine, November 16, 1981.

* * *

† Work supported in part by NASA and the Natural Sciences and Engineering Research Council of Canada.

‡ Work supported by NASA and CalSpace.

§ Work supported by the U.S. Office of Naval Research and the Netherlands Organization for the Advancement of Pure Research (ZWO).

‖ Work supported in part by the U. S. Office of Naval Research.

b. Experimental Solid-State Physics and Quantum Electronics*

Y. Ron Shen, Investigator

1. DETECTION OF MOLECULAR MONOLAYERS BY OPTICAL SECOND HARMONIC GENERATION†

Chenson K. Chen, Tony F. Heinz, Daniel Ricard, and Y. Ron Shen

Detection of molecular monolayers at an interface is a subject of great importance in surface science. Various techniques have been invented for this purpose. Recently, we have been interested in developing nonlinear optical techniques for detecting adsorbed molecules. The second-order nonlinear optical effects are particularly interesting. In a medium with inversion symmetry, the second-order nonlinear susceptibility vanishes in the bulk in the electric-dipole approximation. The surface layers of atoms or molecules, however, do not possess inversion symmetry. This second-harmonic generation (SHG) from molecular monolayers is easily observable. This is particularly true in the presence of a surface enhancement due to the local-field correction resulting from surface roughness.[1]

We have studied SHG by adsorbed molecules on silver in an electrolytic process. The experiment

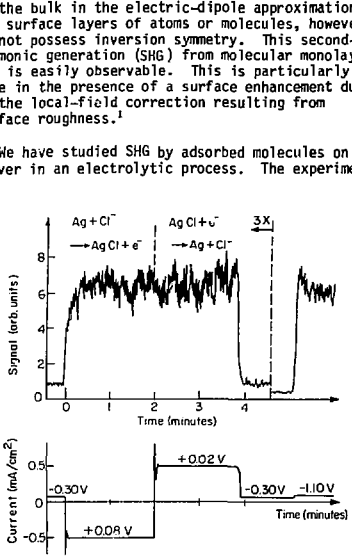

Fig. 1. Current and diffuse second-harmonic reflection as functions of time during and after an electrolytic cycle. The voltages listed on the lower curve are V_{Ag-SCE}. 0.05 M pyridine was added to the 0.1 M KCl solution following the completion of the electrolytic cycle.

(XBL 8012-13338)

*This work was supported by the Director, Office of Energy Research, Office of Basic Energy Sciences, Materials Sciences Division of the U.S. Department of Energy under Contract No. DE-AC03-76SF00098.

was carried out with the use of a Q-switched Nd:YAlG (neodymium-doped yttrium aluminum garnet) laser operating at 1.06 μm, 10 pulses/sec, and a 10 nsec pulse width.

Second-harmonic reflection from the silver surface was easily detected, even with a laser energy of < 0.6 mJ/pulse over 0.2 cm². By monitoring the SH signal during the electrolytic cycle, the change in the signal resulting from the appearance and disappearance of AgCl could be observed, as shown in Fig. 1. The signal rose and fell rapidly at the beginning and end of the cycle, and changed relatively slowly during the cycle. This result suggests that the SH signal mainly originated from a few layers of AgCl at the surface. This is expected since bulk AgCl has inversion symmetry. At the end of the cycle, when pyridine (0.05 M) was added in the solution, and the bias voltage was sufficiently negative, $V_{Ag-SCE} < -0.6$ V, a monolayer of pyridine would be adsorbed on Ag. Figure 1 shows that a 50 time increase of the SHG signal was actually observed due to the presence of the pyridine monolayer.

* * *

†Brief version of Phys. Rev. Lett. 46, 1010 (1981) (LBL-12003).

[1] C. K. Chen, A. R. B. de Castro, and Y. R. Shen, Phys. Rev. Lett. 46, 145 (1981).

2. STUDIES OF MOLECULAR ADSORPTION ON SILVER IN AN ELECTROLYTIC SOLUTION†

Tony Heinz, Chenson K. Chen, Daniel Ricard, and Y. Ron Shen

Molecular monolayers adsorbed on a rough silver surface can be readily detected by optical second harmonic generation (SHG). We can, therefore, use it for an *in situ* study of the equilibrium behavior of molecular adsorption at a roughened Ag-electrode interface. This is demonstrated by the measured adsorption isotherm in Fig. 1 for pyridine in 0.1 M KCl solution. The results can be fitted by the simple Langmuir equation, from which an adsorption energy of $\Delta G = 5.7$ kcal/mole is deduced.

Lacking inversion symmetry, the free pyridine molecule has an electric-dipole contribution to the second-order non-linear polarizability $\alpha^{(2)}$. Therefore, a simple alignment of the molecules upon adsorption could explain the observed SHG. For the adsorption of centrosymmetric molecules, such an alignment alone should not yield a detectable SHG. We have, however, observed a SH signal associated with the adsorption of a monolayer of the centrosymmetric molecule pyrazine on an electrochemically treated silver surface. This indicates the broken inversion symmetry of the adsorbed molecules through interaction with the metal, and underscores the sensitivity of SHG to the details of surface

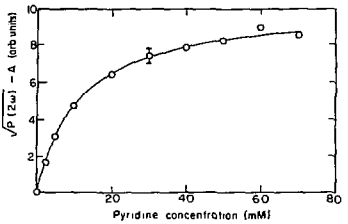

Fig. 1. *Equilibrium second harmonic signal* ($\sqrt{P(2\omega)} - A$) *versus bulk pyridine concentration. The solid Curve is a theoretical fit to the experimental data using the Langmuir model.*

(XBL 815-5824)

structure. Values for the effective second-order nonlinear polarizabilities of adsorbed pyridine and parazine on Ag are deduced from measurements.

* * *

†*Brief version of Chem. Phys. Lett.* 83, 180 (1981) (LBL-12735) and LBL-12808, Chem. Phys. Lett. (to be published).

3. EFFECT OF EXTENDED SURFACE PLASMONS ON SURFACE -ENHANCED RAMAN SCATTERING†

Harry W. K. Tom, Chenson K. Chen, A. Rubens B. de Castro, and Y. Ron Shen

We have designed an experiment to separate the contribution of extended surface plasmons to surface enhanced Raman scattering (SERS) from that of localized surface plasmons and metal-molecule interaction. This was done by propagating an extended surface plasmon wave on an electrolytically cycled AG surface. From the measured wave propagation properties, the surface macroscopic field $E(\omega)$ could be calculated. The observed Raman signal from the adsorbed molecules was clearly further enhanced in addition to the surface enhancement due to roughness, but the enhancement could be fully accounted for by the enhancement in the average macroscopic field at the metal-liquid interface.

* * *

†Brief version of LBL-13027, Solid State Comm. (to be published).

4. ANHARMONICITY, PHONON LOCALIZATION, TWO-PHONON BOUND STATES, AND VIBRATIONAL SPECTRA†

J. C. Kimball,‡ C. Y. Fong,‡ and Y. Ron Shen

Neither local modes nor extended phonons precisely describe the excitations of anharmonic solids. A simple model Hamiltonian presented here characterizes the transition from local oscillator to optical phonon which would take place if one could continuously increase the phonon dispersion. The model is used to describe two types of transitions: a phonon-localization transition which is the analog of the Mott transition for electrons, and a spectral transition associated with the appearance of two-phonon bound states. In real materials, a sharp phonon-localization transition is probably not achievable, but striking spectral effects may be observable for some systems which are marginally able to produce two-phonon bound states.

* * *

†Brief version of Phys. Rev. B 23, 4946 (1981), (LBL-12153).
‡Department of Physics, University of California, Davis, CA 95616.

5. LASER INTERACTION WITH MOLECULAR BEAMS

Y. Ron Shen, in collaboration with Yuan T. Lee's group; see section on Advanced Isotope Separation Technology.

1981 PUBLICATIONS AND REPORTS

Refereed Journals

1. T. F. Heinz, C. K. Chen, D. Ricard, and Y. R. Shen, "Optical Second-Harmonic Generation from a Monolayer of Centrosymmetric Molecules Adsorbed in Silver," Chem. Phys. Lett. 83, 180 (1981), LBL-12735.

†2. S. D. Durbin, S. M. Arakelian, and Y. R. Shen, "Laser-Induced Diffraction Rings from a Nematic Liquid Crystal Film," Optics Lett. 6, 411 (1981).

3. J. C. Kimball, C. Y. Fong, and Y. R. Shen, "Anharmonicity, Phonon Localization, Two-Bound States and Vibrational Spectra," Phys. Rev. B 23, 4946 (1981), LBL-12153.

4. C. K. Chen, T. F. Heinz, D. Ricard, and Y. R. Shen, "Detection of Molecular Monolayers by Optical Second Harmonic Generation," Phys. Rev. Lett. 46, 1010 (1981), LBL-12003.

†5. Peixian Ye and Y. R. Shen, "Four-Wave Mixing and Optical-Field Induced Helical Structure in Liquid Crystalline Materials," Appl. Phys. 25, 49 (1981).

6. C. K. Chen, A. R. B. de Castro, and Y. R. Shen, "*Surface Enhanced Second Harmonic Generation*," Phys. Rev. Lett. 46, 145 (1981), LBL-11596.

7. Y. T. Lee and Y. R. Shen, "Studies with Crossed Laser and Molecular Beams," Phys. Today 33, 52 (1980), LBL-11105.

8. M. W. Sigrist, D. J. Krajnovich, F. Huisken, Z. J. Zhang, Y. T. Lee, and Y. R. Shen, "Laser-Induced Dissociation of Monomers and Dimers of Bromine," Helv. Phys. Acta 53, 289 (1980), LBL-10991.

†9. N-M. Chao, K. C. Chu, and Y. R. Shen, "Local Refractive Index Measurement on a Cholesteric Liquid Crystal Using the Surface Plasmon Technique," Mol. Cryst. Liq. Cryst. 67, 261 (1981).

10. Y. R. Shen, "A Note on Two-Phonon Coherent AntiStokes Raman Scattering," J. Ram. Spec. 10, 110 (1981), LBL-10715.

†11. S. D. Durbin, S. M. Arakelian, and Y. R. Shen, "Optical Field Induced Birefringence and Freedericksz Transition in a Nematic Liquid Crystal," Phys. Rev. Lett. 47, 1411 (1981).

Other Publications

1. Y. R. Shen, C. K. Chen, and A. R. B. de Castro, "Surface Nonlinear Optics," in Lasers and Applications, W. O. N. Guimaraes, C-T. Lin, and A. Mooradian, eds. (Springer-Verlag, Berlin, 1981), p.77, LBL-11252.

2. A. R. B. de Castro, C. K. Chen, and Y. R. Shen, "Surface Enhanced Second Harmonic Generation," Bull. Am. Phys. Soc. 26, 379 (1981), LBL-11946 ABS.

3. C. K. Chen, T. F. Heinz, D. Ricard, and Y. R. Shen, "Detection of Adsorbed Molecules by Second-Harmonic Generation," Bull. Am. Phys. Soc. 26, 379 (1981), LBL-11947 ABS.

4. H. Tom, C. K. Chen, Y. R. Shen, and A. R. B. de Castro, "Surface Enhanced Raman Scattering with Surface Plasmon Excitation," Bull. Am. Phys. Soc. 26, 338 (1981), LBL-11948 ABS.

†5. P. Sheng and Y. R. Shen, "Nematic-Isotropic Phase Transition at Substrate-Liquid Interface," Bull. Am. Phys. Soc. 26, 274 (1981).

†6. S. D. Surbin, S. M. Arakelian, and Y. R. Shen, "Laser-Induced Director Reorientation in a Nematic Liquid Crystal," Bull. Am. Phys. Soc. 26, 274 (1981).

7 J-L. Oudar and Y. R. Shen, "Theoretical Aspects of Four-Wave Mixing Spectroscopy with Multiple Resonances," Digest of Tech. Papers on the Internatl. Conf. on Excited States and Multiresonant Nonlinear Optical Processe in Solids, 1981, p.26, LBL-12154.

8. J. C. Kimball, C. Y. Fong, and Y. R. Shen, "Anharmonicity and Phonon Localization," Bull. Am. Phys. Soc. 26, 281 (1981).

9. Y. R. Shen, C. K. Chen, T. F. Heinz, and D. Ricard, "Surface-Enhanced Nonlinear Optical Effects and Detection of Adsorbed Molecular Monolayers," in Laser Spectroscopy V, A. R. W. McKellar, T. Oka, and B. P. Stoicheff, eds. (Springer-Verlag, Berlin, 1981), p.412, LBL-12930.

10. J. M. Lisy, M. F. Vernon, A. Tramer, H. S. Kwok, D. J. Krajnovich, Y. R. Shen, and Y. T. Lee, "Infrared Vibrational Predissociation Spectroscopy of Small Molecular Clusters," in Laser Spectroscopy V, A. R. W. McKellar, T. Oka, and B. P. Stoicheff, eds. (Springer-Verlag, Berlin, 1981), p.324, LBL-12981.

LBL Reports

1. Peixian Ye and Y. R. Shen, "Transient Four-Wave Mixing and Coherent Transient Optical Phenomena," LBL-13462.

2. H. W. K. Tom, C. K. Chen, A. R. B. de Castro, and Y. R. Shen, "Effect of Extended Surface Plasmons on Surface Enhanced Raman Scattering, LBL-13027.

3. M. F. Vernon, J. M. Lisy, H. S. Kwok, D. J. Krajnovich, A. Tramer, Y. R. Shen, and Y. T. Lee, "Vibrational Predissociation of Benzene Dimers and Trimers by the Crossed Laser-Molecular Beam Technique," LBL-12895.

4. C. K. Chen, T. F. Heinz, D. Ricard, and Y. R. Shen, "Equilibrium and Transient Study of Adsorption of Pyridine on Silver in an Electrolytic Solution," LBL-12808.

5. C. K. Chen, "Nonlinear Optics at Interfaces," (Ph.D Thesis), LBL-12084.

6. Y. R. Shen, "Nonlinear Optical Techniques for Surface Studies," LBL-13365.

Invited Talks

1. Y. R. Shen, "Surface Nonlinear Optics," Topical Meeting on Tunable Lasers, Army Research Office, Keystone, CO, April 1-3, 1981; Sandia National Laboratory, Livermore, CA, July 10, 1981; General Motors Research Laboratories, Warren, MI, May 1, 1981.

2. Y. R. Shen, C. K. Chen, T. F. Heinz, and D. Ricard, "Surface Enhanced Nonlinear Optical Effects and Detection of Adsorbed Molecular Monolayers," Fifth International Conference on Laser Spectroscopy, Jasper Park Lodge, Alberta, Canada, June 26-July 3, 1981.

3. J. M. Lisy, M. F. Vernon, A. Tramer, H. S. Kwok, D. J. Krajnovich, Y. R. Shen, and Y. T. Lee, "Infrared Vibrational Predissociation Spectroscopy of Small Molecular Clusters," Fifth International Conference on Laser Spectroscopy, Jasper Park Lodge, Alberta, Canada, June 26-July 3, 1981.

4. D. Krajnovich, Z. Zhang, F. Huisken, Y. R. Shen, and Y. T. Lee, "The Effects of Reagent Translational and Vibrational Energy on the Dynamics of Endothermic Reactions," XIIth International Confer-

ence on the Physics of Electronics and Atomic Collisions, Gatlinburg, TN, July 15-22, 1981.

5. Y. R. Shen, "Nonlinear Optical Techniques for Surface Studies," 29th Midwest Solid State Conference on Novel Materials and Techniques in Condensed Matter, Argonne National Laboratory, Argonne, IL, September 25-26, 1981.

6. Y. R. Shen, "Nonlinear Optical Effects at Interfaces and in a Liquid Crystal Film," IBM Research Laboratories, Yorktown Heights, NY, August 10, 1981.

7. Y. R. Shen, "Surface Nonlinear Optical Effects and Applications to Surface Physics," University of Toledo, Toledo, OH, September 23, 1981.

8. C. K. Chen and Y. R. Shen, "Nonlinear Optics at an Interface," Gordon Conference, Wolfeboro, NH, August 3-7, 1981.

9. J-L. Oudar and Y. R. Shen, "Theoretical Aspects of Four-Wave Mixing Spectroscopy with Multiple Resonances, Internatl. Conf. on Excited States and Multiresonant Nonlinear Optical Processes in Solids, Aussois, France, March 18-20, 1981.

* * *

†Work supported by the National Science Foundation under Grant DMR78-18826.

c. Excited Quantum Fluids in Solids*

Carson D. Jeffries, Investigator

Introduction. The objective of this work is to study quantum fluids and other excited states in solids. Being studied are the formation and decay mechanisms of excitons in semiconductors, and their condensation into an electron-hole metallic liquid. Excitons and liquid drops can be confined in a strain well. Their properties are important for a detailed understanding of electron-hole interactions. In photo excited Ge under an increasing electric field, oscillations are observed which undergo period doubling bifurcations, eventually becoming noise. This is an example of bifurcation as a route to chaotic behavior in nonlinear systems. Theorists have postulated that such behavior is universal. Measurements on nonlinear semiconducting systems are in approximate agreement with the predicted universal behavior and indicate that noisy instabilities in solids can now be understood and even controlled, with important technical applications. In dislocated Ge a novel anisotropic magnetic resonance is observed from the electrons at dislocated dangling bonds. Detailed measurements disclose a spin-Peierls distortion of the bond angle and the existence of a long-lived dislocation conduction band with spin dependent mobility. The method used is highly sensitive and is a new quantitative microscopic tool for dislocation studies.

1. CORRELATION IN THE ELECTRON-HOLE LIQUID IN Ge†

J. C. Culbertson, J. E. Furneaux,‡ and C. D. Jeffries

The electron-hole liquid (EHL) is a unique system: it is a two component e-h fermi liquid existing, along with free excitons (FE), in optically excited Ge at low temperatures. Many properties (such as binding energy, density, lifetime, surface tension) have been measured as a function of applied stress. The enhancement factor $g_{eh}(o)$, the ratio of the electron density at the hole to the mean density, is a measure of the e-h correlation function at zero separation; its measurement provides a sensitive check on many-body theory approximation schemes.

The measurements are done in a FE-EHL system confined inside a stress-induced potential well, which provides accurately defined spatial distributions far from the crystal surfaces. Measured are the FE and EHL decay rates, the luminescence line shapes, and steady luminescence vs excitation power for a set of crystal stresses.

The measured enhancement factors are plotted in Figure 1, along with two theoretical curves, (a) and (b);§ (a) is a refinement of (b) and takes

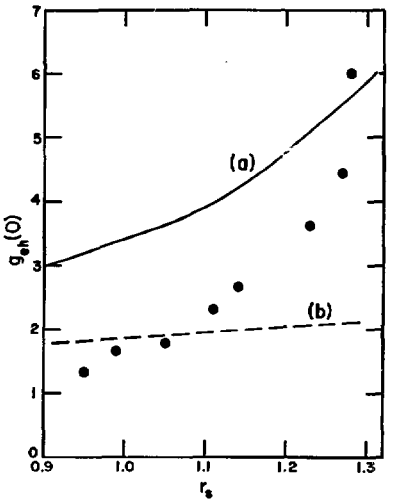

Fig. 1 Measured enhancement factor $g_{eh}(o)$ vs the exciton Bohr radius r_s (black dots). (XBL 8112-12788)

account of multiple scatterings to infinite order. However, neither model includes electron-hole band anisotropy. It is expected that a more refined theory will be developed to fit the data.

* * *

†Brief version of LBL-13739.
‡Present address: Code 6873, Naval Research Laboratory, Washington, D.C. 20375.
§P. Vashishta et al., Phys. Rev. B10, 5108 (1974).

2. BIFURCATION AND CHAOTIC BEHAVIOR IN NONLINEAR SEMICONDUCTOR PHENOMENA†

J. Testa, J. Perez, and C. Jeffries

It has been proposed[1] that the onset of instabilities and noise in many nonlinear physical systems may be universally understood qualitatively by the computed behavior of a simple deterministic recursion relation $x_{j+1}=\lambda x_j \times (1-x_j)$, where x represents the variable of interest, and λ is a control parameter. The prediction for a periodic system

*This work was supported by the Director, Office of Energy Research, Office of Basic Energy Sciences, Materials Sciences Division of the U.S. Department of Energy under Contract No. DE-AC03-76SF00098.

driven at frequency f is: as λ is increased, successive frequency bifurcations occur at threshold values λ_n, such that $(\lambda_n-\lambda_\infty) \approx K\delta^{-n}$, n=1,2,3---, where $\delta = 4.669$ is a universal number; at each bifurcation a new subharmonic f/n appears in the power spectrum at $\Delta = 13$ db below f/(n-1); at λ_∞, there is a transition to a chaotic (noisy) region; for $\lambda > \lambda_\infty$, noise bands merge in a reverse bifurcation, with narrow windows of noiseless periodic motion at specific subharmonics. The objective is to test these remarkable predictions for nonlinear semiconductors.

An LC resonant circuit is made nonlinear by the use of a reversed biased abrupt junction Ge diode as the capacitive element. It is driven at fixed frequency f by a driving voltage V which is increased, corresponding to increasing the parameter λ. A spectrum analyzer records the power spectrum of the developed voltage across the nonlinear capacitor. The amplitude of this voltage is displayed *vs V by a sampling technique*, thus generating a bifurcation diagram.

The results are in qualitative agreement with the predictions: periodic bifurcation is observed up to n=32 (see Fig. 1); noise at the threshold for

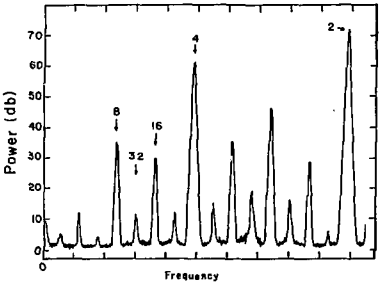

Fig. 1 Power spectrum of anharmonic oscillator driven at f=92 kHz, showing subharmonics at *f/n*, for *n*=2, 4, 8, 16, 32.

(XBL 821-7683)

chaos; periodic windows in the chaotic region are observed at the predicted subharmonic ordering; bifurcation to n=24 is observed within the wide n=3 window. Experimental values δ=4 and Δ=12 db are observed. It is planned to use this model to interpret a wide variety of chaotic behaviors observable in excitations in solids.

* * *

†Brief version of LBL-13719.
[1]See, e.g., M. J. Feigenbaum, Los Alamos Science 1, 4 (1980).

3. ELECTRIC DETECTION OF SPIN RESONANCE OF ELECTRONS AT DISLOCATIONS IN Ge†

E. J. Pakulis and C. D. Jeffries

Dislocations in Ge are of theoretical interest and of practical importance. However, microscopic information such as the bond angles at dislocations has not previously been known. A method for observing these angles by electron spin resonance has been developed.

The method consists of inducing microwave spin resonance of the electrons at dislocations in crystals of Ge, which are high-Q self-resonant cavities. The microwave magnetic field induces spin flips, which produce a measurable absorption *if* there are enough spins. Optically excited free carriers will undergo spin dependent scattering *with the spins on* the dangling bonds (see Fig. 1) giving rise to a

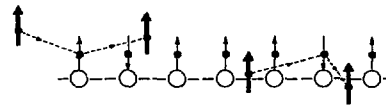

Fig. 1 Schematic of spin dependent scattering of excited electrons (bold arrows) by dangling bonds along a dislocation line.

(XBL 8111-12859)

change in the sample conductivity, sensitivity measured by the microwave *electric* field, hence electric detection of spin resonance.

Samples of n-type dislocated Ge at 2°K under optical pumping showed 24 anisotropic resonance lines, which fit to a simple axially symmetric g tensor with six-fold principal axes at 1.2° from each (111) axis. This distortion may be intrinsic, or due to an instability of either the spin-Peierls type or the dimerization type. There is evidence for an optically excited long-lived (4 hours) dislocation conduction band. This new sensitive method can detect and measure distortions of dislocations at low densities and will be extended to other crystals.

* * *

†Brief version of LBL-13315.

1981 PUBLICATIONS AND REPORTS

Refereed Journals

1. E. J. Pakulis and C. D. Jeffries, "Observation of a novel Electron Paramagnetic Resonance in Ge," Phys. Rev. Lett. 47, Dec. 21, 1981, LBL-13315.

LBL Reports

1. S. M. Kelso, "Energy- and Stress-Dependent Hole Masses in Germanium and Silicon," Phys. Rev. B, Jan. 15, 1982, in press, LBL-12854.

2. S. M. Kelso, "Calculation of Properties of the Electron Hole Liquid in Uniaxially Stressed Ge and Si," sub. to Phys. Rev. B, LBL-13387.

3. J. C. Culbertson and J. E. Furneaux, "Measurement of the Density Dependence of the Electron-Hole Liquid Enhancement Factor in Ge," LBL-13739.

4. J. Testa, J. Perez, and C. Jeffries, "Evidence for Bifurcation and Universal Chaotic Behavior in Nonlinear Semiconducting Devices," LBL-13719.

Talks

1. J. C. Culbertson, J. E. Furneaux, and C. D. Jeffries, "The Enhancement Factor for the Strain Confined Electron-Hole Liquid in Ge," BAPS 26, 486 (1981), LBL-11919.

2. J. E. Furneaux, J. C. Culbertson, and C. D. Jeffries, "Recombination Mechanisms for Strain Confined Excitons in Ge," BAPS 26, 487 (1981) LBL-11920.

3. E. J. Pakulis and C. D. Jeffries, "Photo-Induced Emissive Spin Resonance in Ge Single Crystals," BAPS 26, 223 (1981), LBL-12056.

d. Time-Resolved Spectroscopies in Solids*

Peter Y. Yu, Investigator

Introduction. When light strikes a solid surface, in most cases the energy in the radiation is absorbed by electrons in the solid. Eventually part of this energy comes out of the solid as light and part of it is retained in the solid as heat. The processes involved in the conversion of optical energy into heat occur in picoseconds (10^{-12} sec), so they are most conveniently studied with picosecond laser pulses. It is the purpose of this project to investigate these processes both theoretically and experimentally.

1. NON-THERMALIZED PHOTOLUMINESCENCE IN Cu_2O†

N. Caswell,‡ J. Weiner and P. Y. Yu

Typically one interprets photoluminescence lineshapes by assuming that the optically excited electrons reach a thermal equilibrium with the crystal lattice. However, in many samples, such as highly doped or amorphous semiconductors, the electron lifetime is too short for it to reach thermal equilibrium. So far there has been no successful attempt to understand the lineshapes of such non-thermalized emission.

We have chosen Cu_2O to study this problem because much is known about the properties of Cu_2O. This knowledge enables us to calculate the photoexcited electron distribution and hence the emission lineshape in Cu_2O, with the lifetime of the electron as the only adjustable parameter. With a lifetime of 30 picoseconds we are able to explain all the emission spectra of Cu_2O as a function of temperature and excitation frequencies.

We are now applying the calculation to different systems, namely, very pure semiconductors, in which formation of exciton-polaritons cause the emission lineshape to deviate from a thermalized distribution.

* * *

†This work was supported in part by National Science Foundation Grant No. DMR7919463 (see LBL-12990).
‡Present address: IBM T. J. Watson Research Center, Yorktown Heights, NY 10598.

*This work was supported by the Director, Office of Energy Research, Office of Basic Energy Sciences, Materials Science Division of the U.S. Department of Energy under Contract No. DE-AC03-76SF00098.

2. WORK IN PROGRESS

Lifetime of Photoexcited Free Carriers in GaAs

J. Weiner and P. Y. Yu

Photoexcited electrons in pure GaAs will radiatively recombine in about 1 nsec. If traps are present due to deep impurity levels the electrons will disappear much faster due to trapping at these deep levels. Insulating GaAs doped with deep impurities such as Cr and O are now commonly used as substrates for growing from the liquid phase epitaxal layers of GaAs for devices. It is important to determine the rate of trapping of carriers by these deep impurities.

We have constructed a delayed coincidence photon counting system capable of measuring the lifetime of photoexcited carriers as short as 100 psec. In pure GaAs we found the lifetime of these carriers to be 1.5 ± 0.1 nsec at ~60°K increasing to 2.0 nsec at ~20°K. The lifetime of the photo-excited carriers decreases to ~80 psec in GaAs doped with $1.6 \times 10^{+17}$ cm^{-3} of Cr.

When the intensity of the exciting radiation is increased we find that the photoexcited electrons first form a hot plasma which then cools to the lattice temperature in about 1 nsec. The density of this plasma and the phonon temperature in GaAs under intense radiation is being investigated by time resolved Raman Scattering.

1981 PUBLICATIONS AND REPORTS

Refereed Journals

1. P. Y. Yu and C. Hermann, "Excitation Spectroscopies of Impurities in CdSe," Phys. Rev. B 23, 4097 (1981).

2. P. Y. Yu and L. M. Falicov, "Resonant Electronic Scattering in CdTe: A Probe of Quasibound Excited States," Phys. Rev. B 24, 1144 (1981).

LBL Reports

1. N. Caswell, J. S. Weiner and P. Y. Yu, "A Study of Non-thermalized Luminescence Spectra: The Case of Cu_2O," LBL-12990.

2. N. Caswell and P. Y. Yu, "Physical Origin of the Anomalous Temperature Dependence of the 1s Yellow Exciton Luminescence Intensity in Cu_2O," LBL-13575.

Invited Talks

1. P. Y. Yu, "Study of Exciton Polaritons by Resonant Light Scattering in Solid State and Biomolecular Systems," Castle Hot Springs, Arizona, March 11-14, 1981.

2. P. Y. Yu, "Resonant Light Scattering in Semiconductors—Past, Present and Future," Seminar at Xerox Palo Alto Research Center, Palo Alto, CA, February 27, 1981.

3. P. Y. Yu, "Solid State Physics at Picosecond *Time Scales*," Physics Department Colloquium, U.C. Davis, November 17, 1981.

4. N. Caswell, "Non-thermalized Luminescence *Spectra in* Cu_2O," presented at IBM T. J. Watson Research Center, Yorktown Heights, NY 10598, October 29, 1981.

e. Superconductivity, Superconducting Devices, and 1/f Noise*

John Clarke, Investigator

1. QUANTUM NOISE IN JOSEPHSON JUNCTIONS AND DC SQUIDS†

Roger H. Koch, D. J. Van Harlingen, and John Clarke

In the thermal limit, $eV \ll k_BT$, where V is the bias voltage, the noise in a Josephson tunnel junction is generated by Nyquist noise in the shunt resistance, R. The theory of this noise has been long understood, and is in good agreement with experimental data. However, until recently, there has been little work on noise in the limit $eV \gtrsim k_BT$ where quantum corrections become important. Quantum effects are not only of intrinsic interest, but *also determine the ultimate sensitivity of Josephson* mixers and SQUIDs.

The theory assumes that the resistor produces a current noise with a spectral density $S_I(\nu) = (2h\nu/R)\coth(h\nu/2k_BT)$ at frequency ν. In the limit $T \to 0$, the spectral density reduces to zero point fluctuations, $2h\nu/R$. We have calculated the voltage noise generated across a current-biased junction at frequencies much less than $2eV/h$. We have also extended the theory to compute the noise energy of a dc SQUID, which consists of two shunted junctions incorporated into a superconducting ring with inductance L. The noise energy is defined as $\varepsilon/1\text{Hz} = S_\Phi/2L$, where S_Φ is the spectral density of the magnetic flux noise. In the limit $T \to 0$, we

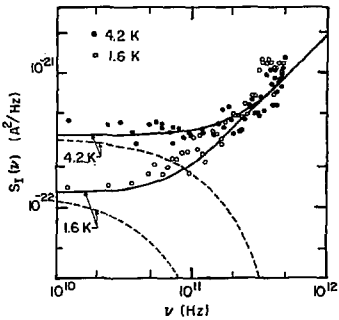

Fig. 1 Measured spectral density of current noise in shunt resistor at 4.2K and 1.6K. Solid lines are $(2h\nu/R)\coth(h\nu/2k_BT)$, dashed lines are $(4h\nu/R)[\exp(h\nu/k_BT) - 1]^{-1}$. (XBL 817-6072).

predict $\varepsilon/1\text{Hz} \approx h$. We have measured the noise in both single junctions and SQUIDs fabricated with suitable parameters to exhibit quantum noise effects. The voltage noise across each device at about 100 kHz was amplified by a cooled LC-resonant circuit, and further amplified by room temperature electronics before being mixed-down to frequencies below 1 kHz, and measured by an on-line PDP-11 computer.

The measured voltage noise for a single junction was in excellent agreement with the theoretical predictions. From the measured noise, we were able to reconstruct the spectral density of the current noise produced by the resistor, as shown in Fig. 1. The agreement between theory and experiment is excellent. The dashed lines, which are the predictions of a theory without the zero point term, fall far below the data at the higher frequencies. A series of SQUIDs has been tested. The best two of them had noise energies below $2h$ when the 1/f noise was subtracted out, and were thus within a factor of 2 of the quantum noise limit.

* * *

†Brief version of LBL-13326.

2. PHONON-INDUCED GAP ENHANCEMENT IN SUPERCONDUCTING ALUMINUM†

Daniel Seligson and John Clarke

A major goal of non-equilibrium superconductivity has been to understand the effect of microwave and ultrasonic radiation on the energy gap, Δ, and critical current, I_c, of thin superconducting films. If energy of the radiation is insufficient to break Cooper pairs (frequency $< 2\Delta/h$), the main effect of the photons or phonons is to induce a change in the quasiparticle distribution. Under appropriate circumstances, this redistribution enhances both Δ and I_c. The purpose of the present experiments is to measure both enhancements simultaneously in Al films irradiated with 9 GHz phonons, and to make a quantitative comparison with the theory.

In the experiment, a traveling-wave-tube amplifier is used to produce 1kW, 1μs pulses of 9 GHz microwaves that are coupled into a re-entrant cavity in the cryostat. The ultrasound is generated by the piezoelectric effect in a quartz rod, one end of which is in a region of high electric field in the cavity. The ultrasound propagates down the rod and is absorbed by an Al film evaporated onto the other end. We measure the critical current of a narrow strip of Al, and determine the energy gap using a tunnel junction.

We find substantial increases in Δ and I_c over the temperature range $0.85 < T/T_c < 0.997$. Figure 1 shows the gap enhancement for a number of values

*This work was supported by the Director, Office of Energy Research, Office of Basic Energy Sciences, Materials Sciences Division of the U.S. Department of Energy under Contract No. DE-AC03-76SF00098.

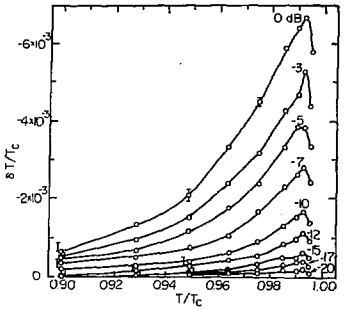

Fig. 1 Effective cooling due to energy gap enhancement, $\delta T/T_c$, of an Al film irradiated with 9 different phonon power levels, vs. reduced temperature. (XBL-8112-12874)

of microwave power, expressed as the temperature δT through which the equilibrium film would have to be lowered to generate the same increase in Δ. The maximum observed value of $\delta T/T_c$ is about 7×10^{-3}. The critical current enhancement falls off much more slowly as the temperature is lowered, and we have observed a maximum cooling $\delta T/T_c$ of about 40×10^{-3}. The reasons for these major differences is being investigated.

* * *

†Brief version of LBL-13749.

3. CHAOS IN JOSEPHSON JUNCTIONS†

Roger H. Koch, John Martinis, and John Clarke

There has recently been intensive study of the properties of non-linear difference equations which, with appropriate choice of parameters, may exhibit chaotic solutions. Although the values of these solutions appear to be random, they are in fact completely determined by the equation. There is considerable interest in investigating the extent to which certain physical systems, which are described by non-linear differential equations, show behavior similar to that of the difference equations.

We have studied Josephson tunnel junctions fabricated to exhibit chaotic behavior. Each junction is shunted with its self-capacitance, C, and a a resistance, R, with substantial self-inductance, L, as shown inset in Fig. 1. The equation of motion of this system is third order in the phase difference across the junction, δ, and contains a non-linear term, $\sin\delta$. These conditions are sufficient to generate chaos provided the parameters are chosen appropriately. Physically, the chaos arises from the mixing of the Josephson frequency and the frequency of the LC-resonant circuit by the non-linearity.

Figure 1(a) shows the measured current-voltage characteristic of a junction exhibiting chaotic behavior. The chaos is manifested as a number of negative resistance regions, most of which are stable and can be retraced in either direction. Figure

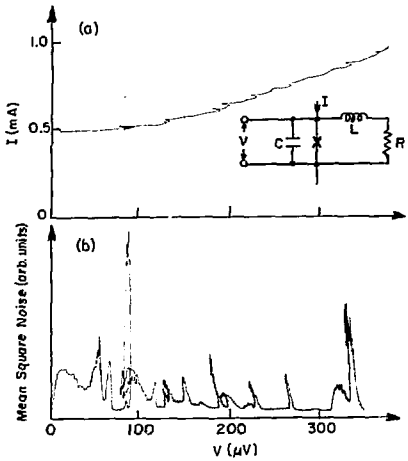

Fig. 1 (a) I-V characteristic of Josephson junction (inset) exhibiting chaotic behavior; (b) shows the mean square noise vs. voltage. (XBL 8112-12995A)

1(b) plots the measured mean square noise across the junction versus voltage. The noise increases rapidly as the characteristic enters the negative resistance region in the direction of increasing current, reaches a maximum at the local minimum in voltage, and decreases as the current is increased further. This behavior has been closely simulated on both analog and digital computers. On the basis of these simulations, we believe that the transition to chaos occurs via intermittency as the current is increased, that is, the Josephson oscillations are interspersed with regions of random behavior. On the other hand, as the current is decreased towards the negative resistance region, the transition occurs via a series of period doubling bifurcations. Detailed studies of the behavior are now being made.

* * *

†Brief version of LBL-13750.

1981 PUBLICATIONS AND REPORTS

Refereed Journals

1. T. Lemberger and J. Clarke, "Charge-Imbalance Relaxation in the Presence of a Pair-Breaking Supercurrent in Dirty, Superconducting Al Films," Phys. Rev. B 23, 1106 (1981), LBL-11406.

2. T. Lemberger and J. Clarke, "Charge-Imbalance Relaxation in the Presence of a Pair-Breaking Interaction in Superconducting AlEr Films," Phys. Rev. B 23, 1088 (1981), LBL-11201.

3. R. Koch, D. Van Harlingen, and J. Clarke, "Quantum Noise Theory for the dc SQUID," Appl. Phys. Lett. 38, 380 (1981), LBL-11729.

4. R. Koch, D. J. Van Harlingen, and J. Clarke, "Koch et al. Respond," Phys. Rev. Lett. 46, 1705 (1981).

5. B. R. Fjordboge, P. E. Lindelof, and J. Clarke, "Charge Imbalance in Superconducting Tin Films Produced by a Supercurrent in the Presence of a Temperature Gradient," J. Low Temp. Phys. 44, 535 (1981), LBL-12262.

6. T. Lemberger, "Charge-Imbalance Fluctuations in Superconductors," Phys. Rev. B 24, 4105 (1981), LBL-12185.

7. R. H. Koch, D. J. Van Harlingen, and J. Clarke, "Observation of Zero Point Fluctuations in a Resistively Shunted Josephson Junction," Phys. Rev. Lett. 47, 1216 (1981), LBL-12134.

8. D. J. Van Harlingen, "Thermoelectric Generation of Charge Imbalance at a Superconductor-Normal Metal Interface," J. Low Temp. Phys. 44, 163 (1981), LBL-12029.

LBL Reports

1. J. Clarke, T. D. Gamble, W. M. Goubau, R. H. Koch, and R. F. Miracky, "Remote-Reference Magnetotellurics: Equipment and Procedures," submitted to Geophys. Pros., LBL-13559.

2. J. Clarke, "SQUID," to be published in Ency. Sci. and Tech., LBL-12136.

3. J. Clarke, "Superconductive Devices," to be published in Ency. Sci. and Tech., LBL-12135.

4. R. H. Koch, D. J. Van Harlingen, and J. Clarke, "Measurements of Quantum Noise in Resistively Shunted Josephson Junctions," submitted to Phys. Rev. B1, LBL-13326.

5. D. J. Van Harlingen, R. H. Koch, and J. Clarke, "Approach to the Quantum Noise Limit in the dc SQUID," submitted to Appl. Phys. Lett., LBL-13668.

6. R. H. Koch, D. J. Van Harlingen, and J. Clarke, "Observation of Quantum Noise Effects in a Resistively Shunted Josephson Junction," LBL-13748.

Other Publications

1. J. Clarke, "Fluctuations Analysis," in SQUID '80, SQUIDs and Their Applications, H. D. Hahlbohm and H. Lubig, eds. (Walter de Gryter, NY, 1980), pp.187-205, LBL-11055.

2. J. Clarke, "Summary and Conclusions," in SQUID '80, SQUIDs and Their Applications, H. D. Hahlbohm and H. Lubig, eds. (Walter de Gryter, NY, 1980), pp. 961-970, LBL-11056.

3. J. Clarke, "Charge Imbalance," Proceedings of the NATO Advanced Study Institute, Maratea, Italy, August 1980, pp.353-422, LBL-11554.

4. T. D. Gamble, W. M. Goubau, N. E. Goldstein, R. Miracky, M. Stark, and J. Clarke, "Magnetotelluric Studies at Cerro Prieto," ACTAS Proceedings, 1981, p.405, LBL-9545.

5. N. E. Goldstein and J. Clarke, "Magnetotelluric Measurements," SQUID Applications to Geophysics, H. Weinstock and W. C. Overton, Jr., eds. (The Society of Exploration Geophysicists, Tulsa, 1981), p.49, LBL-12266.

6. J. Clarke, "Charge Imbalance in Superconductors," Proceedings of the Workshop on Condensed Matter, 1980, Bariloche, Argentina, 1981, p.283.

7. T. Lemberger and J. Clarke, "Measurement of the Charge-Imbalance Relaxation Rate in the Presence of a Pair-Breaking Supercurrent in Dirty Al Films," Bull. Am. Phys. Soc. 26, 243 (1981).

8. R. Lee and J. Clarke, "Microwave Enhancement of the Energy Gap and Critical Current in Superconducting Aluminum Films," Bull. Am. Phys. Soc. 26, 243 (1981).

9. R. H. Koch, D. J. Van Harlingen, and J. Clarke, "Measurement of Zero-Point Noise Using a Josephson Junction," Bull. Am. Phys. Soc. 26, 382 (1981).

10. D. J. Van Harlingen, R. H. Koch, and J. Clarke, "Investigation of the Quantum Noise Limit in dc SQUIDS," Bull. Am. Phys. Soc. 26, 382 (1981).

11. R. H. Koch, D. J. Van Harlingen, and J. Clarke, "Quantum Noise in Josephson Junctions and SQUIDs," Proceedings of 6th International Conference on Noise in Physical Systems, p.359, LBL-12616.

12. T. R. Lemberger, "Superconducting Fluctuations and the Transmission Line Model," Proceedings of the 16th International Conference on Low Temperature Physics, p.163, 1981.

13. D. J. Van Harlingen, R. Koch, and J. Clarke, "DC SQUID near the Quantum Noise Limit," Proceedings of the 16th International Conference on Low Temperature Physics, p.1083, 1981, LBL-12450.

Invited Talks

1. J. Clarke, "SQUIDs: Ultra-Sensitive Detectors and Ultrafast Computers," Physics Colloquium at Cal Tech, February 5, 1981.

2. J. Clarke, "Noise in Josephson Junctions," invited paper at APS March Meeting, Phoenix, Arizona, March 18, 1981.

3. D. J. Van Harlingen, "Thermoelectric Effects in Superconductors," invited paper at 16th International Conference on Low Temperature Physics, Los Angeles, August 19-25, 1981.

4. J. Clarke, "Nonequilibrium Superconductivity and Superconducting Devices," Scientific and Educational Advisory Committee of the Lawrence Berkeley Laboratory, October 6, 1981.

6. J. Clarke, "SQUIDs and Geophysics," Phys. Dept. Colloquium, Univ. of Calif., Berkeley, Oct. 14,1981.

2. Theoretical Solid-State Physics

a. Theoretical Studies of the Electronic Properties of Solid Surfaces*

L. M. Falicov, Investigator

Introduction. This program is concerned with the study of the electronic structure of solid surfaces and interfaces and its consequences for structural, magnetic and chemical properties. The principal investigator and his collaborators formulate theories and models and perform calculations which are either prototypes of important real situations or "realistic" calculations of specific properties. In all parts of this program there is a constant and fruitful interaction with experimental groups at LBL, both within MMRD (Profs. Somorjai and Shirley) and in other Divisions (Prof. E.E. Haller, Engineering and Technical Services Division) as well as in other laboratories (e.g. Prof. Y. Petroff at L.U.R.E., Orsay, France). These experimental-theoretical collaborations result, in some cases, in publications of mixed character in which a given problem is presented both as an experimental result and as an exposition of its underlying theory.

1. THEORETICAL STUDIES OF THE ELECTRONIC, CHEMICAL AND MAGNETIC PROPERTIES OF TRANSITION- AND NOBLE-METAL OVERLAYERS ON TRANSITION- AND NOBLE-METAL SUBSTRATES

L.M. Falicov and Jerry D. Tersoff

The physical properties of metallic overlayers on metallic substrates are of enormous physical interest and of considerable practical importance in catalysis and magnetic devices. In this research project we are studying the electronic configurations and their attendant magnetic and chemical properties of transition and noble metal perfect and imperfect surfaces, overlayers (partial or complete) of transition metals on noble-metal substrates and transition-noble-metal interfaces. The calculations are selfconsistent, are based on the LCAO (or tight-binding) scheme and are performed numerically in the Computation Center of the Lawrence Berkeley Laboratory.

The main results, found in several investigations, are:
(1) There seems to be a direct relationship between catalytic activity and number of unoccupied d states in Ni metal.
(2) The width, position and occupancy of the local d states show simple trends as a function of the Ni site coordination.
(3) For Ni (and similarly, for Pt) sites of highest coordination tend to be the most active sites on a surface, provided they are accessible to adsorbate molecules.
(4) Copper shows little activity, regardless of site coordination.
(5) There is a significant depression of local magnetic moments at the Ni-Cu interface. The Ni magnetization is reduced by $0.46\mu_B$ at the interface layer.
(6) There is no appreciable penetration of the magnetization into the Cu.
(7) The loss of magnetization at the Ni interfaces is attributed to the changing shape of the Ni density of states at the Fermi level. Hybridization between Ni d states and Cu conduction band states also contributes to this loss.

In order to corroborate these results we have calculated the electronic and magnetic properties of artificially ordered Ni-Cu alloys. We have calculated pure Ni, Ni_3, NiCu, $NiCu_3$ and pure Cu. We find the magnetic moments per Ni atom to be:

Alloy	Ni	Ni_3Cu	NiCu	$NiCu_3$	Cu
$\mu(\mu_B)$	0.62	0.47	0.09	0.00	0.00

The reduction in magnetization is due to three physical mechanisms:
(1) Decreased d character of the states at E_F;
(2) Rounding and loss of structure in the projected Ni density of states;
(3) Filling of the d band.
These mechanisms are equally applicable to the disordered alloys.

2. THEORETICAL STUDY OF LITHIUM INTERCALATION IN TRANSITION-METAL DICHALCOGENIDES

L.M. Falicov and Roberto Osório

We have made considerable progress in understanding the intercalation of lithium in ($Li_x Ti_{1-y} Ta_y S_2$). The disordered inherent in the random location of the Ti and Ta metal atoms produces a large variety of new effects in the thermodynamics of the intercalation of lithium in these layered-structure alloys. Work has progressed to the point in which new results will be ready for publication within the next six months.

3. WORK IN PROGRESS

We are currently continuing the research described under Sections 1 and 2. In particular we are in the

*This work was supported by the Director, Office of Energy Research, Office of Basic Energy Sciences, Materials Sciences Division of the U.S. Department of Energy under Contract No. DE-AC03-76SF00098.

process of investigating the difference in magnetic behavior between a Ni monolayer in Cu(100) and on Cu(111). Indications are that the two faces behave in completely different ways, with the magnetization remaining in one face and being absent in the other.

1981 PUBLICATIONS AND REPORTS

Refereed Journals

†1. L.M. Falicov and C.A. Balseiro, "Soft Phonons and Superconducting Quasiparticles: A New Raman-active Hybrid Mode", J. Raman Spectroscopy 10, 251 (1981).

†2. P. Thalmeier and L.M. Falicov, "Model Calculation of Oscillatory Magnetic Breakdown in Metals with Multiply Degenerate Bands", Phys. Rev. B 23, 2586 (1981).

†3. A.M. Stein, G.G. Cabrera and L.M. Falicov, "Short-range-order Effects on the ESR Spectra of a Spin Cluster", Phys. Rev. B 24, 4391 (1981).

†4. P. Schlottmann and L.M. Falicov, "Theory of Intermediate Valence for Systems with Two Magnetic Configurations", Phys. Rev. B 23, 5916 (1981).

5. J. Tersoff and L.M. Falicov, "Electronic Structure and Local Atomic Configurations of Flat and Stepped (111) Surfaces of Ni and Cu", Phys. Rev. B 24, 754 (1981). LBL-12238

†6. P.Y. Yu and L.M. Falicov, "Resonant Electronic Scattering in CdTe: A Probe of Quasibound Excited States", Phys. Rev. B 24, 1144 (1981).

†7. P. Schlottmann and L.M. Falicov, "Local Susceptibility Calculation for Intermediate-Valence Solids", phys. stat. sol. (b) 107, 165 (1981).

†8. Y.R. Lin-Liu, L.M. Falicov and W. Kohn, "First-order Phase Transitions in Intermediate-valence Solids--a Theory Based on Metallic Hydrogen", Phys. Rev. B 24, 5664 (1981).

9. R. Osório and L.M. Falicov, "Cluster-variation Method for the Triangular Lattice Gas", J. Phys. Chem. Solids 43, 73 (1981). LBL-11474, LBL-11475.

LBL Reports

†1. J. Tersoff and L.M. Falicov, "Calculation of Electronic and Magnetic Properties of Ni Films on Cu(100)", LBL-13058.

2. L.M. Falicov, "Spin Waves at Surfaces and Steps in Ferromagnets and Antiferromagnets", LBL-13220.

3. L.M. Falicov, "Summary: Disordered Systems in Perspective", LBL-13331.

4. J. Tersoff and L.M. Falicov, "Interface Magnetization--Cu on Ni(100)", LBL-13624.

5. J. Tersoff and L.M. Falicov, "Calculation of Magnetization in Ordered Ni-Cu Alloys", LBL-13625.

Other Publications

†1. L.M. Falicov, "Level Quantization and Broadening for Band Electrons in a Magnetic Field: Magneto-Optics Throughout the Band", in Theoretical Aspects and New Developments in Magneto-Optics (1980), *edited by J.T. Devreese (Plenum, New York*, 1981), p. 1.

†2. P. Schlottmann and L.M. Falicov, "Theory of Magnetic Properties of Intermediate Valence for Systems with Two Magnetic Configurations", in *Valence Fluctuations in Solids, edited by* L.M. Falicov, W. Hanke and M.B. Maple (North-Holland, Amsterdam, 1981), p. 293.

†3. Y.R. Lin-Liu, L.M. Falicov and W. Kohn, "Equation of State on Intermediate Valence Solids--a Theory Based on Metallic Hydrogen", in Valence *Fluctuations in Solids, edited by* L.M. Falicov, W. Hanke and M.B. Maple (North-Holland, Amsterdam, 1981), p. 361.

†4. T. Lin and L.M. Falicov, "Diatomic-molecule Model for a Mixed-valence System", in Valence Fluctuations in Solids, edited by L.M. Falicov, W. Hanke and M.B. Maple (North-Holland, Amsterdam, 1981), p. 393.

†5. L.M. Falicov and J.L. Morán-López, "Theory of Surface Effects in Binary Alloys", in Simposia. Física de la Materia Condensada (Physics of Condensed Matter) edited by M. Kiwi (Equinoccio, Editorial de la Universidad Simon Bolivar, Caracas, Venezuela, 1980) p. 37.

Contributed Papers

1. L.M. Falicov, "Potential of a Positive Test Charge in Germanium (Application to Hydrogen)", Meeting of the American Physical Society, March 17, 1981.

2. L.M. Falicov, "An Electronic Theory of Short-Range Order in Binary Alloys", Meeting of the APS, March 18, 1981.

3. L.M. Falicov, "Magnetic Excitations Near Interfaces of an Antiferromagnetic Insulator Model", Meeting of the APS, March 18, 1981.

4. L.M. Falicov, "Local Orbital Fluctuations and Catalytic Activity of Flat and Stepped Surfaces--Cu and Ni(111)", Meeting of the APS, March 20, 1981.

5. J.L. Morán-López and L.M. Falicov, "Theory of Hydrogen Chemisorption on Ferromagnets", 28th National Symposium of the American Vacuum Society, November 5, 1981.

Invited Talks

Professor Falicov presented a grand total of eleven talks at seven different institutions on eight different subjects.

* * *

†Work supported in part by National Science Foundation Grant No. DMR7803408.

b. Theoretical Solid-State Physics*

Marvin L. Cohen, Investigator

Introduction. Much of the research is aimed at explaining or predicting properties of solids using as little experimental input as possible. A large effort involves the use of total energy calculations to predict static and vibrational structural properties. The input in these calculations is the atomic number, atomic mass, and a finite number of structures to test. Another part of the program is devoted to surface and interface physics. In addition to electronic calculations of surface and interface states, the total energy approach is used to predict surface geometries. In other areas, calculations are being done on the electronic structure of high temperature superconductors, stacking faults, and line dislocations. In all cases, careful comparisons with experiment are made. A long term goal is to predict structures of new useful materials.

1. TOTAL ENERGY CALCULATIONS

During the past three years, this program has focused on the development of pseudopotential total energy techniques and applications to group IV semiconductors. Recently, the method has been extended to metals, and a Hellmann-Feynman force constant model allows more convenient calculations of surface structure and phonon spectra.

Comparisons with all-electron methods have been done to demonstrate the accuracy of the pseudopotential approach in which only the properties of the valence electrons outside the core are considered.

The calculated bulk properties for Be and Al listed in Tables I and II respectively demonstrate the successes of the method. The input is the atomic number and atomic mass.

Table I
Beryllium

Structural Properties:

	a(Å)	c(Å)	c/a	cohesive energy (Ry/atom)
theory	2.25	3.57	1.58	0.294
expt.	2.2858	3.5842	1.568	0.244
error	~1.5%	<1%	~1%	~20%

Poisson Ratio:

theory	-0.0517
expt.	-0.03 to -0.06

Table II
Aluminum

Structural Properties:

	a_0(Å)	bulk modulus ($\times 10^{12}$ dyn/cm^2)	cohesive energy (Ry)
theory	4.01	0.715	0.268
expt.	4.02	0.722	0.25
error	(<1%)	(~1%)	(~7%)

Phonon Frequencies: ($\times 10^{13}$ rad/sec)

	L(100)	T(100)	L(111)	T(111)
theory	6.11	3.63	6.21	2.74
expt.	6.08	3.65	6.06	2.63
error	(<1%)	(~1%)	(~3%)	(~4%)

Mode Grüneisen Parameters: γ

	L(100)	T(100)	L(111)	T(111)
theory	1.71	2.83	2.10	2.37
expt.	average $\langle\gamma\rangle$ = 2.18			

2. SURFACES AND INTERFACES

An ongoing effort in calculating the electronic structure of surfaces and interfaces has yielded new results for two chemisorption problems: Al on GaAs(110) and Pd on Si(111). In these cases as in the case of a clean surface or interface, the input to the self-consistent pseudopotential calculation necessarily included an experimentally determined model for the surface geometry. Recent total energy calculations using a Hellmann-Feynman force scheme have yielded results for clean surface geometries allowing the possibility of a complete theoretical calculation for electronic and structural properties.

For Si(001) and Si(111), the calculation involves a minimization of the Hellmann-Feynman forces. The atoms are moved until the forces are close to zero.

For Si(001), an asymmetric dimer model results. For Si(111), a (1x1) structure is found with an antiferromagnetic spin ordering. Experiments are in progress to test these results.

3. ELECTRONIC STRUCTURE

The pseudopotential approach was used to calculate the electronic structure of a variety of sys-

*This work was supported by the Director, Office of Energy Research, Office of Basic Energy Sciences, Materials Sciences Division of the U.S. Department of Energy under Contract No. DE-AC03-76SF00098 and also by National Science Foundation Grant No. DMR-7822465.

tems including V_3Si, a ZnS stacking fault, and a partial dislocation in Si.

For V_3Si, the electronic charge density and band structure were analyzed to explain the bonding features of this material. This calculation is one in a series of calculations done for A15 materials. These studies have also yielded an analysis and a determination of effective radii and volumes for elements in A15 compounds.

The calculations for the rotation twin stacking fault in β-ZnS and for the electronic structure of a 30° partial dislocation in Si illustrate the flexibility and power of modern electronic structure schemes and demonstrate that accurate studies of complex systems are now possible.

4. WORK IN PROGRESS

Total energy calculations for III-V semiconductors are being done to determine static and vibrational properties and to predict the structure of high pressure modifications. Extensions of this method when applied to phonons are yielding full dispersion curves. The role and accuracy of the pseudopotential scheme in the total energy formalism is being examined in detail.

1981 PUBLICATIONS AND REPORTS

Refereed Journals

1. J. Ihm, J. R. Chelikowsky, and M. L. Cohen, "Electronic Structure of a Pd Monolayer on a Si(111) Surface," Phys. Rev. B 22, 4610 (1980).

2. M. L. Cohen, "Pseudopotential Theory for Surface and Bulk Properties of Semiconductors" in Proc. 15th Int. Conf. Physics of Semiconductors, Kyoto, 1980, J. Phys. Soc. Japan 49, 13 (1980).

3. J. Ihm and M. L. Cohen, "Equilibrium Properties and the Phase Transition of Grey and White Tin," Phys. Rev. B 23, 1576 (1981).

4. P. K. Lam and M. L. Cohen, "Effective Radii and Volumes for Elements in A15 Compounds," Phys. Letters 81A, 457 (1981).

5. J. Ihm, M. T. Yin, and M. L. Cohen, "Quantum Mechanical Force Calculations in Solids: The Phonon Spectrum of Si," Solid State Commun. 37, 491 (1981).

6. J. E. Northrup and M. L. Cohen, "Electronic Structure of the Rotation Twin Stacking Fault in β-ZnS," Phys. Rev. B 23, 2563 (1981).

7. J. Ihm, M. L. Cohen, and S. F. Tuan, "Demons and Superconductivity," Phys. Rev. B 23, 3258 (1981).

8. J. R. Chelikowsky, D. J. Chadi, and M. L. Cohen, "Electronic Structure of the Al-GaAs(110) Surface Chemisorption System," Phys. Rev. B 23, 4013 (1981).

9. P. K. Lam and M. L. Cohen, "Electronic Charge Density and Bonding in V_3Si," Phys. Rev. B 23, 6371 (1981).

10. M. L. Cohen, "Pseudopotential Calculations for Ideal Interfaces" in Surfaces and Interfaces in Ceramic and Ceramic-Metal Systems, eds. J. Pask and A. Evans (Plenum Press, New York, 1981), p. 1.

11. M. T. Yin and M. L. Cohen, "Microscopic Theory of the Static Structural Properties and Phase Transformation of Ge," Solid State Commun. 38, 625 (1981).

12. M. T. Yin and M. L. Cohen, "Theoretical Determination of Surface Atomic Geometry: Si(001)-(2x1)," Phys. Rev. B 24, 2303 (1981).

13. M. L. Cohen, "Pseudopotentials and Crystal Structure" in Structure and Bonding in Crystals, Vol. 1, eds. M. O'Keeffe and A. Navrotsky (Academic Press, New York, 1981), p. 25.

14. P. K. Lam and M. L. Cohen, "Ab Initio Calculation of the Static Structural Properties of Al," Phys. Rev. B 24, 4224 (1981).

Reports

1. J. E. Northrup, M. L. Cohen, J. R. Chelikowsky, J. Spence, and A. Olsen, "The Electronic Structure of the Unreconstructed 30° Partial Dislocation in Silicon," UCB Physics Dept. preprint.

2. A. K. McMahon, M. T. Yin, and M. L. Cohen, "Comparison of Methods for the Calculation of Phase Stability in Silicon," UCB Physics Dept. preprint.

3. M. T. Yin and M. L. Cohen, "Ground State Properties of Diamond," UCB Physics Dept. preprint.

4. J. E. Northrup, J. Ihm, and M. L. Cohen, "Spin Polarization and Atomic Geometry of the Si(111) Surface," UCB Physics Dept. preprint.

5. M. L. Cohen, "Calculations of Properties of Materials," UCB Physics Dept. preprint.

6. M. Y. Chou, P. K. Lam, and M. L. Cohen, "Ab Initio Calculation of the Static Structural Properties of Be," UCB Physics Dept. preprint.

7. M. T. Yin and M. L. Cohen, "On the Ab Initio Pseudopotential Theory for the Ground State Properties of Solids," UCB Physics Dept. preprint.

8. M. T. Yin and M. L. Cohen, "Ab Initio Calculation of Phonon Frequencies of Al," UCB Physics Dept. preprint.

9. M. T. Yin and M. L. Cohen, "Ab Initio Calculation of the Phonon Dispersion Relation: Application to Si," UCB Physics Dept. preprint.

10. J. C. Phillips and M. L. Cohen, "Molecular Models of Giant Photocontractive Evaporated Chalcogenide Films," UCB Physics Dept. preprint.

11. S. Froyen and M. L. Cohen, "High Pressure Phases of a III-V Semiconductors: A Microscopic Theory," UCB Physics Dept. preprint.

12. S. G. Louie, S. Froyen, and M. L. Cohen, Nonlinear Ionic Pseudopotentials in Spin Density Functional Calculations," UCB Physics Dept. preprint.

C. Materials Chemistry

1. Chemical Structure

a. Low Temperature Properties of Materials*

Norman E. Phillips, Investigator

Introduction. The goal of this program is to contribute to an understanding of the properties of materials by comparing experimental data, usually on low-temperature heat capacities, with models or microscopic theories. Such comparisons are usually most useful at low temperatures, and the measurements have therefore been confined to the region below 25 K. Measurements can be made under pressure and in high magnetic fields. Since the accuracy of heat capacity data is critically dependent on the accuracy of temperature measurements, the maintenance and improvement of a laboratory temperature scale, and its extension to the millikelvin region where the thermodynamic scale is not well established, are important parts of the program.

1. COMPARISON OF AN NBS "FIXED POINT DEVICE" WITH CERIUM MAGNESIUM NITRATE AND NUCLEAR ORIENTATION THERMOMETERS†

W. E. Fogle, E. W. Hornung, M. C. Mayberry, and N. E. Phillips

Temperatures in the mK region have usually been derived from established scales near 1 K by the extrapolation of the magnetic susceptibility of cerium magnesium nitrate (CMN) according to the Curie-Weiss relation, $\chi = C(T - \Delta)^{-1}$. The high-temperature fits, however, do not determine the value of Δ to the accuracy necessary for many measurements at low temperatures. For example, 30% discrepancies in the reported heat capacities of ^{3}He probably derive in some part from errors in Δ. The further development of ^{3}He/mK physics requires substantial improvement in absolute temperature measurements. Nuclear orientation (NO) and noise thermometers are among the most promising for the purpose. These thermometers are not suitable as working thermometers, but they can be used as the basis for low-temperature calibrations of CMN thermometers. An important related development is the distribution by the National Bureau of Standards of a "fixed point device" based on critical temperatures of superconductors that permits comparison of absolute temperature measurements at different laboratories.

As part of a program to obtain accurate data on the heat capacity of ^{3}He, we have intercompared several CMN thermometers, an NO thermometer that incorporates a number of refinements over earlier versions, and an NBS SRM 768 fixed point device. The major conclusions are: (1) The values of Δ for two rather similar types of CMN thermometers differ by 1 mK. (2) Independently of the correct values of Δ, the lowest temperature point on the NBS device is inconsistent with the temperatures assigned to the highest four. (3) Inclusion of the NO data shows that the two values of Δ are 0.0 ± 0.1 and 0.95 ± 0.1 mK, and that the NBS device gives the four highest temperatures to within the stated accuracy, but the fifth, and lowest, is too low by 8%. All of these results have significant implications for low-temperature thermometry and calorimetry.

* * *

†Brief version of postdeadline paper presented at LT16, Los Angeles, August 1981; Physica, to be published (LBL-13790).

2. PRESSURE AND FIELD DEPENDENCE OF THE LOW-TEMPERATURE HEAT CAPACITY OF α-CERIUM†

James D. Boyer and Norman E. Phillips

In metallic Ce the differences in energy between the 4f levels and the Fermi level are small and sensitive to both temperature and volume. As a consequence the various allotropic forms show an extraordinary richness of properties and provide a unique opportunity for study of the effect of 4f occupancy on metallic properties. The electronic structure of the nonmagnetic α-Ce is of particular interest because this phase bridges the gap between the magnetism of the low pressure, isomorphic γ-Ce and the occurrence of superconductivity.

As a contribution to an understanding of the electronic structure of α-Ce, the specific heat was measured between 0.3 and 20 K, at pressures to 9 kbar, and in magnetic fields to 76 kOe. The results give the Debye characteristic temperature, θ_D, and the coefficient of the electronic heat capacity, $\gamma = (1/3)\pi^2k^2(1 + \lambda)N(E_F)$, where $N(E_F)$ is the density of electronic states at the Fermi energy, and λ is the electron mass enhancement, usually dominated by the electron-phonon component, λ_{ep}, but in this case possibly including a spin-fluctuation component, λ_{sf}.

The volume dependence of γ and θ_D are shown in Fig. 1. Several models based on localized 4f states, with parameters derived from a relation between unit cell dimensions and valence, give a volume dependence of $N(E_F)$ that is in good agree-

*This work was supported by the Director, Office of Energy Research, Office of Basic Energy Sciences, Material Sciences Division of the U. S. Department of Energy under Contract No. DE-AC03-76SF00098.

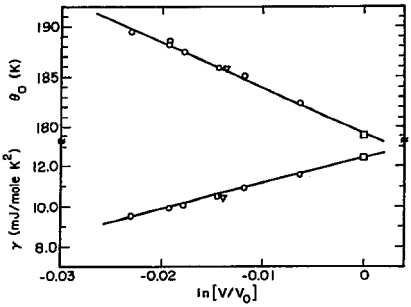

Fig. 1. Volume dependence of γ and θ_0 for α-Ce. (XBL 8112-12751)

ment with $\gamma(V)$. Recent band structure calculations give ($N(E_F)$ and, together with $\theta_0(V)$, $\lambda_{ep}(V)$. The predicted volume dependence of γ is an order of magnitude smaller than observed. Nevertheless, other evidence on the 4f character of the conduction electrons in both γ- and α-Ce show that the band theoretical description is at least approximately correct. The heat capacity data then require, and permit an estimate of, a volume dependent λ_{sf} which also explains the occurrence of superconductivity near the high pressure limit of the phase.

* * *

†Brief version of LBL-13793 and part I of LBL-13645.

3. PRESSURE DEPENDENCE OF THE LOW-TEMPERATURE HEAT CAPACITY OF TEFLON†

James D. Boyer and Norman E. Phillips

Reflecting the general interest in amorphous materials, the low-temperature heat capacity of morphous dielectrics, including polymers, has recently received considerable attention. It is substantially greater than that calculated for the low-frequency acoustic phonons, and above 1 K the excess typically has the form of a sum of two Einstein functions. For linear polymers the acoustic phonon contribution is usually represented by the Tarasov model—the sum of 3-dimensional and (modified) 1-dimensional Debye functions with characteristic temperatures θ_3 and θ_1. Data on the heat capacity of polytetrafluoro-ethylene (teflon), originally obtained in connection with the use of teflon as a pressure transmitting medium in low-temperature calorimetry, appear to be the only data on the pressure dependence of the heat capacity of amorphous dielectrics.

The useful data extend from 1 to 20 K and to a

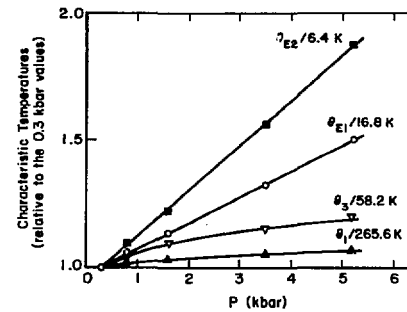

Fig. 1. Pressure dependence of the characteristic temperatures of teflon, relative to the 0.3 kbar values which are indicated for each curve. (XBL 821-7500)

pressure of 5.2 kbar. They are well represented by θ_3, θ_1, and the sum of two Einstein functions, with characteristic temperatures θ_{E1} and θ_{E2}, representing, respectively, 0.75 and 0.036% of the modes, and a Tarasov function. The pressure dependence of the four characteristic temperatures is shown in Fig. 1, where the 0.3 kbar values are also indicated. It is striking that even though the Einstein functions represent less than 1% of the modes, they account for 50% of the maximum pressure dependence. This suggests their association with parts of the chains adjacent to voids. (For both polymethyl methacrylate and polystyrene, pairs of Einstein functions, similar with respect to both numbers of modes and characteristic temperatures, were associated with vibrations of side chains at voids, but such an interpretation could not apply to teflon.) The relatively weak pressure dependence of θ_1 is consistent with its usual identification with longitudinal in-chain vibrations.

* * *

†Brief version of LBL-13794 and Part III of LBL-13645.

4. WORK IN PROGRESS

A search for "phason" anomalies in the specific heat of the alkali metals offers one of the best methods of testing the prediction of charge-density-wave ground states in these metals (see LBL-13791). Recent improvements in the laboratory temperature scale below 1 K make such a search practical, and the project has been undertaken.

Improvements in the precision, to ~0.01%, of heat capacity measurements, led to the identification of anomalies associated with spin-glass ordering in CuMn (see Ref. 1). This work is being extended to investigate the effects of concentration and heat treatment of the anomalies, and is

being supplemented by susceptibility measurements on the same samples.

The measurements with NO and CMN thermometers and on the heat capacity of ^{3}He are being continued.

Additional applications of the high-pressure calorimeter to materials with unstable 4f levels are planned.

* * *

1. W. E. Fogle et al., Phys. Rev. Lett. 47, 352 (1981); LBL-13154.

1981 PUBLICATIONS AND REPORTS

Refereed Journals

1. William E. Fogle, James D. Boyer, Norman E. Phillips, and John Van Curen, "Calorimetric Investigations of Spin-Glass Ordering in CuMn," Phys. Rev. Lett. 47, 352 (1981); LBL-13154.

2. M. D. Núñez-Regueiro, K. Matho, W. E. Fogle, and N. E. Phillips, "Heat Capacity of Dilute CuMn in Strong Magnetic Fields," Physica 107B, 315 (1981); LBL-13788.

3. William E. Fogle, James D. Boyer, Norman E. Phillips, and John Van Curen, "Nature of the Heat Capacity Anomaly in CuMn at T_{sg}," Physica 170B, 633 (1981); LBL-13789.

LBL Reports

1. Norman E. Phillips, "Phason Anomalies in Alkali Metals," LBL-13791.

2. William E. Fogle, James D. Boyer, and Norman E. Phillips, "Verification of a Laboratory Temperature Scale by Heat Capacity Measurements on Copper: The Low-Temperature Heat Capacity of Gold," LBL-13792.

3. James D. Boyer and Norman E. Phillips, "Pressure Dependence of the Low-Temperature Heat Capacity of Teflon," LBL-13794.

4. James D. Boyer, Norman E. Phillips and K. A. Gschneidner, Jr., "Pressure Dependence of the Low-Temperature Heat Capacity of α-Cerium," LBL-13793.

5. James D. Boyer (thesis), "I. The Pressure Dependence of the Low-Temperature Heat Capacity of α-Cerium; II. A Semi-Automatic Low-Temperature Calorimetry System; III. The Pressure Dependence of the Low-Temperature Heat Capacity of Teflon," LBL-13645.

Other Publications

1. W. E. Fogle, E. W. Hornung, M. C. Maybery, and Norman E. Phillips, "Experiments with Powdered CMN Thermometers between 10 mK and 4 K, and a Comparison with an NBS SRM 768 Fixed Point Device," post-deadline paper presented at TL16, Los Angeles, August 1981, LBL-13790.

b. Electrochemical Processes*

Charles W. Tobias, Investigator

Introduction. The purpose of this program is to advance scientific methods for the analysis of scale-dependent cell processes and to provide means by which the design and operation of such processes may be optimized with respect to energy efficiency and capital cost. Physical description and quantitative characterization of transport of charged and uncharged species to and from electrode surface by convective diffusion are core interests. The analysis of high rate processes, such as electromachining and electroforming, is undertaken to point the way to new applications in electrometallurgy. A smaller part of this program is devoted to the exploration of novel electrochemical processes.

1. EFFECTS OF SUSPENDED PARTICLES ON THE RATE OF MASS TRANSFER TO A ROTATING DISK ELECTRODE†

D. J. Roha, R. H. Muller, and C. W. Tobias

Particles of solid nonconducting materials have long been used to promote mass transfer to immersed surfaces. In particular, solids suspended in a liquid rapidly flowing tangentially to a wall can increase the rate of heat and mass transport to the wall many times over the rate in a medium without particles. To facilitate quantitative interpretation of the effect of suspended particles on mass transport to walls, limiting currents for the reduction of ferric cyanide at a rotating disk were determined in the presence of 0-40% by volume of spherical glass beads. Experiments were conducted with six different particle diameters, and with rotation speeds in the range of 387-2700 rpm using both a 0.56-cm and a 1.41-cm radius disk electrode.

It was established that at a given rpm, upon addition of glass beads, the limiting current, i_L, may increase to more than three times its value without solids. This increase in limiting current density is greater at high rotation speeds and with the larger disk electrode. i_L as a function of particle diameter yields a maximum at ~10 μm (Fig. 1). Two mass transfer models are offered to explain this behavior; both assume that the beads are in contact with the disk electrode and moving parallel to its surface. In the "sur-

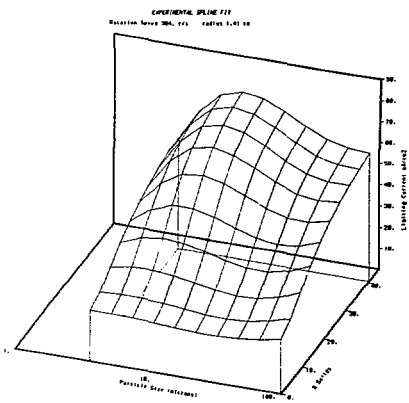

Fig. 1. Experimental limiting current density as expressed by the cubic spline function of volume fraction solids and particle size at 304 radians/s disk rotation speed. (XBL 8011-12779)

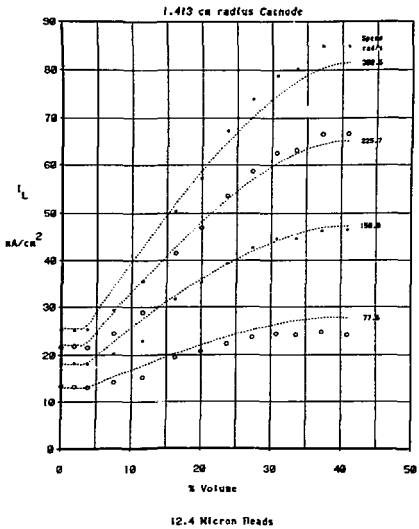

Fig. 2. Experimental data points and the limiting current density predicted by the particle film model as a function of volume concentration glass beads. (XBL 815-9642)

*This work was supported by the Director, Office of Energy Research, Office of Basic Energy Sciences, Materials Sciences Division of the U.S. Department of Energy under Contract No. DE-AC03-76SF00098.

face renewal" model it is assumed that complete mixing takes place with the passage of each bead and the boundary layer is replaced with fresh bulk solution; while with the "particle film" model it is assumed the bead and a clinging film of fluid rotate together. The film promotes mass transfer by alternately adsorbing and desorbing the diffusing species. The "particle film" model best explains the observed behavior of the limiting current density (Fig. 2).

Calculations of required stirring power, versus observed i_L, show that adding beads to increase i_L consumes far less additional power than does increasing the rotation speed.

* * *

†Brief version of LBL-12737.

2. ELECTROCHEMICAL MACHINING OF CEMENTED TITANIUM CARBIDE†

Corinne Coughanowr, R. H. Muller and C. W. Tobias

Titanium carbide has become important in industrial applications for its qualities of low density, high hardness, superior oxidation resistance, and the retention of these qualities at elevated temperatures (1000°C). Since the pure compound is very brittle, a binder is added to impart toughness and impact resistance; nickel is frequently chosen as the binder. The feasibility of using electrochemical machining (ECM) to shape pure titanium carbide has been established in previous work.[1] In the present study the ECM of a cemented TiC/Ni composite, containing nominally 10% Ni, has been investigated and compared to the ECM of the pure components, TiC and nickel. The objectives were to see whether the ECM behavior of the composite could be predicted from its components and to determine what the optimum ECM conditions for yielding a smooth surface finish on TiC/Ni might be.

Cylindrical cavities were electrochemically machined in the three materials with applied voltages of 10-24, and toolpiece advancement rates of 0.2 to 1.2 mm/min. Overvoltage and valence of dissolution were derived from electrical measurements; surface topography, and composition were investigated by means of scanning electron microscopy, energy dispersive x-ray analysis, and scanning Auger microanalysis.

The valences of dissolution were determined to be 3.0, 6.6 and 6.5 for nickel, TiC, and TiC/Ni respectively. All three materials yielded straight-line polarization curves, indicating active dissolution. Overvoltages were 0.7 volts for nickel, 4.2 volts for TiC, and 3.0 volts for TiC/Ni.

There was evidence of an oxide layer after ECM on nickel and on TiC/Ni, but not on TiC. Nickel content on the surface of the composite was higher after ECM than before. Light regions in the SEM micrograph (Fig. 1(a)) are rich in nickel (Fig. 1(b)). A porous, nickel-rich layer results from the preferential dissolution of the TiC phase over the Ni phase over the entire range of ECM conditions investigated. It therefore does not appear that ECM operating conditions can be found which yield a very smooth surface finish.

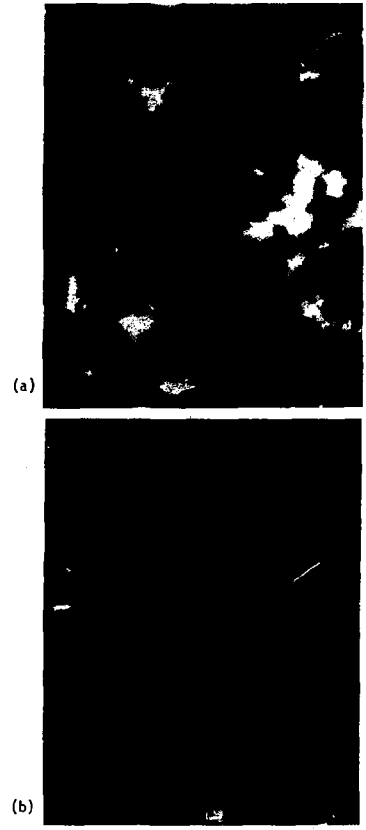

Fig. 1. Surface at bottom of hole drilled electrochemically in TiC/Ni, at 15 V applied voltage and 0.5 mm/min toolpiece advancement rate; (a) SEM micrograph at 10,000x, (b) x-ray map for nickel, corresponding to (a).
((a) XBB 810-11349; (b) XBB 810-11351)

* * *

†Short version of LBL-13682.

1. B. A. Dissaux, "Electrochemical Machining of Carbides and Borides," M. S. Thesis, University of California, Berkeley (1978), LBL-8023.

3. A STUDY OF ELECTROPOLISHING OF FERROUS ALLOYS USING ROTATING DISK ELECTRODES

T. Hryniewicz, R. H. Muller and C. W. Tobias

Electropolishing of most nonferrous metals and stainless steels produces smooth, bright, and reflective surfaces that exhibit superior corrosion resistance compared to untreated metals. These features may be achieved with plain carbon or low-alloy steels. This project was aimed at the elucidation of electropolishing of ferrous materials ranging from pure iron through carbon steels, with increasing carbon content, to a few low-alloy steels. The characteristics of electropolishing stainless and acid-proof steels are well known, and for this reason were not considered in this research.

A rotating disk electrode system has been used to study surface layer formation during ECP in order to control the mass-transport process. The experiments included polarization measurements and dissolution in different parts of the polarization curve (on the plateau c.d. and higher). Investigations were carried out over wide ranges of applied current density, mass loss, and current efficiency.[1] Changing the rotating speed of the sample influences the current density in potentiostatic operations, resulting in different surface finishes. At low potentials, the dissolution results in etched surfaces. Electropolishing conditions may result even at high rotating speeds (above 3000 rpm), which indicates that a viscous layer is not a necessary criterion for the process to occur.

Microscopic observations showed that, contrary to what has been reported in the literature, there is no direct relation between the carbon content in steel and the surface finish after electropolishing. Composition of the surface layer before and after electropolishing has been evaluated using Auger spectroscopy. Surface layers formed on carbon steel under electropolishing conditions are 15 to 20 times thinner than those formed under etching conditions. As expected, after electropolishing, oxygen is the dominant component in the top 10 Å.

* * *

1. T. Hryniewicz, R. H. Muller and C. W. Tobias, "A Study of Electropolishing of Ferrous Alloys Using Rotating Disk Electrodes." LBL-12879 (June 1981).

1981 PUBLICATIONS AND REPORTS

Refereed Journals

1. J. B. Riggs, R. H. Muller and C. W. Tobias, "Prediction of Work Piece Geometry in Electrochemical Cavity Sinking," Electrochimica Acta 26, 961-969 (1981).

2. C. W. Tobias, "The Coming of Age of Electrochemical Engineering," AIChE Symposium Series 204, 77 (1981).

†3. C. W. Tobias and H. H. Law, "The Morphology of Potassium Deposited from Propylene Carbonate Electrolyte," Proceeedings of the Symposium on Electrocrystallization, Rolf Weil, editor, Proceedings vol. 81-6, The Electrochemical Society, June, 1981.

‡4. P. C. Foller and C. W. Tobias, "The Effect of Electrolyte Anion Adsorption on Current Efficiencies for the Evolution of Ozone," J. Phys. Chem. 85, 3238 (1981) [Joel H. Hildebrand Centennial Issue].

LBL Reports

1. P. J. Sides (with C. W. Tobias), "Bubble Dynamics at Gas Evolving Electrodes," Ph.D. dissertation, University of California, Berkeley, LBL-11849.

†2. G. A. Prentice, "Modeling of Changing Electrode Profiles," Ph.D. dissertation, University of California, Berkeley, LBL-11694, December 1980.

†3. G. A. Prentice and C. W. Tobias, "A Survey of Numerical Methods and Solutions of Current Distribution Problems," accepted for publication in the Journal of the Electrochemical Society, LBL-12191, January 1981.

†4. G. A. Prentice and C. W. Tobias, "Finite Difference Calculation of Current Distributions at Polarized Electrodes," accepted for publication in the AIChE Journal, LBL-11058.

†5. G. A. Prentice and C. W. Tobias, "Deposition and Dissolution on Sinusoidal Electrodes," accepted for publication in the Journal of the Electrochemical Society, LBL-12167, January, 1981.

†6. G. A. Prentice and C. W. Tobias, Simulation of Changing Electrode Profiles," accepted for publication in the Journal of the Electrochemical Society, LBL-12192, January 1981.

7. C. W. Tobias, F. McLarnon and R. H. Muller, "Interferometric Study of Combined Forced and Natural Convection," Journal of the Electrochemical Society (LBL-13032 preprint), July, 1981.

8. C. W. Tobias and P. J. Sides, "Resistance of a Planar Array of Spheres; Gas Bubbles on an Electrode," submitted to the Journal of the Electrochemical Society, LBL-11849.

9. T. Hryniewicz, R. H. Muller and C. W. Tobias, "Electropolishing of Steel Rotating Disk Electrodes, LBL-12879, July, 1981.

10. T. Tsuda and C. W. Tobias, "The Influence of Lead Ions on the Macromorphology of Electrodeposited Zinc," M. S. thesis, University of California, Berkeley (1981), LBL-13057.

†11. A. Kindler (with C. W. Tobias), "The Morphology of Electrodeposited Copper," Ph.D. dissertation, University of California, Berkeley (1981), LBL-12838.

†12. P. Cettou and C. W. Tobias, "Bubble Dynamics at Electrode Surfaces," LBL-13632, December 1981.

13. C. Coughenowr (with R. H. Muller and C. W. Tobias), "Electrochemical Machining of Cemented Titanium Carbide," M.S. thesis, University of California, Berkeley, December 1981, LBL-13682.

Other Publications

Book Edited

H. Gerischer and C. W. Tobias, Advances in Electrochemistry and Electrochemical Engineering, Wiley-Interscience, New York, vol. 12, November 1981.

Patent Applications Filed by the Regents of the University of California

1. Electrolytic Process for the Production of Ozone (serial No. 06/154,584) U. C. File: 89-79. Filed May 29, 1980, amended July 17, 1981.

2. Improved Electrodes for Ozone Production (Serial No. 263,155) U. C. File 14-81. Filed May 21, 1981.

3. Improved Electrolytic Process for the Production of Ozone. A single patent application, "Improved Electrolytic Process for the Production of Ozone" corresponding to the above two applications was filed in the European Patent Office, designating all member countries, except Luxemberg, No. 81302353.B, June 10, 1981. Canadian patent application for the above was also filed in May 1981. Patent No. 1 lists as co-inventors P. C. Foller and C. W. Tobias. Patents No. 2 and 3 list as co-inventors P. C. Foller, M. L. Goodwin, and C. W. Tobias.

Invited Talks

†1. R. T. Atanasoski, H. H. Law and C. W. Tobias, "Determination of Water in Propylene Carbonate Electrolytes by Cyclic Voltametry," Meeting of the Electrochemical Society, Minneapolis, Minn., May 10-15, 1981; Extended Abstracts, vol. 81-1, no. 392, p. 985-986 (based on LBL-11847).

2. P. J. Sides and C. W. Tobias, "A Close View of Gas Evolution," invited paper, Meeting of the Electrochemical Society, Minneapolis, MN, May 10-15, 1981; Extended Abstracts, vol. 81-1, no. 392, p. 985-986 [based on LBL-11849].

†3. P. C. Foller and C. W. Tobias, "The Effect of Electrolyte Anion Adsorption on Current Efficiencies for the Evolution of Ozone," invited paper, Meeting of the Electrochemical Society, Minneapolis, MN, May 10-15, 1981; Extended Abstracts, vol. 81-1, no. 478, p. 1182-83.

4. C. W. Tobias, "Electrochemical Engineering of Batteries," invited lecture, Short Course, Continuing Education Institute, Cherry Hill, NJ, June 22-26, 1981.

5. C. W. Tobias, "Prospects of the Electrochemical Technology," invited lecture, W. R. Grace Research Center, Columbia, MD, September 18, 1981.

†6. Philippe Cettou and C. W. Tobias, "The First Generation of Bubbles on Gas-Evolving Electrodes," contributed paper, Meeting of the Electrochemical Society, Denver, CO., October 11-16, 1981; Extended Abstracts, vol. 81-2, no. 584, p. 1401 [based on LBL-13632].

†7. H. H. Law and C. W. Tobias, "The Cathodic Overpotential of Potassium in $KAlCl_4$-Propylene Carbonate Electrolyte," contributed paper, Meeting of the Electrochemical Society, Denver, CO., October 11-16, 1981; Extended Abstracts, vol. 81-2, no. 585, p. 1403 [based on LBL-11487].

8. C. W. Tobias, "On the Nature of Electrolytic Gas Evolution," invited lecture, Department of Chemical Engineering, University of Houston, November 6, 1981.

* * *

†Supported by the Division of Electrochemical Systems Research, Office of Conservation and Renewable Energy, U. S. Department of Energy.
‡Supported entirely from University funds.

2. High Temperature and Surface Chemistry

a. High Temperature Thermodynamics*

Leo Brewer, Investigator

Introduction. High temperature chemistry is characterized by the occurrence of unusual species and phases that are often unstable at conventional temperatures. Because of the difficulty of carrying out measurements under conditions where it is often difficult to contain the materials and to avoid contamination, it is important to design experiments to yield information that can be used with predictive models. In this manner, one can often calculate chemical behavior under conditions where measurements have not been made or would not be practical.

In the past, our research has aimed mostly at improving our understanding of the behavior of gases at high temperatures and of refractory containment materials. At present, our main thrust is aimed at improving our understanding of the thermodynamics of metallic alloys. For many alloys, we have a good understanding of the interactions and have quantitative predictive models which alow prediction of the behavior of unstudied alloys. As an example, last year, we published a tabulation of the thermodynamic properties and phase diagrams of one hundred binary systems of molybdenum. However, there are some systems for which our understanding is not adequate to allow such quantitative predictions. Our research is aimed at such systems.

Although we will report on other studies, our main thrust at present is to characterize the very stable intermetallic compounds that result from the reaction of transition metals from the left hand side of the periodic table, which do not have enough electrons to use all of their bonding orbitals, with transition metals from the right hand side, which have so many valence electrons that they are paired in nonbonding orbitals. Our earlier studies have demonstrated the vigor of such reactions and the unusual properties of the resulting phases. It has been difficult to find reliable methods of determining the thermodynamic properties of these phases. Ordinary calorimetric methods are unusable because of the insolubility of the phases. A variety of other techniques have been considered. Each has posed severe experimental problems under the conditions that must be used. The several methods being used will be described below.

*This work was supported by the Director, Office of Energy Research, Office of Basic Energy Sciences, Materials Science Division of the U. S. Department of Energy under Contract No. DE-ACD3-76SF00098.

1. USE OF GASEOUS EQUILIBRATION TO CHARACTERIZE STABILITY OF STRONGLY INTERACTING INTERMETALLIC PHASES†

Bea-Jane Lin, John Gibson, and Drucilla G. Davis

Oxides such as Ta_2O_5 in equilibrium with H_2O/H_2 gaseous mixtures or nitrides such as ZrN in equilibrium with N_2 gas provide systems with known activity of the metal when thermodynamic data for the oxides or nitrides are available. The determination of the composition of a binary alloy, e.g., $TaIr_x$ in equilibrium with a given H_2O/H_2 ratio provides a value of the activity and activity coefficient of the tantalum in that composition. The values obtained by gaseous equilibration can also be checked for single compositions by equilibration of graphite and a metal carbide, e.g., ZrC, with an alloy such as $ZrRh_x$. Even the gaseous equilibration method is limited to a rather narrow range of compositions for the strongly interacting acid-base phases resulting from the interaction of a transition metal like Ta with vacant d orbitals with a metal like Ir with nonbonding electron pairs because the activities change very rapidly with composition for such systems.

It is important to have such methods to provide checks of EMF measurements made using high temperature solid electrolyte cells which can cover a wide composition range. There are unsuspected systematic errors in the EMF measurements which are often difficult to detect. We are trying to obtain independent checks of EMF measurements using thoria and zirconia electrolytes. It would be desirable to carry out experiments at as low a temperature as possible because the accuracy of measurements decreases as the temperature increases. A thermal balance was used to carry out gaseous equilibration between H_2O/H_2 gas and Ta_2O_5/Ta at temperatures up to 1000°C. However, it was found that equilibration was too slow for these refractory systems and it has been necessary to go to higher temperatures. For some of the systems involving equilibration with graphite or with nitrogen, even temperatures close to 2000°C were inadequate. By use of a graphite tube furnace that can be operated between 2000 and 2500°C, it has been possible to obtain satisfactory values for a variety of transition metal systems.

However, in view of the limited range that can be covered with nitrogen equilibration, we are taking the next step of measuring the equilibrium pressures of the metallic gaseous atoms using a mass spectrometer in the laboratory of Professor Karl Gingerich of Texas A&M University. Data gathered by these various methods should allow us to develop models that will yield predictions of practical accuracy for even the most strongly interacting systems.

* * *

†Taken in part from LBL-13466 (Bea-Jane Lin).

2. GRADIENT FURNACE USE FOR DETERMINATION OF THE HEXAGONAL PHASE STABILITY IN THE COBALT-MOLYBDENUM SYSTEM†

Drucilla G. Davis and Michael Cima

Developing from the ideas of Lewis, Pauling, and Hume-Rothery, N. Engel has presented a theory of metallic bonding that has been very fruitful in providing reliable predictions of transition metal phase diagram behavior. However, objections have been raised to two important aspects of the Engel theory: (1) the extensive promotion of electrons from the ground state of the gaseous atom with increase of the number of bonding electrons, e.g., $3d^7 4s^2$ to the valence state d^6sp for hcp Co and $d^{5.5}sp^{1.5}$ for ccp Co, and (2) the transfer of electrons from less electropositive to more electropositive metals for generalized-Lewis-acid-base reactions. From consideration of the relationship between s,p electron concentrations and the crystal structure and the transfer of electrons from Co to Mo, the Engel theory predicts that addition of Mo should stabilize hcp Co over ccp Co. The presently accepted phase diagram for the Co-Mo system is in contradiction to the prediction in that no stabilization of hcp Co is shown.

The system is difficult to study at the temperature of the hcp-ccp transformation because of slow equilibration. At too high a temperature where equilibration could be rapid, the hcp phase is unstable. At too low a temperature, equilibration is too slow, and that is why previous investigators have missed the stability range of the hcp phase in the Co-Mo system. To find this range, a gradient furnace was used in which samples could be heated along a gradient to find the region in which equilibration could be obtained. Liquid fluxes were used to catalyze the equilibration. Our experiments clearly show that Mo increases the stability range of hcp Co from an upper limit of 427°C for pure Co to 849°C upon addition of 5 at% Mo in confirmation of the predictions of the Engel theory.

The combination of the gradient furnace with addition of catalysts to accelerate equilibration will be used for other sluggish systems. The temperature at which Mo_2S_3 decomposes to Mo and MoS_2 is very uncertain. These techniques are now being used to fix the stability range of Mo_2S_3.

* * *

†Brief version of LBL-13243.

3. WORK IN PROGRESS

Measurements of thermodynamic activity in the range 1500 to 2500°C will continue using carbide and nitride equilibria as well as mass spectroscopic measurements for intermetallic alloys. These results will be used to check the EMF measurements using solid electrolyte cells at temperatures around 1000°C. As the data accumulate, they will be combined with phase diagram information to completely elucidate the thermodynamic behavior of key transition metal systems. When necessary, portions of phase diagrams will be characterized using x-ray diffraction and metallographic techniques as well as the gradient furnace technique. The experimental program will be integrated with extensions of the Engel theory of metals to the quantitative characterization of strongly interacting acid-base phases and to predictions of a variety of properties of the transition metal systems.

1981 PUBLICATIONS AND REPORTS

Refereed Journals

†1. G. M. Rosenblatt, "Estimation of Activity Coefficients in Concentrated Sulfite-Sulfate Solutions," AIChE Journal 27, 619-26 (1981).

LBL Reports

†1. Bea-Jane Lin (Ph.D. thesis), "Solid-Gas Equilibria in $CaSO_3$-H_2O System and Lewis-Acid-Base Alloys," LBL-13466.

2. Drucilla G. Davis (Ph.D. thesis), "The Hexagonal Close Packed Phase Stability in the Cobalt-Molybdenum System: Further Confirmation of the Brewer-Engel Theory," LBL-13243.

3. Leo Brewer, "Estimation of Thermodynamic Data and Phase Diagrams Using HP-65 Calculator Programs," LBL-4994.

†4. Leo Brewer, "Thermodynamic Data for Flue-Gas Desulfurization Processes," LBL-11758.

5. M. Salmeron, L. Brewer, and G. A. Somorjai, "The Structure and Stability of Surface Platinum Oxide and of Oxides and Other Noble Metals," LBL-12411.

Other Publications

1. Leo Brewer, "Bibliography on the High-Temperature Chemistry and Physics of Materials, Vol. 25, Part 2, Gases: (A) Spectroscopy of Interest to High-Temperature Chemistry, and (B) Reactions Between Gases and Condensed Phases," published by IUPAC Commission on High Temperatures and Refractory Materials, edited by M. G. Hocking and V. Vasantasree, London, 1981.

2. L. Brewer, Editor, Proceedings of Flue-Gas Desulfurization Conference, Morgantown, West Virginia, November 6-7, 1980, 363 pp., CONF-801176, September, 1981 and author of paper no. 16, pp. 303-55; also available as LBL-11758 as listed above.

†3. Gerd Rosenblatt, "The Use of Pitzer's Equations to Estimate Activity Coefficients in FGD Scrubber Systems," paper no. 15, pp. 266-302, in Proceedings of Flue-Gas Desulfurization Confer-

ence, Morgantown, West Virginia, November 6-7, 1980, CONF-801176, September, 1981.

4. Leo Brewer, "Compilation of Thermodynamic and Phase Information for the Binary Systems of Molybdenum," Bulletin of Alloy Phase Diagrams 1(2), 40-2 (1980).

5. Leo Brewer, "The Role and Significance of Empirical and Semiempirical Correlations," Structure and Bonding in Crystals, Vol. I, Academic Press, 1981, LBL-10736.

Invited Talks

†1. L. Brewer, "Thermodynamic Values for Desulfurization Processes," American Chemical Society Symposium, March 29-31, 1981, Atlanta, Georgia.

2. L. Brewer, "Teaching Thermodynamics Backwards," American Chemical Society Symposium, March 29-31, 1981, Atlanta, Georgia.

3. L. Brewer, "Abnormal Properties of the Transition Metals and Their Alloys," Symposium on Thermochemistry of Intermetallic Compounds, The Electrochemical Society, May 10-12, 1981, Minneapolis, Minnesota.

4. L. Brewer, "Frontiers in Chemical Research" Lectures, Texas A&M University, College Station, Texas, September 21-25, 1981.

5. D. Davis, "The Cobalt-Molybdenum Binary System," Bay Area High Temperature Science and Technology Conference, Ames Laboratory, Moffett Field, California, October 29, 1981.

* * *

†This work was supported by the Assistant Secretary for Fossil Energy, Office of Coal Research, Advanced Environment Control Division of the U. S. Department of Energy under Contract No. DE-AC03-76SF00098 through the Morgantown Energy Technology Center, Morgantown, WV.

b. Chemistry and Materials Problems in Energy Production Technologies*

Donald R. Olander, Investigator

Introduction. The objective of this project is to obtain basic understanding of several technological problems that are encountered in energy production systems, with principal emphasis on fission reactors. The specific projects deal with the behavior of uranium dioxide, Zircaloy cladding, and fission products of reactor fuel elements, the performance of nuclear waste repositories in salt deposits and the chemistry of silicon single crystal growth by pyrolysis of silane. High-temperature mass spectrometry is utilized in many of the studies.

This experimental program is moving toward chemical and materials problems of concern in nuclear reactor safety. These include the oxidation of Zircaloy by steam-hydrogen mixtures, the reaction of molten Zircaloy and uranium dioxide, surface diffusion on UO_2, vaporization of UO_2 containing simulated fission products, the chemical nature of cesium and iodine released from irradiated fuel, and stress corrosion crack propagation in Zircaloy.

1. WATER AND BRINE MOVEMENT IN SALT CONTAINING NUCLEAR WASTES†

Donald R. Olander

This project analyzes the effect of thermal loading on the performance of repositories for disposal of high level nuclear wastes in geologic salt formations. The object of the analysis is to predict the amount of water and/or brine transported to the drillhole containing the nuclear wasteform.

Both brine inclusion migration and vapor transport by Knudsen and bulk diffusion in interconnected porosity are treated. Inclusions move under the influence of the temperature gradient to the grain boundary, where they are trapped and deliver their brine to the interconnected pores. Further transport of water occurs via the vapor phase in the pores. During nuclear heating, the porosity can change because of the trapping of inclusions from within the salt crystals and by thermomechanical effects (thermal and lithostatic stresses and creep consolidation).

The calculations show that the most important parameters affecting water release are the extent of porosity closure by thermomechanical effects, the permeability of the salt to gas, and the fraction of the intra- and intergranular brine that communicates with the interconnected pores. Judicious choice of the parameters produces water release rates that are comparable to those observed in field tests.

* * *

†Summary of paper submitted to Nucl. Technol. (LBL-13652). This work was partially supported by the Office of Nuclear Waste Isolation of the DOE.

2. THERMOCHEMISTRY OF FISSION PRODUCTS IN REACTOR FUEL RODS†

Rajiv Kohli

The chemical interactions between fission products, fuel, and cladding are important in assessing the mechanism of pellet-cladding interaction (PCI), which occasionally afflicts the fuel rods of light water reactors. To accomplish this assessment, the thermochemistry of the possible reactions of fission products with each other, the fuel, and the Zircaloy cladding must be understood for intact fuel rods.

Using available thermomechanical data and measured in-reactor oxygen potentials (-90 to -130 kcal/mole) equilibrium calculations have been performed for the most plausible reactions involving the fission products Cs, Rb, I, Br, Se, Te, Mo, Zr, and Ba.

The calculations show that the alkali metals will react with the fuel to form ternary oxides; in addition, Cs and Rb can form compounds with the halogens, molybdenum and zirconium. In particular, the high vapor pressures of the molybdates of the alkali metals provides a means of transporting Mo to the cladding where it can cause embrittlement.[1] The calculations also suggest that the role of the halogens (especially iodine) in PCI fuel rod failures may be less important than current theories suggest. Cesium and rubidium zirconates are predicted to exist in the fuel-cladding gap. Te and Se are most likely to move to the cladding as elements.

* * *

†Brief version of paper published Proc. Carl Wagner Symp. on Metall. Thermochemistry and Electrochemistry (June 1981).

1. R. Kohli and F. Holub, J. Nucl. Mater. 9B, 116 (1981).

3. FISSION PRODUCT BEHAVIOR IN REACTOR FUEL RODS UNDER ACCIDENT CONDITIONS†

Rajiv Kohli

Fission product release from fuel elements in which the cladding has been ruptured provides the source term that drives calculations of the radio-

*This work was supported by the Director, Office of Energy Research, Office of Basic Energy Sciences, Materials Sciences Division of the U.S. Department of Energy under Contract No. DE-AC03-76SF00098.

logical consequences of such an accident. The chemical form of the fission products can be established by thermochemistry if the environment at the point of release is specified (i.e., whether or not liquid water is present and if not, the magnitude of the oxygen potential of the vapor phase contacting the fuel). The analysis thus encompasses gas-solid thermochemistry as well as the aqueous chemistry of fission product species in high temperature high pressure water.

The gas-solid calculations are similar to those described in the preceding summary, except that higher oxygen potentials are chosen to represent the following accident conditions: 1) water/steam/hydrogen with oxygen potentials from -90 to -65 kcal/mole; 2) steam/air with an oxygen potential of -20 kcal/mole; and 3) air with an oxygen potential of -3 to -20 kcal/mole. When liquid water contacts the ruptured rod, the aqueous thermochemistry of the fission products is treated by constructing Eh-ph diagrams for the temperature range 50-600 K.

Based on these calculations, Cs and Rb hydroxides, molybdates, and iodides are predicted. Tellurium appears as $TeO(OH)_2$ and Ru and Mo appear as the trioxides. Only under very oxidizing conditions does iodine remain in elemental (and hence very mobile) form.

* * *

†Summary of work reported in Trans. Amer. Nucl. Soc. 39, 384 (1981) and to be reported at the Electrochemical Society meeting Montreal, May 1982.

4. EXTRAPOLATION OF LOW TEMPERATURE VAPOR PRESSURE DATA OF URANIUM CARBIDE TO THE LIQUID REGION†

F. Tehranian and D. R. Olander

Knowledge of the high temperature thermodynamic properties of refractory nuclear ceramics is necessary for assessing the consequences of potential accidents involving fuel melting. Methods of extrapolating the partial vapor pressures of the gaseous uranium oxides from measurements over $UO_2(s)$ through the melting point into the liquid region have been developed, but comparable treatment of uranium carbides has not been reported.

In this work the liquid uranium carbide was considered as a nonideal molecular solution of U, UC and UC_2. Nikol'skii's[1] result for the solid UC was then modified to estimate uranium pressures and carbon activities in the liquid region. Partial molar thermodynamic parameters for the components in the liquid are assumed to differ from those in the solids by the entropy of fusion of each. The standard free energies of formation of the gaseous compounds were used to calculate the composition of the vapor.

The equations derived give the partial pressures of each species, the total pressure, and the carbon-to-uranium ratio in the vapor phase as functions of temperature and carbon-to-uranium ratio in the liquid. Good agreement with the P_{tot}-T estimates by Finn et al.[2] was found.

* * *

†Summary of paper submitted to High Temp. Sci. (LBL-13345)

1. S. S. Nikol'skii, Teplofiz, vys. Temp. 7, 873 (1969)
2. P. A. Finn et al., Proc. of Topical Meeting on Advanced LMFBR Fuels, p. 189, Tuscon, AZ, Oct. 1977.

5. THE ZIRCONIUM-IODINE REACTION BY MODULATED MOLECULAR BEAM MASS SPECTROMETRY

Mehdi Belooch

Pellet-cladding interaction (PCI) failures in a light water reactor (LWR) tend to occur in rods that have been irradiated to significant burnup and then subjected to power increases. It is believed that this type of failure is due to stress corrosion cracking (SCC) of the cladding. The chemical substances responsible for this kind of failure have not yet been positively identified. However, iodine, an abundant fission product, has long been known to promote SCC of Zircaloy at reactor operating temperatures and is suspected to be the species involved in PCI-SCC cladding failures.[1] Although the mechanical aspects of iodine SCC have been widely investigated, little information is available on the kinetics and mechanism of the zirconium-iodine reaction.

A modulated beam of iodine was directed against a zirconium target in an ultra high vacuum system. The reflected reactant and reaction products were detected with a mass-spectrometer and processed by lock-in amplifier to determine the apparent reaction probability and the phase lag, from which the desired reaction kinetic information was extracted. The beam intensity, modulation frequency as well as target temperature could be varied.

Figure 1 shows the apparent reaction probability and phase lag as a function of zirconium target temperature at fixed modulation frequency and beam intensity. Zirconium tetraiodide and atomic iodine were the only detectable reaction products. The apparent reaction probability of ZrI_4 goes through a maximum at about 600 K. The decline in the reactivity at lower temperatures is partially due to the demodulation effect. The iodine atom signal increases with temperature and levels off at about 850 K. These results demonstrate that iodine volatizes zirconium with very high efficiency at temperatures of importance in fuel element operation (600 K). Consequently, removal of zirconium by iodine could be an important aspect of stress corrosion cracking of Zircaloy cladding.

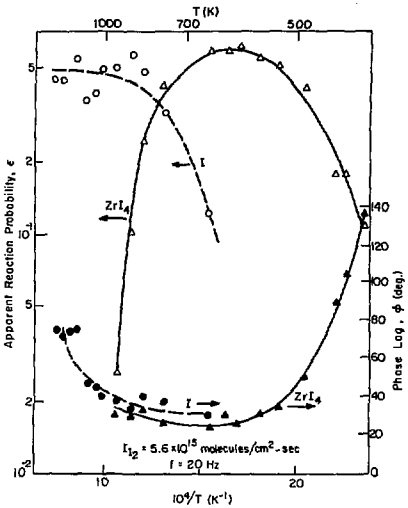

Fig. 1. Reaction probabilities and phase lags for ZrI_4 and I products of the Zr/I_2 reaction.
(XBL 8112-13162)

* * *

1. J. T. A. Roberts, E. Smith, N. Furhrman, and D. Cubicciotti, Nucl. Technol., 35, 131 (1977)

6. THE KINETICS OF LASER PULSE VAPORIZATION OF URANIUM DIOXIDE BY MASS SPECTROMETRY†

Chuen-horng Tsai and D. R. Olander

Safety analyses of nuclear reactors require knowledge of the evaporation behavior of UO_2 at temperatures well above the melting point, 3140 K. Currently used in analyses are the extrapolations from the static measurements performed well below the temperature range of interest, based upon a few thermophysical or thermochemical models.

In this study, sub-millisecond transient heating of a small spot on a UO_2 specimen was accomplished by laser pulsing, which generates surface temperature excursions with maxima ranging from 3700 to 4300 K. The surface temperature transient was monitored by a fast-response automatic optical pyrometer. A computer program was developed to simulate the laser heating process and to calculate the surface temperature evolution.[1] As a result of surface heating, the solid vaporizes. A quadrupole mass spectrometer was used to identify and analyze the major vapor species and to measure the rate of evaporation from the target surface. The partial vapor pressure of each species in the vapor jet was obtained.

For the partial pressure of UO_2, the pressure-temperature data shown in Fig. 1 fall inside the confidence limits recommended on the literature assessment report.[2] The vapor pressure and the vapor composition deduced from the experiments favor Blackburn's model[3] for calculating the equilibrium partial pressure of each species. The data also suggest that equilibrium vaporization based on the Hertz-Langmuir equation, after taking into account the oxygen depletion on the surface, successfully describe the transient vaporization process. The measured time-of-arrival and the width of the mass spectrometric signals agree better with a free molecular model (collisionless expansion) than with a hydrodynamic model (collision-dominated continuum flow). The fact that no dimers were measured also suggests that collisions are negligible in the expansion into vacuum. The degree of ionization in the hot vapor, which was estimated from the mass spectrometer measurement of thermionic ions, is in good agreement with the calculation from Saha's equation and effective "un-isolated" ionization potential.[4]

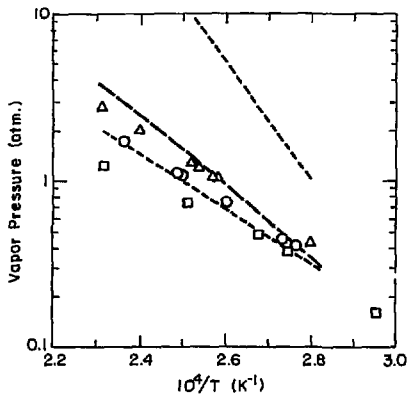

Fig. 1. The pressure-temperature relation for UO_2.
Blackburn's Model for UO_2 partial pressure.[3]
▬ ▬ Recommended limits of total vapor pressure in Ref. 2.
△ This work fitted to log p = 26.81 - 26089/T - 5.594 log T for UO_2 partial pressure (calculated temp).
○ This work fitted to log p = 24.22 - 24238/T - 5.033 log T for UO_2 partial pressure (measured temp).
□ Mach disk photographic measurements for total pressure (measured temp).
(XBL 8112-13163)

* * *

†Brief version of LBL-13679.

1. C. H. Tsai, LBL-12125, Jan. 1981.
2. IAEA Specialists' Meeting on Equations of State of Materials of Relevance to the Analysis of HCDA, IWGFR/26, June 1978.
3. P. E. Blackburn, J. Nucl. Mater. 46, 244 (1973).
4. H. U. Karow, KfK - 2390, Feb. 1977.

1981 PUBLICATIONS AND REPORTS

Refereed Journals

1. D. R. Olander, "Interpretation of Tracer Surface Diffusion Experiments on UO_2 - Roles of Gas and Solid Transport Processes," J. Nucl. Mater. 90, 243 (1981).

2. S. Shann and D. R. Olander, "Correlation of Failure Times for Iodine Stress Corrosion Cracking of Zircaloy," Nucl. Technol. 53, 407 (1981).

3. Rosa Yang and D. R. Olander, "Behavior of Metallic Inclusions in Uranium Dioxide," Nucl. Technol. 54, 223 (1981).

4. D. R. Olander, A. J. Machiels and E. Muchowski, "Migrations of Gas-Liquid Inclusions in Single Crystals of Potassium and Sodium Chlorides," Nucl. Sci. and Engr. 79, 212-227 (1981).

5. D. R. Olander, "The Theory of Uranium Enrichment by the Gas Centrifuge," Prog. in Nucl. Energy, 8, 1-33 (1981).

6. R. Kohli, "Chemical Thermodynamics of Complex Systems: Fission Product Behavior in LWR Fuel Elements," in Proc. Carl Wagner Symposium on Met. Thermo and Electrochem, N. A. Gokcen, ed., 309-326, Met. Soc. AIME, June 1981.

LBL Reports

1. R. Kohli, "Reaction Behavior of Zircaloy With Simulated Fission Products," LBL-12069 (Jan. 1981).

2. R. Kohli, "Oxygen Embrittlement of Zircaloy-2 on Long-Term Exposure to Alkaline Earth and Rare Earth Oxides," LBL-12993 (July 1981).

3. R. Kohli, "The Effects of Long-Term Exposure to Simulated Fission Products on the Properties of Zircaloy-2," LBL-13205 (Aug. 1981).

4. R. Kohli, "The Production of Titanium From Ilmenite: A Review," LBL-13705 (Dec. 1981).

5. C. H. Tsai, "Numerical Simulation of Transient, Incongruent Vaporization Induced by High Power Laser Irradiation," LBL-12125 (Jan. 1981).

6. D. R. Olander, "VAPMIG - A Model of Brine Migration and Water Transport in Rock Salt Supporting a Temperature Gradient," LBL-13562 (Nov. 1981).

7. F. Tehranian and D. R. Olander, "Extrapolation of Low Temperature Vapor Pressure Data of Uranium Carbide to the Liquid Region," LBL-13345 (Sept. 1981).

8. D. R. Olander, A. J. Machiels, M. Balooch, and S. Yagnik, "Thermal Gradient Migration of Brine Inclusions in Synthetic Alkali Halide Single Crystals," LBL-12163 (Jan. 1981).

9. D. R. Olander, "A Mechanistic Analysis of Ruthenium Transport in UO_2," LBL-12550 (April 1981).

10. S. H. Shann, "Radiation Enhancement of Stress Corrosion Cracking of Zircaloy," LBL-13200 (Sept. 1981).

11. C. H. Tsai, "The Kinetics of Laser Pulse Vaporization of Uranium Dioxide by Mass Spectrometry," LBL-13679 (Nov. 1981).

Other Publications

1. S. Y. Zhou and D. R. Olander, "The Redistribution of Ruthenium in UO_2 in a Temperature Gradient," Trans. Amer. Nucl. Soc. 38, 314 (1981).

2. A. J. Machiels, S. Yagnik, and D. R. Olander, "Thermomigration of Two-Phase Inclusions in Salt," Trans. Amer. Nucl. Soc. 38, 168 (1981).

3. D. R. Olander, A. Machiels, S. K. Yagnik, and R. Kohli, "The Mechanism of Intragranular Migration of Brine Inclusions in Salt," Trans. Amer. Nucl. Soc. 38, 169 (1981).

4. K. C. Kim and D. R. Olander, "Oxygen Diffusion in UO_{2-x}," Trans. Amer. Nucl. Soc. 39, 382 (1981).

5. R. Kohli, "A Thermodynamic Assessment of the Behavior of Cesium and Rubidium in Reactor Fuel Elements," in Proc. Intl. Seminar on Materials Behavior and Physical Chemistry in Liquid Metal Systems, Karlsruhe, West Germany, 1981.

6. R. Kohli, "Behavior of Fission Products in LWR Fuel Rods Under Accident Conditions," Trans. Amer. Nucl. Soc. 39, 384 (1981).

7. R. Kohli, "A Thermodynamic Analysis of Fission Product Reaction Behavior in Reactor Fuel Elements," Electrochem. Soc. Extended Abstracts, 81, 856 (1981).

Invited Talks

1. D. R. Olander and S. H. Shann, "Iodine and Metal Iodide Stress Corrosion Cracking of Zircaloy," American Nuclear Society Topical Meeting on Reactor Safety Aspects of Fuel Behavior, Sun Valley, ID, Aug. 5, 1981.

2. D. R. Olander, "Brine Migration Model Development," National Waste Terminal Storage Performance Assessment meeting, DOE/HQ, Germantown, MD, May 27, 1981.

3. C. H. Tsai and D. R. Olander, "Vaporization Kinetics of Uranium Dioxide by Mass Spectrometry," Bay Area Conference on High Temperature Science and Technology, NASA-Ames Research Center, Oct. 29, 1981.

4. R. Kohli, "Chemical Thermodynamics of Fission Products in LWR Fuel Elements," paper presented at the Carl Wagner Commemorative Symposium, Chicago, Feb. 24-26, 1981.

5. R. Kohli, "Behavior of Cesium and Rubidium in LWR Fuel Rods," paper presented at an Intl. Conf. on Physical Chemistry and Materials Behavior, Kernforschungszentrum Karlsrühe, West Germany, March 24-26, 1981.

6. R. Kohli, "Fission Product Thermodynamics," paper presented at the 11th Bay Area High Temp. Conf., U.C. Davis, April 23, 1981.

7. R. Kohli, "Thermochemistry of Fission Products in Reactor Fuel Rods," paper presented at the Intl. Conf. on Themochemistry of Intermetallic Compounds, Minneapolis, May 11-13, 1981.

c. Plasma Enhanced Deposition of Thin Films*

Dennis W. Hess, Investigator

Introduction. Thin films are used in a wide spectrum of applications, including optical coatings, solar cells, and integrated circuits. Each application requires films with precise properties, tailored for that purpose. Thus, it is imperative that the fundamental relationships between film properties and the deposition techniques used for film formation be established.

An rf glow discharge or plasma presents a unique environment in which to carry out chemical reactions leading to film deposition. Because of the high energy electrons present in the plasma, chemical reactions that normally require elevated temperatures (> 500°C) to proceed at a measurable rate can be carried out at room temperature. Further, due to the ion and electron bombardment of the film materials during deposition, materials with unique chemical, electrical, magnetic, and optical properties can be synthesized.

Studies on the plasma-enhanced-deposition (PED) of transition metal oxides are described in the following sections. X-ray diffraction, transmission electron microscopy, and photon-assisted electrolysis are used to investigate materials properties as functions of deposition parameters.

1. PLASMA-DEPOSITED TITANIUM OXIDE PHOTOANODES

Larry M. Williams and D. W. Hess

The current demand for solar energy conversion and storage has kindled an interest in photoelectrochemical systems. Inexpensive materials that display high cell efficiencies and low anode corrosion are needed. Plasma-enhanced deposition is a technique capable of film formation on virtually any substrate material over a wide temperature range.

An rf glow discharge is ignited in a mixture of titanium tetrachloride and oxygen, and titanium oxide films are deposited on various substrate materials. The grain size and crystal structure of the films are studied as a function of rf power and substrate temperature. The photoelectrochemical performance of the films is determined and evaluated in light of the film structure.

Photoanode performance is found to be a strong function of film deposition temperature (Fig. 1). Investigation of the crystallite size in these films demonstrates that low photo-current corresponds to essentially amorphous films, while at temperatures above 300°C, crystalline material

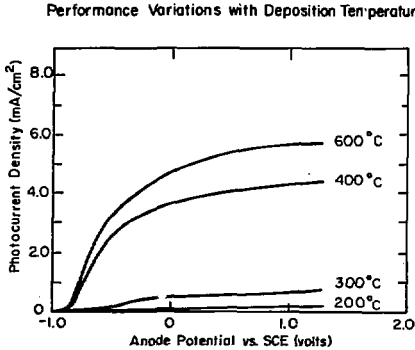

Fig. 1. Photocurrent versus anode potential for titanium oxide films plasma deposited at various substrate temperatures. Plasma conditions are 0.1 W/cm² and 0.2 torr. (XBL 818-6379)

(anatase and/or rutile) appears. Single crystal film growth seems possible at temperatures less than 800°C, since preferred orientation has been indicated by TEM at temperatures between 600°C and 700°C. The performance of the best plasma-deposited photoanodes is equivalent to that obtained with single crystal titanium oxide and with thermally oxidized titanium.

2. STRUCTURE AND MAGNETIC PROPERTIES OF PLASMA DEPOSITED IRON OXIDE FILMS†

Christopher S. Blair and D. W. Hess

Magnetic thin films have been of great interest for many years. The applications range from magnetic recording tape to magnetic discs for computer memories to magnetic recording heads to magnetic bubble devices. Plasma-enhanced deposition offers a method of controlling the structure and the properties of iron and iron oxide films, so that specific properties can be obtained by variation of deposition parameters.

Iron and iron oxide films are deposited by striking a glow discharge in iron pentacarbonyl vapor or in iron pentacarbonyl plus oxygen. The magnetic properties of the resulting films are studied with a hystereisigraph, and are related to

*This work was supported by the Director, Office of Energy Research, Office of Basic Energy Sciences, Materials Sciences Division of the U.S. Department of Energy under Contract No. DE-AC03-76SF00098.

the crystal structure and chemical composition via x-ray diffraction and atomic absorption spectroscopy.

At a power density of 0.08 W/cm^2 and with pure iron pentacarbonyl, α-Fe and a trace of Fe_3O_4 and/or α-Fe_2O_3 crystallites are observed in the deposited film. The films are magnetic, with a coercive force of 4-10 oersteds and a saturation magnetization ranging from 1.5 to 2.0 x 10^{-4} webermeter/kilogram, within the temperature range 200°C-300°C. As oxygen is added to the iron pentacarbonyl, the α-Fe crystallites disappear and α-Fe_2O_3 appears. These films display no magnetic properties. However, the oxides are semiconducting, and are being investigated as possible photoanode materials.

* * *

†Brief version of "Plasma Processing," ed. by R. G. Freiser and C. J. Mogab, The Electrochemical Society, Inc. 1981, p. 30.

1981 PUBLICATIONS AND REPORTS

Refereed Journals

†1. K. Tokunaga, F. C. Redeker, D. A. Danner, and D. W. Hess, "Comparison of Aluminum Etch Rates in CCl_4 and BCl_3 Plasmas," J. Electrochem. Soc., 128, 851 (1981).

Other Publications

1. D. W. Hess, "The Si-SiO_2 Interface: Current Understanding of Chemical and Electronic Defects," in J. Pask and A. Evans, eds., "Surfaces and Interfaces in Ceramic and Ceramic-Metal Systems," Plenum Press, New York, 1981, p. 335.

Invited Talks

†1. D. W. Hess, "Plasma Etching of Thin Films in the Fabrication of Integrated Circuits," AIChE Meeting, Detroit, MI, August 17-21, 1981.

* * *

†Supported by the National Science Foundation under Grant No. ECS-8021508.

d. Electrochemical Phase Boundaries*

Rolf H. Muller, Investigator

Introduction. The purpose of this work is to advance the understanding of boundary layers and thin films at electrochemical interfaces. Boundary layers control the chemical environment in which electrode processes take place and are often responsible for limiting the specific rate at which reactions can be conducted. Thin films at electrodes control the chemical properties of most materials in liquid environments and often represent the dominant resistance in metal deposition and dissolution reactions. New optical techniques for the observation of electrode surfaces in liquid media are developed and used. They include ellipsometry combined with Auger spectroscopy, interferometry, thin film interference, and Doppler velocimetry.

Work on high-rate electrodeposition and dissolution, conducted jointly with C. W. Tobias, is described under "Electrochemical Processes." Applied research, "Anodic Surface Layers on Battery Materials," supported by the Division of Energy Storage, Office of Conservation and Renewable Energy, DOE, is reported under "Electrochemical Energy Storage."

1. SPECTROSCOPIC ELLIPSOMETRY OF MODEL INHIBITOR SYSTEMS†

Joseph C. Farmer and R. H. Muller

Surface active agents have long been used on an empirical basis to control surface finish in electrolytic metal deposition and dissolution. Apart from observed increases of overpotential, little understanding of the functioning of these agents is available, despite the great technical importance of their use, and that of unavoidable impurities. This work was undertaken to determine the amounts of adsorbed materials present on metal surfaces during electrodeposition and their effect on the microtopography of electrodeposited metals by use of in situ optical observations. Synthetic dyes of high purity have been used as model substances of surface active materials. Their strong optical absorption makes it possible to detect very small amounts and the optical properties can be chosen to be different from those of substrate and deposit, which simplifies the interpretation.

The effect of Rhodamine-B on the electrodeposition of lead on copper and silver single crystals in acidic sodium perchlorate solutions has been investigated. This system satisfies the optical requirements, shows an altered deposit brightness, unusually high overpotential and diffusion-related hysteresis of inhibitory effects. A well-defined underpotential deposition region allows one to observe the initial stages of metal deposition which precede the formation of a bulk metal phase. Optical measurements were obtained in situ with a self-compensating spectroscopic ellipsometer[1] and light scattering equipment.[2] Electrode surfaces were also examined by scanning electron microscopy. For comparison with measured spectral data, predicted spectra were computed for different microporous structures and multiple layers.

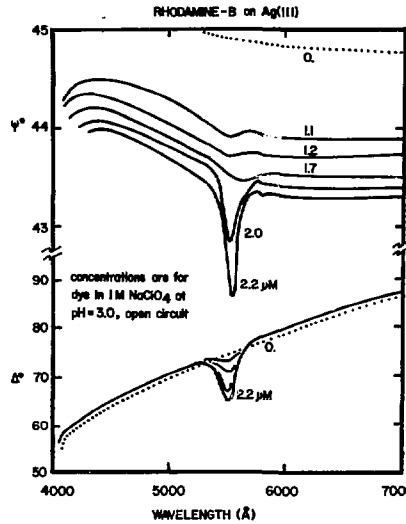

Fig. 1. Spectroscopic ellipsometry of an Ag (111) surface at 75° angle of incidence in 1 M $NaClO_4$, pH 3.0 with different concentrations of Rhodamine-B at open circuit. (XBL 8112-13106)

Adsorption isotherms have shown Rhodamine-B to saturate copper and silver surfaces at a concentration of 2.3μM and 4μM in the absence and presence of 5mM lead, respectively. Spectroscopic ellipsometer data are illustrated in Fig. 1. Orientation of the dye molecules on the substrate has been inferred from the measured birefringence. Underpotential and bulk deposition of lead are shifted to more cathodic potentials. Deposit roughness and porosity are increased; the dye is incorporated in the deposit. Further studies of

*This work was supported by the Director, Office of Energy Research, Office of Basic Energy Sciences, Materials Sciences Division of the U.S. Department of Energy under Contract No. DE-AC03-76SF00098.

film structure will be conducted by use of immersion and ion etching techniques.

* * *

†Short version of LBL-13738, December 1981.
1. LBL-12000, June 1981, p. 205.
2. LBL-12965

2. NUCLEATION AND GROWTH OF ANODIC SILVER OXIDE FILMS: LIGHT SCATTERNG AND ELLIPSOMETRY†

R. H. Muller, W. J. Plieth,‡ and J. C. Farmer

The formation of anodic oxide layers on silver had been interpreted previously[1] as involving several successive processes that include the nucleation and growth of particulate films. Since particle sizes were found to be well below the wavelength of light, their effect was represented by optically equivalent films for the interpretation of the ellipsometer measurements. Even such small particles can, however, result in measurable light scattering, and this work was undertaken to compare scattering and ellipsometer measurements.

Ellipsometer parameters were measured by the same automatic ellipsometer used for the earlier studies except that the instrument had been modified by the use of an argon ion laser (Lexel Model 57, 514 nm) as a light source and a microcomputer (LSI-11) for data acquisition. The laser is essential for scattering experiments with rough surfaces. Scattered light was collected with a fiber-optics probe which was rotated in the plane of incidence around the electrode. Scanning electron micrographs were obtained of several electrode surfaces after current interruption at time intervals characteristic of the different stages of light scattering from the surface.

The time-dependence of light scattering is characterized by an initial period, during which no change is detected, followed by a linear increase in scattered intensity and a later decline. Nucleation of the oxide phase is indicated by a peak in the measured electrode potential. After a short period of growth of the nuclei from supersaturated solution, light scattering becomes significant and ellipsometer parameters change rapidly. At this stage (14% of maximum), a typical particle size of 1000 Å has been determined from SEM pictures; 79% would be expected for the stoichiometric amount of oxide distributed in nonporous, spherical particles with the observed number density. At maximum scattering intensity, typical particle size is 1500 Å, the same as expected. After a decline in scattering intensity to 64% of the maximum, typical particle size is found to be 5000 Å. The change in scattering intensity can be attributed to changing particle size at constant number density. Scattering efficiency decreases as the size of particles exceeds the wavelength of the light and their close spacing results in multiple scattering and light trapping. The present study supports the previous multi-dimensional interpretation of ellipsometer measurements in which an oxidation mechanism involving nucleation and growth of oxide particles via a dissolution-precipitation mechanism had been proposed.

* * *

†Short version of LBL-12965.
‡Free University Berlin, West Germany.
1. R. H. Muller and C. G. Smith, Surf. Sci 76, 375 (1980).

3. NONCIRCULAR COLLISION CROSS-SECTIONS OF INDUCED ELECTRIC DIPOLES†

Joseph C. Farmer

Knowledge of the aerodynamic collision cross-section between pairs of small particles is important in calculating efficiencies of mist and dust collection equipment such as spray scrubbers and acoustic agglomerators, and is central to understanding droplet growth mechanisms in clouds. In principle, collision efficiencies can be enhanced by using external electric fields to induce dipole moments in particles, thereby extending the distance of interaction between collision partners. For specific orientations of the electric field with respect to the direction of particle motion, a net attraction results.

To determine collision efficiencies from first principles requires that a series of three-dimensional particle trajectories be calculated taking into account deflection of a smaller particle by local flow and electric field around the larger particle. From grazing particle trajectories the area of the collision cross-section, hence the aerodynamic collision efficiency, can be computed as seen by an observer upstream of the larger (collector) particle. Six simultaneous, differential equations describing the particle trajectories were integrated numerically by a Runge-Kutta algorithm.

It has been found that previous calculations, including perpendicular orientations of the flow and electric fields, have inadvertently assumed circular cross-sections.[1,2] Such incorrect assumptions can lead to significant errors in collision efficiency estimates (too optimistic by a factor of 3 for inertial capture).

Trajectory calculations were made for two particles of 20 and 8μm diameters colliding under the influence of gravity (inertial capture regime) and polarized by 0, 30, 70 or 100 kV/m external electric fields with both parallel and perpendicular orientations of electric and flow fields. Circular collision cross-sections for parallel orientations were computed for comparison with noncircular cross-sections for perpendicular orientations. In perpendicular electric field orientations, aerodynamic collision cross-sections become highly noncircular even at 30 kV/m, and trends in the relative sizes are not as obvious as those for the parallel case. The cross-sections elongate in the direction of the poles with the formation of lobes and narrow regions around the equator. Increasing the field strength to 70 kV/m further increases the noncircularity. At 100 kV/m, the cross-section separates into a lobe above both poles.

* * *

†Short version of LBL-12863.

1. Lindblad, N. R., Semonin, R. G. (1963), J. Geophys. Res., 68, 1051.
2. Plumlee, H. R., Semonin, R. G. (1965), Tellus, XVII, 356.

4. ELECTROCHEMICAL PROPERTIES OF METAL CLUSTERS†

W. J. Plieth‡

Small particles are known to have properties which are quite different from those of bulk material. Surface-enhanced Raman scattering may be caused by the optical properties of small metal particles. This work contributes to the understanding of electrochemical procedures used for the activation of surfaces for Raman studies.

A theoretical analysis of electrochemical properties of small metal particles has been conducted. Approximate equations are given for the relationship between the particle size and the surface charge, the potential of zero charge, the surface potential, work function and related quantities. The influence of these properties on redox reactions, electrosorption and chemisorption are discussed. The results are used to explain experimental observation in connection with the surface-enhanced Raman effect.

* * *

†Short version of LBL-12955, June 1981.
‡Free University, Berlin, Germany.

5. WORK IN PROGRESS

A study on the effect of surface topography on the stability of electrolyte films on electrode surfaces is being conducted. Despite the importance of such films for the functioning of gas-consuming electrodes and corrosion processes, the force balance responsible for film-formation is not well understood. This work takes advantage of previous developments on the theory of thin film interference.

The effect of turbulence promoters on electrochemical mass transport in a flow channel, previously studied by interferometry, is investigated by limiting current and pressure drop measurements in order to define transport conditions for optimum energy efficiency (with C. W. Tobias).

A previous study of the effect of suspended inert solid particles on electrochemical mass transport will be extended to different solids and flow situations (with C. W. Tobias).

1981 PUBLICATIONS AND REPORTS

Refereed Journals

1. D. B. Riggs, R. H. Muller and C. W. Tobias, "Prediction of Work Piece Geometry in Electrochemical Cavity Sinking," Electrochim. Acta 26, 961 (1981); LBL-6282.

LBL Reports

1. T. Hryniewics, R. H. Muller and C. W. Tobias, "A Study of Electropolishing of Ferrous Alloys Using Rotating Disk Electrodes," LBL-12879.

2. David J. Roha, "Effects of Suspended Particles on the Rate of Mass Transfer to a Rotating Disk Electrode," M.S. thesis, LBL-12737 (with C. W. Tobias).

3. W. J. Plieth, "On the Electrochemical Properties of Small Clusters of Metal Atoms and their Role in the Surface-Enhanced Raman Scattering," LBL-12955.

4. Joseph C. Farmer, "Noncircular Collision Cross-Sections of Induced Electric Dipoles," LBL-12863.

5. F. R. McLarnon, R. H. Muller and C. W. Tobias, "Interferometric Study of Combined Forced and Natural Convection," LBL-13032.

e. Solid-State and Surface Reactions*

Gabor A. Somorjai, Investigator

Introduction. The research program is centered on studies of 1) catalyzed surface reactions and investigations of 2) the atomic structure and chemical composition of solid surfaces and adsorbed monolayers. The kinetics and mechanisms of catalytic surface reactions are studied using well characterized crystal surfaces at low and high pressures by utilizing a combination of surface science techniques.

The materials that are the focus of our studies are platinum, rhodium, iron and its compounds, alkali metals, and bimetallic alloys. The adsorbates and reactants are mostly hydrocarbons, oxygen, hydrogen and water.

Part of the investigation is directed toward atomic scale understanding of the structure and catalytic behavior of metal surfaces. The other part is aimed at developing new catalysts which substitute for precious metals and exhibit high rates and selectivity.

Surface Structure and Chemisorption by Low Energy Electron Diffraction

1. THE STRUCTURE OF EPITAXIALLY GROWN METAL LAYERS ON SINGLE CRYSTAL SURFACES OF OTHER METALS: GOLD ON Pt(100) AND PLATINUM ON Au(100)

J. W. A. Sachtler, M. A. Van Hove, J. P. Biberian, and G. A. Somorjai

In these experiments, gold was evaporated onto Pt(100) and platinum was evaporated onto a Au(100) single crystal surface. Deposition of gold onto Pt(100) removed the $\begin{pmatrix} 14 & 1 \\ -1 & 5 \end{pmatrix}$ reconstructed surface structure and at a coverage of about 0.5 monolayer a (1x1) pattern fully developed, which remained unchanged up to two gold monolayers. Multilayers of gold produced (1x5) and (1x7) surface structures after annealing. These observations can be explained by the formation of a hexagonal top atomic layer on a substrate that retains a square lattice. The well known structure of clean Au(100) did not form, even at 32 layers of gold on Pt(100). Platinum deposited onto Au(100) removed its surface reconstruction yielding a fully developed (1x1) pattern at about one-half monolayer. This pattern remained unchanged upon further platinum deposition. The growth mechanism is inferred from the variation of the Auger signal intensities of the substrate and adsorbate metals with coverage of the adsorbate. Platinum on Au(100) forms microcrystallites (Volmer-Weber type growth), while gold on Pt(100) grows layer-by-layer (Frank-van der Merwe growth mechanism).

2. THE SURFACE RECONSTRUCTIONS OF THE (100) CRYSTAL FACES OF IRIDIUM, PLATINUM AND GOLD: I. EXPERIMENTAL OBSERVATIONS AND POSSIBLE STRUCTURAL MODELS. II. STRUCTURAL DETERMINATION BY LEED INTENSITY ANALYSIS

M. A. Van Hove, R. J. Koestner, P. C. Stair, J. P. Biberian, L. L. Kesmodel, I. Bartos, and G. A. Somorjai

The structures of the reconstructed Ir(100), Pt(100) and Au(100) surfaces have been investigated. Low energy electron diffraction (LEED) patterns were analyzed and LEED intensity vs energy data measured. A variety of structures is observed by LEED: Ir(100) exhibits a relatively simple (1x5) pattern; Pt(100) shows a series of closely-related patterns, a typical representative of which has a $\begin{pmatrix} 14 & 1 \\ -1 & 5 \end{pmatrix}$ structure; Au(100) usually exhibits a c(26x68) pattern, often inaccurately described in the literature as a (20x5) pattern. The reconstruction of Au(111) was also considered for comparison. Various plausible structural models were discussed, and laser simulation was used to reduce the number of these models.

The investigation of the reconstructions of the Ir(100) and Pt(100) crystal surfaces was completed with an extensive analysis of LEED intensities, using dynamical (multiple scattering) calculations. It was found that a hexagonal rearrangement of the top monolayer is a likely explanation of the surface reconstruction. This hexagonal layer would have a registry involving bridge sites on the next square unit cell metal layer, and it is contracted and buckled. Bond length contractions parallel and perpendicular to the surface occur; the Pt top layer is rotated by a small angle (0.7°) with respect to the substrate.

A second model that cannot be definitively ruled out by the LEED analysis, but disagrees with ion-scattering data, involves shifted close-packed rows of top-layer atoms and requires domain structures in the case of Pt and Au. Charge-density-wave and missing-row models are ruled out by our structure analysis. A correlation was found between the occurrence of surface reconstructions on metals and a small ratio of their Debye temperature to their melting point. This correlation singles out mainly the 5d metals as having a propensity to surface reconstruction. The effects of adsorbates on the reconstructions were also discussed.

*This work was supported by the Director, Office of Energy Research, Office of Basic Energy Sciences, Materials Sciences Division of the U.S. Department of Energy under Contract No. DE-AC03-76SF00098.

3. A SURFACE CRYSTALLOGRAPHY STUDY BY DYNAMICAL LEED OF THE $(\sqrt{3} \times \sqrt{3})R30^\circ$ CO STRUCTURE ON THE Rh(111) CRYSTAL SURFACE

R. J. Koestner, M. A. Van Hove, and G. A. Somorjai

The atomic positions of the Rh(111) + $(\sqrt{3} \times \sqrt{3})R30^\circ$ CO and CO_2 surfaces were analyzed by dynamical LEED. The Rh(111) + $(\sqrt{3} \times \sqrt{3})R30^\circ$ CO and CO_2 systems produce identical I-V curves, confirming the dissociation of CO_2 to CO on this surface. The adsorbed CO was found to stand perpendicular to the surface with the carbon end down at an atop site (that is, terminally bonded). The CO overlayer spacings are $d_{RhC} = 1.95 \pm 0.1$ Å and $d_{CO} = 1.07 \pm 0.1$ Å. This geometry yields a Zanazzi-Jona R-factor of 0.40 and a Pendry R-factor of 0.50.

4. PULSE COUNTING LOW ENERGY ELECTRON DIFFRACTION INSTRUMENT

J. E. Katz, D. F. Ogletree, U. Bardi, and G. A. Somorjai

The new LEED instrument uses a channel plate to increase the diffracted intensity, permitting the use of incident electron currents of a few picoamperes, thus eliminating beam damage on the surface under study. The use of a position sensitive detector (resistive anode) will permit the recording of the diffraction pattern by means of a two-dimensional position sensitive digitizer. The system is designed to use a computer to record and store the diffracted beam intensities as a function of the incident beam energy. In the first stages of development, however, the diffracted pattern will simply be displayed on an oscilloscope screen.

All the parts necessary for the construction of the LEED optical resistive anode assembly, are presently on hand. The system will be mounted for the first testing in an existing Ultek UHV system. The two-dimensional position detector and the channel plate supply have been built, and we plan to borrow and use existing retarding grids and electron gun power supplies for the initial test and set up.

We estimate that the basic LEED system will be operational early in 1982. The successive development of a computerized data collection system will greatly increase the usefulness and versatility of the system.

5. POTASSIUM AND POTASSIUM OXIDE MONOLAYERS ON THE PLATINUM (111) AND STEPPED (755) CRYSTAL SURFACES. A LEED, AES, AND TDS STUDY

E. L. Garfunkel and G. A. Somorjai

The adsorption of potassium and the coadsorption of potassium and oxygen on the Pt(111) and stepped Pt(755) crystal surfaces were studied by AES, LEED, and TDS. Pure potassium adlayers were found by LEED to be hexagonally ordered on Pt(111) at coverages of $\theta_K = 0.9 - 1$. The monolayer coverage was 5.4×10^{14} K atoms/cm^2 (0.36 times the atomic density of the Pt(111) surface). Orientational reordering of the adlayers, like that of noble gas phase transitions on metals, was observed. The heat of desorption of K decreased, due to depolarization effects, from 60 kcal/mole at $\theta_K = 1$ on both Pt(111) and Pt(755). Exposure to oxygen thermally stabilizes a potassium monolayer, increasing the heat of desorption from 25 kcal/mole to 50 kcal/mole. Both potassium and oxygen were found to desorb simultaneously, indicating strong interactions in the adsorbed overlayer. LEED results on Pt(111) further indicate that a planar K_2O layer may be formed by annealing coadsorbed potassium and oxygen to 750 K.

6. SURFACE DEBYE TEMPERATURES OF Rh(100) and (111) SURFACES

D. G. Castner, J. E. Black, D. Castiel, R. F. Wallis, and G. A. Somorjai

Surface Debye temperatures have been measured for rhodium (100) and (111) surfaces using a conventional low-energy-electron-diffraction/Auger-electron-spectroscopy system. The 00 beam intensities were measured with a spot photometer and the crystal temperature was monitored with a Pt vs Pt-10 at% Rh thermocouple. From the intensity vs temperature curve, a Debye temperature was calculated for each beam voltage. The surface Debye temperatures were then estimated from plots of Debye temperature vs beam voltage. Using three-constant and five-constant lattice-dynamical models, we have made calculations of the bulk phonon dispersion curves and the surface Debye temperatures. A comparison is given of the experimental and theoretical results for the surface Debye temperatures.

7. THE STRUCTURE AND STABILITY OF SURFACE PLATINUM OXIDE AND OF OXIDES OF OTHER NOBLE METALS

M. Salmeron, L. Brewer, and G. A. Somorjai

The formation and stability of surface layers of platinum oxides in platinum single crystals has been studied in ultrahigh vacuum. Low energy electron diffraction (LEED) was used to identify the ordered structures that formed on the surface of Pt(111), Pt(332), and Pt(110). It appears that these structures can be related to hexagonal planes of PtO_2. The cleanliness of the surface was monitored by Auger electron spectroscopy (AES). The presence of impurities like Ca and Si must be avoided as they oxidize before the Pt. It is shown that the Pt oxide layers are stabilized by the very slow kinetics of oxygen diffusion to the surface which is responsible for the observed long life of the oxide layers under most catalytic reactions that are carried out at temperatures below 500°C. The stability of other oxides of noble metals that have been observed in UHV studies is also reviewed.

8. ADSORPTION AND BONDING OF BUTANE AND PENTANE ON THE Pt(111) CRYSTAL SURFACES: EFFECTS OF OXYGEN TREATMENTS AND DEUTERIUM PREADSORPTION

M. Salmeron and G. A. Somorjai

The adsorption of C_4H_{10} and C_5H_{12} on Pt(111)

was studied by thermal desorption spectroscopy. The hydrocarbons show a first order desorption process with peak temperatures of 166 and 195 K. Kinetic parameters obtained were $\nu = 9.4 \times 10^{10}$ sec^{-1}, $E = 8.2$ kcal/mol for C_4H_{10}, and $\nu = 3.7 \times 10^{11}$ sec^{-1}, $E = 10.2$ kcal/mol for C_5H_{12}. Multilayers of both hydrocarbons are formed at 110 K and high exposures. The presence of subsurface oxygen introduces new adsorption sites and decreases the exposure needed for multilayer formation. Preadsorbed deuterium interacts repulsively with the adsorbed hydrocarbons, lowering its desorption temperatures.

9. DYNAMICAL AND APPROXIMATE LEED THEORIES APPLIED TO LAYERS OF LARGE MOLECULES

M. A. Van Hove and G. A. Somorjai

A theoretical study is carried out of the application of the combined space method (CSM) in low energy electron diffraction (LEED) from large molecules, for which rings of six carbon atoms arranged in periodic layers are chosen. A marked sensitivity of calculated intensity-energy (I-V) curves to variations of the geometry of these rings is exhibited. The reduction of the computation effort through approximations characterized by various degrees of neglect of multiple scattering is explored. It is shown that efficient approximate methods can be applied in the structural determination of large molecules at surfaces, at the very least in preliminary unrefined searches through sets of plausible structures. A new class of approximations based on near-neighbor multiple scattering is proposed that has efficient features for multiple use in structural searches.

10. THE DESORPTION, DECOMPOSITION, AND DEUTERIUM EXCHANGE REACTIONS OF UNSATURATED HYDROCARBONS (ETHYLENE, ACETYLENE, PROPYLENE, AND BUTENES) ON THE Pt(111) CRYSTAL FACE

M. Salmeron and G. A. Somorjai

The desorption and thermal desorption of C_2H_2, C_2H_4, C_3H_6, and C_4H_8 (cis and trans-) on Pt(111) has been studied as a function of coverage. The undissociated olefin molecules, in the monolayer coverage range, desorb at 285 ± 4 K, 280 ± 5 K, and 261 ± 6 K for C_2H_4, C_3H_6, and C_4H_8, respectively. At high exposures, multilayers of C_3H_6 and C_4H_8 formed while the Pt(111) crystal was maintained at 110 K. The desorption temperatures of these multilayers are 139 ± 5 K and 150 ± 8 K for C_3H_6 and C_4H_8 respectively. After the partial desorption of the undissociated molecules, the remaining adsorbed hydrocarbons decompose to yield desorbing H_2 and partially dehydrogenated surface species. The three olefins give rise to a sharp H_2-desorption peak at 297 ± 4, 296 ± 4, and 294 ± 5 K for C_2H_4, C_3H_6, and C_4H_8, respectively. The remaining surface species undergo a further dehydrogenation reaction that gives rise to another sharp desorption peak at 492 ± 6, 436 ± 5, and 381 ± 5 K, respectively. At even higher temperatures a series of three more H_2 peaks, at similar temperatures for all the hydrocarbons, appear at ~ 550, 640, and 710 K. These H_2 peaks represent the final and complete dehydrogenation of the hydrocarbon fragments on the Pt(111) surface. The H_2 desorption spectrum of C_2H_2 is very similar to that of C_2H_4 except for the absence of the first H_2 peak at 297°K. D_2 coadsorption produces changes in the binding of the hydrocarbon molecules on the Pt surface. Limited D incorporation into the undissociated hydrocarbon molecules has been observed to occur through H-D exchange in the coadsorption experiments. At higher temperatures, the stable room temperature phase on all these hydrocarbons undergoes extensive H-D exchange when exposed to D_2 without decomposition.

11. THE GROWTH AND CHEMISORPTION PROPERTIES OF Ag AND Au MONOLAYERS ON PLATINUM SINGLE CRYSTAL SURFACES: AN AES, TDS, AND LEED STUDY

P. W. Davies, M. Quinlan, and G. A. Somorjai

The growth and chemisorptive properties of monolayer films of Ag and Au deposited on both the Pt(111) and the stepped Pt(553) surfaces were studied using Auger electron spectroscopy (AES), thermal desorption spectroscopy (TDS), and low energy electron diffraction (LEED). AES studies indicate that the growth of Au on the Pt(111) and Pt(553), and Ag on the Pt(111) proceeds via a Stranski-Krastanov mechanism, whereas the growth of Ag on the Pt(533) surface follows a Volmer-Weber mechanism.

Au dissolved into the bulk Pt crystal above 800 K, whereas Ag desorbs above 900 K. TDS studies of Ag-covered Pt surfaces indicate that the Ag-Pt bond is ~ 25 kJ mol^{-1} stronger (283 kJ mol^{-1}) than the Ag-Ag bond (254 kJ mol^{-1}). On the Pt(553) surface the Au atoms are uniformly distributed between terrace and step sites, but Ag preferentially segregates to the terraces.

The decrease in CO adsorption on the Pt crystal surfaces is in direct proportion to the Ag or Au coverage. No CO adsorption could be detected for Ag or Au coverages above one monolayer at 300 K and 10^{-8} torr. The heat of adsorption of CO on Pt is unaltered by the presence of Ag or Au.

12. THE STRUCTURES OF SMALL HYDROCARBON MOLECULES ON Rh(111) STUDIED BY LOW ENERGY ELECTRON DIFFRACTION: ACETYLENE, ETHYLENE, METHYLACETYLENE, AND PROPYLENE

M. A. Van Hove, R. J. Koestner, and G. A. Somorjai

Ethylene ($H_2C{=}CH_2$) deposited on Rh(111) at temperatures between 230 and 270 K produces a sharp (2x2) pattern at 1/4 monolayer coverage. The surface species obtained in this way is ethylidyne (>C-CH_3), bonded to three metal atoms and standing perpendicularly to the metal surface. It is identical to the ethylidyne species found on Pt(111) in similar circumstances. It can also be obtained from acetylene (H-C≡C-H) by coadsorption of H_2.

The (2x2) ethylidyne species on Rh(111) can be converted under gentle heating or addition of H_2 to a species having a c(4x2) pattern and the same

1/4 monolayer coverage. High resolution electron energy loss spectroscopy indicates that the ethylidyne species is maintained. However, dynamical LEED calculations do not agree well with experiment for this structure or any other structure.

Propylene ($H_2C{=}CH{-}CH_3$) deposited on Rh(111) at temperatures between 230 and 270 K produces a (2x2) pattern with weak diffuse spots in extra $(2\sqrt{3} \times 2\sqrt{3})R30^\circ$ positions. The I-V curves of the (2x2) spots are nearly identical to those of (2x2) ethylidyne. Prolonged exposure to propylene produces a sharp $(2\sqrt{3} \times 2\sqrt{3})R30^\circ$ pattern with concurrent changes in the I-V curves. We suggest that a propylidyne species ($>C{-}CH_2{-}CH_3$) has been obtained whose $>C{-}C$ base is identical to that of ethylidyne. The extra methyl groups ($-CH_3$) on neighboring molecules interact with each other because of their size and can produce the $(2\sqrt{3} \times 2\sqrt{3})R30^\circ$ unit cell. LEED calculations are in progress to check this model and determine the various structural parameters.

Both propylene and methylacetylene ($H{-}C{\equiv}C{-}CH_3$) can produce c(4x2) patterns with I-V curves identical to those of the c(4x2) species obtained from ethylene and acetylene.

A new theoretical approximation is used in a first stage of this LEED analysis: the multiple scattering is ignored within the molecular overlayer, but not in other parts of the surface, including between the substrate and the overlayer.

13. ARRANGEMENT OF CO MOLECULES ADSORBED ON LOW INDEX METAL SURFACES: A COMPARISON BETWEEN LEED AND HREELS OR IRS

J. P. Biberian and M. A. Van Hove

The adsorption of carbon monoxide on low index metal surfaces has been the object of intense research, presenting some apparently conflicting results. Thus, for three systems, CO on Cu(100), on Cu(111) and on Ru(0001), HREELS or IRS show only one C-O stretching frequency while an interpretation of the LEED diagram with a compact monolayer of CO gives at least two adsorption sites. A reexamination of these systems with a model based on a finite coincidence unit cell and one adsorption site, allows a better interpretation of all the data. Laser simulation of LEED is used to test this interpretation and to determine molecular positions within the larger coincidence unit cells.

Electron Spectroscopy Studies of Solid Surfaces and Adsorbates

1. THE STRONG INFLUENCE OF POTASSIUM ON THE ADSORPTION OF CO ON PLATINUM SURFACES: A TOS AND HREELS STUDY

E. L. Garfunkel, J. E. Crowell and G. A. Somorjai

The chemisorptive properties of carbon monoxide on the Pt(111) crystal face were observed to change markedly in the presence of potassium. Upon deposition of half a monolayer of potassium the saturation coverage adsorption energy of CO increased from 27 to 39 kcal/mole. High resolution electron energy loss spectroscopy (HREELS) showed a 475 cm^{-1} decrease in the bridge bonded CO vibrational frequency to as low as 1400 cm^{-1}, while CO preferentially occupied bridge bonded rather than linearly bonded surface sites in the presence of potassium. These large variations appear to be caused by enhanced electron back-donation from the platinum into the $2\pi^*$ antibonding orbitals of CO.

2. ELECTRON SPECTROSCOPY STUDIES OF THE CLEAN THORIUM AND URANIUM SURFACES: THE CHEMISORPTION AND INITIAL STAGES OF REACTION WITH O_2, CO and CO_2

W. McLean, C. A. Colmenares, R. L. Smith, and G. A. Somorjai

The adsorption of O_2, CO and CO_2 on the thorium (111) crystal face and on polycrystalline α-uranium has been investigated by x-ray photoelectron spectroscopy (XPS), Auger electron spectroscopy (AES), and secondary ion mass spectroscopy (SIMS) at 300 K. Oxygen adsorption on both metals resulted in the formation of the metal dioxide. CO and CO_2 adsorption on Th(111) produced species derived from atomic carbon and oxygen; the presence of molecular CO was also detected. Only atomic carbon and oxygen were observed on uranium. Elemental depth profiles by AES and SIMS indicated that the carbon produced by the dissociation of CO or CO_2 diffused into the bulk of the metals to form a carbide, while the oxygen remained on their surfaces as an oxide.

3. DESIGN AND CONSTRUCTION OF A HIGH STABILITY, LOW NOISE, POWER SUPPLY FOR USE WITH HIGH RESOLUTION ELECTRON ENERGY LOSS SPECTROMETERS

J. E. Katz, P. W. Davies, J. E. Crowell, and G. A. Somorjai

The design and construction of a high stability, low noise, power supply that provides potentials for the lens and analyzer elements of a 127° Ehrhardt-type high resolution electron energy loss spectrometer (HREELS) is described. The supply incorporates a filament emission-control circuit and facilities for measuring electron beam current at each spectrometer element, thus facilitating optimal tuning of the spectrometer. Spectra obtained using this supply are shown to have a fourfold improvement in signal-to-noise ratio and a higher resolution of the vibrational loss features when compared with spectra taken using a previously existing supply based on passive potential divider networks.

Molecular Beam-Surface Interactions

1. DETECTION OF ROTATIONAL ENERGY TRANSFER IN NO BY LASER IONIZATION DURING MOLECULAR BEAM-SURFACE SCATTERING

M. Asscher, W. L. Guthrie, T. H. Lin, and G. A. Somorjai

A detector was constructed to extend molecular beam-surface scattering energy transfer studies to include measurement of the energy distribution in rotational and vibrational modes. The internal energy distribution is measured by the use of tuneable UV radiation from a dye laser. A quartz lens is used to focus the laser light within the differentially pumped detector chamber, producing sufficient intensity for multiphoton ionization of the molecule under study. Prior to the scattering experiment in the UHV scattering chamber a gas phase spectrum of NO was taken using two-photon ionization in the 225-227 nm range. This detector proved to be extremely sensitive. It can resolve a complete rotational spectrum from as little as 10^{-10} torr of NO with a laser energy of ~ 50 μJ/pulse. By tuning the laser one can obtain complete information about the post-scattering rotational and vibrational population, which is essential for the understanding of the dynamics of inelastic scattering of molecules from surfaces. We are using this technique to study translational to rotational energy transfer in NO inelasticity scattered from a Pt(111) surface. This study will complement translational energy measurements of the same system.

Studies of Catalyzed Surface Reactions

1. THE REACTIVITY AND COMPOSITION OF STRONGLY ADSORBED CARBONACEOUS DEPOSITS ON PLATINUM. MODEL OF THE WORKING HYDROCARBON CONVERSION CATALYST

S. M. Davis, F. Zaera, and G. A. Somorjai

The role of strongly adsorbed hydrocarbon deposits in reforming catalysis on a series of flat, stepped, and kinked platinum single crystal surfaces at atmospheric pressures and temperatures between 300 and 700 K has been established and a model has been developed for the working structure and composition of the active catalyst surface. Restart reaction studies and reaction rate studies using platinum surfaces precovered with carbonaceous overlayers containing carbon-14 were used to investigate the catalytic activity and selectivity of carbon-covered platinum in hydrocarbon hydrogenation, dehydrogenation, and skeletal rearrangement.

Quantitative hydrogen thermal desorption studies were carried out as a function of surface structure and reaction temperature to determine 1) the composition, and 2) the energetics for sequential dehydrogenation of carbonaceous deposits derived from a variety of adsorbed hydrocarbons including isobutane, neopentane, n-hexane, and cyclohexene. Carbon monoxide adsorption thermal desorption methods were developed to titrate uncovered platinum surface sites before and after reaction rate studies. The uncovered site concentrations were correlated with the total surface carbon coverage as determined by Auger electron spectroscopy and the catalytic activity and selectivity of carbon-covered platinum.

These experiments together with results from related structure sensitivity, thermal desorption, deuterium exchange, and radiotracer studies revealed that the primary role of the disordered carbon deposit is that of a nonselective poison that blocks platinum surface sites from incident reactant molecules. The most important chemical properties of the carbonaceous deposit are its abilities to store and exchange hydrogen with reacting surface species and to provide desorption sites for product molecules. The growth mechanism of this carbonaceous deposit is sensitive to the structure of the reacting hydrocarbon, and its morphology appears to vary continuously from two-dimensional at low reaction temperatures (< 550 K) to three-dimensional for temperatures higher than about 600 K.

2. IRON SINGLE CRYSTALS AS AMMONIA SYNTHESIS CATALYSTS: EFFECT OF SURFACE STRUCTURE ON CATALYST ACTIVITY

N. D. Spencer, R. C. Schoonmaker, and G. A. Somorjai

The catalysis of ammonia synthesis by three iron single crystal faces was investigated. At 798 K and a total pressure of 20 atm of a stoichiometric mixture of hydrogen and nitrogen, the relative rates of ammonia formation were found to be 418:25:1 for Fe(111), Fe(100), and Fe(110) samples, respectively. The activation energy for ammonia synthesis on the Fe(111) surface was determined as 19.4 Kcal/mole^{-1}. Significant quantities of nitrogen were found to be present in the bulk and on the surface of the iron samples after catalytic runs. This is the first study in which ammonia synthesis activity has been directly correlated with surface crystallographic structure under well-defined, high pressure conditions.

3. HIGH PRESSURE STUDIES OF THE Au-Pt SYSTEM: THE EFFECT OF GOLD ON HYDROCARBON CONVERSION REACTIONS

J. W. A. Sachtler and G. A. Somorjai

The conversion of n-hexane was investigated on the Pt(111) crystal surface as a function of gold surface concentration. Gold, when evaporated onto platinum, decreased the rates of all competing hydrocarbon reactions in proportion to the gold surface concentration. When gold was diffused into the platinum crystal lattice large changes in both the rate and the selectivities of the reactions occurred. Isomerization rates increased by a factor of two while the rate of hydrogenolysis decreased exponentially with gold coverage. The rate of dehydrocyclization decreased linearly with gold surface concentration. The large changes in the reaction selectivities are likely to be due to the rapid decrease in the concentration of three-

fold sites in the (111) platinum surface as gold diffuses into the platinum lattice.

4. WORK IN PROGRESS

The surface structure, chemisorption properties and chemical reactivity of molybdenum crystals, the molybdenum-sulfur and molybdenum-oxygen systems are being explored. The main reactions of interest are hydrodesulfurization, methane oxidation and dehydrocyclization.

The effects of metal monolayers condensed onto crystal faces of other transition metals on the catalyzed hydrocarbon reactions are being explored. Work on the Pt-Ti, Pt-Zr, Pt-Re and Pt-Au systems are in progress.

Ammonia synthesis over rhenium surfaces is investigated. This is a new catalyst for this reaction that appears to be more active than iron.

High resolution electron energy loss studies are being carried out on hydrocarbon fragments that remain on the platinum and rhodium catalyst surfaces after high pressure catalytic reactions.

1981 PUBLICATIONS AND REPORTS

Refereed Journals

1. M. A. Van Hove, R. J. Koestner, P. C. Stair, J. P. Biberian, L. L. Kesmodel, and G. A. Somorjai, "The Surface Reconstructions of the (100) Crystal Faces of Iridium, Platinum, Gold: [I] Experimental Observations and Possible Structural Models," Surf. Sci. 103, 189 (1981); LBL-10340.

2. M. A. Van Hove, R. J. Koestner, P. C. Stair, J. P. Biberian, L. L. Kesmodel and G. A. Somorjai, "The Surface Reconstructions of the (100) Crystal Faces of Iridium, Platinum, and Gold: [II] Structural Determination by LEED Intensity Analysis," Surf. Sci. 103, 218 (1981); LBL-10340.

3. L. H. Dubois, P. K. Hansma and G. A. Somorjai, "Evidence for an Oxygen Intermediate in the Catalytic Reduction of NO by CO on Rhodium Surfaces," J. Catal. 65, 318 (1980); LBL-10061.

4. W. Guthrie, J. Sokol and G. A. Somorjai, "The Decomposition of Ammonia on the Flat (111) and Stepped (577) Platinum Crystal Surfaces," Surf. Sci. 109, 390 (1981); LBL-10536.

5. L. H. Dubois, P. K. Hansma and G. A. Somorjai, "The Application of HREELS to the Study of Model Supported Metal Catalysts," Appl. of Surf. Sci. 6, 173 (1980); LBL-10733.

6. W. D. Gillespie, R. K. Herz and G. A. Somorjai, "Cyclohexane Dehydrogenation and Hydrogenolysis Catalyzed by Platinum Single Crystals at Atmospheric Pressure," J. Catal. 67, 371 (1981); LBL-10576.

7. J. W. A. Sachtler, M. A. Van Hove, J. P. Biberian and G. A. Somorjai, "Enhanced Reactivity of Ordered Monolayers of Gold on Pt(100) and Platinum on Au(100) Single Crystal Surfaces," Phys. Rev. Lett. 45, 1601 (1980); LBL-10840.

8. D. G. Castner, L. H. Dubois, B. A. Sexton and G. A. Somorjai, "Evidence for CO Dissociation on Rhodium Surfaces," Surf. Sci. 103, L-134 (1981); LBL-11205.

9. R. J. Koestner, M. A. Van Hove and G. A. Somorjai, "A Surface Crystallography Study by Dynamical LEED of the CO-($\sqrt{3} \times \sqrt{3}$)R30° Structure on the Rh(111) Crystal Surface," Surface Sci. 107, 439 (1981); LBL-11263.

10. G. A. Somorjai, "The Catalytic Hydrogenation of CO: The Formation of C_1 Hydrocarbons," Catal. Rev.-Sci. Eng. 23, 189 (1981); LBL-11354.

11. S. T. Ceyer, W. J. Siekhaus, and G. A. Somorjai, "Design of a Molecular Beam Surface Scattering Apparatus for Velocity and Angular Distribution Measurements," J. Vac. Sci. Technol. 19, 726 (1981); LBL-11553.

12. L. H. Dubois and G. A. Somorjai, "The Application of HREELS to the Characterization of Adsorbed Molecules on Rhodium Single Crystal Surfaces," ACS Symposium Series 137, A. T. Bell and M. L. Hair, eds., ACS, (1980); LBL-10188.

13. G. A. Somorjai, "Surface Science and Heterogeneous Catalysis," Lecture, Swiss Chemical Soc., Zurich, Switzerland, May 14, 1980, Chimia Vol. 35, 1 (1981); LBL-11690.

14. W. D. Gillespie, R. K. Herz, E. E. Petersen, and G. A. Somorjai, "The Structure Sensitivity of n-Heptane Dehydrocyclization and Hydrogenolysis Catalyzed by Platinum Single Crystals at Atmospheric Pressures," J. Catal. 70, 147 (1981); LBL-11704.

15. T. H. Lin and G. A. Somorjai, "Modulated Molecular Beam Scattering of CO and NO from Pt(111) and the Stepped Pt(557) Crystal Surfaces," Surface Sci. 107, 573 (1981); LBL-11787.

16. S. M. Davis, G. E. Gordon, M. Press, and G. A. Somorjai, "A Radiotracer Technique for Adsorption and Catalysis Studies: Application to ^{14}C-Benzene Chemisorption and Rehydrogenation on Pt(111)," J. Vac. Sci. Technol. 19, 231 (1981); LBL-12005.

17. J. W. A. Sachtler, J. P. Biberian, and G. A. Somorjai, "The Reactivity of Ordered Metal Layers on Single Crystal Surfaces of Other Metals: Au on Pt (100) and Pt on Au(100)," Surface Sci. 110, 43 (1981); LBL-12111.

18. M. Salmeron and G. A. Somorjai, "Oxygen Induced Dissolution and Segregation of Silicon in Platinum Single Crystals," J. Vac. Sci. Technol. 19, 722 (1981); LBL-12151.

19. D. G. Castner, J. E. Black, D. Castiel, R. F. Wallis, and G. A. Somorjai, "Surface Debye Temperatures of Rh(100) and (111) Surfaces," Phys. Rev. 12, No. 14 (1981).

20. M. A. Van Hove and S. Y. Tong, "Computation

Procedure of the Combined Space Method," Proc. Conf. on Determination of Surface Structure by LEED, Plenum, NY, 1981.

21. M. A. Van Hove and R. J. Koestner, "R-Factors in LEED: Comparison of Different R-Factors, Coincidence of Beam R-Factor Minima, and Structural Search Strategies," Proc. Conf. on Determination of Surface Structure by LEED, Plenum, NY, 1981.

22. M. A. Passler, A. Ignatiev, B. W. Lee, D. Adams and M. A. Van Hove, "The Use of Reliability Factors for Surface Structure Determination of W(100)c(1x1)-H," Proc. Conf. on Determination of Surface Structure by LEED, Plenum, NY, 1981.

23. J. P. Biberian and M. A. Van Hove, "Arrangement of CO Molecules on Low Index Metal Surfaces: A Comparison Between LEED and HREELS or IRS," Proc. of the 1980 Conf. on Vibrations at Surfaces, Namur, Belgium.

24. D. L. Adams, H. B. Nielsen, M. A. Van Hove and A. Ignatiev, "LEED Study of the Pt(110)-(1x2) Surface," Surf. Sci. 104, 47 (1981).

Other Publications

1. G. A. Somorjai, Chemistry in Two Dimensions: Surfaces, Cornell University Press, 1981. Book.

LBL Reports

1. S. M. Davis and G. A. Somorjai, "Deuterium Exchange Reactions of n-Hexane and n-Heptane Catalyzed over Platinum Single Crystal Surfaces," J. Phys. Chem., LBL-12149.

2. S. Ferrer, J. M. Rojo, M. Salmeron and G. A. Somorjai, "The Role of Surface Irregularities (Steps, Kinks) and Point Defects on the Chemical Reactivity of Solid Surfaces," Philosophical Magazine, 1981.

3. S. M. Davis and G. A. Somorjai, "Surface Reactions," in Encyclopedia of Materials Science and Engineering, M. B. Bever, ed., Pergamon Press, NY, 1982, LBL-12372.

4. M. Salmeron, L. Brewer and G. A. Somorjai, "Structure and Stability of Platinum Oxide and Other Oxides of Noble Metals," Surf. Sci. 110, 227 (1981), LBL-12411.

5. M. Salmeron and G. A. Somorjai, "Adsorption and Bonding of Butane and Pentane on the Pt(111) Crystal Surfaces. Effects of Oxygen Treatments and Deuterium Preadsorption," J. Phys. Chem., LBL-12617.

6. R. J. Koestner, J. C. Frost, P. C. Stair, M. A. Van Hove and G. A. Somorjai, "Evidence of Alkylidyne Structure for C_3 and C_4 Unsaturated Hydrocarbons Adsorbed on a Pt(111) Single Crystal Surface," LBL-12780.

7. M. A. Van Hove and G. A. Somorjai, "Dynamical and Approximate LEED Theories Applies to Layers of Large Molecules," LBL-12803.

8. M. Salmeron and G. A. Somorjai, "The Desorption, Decomposition, and Deuterium Exchange Reactions of Unsaturated Hydrocarbons (Ethylene, Acetylene, Propylene, and Butenes) on the Pt(111) Crystal Face," J. Phys. Chem. (1982), LBL-12857.

9. P. W. Davies, M. Quinlan and G. A. Somorjai, "The Growth and Chemisorption Properties of Ag and Au Monolayers on Platinum Single Crystal Surfaces: An AES, TDS, and LEED Study," LBL-12946.

10. G. A. Somorjai, "The Surface Science of Heterogeneous Catalysis. Possible Applications in Atmospheric Sciences," J. Geophys. Res., LBL-12986.

11. G. A. Somorjai, "Study of the Structure of Adsorbed Molecules on Solid Surfaces by HREELS and LEES," Proc. 9th Intl. Conf. on Atomic Spectroscopy, XXII CSI, Tokyo, Sept. 1981, Pure and Appl. Chem., LBL-12996.

12. W. McLean, C. A. Colmenares, R. L. Smith and G. A. Somorjai, "Electron Spectroscopy Studies of the Clean Thorium and Uranium Surfaces. The Chemisorption and Initial Stages of Reaction with O_2, CO, and CO_2," Phys. Rev. B.

13. N. D. Spencer, R. C. Schoonmaker and G. A. Somorjai, "Structure Sensitivity in the Iron Catalysed Synthesis of Ammonia," Nature (1981), LBL-13162.

14. G. A. Somorjai, Scientific American Article, LBL-13163.

15. M. Langell and G. A. Somorjai, "The Composition and Structure of Oxide Films Grown on the (110) Crystal Face of Iron," LBL-13203.

16. E. L. Garfunkel and G. A. Somorjai, "Potassium and Potassium Oxide Monolayers on the Pt(111) and Stepped (755) Crystal Surfaces," Surface Sci., LBL-13293.

17. N. D. Spencer, R. C. Schoonmaker and G. A. Somorjai, "Iron Single Crystal as Ammonia Synthesis Catalysts: Effect of Surface Structure on Catalyst Activity," J. Catal. (1982), LBL-13294.

18. M. A. Van Hove, R. J. Koestner and G. A. Somorjai, "The Structures of Small Hydrocarbon Molecules on Rh(111) Studied by Low Energy Electron Diffraction: Acetylene, Ethylene, Methylacetylene, and Propylene," J. Vac. Sci. Technol., LBL-13300.

19. T.-H. Lin, W. L. Guthrie and G. A. Somorjai, "The Angular and Velocity Distribution of NO Scattered from the Pt(111) Crystal Surface," LBL-13347.

20. E. L. Garfunkel, J. E. Crowell and G. A. Somorjai, "The Strong Influence of Potassium on the Adsorption of CO on Platinum Surfaces: A TDS and HREELS Study," J. Phys. Chem., LBL-13349.

21. S. M. Davis, W. D. Gillespie and G. A. Somorjai, "Deuterium Isotope Effects for Hydrocarbon Reactions Catalyzed over Platinum Single Crystal Surfaces," J. Phys., LBL-13363.

22. Stephen Mark Davis, Ph.D. thesis, "Hydrocarbon Catalysis Over Platinum Single Crystal Sur-

faces: The Role of Adsorbed Carbon Deposits and Other Chemical Additives," (1981).

23. William Douglas Gillespie, Ph.D. thesis, "The Pressure, Structure and Composition Dependence of Catalyzed Hydrocarbon Reaction Over Platinum Single Crystal Surfaces," (1981).

Invited Talks

1. G. A. Somorjai, "Surface Science of Heterogeneous Catalysis," University of Nebraska, Lincoln, February 27, 1981.

2. G. A. Somorjai, "Surface Structure of Catalysis," ACS Meeting, Atlanta, GA, March 30, 1981.

3. G. A. Somorjai, "The Structures and Selective Catalysis of Hydrocarbons on Pt Crystal Surfaces," Kendall Award in Colloid and Surface Chemistry, April 1, 1981.

4. G. A. Somorjai, "Surface Science of Energy Conversion, and Catalysis on the Atomic Scale--"The Case History of Platinum," Mack Memorial Lectures, Ohio State and Columbia, April 30, 1981.

5. G. A. Somorjai, "Catalyzed Reactions of C and CO with Water Vapor and Hydrogen," Conference on Catalysis, NBS, Washington, DC, May 6 and 7, 1981.

6. G. A. Somorjai, "The Structure and Reactivity of Organic and Metal Monolayers on Platinum: The Building of New Metal Catalysts," Garden Research Conference, 50th Anniversary, Frontiers of Science, New London, NH, June 24, 1981.

7. G. A. Somorjai, "The Surface Science of Heterogeneous Catalysis: Possible Applications to Atmospheric Sciences," Workshop/Conference on Heterogeneous Catalysis in Atmospheric Chemistry, Albany, NY, June 29, 1981.

8. G. A. Somorjai, "The Surface Crystallography of Hydrocarbon Molecules Adsorbed on the Platinum and Rhodium (111) Surfaces," XIIth Congress and General Assembly, Chairman, Microsymposia, Ottawa, Canada, August 25, 1981.

9. G. A. Somorjai, "The Chemisorption of CO and CO_2 on Gold-Supported ThO_2 Films," 28th National Symposium, American Vac. Society, Boston, MA, September 10, 1981.

10. G. A. Somorjai, "The Surface Science of Heterogeneous Catalysis," Hokkaido University, Hokkaido, Japan, September 5, 1981.

11. G. A. Somorjai, "The Activity of Carbon and Metal Monolayers on Pt for Hydrocarbon Conversion: The Building of New Metal Catalysts," Tokyo Institute of Technology, Tokyo, Japan, September 7, 1981.

12. G. A. Somorjai, "Study of the Structure of Adsorbed Molecules on Solid Surfaces by High Resolution Electron Energy Loss Spectroscopy and LEED," 9th. Intl. Conf. on Atomic Spectroscopy, Tokyo, Japan, September 8, 1981.

13. G. A. Somorjai, "The Atomic Scale Ingredients of Heterogeneous Catalysis," Tsukuba Science City, Japan, September 9, 1981.

14. G. A. Somorjai, "Surface Monolayer Analysis by Electron Scattering and Emission," Symposium on Microbeam Analysis, Lake Biwa, Japan, September 10, 1981.

15. G. A. Somorjai, "New Techniques and Recent Trends in Surface Characterization," Symposium on Analytical Spectroscopy, Kyoto, Japan, September 12, 1981.

16. G. A. Somorjai, "The Chemistry of Monolayers on Surfaces: Structure and Bonding," Dreyfus Lectures, University of Colorado, Boulder, CO, September 16, 1981; "The Atomic Scale Ingredients of Heterogeneous Catalysis," Dreyfus Lectures, September 17, 1981; "The Building of New High Technology Heterogeneous Catalysts for Energy Conversion," Dreyfus Lectures, September 18, 1981.

17. G. A. Somorjai, "The Surface Science of Heterogeneous Catalysis. The Building of New High Technology Catalysts," R and D and the Chemical Industry in the 80's, Ashland Chem. Co., Columbus, OH, October 5-7, 1981.

18. G. A. Somorjai, "Surface Science of Heterogeneous Catalysis," U.C. Davis, Department of Chemistry Seminar, Davis, CA, November 3, 1981.

19. G. A. Somorjai, "The Surface Science of Heterogeneous Catalysis," The Robert A. Welch Foundation, Houston, TX, November 10, 1981.

20. G. A. Somorjai, "The Design of New Heterogeneous Catalysts," AIChE Symposium, New Orleans, LA, November 12, 1981.

21. M. A. Van Hove, "The Structure of Ethylene Adsorbed on Rh(111) Determined by a Dynamical Low Energy Electron Diffraction Analysis," American Physical Society Meeting, Phoenix, AZ, March 16, 1981.

22. M. A. Van Hove, "The Structure of Small Hydrocarbon Molecules Adsorbed on Pt(111) and Rh(111)," NASA-Ames, Moffett Field, CA, March 31, 1981.

23. M. A. Van Hove, "Recent Surface Structure Determinations by Low Energy Electron Diffraction: Metal Surface Reconstructions, Adsorbed Molecules," University of California, Santa Barbara, June 5, 1981.

24. M. A. Van Hove, "The Structure of Small Hydrocarbon Molecules Adsorbed on Pt and Rh(111), Studies by LEED and HREELS," Exxon Research Laboratories, Linden, NJ, August 3, 1981.

25. M. A. Van Hove, "Phase Transitions in Molecular Overlayers on Pt and Rh(111)," Conference on Phase Transitions on Surfaces, Orono, Maine, August 6, 1981.

26. M. A. Van Hove, "Recent Structure Determinations by LEED: Clean Metal Surface Reconstructions," Brookhaven National Laboratory, Upton, NY, August 10, 1981.

27. M. A. Van Hove, "Recent Structure Determinations by LEED: Clean Metal Surface Reconstructions and Adsorbed Molecules," University of Wisconsin-Milwaukee, August 18, 1981.

28. M. A. Van Hove, "The Structures of Small Hydrocarbon Molecules on Rh(111) Studies by Low Energy Electron Diffraction: Acetylene, Ethylene, Methylacetylene and Propylene," American Vacuum Society Meeting, Anaheim, CA, November 5, 1981.

I. Nuclear Magnetic Resonance*

A. Pines, Investigator

Introduction. Techniques have been developed using nuclear magnetic resonance (NMR) to study the structure and dynamics of atoms and molecules, for example those in liquid crystals and in matter undergoing photochemical reaction or subjected to magnetic fields. The studies are interesting from a theoretical standpoint, e.g., the way in which molecules absorb groups of photons in multiple quantum spectroscopy, and are also providing information about the properties of several classes of materials.

Multiple quantum spectroscopy (the selective absorption of groups of photons) has been developed and applied to the study of molecular conformations and dynamics, high resolution NMR in inhomogeneous magnetic fields, and anisotropic diffusion in liquid crystals. Time-resolved photochemistry in magnetic fields yields isotope enrichment through the magnetic isotope effect and allows the study of molecules in optically excited crystals.

1. ANISOTROPIC DIFFUSION IN LIQUID CRYSTALS

D. B. Zax and A. Pines

A quantitative measure of the rate of molecular diffusion is important in a number of areas of chemical research. These measurements are particularly important to an understanding of fundamental processes in membranes and lipid bilayers. Liquid crystals have been proposed as models for such systems. Pulsed spin echo techniques, which have traditionally provided the most reliable measure of diffusion rates in isotropic systems, are not directly applicable to these anisotropic systems. The same ordering that makes these systems function as orienting environments results in only partial averaging of the dipolar interaction and often precludes the formation of a spin echo.

Using multiple quantum spin echo techniques, the effect of the dipolar interactions can be largely overcome. Furthermore, multiple quantum spin echoes have been shown to be far more sensitive to diffusion than the standard NMR techniques. This is a particular advantage in an ordered system where diffusion is expected to be slow.

Experiments have been performed on benzene dissolved in a nematic phase liquid crystal (Fig. 1). We have found $D = 1.25 \pm 0.15 \times 10^{-6} cm^2/sec$ parallel to the liquid crystal director axis and $D = 9.95 \pm 0.15 \times 10^{-6} cm^2/sec$ perpendicular to the axis of orientation. This yields a $D_{\parallel}/D_{\perp} = 1.3$, which is close to the $\pi/2$ expected from a simple theory. Further work will investigate the effect of shape on the anisotropy of diffusion of small molecules dissolved in nematic phases, and diffusion in discotic phases.

Fig. 1. Anisotropic diffusion of benzene in a nematic liquid crystal matrix. (XBL 8112-13092)

2. DOUBLE QUANTUM COHERENCE OF SPIN 1 IN LIQUIDS†

Y. S. Yen, D. P. Weitekamp, and A. Pines

Pulse sequences developed to excite double quantum coherence of spin 1 nuclei in solids are ineffective in liquids where the motional average of the quadrupole coupling vanishes. However, through resolved J couplings, double quantum coherence can be obtained using the magnetization of neighboring heteronuclei.

The observation of double quantum coherence in ^{14}N, a quadrupolar nucleus of spin 1, by heteronuclear coherence transfer was demonstrated in the ammonium ion system. Figure 1 shows the ^{14}N double quantum transition lines of an ammonium nitrate solution as detected through the protons. The

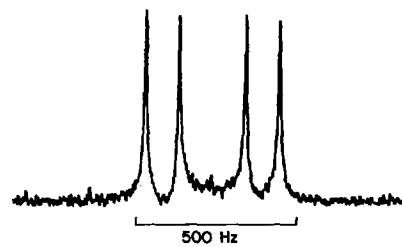

Fig. 1. Proton detected ^{14}N double quantum magnitude spectrum of an 8 molar ammonium nitrate solution. (XBL 819-4950)

*This work was supported by the Director, Office of Energy Research, Office of Basic Energy Sciences, Materials Sciences Division of the U.S. Department of Energy under Contract No. DE-AC03-76SF00098.

indirect detection scheme benefits from the high sensitivity of proton NMR. The double quantum multiplet splitting is 2J, and thus offers inherently better resolution than is possible in the single quantum spectrum. Linewidth measurement of the double quantum lines contributes additional information to the relaxation dynamics of ^{14}N in isotropic solution.

* * *

†Brief review of LBL-13434, Y. S. Yen and D. P. Weitekamp, J. Mag. Res. (in press).

3. MOLECULAR CONFORMATION IN LIQUID CRYSTALS†

S. Sinton, G. Drobny, and A. Pines

The study of the conformation of aromatic units in liquid crystal molecules is important in understanding the physics and chemistry of their various fascinating phases. This can usually only be accomplished with deuterium isotope substitution and complex analysis of the NMR spectra. However, multiple quantum transitions are extremely sensitive to correlations, both static and dynamic, between the protons of a molecule and are usually resolvable and simple to analyze. We have used this to study the conformations of a number of liquid crystal systems and the relationship of these conformations to the macroscopic phases. For example, in the nematic phase of cyanobiphenyl systems, the conformation of the biphenyl group could be analyzed by fitting the 6- and 7-quantum spectra (the normal 1-quantum spectrum has ~ 1000 lines and can hardly be analyzed) to theoretical models of the order parameters and biphenyl dihedral angle.

Aliphatic chain configurations can also be studied, since the multiple quantum spectra are extremely sensitive to inter-segment dipole-dipole couplings (Fig. 1). The best fit is found to be a model with all trans and two conformations with gauche defects.

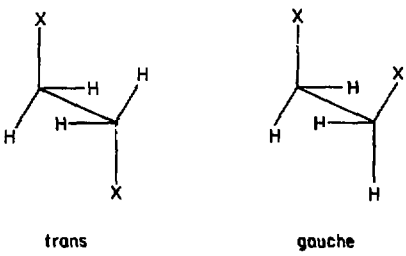

Fig. 1. Trans and gauche configuration of an aliphatic chain. Such chain configurations along an oriented chain are being studied using high multiple quantum transitions. (XBL 811-7662)

* * *

†Based in part on LBL-13604.

4. SELECTIVE EXCITATION OF HIGH n-QUANTUM TRANSITIONS†

W. S. Warren, D. P. Weitekamp, Y. S. Yen, J. R. Garbow, and A. Pines

The question of whether a molecule can be used to absorb and emit photons only in groups of n has been treated further. A number of pulse sequences have been introduced which in effect induce excitation by only resonant groups of n photons. This causes only n-quantum transitions even when many other transitions might be resonant. The theory explains how this is done by using repeated phase shifts of $2\pi/n$ in the radiation to build up the selected coherences with all other coherences interfering destructively. Coherent averaging theory was extended to describe selective sequences and together with time reversal excitation produces efficient n-quantum pumping which is selective to arbitrarily high order in the average Hamiltonian. The selectivity produces an enormous enhancement of the high n-quantum coherences (or populations) which are normally very weak when governed by an incoherent statistical process. For example, the 12-quantum transition in a many spin crystal can be enhanced by four or five orders of magnitude.

* * *

†Based in part on LBL-11885.

5. NOISE IN TWO DIMENSIONAL SPECTROSCOPY†

D. P. Weitekamp and A. Pines

In two dimensional NMR spectroscopy, a recent area of enormous value, the observable magnetic dipole radiation is recorded in a period t_2 as a function of variable evolution times t_1. Fourier transformation of the resulting signal $g(t_1,t_2)$ yields a two dimensional spectrum $\hat{g}(\omega_1,\omega_2)$. It has long been observed that such experiments are subject to noise contributions which play no role in the traditional one dimensional experiments. Its existence has been attributed arbitrarily to instrumental instability but no theory of its statistical nature or methods for its elimination or minimization have been previously proposed. Experience in our laboratory shows this "t_1 noise" to be the dominant contribution limiting the sensitivity and applicability of two dimensional experiments. We have developed a simple model of t_1 noise as resulting from random fluctuations in the transfer function characteristic of the measurement process. The model predicts a positive dependence of the observed noise on signal amplitude which has been confirmed in several ways. The model and experiments demonstrate that t_1 noise is multiplicative in contrast to usual thermal mechanisms which produce additive noise. This understanding has allowed us an approach to minimization of t_1 noise and enhancement of two dimensional sensitivity by the use of pulsed field gradients,

coherence transfer echoes and selective excitation sequences.

* * *

†Brief review of LBL-13557.

6. HIGH RESOLUTION NMR IN INHOMOGENEOUS FIELDS

J. R. Garbow, D. P. Weitekamp, and A. Pines†

The homogeneity of the external magnetic field often places a limitation on the obtainable resolution in NMR experiments. Multiple quantum transitions are particularly susceptible to this inhomogeneous broadening, the broadening being linear in the multiple quantum order, n. In addition, the phases (and intensities) of individual multiple quanta are generally random, being dependent upon the details of the coherent excitation. These two effects can lead to a loss of information in multiple quantum spectra. Using total spin coherence, the effects of magnetic field inhomogeneity can be completely removed.

The total spin coherence is the highest order multiple quantum transition in a coupled spin system, the one between the extreme energy states. This single transition serves as both the initial and final condition from this highest order to one selective order. Times are chosen so that only transitions belonging to this selected order echo, yielding spectra that are totally free of inhomogeneous broadening. Preserved in the resulting sharp line spectra are all chemical shifts and spin-spin couplings as shown in Fig. 1 of partially oriented acetaldehyde along with a profile of the magnetic field in which the spectrum was taken.

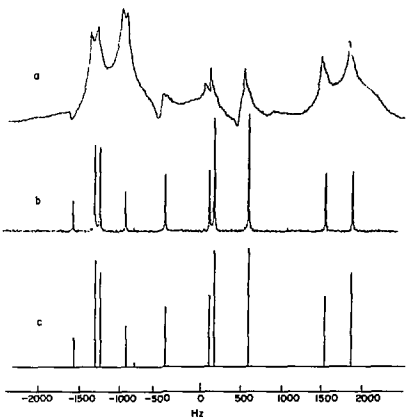

Fig. 1. Removal of inhomogeneous broadening by total spin coherence transfer echo spectroscopy. (a) the single quantum Fourier transform proton spectrum of acetaldehyde in a nematic liquid crystal was taken in an inhomogeneous field and then (b) with a coherence transfer pulse sequence yielding lines with widths limited only by homogeneous broadening. The simulation of this AB_3 system is shown in (c) demonstrating that there are no distortions in line positions. The lines of E symmetry are absent because they do not correlate with the total spin transition.
(LBL 811-7538)

* * *

†D. P. Weitekamp, J. R. Garbow, J. B. Murdoch, and A. Pines, J. Am. Chem. Soc. 103, 3578 (1981); LBL-12085.

1981 PUBLICATIONS AND REPORTS

Refereed Journals

1. D. Wemmer, D. J. Ruben, and A. Pines, "NMR Study of Molecular Reorientation under Fivefold Symmetry - Solid Permethylferrocene," J. Chem. Soc., 103, 28 (1981); LBL-10563.

2. G. Drobny, A. Pines, S. Sinton, W. S. Warren, and D. P. Weitekamp, "Selectivity in Multiple-Quantum Spectroscopy," Phil. Trans. R. Soc. Lond. A 299, 585 (1981); LBL-11157.

3. W. S. Warren and A. Pines, "Analogy of Multiple-Quantum NMR to Isotopic Spin Labeling," J. Am. Chem. Soc., 103, 1613 (1981); LBL-11345.

4. W. S. Warren and A. Pines, "Experiments on Selective Excitation of Multiple Quantum Transitions in NMR Spectroscopy," J. Chem. Phys., 74, 2808 (1981); LBL-11916.

5. D. P. Weitekamp, J. R. Garbow, J. B. Murdoch, and A. Pines, "High Resolution NMR in Inhomogeneous Magnetic Fields: Application of Total Spin Coherence Transfer Echoes," J. Am. Chem. Soc., 103, 3578 (1981); LBL-12085.

6. S. Emid, J. Smidt, and A. Pines, "Dipolar Relaxation by Rotation in Spin Space," J. Mag. Res., 45, 94 (1981).

For further references, see article on Coal Liquefaction Alloy Test Program.

LBL Reports

1. W. S. Warren and A. Pines, "Simple Pulse Sequences for Selective Multiple-Quantum Excitation," LBL-13006.

2. Y. S. Yen and D. P. Weitekamp, "Indirect Detection of Spin 1 Double Quantum Coherence in Liquids," LBL-13434 (submitted for publication, J. Mag. Reson.).

3. D. P. Weitekamp, J. R. Garbow, and A. Pines, "Search Procedure for Optimizing High Order Multiple Quantum Transition Intensities," LBL-13557 (submitted for publication, J. Mag. Reson.).

4. Larry Lee Sterna, "Effect of Nuclear Spin on Chemical Reactions and Internal Molecular Rotation," Ph.D. thesis, Berkeley, December 1980, LBL-10594.

5. Jau-Huei Tang, "Study of Correlations in Molecular Motion," Ph.D. thesis, Berkeley, November 1981, LBL-13605.

6. Steven William Sinton, "NMR Studies of Oriented Molecules," Ph.D. thesis, Berkeley, November 1981, LBL-13604.

7. Gary Drobny, "NMR Studies of Liquid Crystals and Molecules Dissolved in Liquid Crystals," Ph.D. thesis, Berkeley, LBL-13736.

Invited Talks

1. A. Pines, "Study of Molecular Conformation and Dynamics in Polymers," Monsanto Research Corporation, St. Louis, MO, February 1981, seminar.

2. A. Pines, "Nuclear Magnetic Resonance with Lots of Photons," Robert W. Vaughan Lectureship in Chemical Engineering, California Institute of Technology, Pasadena, March 5, 1981.

3. A. Pines, "Selective Excitation in Multiple Quantum Spectroscopy," 5th European Experimental NMR Conference, Konigstein, West Germany, May 1981, invited talk.

4. A. Pines, "Recent Developments in Multiple Quantum NMR," 23rd Rocky Mountain Conference, Denver, CO, August 2-6, 1981, invited lecture.

5. A. Pines, "Recent Developments in Multiple Quantum Spectroscopy," 5th Specialized Colloque Ampere, Uppsala, Sweden, August 17-21, 1981, invited lecture.

6. A. Pines, "Selective n-Quantum Excitation," Gordon Research Conference on Magnetic Resonance, Wolfeboro, NH, June 15-19, 1981, invited talk.

7. A. Pines, series of lectures on Modern Multiphoton Techniques, IBM Research Division, Danebury, CT, October 26, 1981.

8. A. Pines, "Free Induction Decay - Where Does It Go?" Department of Chemistry, Harvard University, Cambridge, MA, October 28, 1981, seminar.

9. A. Pines, "NMR with Lots of Photons," The Guy Allen Lecture in Physical Chemistry, Yale University, New Haven, CT, October 30, 1981.

10. A. Pines, "Free Induction Decay - Where Does It Go?" Department of Chemistry, The University of Utah, Salt Lake City, December 8, 1981, research seminar.

11. G. Drobny, "Selective Excitation in Multiple Quantum Spectroscopy," 22nd ENC Conference, Asilomar, CA, April 5-9, 1981, invited talk.

12. J. R. Garbow, A. Pines and D. P. Weitekamp, "High Resolution Measurement of Local Fields Using Multiple Quantum NMR," poster presentation, 22nd ENC Conference, Asilomar, CA, April 5-9, 1981.

13. A. Pines, "NMR With Lots of Photons," The Guy Allen Lecture in Physical Chemistry, Yale University, New Haven, CT, October 30, 1981.

14. A. Pines, "Free Induction Decay - Where Does it Go?" Department of Chemistry, The University of Utah, Salt Lake City, seminar, December 8, 1981.

15. A. Pines, "Mobil Research and Development," Princeton, NJ, seminar, December 10, 1981.

II Chemical Sciences

A. Fundamental Interactions

1. Photochemical and Radiation Studies

a. Photon-Assisted Surface Reactions, Materials, and Mechanisms*

Gabor A. Somorjai, Investigator

Introduction. This project explores photocatalyzed chemical reactions that take place at the solid-vapor interface. These reactions include the photo-dissociation of water (H_2O) to produce hydrogen and oxygen and the photon assisted reactions of carbon dioxide (CO_2) and water to produce simple hydrocarbons (photosynthesis). The purpose of these studies is to explore the mechanism of photon-assisted surface reactions and then establish the optimum conditions (of surface structure, composition, temperature and reactant mixture) to maximize the rate of production of the desired chemicals (hydrogen and/or hydrocarbons). The materials that are being used include strontium titanate, iron oxides and silicates and rhenium sulfide.

1. PHOTODISSOCIATION OF WATER ON IRON-BASED OXIDE SURFACES

C. Leygraf and G. A. Somorjai

Fe_2O_3 is a promising material for the photo-assisted dissociation of water because of its small band gap (~ 2.2 eV) and chemical stability. The band positions for this semiconductor relative to the H^+/H_2 and O_2/H_2O redox energy levels are, however, unfavorable. Thus, an external bias is required in order to shift the band positions of Fe_2O_3 so that photodissociation of water can occur. Work is in progress to dope Fe_2O_3 with Si and with metals of low electron affinity in order to achieve a better matching between the band positions and the redox energy levels of H_2O. Photoelectrochemical measurements of synthesized iron-based oxides show that when introducing a few percent of SiO_2 into Fe_2O_3 the resulting n-type semiconductor requires at least 125 mV less external bias than pure Fe_2O_3 for the photodissociation of water.

2. THE COMPOSITION AND STRUCTURE OF OXIDE FILMS GROWN ON THE (110) CRYSTAL FACE OF IRON†

M. Langell and G. A. Somorjai

Epitaxial oxide layers of Fe_3O_4-like composition and symmetry have grown on Fe(110) crystals exposed to oxygen gas. The epitaxial relationship between the oxide and the Fe(110) substrate is elucidated and the orientation of the oxide film has been explained in terms of the close registry between the Fe(110) and Fe_3O_4(111) crystal lattices. Both the structure and composition of the iron oxide epitaxies are a function of substrate temperature and oxygen pressure, and an oxide nucleation point has been observed over only part of the temperature-pressure range investigated. While oxide surfaces with Fe_2O_3-like composition have been observed, they are disordered and are only approximately one monolayer in thickness.

3. WORK IN PROGRESS

An apparatus has been constructed to simultaneously measure the photocurrent and the gas evolution during the photon assisted dissociation of water. This instrument is being used to evaluate the iron based doped oxides for photodissociation activity.

ReS_2 and MoS_2 as well as FeS_2 are being evaluated for possible photoactivity.

* * *

†Brief version of LBL-13203.

1981 PUBLICATIONS AND REPORTS

Refereed Journals

1. S. Ferrer and G. A. Somorjai, "UPS Study of the Adsorption of Oxygen on Reduced $SrTiO_3$ Surfaces," J. Appl. Phys. 52, 4792 (1981); LBL-11614.

2. S. Ferrer and G. A. Somorjai, "Evidence for Photodissociation of Water Vapor on Reduced $SrTiO_3$(111) Surfaces in a High Vacuum Environment. Relationship Between the Rate of Hydrogen Evolution and the Surface Concentration of Ti^{3+} Species," Phys. Chem. Lett. 85, 1464 (1981); LBL-11661.

3. R. G. Carr and G. A. Somorjai, "Hydrogen Production from Photolysis of Steam Adsorbed onto Platinized $SrTiO_3$," Nature 290, 576 (1981); LBL-11872.

4. F. T. Wagner, S. Ferrer and G. A. Somorjai, "Surface Aspects of Hydrogen Photogeneration on Titanium Oxides," in Photoeffects at Semiconductor-Electrolyte Interfaces, ed. A. J. Nozik, ACS Symposium Series 146, Washington, 1981; LBL-11456.

*This work was supported by the Director, Office of Energy Research, Office of Basic Energy Sciences, Chemical Sciences Division of the U.S. Department of Energy under Contract No. DE-AC03-76SF00098.

Other Publications

1. G. A. Somorjai, Chemistry in Two Dimensions: Surfaces, Cornell University Press, 1981. Book.

LBL Reports

1. M. Langell and G. A. Somorjai, "The Composition and Structure of Oxide Films Grown on the (110) Crystal Face of Iron," LBL-13203.

2. F. T. Wagner, "Photocatalytic Hydrogen Production from Water and Intermetallic Compound Formation on Single Crystal Surfaces of Titanium Oxides," Ph.D. thesis, July 1981.

3. Roger Gladwin Carr, "Photo-induced Reactions of Gases Adsorbed Onto Semiconductor Surfaces," Ph.D. thesis, November 1981.

Invited Talks

1. G. A. Somorjai, "Hydrogen Production From Photolysis of Steam Adsorbed Onto Platinized $SrTiO_3$," 5th DOE Solar Conference, Brookhaven National Laboratory, Upton, NY, May 28, 1981.

b. Photochemistry of Materials in the Stratosphere*

Harold S. Johnston, Investigator

1. NITROGEN OXIDES AND THE SST CONTROVERSY TEN YEARS LATER: A CASE STUDY IN THE USE OF SCIENCE FOR DECISION MAKING

Harold S. Johnston

A decade ago it was generally felt that the atmosphere is so massive that human activity could not bring about significant atmospheric perturbations on the global scale. In 1970 it was pointed out that natural ozone is destroyed catalytically by the oxides of nitrogen (NO, NO_2) at partial pressures 10^{-3} to 10^{-2} that of ozone itself, and a year later it was shown that the then planned 500 supersonic transports (SST) flying as scheduled at 20 kilometer altitude would more or less double stratospheric NO_x on the global scale. Including the primitive knowledge of the stratosphere available in 1971, model calculations for various plausible scenarios indicated global-average ozone reductions between 3 and 23% for this NO_x perturbation.

Over the intervening 10 years, there has been extensive observational, laboratory, and theoretical research on stratospheric ozone problems, including the discovery in 1974 of the effect of organic chlorides. These new measurements and considerations of atmospheric motions have been incorporated in a sequence of models that necessarily change as often as significant new data are obtained. Using a given model of atmospheric motions and a standard input of NO_x at 17 and at 20 kilometers, the atmospheric scientists at Lawrence Livermore National Laboratory have calculated the change of the ozone vertical column for the sequence of chemical models between 1974 and 1981 as shown in Fig. 1.

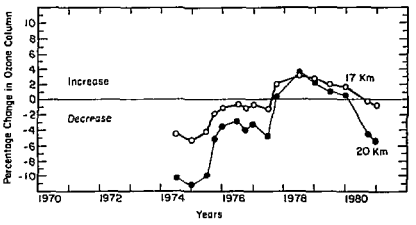

Fig. 1. History of the calculated change in the ozone vertical column for standard nitric oxide injections at 17 and at 20 km altitude as calculated by the Lawrence Livermore Laboratory model. These calculations were made with the same model for atmospheric motions, but they vary with changed perceptions of how to treat solar radiation, in identity of important species, and in values of photochemical rate coefficients.
(XBL 824-9049)

A three-year crash program of research by the Department of Transportation with standard NO_x injection at 20 km led in 1974 to a calculated 10% ozone reduction. After recognition of chlorine as an important stratospheric species, the model indicated a 4 or 5% ozone reduction. The changes in predictions since then have primarily depended on new results concerning hydroxyl radicals, since these tie up the catalytically active NO_x (HO + NO_2 → HNO_3) and free the catalytically active form of ClX (HO + HCl → H_2O + Cl). Several new studies indicated a shift between HOO and HO, and the model calculated an increase in the ozone column during 1978-80. Recently several further studies have found that HO and HOO are removed faster than previously thought, and in 1981 the model again predicts an ozone decrease for stratospheric NO injections. The changing predictions in Fig. 1 reflect the evolution of this field of science from a primitive state in 1971 to a highly, but still not fully, developed state in 1981.

* * *

†Brief version of a paper presented at AAAS Symposium, Toronto, January 1981. (LBL-12251)

2. HIGH-RESOLUTION ABSORPTION SPECTRUM OF THE NITRATE FREE RADICAL†

William J. Marinelli, Diane Swanson, and Harold S. Johnston

The nitrate free radical (NO_3) plays a minor, but not negligible role, in several stratospheric reactions. Its concentration in the atmosphere and in the laboratory is measured by light absorption at 662 nm. Recent determinations of the absorption cross-section at the 662 peak have differed by about 35%. This study was undertaken to establish the shape of this absorption peak and to see if this zero-zero vibrational peak shows any fine structure.

Small amounts of NO_3 are produced as free-radical intermediate in a system of N_2O_5 and ozone. A CW argon-ion laser was used to excite a tunable dye laser, which could be operated at moderate (0.05 nm) or very high (0.0003 nm) resolution. Absorption spectra were obtained in a cell 2 meters long, and corrections were made for ozone.

The absorption spectrum showed no fine structure at high resolution, and its shape was accurately determined. It was shown that recent absolute spectra gave the same integrated absorption (within 3%) over this peak, even though the values at the peak were different. One of these studies had poor resolution and an apparent discrepancy was due to this feature.

*This work was supported by the Director, Office of Energy Research, Office of Basic Energy Sciences, Chemical Sciences Division of the U.S. Department of Energy under Contract No. DE-AC03-76SF00098.

* * *

†Brief version of LBL-13699, November 1981.

3. PRIMARY PRODUCTS IN THE PHOTOLYSIS OF CHLORINE NITRATE†

William J. Marinelli and Harold S. Johnston

Chlorine nitrate ($ClONO_2$), being produced by the combination of NO_2 and ClO, ties up two ozone-destroying catalysts in the stratosphere. In this way an increase in chlorine plays a double role, it tends directly to reduce ozone but it also reduces an ozone destroyer (NO_2). The photolysis of chlorine nitrate returns it to the active ozone-destroying species, but there is considerable uncertainty as to the primary products of this process.

Chlorine nitrate was photolyzed by a pulse of ultraviolet radiation from an excimer laser, and the NO_3 product was followed by absorption of visible light from an argon ion excited dye laser. The photolyzing beam and the probing beam were propagated coaxially down a 2 meter long reaction tube, and the concentration of NO_3 was followed for about 2 milliseconds before and after the photolyzing pulse.

Results were obtained over a range of intensities of the photolyzing pulse, at two different total pressures, and with different carrier gases. The results are shown in Fig. 1. The primary quantum yield for NO_3 production is

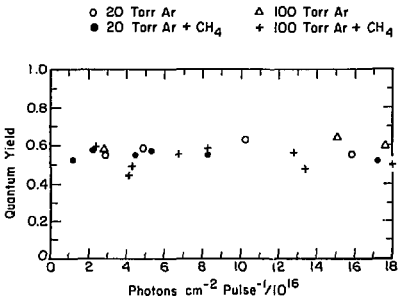

Fig. 1. Observed primary quantum yield of NO_3 from the photolysis of chlorine nitrate.
(XBL 8111-12363)

0.55 ± 0.1. These results indicate that Cl + NO_3 is the major product channel; but parallel channels, such as ClO + NO_2, are not excluded.

* * *

†Brief version of LBL-13473, December 1981.

4. INTEGRATED ABSORPTION COEFFICIENTS FOR SEVERAL VIBRATION-ROTATION TRANSITIONS OF THE GAS-PHASE HYDROXYL RADICAL USING A TUNABLE DIODE LASER†

James R. Podolske and Harold S. Johnston

Although transition frequencies of the hydroxyl radical are known accurately, information on integrated absorption coefficients has been restricted to theoretical calculations and to inference from emission studies.

In this study a narrow line-width tunable diode laser was coupled with a molecular modulation spectrometer directly to measure the integrated absorption coefficients of several vibration-rotation transitions of the hydroxyl radical. An example of the data is given by Fig. 1. At a

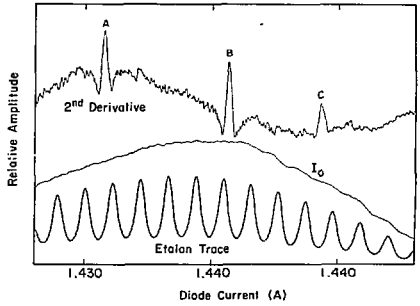

Fig. 1. Diode laser signal near 3407.75 cm^{-1} as scanned by variation of current through the diode. I_0, a single emission mode. Upper curve: B, H_2O calibration line at 3407.826 cm^{-1}; A, HO at 3407.607 cm^{-1}; C, HO at 3407.989 cm^{-1}. Lower curve: wavelength scale based on B.
(XBL 818-11461)

fixed low temperature, the output of the diode laser is scanned through a single mode, I_0, and second derivative spectra are displayed. Band B is a well-known very weak absorption by water at 3407.826 cm^{-1}; the wavelength scale is established relative to B by the etalon trace; and bands A (3407.607 cm^{-1}) and C (3407.989 cm^{-1}) are absorptions by the HO radical. The absolute intensities of A and C are derived from the known absolute intensity of water at B and from the absolute concentration of HO as established by molecular modulation experiments involving the photolysis of ozone in the presence of water vapor.

These absolute integrated absorption coefficients should permit quantitative optical analysis for HO in the atmosphere, in flames, and in other environments.

* * *

†Brief version of material in LBL-13218, September 1981.

5. RATE CONSTANT FOR THE RESONANT ENERGY TRANSFER BETWEEN ELECTRONICALLY EXCITED OXYGEN, $O_2(^1\Delta_g)$, AND THE HOO FREE RADICAL†

James R. Podolske and Harold S. Johnston

Although it has been known for some time that the resonant energy-transfer reaction $HO_2(^2A'') + O_2(^1\Delta_g) \rightarrow HO_2(^2A') + O_2(^3\Sigma_g^-)$ occurs at a fast rate, the rate constant for this reaction had not been measured, and the reaction is not included in atmospheric or laboratory models.

The response of ozone to ultraviolet light without and with added water vapor was studied, and the results were shown to contradict current kinetic models unless the above reaction is included. If the value 8×10^{-11} cm^{-3} s^{-1} is used for the reaction $HO + HOO \rightarrow H_2O + O_2$, then the rate constant for the energy transfer reaction is 4×10^{-11} cm^{-3} s^{-1}.

Although this reaction is probably unimportant in atmospheric models, it is very important in laboratory studies involving ozone and water. The neglect of this reaction in such laboratory studies explains some of the large discrepancies reported by different workers for the rate of the reaction $HO + HOO \rightarrow H_2O + O_2$.

* * *

†Brief version of material in LBL-13218, September 1981.

6. THE RATE OF REACTION OF HYDROXYL RADICALS WITH NITRIC ACID AS A FUNCTION OF TEMPERATURE†

William J. Marinelli and Harold S. Johnston

Recently, Ravishankara and co-workers[1] reported that the reaction $HO + HNO_3 \rightarrow H_2O + NO_3$ has a rate that increases as temperature decreases over the range 400 to 200 K. This unexpected finding is one of the major features causing the 1981 change in Fig. 1 of report 1, that is, the large increase in ozone depletion calculated for NO_x injections in the stratosphere. This result appeared very strange in terms of gas-phase reaction rate theory, and a careful reinvestigation was undertaken.

Hydroxyl radicals were produced by partial photolysis of HNO_3 at 249 nm by a pulsed excimer laser, and their relative concentrations were followed as a function of time by hydroxyl radical resonance fluorescence. Rate constants were obtained with good precision as a function of temperature (Fig. 1). The result between 218-363 K is: $k = (1.5 \pm 0.4) \times 10^{-14} \exp(644 \pm 79/T)$ cm^3 s^{-1}, which agrees closely with the value between 224 and 366 K reported by Ravishankara et al.: $k = 1.5 \times 10^{-14} \exp(649/T)$.

The unusual result by Ravishankara is confirmed by this study, and thus the far ranging impact of this result on both NO_x and ClX perturbation calculations is supported.

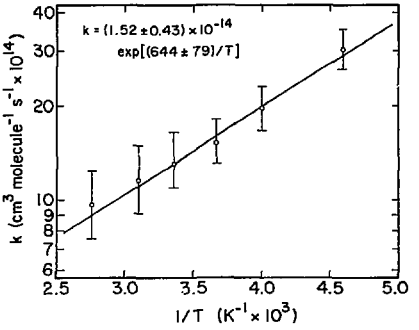

Fig. 1. Arrhenius plot for the reaction of HO with HNO_3 from 218-363 K, showing negative activation energy. (XBL 8111-12366)

* * *

†Brief version of material in LBL-13473, December 1981.

1. P. H. Wine, A. R. Ravishankara et al., J. Geophys. Res. 86, 1105 (1981).

1981 PUBLICATIONS AND REPORTS

Refereed Journals

1. H. H. Nelson, W. J. Marinelli and H. S. Johnston, "The Kinetics and Product Yield of the Reaction of HO with HNO_3," Chem. Phys. Lett. 78, 495 (1981); LBL-12096.

2. G. S. Selwyn and H. S. Johnston, "Ultraviolet Absorption Spectrum of Nitrous Oxide as Function of Temperature and Isotopic Substitution," J. Chem. Phys. 74, 3791 (1981); LBL-11234.

LBL Reports

1. H. H. Nelson and H. S. Johnston, "The Kinetics of the Reaction of Cl with ClNO and $ClNO_2$ and the Photochemistry of $ClNO_2$," accepted for publication in J. Phys. Chem, LBL-13177.

2. M. Kowalczyk, "Molecular Beam Chemiluminescence Studies of the NO + O_3 Reaction and Modeling of Global NO_2 Distribution," Ph.D. thesis, University of California, Berkeley, November 1980, LBL-12106.

3. James R. Podolske, "Integrated Absorption Coefficients for Several Vibration-Rotation Transitions of the Gas-Phase Hydroxyl Radical Using a Tunable Diode Laser," Ph.D. thesis, University of California, Berkeley, September 1981, LBL-13218.

4. William J. Marinelli, "The Photochemistry of HNO_3 and $ClNO_3$," Ph.D. thesis, University of California, Berkeley, December 1981, LBL-13473.

Invited Talks

1. H. S. Johnston, "The Nitrogen Oxides Controversy," American Association for the Advancement of Science Symposium, Toronto, Ontario, Canada, January 8, 1981, LBL-12251.

2. Chemical Physics

a. Energy Transfer and Structural Studies of Molecules on Surfaces*

Charles B. Harris, Investigator

1. ENERGY TRANSFER STUDIES BETWEEN ADSORBED MOLECULES AND Ag SURFACES IN ULTRAHIGH VACUUM†

C. B. Harris, H. J. Robota, and P. M. Whitmore

The importance of electric fields localized at metal surfaces and the collective excitations of electrons at the metal surface in affecting molecular properties of adsorbates has recently received a great deal of attention. In order to study these interactions, an experimental configuration which can easily be adapted to a number of experiments involving metal surface excitations was utilized.

Counterpropagating optical paths for a rotating analyzer spectroscopic ellipsometer and a tunable dye laser excitation source allow measurement and precise control of the thickness of deposited layers on the metal surface as well as a means of investigating their optical response functions. State-selective excitation of the adsorbate is obtained by means of a tunable laser system, and an f/1 collection lens located inside the vacuum chamber is used to collect luminescence and couple the signal to external optics.

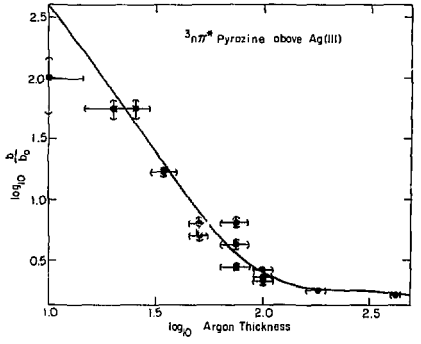

Fig. 1. Normalized decay rate vs. argon thickness for $^3n\pi^*$ pyrazine above Ag(111). Curve is calculated from a classical model.

(XBL 819-6592)

This system was recently applied to the study of nonradiative energy transfer from the $^3n\pi^*$ state of 1,4 diazabenzene to an Ag(111) surface. Following the laser pulse, the time dependence of the emission decay was time averaged and the resulting decay curve at a single thickness of argon is obtained. Figure 1 shows the experimental energy transfer rates vs distance from the Ag(111) surface and a comparison with the distance dependent rate calculated from a theoretical model.[1]

* * *

†Brief version of LBL-13031 (In press, JCP Communication 1981).

1. R. R. Chance, A. Prock and R. Silbey, Adv. in Chem. Phys. 37,1 (1978).

2. ROLE OF SURFACE PLASMONS IN ENERGY TRANSFER TO METAL SURFACES THROUGH NEAR FIELD DIPOLE COMPONENTS†

C. B. Harris, P. M. Whitmore, and H. J. Robota

The coupling of surface plasmons to excited states of adsorbed molecules can play an important role in determining the spectroscopic and chemical behavior of the adsorbates. Using a classical model that uses bulk optical properties and geometrical boundaries to describe the interaction of a dipolar field with a surface, excellent agreement with the experimental data was obtained (cf. Fig. 1 of article 1) down to a distance of 10 Å.

Energy transfer from an excited dipole near a metal surface occurs through the near-field components of the dipole electric field (i.e., those components with a $1/R^2$ and $1/R^3$ spatial dependence). In general, the metal can accept the energy either through the excitation of surface plasmons or by driving the nearly free electrons, which then dissipate the energy through bulk scattering processes. In Fig. 1a the total decay rate of $^3n\pi^*$ pyrazine on silver has been separated into the relative probability for decay into photons (RD), surface plasmons (SP), and bulk dielectric losses ("lossy surface waves," LW). The energy of $^3n\pi^*$ pyrazine (3.3 eV) lies very close to the silver surface plasmon resonance (at 3.6 eV) and hence energy transfer to the silver surface plasmons is efficient and long range. By contrast, the same breakdown of the total decay rate on nickel (cf. Fig. 1b) shows that energy transfer to nickel surface plasmons is almost zero. Here, however, the bulk dielectric losses are much more efficient on nickel than on silver, so the "lossy surface waves" become very effective at long range as well as short range.

*This work was supported by the Director, Office of Energy Research, Office of Basic Energy Sciences, Chemical Sciences Division of the U.S. Department of Energy under Contract No. DE-AC03-76SF00098.

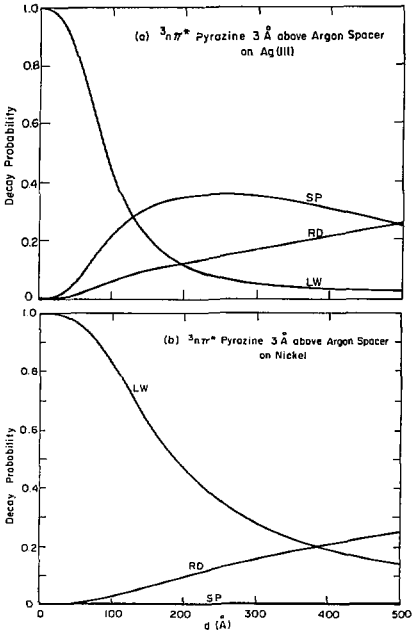

Fig. 1. Calculated probability for decay into photons (RC), surface plasmons (SP), and lossy waves (LW) for $^3n\pi^*$ pyrazine on a) Ag(111) and b) nickel. (XBL 8110-6896A)

* * *

†Brief version of LBL-13780.

3. THE MODIFICATION OF SURFACE OPTICAL RESPONSE THROUGH CHEMISORPTION†

C. B. Harris, H. J. Robota, and P. M. Whitmore

Studies of bond formation between a metal surface and chemisorbed species have focused primarily on the specific changes in the electronic orbitals of the adsorbate while the changes in the electronic states of the metal substrate have only been dealt with in very general terms. The chemisorption-induced changes in the electronic properties of an Ni(111) surface were studied for a wide variety of adsorbates, and a uniform modification of the surface optical properties was found that does not change significantly for different chemisorbed species. These changes have been accounted for by means of a chemical effect on the metal band structure at the surface.

The experiments were performed by analyzing the changes in the optical response function of an Ni(111) surface before and after chemisorption. Changes in the optical response induced by chemisorption could be seen in the absorption coefficient of the overlayer phase. A new, broad absorption feature centered at 4.2 eV was found for all chemisorbed species. This feature is explained as an enhancement of the Λ_1-Λ_3 Ni interband absorption as shown in Fig. 1. Upon chemisorption, the surface state on the (111) surface is quenched resulting in a redistribution of electron density at the surface. The enhancement appears band selective along a symmetry axis normal to the surface (i.e., along the (1/2 1/2 1/2) direction) and is explained in terms of an increase in the p_z character in the Λ_1 band and thus an increase in the matrix element with the Λ_3 band in the optical transition. The conclusions of this study are general and should be applicable to a wide variety of metal-chemisorbed systems.

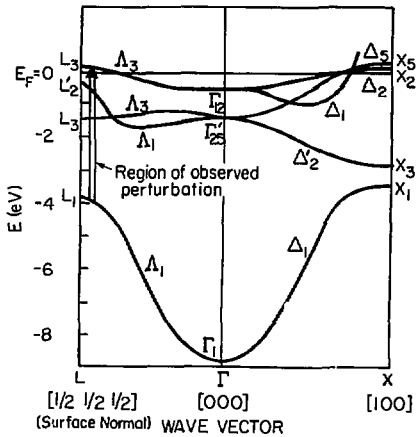

Fig. 1. Modification of nickel band structure after chemisorption on the (111) surface. (XBL 818-6205A)

* * *

†Brief version of LBL-11837 (In press, J. Chem. Phys. 1981).

4. LASER RAMAN STUDIES OF ADSORBATES ON Ag(110) AND Ag(111) SURFACES†

C. B. Harris and G. M. Goncher

During the past several years surface enhanced Raman spectra (SERS) have been observed by many investigators for adsorbates on a variety of Ag, Au and Cu substrates. The lack of surface characterization in many of these studies makes comparison and theoretical interpretation of results extremely difficult. Consequently, single crystal silver(110) and (111) surfaces prepared and characterized by several different methods were studied in UHV conditions.

Surfaces that provided an enhanced Raman signal exhibited roughness on a scale of ~ 1 μm, while surfaces with roughness ≤ 100 Å showed no enhancement. Surface roughness was determined using scanning electron microscopy and electron beam induced surface luminescence. The Raman enhancement on rough surfaces persisted well past the first layer of adsorbed molecules (see Fig. 1), with the first monolayer showing an enhancement approximately 10x that of subsequent layers. The maximum enhancement of pyridine Raman cross-sections observed in these studies was 500x, in contrast to much higher enhancements observed at electrochemically roughened electrode surfaces.

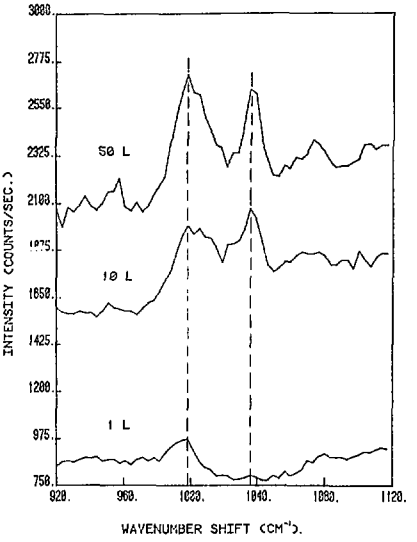

Fig. 1. Surface Raman spectra of pyridine on sputtered Ag(110) at varying pyridine coverages (514.5 nm excitation). (XBL 8112-13186)

These results indicate that there is more than one enhancement mechanism active for the surfaces prepared in these studies, one component being a long range electromagnetic interaction of the molecule with the dipole fields of the surface.

* * *

†Brief version of LBL-13779.

5. SEPARATION OF THE REPULSIVE AND ATTRACTIVE INTERMOLECULAR POTENTIALS IN LIQUIDS FROM THE TEMPERATURE DEPENDENCE OF PICOSECOND COHERENT STOKES SCATTERING†

C. B. Harris, A. Harris, M. Berg, and S. M. George

The effect of attractive and repulsive parts of the intermolecular potential on vibrational dynamics in liquids can be studied using nonlinear picosecond techniques. These techniques allow one to separate rapidly fluctuating, short range, repulsive perturbations of molecular vibrational states from slowly fluctuating, long range, attractive perturbations.

Using a selective picosecond method that separates these effects, the temperature dependence of homogeneous and inhomogeneous contributions to the scattering were studied. These experiments provide a unique method for assessing

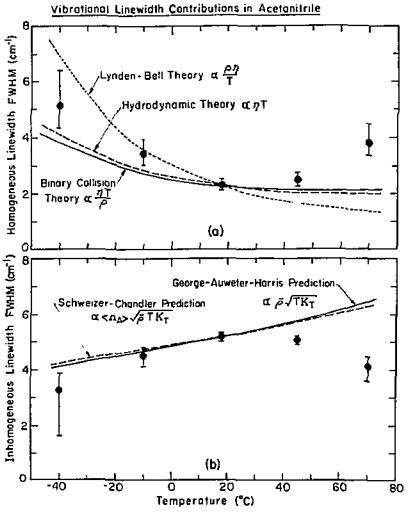

Fig. 1. Measured vibrational linewidth contributions in acetonitrile compared to theoretical predictions. (XBL 8112-13160)

the effects of long and short range forces on liquid structure and dynamics.

The results for liquid acetonitrile from -40°C to +70°C are shown in Fig. 1. The homogeneous linewidth is a factor of two greater at -40°C than at +45°C, showing that the dephasing rate increases at low temperature. The intermolecular collision rate also increases at low temperature due to greater liquid density and viscosity. This indicates that repulsive collisions probably dominate the homogeneous dephasing rate. The inhomogeneous linewidth decreases at low temperatures in agreement with a proposed[1] density fluctuation model. This model attributes inhomogeneous broadening to variations in long range forces acting on the vibrators, due to local density fluctuations which average slowly on the dephasing time scale.

* * *

†Partially supported by a grant from the National Science Foundation. Brief version of LBL-13781.

1. S. M. George, H. Auweter and C. B. Harris, J. Chem. Phys. 73, 5573 (1980).

6. A HIGH POWER PICOSECOND LASER SYSTEM OPTIMIZED FOR COHERENT STIMULATED STOKES SCATTERING EXPERIMENTS IN LIQUIDS†

C. B. Harris, S. M. George, A. Harris, and M. Berg

Picosecond light pulse experiments require stable and reliable picosecond light pulse lasers. Nonlinear picosecond experiments demand high power picosecond pulses with reproducible pulse amplitudes. For maximum time resolution, nonlinear picosecond experiments also require pulses with rapidly rising edges.

A stable and reliable passively mode-locked

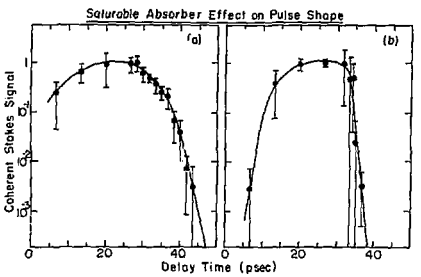

Fig. 1. Saturable absorber effect on picosecond pulse shape. (XBL 8112-13166)

Nd:glass laser was constructed by maximizing the thermal and mechanical stability of each aspect of the laser design. This optimized laser was able to produce picosecond pulse trains for 12 hours. Picosecond pulses with reproducible amplitudes were consistently selected from the pulse trains by a Pockels cell driven by a low-jitter electronic circuit. After amplification, these pulses were passed through a saturable absorber that compressed the pulse and established a very rapid rising edge of 0.7 picoseconds on the pulse.

Pulse shapes measured by coherent Stokes Raman scattering are shown in Fig. 1. Fig. 1(a) shows the pulse shape without use of a saturable absorber and Fig. 1(b) displays the pulse shape with a saturable absorber.

* * *

†Partially supported by a grant from the National Science Foundation. Brief version of LBL-11963 (Review of Scientific Instruments, 52, 852 1981).

7. PICOSECOND PULSE COMPRESSION USING KODAK HEPTAMETHINE PYRILIUM DYE NO. 5 AS A SATURABLE ABSORBER†

C. B. Harris, M. Berg, S. M. George, and A. Harris

Experiments combining nonlinear optics and coherence effects have allowed the probing of ultrafast phenomena which were previously inaccessible. The time resolution of these experiments is critically dependent on the rising edge characteristics of the light pulses used. The ability of saturably absorbing dyes to shorten the leading edge of light pulses has been predicted on the basis of a rate equation. However, calculations on a model including coherence effects have suggested that optical nutation can cause amplitude modulation with high energy pulses.

A study on the effect of saturable absorbers on picosecond pulses was undertaken with the goal of optimizing the experimental time resolution while maintaining pulse quality. Kodak dye No. 9860 was compared to the more rapidly relaxing Kodak heptamethine pyrilium dye No. 5.

The results show that dye No. 5 reduces the overall width of the light pulses more than dye No. 9860 (cf. Fig. 1), but at a significantly greater loss in intensity. This difference can be attributed to the faster relaxation time of dye No. 5. Although dye No. 9860 does not reduce the pulse width as much as dye No. 5, No. 9860 gives a higher power pulse with a dramatically sharpened rising edge. This sharpening leads to a resolution of 0.7 ps in coherent dephasing experiments. These high power pulses were also found to be bandwidth limited and free from amplitude modulation.

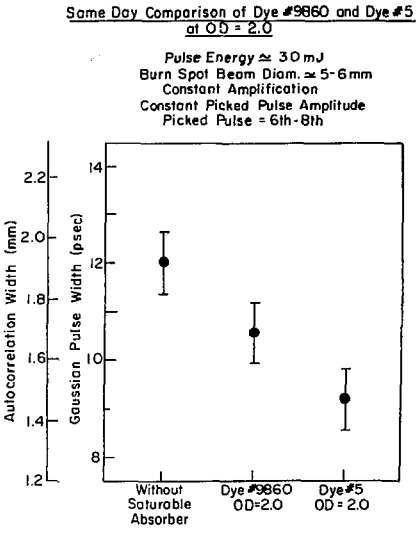

Fig. 1. Comparison of the effect of saturable absorber dyes No. 5 and No. 9860 on the pulse autocorrelation width. (XBL 814-5561)

* * *

†Partially supported by a grant from the National Science Foundation. Brief version of LBL-12695.

1981 PUBLICATIONS AND REPORTS

Refereed Journals

†1. S. M. George and C. B. Harris, "A Passively Mode-Locked Oscillator Optimized for TEM_{00} Selectivity and Long Term Stability and Reliability," Review of Scientific Instruments, 52, 852 (1981); LBL-11963.

2. J. L. Chao, "Applications of the Optical Multichannel Analyzer for (1) Low Light Level Signal Averaging and (2) 2-D Mode Detection of Picosecond Laser Generated Raman Spectra," Applied Spectroscopy, 35, 3 (1981) LBL-11391.

3. H. J. Robota, P. M. Whitmore, and C. B. Harris, "Optical Properties of Molecules Chemisorbed on the Ni(111) Surface," J. Chem. Phys. in press, (1981), LBL-11837.

4. P. M. Whitmore, H. J. Robota, and C. B. Harris, "Electron Energy Transfer from Pyrazine to a Silver(111) Surface Between 10 Å and 400 Å," J. Chem. Phys. Communications, in press, (1981); LBL-13031.

LBL Reports

†1. S. M. George, M. Berg, A. L. Harris, and C. B. Harris, "Picosecond Pulse Shortening Using Dye No. 5 as a Saturable Absorber," LBL-12695.

†2. S. Marks, "The Role of Energy Exchange in Vibrational Dephasing Processes in Liquids and Solids," Ph.D. thesis (1981), LBL-13124.

3. H. J. Robota, "Optical Absorption Spectroscopy of Molecules Adsorbed on Ni(111) and Energy Transfer from the $^3n\pi^*$ state of Pyrazine to Ni(111) and Ag(111) Surface," Ph.D. thesis (1981), LBL-13623.

4. P. M. Whitmore, H. J. Robota, and C. B. Harris, "Role of Surface Plasmons in Energy Transfer to Metal Surfaces Through Near Field Dipole Components," LBL-13780.

5. G. M. Goncher and C. B. Harris, "Laser Raman Studies of Adsorbates on Ag(110) and Ag(111) Surfaces," LBL-13779.

6. A. L. Harris, S. M. George, M. Berg, and C. B. Harris, "Separation of the Repulsive and Attractive Intermolecular Potentials in Liquids from the Temperature Dependence of Picosecond Coherent Stokes Scattering," LBL-13781.

Invited Talks

1. C. B. Harris, "The Structure and Dynamics of Liquids on a Picosecond Timescale," Columbia University, NY, October 1980.

2. C. B. Harris, "The Structure and Dynamics of Liquids on a Picosecond Timescale," University of California, Berkeley, CA, October 1980.

3. C. B. Harris, "The Use of Nonlinear Optics to Study the Dynamics of Liquids on a Picosecond Timescale," Institut für Physikalische Chemie der Universität München, Munich, West Germany, January 1981.

4. C. B. Harris, "The Structure and Dynamics of Liquids on a Picosecond Timescale," Rijksuniversiteit te Leiden, Leiden, The Netherlands, March 1981.

5. C. B. Harris, "A Fundamental Theory for Charge and Quantization," University of Groningen, Groningen, The Netherlands, April 1981.

6. C. B. Harris, "Use of Nonlinear Optics on a Picosecond Timescale to Study the Structure and Dynamics of Liquids: Distinguished Lecture Series Part I," University of Texas, Austin, TX, March 1981.

7. C. B. Harris, "Use of Nonlinear Optics on a Picosecond Timescale to Study the Structure and Dynamics of Liquids: Distinguished Lecture Series Part II," University of Texas, Austin, TX, March 1981.

8. C. B. Harris, "Use of Nonlinear Optics on a Picosecond Timescale to Study the Structure and Dynamics of Liquids: Distinguished Lecture Series Part III," University of Texas, Austin, TX, March 1981.

9. C. B. Harris, "Optical Spectroscopy of Molecules Chemisorbed on Metal Surfaces: Distinguished Lecture Series Part I," University of Texas, Austin, TX, March 1981.

10. C. B. Harris, "Optical Spectroscopy of Molecules Chemisorbed on Metal Surfaces: Distinguished Lecture Series Part II," University of Texas, Austin, TX, March 1981.

11. C. B. Harris, "Picosecond Studies of Liquid State," Max Planck Institut for Laser and Plasma Physics, Garching, West Germany, April 1981.

12. C. B. Harris, "Structure and Dynamics of Liquids on a Picosecond Timescale," Universität Bayreuth, Bayreuth, West Germany, May 1981.

13. C. B. Harris, "Energy Transfer Processes on Metal Surfaces," Technische Universität München, Garching, West Germany, May 1981.

14. C. B. Harris, "Can Space-Time be a Limiting Symmetry of a More General Geometry?" Institut für Theoretische Physik, Universität Stuttgart, Stuttgart, West Germany, June 1981.

15. C. B. Harris, "Optical Studies of Chemisorption and Energy Transfer on Metal Surfaces," Laboratoire de Spectrometrie Physique Universite I Grenoble, France, June 1981.

16. C. B. Harris, U.S. France Seminar on Laser and Theoretical Studies of Molecular Dynamics in the Condensed Phase, Talloires Haute-Savoice, France, June 1981.

b. Molecular Beam Spectroscopy*

John S. Winn, Investigator

Introduction. This program derives fundamental spectroscopic information on various types of molecular species using molecular beam methods. Molecular beams offer the advantages of a collision-free environment as well as the opportunity to prepare species that are either unstable or very scarce in a bulk static equilibrium sample of gas. The species that have been of greatest interest have been weakly-bound molecules, which are the precursors of nucleated condensed phases, and metal carbonyls, which are potential materials for catalysts and novel thin-film structures.

1. MECHANISMS OF METAL CARBONYL DISSOCIATIONS

Brian C. Hale, William E. Hollingsworth, David V. Horák, and John S. Winn

The volatility of metal carbonyls offers the prospect of producing gas phase transition metal atoms at low temperatures. Previous work[1] has shown that electronic energy transfer to a metal carbonyl cleaves all metal-ligand bonds in a single collision. Continuing work has focused on other processes that can effect dissociation.

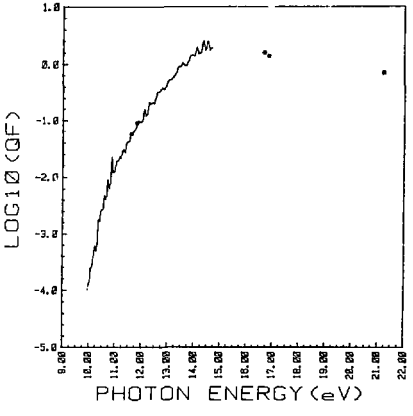

Fig. 1. Log of the relative visible quantum fluorescence of Fe* from VUV photolysis of $Fe(CO)_5$ versus VUV photon energy. Discrete points represent Ar, Ne, and He resonance lines.

(XBL 821-7570)

Vacuum ultraviolet radiation possesses sufficient energy to dissociate a monometal carbonyl such as $Fe(CO)_5$. The wavelength dependence of such a process is demonstrated in Fig. 1, in which the logarithm of the relative Fe* quantum fluorescence is plotted versus the incident photon energy. Dispersed radiation from a H_2 VUV lamp crossed a molecular beam of $Fe(CO)_5$ while Fe* fluorescence in the visible was monitored at right angles. (The five discrete points correspond to Ar, Ne, and He atomic resonance radiation sources.)

These data probe the dissociation continuum of $Fe(CO)_5$, and the shape of the curve contains dynamical information on the dissociation process itself. Both these data and data not shown here show distinct differences between VUV dissociation and electronic energy transfer dissociation. These studies indicate the possible use of photochemical control of practical processes such as thin film deposition, and research into these areas is underway.

* * *

1. D. C. Hartman, W. E. Hollingsworth, and J. S. Winn, J. Chem Phys. 72, 833 (1980).

2. MOLECULAR BEAM ELECTRIC RESONANCE SPECTROSCOPY†

Henry S. Luftman, Michael Maier, Susan A. Sherrow, and John S. Winn

The study of the structures of weakly bonded (van der Waals) molecules[1] can elucidate the intermolecular forces and electronic structure changes that are precursors to macroscopic condensation phenomena and that govern the equation of state of weakly interacting systems. Molecules consisting of one or more rare gas atoms attached to simple dipolar molecules (such as ArOCS, HeClF, and Ar_2ClF) can be formed as stable species in the collision free environment of a supersonic molecular beam, and the equilibrium nature of the intermolecular potential that binds these clusters can be probed by various spectroscopies.

A high resolution supersonic molecular beam electric resonance spectrometer has been built for this research. The trajectory of a beam of dipolar molecules in an inhomogeneous electric field is dependent on the rotational state distribution of the molecules. Radio frequency and microwave region rotational transitions of linewidth ~ 1 kHz are detected by the change in beam trajectory that accompanies such transitions. Thus, a mass spectrometer flux is monitored rather than a radiation field power level. The high intensity supersonic molecular beam source creates an environment that allows the formation of these van der Waals mole-

*This work was supported by the Director, Office of Energy Research, Office of Basic Energy Sciences, Chemical Sciences Division of the U.S. Department of Energy under Contract No. DE-AC03-76SF00098.

cules with predominant rotational population in the more favorable lower energy rotational states.

Spectra have been obtained for ClF, OCS, and ArOCS along with detailed refocusing and transition studies of OCS over a wide range of source pressures, temperatures, mixture compositions, and nozzle diameters. *Computer simulations of the* molecular ensemble's trajectory give good qualitative agreement with the observed behavior. These studies characterize the beam velocity profile and internal state distribution, quantities that govern spectral resolution and signal intensity, respectively. Refocusing studies of Ar_2ClF and predicted spectra based on anticipated molecular geometries are being done in preparation for spectral searches.

* * *

†Supported in part by grants from the National Science Foundation and the ACS Petroleum Research Fund.

1. J. S. Winn, Acc. Chem. Res. 14, 341 (1981).

1981 PUBLICATIONS AND REPORTS

Refereed Journals

1. J. S. Winn, "Analytic Potential Functions for Diatomic Molecules: Some Limitations," J. Chem. Ed. 58, 38 (1981); LBL-10171.

2. J. H. Goble and J. S. Winn, "Analytic Potential Functions for Weakly Bound Molecules. III. Bonding in the Alkaline Earth Diatomics," Chem. Phys. Lett. 77, 168 (1981); LBL-11708.

3. J. S. Winn, "Implications of the Virial Theorem on the Descriptions of Weak Bonds," J. Chem. Phys. 74, 608 (1981); LBL-12241.

4. D. C. Hartman and J. S. Winn, "Chemiluminescent Chemi-ionization: Ar* + Ca and the $CaAr^+$ Emission Spectrum," J. Chem. Phys. 74, 4320 (1981); LBL-10168.

5. J. S. Winn, "A Systematic Look at Weakly Bound Diatomics," Acc. Chem. Res. 14, 341 (1981); LBL-12896.

LBL Reports

1. J. H. Goble, W. E. Hollingsworth, and J. S. Winn, "Resonant Light Absorption by an Excitive Penning Ionization Collision," LBL-13045, August 1981.

Invited Talks

1. J. S. Winn, "Laser Fluorescence of Trapped CH^+," Faraday Discussion No. 71, High Resolution Spectroscopy, Bristol, England, April, 1981.

2. J. S. Winn, "Mechanisms of Metal Carbonyl Dissociations and Thin Film Applications," IBM Yorktown Heights Research Laboratory seminar, May 1981.

3. J. S. Winn, "Gas Phase Transition Metal Chemistry from Metal Carbonyl Dissociation," U.C. Santa Cruz Research Seminar in Chemistry, November 1981.

c. Selective Photochemistry*

C. Bradley Moore, Investigator

1. KINETICS OF TRANSIENT SPECIES OF IMPORTANCE IN COMBUSTION CHEMISTRY†

Andrew O. Langford and C. Bradley Moore

A better understanding of combustion processes is essential to the more efficient and cleaner use of hydrocarbon fuels. Such understanding is by no means straightforward since the bulk combustion process consists of myriad elementary reactions. A good example is the proposed mechanism for methanol oxidation which includes 84 elementary reactions starting from methanol and oxygen. Rate constants for many of these reactions have not been directly determined and only indirect or estimated values exist, making quantitative modeling of these systems realistically impossible. Among the most uncertain rate constants are those for reactions of small polyatomic radicals such as HCO and CH_2. The laser photolysis/laser resonance absorption apparatus developed in our laboratory has been used to study reactions of these species through absorption in the visible. To date, rate constants for the reactions of HCO(DCO) with NO and O_2 have been determined (Fig. 1). The large magnitudes of these rate constants and the fact that DCO reacts more rapidly than HCO suggests that reaction occurs through a collision complex (e.g., ONC(H)O).

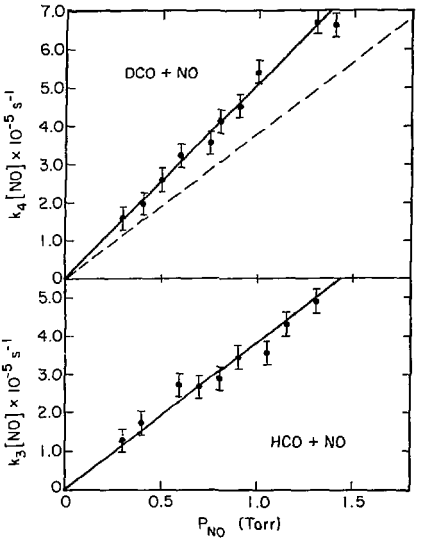

Fig. 1. Pseudo first order rate constants for reactions HCO + NO → HNO + CO and DCO + NO → DNO + CO. The dashed line in the upper panel is identical to the solid line of the lower panel and shows the unusual isotope effect $k_D > k_H$.
(XBL 822-7807)

A study of reaction and singlet-triplet quenching of $CH_2(^1A_1)$ with CH_2CO, O_2, H_2 and hydrocarbons is nearing completion. An IR probe source and detection system is being developed so that $CH_2(^3B_1)$, CH_3 and other radicals without convenient electronic spectra may be studied.

* * *

†Brief version of LBL-13870 to be published in the Journal of Chemical Physics.

2. HIGH OVERTONE SPECTROSCOPY†

James S. Wong and C. Bradley Moore

The high overtone spectra of hydrogen stretching vibrations of polyatomic molecules are best described as local modes.[1] Each inequivalent hydrogen absorbs at a different frequency. The spectrum of propene (Fig. 1) illustrates the easy

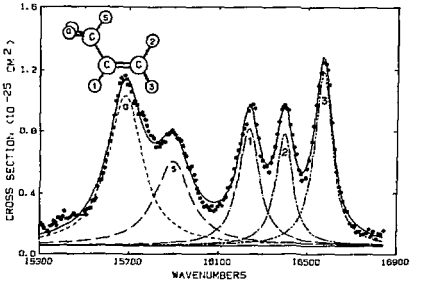

Fig. 1. The v = 0 → 6 absorption spectrum of propene. The methyl and olefinic H's absorb very different frequencies. The three distinguishable olefinic H's are cleanly resolved. The methyl H-atom in the plane of the three C-atoms absorbs at a slightly different frequency from those out-of-plane. (XBL 818-11027)

*This work was supported by the Director, Office of Energy Research, Office of Basic Energy Sciences, Chemical Sciences Division of the U.S. Department of Energy under Contract No. DE-AC03-76SF00098.

resolution of chemical differences. Spectra were recorded for a wide variety of hydrocarbons and halogenated hydrocarbons and show a strong correlation between bond length, observed frequency, and anharmonicity. The vibrational energy levels and hence the potential function for C-H bonds is well described by a single parameter for energies up to at least half the dissociation limit. Absolute intensities for the $v = 0 \rightarrow 6$ transition vary from 0.5 to 1.7 x 10^{-23} cm^2 cm^{-1} $molecule^{-1}$. Thus it is risky to use the integrated area of a peak to count the number of equivalent H's absorbing at that frequency. The variation in intensity must be due to variation in the dipole moment expansion (electrical anharmonicity) since there is no correlation with the $\omega_e x_e$ value (mechanical anharmonicity).

Hydrogens that are usually thought to be chemically identical, s and a positions on a methyl group, or axial and equatorial bonds on a cycloalkane, exhibit resolvable absorptions in high overtone spectra. Work currently underway is aimed at using this selectivity in excitation to produce specific reaction products by bond-selective vibrational photochemistry.

* * *

†Brief version of LBL-13442 accepted by The Journal of Physical Chemistry and LBL-13872 submitted to the Journal of Chemical Physics.

1. B. R. Henry, Acc. Chem. Res. 10, 207 (1977).

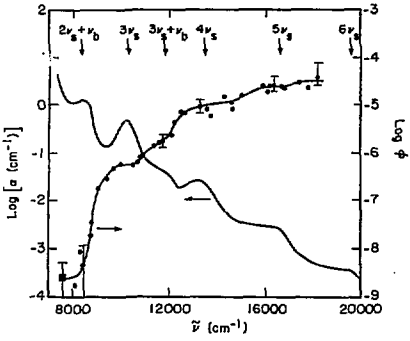

Fig. 1. Log_{10} quantum yield for photoionization of water at 283 ± 1 K as a function of photon energy. A line is drawn through the experimental points. The absorption spectrum of water is shown as the dependence of log_{10} of the natural absorption coefficient $[I/I_0 = \exp\{\alpha\ell\}]$ on wavenumber. Band assignments are shown with subscripts b and s representing bending and stretching modes, respectively. (XBL 822-7808)

3. DISSOCIATIVE IONIZATION OF WATER INDUCED BY SINGLE-PHOTON VIBRATIONAL EXCITATION†

Wesley C. Natzle, D. M. Goodall‡ and C. Bradley Moore

Single-photon vibrational photochemistry in liquids must compete with rapid loss of vibrational excitation to the solvent. As a result, when these reactions do occur they may exhibit high bond or mode selectivity.[1] The proton transfer reaction

$$H_2O(\ell) + h\nu \rightarrow H^+(aq) + OH^-(aq),$$

$$H_{238} = 14.5 \text{ kcal/mole}$$

occurs with measurable quantum yield.[2]

Figure 1 shows the photoionization quantum yield as a function of excitation wavenumber, $\tilde{\nu}$. Superimposed on the trend of increasing ϕ with increasing $\tilde{\nu}$ is a pattern which correlates with the absorption spectrum. The quantum yield rises rapidly on the low frequency side of a band and is relatively constant through the band center and high frequency wing. Since more strongly H-bonded water molecules absorb at lower frequency, the quantum yield per unit of input energy is higher for excitation of more strongly hydrogen-bonded groups. The small hump in the quantum yield at the $3\nu_s + \nu_b$ overtone shows that excitation of the bending vibration is effective in causing ionization, though perhaps not as much as an equal energy of stretching excitation. The low quantum yield at high frequency shows that vibrational relaxation competes effectively with formation and separation of ion pairs. The present data combined with forthcoming data as a function of temperature and isotopic substitution should provide a basis for further qualitative mechanistic conclusions.

* * *

†Brief version of J. Phys. Chem. 85, 2882 (1981); (LBL-13441).

‡Permanent address: Department of Chemistry, University of York, York, United Kingdom.

1. C. B. Moore and I. W. M. Smith, Faraday Disc. Chem. Soc. 67, 146 (1979).
2. B. Knight, D. M. Goodall, and R. C. Greenhow, J. Chem. Soc. Faraday Trans. II 75, 841 (1979).

1981 PUBLICATIONS AND REPORTS

Refereed Journals

†1. B. H. Johnston, A. H. Kung, C. B. Moore, and J. E. Hearst, "Kinetics of Formation of DNA Cross-links by 4"-Aminomethyl-4,5', 8-Trimethylpsoralen," Biochemistry 20, 735 (1981); LBL-12164.

‡2. W. C. Natzle, C. B. Moore, D. M. Goodall, W. Frisch, and J. F. Holzwarth, "Dissociative Ionization of Water Induced by Single-Photon Vibrational Excitation," J. Phys. Chem. 85, 2882 (1981); LBL-13441.

Other Publications

1. J. S. Wong and C. B. Moore, "Laser Photoacoustic Spectroscopy of High Vibrational Overtones," Proceedings of the Second International Topical Meeting on Photoacoustic Spectroscopy, Berkeley, CA, June 1981; LBL-12523.

‡2. J. S. Wong and C. B. Moore, "Vibrationally Highly Excited Molecules and Intramolecular Mode Coupling Through High Overtone Spectroscopy," Proceedings of the 28th International Union of Pure and Applied Chemistry Congress, Vancouver, B.C., Canada, August 16-22, 1981; LBL-13439.

LBL Reports

‡1. Linda Young, "Vibrational Relaxation of Matrix Isolated CH_3F and HCl," (Ph.D. thesis) LBL-13440.

2. James Stephen Wong, "High Overtone Spectroscopy of Polyatomic Molecules," (Ph.D. thesis) LBL-13868.

‡3. J. S. Wong, R. A. MacPhail, C. B. Moore, and H. L. Strauss, "Local Mode Spectra of Inequivalent C-H Oscillators in Cycloalkanes and Cycloalkenes," LBL-13442.

‡4. A. O. Langford and C. B. Moore, "The Reaction of Formyl Radicals with NO and O_2: Absolute Rate Constants and Kinetic Isotope Effects," LBL-13870.

‡5. L. Young and C. B. Moore, "Vibrational Relaxation of CH_3F in Inert Gas Matrices," LBL-13871.

‡6. J. S. Wong and C. B. Moore, "Inequivalent C-H Oscillators of Gaseous Alkanes and Alkenes in Laser Photoacoustic Overtone Spectroscopy," LBL-13872.

Invited Talks

1. C. Bradley Moore, "Laser-induced Chemical Reactions," University of California, Berkeley, CA, Department of Chemistry Physical Chemistry Seminar, January 12, 1981.

2. C. Bradley Moore, "IR Laser-induced Unimolecular Reactions," Stanford Research Institute, Menlo Park, CA. Chemical Kinetics Laboratory colloquim, February 25, 1981.

3. C. Bradley Moore, "Selectivity in Laser Photochemistry," Iowa State University, Ames, IA, Department of Chemistry Colloquim. April 4, 1981.

4. C. Bradley Moore, "Laser Photochemistry," National Research Council of Canada (Ottawa) Seminar, April 6, 1981.

5. C. Bradley Moore, "Selectivity in Laser-induced Reactions," Indiana University, Bloomington, IN, Department of Chemistry Seminar, April 8, 1981.

6. C. Bradley Moore, "Recent Advances in Photochemistry," Stanford University Department of Chemistry Seminar, April 15, 1981.

7. C. Bradley Moore, "Selectivity in Laser Photochemistry," University of Chicago, Chicago, IL, Department of Chemistry Seminar, April 27, 1981.

8. C. Bradley Moore, "Vibrational Relaxation of HCl in Rare Gas Matrices," Gordon Conference on Molecular Energy Transfer, Wolfeboro, NH, June 29-July 3, 1981.

9. C. Bradley Moore, "Vibrationally Excited Molecules: Spectroscopy, the Dynamics and Photochemistry," International Union of Pure and Applied Chemistry, 28th Congress, Vancouver, BC, Canada. Keynote Lecture of Symposium on Laser Chemistry, August 16-22, 1981.

10. C. Bradley Moore and A. O. Langford, "Laser Flash Kinetic Spectroscopy with Transient Concentration Measurement by cw Lasers," American Chemical Society Symposium on "New Techniques in Chemical Kinetics," National Meeting, New York, NY, August 23-28, 1981.

11. C. Bradley Moore, "Energy Transfer in Polyatomic Molecules: Collisions, Half-Collisions and No Collisions," Joint Institute for Laboratory Astrophysics, University of Colorado, Boulder, Colloquim, October 30, 1981.

12. C. Bradley Moore, "Vibrationally Excited Molecules-Spectroscopy, Energy Transfer and Chemical Reaction," Swarthmore College, Swarthmore, PA, Department of Chemistry. Lecture part of "Chemistry Along a Laser Beam," The Dreyfus Lecture Series, December 2, 1981.

* * *

†Partially supported by the National Science Foundation.

‡Partially supported by the U.S. Army Research Office, Triangle Park, NC.

§Partially supported by the U.S. Army Research Office, Triangle Park, NC, and the National Science Foundation.

d. Physical Chemistry with Emphasis on Thermodynamic Properties*

Kenneth S. Pitzer, Investigator

Introduction. The general objective is the discovery and development of methods of calculation of thermodynamic and related properties of important chemical systems by use of quantum and statistical mechanics together with experimental measurements for key systems. Current efforts include relativistic quantum mechanical methods for the calculation of energies, bond distances, and other properties of the ground and excited states of molecules containing very heavy atoms where the conventional nonrelativistic methods are inadequate. Such results are important in evaluation of possible laser systems and for models of catalytic entities including heavy atoms such as platinum.

Other areas of recent or current interest include applications of advanced symmetry theory to chemical problems and the statistical mechanics of ionized systems - plasmas as well as electrolyte solutions.

Some related research applying the earlier results of this project to geochemical problems is supported by DOE through the Earth Sciences Division at LBL and is discussed in the latter's annual report.

1. AB INITIO EFFECTIVE CORE POTENTIALS INCLUDING RELATIVISTIC EFFECTS: A PROCEDURE FOR THE INCLUSION OF SPIN-ORBIT COUPLING IN MOLECULAR WAVEFUNCTIONS†

W. C. Ermler,‡ Y. S. Lee,‡ P. A. Christiansen,‡ and K. S. Pitzer

While there are several relativistic effects in electron structure calculations for molecules including very heavy atoms, it is the spin-orbit term that introduces major complications as compared to nonrelativistic methods. This paper presents a new method that greatly reduces these extra complications arising from the spin-orbit terms.

The key step is the identification of the spin-orbit operator as the difference in effective potentials for $j = \ell + 1/2$ and $j = \ell - 1/2$ for a given ℓ value times the appropriate projection operator. In contrast to the empirical methods in current use elsewhere, this is a rigorously defined *ab initio* operator.

With this new spin-orbit operator one may rigorously set up the relativistic molecular calculations in the same general pattern as for a nonrelativistic basis. The other relativistic effects change the numerical values of various terms but do not introduce new terms. Electron correlation is introduced by the configuration interaction method as a final step. The spin-orbit terms can be introduced in this same final step. One must expand the list of configurations and deal with complex as well as real terms but the general form of the calculation remains unchanged. Thus the new programs can be developed as modifications of existing computer codes and the calculational costs are not unduly greater for the relativistic basis.

* * *

†Brief version of Chem. Phys. Lett., 81, 70 (1981). (LBL-12158)

‡A collaborative effort with former members of this research group. Present addresses: for W. C. E., Stevens Institute of Technology, Hoboken, NJ 07030; for Y. S. L., University of Chicago, James Franck Institute, Chicago, IL 60637; for P. A. C., Clarkson College of Technology, Potsdam, NY 13676.

2. IMPROVED AB INITIO EFFECTIVE POTENTIALS FOR Ar, Kr, and Xe WITH APPLICATIONS TO THEIR HOMONUCLEAR DIMERS†

P. A. Christiansen,‡ K. S. Pitzer, Y. S. Lee,‡ J. H. Yates,‡ W. C. Ermler,‡ and N. W. Winter§

This research, undertaken cooperatively with Lawrence Livermore National Laboratory (LLNL), was designed to yield characteristics of potential high-energy laser systems. The results also constitute a test of our system of effective core potentials by comparisons with all-electron calculations for some of the species investigated.

The new system[1] of effective potentials derived from "shape consistent" pseudo-orbitals had been tested by comparison with all-electron calculations for molecules with relatively light atoms with excellent agreement. The present calculations extend such comparisons to molecules and molecular ions including much heavier atoms. The agreement obtained is again excellent; the species considered were Ar_2, Ar_2^+, Kr_2, Kr_2^+, Xe_2, Xe_2^+. The results will be used at LLNL in studies of lasers.

* * *

†Brief version of LBL-13035, July 1981, J. Chem. Phys. 74, 1162 (1981).

‡A collaborative effort involving former members of this research group. Present addresses: P. A. C., Clarkson College of Technology, Potsdam, NY 13676; Y. S. L., James Franck Institute, Chicago, IL 60637; J. H. Y., and W. C. E., Stevens Institute of Technology, Hoboken, NY 07030.

§Lawrence Livermore National Laboratory.

1. P. A. Christiansen, Y. S. Lee, and K. S. Pitzer, J. Chem. Phys. 71, 4445 (1979).

*This work was supported by the Director, Office of Energy Research, Office of Basic Energy Sciences, Chemical Sciences Division of the U.S. Department of Energy under Contract No. DE-AC03-76SF00098.

3. RELIABLE STATIC ELECTRIC DIPOLE POLARIZABILITIES FOR HEAVY ELEMENTS†

Phillip A. Christiansen,‡ and Kenneth S. Pitzer

While our primary interest is in energies of dissociation, the polarizability is another property of considerable significance. Polarizability values are useful in explaining and predicting a large variety of atomic and molecular collision phenomena. This research was undertaken to test whether our relativistic effective potential methods would be successful in the accurate calculation of polarizabilities.

The major advance over previous calculations is the use of our new system[1] of effective potentials based on "shape consistent" pseudo-orbitals for the heavy atoms. The basis sets and the general structure of calculations methods followed the best current practice in all other respects.

The atoms of cesium and rubidium were chosen for the calculations because accurate experimental values are available for test comparisons and they are heavy enough to make relativistic effects significant. It was found that electron correlation must be included through appropriate configuration interaction methods but that one then obtained excellent agreement. In contrast, the polarizability of Cs calculated by use of Phillips-Kleinman effective potentials was too small by about 20%.

* * *

†Brief version of LBL-13256, August 1981, in press Chemical Physics Letters.

‡Present address: Clarkson College of Technology, Potsdam, NY 13676.

1. P. A. Christiansen, Y. S. Lee, and K. S. Pitzer, J. Chem. Phys. 71, 4445 (1979).

4. SOME RECENT APPLICATIONS OF GROUP THEORY TO CHEMICAL PHYSICS†

K. Balasubramanian

Group theory is potentially useful in simplification of several problems in chemical physics by way of achieving symmetry reductions, classification and correlation of spectroscopic states in dynamical processes, partitioning spin functions in accordance to their transformation properties, etc. There are several problems in chemical physics such as symmetry simplifications in configuration interaction, nuclear spin statistics of rigid and non-rigid molecules, correlation of rovibronic levels and nuclear spin species, etc. that are still not completely solved for general systems. We undertake this investigation with the intent of solving such problems.

We use, in general, group theoretical generator methods to solve the problems mentioned earlier. These generator methods provide for generating functions wherein coefficients of the various terms in the generating functions are the quantities of interest. For example, such generators can be developed using elegant group theoretical techniques for the character tables of the symmetry groups of nonrigid molecules and NMR groups, etc.

An efficient generator method was developed for the nuclear spin statistics of molecules that is of considerable interest in molecular spectroscopy. It was shown that group structures called generalized character cycle index (GCCI) which can be obtained from the character tables are generators of nuclear spin statistics. Rovibronic levels of molecules exhibiting large amplitude motions were correlated using these techniques. Symmetry simplifications were introduced in configuration interaction by partitioning symmetry allowed space types into equivalence classes. Most of these techniques are now computerized.

* * *

†A brief version of reports LBL-11659, LBL-11851, LBL-12025, LBL-12406, LBL-12644, LBL-12645, LBL-12724, LBL-12762, LBL-12809, LBL-13001, LBL-13692, LBL-13693, and LBL-13694; some of these have now been published with the journal references given in the list of publications.

5. WORK IN PROGRESS

The new system described in report 1 above for relativistic electron structure calculations for molecules containing very heavy atoms has been implemented. The first application was to TlH which was chosen because Tl has a very large spin-orbit splitting. Also there are several experimental spectra for comparison with our calculations. Our nearly complete results show good agreement within the respective uncertainties of experiment and numerical approximation of calculation. The spectral features near dissociation are somewhat confusing and we hope that detailed calculations for those states will help us interpret the experimental results.

TlH has, in first approximation, just a single electron pair bond but the relativistic effects complicate its description considerably. As a next example we are investigating Pb_2 where there is, in essence, a double bond, but again with all of the complications of a large spin-orbit effect. Thus Pb_2 will be a severe test of the new calculation system.

1981 PUBLICATIONS AND REPORTS

Refereed Journals

1. Phillip A. Christiansen and Kenneth S. Pitzer, "Electronic Structure and Dissociation Curves for the Ground States of Tl_2 and Tl_2^+ from Relativistic Effective Potential Calculations," J. Chem. Phys. 74, 1162 (1981); LBL-11312.

2. Kenneth S. Pitzer and Phillip A. Christiansen, "Relativistic Modifications of Covalent Bonding in Heavy Elements: Calculations for TlH," Chem. Phys. Lett. 77, 589 (1981); LBL-11611.

3. K. Balasubramanian, "A Method for Nuclear Spin Statistics in Molecular Spectroscopy," J. Chem. Phys. 74, 6824 (1981); LBL-11659.

4. Kenneth S. Pitzer, "Dissociation Energies of Molecules with Very Heavy Atoms from Mass Spectrometry," J. Chem. Phys. 74, 3078 (1981); LBL-11763.

5. K. Balasubramanian, "Comments on McBride's Completion of Kroner's Proof that Hydrogens of Benzene are Homotopic," Theoretica Chimica Acta, 59, 91 (1981); LBL-12025.

6. Walter C. Ermler, Yoon S. Lee, Phillip A. Christiansen, and Kenneth S. Pitzer, "Ab Initio Effective Core Potentials Including Relativistic Effects. VI. A Procedure for the Inclusion of Spin-Orbit Coupling in Molecular Wavefunctions," Chem. Phys. Lett. 81, 70 (1981); LBL-12158.

7. K. Balasubramanian, "Generating Functions for the Nuclear Spin Statistics of Non-rigid Molecules," J. Chem. Phys. 75, 4572 (1981); LBL-12406.

8. Phillip A. Christiansen, K. S. Pitzer, Y. S. Lee, J. H. Yates, W. C. Ermler, and N. W. Winter, "Improved Ab Initio Effective Potentials for Ar, Kr, and Xe with Applications to their Homonuclear Dimers, J. Chem. Phys. 75, 5410 (1981); LBL-13035.

LBL Reports

1. K. Balasubramanian, "Symmetry Simplifications of Space Types in Configuration Interaction Induced by Orbital Degeneracy," LBL-11851.

2. Kenneth S. Pitzer, "Thermodynamics of Electrolyte Solutions over the Entire Miscibility Range," LBL-12377.

†3. P. S. Z. Rogers, Daniel J. Bradley, and Kenneth S. Pitzer, "Densities of Aqueous Sodium Chloride Solutions from 75°C to 200°C at 20 Bar," LBL-12407.

4. K. Balasubramanian, "An Algorithm for the Generation of Nuclear Spin Species and Nuclear Spin Statistical Weights," LBL-12644.

5. K. Balasubramanian, "Computer Generation of Nuclear Spin Species and Nuclear Spin Statistical Weights," LBL-12645.

6. K. Balasubramanian, "Symmetry Operators of Generalized Wreath Products and Their Applications to Chemical Physics," LBL-12724.

†7. J. Christopher Peiper and Kenneth S. Pitzer, "Thermodynamics of Aqueous Carbonate Solutions Including Mixtures of Sodium Carbonate, Bicarbonate and Chloride," LBL-12725.

8. K. Balasubramanian, "The Symmetry Groups of Chemical Graphs," LBL-12762.

9. K. Balasubramanian, "A Method for Constructing Isomerization Reactions," LBL-12809.

10. K. Balasubramanian, "Spectra of Chemical Trees," LBL-13001.

11. Phillip A. Christiansen and Kenneth S. Pitzer, "Reliable Static Electric Dipole Polarizabilities for Heavy Elements," LBL-13256.

12. K. Balasubramanian, "Computer Generation of Isomers," LBL-13692.

13. K. Balasubramanian, "Computer-assisted Enumeration of NMR Signals," LBL-13693.

14. K. Balasubramanian and M. Randić, "The Characteristic Polynomials of Structures with Pending Bonds," LBL-13694.

Invited Talks

1. K. Balasubramanian, "Applications of Group Theory to Dynamic NMR Effects," Third Annual West Coast Theoretical Chemistry Conference on Molecular Structure and Interactions, NASA Ames Research Center, Moffett Field, CA, April 1981.

2. Kenneth S. Pitzer, "The Treatment of Ionic Solutions over the Entire Miscibility Range," Plenary Lecture at the Annual Meeting of the Bunsen Gesellschaft, Marburg, West Germany, May 1981, LBL-12761.

3. K. Balasubramanian, "Some Recent Applications of Group Theory to Chemical Physics," University of Oregon, Eugene, OR, June 1981.

4. K. Balasubramanian, "Symmetry Operators of Generalized Wreath Products," SIAM Conference of Applications of Discrete Mathematics, Troy, NY, June 1981.

5. K. Balasubramanian, "Operator Methods in Spectroscopy," American Conference on Theoretical Chemistry, University of Colorado, Boulder, CO, July 1981.

6. K. Balasubramanian, "Computer-assisted Techniques in Spectroscopy," 28th IUPAC Congress, University of British Columbia, Vancouver, B.C., August 1981.

7. Kenneth S. Pitzer, "Electron Structures of Molecules with Very Heavy Atoms using Effective Core Potentials," NATO Advanced Study Institute, Vancouver, B.C., August 1981.

†8. Kenneth S. Pitzer and P. S. Z. Rogers, "Equation of State for Aqueous Sodium Chloride," 28th IUPAC Congress, University of British Columbia, Vancouver, B.C., August 1981.

* * *

†This work was supported by the Director, Office of Energy Research, Office of Basic Energy Sciences, Division of Engineering, Mathematics and Geosciences of the U.S. Department of Energy under Contract No. DE-AC03-76SF00098.

e. Molecular Interactions*

William A. Lester, Jr., Investigator

Introduction. This is a new project for FY 1982. The purpose is to extend the understanding of the dynamics of molecular processes by theoretical studies of the electronic structure and collision dynamics of prototype systems. Rigorous ab initio methods-Hartree-Fock (HF), multiconfiguration Hartree-Fock (MCHF), and configuration interaction (CI) - implemented in efficient computer software provide the basis for computations of reaction pathways, potential energy surfaces, and molecular properties. Such data are essential for theories of collisional energy transfer (rotational, vibrational, and electronic), chemical reaction, and photodissociation. These areas are of current interest because of improved measurements of state-to-state cross sections and rate constants facilitated by advances in laser and molecular beam technology. Because of the practical importance of combustion, emphasis is placed on the elucidation of elementary chemical steps of combustion in the selection of prototype molecular systems.

1. WORK IN PROGRESS

William A. Lester, Jr., Michel Dupuis, and Vladimir Z. Kresin

The determination of critical regions of potential energy surfaces that dominate chemical reactions and photo-induced properties are under investigation. One study involves the computation of low-lying potential energy surfaces for selected systems of combustion interest that produce formyl (HCO) radicals in the ground and first-excited states. The initial effort is focused on the reaction $H_2CO + OH \rightarrow HCO + H_2O$. Also underway is the computation of the barrier height for H_2CO photodissociation using MCHF and MCHF-CI wavefunctions.

An adiabatic theory of polyatomic photodissociation developed in the past year is now being applied to CS_2 ($2\ ^1B_2$), for which a number of independent measurements have recently been reported. In progress are computations of the excited-state force constants using MCHF wavefunctions, an analytical method for the evaluation of the first derivatives with respect to nuclear coordinates, and a finite difference method to compute the force constants. Preliminary calculations of the geometry and vibrational frequencies of CS_2 ($1\ ^1B_2$) using these procedures are in excellent agreement with experiment. Reliable experimental data for the geometry and force constants of the $2\ ^1B_2$ state are not available.

The adiabatic theory of polyatomic photodissociation forms the basis of an adiabatic theory of chemical reactions that is under development. This work is promising because it bypasses the common difficulty of a mixed basis set that arises in formulations that use Hamiltonians for both reactants and products.

Because of our capability to compute vibrational frequencies with multi-reference wave functions, radicals can be studied. In progress are studies of the vinyl radical (using a generalized valence bond wave function) and allyl radical (using a MCHF wave function).

The electronic structure capability which is embodied in the group's computer program HONDO is being extended to enable the computation of energy barriers, analytical force constants, infrared intensities and equilibrium, transition state, and barrier geometries for multi-reference wavefunctions.

1981 PUBLICATIONS AND REPORTS

Refereed Journals

1. D. Spangler, J. J. Wendoloski, M. Dupuis, M. M. L. Chen, and H. F. Schaefer, III, "Geometry and Electronic Structure of $(CO)_3NiCH_2$. A Model Transition-Metal Carbene," J. Am. Chem. Soc. 103, 3985 (1981); LBL-10650.

2. M. Dupuis, "Energy Derivatives for CI Wavefunctions," J. Chem. Phys. 74, 5758 (1981); LBL-11163.

3. L. D. Thomas, M. H. Alexander, B. R. Johnson, W. A. Lester, Jr., J. C. Light, K. D. McLenithan, G. A. Parker, M. J. Redmon, T. G. Schmaltz, D. Secrest, and R. B. Walker, "Comparison of Numerical Methods for Solving the Second-Order Differential Equations of Molecular Scattering Theory," J. Comp. Phys. 41, 407 (1981); LBL-11233.

4. T. Takada, M. Dupuis, and H. F. King, "Molecular Symmetry III: Second Derivatives of the Energy with Respect to Nuclear Coordinates," J. Chem. Phys. 75, 332 (1981); LBL-12057.

5. V. Z. Kresin, "The Properties of Superconductor - Semimetal (or Semiconductor) Systems," Physica 107B, 13 (1981); LBL-12510.

6. Y. Osamura, H. F. Schaefer, III, M. Dupuis, and W. A. Lester, Jr., "A Unimolecular Reaction $ABC \rightarrow A + B + C$ Involving Three Product Molecules and a Single Transition State. Photodissociation of Glyoxal: $HCOHCO \rightarrow H_2 + CO + CO$," J. Chem. Phys. 75, 5828 (1981); LBL-12841.

LBL Reports

1. M. Dupuis and B. Liu, "The 'Super CI' MCHF Program in ALCHEMY," LBL-12157.

*This work is supported by the Director, Office of Energy Research, Office of Basic Energy Sciences, Chemical Sciences Division of the U.S. Department of Energy under Contract No. DE-AC03-76SF00098 and by the National Science Foundation.

2. V. Z. Kresin and W. A. Lester, Jr., "A New Adiabatic Approach to the Photodissociation of Polyatomic Molecules," LBL-12317.

3. V. Z. Kresin, "Collective Excitations in π-Electron Systems," LBL-12576.

4. M. Dupuis and J. Pacansky, "Theoretical Study of Cyclopropane and Cyclopropyl Radical: Structure and Vibrational Analysis," LBL-12608.

5. V. Z. Kresin, "Influence of the Electron-Phonon Coupling on Superconducting Contact and the Properties of Superconductor-Semimetal (or Semiconductor) Systems," LBL-12699.

6. M. Dupuis, J. J. Wendoloski, T. Takada, and W. A. Lester, Jr., "Theoretical Study of Electrophilic Addition: $O(^3P) + C_2H_4$," LBL-12756.

7. M. Dupuis, J. J. Wendolski, and W. A. Lester, Jr., "Electronic Structure of Vinoxy Radical CH_2CHO," LBL-12815.

8. V. Z. Kresin and W. A. Lester, Jr., "Theory of Polyatomic Photodissociation: Adiabatic Description of the Dissociative State and Translation Vibration Interaction," LBL-12861.

I. Chemical Dynamics Studies*

Bruce H. Mahan, Yuan T. Lee, and John S. Winn, Investigators

Introduction. This research probes the dynamics of single bimolecular collisions between small gas phase species. The spectroscopy of the collision partners (or of the collision products) is used to advance the understanding of elementary chemical *reaction processes. Particular emphasis has been* placed on processes involving molecular ions, such as one finds in discharge, plasma, and certain combustion environments. The new technique of laser induced fluorescence spectroscopy of molecular ions confined to a radio-frequency trap is of particular value to these studies.

1. ELECTRON IMPACT PRODUCTION OF CH^+ FROM METHANE†

Bruce H. Mahan and Anthony O'Keefe

While it is well known from conventional mass spectrometry that CH^+ is among the fragment ions produced by electron bombardment of CH_4, the dynamic distribution of energy among the fragments had not been previously measured. Such information is of general use to the theories and applications of polyatomic molecular fragmentation in general.

By storing nascent CH^+ fragments under collision free conditions, a sufficient number may be accumulated to allow their internal energy distribution to be probed by laser-induced fluorescence. A laser-induced fluorescence spectrum can be interpreted to yield vibration-rotation state distributions in the ground electronic state of the *probed species.*

Such an interpretation for the CD^+ fragment from CD_4 is shown in Fig. 1. The analysis indicates a rotational temperature of ~ 1550 K in the lowest two vibrational levels of CD^+, and further analysis indicates a *vibrational temperature* ~ 3×10^4 K. Similar results hold for CH^+; no isotope effect is apparent.

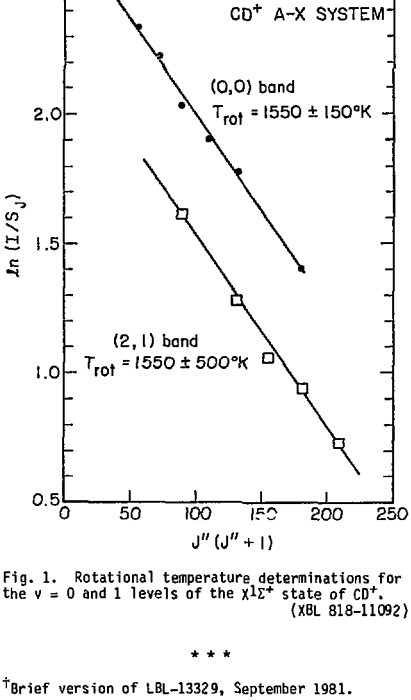

Fig. 1. Rotational temperature determinations for the v = 0 and 1 levels of the $X^1\Sigma^+$ state of CD^+. (XBL 818-11092)

* * *

†Brief version of LBL-13329, September 1981.

2. CHARGE TRANSFER FROM N_2 AND Ar TO N_2^+ †

Bruce H. Mahan, Cecilia Martner,‡ and Anthony O'Keefe

Charge transfer collisions are common ways of redistributing charge and releasing energy in discharge and general plasma environments. The dynamics of such reactions have not been studied in detail due to the lack of spectroscopic probes (of sufficient resolution) of the ion's internal state.

N_2^+ is created and stored under conditions that permit a variable, yet controlled number of collisions with a neutral gas to occur. After a selected time period, the state distribution of these ions is interrogated by the laser-induced fluorescence method.

The results of N_2^+/Ar collisions are especially

*This work was supported by the Director, Office of Energy Research, Office of Basic Energy Sciences, Chemical Sciences Division of the U.S. Department of Energy under Contract No. DE-AC03-76SF00098.

instructive. N_2^+ (v = 0) cannot charge transfer with Ar; only rotationally inelastic collisions are observed. N_2^+ (v = 1) can charge transfer with Ar; rapid depletion of this state of the ion is observed after only 10 or so collisions.

* * *

†Brief version of LBL-13560, November 1981.

‡Associated with the Department of Chemistry, U.C. Berkeley.

1981 PUBLICATIONS AND REPORTS

Refereed Journals

1. B. H. Mahan and A. O'Keefe, "Radiative Lifetimes of Excited Electronic States of Molecular Ions," Astro. J. 248, 1209 (1981).

LBL Report

1. A. O'Keefe, "Laser Induced Fluorescence Studies of Fragment Ions: CH^+ and CD^+," (Ph.D. thesis), LBL-13258.

g. Theory of Atomic and Molecular Collision Processes*

William H. Miller, Investigator

1. REACTION PATH MODEL FOR POLYATOMIC REACTION DYNAMICS†

S. K. Gray, S.-h. Shi, C. J. Cerjan,‡ and W. H. Miller

The reaction path Hamiltonian[1] models a polyatomic molecular system as motion along a reaction coordinate (the steepest descent path through a transition state from reactants to products) plus locally harmonic modes transverse to it. Applications based on it show that tunneling effects can be very significant in the collisionless unimolecular decomposition of formaldehyde, $H_2CO \rightarrow H_2 + CO$, and the unimolecular rearrangement of vinylidene, $H_2C{=}C: \rightarrow HC{\equiv}CH$.

Most recently it has been shown how vibrationally inelastic effects, i.e., energy transfer between the reaction coordinate and the transverse vibrational modes, can be incorporated. The semiclassical perturbation-infinite order sudden (SCP-IOS) approximation that has been developed is simple enough to permit application to polyatomic systems, and tests on simpler systems show it to be of useful semiquantitative accuracy. It has been shown how this SCP-IOS reaction path model can be applied not only to tunneling effects on rate constants, but also to product state distributions, line widths of local mode overtones, and to mode-specific effects in polyatomic reactions.

* * *

†Abstracted from J. Am. Chem. Soc. 103, 1900, 1904 (1981), and J. Chem. Phys. 75, 2258 (1981) and J. Phys. Chem. 00, 0000 (1981). All calculations involved in this work were carried out on a Harris minicomputer supported by National Science Foundation Grant CHE79-20181.

‡Postdoctoral fellow supported by National Science Foundation Grant CHE79-20181.

1. W. H. Miller, N. C. Handy, and J. E. Adams, J. Chem. Phys. 72, 99 (1980).

2. MODE-SPECIFICITY IN UNIMOLECULAR REACTION DYNAMICS†

B. A. Waite and W. H. Miller

It has been implicitly assumed that whether or not a unimolecular reaction behaves statistically or mode-specifically, i.e., whether the decay rate depends only on the total energy in the molecule, depends only on whether or not the classical mechanics of the intra-molecular motion is ergodic or quasiperiodic. Earlier work[1] of ours has tended to refute this assumption, and the present results are even more definitive.

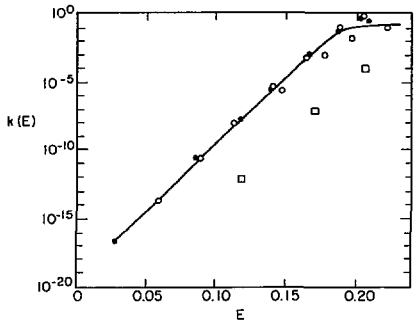

Fig. 1. Rate constant versus energy for metastable states of the Henon-Heiles Hamiltonian. Solid points, squares, and circles denote A_1, A_2, and E states, respectively, and the solid curve is the result of microcanonical transition state theory. (XBL 8010-7395)

The Henon-Heiles model is a system of two coupled oscillators that has been extensively studied with regard to the ergodic/quasiperiodic character of its classical dynamics; the motion shows a well-defined transition from quasiperiodic-to-ergodic character at an energy of about half the classical dissociation energy. In the present work all the complex eigenvalues for the quantum mechanical version of the system have been calculated; the real part of a complex eigenvalue is the energy of the metastable state, and the imaginary part gives its decay rate.

Figure 1 is a plot of unimolecular decay rate versus energy for these metastable states. The points are the results of the quantum calculation, and the important observation is that they are completely statistical in character, i.e., the decay rate is a smooth function of the total energy, showing no hints at all of mode-specific behavior. (The dissociation energy is 0.17 in the units of Fig. 1.) Furthermore, these rigorously computed quantum values are in good quantitative agreement with a simple statistical theory (microcanonical transition state theory), which is the solid curve in Fig. 1.

* * *

†Abstracted from J. Chem. Phys. 74, 3910 (1981). All calculations involved in this work were carried out on a Harris minicomputer supported by

*This work was supported by the Director, Office of Energy Research, Office of Basic Energy Sciences, Chemical Sciences Division of the U.S. Department of Energy under Contract No. DE-AC03-76SF00098.

National Science Foundation Grant CHE79-20181.
1. B. A. Waite and W. H. Miller, J. Chem. Phys. 73, 3713 (1980).

3. CLASSICAL MODELS FOR ELECTRONICALLY NON-ADIABATIC COLLISION PROCESSES.†

A. E. Orel, D. P. Ali, and W. H. Miller

This work shows how the electronic degrees of freedom in a molecular collision process can be modeled as classical degrees of freedom. The advantage in such an approach is that a classical trajectory simulation of collision processes can be carried out that treats the electronic and heavy particle (i.e., translation, rotation, and vibration) degrees of freedom in a dynamically consistent way. Earlier work has shown that approaches that are not dynamically consistent will miss certain features in the collision dynamics.

This work explores several different ways of modeling the electronic degrees of freedom classically. A previously developed approach is applied to the quenching of bromine atoms by hydrogen

$$Br^* + H_2 \rightarrow Br + H_2^{\ddagger} \quad ,$$

and as indicated, much of the electronic energy goes into vibrational excitation of H_2. Another, entirely new approach--essentially a classical mechanical version of valence bond theory--is also developed and applied to several examples. This latter model not only approximates the electronically nonadiabatic effects classically, but it also models the electronic potential energy surfaces classically!

* * *

†Abstracted from Chem. Phys. Lett. 79, 137 (1981) and J. Chem. Phys. 74, 6075 (1981). All calculations involved in this work were carried out on a Harris minicomputer supported by National Science Foundation Grant CHE79-20181.

1981 PUBLICATIONS AND REPORTS

Refereed Journals

1. S. K. Gray, W. H. Miller, Y. Yamaguchi, and H. F. Schaefer, "Tunneling in Unimolecular Decomposition of Formaldehyde, a More Quantitative Study," J. Amer. Chem. Soc. 103, 1900 (1981); LBL-11361.

2. Y. Osamura, H. F. Schaefer, S. K. Gray and W. H. Miller, "Vinylidene, a Shallow Minimum on the C_2H_2 Potential Energy Surface: Static and Dynamical Considerations," J. Amer. Chem. Soc. 103, 1904 (1981); LBL-11625.

3. B. A. Waite and W. H. Miller, "Mode-Specificity in Unimolecular Reaction Dynamics: The Henon-Heiles Potential Energy Surface," J. Chem. Phys. 74, 3910 (1981); LBL-11765.

4. A. E. Orel, D. P. Ali and W. H. Miller, "Classical Model for Electronically Non-Adiabatic Collision Processes: Resonance Effects in Electronic-Vibrational Energy Transfer," Chem. Phys. Lett. 79, 137 (1981); LBL-11853.

5. W. H. Miller and A. E. Orel, "Classical Trajectory Models for Electronically Non-Adiabatic Collision Processes: A Classical Valence Bond Model for Electronic Degrees of Freedom," J. Chem. Phys. 74, 6075 (1981); LBL-11928.

6. W. H. Miller and S.-h. Shi, "Unified Semiclassical Perturbation and Infinite Order Sudden Approximation, with Application to the Reaction Path Hamiltonian Model," J. Chem. Phys. 75, 2258 (1981); LBL-12554.

7. C. J. Cerjan and W. H. Miller, "On Finding Transition States," J. Chem. Phys. 75, 2800 (1981); LBL-12575.

8. C. J. Cerjan, S.-h. Shi, and W. H. Miller, "Applications of a Simple Dynamical Model to the Reaction Path Hamiltonian: Tunneling Corrections to Rate Constants, Product State Distributions, Line Widths of Local Mode Overtones, and Mode-Specificity in Unimolecular Decomposition," J. Phys. Chem. (Accepted for publication); LBL-12842.

Other Publications

1. W. H. Miller, Reaction Path Hamiltonian for Polyatomic Systems: Further Developments and Applications, in "Potential Energy Surfaces and Dynamical Calculations," ed. D. G. Truhlar, Plenum Press, 1981, p. 265.

Invited Talks

1. Conference on Theoretical Approaches to Dynamics, Austin, TX, March 1-4, 1981, "Classical Valence Bond Model for Electronically Non-Adiabatic Collision Processes."

2. Sanibel Symposium on Atomic, Molecular, and Solid State Theory, Collision Phenomena, and Computational Quantum Chemistry, Daytona Beach, FL, March 8-13, 1981, "Classical Valence Bond Model for Electronically Non-Adiabatic Collision Processes."

3. The Camille and Henry Dreyfus Lecture, University of Kansas, April 2, 1981, "An Approach to Polyatomic Reaction Dynamics."

4. American Conference on Theoretical Chemistry, Boulder, CO, June 22-26, 1981, "A Reaction Path Model for Polyatomic Reaction Dynamics: Tunneling, Vibrational Inelasticity, and Mode-Specificity."

5. Gordon Research Conference on Molecular Energy Transfer, Wolfboro, NH, June 29-July 3, 1981, "To What Extent Can Current Theoretical Models Accurately Describe the Dynamics of Electronic Energy Transfer in Gases?"

h. Photoelectron Spectroscopy*

David A. Shirley, Investigator

Introduction. This project is dedicated to the study of new phenomena by the use of photoelectron spectroscopy. Of special importance is utilization of synchrotron radiation in the energy range 5-4000 eV.

Experiments on atoms and molecules have demonstrated several new phenomena in 1981. Molecular shape resonances near K-edges were observed for the first time by photoemission (article 1), as were multichannel resonant interference profiles (article 3). Angular distribution phenomena were studied (articles 2, 5, and 6). Ultrahigh resolution photoelectron spectra yielded high-accuracy spectroscopic constants for H_2^+, D_2^+, and HD^+ (article 4). Multiphoton photoelectron spectra of two chlorofluorocarbons yielded detailed structure, elucidating the path of photoionization (article 7).

The 800-4000 eV JUMBO monochromator was thoroughly characterized in 1981 (article 8). Off-normal photoelectron diffraction was analyzed (articles 9 and 10). Finally, band-structure studies were extended to high energies (article 11) and to stepped (article 12) and antiferromagnetic (article 13) surfaces.

1. SHAPE RESONANCES IN K-SHELL AND AUGER PHOTOELECTRON DISTRIBUTIONS FROM CO, CO_2, AND N_2†

C. M. Truesdale, D. W. Lindle, P. H. Kobrin, U. Becker,‡ H. G. Kerkhoff,‡ S. Southworth, and D. A. Shirley

K-shell photoabsorption can be highly anisotropic below the photoionization threshold because symmetry selection rules govern the transitions to discrete excited states. Above the threshold, continuum photoabsorption also varies with the relative orientation of the molecular axes and the photon polarization vector. "Shape resonances" have been predicted[1] in both the absorption cross-section and the angular distribution of electrons near threshold. These resonances can be regarded as arising through scattering of outgoing auger electrons and photoelectrons excited from the K shell by the anisotropic molecular field. Although extensively discussed,[2-4] K-shell shape resonances had not been previously observed in free molecules.

Synchrotron radiation at the Stanford Synchrotron Radiation Laboratory, combined with a double-angle time-of-flight electron spectrometer, have enabled us to observe shape resonances for the first time, near the K-shell thresholds in CO, CO_2, and N_2. Shape resonance behavior was observed in both the partial cross-sections and the asymmetry parameters of photoelectrons. For CO_2, the asymmetry-parameter shape resonance is shown in Fig. 1, together with the theoretical prediction.

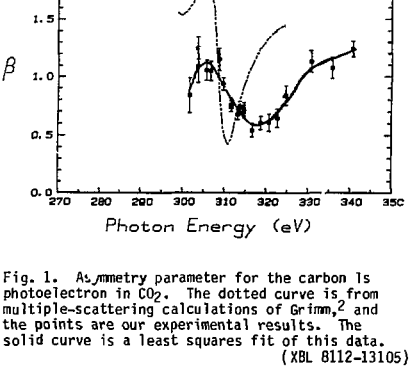

Fig. 1. Asymmetry parameter for the carbon 1s photoelectron in CO_2. The dotted curve is from multiple-scattering calculations of Grimm,[2] and the points are our experimental results. The solid curve is a least squares fit of this data. (XBL 8112-13105)

The Auger electrons from N_2 and the carbon Auger electrons from CO and CO_2 show strong resonances due to excitations of their K electrons to bound Rydberg ($\sigma \rightarrow \pi$) states. The carbon Auger group of CO_2 also shows a resonance during photoionization ($\sigma \rightarrow \sigma$).

* * *

†Brief version of LBL-12873 and subsequent reports.

‡Institut für Strahlungs und Kernphysik, Fachbereich Physik, Technische Universität Berlin, West Germany.

1. J. L. Dehmer, J. Chem. Phys. 56, 4496 (1972).
2. F. A. Grimm, Chem. Phys. 53, 71 (1980).
3. J. L. Dehmer and D. Dill, Phys. Rev. Lett. 35, 213 (1975), J. L. Dehmer and D. Dill, J. Chem. Phys. 65, 5327 (1976).
4. D. Dill, J. R. Swanson, S. Wallace, and J. L. Dehmer, Phys. Rev. Lett. 45, 1393 (1980).

*This work was supported by the Director, Office of Energy Research, Office of Basic Energy Sciences, Chemical Sciences Division of the U.S. Department of Energy under Contract No. DE-AC03-76SF00098. It was performed at the Stanford Synchrotron Radiation Laboratory, which is supported by the NSF through the Division of Materials Research.

2. ELECTRON SPECTROSCOPY STUDY OF INNER-SHELL PHOTOEXCITATION AND IONIZATION OF Xe†

S. Southworth, U. Becker,‡ C. M. Truesdale, P. H. Kobrin, D. W. Lindle, and D. A. Shirley

In the photon energy range $h\nu \approx 65$–700 eV, the photoabsorption cross section of Xe is dominated by the excitation and ionization of the inner-subshell 4d electrons. Photoemission of the outer-shell 5p and 5s electrons is modified by many-electron interactions with the 4d subshell.[1] In addition, photoemission of a 4d electron leaves an excited ionic state which decays by ejection of secondary Auger electrons. Resonant photoexcitation of the 4d → np Rydberg states produces highly excited Xe atoms that can decay by various autoionization processes. Hence, experimental and theoretical studies of inner-shell photoionization processes of Xe provide a direct probe of the many-electron nature of atoms.

We have used synchrotron radiation to study inner-shell photoionization of Xe by measuring the angular distribution asymmetry parameters (β) and, in certain cases, the branching ratios and partial cross sections of photoelectrons and Auger electrons. The broad continuum provided by the synchrotron radiation allowed measurements to be made over a wide energy range. In particular, the tunability of the monochromatized synchrotron radiation allowed the study of autoionization processes upon resonant excitation of the 4d → np Rydberg levels.

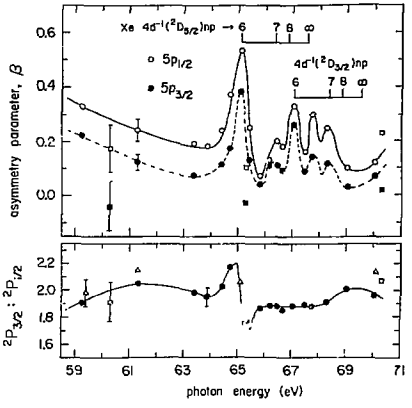

Fig. 1. Asymmetry parameters (β) and branching ratio for the Xe $5p_{3/2}$ and $5p_{1/2}$ photoelectrons measured through the 4d → np autoionizing resonances. Circles represent this work; squares represent Krause et al.,[2] triangles represent Wuillenmier et al.[3] For clarity, only representative error bars are shown. Lines are drawn through the data points as an aid in viewing the figure. (XBL 8110-11759)

Electron spectra recorded in the energy region of the 4d → np resonances show that these states decay predominantly by Auger processes rather than by autoionization processes in which the 5p and 5s electrons are ejected. However, even though the resonances have a relatively small effect on the $5p_{3/2}$ and $5p_{1/2}$ partial cross sections, the photoelectron asymmetry parameters display resonant oscillations (see Fig. 1). In contrast, we observed no resonant variation of β for the 5s photoelectrons.

* * *

†Brief version of LBL-13697, to be submitted to Phys. Rev. A.

‡Institut für Strahlungs- und Kernphysik, Fachbereich Physik, Technische Universität Berlin.

1. M. Ya Amusia, Comm. Atom. Molec. Phys. 8, 61 (1979).
2. Krause et al., Phys. Rev. A24, 1374 (1981).
3. Wuillenmier et al., Phys. Rev. A16, 646 (1977).

3. AUTOIONIZING RESONANCE PROFILES IN THE PHOTOELECTRON SPECTRA OF ATOMIC CADMIUM†

P. H. Kobrin, U. Becker, S. Southworth, C. M. Truesdale, D. W. Lindle, and D. A. Shirley

Autoionization in atoms gives rise to resonance profiles in photoabsorption as described by Fano. The branching ratios to each of the final-ionic states may vary dramatically at the autoionizing energy.[1] If the partial cross-sections for formation of each of the final-ionic states is measured, then it is possible to observe separate resonance profiles for each partial cross-section. These profiles provide more detailed information on the autoionization process than does a single photoabsorption profile. Other sensitive probes of the autoionization process are available in the measurement of the angular distributions and spin polarizations of the emitted electrons in the neighborhood of a resonance.

We have used double-angle time-of-flight photoelectron spectroscopy with tunable synchrotron radiation to measure the largest set of profiles yet obtained for an atomic autoionizing resonance.[2] In particular, the partial cross-section profiles for the $4d^{10}5s\ ^2S_{1/2}$, $4d^95s^2\ ^2D_{5/2}$, $4d^95s^2\ ^2D_{3/2}$, and $4d^{10}5p\ ^2P_{3/2,1/2}$ ionic states and the angular distribution profiles for the $4d^95s^2\ ^2D_{5/2}$ and $4d^95s^2\ ^2D_{3/2}$ photoelectrons from atomic Cd have been measured in the region of the $Cd(4d^{10}5s^2)\,^1S_0 + h\nu \rightarrow Cd^*[4d^9(5s5p\ ^3P)]\,^2P_{3/2}6s\ ^1P_1$ double electron excitation absorption feature at 588 Å in the Cd absorption spectrum. Figures 1 and 2 show some of these profiles.

* * *

†Brief version of LBL-13304.

1. R. A. Rosenberg, M. G. White, G. Thornton, and D. A. Shirley, Phys. Rev. Lett. 43, 1384 (1979).

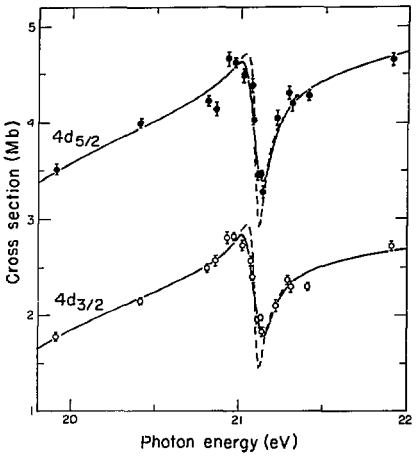

Fig. 1. The partial cross-section measurements of the $4d^9 5s^2\ ^2D_{5/2}$ and $4d^9 5s^2\ ^2D_{3/2}$ ionic states of Cd^+. The solid curves are fits to theoretical lineshapes. In the dashed curves the monochromator broadening has been deconvoluted.

(XBL 8110-7353)

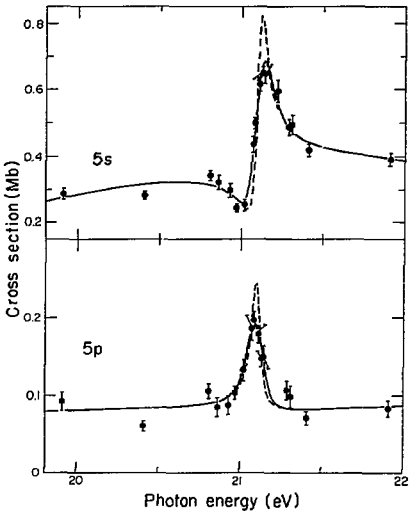

Fig. 2. Same as Fig. 1, for the $4d^{10}5s\ ^2S_{1/2}$ and $4d^{10}5p\ ^2P_{3/2,1/2}$ ionic states. Note the dramatically different energy dependences for the various states.

(XBL 8110-7349A)

4. ROTATIONALLY-RESOLVED PHOTOELECTRON SPECTROSCOPY OF n-H_2, p-H_2, HD, AND D_2†

J. E. Pollard, D. J. Trevor, J. E. Reutt, Y. T. Lee, and D. A. Shirley

The photoelectron spectra of hydrogen and its isotopes can provide information on the energetics of the molecular ions and on the relative photoionization cross sections for transitions to the various rotation-vibration energy levels. Although several measurements of these spectra have been reported, there still exists a need for data of higher resolution and sensitivity, particularly for the upper vibrational states of the ions that are usually obscured by the spectrometer background. The Doppler broadening for these light molecules, which can be as large as 20 MeV at 584 Å, has limited the resolution obtained in previous experiments.

We have measured the 584 Å photoelectron spectra of n-H_2, p-H_2, HD, and D_2 at a resolution of 11 meV FWHM with an apparatus which uses a supersonic molecular beam source to remove Doppler broadening.[1] The spectra reveal considerably more rotational structure than was observed in earlier experiments, and because of the very low spectrometer background, transitions are observed for states up to one or two vibrational quanta from the dissociation limit. The rotational population distribution of the initial-state molecules can be varied considerably by adjusting the stagnation temperature and pressure, and this provides a useful tool for greatly enhancing or reducing transitions from rotationally-excited states of the neutrals. We have obtained values for the rotational and vibrational constants of H_2^+, HD^+, and D_2^+, as well as relative intensities for all observed vibrational levels.

Figure 1 shows the spectrum of n-H_2 taken with a nozzle temperature of 473 K. For each ionic vibrational state the observed rotational structure is primarily the Q branch ($J''=J'$), and the distribution of rotational intensities reflects the rotational populations of n-H_2 at a temperature somewhat below 473 K. The rotational relaxation of H_2 can be readily measured by taking spectra at successively higher backing pressures. The rotationless ($J'' = J' = 0$) spectra of p-H_2, HD, and D_2 have been obtained by running at a nozzle temperature of 77 K, thereby providing us with accurate vibrational differences (ΔG-values). These

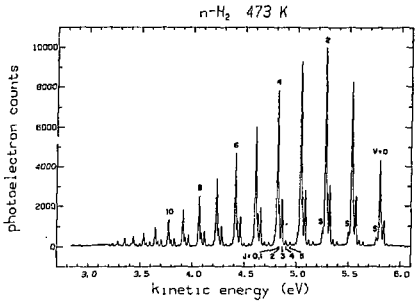

Fig. 1. The 584 Å spectrum of n-H_2 expanded through a 70 μm diam nozzle from a stagnation pressure of 600 torr at 473 K.

(XBL 8111-12586)

results are found to be consistent with the extensive tabulations of energy levels available from theory.[2]

* * *

†Brief version of LBL-13696.

1. J. E. Pollard, D. J. Trevor, Y. T. Lee, and D. A. Shirley, Rev. Sci. Instrum. 52, 1837 (1981).
2. G. Hunter, A. W. Yau, and H. D. Pritchard, At. Data Nucl. Data Tables 14, 11 (1974).

5. PHOTOELECTRON ANGULAR DISTRIBUTIONS FROM H_2 AND D_2†

S. Southworth, W. D. Brewer,‡ C. M. Truesdale, P. H. Kobrin, D. W. Lindle, and D. A. Shirley

The relatively simple two-electron structure of H_2 has made it a prototype system for study in the development of theoretical models of molecular photoionization. Of particular interest is the photoelectron asymmetry parameter β, which characterizes the angular distribution. Several theoretical calculations of $\beta(H_2)$ have been published (see Fig. 1). All of the theoretical calculations predict a large asymmetry and a slow variation of $\beta(H_2)$ with energy, but they differ in the precise magnitude of $\beta(H_2)$ and in the slope of the energy variation.

In view of the discrepancies among the theoretical and previous experimental values, and because we have an apparatus that is relatively free of the systematic errors usually inherent in β measurements, we have made another set of measurements of $\beta(H_2)$ using synchrotron radiation. We also measured $\beta(D_2)$ to look for variations between the isotopes. Our measurements of $\beta(H_2)$ and $\beta(D_2)$ represent the total photoelectron bands, i.e., summed over all rotational and vibrational transitions.

As shown in Fig. 1, our measurements agree well

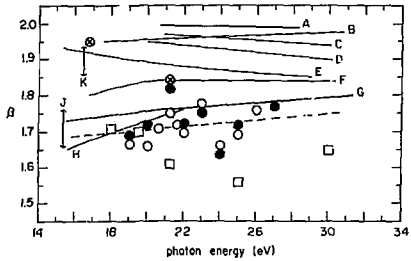

Fig. 1. Experimental β values for H_2 and D_2 with theoretical calculations for H_2. Experimental: ○ = present results for H_2; ● = present results for D_2; □ = Marr et al. results for H_2; ⊕ = Morgenstern et al. results for H_2. The dashed line is a least-squares fitted line through the present results for H_2 and D_2. Theoretical curves: A = Chow Chiu and Samanta; B = Ritchie and Tambe; C = Thiel; D = Dutta et al.; E = Hirota; F = Itikawa; G = Tully et al.; H = Shaw and Berry. Theoretical calculations at one energy: J = Dill, K = Chandra.

(XBL 817-10543)

with a few of the theoretical calculations, but most of the calculations predict asymmetries that are too large. Virtually identical β values were observed for H_2 and D_2, which is the result obtained in a fixed-nuclei model where vibrational and rotational structure is neglected. The equivalence of $\beta(H_2)$ and $\beta(D_2)$ indicates that the rotational structure in the photoionization process is not strongly modified by rotation-vibration or electronic-nuclear interactions.

* * *

†Brief version of LBL-12922, to be published in J. Electron Spectrosc.

‡Institut für Atom und Festkörperphysik, Freie Universität Berlin, West Germany.

6. PHOTOIONIZATION CROSS SECTIONS AND PHOTOELECTRON ASYMMETRIES OF THE VALENCE ORBITALS OF NO†

S. Southworth, C. M. Truesdale, P. H. Kobrin, D. W. Lindle, W. D. Brewer,‡ and D. A. Shirley

Synchrotron radiation has made possible the technique of wavelength-dependent photoelectron spectroscopy, which allows the measurement of partial photoionization cross sections $\sigma(\epsilon)$ and photoelectron angular distribution asymmetry parameters $\beta(\epsilon)$ over a range of incident photon energy. The spectral variation of $\sigma(\epsilon)$ and $\beta(\epsilon)$ characterizes the electronic structure and photoionization dynamics. Such measurements provide a sensitive test for the accuracy of theoretical photoionization calculations. The multiple-scattering model (MSM)[1,2] of molecular photo-

ionization was recently applied to the calculation of $\sigma(\epsilon)$ and $\beta(\epsilon)$ for the orbitals of NO, and we have made the corresponding measurements for the valence orbitals over the photon energy range 16-31 eV.

The measurements were made at the Stanford Synchrotron Radiation Laboratory using our double-angle time-of-flight electron spectrometer. With this spectrometer, the entire photoelectron spectrum is recorded simultaneously at two angles, which greatly increases the collection efficiency and the signal/noise ratio. This technique also greatly reduces or eliminates certain systematic errors in the measurement of photoelectron asymmetry parameters $\beta(\epsilon)$.

Maxima observed in the partial cross section measurements for the 2π, 5σ, and 4σ molecular orbitals of NO are attributed to a shape resonance in the σ ionization continuum, as predicted by the MSM calculations. For the 2π orbital, a second, stronger resonance feature was observed that is not predicted by the MSM and is tentatively attributed to shape resonances in the π and δ ionization channels. The MSM calculations of photoelectron asymmetries for the 1π and 5σ orbitals are in very good agreement with the measured $\beta(\epsilon)$ values. However, for the 2π and 4σ orbitals, the theoretical $\beta(\epsilon)$ curves are shifted strongly from the measured values. In summary, the MSM theory is partially successful in predicting the measured $\sigma(\epsilon)$ and $\beta(\epsilon)$ values of NO, but certain strong discrepancies remain between theory and experiment.

* * *

†Brief version of LBL-12907, to be published in J. Chem. Phys.

‡Institut für Atom und Festkörperphysik, Freie Universität Berlin, West Germany.

1. D. Dill and J. L. Dehmer, J. Chem. Phys. 61, 692 (1974).
2. S. Wallace, D. Dill, and J. L. Dehmer, J. Chem. Phys., to be published; S. Wallace, Ph.D. thesis, Boston University, 1980.

7. MULTIPHOTON IONIZATION PHOTOELECTRON SPECTROSCOPY OF CCl_2F_2 AND CCl_3F†

D. J. Trevor, J. W. Hepburn, J. E. Pollard, Y. T. Lee, and D. A. Shirley

Multiphoton ionization is a rapidly growing technique, permitting the study of many otherwise inaccessible states, as well as providing an ultrasensitive analytical method for single atom detection.[1] In this method high power visible or near ultraviolet lasers are used in the multiple-photon excitation scheme to achieve sufficient energy to ionize the molecule or atom. However, in contrast to a single photon ionization, the multiphoton ionization of many polyatomics is accompanied by extensive fragmentation. To understand the mechanism of this fragmentation, the energy partitioning in the ionization continuum must be examined. Photoelectron spectroscopy is a unique tool in this regard and has significantly aided our understanding of multiphoton ionization.

We have measured the photoelectron spectra and mass spectra resulting from multiphoton ionization of CCl_2F_2 and CCl_3F with approximately 25 MW/cm^2 ArF (193 nm) radiation.[2] These experiments were performed by crossing a collimated supersonic molecular beam with the focused (50-cm lens) laser beam. The resulting photoelectrons were analyzed with an electrostatic spectrometer (20 meV FWHM), or the photoions detected with a quadrupole mass spectrometer.

The recorded mass spectra indicated extensive fragmentation producing a significant fraction of diatomic fragment ions, CF^+ and CCl^+. The photoelectron spectra are shown in Fig. 1. Especially in CCl_2F_2, a distinct vibrational sequence is observed and assigned to CF^+. This ion must have been produced by two photon ionization of CF that

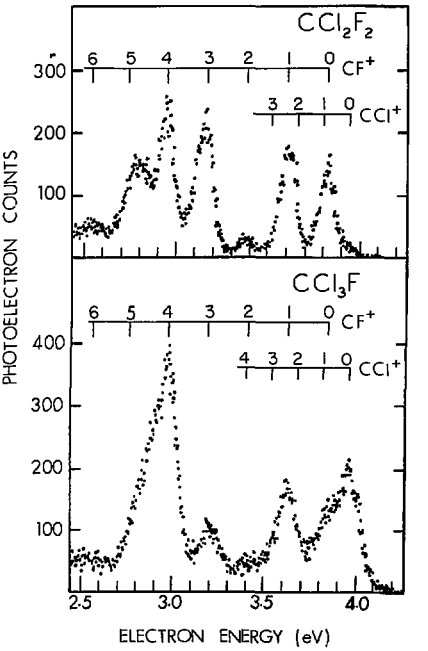

Fig. 1. Multiphoton ionization photoelectron spectra of supersonic beams of CCl_2F_2 and CCl_3F taken with an ArF (193 nm) laser. This data is the direct sum of several scans without correction for decreasing laser power. The abscissa is also uncorrected for a constant offset (< 0.5 eV) that could not be determined in this series of experiments.

(XBL 8111-12470)

itself is produced by a two photon or two consecutive single photon dissociations of CCl_2F_2. The spacings of these peaks and intensities are in agreement with this assignment. Several of these features and an additional shoulder to lower binding energy are observed in the CCl_3F spectra; this has been tentatively assigned to CCl^+. These measurements have demonstrated the importance of neutral photodissociation in multiphoton ionization.

* * *

†Brief version of LBL-13752.

‡We acknowledge the San Francisco Laser Center for the use of the laser.

1. P. M. Johnson, Acc. Chem. Res. 13, 20 (1980).
2. J. W. Hepburn, D. J. Trevor, J. E. Pollard, D. A. Shirley, and Y. T. Lee, submitted to J. Chem. Phys.

8. A DOUBLE-CRYSTAL MONOCHROMATOR FOR THE ENERGY REGION 550-5000 eV†

Z. Hussain, E. Umbach,‡ J. J. Barton, C. C. Bahr, and D. A. Shirley

A serious constraint on experimental spectroscopy is the limited energy range over which suitable light sources are available. Before the utilization of high-energy electron accelerators, intense tunable light sources were available only for energies up to the ultraviolet range ($h\nu \leq 10$ eV). During the 197Ds synchrotron radiation, with appropriate monochromators, has extended this range considerably. The unique properties of synchrotron radiation has resulted in new experimental developments in various fields of science which have led to a rapid growth of synchrotron radiation facilities in many countries.[1] At present, the widest energy range is covered at the Stanford Synchrotron Radiation Laboratory (SSRL).

With the explicit goal of closing the gap in available photon energies provided by vacuum grating monochromators ($h\nu \leq 800$ eV) and crystal monochromators operated under an atmospheric pressure of helium (≥ 3 keV), a double-crystal vacuum monochromator (JUMBO) has been developed at SSRL. The monochromator presently covers the spectral range from 550 to 5000 eV.[2] The crystals that make this energy range accessible are shown in Fig. 1. Also shown are the elements with absorption edges in this energy region, as indicated. The importance of this monochromator is obvious from the fact that all elements heavier than oxygen are accessible. Monochromator crystals such as beryl(10$\bar{1}$0), InSb(111), Ge(111) and β-alumina (0002) have already been tested. The diffracting crystal beryl--a naturally occurring mineral--with 2d spacing of 15.96 Å between (10$\bar{1}$0) planes provides highly monochromatic light of good intensity from 800 to 2000 eV. The intensity above ~1550 eV has structure and is attenuated by the absorption above the Al and Si K edges. To demonstrate the inherent resolution capabilities of the monochromator crystals, double-crystal rocking-curve values at various energies are also shown in the figure. The full widths at half maximum height of the rocking curves from beryl crystals are from

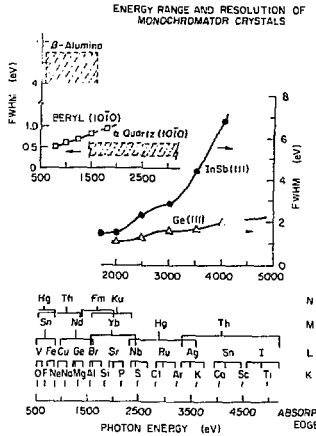

Fig. 1. Experimentally determined rocking curves are shown for the monochromator crystals tested in JUMBO. Incomplete measurements of the rocking curves for β-alumina and α-quartz limit these curves to the shaded areas shown. Absorption edges for selected elements accessible to JUMBO are indicated below.

(XBL 822-8025)

0.5 to 0.9 eV in the energy region 800-1800 eV. InSb(111) can be used from 1680 to 4300 eV. These crystals are specifically suitable for work on the important K edge of Si. Ge(111) crystals exhibit excellent diffraction properties, thermal stability and resolving power. To expand the spectral range further, we have recently tested a pair of β-alumina(0002) crystals with 2d = 22.49 Å. These crystals cover the energy range from ~550 to 1500 eV but are found to provide relatively poor resolution of ~6-7 eV. However, one may expect to get an improvement in resolution by at least a factor of 2-3 if a good quality crystal becomes available. The energy range needed for the Al K edge, which cannot be reached by InSb(111) or Ge(111) and is not covered by beryl satisfactorily, can be spanned by α-quartz (1010) crystals which are known to have resolution better than 0.5 eV. However, the presence of Si (Si K edge = 1840 eV) limits the effectively useful energy range to only ~1470-1840 eV.

By employing beryl, InSb, Ge, and β-alumina crystals, and with the present capability of changing four pairs of crystals in situ JUMBO can now cover nearly the full energy range 550-5000 eV. Novel studies of bulk and surface properties of materials by angle-resolved photoemission, x-ray induced Auger spectroscopy, photon-stimulated ion desorption and extended x-ray absorption fine structure studies have demonstrated the broad use-

fulness of this previously inaccessible energy region of the electromagnetic spectrum (e.g., see article 11).

* * *

†Brief version of LBL-12729.

‡Permanent address: Physik Department, Technische Universität, München, West Germany.

1. H. Winick and S. Doniach, Editors, Synchrotron Radiation Research (Plenum Press, New York, 1980).
2. Z. Hussain, E. Umbach, D. A. Shirley, J. Stöhr, and J. Feldhaus, Nucl. Instr. and Meth. (to appear).

9. NORMAL PHOTOELECTRON DIFFRACTION STUDIES OF SELENIUM AND SULFUR OVERLAYERS ON Ni(011) and Ni(111)†

D. H. Rosenblatt, S. D. Kevan,‡ J. G. Tobin, R. F. Davis,§ M. G. Mason,‖ D. R. Denley,¶ D. A. Shirley, and S. Y. Tong**

Normal photoelectron diffraction (NPD), a technique combining angle-resolved photoemission with synchrotron radiation, has been shown to be an accurate method of determining the structure of atomic and molecular overlayers on single crystal metal surfaces. In this work, NPD is used to study adsorbate/substrate systems which have not yet been studied by any other accurate structural technique.

In the NPD technique, the photoemission intensity of an adsorbate core level is measured normal to the surface as a function of photon (and thus kinetic) energy. An intensity-kinetic energy curve similar to a low energy electron diffraction (LEED) I-V curve is generated which, when compared to theoretical curves, may yield a surface structure.

NPD has been used to study the structure of c(2x2)S and c(2x2)Se on Ni(011). In the latter case, Se is found to be situated above the hollows in the Ni(011) surface, at a perpendicular distance ($d_\perp$) of 1.10 Å above the surface (Fig. 1). For an annealed p(2x2)Se overlayer on Ni(111), the Se atoms are found to be bonded only to those threefold hollow sites in the (111) surface that have a vacancy in the second layer. NPD is shown to be particularly well suited for studying disordered adsorbate systems and systems which have two-dimensional order but contain domains of two different adsorption sites.

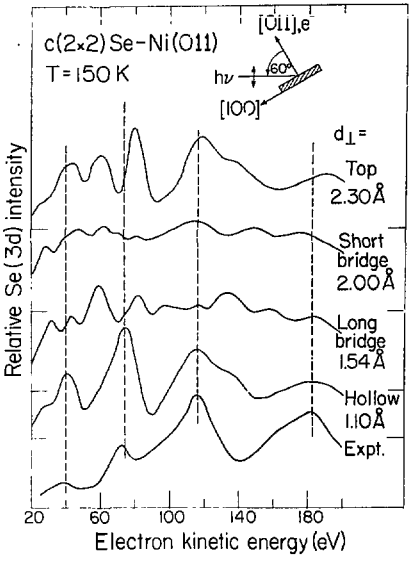

Fig. 1. Experimental NPD results for c(2x2)Se-Ni(011) compared with calculated curves for the experimental arrangement shown. (XBL 811-12022)

* * *

†Brief version of LBL-13410, Dec., 1981, to be submitted to Phys. Rev. B.

‡Bell Labs, Murray Hill, NJ 07974,
§Research Laboratories, Polaroid Corporation, Waltham, MA 02154.
‖Research Laboratory, Eastman Kodak, Rochester, NY 14650.
¶Shell Development Company, Houston, TX 77001.
**Department of Physics, University of Wisconsin, Milwaukee, WI 53201.

10. OFF-NORMAL PHOTOELECTRON DIFFRACTION STUDY OF THE c(2x2) SELENIUM OVERLAYER ON Ni(001)†

D. H. Rosenblatt, S. D. Kevan,‡ J. G. Tobin, R. F. Davis,§ M. G. Mason,‖ D. A. Shirley, and S. Y. Tong¶

Angle-resolved photoemission, in conjunction with synchrotron radiation, has become an effective tool for studying the morphological structure of surfaces. In this work, the technique of off-normal photoelectron diffraction (PD), is shown to be capable of determining accurate surface structures. The important structural parameter in PD is $d_\perp$, the perpendicular interplanar spacing between the adsorbate layer and the top substrate layer of an ordered surface.

Photoelectron diffraction can be observed by measuring the angle-resolved photoemission intensity from a core level of an adsorbate atom or molecule bonded to a single crystal metal surface. If the photon energy is varied and the core-level photoelectrons are collected in a small cone of solid angle, diffraction of the photoelectrons can yield an oscillatory dependence of the photoelec-

tron intensity on kinetic energy. Structural information can then be derived from a comparison of experimental and theoretical PD curves.

Off-normal photoelectron diffraction data for the c(2x2)Se-Ni(001) system have been compared with calculations to confirm the accepted fourfold hollow site geometry. The best theory-experiment fit is found for a $d_\perp$ spacing of 1.55 Å (see Fig. 1), in agreement with normal photoelectron diffraction and low energy electron diffraction results. A detailed R-factor analysis indicates that the fit is very good, especially at smaller polar angles of electron emission. This work represents the first structure determination by off-normal PD.

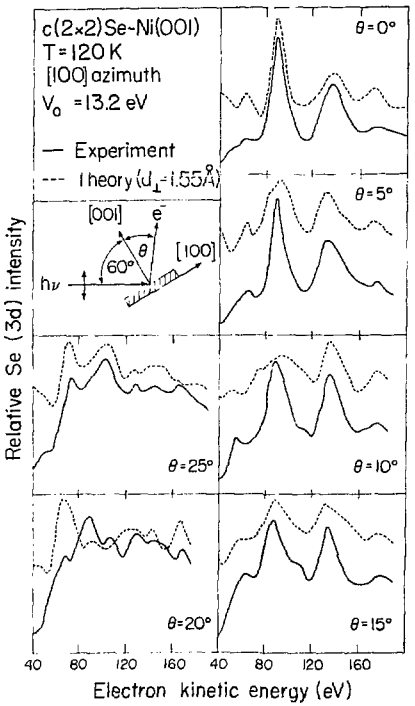

Fig. 1. Experimental off-normal PD data for the [100] azimuth (solid curves) compared with theoretical calculations for the hollow site with $d_\perp$ = 1.55 Å (dashed curves).

(XBL 8111-12015)

* * *

†Brief version of LBL-13268, December 1981. To be submitted to Phys. Rev. B.
‡Bell Labs, Murray Hill, NJ 07974.
§Research Laboratories, Polaroid Corporation, Waltham, MA 02154.
‖Research Laboratory, Eastman Kodak, Rochester, NY 14650.
¶Department of Physics, University of Wisconsin, Milwaukee, WI 53201.

11. ANGLE-RESOLVED PHOTOEMISSION STUDY OF THE VALENCE BANDS OF W(011) IN THE ENERGY RANGE 1000-1250 eV†

Z. Hussain, E. Umbach,‡ J. J. Barton, J. G. Tobin, and D. A. Shirley

Angle-resolved photoemission experiments have been carried out on the valence bands of W(011) using a new UHV double crystal monochromator at SSRL in the energy region 1100-1250 eV (see article 8) to address two fundamental questions pertaining to photoemission from metals:[1] 1) What is the dominant source of Brillouin-zone averaging in valence-band experiments at photon energies of ~ 1-keV, phonon-assisted nondirect transitions arising from lattice vibrations[2] and/or complexities in the final-state electronic wave function due to scattering or component mixing by the crystal potential?[3] Either mechanism would suppress the importance of wave-vector conservation as a useful selection rule in determining which initial region in the Brillouin zone is involved in the emission. The presence of phonon effects would imply a strong temperature dependence in ARP spectra. Inasmuch as phonon effects can be reduced at low temperatures and/or by selecting a system with a large Debye Waller factor, one would expect to observe a strong excitation-energy dependence in ARP valence-band spectra if complexities in the final state electronic wave function are not important or vice versa. 2) If direct transitions (DT) can be observed in ARP at higher energies under certain conditions, is it possible to analyze the data using a simple DT model previously shown to apply rather well to photoemission studies in the 40-150 eV range?[4]

Experimental valence-band spectra along normal emission direction at excitation energies of 1100 eV, 1150 eV, 1175 eV, and 1200 eV, together with theoretically expected curves based on a simple DT model are shown in Fig. 1. There are marked changes in the relative intensities of the two prominent peaks at binding energies of ~ 2.3 eV and ~ 4.8 eV, in very good agreement with the simple DT model. It has also been observed that these spectra exhibit very strong temperature dependences, such that at high temperatures they converge to nearly the same shape. This behavior is consistent with a strong DT component at lower temperatures and complete zone averaging due to phonon effects at higher temperatures.

We conclude that direct transitions can be observed in ARP valence-band spectra obtained at excitation energies of ~ 1 keV from materials with large Debye-Waller factors. Phonon-assisted

non-direct transitions, rather than final-state complexity, are the dominant source of the Brillouin-zone averaging. A simple bulk direct-transition model with plane-wave final states and constant matrix elements gives a good description

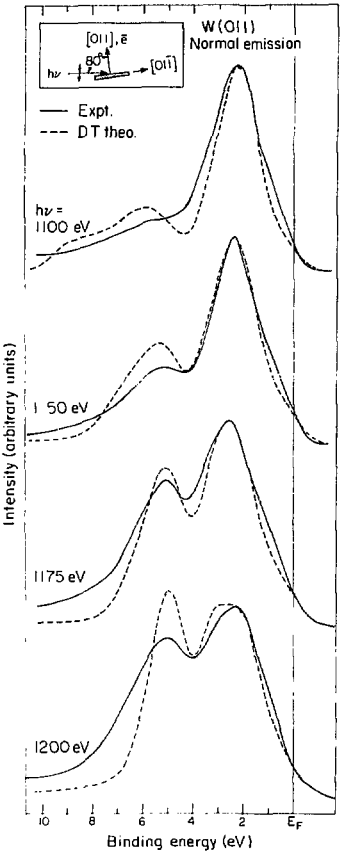

Fig. 1. Valence-band photoemission spectra obtained for the normal electron emission direction at four different excitation energies, compared with direct-transition theory. The theoretical curves were obtained from a weighted sum of the pure direct-transition curves and the density of states. The experimental geometry is also shown in the inset.

(XBL 817-2380)

of spectral changes with photon energy. Furthermore, future ARP experiments with variable photon energies in the presently available region of 800-1500 eV, combined with more favorable conditions of low temperatures ($\leq$ 100 K) and higher analyzer angular resolution ($\leq 2°$), could provide a rather straightforward technique for studying the band structures of solids.

* * *

†Brief version of LBL-12672.

‡Permanent address: Physik Department, Technische Universität München, West Germany.

1. Z. Hussain, E. Umbach, J. J. Barton, J. G. Tobin, and D. A. Shirley. Submitted to Phys. Rev. B.
2. N. J. Shevchik, J. Phys. C 10, 555 (1977); Phys. Rev. B 16, 3482 (1977).
3. F. R. McFeely, J. Stohr, G. Apai, P. S. Wehner, and D. A. Shirley, Phys. Rev. B 14, 3273 (1976).
4. Z. Hussain, S. Kono, L.-G. Petersson, C. S. Fadley, and L. F. Wagner, Phys. Rev. B 13, 724 (1981).

12. ANGLE-RESOLVED PHOTOEMISSION STUDIES OF THE VALENCE BAND STRUCTURE OF STEPPED CRYSTAL SURFACES: Cu(S)-[3(111)x(100)]†

R. F. Davis,‡ R. S. Williams,§ S. D. Kevan,‖ P. S. Wehner,¶ and D. A. Shirley

Detailed angle-resolved photoemission (ARP) studies of Group VIII and IB metals have shown that the peak structures in valence-band photoelectron energy distribution curves (EDCs) arise mainly from energy and crystal momentum-conserving direct electronic transitions near or at the surface, thereby facilitating the development of empirical valence-band dispersion relations $E_n(\vec{k}_i)$ which generally show excellent agreement with bulk valence band structure calculations.[1] However, in each case, the surface studied was a low-Miller-index plane [i.e., (100), (110), or (111)]. We report angle-resolved normal photoemission (ARNP) valence-band studies of the Cu(211) stepped crystal face. These experiments directly address a number of important problems in photoemission from metals. Low k-space symmetry induces a complete nondegeneracy of the energy levels at most reduced k points along the [211] line thereby complicating the data analysis; the relatively large surface unit cell gives rise to a set of small two-dimensional reciprocal lattice vectors which may induce surface Umklapp effects; and the clean Cu(211) surface develops a stable stepped structure after annealing. The electronic structure of stepped and kinked surfaces is of considerable interest because the step and/or kink atoms on such surfaces are believed to influence surface reactivity.[2]

Employing synchrotron radiation in the energy range 9 eV $\leq h\nu \leq$ 34 eV, we have performed ARP experiments with Cu(S)-[3(111)x(100)] in the normal emission geometry, yielding empirical valence-band $E_n(\vec{k}_i)$ curves along the [211] direction in k-space from EDC peak positions. As shown graphically in Fig. 1, the experimental band positions agree well

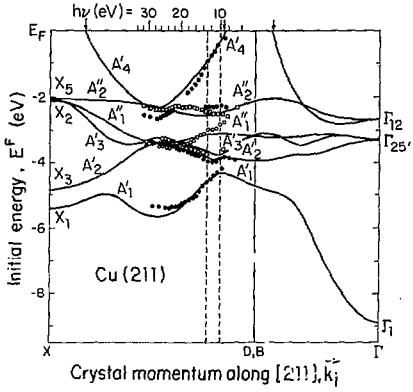

Fig. 1. Empirical (symbols) and theoretical (solid lines) valence-band dispersion relations for Cu(211). A partial photon energy scale is indicated for $\vec{k}$ states at the Fermi level E_F. (XBL 816-3265)

with theoretical[3] bulk Cu bands interpolated along [211] ($\Gamma \rightarrow B$, $D \rightarrow X$).

The four major results of this work are summarized: 1) it is possible to determine experimental valence-band dispersion relations for non-low-index directions; 2) valence-band dispersion relations for stepped Cu(211) show excellent agreement with bulk valence bands interpolated along the [211] direction; 3) the quasi-free electron model describes photoelectron dispersion relations (no surface Umklapp effects were observed), but the one-electron bulk conduction bands do not; 4) there is no evidence for band-gap photoemission; and 5) these studies suggest that the stepped structure of the Cu(211) surface does not significantly perturb its bulk-like electronic structure, a result which was anticipated in previous work.[4]

* * *

†Brief version of LBL-8511, submitted to Phys. Rev. B.

‡Polaroid Corporation, Waltham, MA 02154.

§Department of Chemistry, University of California, Los Angeles, CA 90024.

‖Bell Laboratories, Murray Hill, NJ 07974.

¶Tennessee Eastman Company, Kingsport, TN 37662.

1. See for example, D. A. Shirley, J. Stohr, P. S. Wehner, R. S. Williams, and G. Apai, Physica Scripta 16, 398 (1977); F. J. Himpsel, Appl. Opt. 19, 3964 (1980).
2. G. A. Somorjai, Adv. Catal. 26, 1 (1977); D. W. Blakely and G. A. Somorjai, J. Catal. 42, 181 (1976).
3. G. A. Burdick, Phys. Rev. 129, 138 (1963).
4. R. S. Williams, P. S. Wehner, S. D. Kevan, R. F. Davis, and D. A. Shirley, Phys. Rev. Lett. 41, 323 (1978).

13. VALENCE BAND STRUCTURE OF ANTIFERROMAGNETIC Cr ALONG Δ AND Σ †

R. F. Davis,‡ G. Thornton,§ C. C. Parks, and D. A. Shirley

We have recently performed angle-resolved normal photoemission (ARNP) to establish experimental valence-band dispersion relations, $E_n(\vec{k})$, for the filled or nearly filled d-electron shell of d-band metals[1] in Group VIII and IB elements. In these systems, the direct transition model (DTM) in conjunction with a quasi-free electron parabolic final-state dispersion relation has been used with considerable success. Here we extend these studies to the valence bands of the (100) and (110) faces of chromium (Group VIB). Unlike the previous cases, the Cr metal d-shell is slightly less than half filled, which could lead to many-electron effects in photoemission and a breakdown of the direct transition model. By analogy to the (100) and (110) faces of molybdenum and tungsten,[2] surface states and the one-dimensional density of states may be important in chromium. Finally, uniquely among metals, chromium displays itinerant antiferromagnetic behavior, and the associated spin density wave (SDW) may have an important effect on the electronic structure of chromium as probed by ARNP.

The ARNP spectra of the (100) and (110) faces of Cr were taken with photons in the energy range 6 eV $\leq h\nu \leq$ 32 eV at SSRL employing an apparatus described elsewhere.[1] Using an appropriate final-state dispersion relation, empirical dispersion relations were determined, as summarized in Fig. 1, and compared to the theoretical band structure.

The main conclusions from this work are as follows: 1) the direct transition model works well for chromium as evidenced by peak energy dispersion with hν and a detailed empirical band structure is determined along XΔΓΣM; 2) the antiferromagnetic state and associated spin density wave are directly evidenced in both Cr(100) and Cr(110); 3) an antiferromagnetic band-gap surface state is observed on Cr(110); and 4) the commensurate antiferromagnetic model in the theoretical calculations is probably not accurate, particularly at high symmetry points.

* * *

†Brief version of LBL-13695.

‡Polaroid Corporation, Waltham, MA 02154.

§Department of Chemistry, University of Manchester, Manchester M13-9PL, England.

1. G. Thornton, R. F. Davis, K. A. Mills, and D. A. Shirley, Solid State Commun. 34, 87 (1980) and references therein.
2. I. Terakura, K. Terakura, and N. Hamada, Surf. Sci. 103, 103 (1981) and references therein.
3. J. Kübler, J. Magn. Magn. Mat. 20, 277 (1980).

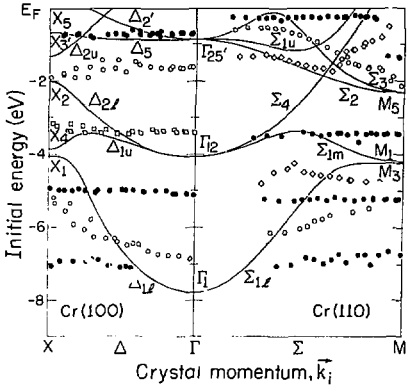

Fig. 1. Dispersion relations for chromium along [100] and [110] in the reduced zone scheme, derived from experimental and theoretical (Ref. 3) curves. Open and closed symbols represent dispersive and nondispersive curves, respectively. Nondispersive empirical curves can be assigned using a density-of-states photoemission mechanism, except for the uppermost ΓΣM curve which corresponds to a $\bar{\Gamma}$ surface state. (XBL 8110-7383)

14. *WORK IN PROGRESS*

Synchrotron radiation in the 50-4000 eV range is being utilized to study several new phenomena recently discovered by this group: normal photoelectron diffraction, condensed-phase photoelectron asymmetry, and core-level photoelectron shape resonances. Also under study are Auger electron angular distributions near threshold.

Electronic band-structure studies are being extended to new types of systems, including thin metallic overlayers, to study the onset of band structure in two-dimensional systems. Metal clusters are also under study to attack this problem from a different direction. Surface structure is also of special interest in the electronic structure work.

Gas-phase research is concentrated in two areas. Time-of-flight measurements with synchrotron radiation are used to study angular distributions of photoelectrons and resonant photoemission phenomena. In a joint project with Y. T. Lee, ultrahigh resolution photoelectron spectroscopy based on molecular beams is yielding new information about small molecules.

1981 PUBLICATIONS AND REPORTS

Refereed Journals

1. M. G. Mason, S. T. Lee, G. Apai, R. F. Davis, D. A. Shirley, A. Franciosi, and J. H. Weaver, "Particle-Size-Induced Valence Changes in Samarium Clusters," Phys. Rev. Lett. 47, 730 (1981); LBL-11810.

2. Z. Hussain, D. A. Shirley, C. H. Li, and S. Y. Tong, "Fourier-Transform Analysis of Normal Photoelectron Diffraction Data for Surface-Structure Determination," Proc. Natl. Acad. Sci. USA 78, 5293 (1981); LBL-11686.

3. S. H. Southworth, P. H. Kobrin, C. M. Truesdale, D. W. Lindle, S. Owaki, and D. A. Shirley, "Photoelectron and Auger Electron Asymmetries: Alignment of $Xe^+(^2D_{5/2})$ by Photoionization," Phys. Rev. A 24, 2257 (1981); LBL-11483.

4. D. H. Rosenblatt, J. G. Tobin, M. G. Mason, R. F. Davis, S. D. Kevan, D. A. Shirley, C. H. Li, and S. Y. Tong, "Normal Photoelectron Diffraction of c(2x2)O(1s)-Ni(001) and c(2x2)S(2p)-Ni(001), with Fourier-transform Analysis," Phys. Rev. B 23, 3828 (1981); LBL-11447.

5. D. A. Shirley, "Photoemission from Solids: The Transition from Solid-State to Atomic Physics," in Inner-Shell and X-Ray Physics of Atoms and Solids, International Conference on X-Ray Processes and Inner-Shell Ionization, Glasgow, Scotland, D. J. Fabian, H. Kleinpoppen, and L. M. Watson, Eds., (Plenum Press, New York, 1981), pp. 455-466; LBL-11276.

6. J. E. Pollard, D. J. Trevor, Y. T. Lee, and D. A. Shirley, "Photoelectron Spectroscopy of Supersonic Molecular Beams," Rev. Sci. Instrum. 52, 1837 (1981); LBL-11250.

7. S. D. Kevan, J. G. Tobin, D. H. Rosenblatt, R. F. Davis, and D. A. Shirley, "Temperature Dependence of Normal-emission Photoelectron Diffraction and Analogies with Extended X-ray-absorption Fine Structure," Phys. Rev. B 23, 493 (1981); LBL-11199.

8. S. D. Kevan, R. F. Davis, D. H. Rosenblatt, J. G. Tobin, M. G. Mason, D. A. Shirley, C. H. Li, and S. Y. Tong, "Structural Determination of Molecular Overlayer Systems with Normal Photoelectron Diffraction: c(2x2)CO-Ni(001) and $(\sqrt{3} \times \sqrt{3})R$ 30° CO-Ni(111)," Phys. Rev. Lett. 46, 1629 (1981); LBL-10024.

9. D. A. Shirley, "Surface and Adsorbate Structural Studies by Photoemission in the hν = 50-500 eV Range," CR in Solid State Materials Science 10, 373 (1981); LBL-9596.

LBL Reports

1. R. F. Davis, R. S. Williams, S. D. Kevan, P. S. Wehner, and D. A. Shirley, "Angle-Resolved Photoemission Studies of the Valence Band Structure of Stepped Crystal Surfaces: Cu(S)-[3(111)x(100)]," LBL-8511.

2. Z. Hussain, E. Umbach, J. J. Barton, J. G. Tobin, and D. A. Shirley, "Angle-Resolved Photoemission Study of the Valence Bands of W(011) in the Photon Energy Range 1100-1250 eV: Observation of Strong Direct Transitions and Phonon Effects," LBL-12672.

3. Z. Hussain, E. Umbach, D. A. Shirley, J. Stöhr, and J. Feldhaus, "Performance and Application of a Double Crystal Monochromator in the Energy Region 800 $\leq h\nu \leq$ 4500 eV," LBL-12729.

4. S. H. Southworth, C. M. Truesdale, P. H. Kobrin, D. W. Lindle, W. D. Brewer, and D. A. Shirley, "Photoionization Cross Sections and Photoelectron Asymmetries of the Valence Orbitals of NO," LBL-12907.

5. S. H. Southworth, W. D. Brewer, C. M. Truesdale, P. H. Kobrin, D. W. Lindle, and D. A. Shirley, "Photoelectron Angular Distributions from H_2 and D_2," LBL-12922.

6. D. H. Rosenblatt, S. D. Kevan, J. G. Tobin, R. F. Davis, M. G. Mason, D. A. Shirley, and S. Y. Tong, "Off-Normal Photoelectron Diffraction Study of the c(2x2) Selenium Overlayer on Ni(001)," LBL-13268.

7. P. H. Kobrin, U. Becker, S. H. Southworth, C. M. Truesdale, D. W. Lindle, and D. A. Shirley, "Autoionizing Resonance Profiles in the Photoelectron Spectra of Atomic Cadmium," LBL-13304.

8. R. F. Davis, "Angular Distribution and Atomic Effects in Condensed Phase Photoelectron Spectroscopy," LBL-13511 (Ph.D. thesis).

9. S. H. Southworth, "Atomic and Molecular Photoelectron and Auger Electron Spectroscopy Studies using Synchrotron Radiation," LBL-13512 (Ph.D. thesis).

10. J. W. Hepburn, D. J. Trevor, J. E. Pollard, D. A. Shirley, and Y. T. Lee, "Multiphoton Ionization Photoelectron Spectroscopy of CCl_2F_2 and CCl_3F," LBL-13752.

Invited Talks

1. D. A. Shirley, Current Status of Surface Structure Studies by Normal Photoelectron Diffraction, 36th Northwest Regional Meeting of the American Chemical Society, Montana State University, Bozeman, MT, June 17-19, 1981.

2. D. A. Shirley, National Overview of Synchrotron Radiation Sources and Facilities, Materials Research Council Meeting, San Diego, CA, July 10, 1981.

3. D. A. Shirley, Photoemission from Solids: Past, Present, and Future, 182nd National Meeting of the American Chemical Society, New York, NY, August 26-27, 1981.

4. D. A. Shirley, Recent Advances in the Study of Band Structures in Solids by Photoelectron Spectroscopy, Surface Science Symposium, Xerox Palo Alto Research Center, Palo Alto, CA, October 20, 1981.

5. D. A. Shirley, Normal Photoelectron Diffraction: A Progress Report, 8th Annual SSRL Users Meeting, Stanford, CA, October 22-23, 1981.

6. D. A. Shirley, Photoelectron Spectroscopy: The Electron's View of Matter, Gilbert Newton Lewis Memorial Lecture, University of California, Berkeley, CA, October 29, 1981.

7. Zahid Hussain, Performance and Application of a Double Crystal Monochromator in the Energy Region 800 $\leq h\nu \leq$ 4500 eV, Second National Conference on Synchrotron Radiation Instrumentation, Cornell University, Ithaca, NY, July 15-17, 1981.

8. Zahid Hussain, Angle-Resolved Photoemission Studies in a Novel Energy Region: 300-4500 eV, IBM Thomas J. Watson Research Center, Yorktown Heights, NY, September 8-10, 1981.

9. Zahid Hussain, Performance and Application of a Double Crystal Monochromator in the Energy Region 800 $\leq h\nu \leq$ 4500 eV, 8th Annual SSRL Users Meeting, Stanford, CA, October 22-23, 1981.

10. Zahid Hussain, Studies of Photoelectron Diffraction, Angle-Resolved Photoemission and Threshold Effects in Auger Spectroscopy in a Novel Energy Region: 800-4500 eV, Materials Research Society Annual Meeting, Boston, MA, November 16-19, 1981.

11. Dennis J. Trevor, High Resolution Ultraviolet Photoelectron Spectroscopy, Seminar on Collision Experiments in their Theoretical Frame, The University of Chicago, Chicago, IL, May 21-23, 1981.

i. Crossed Molecular Beams*

Yuan T. Lee, Investigator

1. $O(^3P) + C_2H_3Br$: REACTIVE SCATTERING†

Guozhong He, R. J. Baseman, R. J. Buss, and Y. T. Lee

Understanding the mechanisms of the reactions of oxygen atoms with unsaturated hydrocarbons is important because they play a major role in combustion processes. Earlier, this group has studied reactions of $O(^3P)$ with C_2H_2, C_2H_4, and C_6H_6, identifying primary products and obtaining product translational energy distributions. A mechanism has been proposed that invokes reactions on several triplet surfaces to explain the observed products and reconcile these findings with the results of others. The reactions presented here and in the following two articles, were chosen to test the validity and generality of the proposed mechanism. The reaction $O(^3P) + C_2H_3Br$ is more complicated than the previous reactions. Because the C-Br bond is weak, migration of the Br atom in the complex may compete in importance with C-Br bond breaking.

The reaction was studied at two collision energies, 7.4 and 12.4 kcal/mole, in a crossed supersonic beam apparatus with rotatable quadrupole mass spectrometry. The angular and velocity distributions of the signal at different masses were used to identify the primary species from which the signals arise. In Fig. 1 are shown the angular distributions of signal from mass 120, 95 and 42. The mass 95 and 42 are also shown corrected for contributions from elastic scattering and from fragmentation of the C_2H_2BrO product in the ionizer. The signal at mass 120 is identified as the product of H atom elimination from the $O-C_2H_3Br$ complex. Mass 95 is the parent ion of CH_2Br produced by C-C bond breaking after Br atom migration. The mass 42 signal is $C_2H_2O^+$ ion arising from ionization of C_2H_3O product from the Br atom elimination.

The three reactions observed here are consistent with the model proposed for the $O + C_2H_4$ reaction. The oxygen attacks C_2H_3Br at either carbon forming one of four triplet biradical intermediates. Reactions on each surface depend on which product states the intermediate correlates to. In $O + C_2H_4$, the only channel under collision-free conditions is loss of an H atom, however in $O + C_2H_3Br$ the weak C-Br bond can be broken on one of the four surfaces and Br migration is possible. No evidence for the formation of 3- or 4-center elimination products is seen. It is not possible to dismiss the 1,2 migration of H atom which would lead to CH_2Br production, although this migration was not observed in the $O + C_2H_4$ reaction.

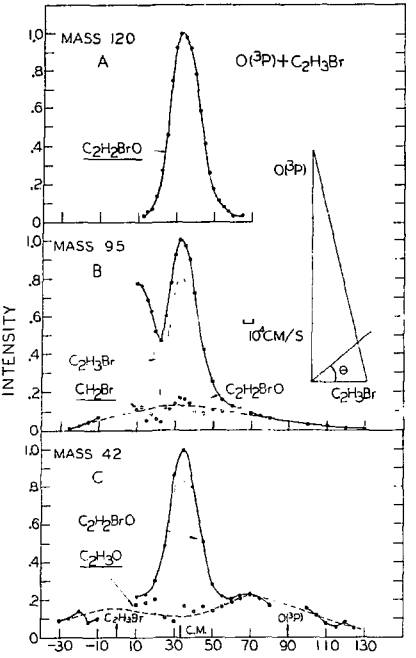

Fig. 1. Angular distribution of product from $O + C_2H_3Br$ at 12.4 kcal/mole collision energy. (A) C_2H_2BrO product. (B) CH_2Br product (open circles) showing subtraction of elastic and fragmentation contributions. (C) C_2H_3O product with subtraction of fragmentation shown.

(XBL 815-9972)

* * *

†Brief version of LBL-12801.

2. $O(^3P) + 1,1-C_2H_2Cl_2$: REACTIVE SCATTERING

Guozhong He, R. J. Baseman, R. J. Buss, and Y. T. Lee

Frequently, the reaction mechanisms that have been proposed for oxygen atom reactions with un-

*This work was supported by the Director, Office of Energy Research, Office of Basic Energy Sciences, Chemical Sciences Division of the U.S. Department of Energy under Contract No. DE-AC03-76SF00098.

saturated hydrocarbons have included as major channels, the 1,2 migration of H atoms. Our studies of these reactions under single collision conditions have suggested that this process is not competitive with simple C-H bond ruptures. These results are supported by several theoretical results that indicate a high barrier to the H atom migration on a triplet surface. The reaction $O(^3P) + 1,1\text{-}C_2H_2Cl_2$ is of interest as a probe of this problem because the migration of an H atom or of a Cl atom leads to distinguishable products.

The apparatus was identical to that in the preceding article. Figure 1 shows angular distributions of signal at three masses, 110, 76 and 51. The H atom elimination produces the characteristic sharp peak at the center of mass angle at mass 110. The angular distribution of mass 76 signal is broadened from the Cl atom elimination and contains a peak at the CM angle from fragmentation of the C_2HCl_2O product. CH_2Cl product is observed at mass 51 with a very broad angular range resulting from recoil of the heavy CClO fragment. No signal was seen at mass 83, $CHCl_2$.

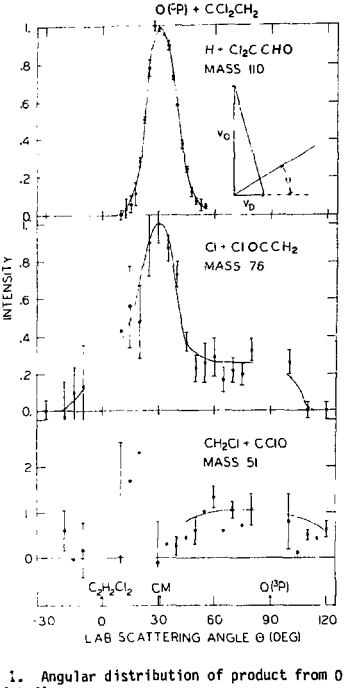

Fig. 1. Angular distribution of product from O + $1,1\text{-}C_2H_2Cl_2$.

(XBL 818-11365)

The reaction products observed here agree well with the proposed O-olefin mechanism. The oxygen attaches to one of the carbons forming a triplet biradical. If the carbon is bonded to two Cl atoms, a Cl atom may be lost or may migrate to the other carbon followed by C-C bond rupture. These two events are each favored on different triplet surfaces. If the oxygen attaches to the carbon containing two H atoms, the only available decay channel is C-H bond breakage because the migration of the H atom has a large barrier. Three or four center elimination of HCl, H_2 or Cl_2 appears to be noncompetitive.

* * *

†Brief version of LBL-11909.

3. $O(^3P)$ + PROPENE: REACTIVE SCATTERING

R. J. Baseman, R. J. Buss, Guozhong He, and Y. T. Lee

Propene is another unsaturated hydrocarbon, important as a fuel, whose reactions with oxygen atoms are poorly understood. A recent near-single collision study[1] of $O + C_3H_6$ has identified four principle reactions; three involve H atom migrations in the complex and one involves the three-center elimination of molecular H_2. None of the proposed reaction routes involves the simple bond cleavage that appears to dominate oxygen-atom reactions with olefins. The present study was aimed at answering this apparent conflict by measurement of products of single collisions.

Angular distributions of ion-product masses were obtained in a crossed beams experiment identical to that described in the previous two reports. The mass 57 product was narrowly distributed about the center of mass angle and identified as arising from C_3H_5O from the H atom elimination. The product of mass 29 cannot be positively identified because it may originate in the ionizer from any of several possible products; C_2H_3O, CHO, CH_2O or C_2H_5.

The mechanism of the oxygen atom-olefin reaction which has been proposed to explain the results of the reactions with C_2H_4, C_2H_3Br and $C_2H_2Cl_2$ would predict that $O + C_3H_6$ would form a complex on one of four potential energy surfaces and the complex would decay by loss of an H atom or of a CH_3 radical. Luntz[2] has observed CH_2CHO product from this reaction with laser induced fluorescence, confirming the CH_3 elimination channel. If we attribute the mass 29 signal, observed here, to fragmentation of the CH_2CHO product in the electron bombardment ionizer, then the results are entirely consistent with the previously studied $O(^3P)$-olefin system as well as with the LIF results. The two principle channels are C-H bond cleavage yielding H + C_3H_5O and methyl radical elimination producing CH_3 + CH_2CHO.

* * *

†Brief version of LBL-12894.

1. B. Blumenberg, K. Hoyermann and P. Sievert, 16th Int. Symp. on Combustion, The Combustion

Institute, Pittsburgh, PA, 1976.
2. A. Luntz, private communication.

4. REACTION DYNAMICS OF THE $H_2^+ + N_2$, CO, and O_2 SYSTEMS†

S. L. Anderson, T. Turner and Y. T. Lee

The reactions of H_2^+, $D_2^+(v)$ with N_2, CO and O_2 were studied as functions of initial ion vibrational states and relative kinetic energies. Cross sections were obtained for the charge transfer (CT) and proton transfer (PT) reactions.

A cross section for a particular reaction is best studied knowing its relative energy and as many of the internal energy states of reactants and products as possible. In particular, calculated potential energy surfaces and trajectories are useful for describing the reaction kinetics. For $H_2^+ + H_2$ and $H_2^+ + Ar$ theoretical calculations were available (Refs. 1 and 2 respectively) to help explain the observed dynamics. However, for $H_2^+ + N_2$, CO, and O_2, potential energy surfaces are not available; the results are explained, whenever possible, with qualitative surfaces and crude correlation arguments.

The apparatus consists of a photoionization source to produce a known vibrational population of H_2^+ ions, a scattering cell filled with reactant neutral molecule biased with respect to the source, and a detection system where product ions are mass analyzed and counted using a Daly detector. The photoions are formed in and guided through the scattering cell by means of an octapole ion guide as described in the literature.[1] Cross sections are calculated for the different vibrational levels of H_2^+, D_2^+ (v = 0-4) and various relative energies-of-collision (center of mass energy = 0-10 eV).

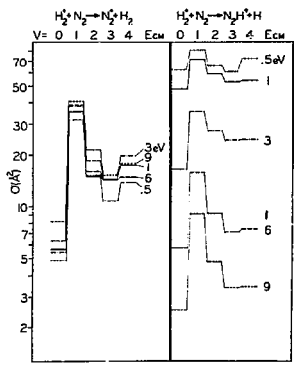

Fig. 1. Charge and proton transfer cross sections as a function of ion vibrational and relative kinetic energy for $H_2 + N_2$. (XBL 817-10697)

The results for $H_2^+ + N_2$ are shown in Fig. 1. The $H_2^+ + N_2$ system behaves very similarly to $H_2^+ + Ar$ owing to the similar nature of the potential energy surfaces. For $H_2^+ + CO$ and O_2, due to the lack of theoretical work available, only the CT results can be fit fairly well calculating the Franck-Condon factors between ion and molecule for both molecules in their initial states, multiplied by an exponential energy defect factor. The above experiments are being analyzed and a paper is being written.[3] The $H_2^+ + He$ system will be studied in the future.

* * *

†Brief version of LBL-13556.

1. S. L. Anderson, F. A. Houle, D. Gerlich, Y. T. Lee, J. Chem. Phys. 75, 2153 (1981). LBL-11976
2. F. A. Houle, S. L. Anderson, D. Gerlich, T. Turner, Y. T. Lee, Chem. Phys. Lett. 82, 392 (1981). LBL-12970
3. To be submitted to J. Chem. Phys.

5. THE LIFETIME OF METASTABLE $(a^4\pi_u)O_2^+$

S. Bustamente, M. Okumura, F. A. Houle, and Y. T. Lee

Obtaining accurate spectroscopic data on molecular ions is difficult because the maximum number density achievable is very low. The photodissociation spectroscopy of trapped ions is a very sensitive technique for this purpose, because absorptions can be detected indirectly by monitoring fragment ions. One well studied system is the first negative band of O_2^+, $b^4\Sigma^- \leftarrow a^4\pi_u$, where the upper level predissociates. The $a^4\pi_u$ state is metastable, and by using the photodissociation signal to measure the $^4\pi$ population, we have measured its radiative lifetime. The metastable decay cannot be accurately measured except under high vacuum. The measurement of this spin forbidden transition can give us information on the spin-orbit coupling of the $a^4\pi_u$ state to other doublet states, especially the nearby $A^2\pi_g$ state.

The apparatus has been previously described,[1] but now has several major improvements. The ionizer creates a mix of metastable and ground state O_2^+ ions. They are focused and mass selected by a 60° sector magnet, then bent 90° into the axis of a laser beam with an electrostatic quadrupole bending field collinear with the laser. After a variable delay, the laser (a YAG pumped dye laser) is pulsed, and any photofragment ions from the dissociation of the remaining metastable ions are detected with a quadrupole mass spectrometer.

The modifications have greatly improved the signal and the quality of the data from that reported earlier. We have found that we are now able to measure small differences in decay rates as a function of laser frequency. The photodissociation signal has contributions from direct dissociation of all levels, and from state-to-state predissociation, and these must be distinguished to obtain true state-resolved decays.

Several other experiments are planned. The

threshold photodetachment spectrum for the CH_2^- ion will resolve the current controversy concerning the interpretation of the photoelectron spectrum of CH_2^- and the singlet/triplet splitting measured from it for the methylene radical. We will also continue studies on the vibrational predissociation of rare gas ion - van der Waal's complexes created in the supersonic expansion of a weak atmospheric pressure plasma. Such work should yield the infrared spectra of ions whose spectra have previously been undetected.

* * *

1. D. K. Gerlich, S. W. Bustamente, L. R. Carlson, H. S. Kwok, and Y. T. Lee, LBL-8580 (1978) 331.

6. RARE GAS-HALOGEN ATOM INTERACTION POTENTIALS FROM MOLECULAR BEAM STUDIES: $I(^2P_{3/2})$ + Kr, Xe $(^1S_0)$.

P. Casavecchia, Guozhong He, R. K. Sparks and Y. T. Lee

Knowledge of the interaction potentials of halogens with rare gases is very useful for understanding the emission spectra and the kinetics of lasing action in an excited rare gas halogen medium. In addition, these interaction potentials reveal the nature of chemical bonding and its importance in van der Waals molecules as well as providing help in understanding termolecular recombination of halogen atoms in rare gas environments.

Angular distributions of $I(^2P_{3/2})$ scattered from Kr and $Xe(^1S_0)$ in the thermal energy range have been measured in a crossed molecular beam apparatus. The data were analyzed using an appropriate elastic scattering analysis, which neglects nonadiabatic coupling as previously used for F-RG, Cl-Xe and Br-RG to obtain the interaction potential curves for the two relevant states (X1/2 and I3/2) governing the scattering. The I-Xe X1/2 potential (ϵ = 0.69 kcal/mole, r_m = 4.30 Å) and I-Kr X1/2 potentials (ϵ = 0.55 kcal/mole, r_m = 4.05 Å) show a slightly stronger interaction than the potential of Xe-Xe and Xe-Kr. The I3/2 potentials for the I-Xe (ϵ = 0.48 kcal/mole, r_m = 4.60 Å) and I-Kr (ϵ = 0.36 kcal/mole, r_m = 4.32 Å) were found to be shallower and to have a minimum at larger internuclear distance than the corresponding rare gas pair potentials.

These iodine-rare gas systems complete a matrix of halogen-rare gas diatomics which have been investigated. From a comparison of the RG-X potentials with the RG-RG analogues and from the trends observed in ϵ and r_m much insight has been gained into the factors governing the peculiar electronic structure.

* * *

†Brief version of LBL-12799.

1981 PUBLICATIONS AND REPORTS

Refereed Journals

1. S. L. Anderson, T. Hirooka, P. W. Tiedemann, B. H. Mahan, and Y. T. Lee, "Photoionization of $(H_2)_2$ and Clusters of O_2 Molecules," J. Chem. Phys. 73, 4779 (1980).

2. C. C. Kahler and Y. T. Lee, "Crossed Molecular Beam Studies of Chemiluminescent Reactions: F_2 + I_2, Br_2, and ICl," J. Chem. Phys. 73, 5122 (1980).

3. Yuan T. Lee and Y. Ron Shen, "Studies with Crossed Laser and Molecular Beams," Physics Today, 33, 52 (1980).

4. P. Casavecchia, R. J. Buss, S. J. Sibener, and Y. T. Lee, "A Crossed Molecular Beam Study of the $O(^1D_2)$ + CH_4 Reaction," J. Chem. Phys. 73, 6351 (1980).

5. Piergiorgio Casavecchia, Guozhong He, Randal K. Sparks, and Yuan T. Lee, "Interaction Potentials for $Br(^2P)$ + Ar, Kr, and $Xe(^1S)$ by the Crossed Molecular Beams Method," J. Chem. Phys. 75, 710 (1981).

6. Richard J. Buss, Robert J. Baseman, Guozhong He, and Y. T. Lee, "Reaction of Oxygen Atoms with Ethylene and Vinyl Bromide," J. Photochem. 17, 389 (1981).

7. Scott L. Anderson, F. A. Houle, D. Gerlich, and Y. T. Lee, "The Effect of Vibration and Translation Energy on the Reaction Dynamics of the H_2^+ + H_2 System," J. Chem. Phys. 75, 2153 (1981).

8. R. K. Sparks, K. Shobatake, L. R. Carlson, and Y. T. Lee, "Photofragmentation of CH_3I: Vibrational Distribution of the CH_3 Fragment," J. Chem. Phys. 75, 3838 (1981).

9. R. J. Buss, P. Casavecchia, T. Hirooka, S. J. Sibener, and Y. T. Lee, "Reactive Scattering of $O(^1D)$ + H_2," Chem. Phys. Lett. 82, 386 (1981).

10. F. A. Houle, S. L. Anderson, D. Gerlich, T. Turner, and Y. T. Lee, "Vibrational Effects in Proton and Charge Transfer in the H_2^+ + Ar System," Chem. Phys. Lett. 82, 392 (1981).

11. J. M. Lisy, Andrzej Tramer, Matthew F. Vernon, and Yuan T. Lee, "Vibrational Predissociation Spectra of $(HF)_n$, n = 2-6," J. Chem. Phys. 75, 4733 (1981).

LBL Reports

1. Dennis J. Trevor, "Photoelectron Photoion Molecular Beam Spectroscopy," Ph.D. thesis, LBL-11434.

2. M. F. Vernon, D. J. Krajnovich, H. S. Kwok, J. M. Lisy, Y. R. Shen, and Y. T. Lee, "Infrared Vibrational Predissocation Spectroscopy of Water Clusters by the Crossed Laser - Molecular Beam Technique," submitted to J. Chem. Phys. November 1981, LBL-11970.

†3. H. S. Kwok, G. Z. He, R. K. Sparks and Y. T. Lee, "On the Photodissociation of Nitromethane at 266 nm," submitted to Int. J. Chem. Kinet. February 1981, LBL-12309

4. J. E. Pollard, D. J. Trevor, Y. T. Lee, and D. A. Shirley, "Photoelectron Spectroscopy of Supersonic Molecular Beams," submitted to Rev. Sci. Instrum. June 1981, LBL-11250.

5. Scott Law Anderson, "The Effect of Vibrational Excitation on the Dynamics of Ion-Molecule Reactions," Ph.D. thesis, LBL-13309.

Other Publications

1. R. K. Sparks, C. C. Hayden, K. Shobatake, D. M. Neumark, and Y. T. Lee, "Molecular Beam Studies of Reaction Dynamics of F + H_2, D_2," in Horizons of Quantum Chemistry, edited by K. Fukui and B. Pullman (D. Reidel Publishing Company, Boston, 1980) p. 91, LBL-9688.

2. H. Haberland, Y. T. Lee and P. E. Siska, "Scattering of Noble-Gas Metastable Atoms in Molecular Beams," in The Excited State in Chemical Physics, Part 2," edited by Dr. J. W. McGowan (John Wiley & Sons, New York, 1981) p. 487, LBL-8959.

Invited Talks

1. Y. T. Lee, "Molecular Beam Studies on Photofragmentation and Vibrational Predissociation," Western Spectroscopy Association Meeting, Asilomar, CA, January 28-30, 1981.

2. Y. T. Lee, "Recent Advances in Molecular Beam Chemistry," Chemistry Department, Johns Hopkins University, Lester P. Kuhn Lecture, March 17, 1981.

3. Y. T. Lee, "Molecular Beam Studies on Reaction Dynamics," Chemistry Department, Pennsylvania State University, College Station, PA, March 19, 1981.

4. James M. Lisy, "Vibrational Predissociation of Small Molecular Clusters," Symposium on van der Waals Molecules, State University of New York, Oneonta, NY, March 19-20, 1981.

5. Y. T. Lee, "Dynamics of Endothermic Reactions Involving Atoms and Polyatomic Molecules," Debye Award Symposium honoring Professor R. B. Bernstein, American Chemical Society Annual Meeting, Atlanta, GA, March 30, 1981.

6. Y. T. Lee, "Energy Splitting Between Singlet and Triplet Methylene," Department of Chemistry, University of Texas, Austin, April 2, 1981.

7. Y. T. Lee, "Molecular Beam Studies on Reaction Dynamics," Third West Coast Theoretical Chemistry Conference, NASA Ames Research Center, April 22-24, 1981.

8. Y. T. Lee, "Reaction of Oxygen Atoms with Unsaturated Hydrocarbons," Chemistry Department, Tsinghua University, Hsinchu, Taiwan, China, May 26, 1981.

9. Y. T. Lee, "Effect of Vibrational and Translational Energies in Endothermic Reactions," Chemistry Department, Taiwan University, Taipei, Taiwan, China, May 28, 1981.

10. Y. T. Lee, "Photofragmentation Translational Spectroscopy," Academia Sincia, Taiwan, China, May 29, 1981.

11. P. Casavecchia, "Interaction Potentials of Ground State Xenon Halides," 8th International Symposium on Molecular Beams, Palais des Festivals, 06400 Cannes, France, June 1-5, 1981.

12. R. J. Buss, "Reactive Scattering of $O(^3P)$ with Unsaturated Hydrocarbons," 8th International Symposium on Molecular Beams, Palais des Festivals, 06400 Cannes, France, June 1-5, 1981.

13. Y. T. Lee, "Vibrational Predissociation Spectroscopy of Hydrogen Bonded Clusters and van der Waals Molecules," V International Conference on Laser Spectroscopy, Jasper Parks, Canada, June 29-July 3, 1981.

14. Y. T. Lee, "The Current Status of the Reactive Scattering Experiment," XII International Conference on the Physics of Electronic and Atomic Collisions, Gatlinburg, TN, July 15-21, 1981.

15. T. Turner, "The Effect of Reagent Vibration on the Dynamics of Reactions of H_2^+ with Simple Molecules," XII International Conference on the Physics of Electronic and Atomic Collisions, Gatlinburg, TN, July 15-21, 1981.

16. Y. T. Lee, Gordon Research Conference on "Dynamics of Molecular Collisions" at Plymouth, NH, July 27-31, 1981.

17. Y. T. Lee, "The Effect of Vibrational Excitation in Ion-Molecule Reactions," 28th International Union of Pure and Applied Chemistry Congress, Vancouver, Canada, August 17-21, 1981.

18. R. J. Baseman, "Mechanisms for Reactions of Oxygen (^3P) Atoms with Unsaturated Hydrocarbons Determined by Crossed Molecular Beams Scattering," American Chemical Society Meeting, "New Techniques in Chemical Kinetics," New York, NY, August 23-28, 1981.

19. Y. T. Lee, "Reactions of Oxygen Atoms with Ethylene and Vinylbromide," X International Conference on Photochemistry, The University of Crete, Iraklion, Crete, Greece, September 9-12, 1981.

20. Y. T. Lee, "Molecular Beam Studies of Bimolecular Reactions: F + H_2 and Li + HF," 50 Years Dynamics of Chemical Reactions Conference, Berlin, West Germany, October 12-15, 1981.

* * *

†Work supported in part by the Office of Naval Research under Contract No. N000014-75-C-0671.
‡ Work supported in part by the Office of Naval Research under Contract No. N000014-77-C-0101.

J. Potential Energy Surfaces for Chemical Reactions*

Henry F. Schaefer III, Investigator

Introduction. This research program has two goals, related yet distinct. The first goal is the development of new theoretical and/or computational methods for the description of "what electrons are doing in molecules," to use the words of Robert S. Mulliken. Specifically, the single outstanding problem in the field is the correlation problem, that of formulating models for going beyond the single-particle or Hartree-Fock approximation. The second goal of our research is to apply these theoretical methods to significant problems of broad chemical interest. Currently, two areas are of special interest: 1) model theoretical studies of chemisorption, metal clusters, and organometallic species and 2) potential energy surfaces which govern gas-phase chemical reactions. Research in the former area is ultimately aimed at a truly molecular understanding of catalysis, a subject critical to future energy requirements, but sometimes approached by trial and error methods. In the latter area our research sometimes tends towards molecules potentially important in interstellar space, atmospheric chemistry and the development of high power laser systems. It is to be emphasized that in recent years theoretical chemistry has become a significant source not only of broad generalities, but also of specific predictions concerning molecular systems which may be very important but inaccessible to experiment.

1. HYDROXYCARBENE (HCOH) AND PROTONATED FORMALDEHYDE: TWO POTENTIALLY OBSERVABLE INTERSTELLAR MOLECULES

Mark R. Hoffmann and Henry F. Schaefer III

Formaldehyde is thought to be the most widespread tetraatomic molecule in interstellar space. Most models of the role of formaldehyde in interstellar space concur that one of its most important reactions is the protonation

$$H_2CO + H_3^+ \rightarrow H_3CO^+ + H_2 \qquad (1)$$

Among possible H_3CO^+ structures, the oxygen protonated geometry (bottom structure in Fig. 1) is the lowest energy isomer. Assuming a purely statistical distribution of products for the dissociative recombination reaction

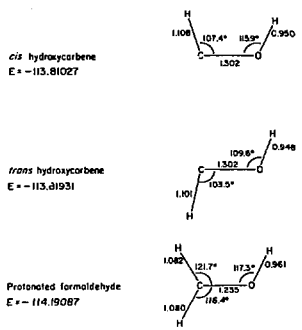

Fig. 1. Theoretical molecular structures of HCOH and H_3CO^+. Bond distances are in Å.
(XBL 824-9060)

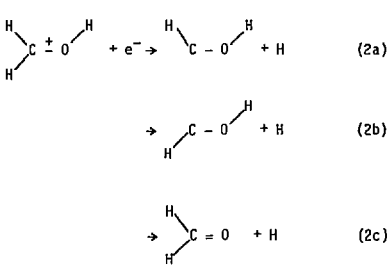

one predicts equal numbers of the three products cis hydroxycarbene (2a), trans hydroxycarbene (2b), and ordinary formaldehyde (2c). Thus it is possible that hydroxycarbene (HCOH) might be an important interstellar molecule, despite the fact that it has never been observed spectroscopically by terrestrial laboratory experiments.

Ab initio molecular electronic structure theory has been used to predict the equilibrium geometries and rotational constants of H_3CO^+ and the cis and trans forms of HCOH. The lowest rotational transition, designated $\Delta E(0_{0,0} \rightarrow 1_{0,1})$, for these three species is predicted to occur at 62.9 GHz (H_3CO^+), 68.1 GHz (cis HCOH), and 68.4 GHz (trans HCOH). It is hoped that these predictions will assist radioastronomers in the identification of these three molecular species in dense interstellar clouds.

*This work was supported by the Director, Office of Energy Research, Office of Basic Energy Sciences, Chemical Sciences Division of the U. S. Department of Energy under Contract No. DE-AC03-76SF00098.

* * *

*Brief version of Astrophys. J. 249, 563 (1981); LBL-12586.

2. BIS(CYCLOBUTADIENE)NICKEL: GEOMETRICAL AND ELECTRONIC STRUCTURE†

Russell M. Pitzer, John D. Goddard, and Henry F. Schaefer III

Surely one of the more important achievements in organometallic chemistry during the past few years was the synthesis of the first cyclobutadiene (CBD) sandwich compound. Hoberg, Krause-Göing, and Mynott reported in 1978 that the octaphenyl compound $Ni(C_4Ph_4)_2$ crystallizes as small, well-formed blue needles, has a melting point of 404°C, and is relatively unreactive. For example, the ligands cannot be replaced by CO, even at 110°C and 1 atm, and the compound is both air stable and unaffected by boiling water. All these observations point to a well-protected nickel atom for which the 18-electron rule is satisfied. At such an early stage in the development of CBD sandwich chemistry, it is not surprising that the unsubstituted $NI(C_4H_4)_2$ has not yet been reported.

The predicted equilibrium geometry of bis (cyclobutadiene) nickel is illustrated in Fig. 1. The final Ni-ring and C-C distances are remarkably close to those of the known $C\ell_2Ni(C_4Me_4)$ crystal structure. The out-of-plane bending of the C-H bonds is, however, opposite in direction to the observed bending angle in the well characterized cyclopentadienyl sandwich ferrocene, $Fe(C_5H_5)_2$. For $Ni(C_4H_4)_2$, the conformer with the two CBD rings eclipsed lies about 1 kcal/mole below the staggered form. It is hoped that some of these predictions concerning nickel CBD sandwiches will be confirmed in forthcoming laboratory studies.

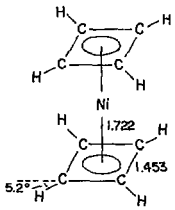

Fig. 1. Predicted equilibrium geometry for bis(cyclobutadiene) nickel, with distances in Å. (XBL 824-9059)

* * *

†Brief version of J. Amer. Chem. Soc. 103, 5681 (1981).

3. A UNIMOLECULAR REACTION ABC → A + B + C INVOLVING THREE PRODUCT MOLECULES AND A SINGLE TRANSITION STATE: PHOTODISSOCIATION OF GLYOXAL†

Yoshihiro Osamura, Henry F. Schaefer III, M. Dupuis, and William A. Lester, Jr.

The spectroscopy, photophysics, and photochemistry of glyoxal ($H-\overset{O}{\overset{\|}{C}}-\overset{O}{\overset{\|}{C}}-H$) has been the subject of intense experimental study in recent years. Perhaps most exhaustively studied has been the internal conversion (radiationless transition) from the lowest $n\rightarrow\pi^*$ singlet state S_1 to the vibrationally excited levels of the S_0 ground state. In light of the remarkable amount of dynamical information available concerning the decay of S_1 glyoxal, it is perhaps surprising that a much less complete mechanistic picture exists for the ensuing photodissociation. The most important fact garnered recently in this regard is that, contrary to previous expectations, glyoxal dissociates from the S_1 zero-point level in the absence of collisions.

In this research it has been shown that the seemingly heretical unimolecular reaction to three products

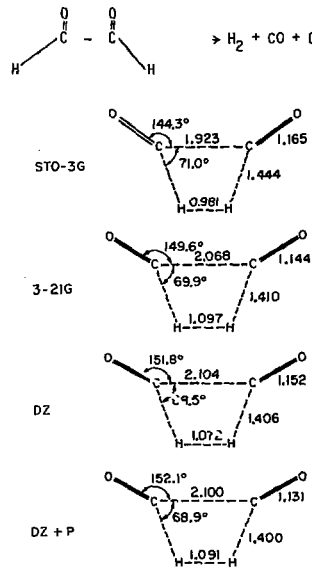

Fig. 1. Transition state geometrical structures for $H-\overset{O}{\overset{\|}{C}}-\overset{O}{\overset{\|}{C}}-H \rightarrow H_2 + CO + CO$. Predictions are at several levels of theory, with bond distances in Å. (XBL 816-3909)

is allowed by orbital symmetry considerations. Moreover, the transition state connecting glyoxal with the three product molecules lies at an energy comparable to that imparted to S_0 after the radiationless transition. Predicted structures (at various levels of theory) for this unorthodox transition state are shown in Fig. 1. At the highest level of theory adopted, the planar C_{2v} structure actually has two imaginary vibrational frequencies, with the larger (2161 i) corresponding to the expected reaction coordinate. However, due to the extreme flatness of the potential energy surface in the direction of the 96 i normal mode, it seems likely that the true (nonplanar at this level of theory) saddle point energy will be only slightly less than that of the constrained C_{2v} stationary point. It is hoped that molecular beam experiments in the MMRD laboratory of Professor Y. T. Lee will confirm these remarkable theoretical predictions.

* * *

†Brief account of J. Chem. Phys. 75, 5828 (1981). (LBL-12841).

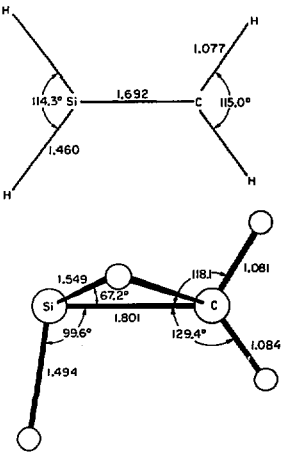

Fig. 1. Theoretical structures for silaethylene and the transition state connecting it with methylsilylene. Bond distances are in Å.

(XBL 817-4D58)

4. THEORETICAL STUDIES OF THE 1,2 HYDROGEN SHIFT: THE CONTROVERSIAL BARRIER HEIGHT BETWEEN SILAETHYLENE AND METHYLSILYLENE.

Yasunori Yoshioka and Henry F. Schaefer III

In an earlier theoretical study, Goddard, Yoshioka, and Schaefer predicted that the isomers $H_2Si{=}CH_2$ and $HSi{-}CH_3$ are nearly degenerate and separated by a large barrier, not less than 25 kcal/mole. In light of this, the publication of dissenting back-to-back communications in the Journal of the American Chemical Society came as something of a surprise to us. Conlin and Wood reported indirect evidence from the pyrolysis of methylsilacyclobutane that the reaction

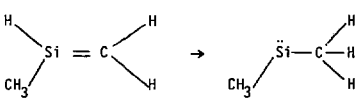

(1)

is rapid, while Michl and West present matrix isolation spectroscopic results which suggest that even at 100 K reaction (1) proceeds rapidly. The latter authors conclude that "unless the additional methyl (group) has a dramatic effect, this (theoretical) result is not compatible with our interpretation. No simple alternatives have occurred to us."

In view of the reports mentioned above, further theoretical investigation was deemed imperative. In the current study a complete double zeta plus polarization basis set was chosen and exhaustive geometrical optimization carried out for both silaethylene and the transition state to methylsilylene. The theoretical structures are summarized in Fig. 1 and the predicted barrier from the silaethylene side is still of the order of 35 kcal/mole. Since the theoretical transition state includes no elements of symmetry, it would appear unlikely that a different, lower energy reaction pathway for

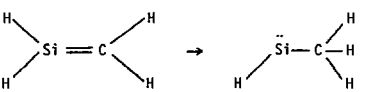

(2)

exists. Barton at Iowa State has suggested an alternate interpretation of the Conlin-Wood experiments, and a different explanation of the Michl-West results would open the way to another triumph for applied theoretical chemistry.

* * *

†Brief version of J. Amer. Chem. Soc. 103, 7366 (1981), LBL-13670.

5. ISOMERIC STRUCTURES OF CH_2LiF, THE PROTOTYPE CARBENOID†

Mark A. Vincent and Henry F. Schaefer II

The term "carbenoid" has been suggested for the description of intermediates that exhibit reactions analogous to those of carbenes, without actually being the free divalent carbon species R_2C:. Methylene donors R_2CAB via

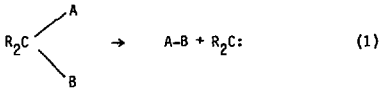

are thus labeled carbenoids when A and B remain weakly associated with the carbon atom at transition states for what would otherwise be free R_2C: carbene reactions. Haloalkalicarbenoids are of special interest in that the formation (1) of the alkali halide is typically such an energetically favorable process that it may facilitate the generation of highly unstable reactive intermediates.

CH_2LiF is the prototype carbenoid, i.e., the simplest molecule that could reasonably be expected to have properties related to those of the heavier halolithiocarbenoids. Nonempirical molecular electronic structure theory has been used in this research to predict the equilibrium geometries, vibrational frequencies, and relative energetics of all plausible isomers of the CH_2LiF system. The predicted theoretical structures are illustrated in Fig. 1.

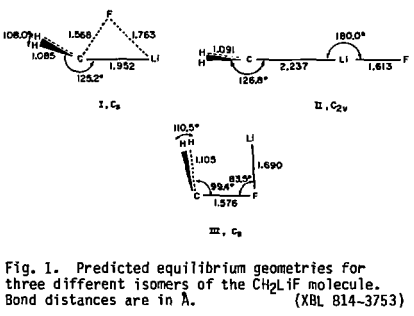

Fig. 1. Predicted equilibrium geometries for three different isomers of the CH_2LiF molecule. Bond distances are in Å. (XBL 814-3753)

Structure I is the absolute minimum on the CH_2LiF hypersurface and is best described by the ion pair valence structure $H_2CLi^+...F^-$. Structure II represents an exceedingly shallow minimum on the energy surface, separated by a barrier of only ~ 1 kcal from structure I and lying 28 kcal higher. Hence we conclude that structure II would not be observable in the gas phase. On the other hand, structure III is a deep secondary minimum, although it lies 25 kcal above structure I. Structure III is best described as $H_2C...FLi$, although some fraction of $H_2CF^-...Li^+$ character is present. Spectroscopic studies by Andrews have demonstrated the existence of two distinct isomers of heavier carbenoids such as $LiCCl_3$ and comparable experimental studies of HC_2LiF would be both welcome and timely.

* * *

†Brief version of LBL-13785.

1981 PUBLICATIONS AND REPORTS

Refereed Journals

1. S. P. So, R. W. Wetmore, and H. F. Schaefer, "Excited Singlet Electronic States of Acetylene: Cis and Trans Structures and Energetics," J. Chem. Phys. 73, 5706 (1980).

2. J. D. Goddard, Y. Yoshioka, and H. F. Schaefer, "Methylsilylene, Silaethylene, and Silylmethylene: Energies, Structures, and Unimolecular Reactivities," J. Amer. Chem. Soc. 102, 7644 (1980).

3. S. C. deCastro, H. F. Schaefer, and R. M. Pitzer, "Electronic Structure of the NH_4^+ Molecular Ion," J. Chem. Phys. 74, 550 (1981).

4. Y. Osamura, J. D. Goddard, H. F. Schaefer, and K. S. Kim, "Near Degenerate Rearrangement Between the Radical Cations of Formaldehyde and Hydroxymethylene," J. Chem. Phys. 74, 617 (1981).

5. H. F. Schaefer, "Approaching the Hartree-Fock Limit for Organotransition Metal Complexes," J. Molec. Structure 76, 117 (1981).

6. Y. Yoshioka, J. D. Goddard, and H. F. Schaefer, "Analytic Configuration Interaction Gradient Studies of SH_4, Sulfurane," J. Chem. Phys. 74, 1855 (1981).

7. Y. Osamura, H. F. Schaefer, S. K. Gray, and W. H. Miller, "Vinylidene: A Very Shallow Minimum on the C_2H_2 Potential Energy Surface. Static and Dynamical Considerations," J. Amer. Chem. Soc. 103, 1904 (1981).

8. M. M. L. Chen, R. W. Wetmore, and H. F. Schaefer, "Mechanism of the H + O_3 Reaction," J. Chem. Phys. 74, 2938 (1981).

9. S. K. Gray, W. H. Miller, Y. Yamaguchi, and H. F. Schaefer, "Tunneling in the Unimolecular Decomposition of Formaldehyde: A More Quantitative Study," J. Amer. Chem. Soc. 103, 1900 (1981).

10. J. G. Goddard, Y. Yamaguchi, and H. F. Schaefer, "Features of the H_2CO Potential Energy Hypersurface Pertinent to Formaldehyde Photodissociation," J. Chem. Phys. 75, 3459 (1981).

11. W. O. Laidig, and H. F. Schaefer, "Large Multiconfiguration Self-Consistent-Field Wavefunctions for the Ozone Molecule," J. Chem. Phys. 74, 3411 (1981).

12. Y. Osamura and H. F. Schaefer, "Internal Rotation Barrier and Transition State for Glyoxal," J. Chem. Phys. 74, 4576 (1981).

13. P. Saxe, H. F. Schaefer, and N. C. Handy, "Exact Solution (Within a Double-Zeta Basis Set) of the Schrödinger Electronic Equation for Water," Chem. Phys. Lett. 79, 202 (1981).

14. Y. Osamura and H. F. Schaefer, "Toward the Spectroscopic Identification of Vinylidene, $H_2C{=}C$:," Chem. Phys. Lett. 79, 412 (1981).

15. P. Saxe, H. F. Schaefer, and N. C. Handy, "Methylene Singlet-Triplet Separation. An Explicit Variational Treatment of Many-Body Correlation Effects," J. Phys. Chem. 85, 745 (1981).

16. D. Spangler, J. J. Wendoloski, M. Dupuis, M. M. L. Chen, and H. F. Schaefer, "Geometry and Electronic Structure of $(CO)_3NiCH_2$. A Model Transition-Metal Carbene," J. Amer. Chem. Soc. 103, 3985 (1981).

17. Y. Yoshioka, J. D. Goddard, and H. F. Schaefer, "Theoretical Challenge to the Experimentally Determined Geometrical Structure of Dimethylsilaethylene," J. Amer. Chem. Soc. 103, 2452 (1981).

18. Y. Yoshioka, H. F. Schaefer, and K. D. Jordan, "Theoretical Investigation of the Electron Affinity of CO_2," J. Chem. Phys. 75, 1040 (1981).

19. L. Farnell, J. Kao, L. Radom, and H. F. Schaefer, "Structures and Stabilities of Isomeric [10] Annulenes," J. Amer. Chem. Soc. 103, 2147 (1981).

20. M. R. Hoffmann and H. F. Schaefer, "Hydroxycarbene (HCOH) and Protonated Formaldehyde: Two Potentially Observable Interstellar Molecules," Astrophys. J. 249, 563 (1981).

21. M. A. Vincent and H. F. Schaefer, "Diborane (4) (B_2H_4): The Boron Hydride Analogue of Ethylene," J. Amer. Chem. Soc. 103, 5677 (1981).

22. R. M. Pitzer, J. D. Goddard, and H. F. Schaefer, "Bis(cyclobutadiene) Nickel: Geometrical and Electronic Structure," J. Amer. Chem. Soc. 103, 5681 (1981).

23. Y. Osamura, Y. Yamaguchi, and H. F. Schaefer, "Analytic Configuration Interaction (CI) Gradient Techniques for Potential Energy Hypersurfaces. A Method for Open-Shell Molecular Wavefunctions," J. Chem. Phys. 75, 2929 (1981).

LBL Reports

1. Y. Osamura, H. F. Schaefer, M. Dupuis and W. A. Lester, Jr., "A Unimolecular Reaction ABC → A + B + C Involving Three Product Molecules and a Single Transition State. Photodissociation of Glyoxal: $HC\overset{O}{\overset{\|}{C}}H \rightarrow H_2 + CO + CO$," LBL-12841.

2. Y. Yoshioka and H. F. Schaefer, "Theoretical Studies of the 1,2 Hydrogen Shift. XI. The Controversial Barrier Height Between Silaethylene and Methylsilylene," LBL-13670.

3. M. A. Vincent and H. F. Schaefer, "Isomeric Structure of CH_2LiF, the Prototype Carbenoid," LBL-13785.

Other Publications

1. B. R. Brooks, W. D. Laidig, P. Saxe, J. D. Goddard, and H. F. Schaefer, "New Directions for the Loop-Driven Graphical Unitary Approach: Analytic Gradients and an MCSCF Procedure," pages 158-176 of "The Unitary Group for the Evaluation of Electronic Energy Matrix Elements," J. Hinze, ed. Volume 22 of Lecture Notes in Chemistry (Springer-Verlag, Berlin, 1981).

3. Atomic Physics

a. Atomic Physics*

R. Marrus, Investigator

Introduction. The atomic physics group is pursuing experiments on the spectroscopy and collision effects of highly-ionized atoms from the Berkeley SuperHILAC. The goal of these experiments is to test theoretical models of such effects. In addition, some of the phenomena under investigation are relevant to magnetic confinement fusion devices (TOKAMAKS) and astrophysical questions. Techniques employed to study these problems include ion trapping and precision UV and optical spectroscopy. Ionized atoms produced in spark sources are also being employed to study spectroscopy of low-ionization states in an ion trap. Forbidden transitions that are of astrophysical and fusion interest have been observed in this environment.

A separate program is in progress using laser spectroscopy to study parity violation in heavy atoms. Such effects have been predicted by the gauge theories, particularly the model of Weinberg and Solam. In prior experiments we have observed the effect and have achieved a rough precision in agreement with the predictions of the Weinberg-Salam model. Another experiment is in progress to confirm this result, using a higher signal-to-noise ratio and expected higher precision.

1. ELECTRON CAPTURE BY Ne^{10+} TRAPPED AT VERY LOW ENERGIES

R. Marrus, M. H. Prior and C. R. Vane

Electron capture by multiply charged ions in collision with neutral atoms is a subject to considerable interest in fusion power research and astrophysics. In both cases, the capture rate plays an important role in determining the population density of a given degree of ionization. Since capture occurs into excited states of the product ion, subsequent radiation can be a serious energy loss process in a fusion reactor, even when the multicharged ions are a minor constituent of the plasma. Experimental study of electron capture by highly charged ions has been made primarily by beam-gas collision techniques, and has been almost entirely confined to the energy range above about 1 keV and charge states less than fully stripped (bare nuclei). We have developed a new technique[1] that allows study of multicharged ion-atom collisions (including fully stripped ions) in a low energy range hitherto unexplored.

The technique uses an electrostatic ion trap to capture low energy (few eV) recoil ions made by impact of a fast heavy-ion beam on a low density target gas. The experiments are carried out at the LBL SuperHILAC using 370-MeV Xe^{38+} beam ions in collision with neon gas at pressures up to a few times 10^{-6} torr. All charge-state neon ions are produced. Initial studies concentrated upon the bare nucleus Ne^{10+}. The trapped ions are detected by inverting the trap potential and sampling a portion of the exiting ion pulse with a commercial radio-frequency quadrupole mass analyzer. Study of the decay of the trapped ion signal versus neon density yields the rate constant for electron capture of the Ne^{10+} ions into all lower charge states. By varying the trap potential, the mean kinetic energy of the ions can be altered in a known way, allowing low resolution study of the velocity dependence of the capture process. Figure 1 shows examples of decay curves obtained at varying neon densities for one trap potential.

These studies show that the cross-section for electron capture by Ne^{10+} over the range of 7 to

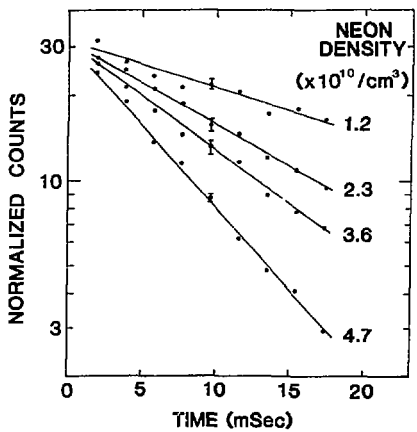

Fig. 1. Decay of trapped Ne^{10+} at a trap potential of 20.7 V for various neon densities. Each curve has been normalized to the same value at t = 0 (the trailing edge of the HILAC beam pulse). Error bars indicate statistical uncertainties of the data. (XBL 809-11944)

*This work was supported by the Director, Office of Energy Research, Office of Basic Energy Sciences, Chemical Sciences Division of the U. S. Department of Energy under Contract No. DE-AC03-76SF00098.

45 eV impact energies on neon atoms is a constant $(2.4 \pm 0.4) \times 10^{-15}$ cm^2. Future work will be extended to the other neon charge states and include collisions with atoms other than neon.

* * *

1. C. R. Vane, M. H. Prior and R. Marrus, Physical Review Letters, 46, 107 (1981).

2. PARITY VIOLATION IN ATOMIC THALLIUM†

E. Commins

The original parity violation experiment was successfully completed and the results were published. The experimental result obtained was a measure of the circular dichroism associated with the transition $6P_{1/2}$ to $7P_{1/2}$ in Tl. The amount of the circular dichroism measured was in good agreement with theoretical calculation based on the Weinberger-Salam model and represents a critical test of modern theory of the weak and magnetic interactions.

As an outgrowth of this work, measurements of the spontaneous emission decay rates of the following thallium excited states were carried out:

$$7^2P_{1/2},\ 7^2P_{3/2},\ 8^2P_{3/2},\ \text{and}\ 6^2D_{3/2}.$$

Knowledge of the lifetimes of these states is important for further refinement of theoretical understanding of parity violation in thallium. The experimental results obtained are in very good agreement with predictions made by Neuffer and Commins[1] and give added support for the validity of their calculations of parity violation.

A great deal of progress was made on the new thallium parity violation experiment, which employs linearly polarized light and an external magnetic field. This work is being carried out by P. Drell and E. Commins. During the past year the apparatus was completed, and includes some new and sophisticated electronic equipment and techniques for reducing background and eliminating its residual systematic effects. Detailed observations of signal strengths and lineshapes were carried out, which conform to our earlier expectations. At the time of writing, we are about ready to take real parity data with conditions of signal intensity and signal to background ratio vastly superior to those of the old experiment. This means that a much more precise measurement should be obtained during the coming year.

* * *

†Brief version of LBL-12165.

1. D. Neuffer and E. D. Commins, Phys. Rev. A16, 844 (1977).

3. CHARGE CHANGING CROSS-SECTION FOR Fe IONS

H. Gould and J. Alonso

Although electron capture and loss of fast ions colliding with atoms have been studied extensively for sixty years, there is almost no experimental information for charge-changing cross sections for very heavy ions at velocities above 10^9 cm/sec. These cross sections are of timely interest for design of heavy ion accelerators and for the use of fast heavy ions as igniters for Pellet fusion, where the electron loss cross sections for partially ionized Pb or U ions are critical in determining the conditions under which the ions can be accelerated, transported, and focused in the reaction vessel.[1]

In our experiment, incident ionization states are obtained by magnetically separating a beam of ions accelerated at the SuperHILAC. After collimation, the ions pass through a differentially pumped 24 cm long charge exchange chamber. The final ionization states are analyzed in a second electromagnet and detected by a 50 cm long position-sensitive gas-filled proportional counter. Data are collected by observing the relative number of ions striking the counter at locations corresponding to the different ionization states as a function of the pressure in the charge exchange chamber.

Figure 1 shows the capture and single electron

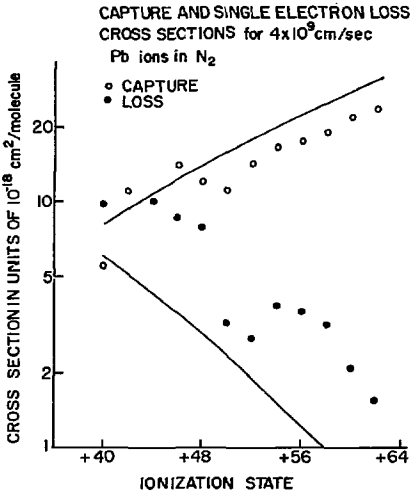

Fig. 1. (XBL 821-7738)

loss cross sections in nitrogen as a function of the ionization state for Fe ions at $V = 4 \times 10^9$ cm/sec. Semiclassical (SC) models have been used to calculate the cross sections for electron capture and loss by fast ions of high charge in light gasses. The results of two such calculations[2,3] multiplied by a factor of two to (imperfectly) account for molecular nitrogen are plotted in Fig. 1. The agreement with experiment for all of the data is on average better than a factor of two. The SC loss calculation works best at the lower ionization states where the independent particle approximation is more appropriate.

* * *

1. Proc. of the Heavy Ion Workshop held at Brookhaven Nat. Lab., October 17-21, 1977, Ed. L. W. Smith, Brookhaven Nat. Lab. Report BNL 50769 (1978). p. 41-58, p136; R. P. Hubbard and D. A. Tidman, Phys. Rev. Lett. 41, 866 (1978).

2. V. S. Nikolaev, Zh. Eksperim I Teor. Fiz. 33, 534 (1957) [Sov. Phys. JETP 6, 417 (1957)].

3. The loss cross section calculation is based upon: N. Bohr, Kgl. Danske Videnskab, Mat. Pys. Medd. 18, No. 8 (1948). N. Bohr and J. Lindhard, Kgl. Danske Videnskab. Selskab, Mat. Phys. Medd. 28, No. 7 (1954).

1981 PUBLICATIONS AND REPORTS

Refereed Journals

1. C. R. Vane, M. H. Prior and R. Marrus, Phys. Rev. Letters, 46, 107 (1981).

2. P. Bucksbaum, E. Commins and L. Hunter, Phys. Rev. Letters, 46, 640 (1981).

3. P. Bucksbaum, E. Commins and L. Hunter, Phys. Rev. D24, 1134 (1981).

B. Processes and Techniques*

1. Chemical Energy

a. Formation of Oxyacids of Sulfur from SO_2*

Robert E. Connick, Investigator

The present work was undertaken to increase the knowledge of the basic chemistry of sulfur dioxide and compounds formed from it in aqueous solutions. Such information is important because of the serious pollution caused by emission of sulfur dioxide in the stack gases of power plants that burn coal. Processes presently in use for controlling such emissions generally depend on absorption of the sulfur dioxide into aqueous solutions of low acidity and on subsequent chemical manipulation. These processes are expensive and unreliable, in part because their complex chemistry is not adequately understood.

The interconversions of sulfur species in solution are important to understand, both as regards mechanisms and rates of reaction. In solutions of S(IV) there are present in varying amounts, depending on the acidity, the species SO_2, HSO_3^-, SO_3H^-, $S_2O_5^{2-}$ and SO_3^{2-}, as well as some minor species present only at high HSO_3^- and SO_2 concentrations. The mechanism and rate at which these species exchange their oxygen with the oxygen of water has been the subject of two earlier investigations.[1,2] The results of these studies are not in good agreement. Use of the nuclear magnetic resonance of oxygen of mass 17 offered a new approach to the problem and gave the possibility of yielding considerable further insight into the mechanism of the exchange.

Experiments with more concentrated solutions of sodium bisulfite than used in earlier work have yielded a rate intermediate between that of the earlier investigators. Dilute solutions will be studied to make the results more comparable, although the NMR method is limited in this respect. The present results also indicate that oxygen exchange occurs rapidly between HSO_3^- and $S_2O_5^{2-}$ apart from the slower exchange with water, probably through the reactions

$$SO_2 + SO_3^{2-} \rightleftarrows S_2O_5^{2-}$$

$$HSO_3^- \rightleftarrows H^+ + SO_3^{2-}$$

This is a result that could only be obtained from the NMR study.

*This work was supported by the Director, Office of Energy Research, Office of Basic Energy Sciences, Chemical Sciences Division of the U. S. Department of Energy under Contract No. DE-AC03-76SF00098.

1981 PUBLICATIONS AND REPORTS

Refereed Journals

†1. I. Nagypál, F. Debreczeni, and R. E. Connick, "NMR Relaxation Studies in Solution of Transition Metal Complexes. I. Exchange Reactions in Aqueous Solution of Copper (II) - Glycine System," Inorg. Chim. Acta 48, 225 (1981).

2. M. Thompson and R. E. Connick, "Hydrolytic Polymerization of Chromium(III). I. Two Dimeric Species," Inorg. Chem. 20, 2279 (1981), LBL-11336.

LBL Reports

1. J. Finholt, M. E. Thompson, and R. E. Connick, "Hydrolytic Polymerization of Chromium(III). II. A Trimeric Species," LBL-12247.

‡2. R. E. Connick and T. G. Braga, "Kinetics of the Oxidation of Bisulfite Ion by Oxygen," LBL-12342 (pp. 118-138).

Invited Talks

‡1. T. G. Braga and R. E. Connick, "Kinetics of the Oxidation of Bisulfite Ion by Oxygen," Meeting of the American Chemical Society, Atlanta, Georgia, March 1981 (Based in part on LBL-12342).

* * *

1. M. Eigen, K. Kustin and G. Maass, Z. Physik. Chem. 30, 130 (1961).
2. R. H. Betts and R. H. Voss, Can. J. Chem. 48, 2035 (1970).

†Work supported by Hungarian National Academy of Sciences.
‡Work supported by the Assistant Secretary for Fossil Energy, Office of Coal Research, Advanced Environment Control Division of the U. S. Department of Energy under Contract No. DE-AC03-76SF00098, through the Morgantown Energy Technology Center, Morgantown, WV.

b. Catalytic Hydrogenation of CO: Catalysis on Well-Characterized Surfaces*

Gabor A. Somorjai, Investigator

and

Catalysis by Supported Metals*

Alexis T. Bell, Investigator

Introduction. The purpose of this program is to develop an understanding of the fundamental processes involved in catalytic conversion of carbon monoxide and hydrogen to gaseous and liquid fuels. Attention is focused on defining the factors that limit catalyst activity, selectivity, and resistance to poisoning, and the relationship between catalyst composition/structure and performance. To meet these objectives a variety of surface diagnostic techniques (LEED, AES, XPS, EELS, IRS, TPD) are used to characterize supported and unsupported catalysts before, during, and after reaction. The information thus obtained is combined with detailed studies of reaction kinetics to elucidate reaction mechanisms and the influence of modifications in catalyst composition and/or structure on the elementary reactions involved in carbon monoxide hydrogenation.

1. THE FORMATION OF OXYGEN CONTAINING ORGANIC MOLECULES BY THE HYDROGENATION OF CO USING LANTHANUM RHODATE CATALYSTS†

P. R. Watson and G. A. Somorjai

A $LaRhO_3$ catalyst was used for the hydrogenation of carbon monoxide at 6 atm pressure and between 225 and 375°C. The oxide is stable to reduction to the metal, but x-ray photoelectron and Auger spectroscopy shows that the active catalyst contains a reactive carbonaceous layer with most of the rhodium in the +1 oxidation state and with some metal present. The presence of large amounts of oxidized rhodium species correlates with the production of large quantities of oxygenated hydrocarbons up to 80+ wt%. The selectivity to different oxygenated products varies with temperature; yields of acetaldehyde and ethanol in excess of 50 wt% are found at temperatures around 300°C.

The activation energies for the formation of all the products except methanol are similar at 28 ± 2 kcal/mole, indicating that they are likely to form from a common CH_x precursor, obtained by dissociative adsorption of CO. Methanol is probably formed from molecular CO with an activation energy of 16 ± 3 kcal/mole. The changes in selectivity with temperature can be explained by competing carbonylation and hydrogenation reactions coupled with changing concentrations of molecular and dissociated CO on the surface.

* * *

†Brief version of LBL-12969.

2. EFFECTS OF DISPERSION ON THE ACTIVITY AND SELECTIVITY OF ALUMINA-SUPPORTED RUTHENIUM CATALYSTS FOR CARBON MONOXIDE HYDROGENATION†

C. S. Kellner and A. T. Bell

The influence of dispersion on the activity and selectivity of supported Group VIII metals for the synthesis of hydrocarbons via CO hydrogenation has been investigated to only a limited degree and is not fully understood. The present study was carried out to establish the manner in which dispersion affects Ru/Al_2O_3 catalysts. In addition to analysis of reaction products, in situ infrared spectroscopy was used to characterize the structure of chemisorbed CO as a function of metal dispersion. For dispersions below about 0.7, there is a moderate decrease in the specific activity for synthesis of methane and C_{2+} hydrocarbons with increasing dispersion, but neither the probability of chain growth nor the olefin to paraffin ratio of the products is greatly affected. Catalysts with dispersions above 0.7 exhibit a very rapid decline in the turnover frequencies for the synthesis of all products. This is accompanied by a slight decrease in the chain growth probability and a very dramatic decrease in the olefin to paraffin ratio. At all dispersion levels, the distribution of hydrocarbon products with number of carbon atoms is of a Schulz-Flory type. The decrease in specific activity with increasing dispersion, for dispersions below 0.7, is attributed to a decrease in the fraction of sites present on planar surfaces of the Ru microcrystallites. The much faster decrease in specific activity, observed for dispersions greater than 0.7, is believed to be due to changes in the electronic properties of the small crystallites with size or to interactions of the crystallites with the support. In situ infrared spectra suggest that only those Ru sites which adsorb one linearly-bound CO molecule per site are active for CO hydrogenation, whereas those adsorbing two CO molecules per site are not active under the conditions used in this study.

* * *

†Brief version of LBL-12429.

*This work was supported by the Director, Office of Energy Research, Office of Basic Energy Sciences, Chemical Sciences Division of the U. S. Department of Energy under Contract No. DE-AC03-76SF00098.

3. STUDIES OF CARBON MONOXIDE HYDROGENATION OVER RUTHENIUM USING TRANSIENT-RESPONSE TECHNIQUES

N. W. Cant and A. T. Bell

An apparatus has recently been completed for studying the dynamics of catalyzed reactions under transient conditions. The gas manifold associated with this apparatus is designed so that a step-function change in either reactant concentration or isotopic composition can be imposed on a catalyst disk contained within a microreactor/infrared cell. The response to such stimuli is followed by mass spectrometric analysis of the gases effluent from the reactor and by rapid acquisition of infrared spectra of adsorbed species using Fourier-transform infrared spectroscopy.

Transient response isotopic tracing was used together with in situ infrared spectroscopy to elucidate the dynamics of several elementary processes believed to occur during CO hydrogenation over ruthenium catalysts. Chemisorbed CO was observed to exchange very rapidly with gas phase CO and under reaction conditions the two species are in equilibrium. A similar conclusion was reached regarding the relationship between gas phase H_2 and adsorbed H-atoms. The dissociation of molecularly adsorbed CO to form atomic carbon and oxygen was found to require vacant surface sites and to be reversible. It was shown that while CO is the principal adsorbed species present on the catalyst surface under reaction conditions, the catalyst also maintains a significant inventory of non-oxygenated carbon but no chemisorbed oxygen. It was also found that the rate at which non-oxygenated carbon undergoes hydrogenation is faster than the rate at which adsorbed CO is hydrogenated. This observation supports the hypothesis that the non-oxygenated carbon is an intermediate in CO hydrogenation.

* * *

†Brief version of LBL-12598.

4. REACTIVE SCAVENGING OF SURFACE SPECIES FORMED DURING HYDROGENATION OF CARBON MONOXIDE OVER RUTHENIUM†

J. A. Baker and A. T. Bell

In earlier studies it was demonstrated that CH_2 and/or CH_3 species produced during CO hydrogenation over Ru can be detected by reactive scavenging using olefinic reagents as scavengers. The present study was designed to investigate a broader range of scavenging reagents and to provide more definitive evidence for the presence of methylene and alkyl groups adsorbed on the catalyst surface.

It was established that cyclohexene, benzene, cyclopentene, and cis-2-butene, added in low concentration to a mixture of CO and H_2, can be used to scavenge hydrocarbon species produced on the surface of Ru during CO hydrogenation. The presence of CH_2 groups is strongly supported by the formation of norcarane and dimethylcyclopropane from cyclohexene and cis-2-butene, respectively. Evidence was also obtained for the presence of methyl and higher molecular weight alkyl groups. The principal support for this conclusion is the observation of alkyl derivatives of cyclohexene and benzene, when cyclohexene or benzene, respectively, was used as a scavenger. Finally, it was observed that each of the scavengers causes a reduction in the probability of hydrocarbon chain growth, α, and that the degree of this effect correlates with the conversion of the scavenger to products containing one or more carbon atoms than the scavenger. From these observations, it was concluded that the species removed by the scavenger participate in the process of hydrocarbon chain growth.

* * *

†Brief version of LBL-13773.

5. WORK IN PROGRESS

a. Electron Spectroscopy Studies of Hydrocarbon Fragments on Rhodium

J. Crowell and G. A. Somorjai

High resolution electron loss spectroscopy (HREELS) detects the vibrational modes of adsorbed molecules and can be used to monitor the organic fragments that are possible reaction intermediates during the CO/H_2 reaction. An apparatus was constructed and completed that can be used to carry out reaction rate studies at high pressures (atmospheres) and to investigate the surface monolayer by HREELS before and after the catalytic reaction. Preliminary studies detected the presence of CH fragments on the Rh (111) crystal face after a CO/H_2 reaction that readily exchange deuterium without change of the adsorbate fragment geometry.

b. Temperature-Programmed Desorption from Supported-Metal Catalysts

A. A. Chin, J. Rieck, and A. T. Bell

Temperature-programmed desorption (TPD) can be used to determine the parameters pertaining to the desorption of molecules adsorbed on a metal surface. An apparatus has been developed for performing TPD investigations using supported-metal catalysts. Desorption can be carried out either in a vacuum chamber or in a flow of ultra-pure helium. The desorbing gases are analyzed by a mass spectrometer which is connected to a data-acquisition system. TPD spectra of up to ten components can be taken simultaneously and stored on a magnetic disk.

Extensive studies of H_2 chemisorption on a Rh/SiO_2 catalyst have been performed. The TPD spectra show two clearly defined features, both of which follow second order kinetics. The activation energy associated with the first peak is 14 kcal/mole and agrees closely with the values reported for H_2 desorption from Rh single crystals. The second peak is characterized by an activation energy of 22 kcal/mole.

1981 PUBLICATIONS AND REPORTS

Refereed Journals

1. D. G. Castner and G. A. Somorjai, "LEED, AES, and Thermal Desorption Studies of the Oxidation of the Rh(111) Surface," Appl. of Surf. Sci. 6, 29 (1980); LBL-9288.

2. D. G. Castner, R. L. Blackadar, and G. A. Somorjai, "CO Hydrogenation over Clean and Oxidized Rhodium Foil and Single Crystal Catalysts. Correlations of Catalyst Activity, Selectivity, and Surface Composition," J. Catal. 66, 257 (1980); LBL-10018.

3. L. H. Dubois, P. K. Hansma, and G. A. Somorjai, "Evidence for an Oxygen Intermediate in the Catalytic Reduction of NO by CO on Rhodium Surface," J. Catal. 65, 318 (1980); LBL-10061.

4. L. H. Dubois, P. K. Hansma, and G. A. Somorjai, "The Application of HREELS to the Study of Model Supported Metal Catalysts," Appl. of Surf. Sci. 6, 173 (1980); LBL-10733.

5. D. G. Castner, L. H. Dubois, B. A. Sexton, and G. A. Somorjai, "Evidence for CO Dissociation on Rhodium Surfaces," Surf. Sci. 103, L-134 (1981); LBL-11205.

6. G. A. Somorjai, "The Catalytic Hydrogenation of CO. The Formation of C_1 Hydrocarbons", Catal. Rev.-Sci. Eng. 23, 189 (1981); LBL-11354.

7. K. I. Tanner and A. T. Bell, "Conversion of Solvent Refined Coal to Liquid Products in the Presence of Lewis Acids," Fuel, 60, 52 (1981).

8. C. S. Kellner and A. T. Bell, "Evidence for H_2/D_2 Isotope Effects on Fischer-Tropsch Synthesis over Supported Ruthenium Catalysts," J. Catal. 67, 175 (1981); LBL-10786.

9. A. T. Bell, "Catalytic Synthesis of Hydrocarbons over Group VIII Metals. A Discussion of the Reaction Mechanism," Catal. Rev.-Sci. Eng., 23, 203 (1981); LBL-11339.

10. "Effects of Metal-Support Interactions on the Synthesis of Methanol Over Palladium," J. Catal. 70, 287 (1981); LBL-11603.

11. C. S. Kellner and A. T. Bell, "The Kinetics and Mechanism of Carbon Monoxide Hydrogenation Over Alumina-Supported Ruthenium," J. Catal. 70, 418 (1981); LBL-12133.

‡12. "Design and Construction of a Reactor for In Situ Infrared Studies of Catalytic Reactions," J. Catal. 71, 216 (1981); LBL-12234.

13. C. S. Kellner and A. T. Bell, "Synthesis of Oxygenated Products from Carbon Monoxide and Hydrogen Over Silica-Supported Ruthenium Catalyst," J. Catal. 71, 288 (1981); LBL-12178.

14. C. S. Kellner and A. T. Bell, "Infrared Studies of Carbon Monoxide Hydrogenation Over Alumina-Supported Ruthenium," J. Catal. 71, 296 (1981); LBL-12132.

LBL-Reports

1. P. R. Watson and G. A. Somorjai, "The Hydrogenation of CO over Rhodium Oxide Surfaces," LBL-12750.

2. P. R. Watson and G. A. Somorjai, "The Formation of Oxygenated Chemicals from Synthesis Gas Using a Lanthanum Rhodate Catalyst," LBL-12969.

3. P. R. Watson and G. A. Somorjai, "The Interaction of CO, CO_2, and O_2 with Rhodium Oxide ($Rh_2O_3 \cdot 5H_2O$): Its Reduction and Catalytic Stability," LBL-13524.

4. C. S. Kellner, "The Mechanism and Kinetics of Fischer-Tropsch Synthesis Over Supported Ruthenium Catalysts," (Ph.D. thesis), LBL-12278.

5. C. S. Kellner and A. T. Bell, "Effects of Dispersion on the Activity and Selectivity of Alumina-Supported Ruthenium Catalysts for Carbon Monoxide Hydrogenation," LBL-12429.

‡6. N. W. Cant and A. T. Bell, "Studies of Carbon Monoxide Hydrogenation Over Ruthenium Using Transient Response Techniques," LBL-12598.

7. S. S. Salim and A. T. Bell, "Effects of Lewis Acid Catalysts on the Hydrogenation and Cracking of Three-Ring Aromatic and Hydroaromatic Structures Related to Coal," LBL-13577.

8. H. Arakawa and A. T. Bell, "Effects of Potassium Promotion on the Activity and Selectivity of Iron Fischer-Tropsch Catalysts," LBL-13578.

9. J. A. Baker and A. T. Bell, "Reactive Scavenging of Surface Species Formed During Hydrogenation of Carbon Monoxide Over Ruthenium," LBL-13773.

* * *

‡Supported in part by the National Science Foundation.

Invited Talks

1. G. A. Somorjai, "Catalyzed Reactions of C and CO with Water Vapor and Hydrogen," DOE Conference on Catalysis, National Bureau of Standards, Washington, DC, May 1981.

2. G. A. Somorjai, "New Techniques and Recent Trends in Surface Characterization," 9th ICAS/XXII CSI Post-Conference Symposium, Osaka, Japan, September 1981.

3. G. A. Somorjai, "Surface Monolayer Analysis by Electron Scattering and Emission," Lake Biwa, Japan, September 1981.

4. G. A. Somorjai, "The Chemistry of Monolayers on Surfaces: Structure and Bonding," Dreyfus Lectures, University of Colorado, Boulder, CO, September 1981.

5. G. A. Somorjai, "Surface Science of Heterogeneous Catalysis," Department of Chemistry, University of California, Davis, CA, November 1981.

6. A. T. Bell, "Hydrocarbon Synthesis Over Catalysts Prepared by Supporting Ru-Cluster Complexes on Alumina," Eastman Kodak Co., Rochester, NY, January 1981.

7. A. T. Bell, "Applications of Fourier Transform Infrared Spectroscopy to the Study of Catalytic Reactions," 181st National ACS Meeting, Atlanta, GA, March 1981.

8. A. T. Bell, "The Mechanism and Kinetics of Fischer-Tropsch Synthesis Over Ruthenium," New England Catalysis Society, Worcester, MA, April 1981.

9. A. T. Bell, "Studies of Catalyzed Reactions Through the Use of Transient Response Techniques," Department of Chemical Engineering, M.I.T., Cambridge, MA, May 1981.

10. A. T. Bell, "Hydrocarbon Synthesis Over Catalysts Prepared by Supporting Ru-Cluster Complexes on Alumina," Department of Chemistry, University of Wisconsin, Milwaukee, WI, April 1981.

11. A. T. Bell, "Studies of Catalyzed Reactions Through the Use of Transient Response Techniques," Department of Chemistry, University of Wisconsin, Milwaukee, WI, April 1981.

12. A. T. Bell, "Effects of Dispersion and Metal-Support Interactions on CO Hydrogenation Over Group VIII Metals," Dow Chemical Co., Freeport, TX, April 1981.

13. A. T. Bell, "Hydrocarbon Synthesis Over Catalysts Prepared by Supporting Ru-Cluster Complexes on Alumina," Department of Chemical Engineering, Rice University, Houston, TX, April 1981.

14. A. T. Bell, "Applications of Fourier Transform Infrared Spectroscopy to In Situ Catalyst Surface Studies," International Conference on Fourier Transform Infrared Spectroscopy, Columbia, SC, June 1981.

15. A. T. Bell, "Applications of Transient Response Techniques to the Study of Fischer-Tropsch Synthesis and Nitric Oxide Reduction," Gordon Conference on Catalysis, New London, NH, June 1981.

16. A. T. Bell, "Propagation of CO/H_2 Reactions," Fuel Science Gordon Conference, Plymouth, NH, July 1981.

17. A. T. Bell, "The Influence of Dispersion and Metal-Support Interactions on CO Hydrogenation," Centrum voor Oppervlaktescheikunde en Colloidale Scheikunde, Katholieke Universiteit Leuven, Leuven, Belgium, August 1981.

18. A. T. Bell, "Applications of Transient Response Techniques to the Study of Catalysis," Laboratorium voor Petrochemische Technick, Rijksuniversiteit, Ghent, Belgium, August 1981.

19. A. T. Bell, "The Mechanism and Kinetics of Fischer-Tropsch Synthesis over Ruthenium," Unité de Recherches Catalyse Hétérogène, Université Libre de Bruxelles, Brussels, Belgium, September 1981.

20. A. T. Bell, "Participation of Hydrogen in the Hydrogenolysis and Hydrogenation of Coal-Related Model Compounds Catalyzed by Zinc Halides," International Conference on Coal Science, Düsseldorf, Germany, September 1981.

21. A. T. Bell, "Mechanism and Kinetics of Fischer-Tropsch Chemistry on Ruthenium," Anglo-American Seminar on the Chemistry of the Reactions of Carbon Monoxide with Hydrogen, Cambridge University, Cambridge, United Kingdom, September 1981.

c. Organometallic Chemistry of Coal Conversion*

K. Peter C. Vollhardt, Investigator

Introduction. The purpose of this work is to develop organic and organo-metallic methodology concerned with furthering the understanding of basic processes in coal conversion. This encompasses studies on the mechanism of the Fischer-Tropsch and other C-C bond forming reactions involving small molecules, the synthesis of potential analogs of surface intermediates in the reduction of carbon monoxide, the substitution of nitrogen and sulfur moieties in coal and coal-derived liquids by other structural units, and the construction of ligands activating potential catalysts.

1. BISCARBYNE CLUSTERS AS HOMOGENEOUS ANALOGS OF FISCHER-TROPSCH INTERMEDIATES ON SURFACES†

David E. Van Horn and K. Peter C. Vollhardt

The synthesis and investigation of homogeneous organometallic species with structural features mimicking those thought to occur on important catalytic surfaces should lead to a better understanding of the factors responsible for good catalytic action. Carbyne metal complexes have recently commanded increasing attention as models for carbyne intermediates in heterogeneous catalysis, particularly the Fischer-Tropsch and related reactions, and alkyne metathesis. The principal investigator has reported a facile and direct entry into $[\mu_3\eta^1 - CR^1][\mu_3\eta^1 - CR^2][(\eta^5 - C_5H_5)Co]_3$ biscarbyne clusters 1 by the reaction of $\eta^5 - C_5H_5Co(CO)_2$ with alkynes. The novel chemistry of these systems is reported.

As shown in Fig. 1, reaction of 1a with iodine gave 1b (70%) and 1c (11%). Exposure of 1b to $AgBF_4$ generated a precipitate which dissolved in CH_3OH to give 1f quantitatively. This species may be regarded as a model for reduced CO on a trinuclear cobalt core.

Surprisingly oxidation of 1d in air (75°C, 19d) leaves the metal cluster untouched but attacks the α-positions in the chain to 1g (40%) and 1h (30%), presumably by a free radical mechanism. Compound 1a undergoes rapid H-D exchange at the apical position (CF_3CO_2D), through the likely intermediacy of a protonated carbene-carbyne cluster. Interestingly exposure of 1d to CF_3SO_3H gives 2, which is edge and not apically protonated, suggesting the latter to be a reactive intermediate in the above exchange.

1 2

a; $R_1 = R_2 = H$
b; $R_1 = I$, $R_2 = H$
c; $R_1 = R_2 = I$
d; $R_1 = R_2 = n\text{-}C_4H_9$
e; $R_1 = R_2 = C_6H_5$
f; $R_1 = CH_3O$, $R_2 = H$
g; $R_1 = CH_3CH_2CH_2\overset{O}{\overset{\|}{C}}$, $R_2 = n\text{-}C_4H_9$
h; $R_1 = CH_3CH_2CH_2CHOH$, $R_2 = n\text{-}C_4H_9$

Fig. 1. (X8L 823-8142)

* * *

†Brief version of J. Chem. Soc. Chem. Commun. 133 (1982) LBL-13759.

2. HYDROCARBON FORMATION ON POLYMER-SUPPORTED η^5-CYCLOPENTADIENYL COBALT†

Linda S. Benner, Patrick Perkins, K. Peter C. Vollhardt, and Timothy W. Weidman

The development of novel catalytic species capable of reducing CO to methane and higher hydrocarbons is of prime importance in an effort to derive liquid fuels from coal by Fischer-Tropsch technology.

Work has been completed on the scope and limitations of a polystyrene supported cobalt based Fischer-Tropsch catalyst. The system appears mononuclear and homogeneous (albeit immobilized), also active in hydroformylation, and unique in its stability, probably a consequence of site-site isolation. A number of homogeneous model systems, while showing hydrogen activation, were inactive in CO reduction.

Further work in this area is directed at novel ligand design aimed at generating activated metal cores.

* * *

†Brief version of A.C.S. Symp. Ser., 152, 165 (1981); LBL-11710.

*This work was supported by the Director, Office of Energy Research, Office of Basic Energy Sciences, Chemical Sciences Division of the U. S. Department of Energy under Contract No. DE-AC03-76SF00098.

3. THE EXTRUSION OF SULFUR MONOXIDE FROM SMALL MOLECULES†

William G. L. Aalbersberg and K. Peter C. Vollhardt

Sulfur monoxide is probably generated in processes designed to oxidatively remove sulfur from coal derived liquids. It also appears to have a role in the production of photochemical smog. One of the key steps in the production of sulfuric acid aerosols is the oxidation of sulfur dioxide to sulfur trioxide. The reaction of two molecules of sulfur dioxide to sulfur trioxide and sulfur monoxide has one of the highest rate constants (5400 $ppm^{-1}min^{-1}$) of the possible atmospheric sulfur dioxide oxidation reactions.

An organic source of SO is thiirane oxide 1, which furnishes ethylene

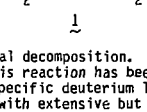

1

and SO on thermal decomposition. The stereochemistry of this reaction has been investigated using a stereospecific deuterium label, and was found to occur with extensive but not complete retention. This suggests that ground state SO is formed by intersystem crossing through intermediate biradicals. This notion is corroborated by recently completed trapping experiments.

* * *

†Brief version of Isr. J. Chem., 21, 145 (1981); LBL-12227.

4. THE MECHANISM OF THE REPPE CYCLOOCTATETRAENE SYNTHESIS FROM ETHYNE†

Robert E. Colborn and K. Peter C. Vollhardt

A presumed heterogeneous Ni(0) catalyst converts ethyne to cyclooctatetraene by a little understood mechanism. Since this is a fundamental and unique organometallic transformation a labeling experiment was undertaken to elucidate some of its mechanistic features.

Singly ^{13}C-labeled ethyne may be cyclized to tetralabeled cyclooctatetraene under N_2 pressure (50-60 psig) by using nickel catalysts under conditions similar to those reported. The resulting cyclopolyolefin is degraded to a C_4-fragment incorporated in dimethylphthalate according to a literature procedure. The latter is analyzed through g.c. mass spectrometry. The peak ratios of the most intense $C_9H_7O_3$ peaks containing various amounts of label rule out cyclobutadienes and benzenes as intermediates, and metathesis mechanisms as part of the nickel catalyzed cyclic tetramerization of ethyne. The label distribution is, however, consistent with a concerted or stepwise coupling mechanism of the four alkyne units.

* * *

†Brief version of J. Am. Chem. Soc., 103, 6259 (1981); LBL-13235. Supported in part by NSF.

5. WORK IN PROGRESS

The mechanism of a novel reaction in which a metal bound thiophene dioxide extrudes SO_2 is being investigated using stereochemical labels.

A biscarbyne double decker shift has been uncovered in which sp-hybridized C-C bonds are simultaneously broken and formed, possibly constituting a model for C-C bond formation in the Fischer-Tropsch reaction. Crossover labeling and kinetic investigations are in progress.

Novel dinuclear cobalt and ruthenium complexes have been synthesized incorporating the fulvalene ligand. Their catalytic potential is under study.

1981 PUBLICATIONS AND REPORTS

Refereed Journals

†1. C. Chang, C. G. Francisco, T. R. Gadek, J. A. King, Jr., E. D. Sternberg, and K. P. C. Vollhardt, "Transition Metal Mediated Carbon-Carbon Bond Formations. A General, Partially Chemo-, Regio-, and Stereospecific Synthesis of Annelated Cyclohexadienes From Acyclic Starting Materials," in B. M. Trost and C. R. Hutchinson, eds., Organic Synthesis Today and Tomorrow, (IUPAC), Pergamon Press, New York, NY (1981), p. 71.

‡2. G. Ville, K. P. C. Vollhardt, and M. J. Winter, "On the Reversibility of η^4-Cyclobutadiene Metal Formation From Complexed Alkynes: Unimolecular Isomerization of Labelled Racemic and Enantiomerically Enriched η^5-Cyclopentadienyl-η^4-cyclobutadiene Cobalt Complexes," J. Am. Chem. Soc., 103, 5267 (1981); LBL-12943.

3. J. M. Huggins, J. A. King, Jr., K. P. C. Vollhardt, and M. J. Winter, "Separation of Diastereomers, Structural Isomers, and Homologs of η^5-Cyclopentadienyl Cobalt and Dinuclear Molybdenum Complexes by Reverse Phase High Performance Liquid Chromatography Using Deoxygenated Solvents," J. Organomet. Chem., 208, 73 (1981); LBL-11801.

4. L. S. Benner, P. Perkins, and K. P. C. Vollhardt, "Hydrocarbon Formation on Polymer-Supported η^5-Cyclopentadienyl Cobalt," A.C.S. Symp. Ser., 152, 165 (1981); LBL-11710.

†5. C. Chang, J. A. King, Jr., K. P. C. Vollhardt, "Intermolecular Cobalt Mediated [2+2+2] Cycloadditions: Regiospecific One Step Construction of Bicyclic Dienes from α,ω-Enynes and Alkynes," J. Chem. Soc., Chem. Commun., 53 (1981).

6. W. G. L. Aalbersberg and K. P. C. Vollhardt, "The Nature of Sulfur Monoxide From Thiirane Oxide: A Stereochemical Test," Isr. J. Chem., 21, 145 (1981); LBL-12227.

7. Y.-H. Lai, W. Tam, and K. P. C. Vollhardt, "Transition Metal Activation of π-Complexed Benzene: Double Nucleophilic Addition," J. Organometal. Chem., 216, 97 (1981); LBL-12459.

‡8. E. R. F. Gesing and K. P. C. Vollhardt, "The Variety of Compounds From The Interaction of 1,5-Diynes with η^5-Cyclopentadienyl Cobalt: 1,6-Bis(trimethylsilyl)-1,5-hexadiyne, a Complete Product Analysis," J. Organometal. Chem., 217, 105 (1981).

†9. Thomas R. Gadek and K. P. C. Vollhardt, "Cobalt Mediated [2+2+2]-Cycloadditions: Stereospecific Intramolecular Co-Cyclization of Internal Di- and Trisubstituted Double Bonds With Terminal Alkynes to Tricyclic Dienes Bearing Angular Methyl Groups," Angew. Chem., 93, 801 (1981); Angew. Chem., Int. Ed. Engl., 20, 802 (1981).

10. L. S. Benner, Y.-H. Lai, and K. P. C. Vollhardt," On the Purported Fischer-Tropsch Alkylation of Benzene: The Reaction of Benzene With Aluminum Trichloride Revisited," J. Am. Chem. Soc., 103, 3609 (1981); LBL-12662.

‡11. R. E. Colborn and K. P. C. Vollhardt, "On the Mechanism of the Reppe Cyclooctatetraene Synthesis From Ethyne: A Labeling Experiment," J. Am. Chem. Soc., 103, 6259 (1981); LBL-13235.

LBL Reports

1. D. E. Van Horn and K. P. C. Vollhardt, "Some Remarkable Reactions of the Biscarbyne Clusters $[\mu_3\eta^1 - CR^1][\mu_3\eta^1 - CR^2][(\eta^5 - C_5H_5)Co]_3$ with Electrophiles," LBL-13759.

Invited Talks

1-4. K. P. C. Vollhardt, "Transition Metal Mediated Carbon-Carbon Bond Making and Breaking Reactions," University of Alberta, University of British Columbia, Victoria University, Simon Fraser University, Canada, January 1981.

5-6. K. P. C. Vollhardt, "The Transition Metal Mediated Conversion of Trimethylsilylalkynes to Complex Organic Molecules," Plenary Lecture, 181st ACS National Meeting, Symposium on Silicon in Organic Synthesis, Atlanta, GA, March 29-April 3, 1981; University of Missouri, St. Louis, November 1981.

7-11. K. P. C. Vollhardt, "Transition Metal Mediated Carbon-Carbon Bond Formations," Plenary Lecture, 10th Conference on Coordination and Metal-Organic Chemistry, Queenstown, New Zealand, May 10-15, 1981; University of Queensland; Australian National University; University of Adelaide; Monash University, Australia, May 1981.

12. K. P. C. Vollhardt, "Remarkable Transformations in the Coordination Sphere of Cobalt," Australian National University, May 1981.

13. K. P. C. Vollhardt, "Transition Metal Catalyzed Routes to Natural Products," Plenary Lecture, Symposium on Synthesis in Organic Chemistry, Oxford, England, July 21-23, 1981.

14-16. K. P. C. Vollhardt, "Transition Metal Mediated Carbon-Carbon and Carbon-Heteroatom Bond Formations, Shell Company, Houston, TX, June 1981; W. R. Grace & Co., Columbia, Maryland, October 1981; Plenary Lecture, 11th ACS Northeast Regional Meeting, Rochester, NY, October 1981.

17-18. K. P. C. Vollhardt, "Transition Metal Mediated [2+2+2] Cycloadditions: A Better Version of the Diels-Alder Reaction?" University of Southern California, Los Angeles, September 1981; University of Arkansas, Fayetteville, October 1981.

19. K. P. C. Vollhardt, "Mechanistic Studies in Transition Metal Mediated Bond Breaking and Making Reactions," University of Missouri, St. Louis, November 1981.

* * *

†Supported in part by NIH.
‡Supported in part by NSF.

d. Synthetic and Physical Chemistry*

William L. Jolly, Investigator

Introduction. The purpose of this project is to use photoelectron spectroscopy to determine the nature of the bonding in significant inorganic and organometallic compounds. By measuring core electron binding energies of appropriate transition metal compounds, it is possible to study the interaction of metal d electrons with various ligands and to identify various modes of ligand-metal bonding which have analogs in the intermediates of catalyzed organic reactions. Core binding energies can also be used, in conjunction with valence shell ionization potentials, to quantify the bonding or antibonding character of molecular orbitals.

1. THE STUDY OF MOLECULAR ELECTRON DISTRIBUTION BY X-RAY PHOTOELECTRON SPECTROSCOPY†

William L. Jolly and Albert A. Bakke

The following "potential equation" has commonly been used to correlate core binding energies with atomic charges:

$$\Delta E_B(A) = \langle \tfrac{1}{r} \rangle \, \Delta Q_A + \sum_{B \neq A} (Q_B/R_{AB}) - \Delta E_R(A),$$

where

$\Delta E_B(A)$ is the change in binding energy,
r is the effective radius of the atom,
Q_A and Q_B are atomic charges,
R_{AB} is the distance between atoms A and B, and
$\Delta E_R(A)$ is the relaxation energy.

The atomic charges that one can derive from binding energy data by simultaneous solution of a suitable set of such equations have qualitative significance, but the derived atomic charges generally cannot be relied upon to account quantitatively for other physical properties that are sensitive functions of valence electron distribution. It is well known, for example, that a reasonable assignment of point-charge atoms cannot account for the dipole moments of molecules with lone pair electrons. It is also known that bond formation involves a build-up of electron density between atoms, a feature lacking in ordinary point-charge models of molecules.

Therefore, we have chosen to use molecular models involving point charge atoms in which fractional negative charges are placed at points between the bonded atoms and at points corresponding to lone pair electron density. Using this model and core binding energies and dipole moments for 17 molecules (including HF, HCl, and all the chloro and fluoro derivatives of methane), we have established atomic charges, effective lone-pair charges, and effective bonding-region charges for these molecules. These parameters allow us to reproduce both the binding energy and dipole moment values with a standard deviation of 0.28 eV (or debye). The model can be readily extended to many other systems and can help in the prediction of binding energies and dipole moments.

* * *

†Brief version of chapter in "Electron Distributions and the Chemical Bond," M. B. Hall and P. Coppens, Eds., Plenum, in press; LBL-13000.

2. THE USE OF CORE ELECTRON BINDING ENERGIES FOR THE QUANTIFICATION OF THE BONDING AND ANTIBONDING CHARACTER OF MOLECULAR ORBITALS†

William L. Jolly

The usual interpretation of a valence-shell photoelectron spectrum consists of little more than the assignment of the various peaks to molecular orbitals (MOs). Knowledge of the ionization potentials corresponding to particular MOs is of limited value to a chemist because the absolute magnitudes of the ionization potentials are not directly related to the bonding or antibonding characters of the MOs.

To ascertain the character of an MO it is necessary to compare its ionization potential with that of a hypothetical nonbonding localized atomic orbital that constitutes a significant part of the MO. We refer to the latter ionization potential as a "localized-orbital ionization potential" (LOIP). We propose that differences in LOIP between compounds are proportional to the corresponding differences in core electron binding energy and that therefore core electron binding energies can be used for the comparison of valence ionization potentials.

We have shown how core and valence ionization potentials for a variety of compounds may be used to evaluate quantitatively the bonding or antibonding character of MOs. The results are in good accord with modern views of the bonding in the compounds. The method should aid photoelectron spectroscopists in the assignment of spectra.

* * *

†Brief version of J. Phys. Chem., 85, 3792 (1981); LBL-11396. This work was partly supported by the NSF, Grant CHE-7926097.

*This work was supported by the Director, Office of Energy Research, Office of Basic Energy Sciences, Chemical Sciences Division of the U. S. Department of Energy under Contract No. DE-AC03-76SF00098.

3. X-RAY PHOTOELECTRON SPECTROSCOPIC STUDY OF ORGANOMETALLIC NITROSYL COMPOUNDS OF CHROMIUM, MOLYBDENUM, AND TUNGSTEN†

H. W. Chen, W. L. Jolly, S. F. Xiang, and P. Legzdins

Previous XPS studies of transition metal nitrosyls and carbonyls have established that NO groups are stronger π acceptors than CO groups and that the ligand core binding energies are linearly related to the corresponding N-O or C-O stretching force constants. In this study we have used XPS to characterize the bonding in families of organometallic nitrosyl complexes.

In the series of compounds $CpM(ND)_2Cl$ (M = Cr, Mo, W), on going from the chromium compound to the tungsten compound the oxygen and nitrogen binding energies markedly decrease and the chlorine binding energy increases. On going from the chromium compound to the tungsten compound, π-acceptor bonding by the NO groups increases, and for compensation of the increased metal atom charge, σ-donor bonding by the chlorine atoms increases. These and other data also show that, in such series of compounds, the oxygen atom of the NO group receives most of the electron density when back-bonding increases.

It appears that, on descending a transition metal family, σ-donation by the NO group increases, and the resultant improved $d\pi$-π^* overlap causes an i[illegible]ease in back-bonding. The stronger σ bonding [illegible]tween the nitrogen and metal atom causes a shift of electron density from nitrogen to metal that compensates for the increase in π^* electron density. Thus, the nitrogen atom charge is almost unchanged.

* * *

†Brief version of Inorg. Chem. 20, 1779 (1981); LBL-11444.

4. AN XPS STUDY OF THIOCARBONYL AND THIONITROSYL COMPLEXES†

H. W. Chen, W. L. Jolly, S. F. Xiang, I. S. Butler, and J. Sedman

To obtain information about the valence electron distribution in transition-metal thiocarbonyl and the corresponding non-thio complexes, we have obtained the gas-phase core electron binding energies of four thiocarbonyl complexes, one thionitrosyl complex, and the corresponding non-thio complexes.

The most significant feature of the data is the approximate constancy of the binding energies of the metal atom and the carbonyl groups upon replacing one of the CO groups by a CS group or replacing an NO group by an NS group. That is, the replacements have little effect on the bonding of the other ligands.

To account for the fact that replacement of CO by CS, or of NO by NS, has little effect on the electron distribution of the remainder of the complex, we conclude that increased back-bonding compensates for the greater donor characters of the CS and NS groups. Hence, the CS and NS groups are better π-acceptors than CO and NO groups, respectively.

* * *

†Brief version of J. Electron Spectrosc. Relat. Phenom. 24, 121 (1981); LBL-11443.

5. WORK IN PROGRESS

XPS spectra of various compounds of the type $RCCo_3(CO)_9$ are being studied to determine the effect of changes in the R group on the cobalt cluster. These molecules are analogs of organic fragments chemisorbed on a metal surface. Members of the tetrahedral series $Co_4(CD)_{12}$ - C_4H_4 and of the 3-membered ring series $Fe_3(CO)_{12}$ - C_3H_6 are being investigated to test the "isolobal" formalism of transition metal cluster compounds.

The LOIP concept, in which core binding energies are used to interpret valence ionization potentials, is being extended to organometallic compounds.

The inlet system of the XPS spectrometer is being modified for the study of short-liveo gaseous species.

1981 PUBLICATIONS AND REPORTS

Refereed Journals

1. H. W. Chen, W. L. Jolly, S. F. Xiang, and P. Legzdins, "X-ray Photoelectron Spectroscopic Study of Organometallic Nitrosyl Compounds of Chromium, Molybdenum, and Tungsten," Inorg. Chem., 20, 1779 (1981); LBL-11444.

2. H. W. Chen, W. L. Jolly, S. F. Xiang, I. S. Butler, and J. Sedman, "An X-ray Photoelectron Spectroscopic Study of Transition-Metal Thiocarbonyl and Thionitrosyl Complexes," J. Electron Spectrosc. Relat. Phenom., 24, 121 (1981); LBL-11443.

3. W. L. Jolly, "Use of Core Electron Binding Energies for the Comparison of Valence-Shell Ionization Potentials and the Quantification of the Bonding and Antibonding Character of Molecular Orbitals," J. Phys. Chem., 85, 3792 (1981); LBL-11396.

LBL Reports

1. A. J. Ricco, A. A. Bakke, and W. L. Jolly, "An XPS Study of the σ- and π-Allyl Groups," June 1980, LBL-12912.

2. S. F. Xiang, A. A. Bakke, H. W. Chen, J. L. Hoskins, T. H. Lee, D. Seyferth, H. P. Withers and W. L. Jolly, "An XPS Study of the Bonding in Alkylidynetricobalt Nonacarbonyl Complexes and Related Compounds," Sept. 1981, LBL-13320.

Other Publications

1. W. L. Jolly and A. A. Bakke, "The Study of Molecular Electron Distribution by X-ray Photoelectron Spectroscopy," chapter in "Electron Distributions and the Chemical Bond," M. B. Hall and P. Coppens, Eds., Plenum, in press, LBL-13000.

2. W. L. Jolly, Book Review: J. K. Burdett, "Theoretical Models of Inorganic Stereochemistry," Nature, 293, 244 (1981).

Invited Talks

1. W. L. Jolly, "The Study of Molecular Electron Distribution by X-ray Photoelectron Spectroscopy," Symposium on Electron Distributions and the Chemical Bond, National A.C.S. Meeting, Atlanta, Georgia, March 1981.

2. W. L. Jolly, "Applications of XPS in Inorganic Chemistry," Symposium on Electron Spectroscopy at Northwest Regional Meeting of A.C.S., Montana State University, Bozeman, June 1981.

e. Chemistry and Morphology of Coal Liquefaction*

Heinz Heinemann, Investigator, with Alexis T. Bell, R. G. Bergman, James W. Evans, Richard H. Fish, E. E. Petersen, A. V. Levy, G. A. Somorjai, and K. Peter C. Vollhardt, Investigators

[See Fossil Energy Section]

f. Electrochemical Systems*

John Newman, Investigator

Introduction. This program includes investigation of electrochemical transport, analysis of mass-transfer rates and current distribution, and design of practical electrochemical systems. Coupled kinetic, mass transfer, and fluid flow phenomena are investigated in semiconductor electrode systems, with emphasis on the optimization of configurational and operating parameters of liquid-junction photovoltaic cells.

1. MATHEMATICAL MODELING OF THE LIQUID-JUNCTION PHOTOVOLTAIC CELL[†]

Mark E. Orazem and John Newman

The liquid-junction photovoltaic cell is an electrochemical system with one or two semiconducting electrodes. This system has undergone intense study since the early 1970s as a means of converting solar energy to chemical or electrical energy. A mathematical model of the liquid-junction photovoltaic cell has been developed that allows prediction of performance characteristics based upon fundamental system properties. This model will eventually be used to aid in the optimization and engineering design of semiconducting electrochemical systems.

The principal elements of a liquid-junction photovoltaic cell are the counterelectrode, the electrolyte, the semiconductor-electrolyte interface, and the semiconductor. The mathematical model of this cell includes the macroscopic transport and kinetic equations that govern the counterelectrode, the electrolyte solution, and the semiconductor, and a microscopic representation of the interface between the semiconductor and the solution. The semiconductor-electrolyte interface couples the macroscopic equations that govern the adjacent bulk phases. Single-step reactions determine the concentrations of individual species and potentials at interfacial planes. Electrical current can pass from the semiconductor to the solution by means of these interfacial reactions.

The model can be used to calculate current-voltage curves for the illuminated and non-illuminated cell. The potential and concentration distributions within the cell can also be calculated. Computed current-voltage curves are presented in Fig. 1 for an n-type GaAs anode in

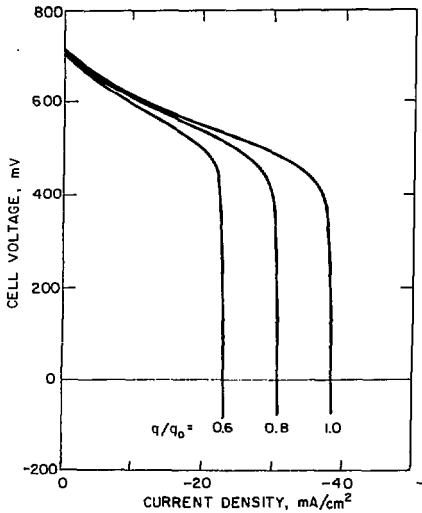

Fig. 1. Computed current-voltage curves for an n-type GaAs anode in contact with a 0.8M K_2Se, 0.1M, K_2Se_2, 1.0M KOH electrolyte.
(XBL 8112-13154)

*This work was supported by the Director, Office of Energy Research, Office of Basic Energy Sciences, Chemical Sciences Division of the U. S. Department of Energy under Contract No. DE-AC03-76SF00098.

contact with a 0.8M K_2Se, 0.1M K_2Se_2, 1.0M KOH electrolyte solution. The counterelectrode is located 0.1 cm from the anode.

Radiative reflection and scattering losses in a cell without interfacial kinetic limitations are seen in Fig. 1 to decrease the limiting current, with only a small decrease in the open-circuit cell voltage. In all cases the cell voltage is highest at open-circuit and decreases sharply as a limiting current is reached. A limiting current is observed due to a limiting concentration of holes in the semiconductor. This model has also been used to show that interfacial kinetic limitations can drastically influence the open-circuit cell voltage, the value of the limiting current, and the shape of the current-voltage curve. A small reaction rate constant is compensated for by increased potential and concentration driving forces. In this way, kinetic limitations influence the cell performance.

* * *

†Brief version of "Theoretical Analysis of Liquid-Junction Photovoltaic Cells," presented by Mark E. Orazem and John Newman at the 159th meeting of the Electrochemical Society, Minneapolis, MN, May 14, 1981.

2. WORK IN PROGRESS

An experimental investigation has begun of the electrosorptive removal of divalent heavy metals from dilute aqueous streams. A bench-top scale, flow-through porous carbon electrode reactor has been constructed. Preliminary experiments have confirmed that monovalent ions can be adsorbed and desorbed onto the porous carbon electrodes.

Experiments are presently being conducted to determine the feasibility of removing mercuric ions from contaminated brine solutions by reduction in a flow-through porous cathode. Mercury concentrations of 50 ppm in 4M NaCl brine were decreased to less than 1 ppm with flow rates as high as 30 bed volumes per hour. Stable steady-state polarization curves and diffusion-limited currents were obtained. Future work will include additional experiments to elucidate further the mass transfer characteristics of this system. Results of these experiments will yield mass-transfer coefficient data which can be used in scale-up.

1981 PUBLICATIONS AND REPORTS

Publications and Technical Reports

1. D. A. Scherson, P. F. Marconi, and J. S. Newman, "On the Short Time Solution for the Concentration Step at the Surface of a Rotating Disk," J. Electrochem. Soc., 127, 2603-2604 (1980).

2. C. G. Law, Jr., P. Pierini, and J. S. Newman, "Mass Transfer to Rotating Disks and Rotating Rings in Laminar, Transition and Fully-developed Turbulent Flow," Intern. J. Heat Mass Transfer, 24, 909-918 (1981).

3. D. A. Scherson and J. S. Newman, "The Variation of Supporting Electrolyte Concentration in Impedance Studies at a Rotating Disk Electrode," J. Electrochem. Soc., 128, 1018-1022 (1981).

4. D. L. Ullman, "Current Limited by Transport Through the Space-Charge Region of a Semiconductor Electrode," J. Electrochem. Soc., 128, 1269-1273 (1981).

LBL Reports

1. Clarence Garlan Law, Jr., "Corrosion of Iron," (Ph.D. thesis). November 1980, LBL-11305.

2. Peter Eugene Pierini, "A Study of Ring and Ring-Disk Electrodes," (Ph.D. thesis). May 1981, LBL-12776.

Papers Presented

1. John Newman, "Corrosion of Iron," Annual Review Symposium of the Materials and Molecular Research Division, Lawrence Berkeley Laboratory, Berkeley, February 10, 1981.

2. M. E. Orazem and J. S. Newman, "Theoretical Analysis of Liquid-Junction Photovoltaic Cells," Minneapolis meeting of the Electrochemical Society, May 14, 1981.

3. Ellen M. Pawlikowski, J. M. Prausnitz, and J. S. Newman, "Phase Equilibria for Aqueous Solutions of Ammonia and Carbon Dioxide: Effects of Salts in the Region 100-150°C," Marburg meeting of Deutschen Bunsen-Gesellschaft, May 29, 1981.

4. Ellen M. Pawlikowski, J. M. Prausnitz, and J. S. Newman, "Vapor-Liquid Equilibrium Calculations for Aqueous Mixtures of Volatile Weak Electrolytes and Other Gases for Coal-Gasification Processes," invited paper at the Second World Congress of Chemical Engineering and World Chemical Exposition, Montreal, October 6, 1981.

g. Surface Chemistry — Application of Coordination Principles*

Earl L. Muetterties, Investigator

The objective of this research is the delineation of the molecular features of hydrocarbon chemisorption on metal surfaces and of the hydrocarbon reactions mediated on these surfaces. Carbon-hydrogen and carbon-carbon bond breaking and making represent the two classes of surface reactions. Our initial efforts have focused on carbon-hydrogen bond scission and formation. These fundamental studies should provide valuable information for the development of more selective catalytic hydrocarbon reactions.

Hydrocarbon chemistry is examined as a function of the metal, the metal surface topography, and surface contaminants like carbon, sulfur and oxygen. To enable this investigation and to exploit the electron spectroscopies and diffraction techniques, all reactions were monitored in an ultra high vacuum system. Nickel and platinum were examined for the hydrogenation and dehydrogenation reactions of acetylene and of cycloalkanes and cycloalkenes.

Acetylene chemisorbed on Pt(111) and Pt(100) react with hydrogen in qualitatively different modes.[1] On Pt(111), the net reaction is hydrogen addition. Analysis of the Pt(111)-C_2D_2 reaction with H_2 established that the initial C-D bonds are not cleaved at 25-130°C to generate Pt-D surface species. In sharp contrast, the net reaction of Pt(100)-C_2D_2 with hydrogen at 25°C is only H-D exchange; there is no net hydrogen addition.

Cyclohexane, cyclohexene and cyclohexadienes adsorbed on nickel and platinum surfaces dehydrogenate to chemisorbed benzene at temperatures of 0-100°C with rates that increase in the order cyclohexane < cyclohexene < cyclohexadiene.[2] Generally, the platinum surfaces were the most active; only the stepped Pt 6(111)x(111) effected a substantial conversion of cyclohexane to benzene. Carbon surface contamination of the Ni(110) surface uniquely led to an enhancement in dehydrogenation capability of this surface. This chemistry is being extended to cycloalkanes and cycloalkenes in general.

* * *

1. E. L. Muetterties, M.-C Tsai, and S. Kelemen, Proc. Natl. Acad. Sci., USA, 78, 6571 (1981).

*This work was supported by the Director, Office of Energy Research, Office of Basic Energy Sciences, Chemical Sciences Division of the U. S. Department of Energy under Contract No. DE-AC03-76SF00098.

1981 PUBLICATIONS AND REPORTS

Refereed Journals

†1. J. R. Bleeke and E. L. Muetterties, "Catalytic Hydrogenation of Aromatic Hydrocarbons. Stereochemical Definition of the Catalytic Cycle for η^3-$C_3H_5Co(P(OCH_3)_3)_3$," J. Am. Chem. Soc., 103, 556 (1981).

†2. A. C. Sievert and E. L. Muetterties, "Arene Transition-Metal Chemistry 5. Arene Ligand Exchange and Reactivity in η^6-Arene Iridium(I) Complexes," Inorg. Chem., 20, 489 (1981).

3. C. M. Friend, J. Stein, and E. L. Muetterties "Coordination Chemistry of Metal Surfaces 2. Chemistry of CH_3CN and CH_3NC on Nickel Surfaces," J. Am. Chem. Soc., 103, 767 (1981).

4. C. M. Friend and E. L. Muetterties, "Coordination Chemistry of Metal Surfaces 3. Benzene and Toluene Interactions with Nickel Surfaces," J. Am. Chem. Soc., 103, 773 (1981).

†5. J. H. Davies, M. A. Beno, J. M. Williams, J. Zimmie, M. Tachikawa, and E. L. Muetterties, "Structure and Chemistry of a Metal Cluster with a Four Coordinate Carbide Cluster Atom," Proc. Natl. Acad. Sci., USA, 78, 668 (1981).

†6. M. Tachikawa and E. L. Muetterties, "Metal Carbide Clusters," Prog. Inorg. Chem., 28, 203 (1981).

†7. G. F. Schmidt, E. L. Muetterties, M. A. Beno, J. M. Williams, "Alkyl-Metal and Aryl-Metal Bond Chemistry in Coordinately Unsaturated Polynuclear Complexes," Proc. Natl. Acad. Sci., USA, 28, 1318 (1981).

†8. S. Slater and E. L. Muetterties, "Chemistry of the Mo-Mo Triple Bond in the $[\eta^5$-$C_5H_5)(CO)(C_{12}H_{20})$ Metallocycle," Inorg. Chem., 20 1237 (1981).

†9. M. A. Beno, J. M. Williams, and E. L. Muetterties, "A Closed Three-Center Carbon-Hydrogen-Metal Interaction. A Neutron Diffraction Study of $HFe_4(\eta^2$-$CH)(CO)_{12}$," J. Am. Chem. Soc., 102, 1485 (1981).

†10. K. D. Tau, E. L. Muetterties, M. R. Thompson, and V. W. Day, "Catalytic Hydrogenation of Aromatic Hydrocarbons 7.," Inorg. Chem., 20, 1237 (1981).

11. E. L. Muetterties, "Molecular Metal Clusters as Catalysts," Catal. Rev.-Sci. Eng., 23, 69 (1981), LBL-12867.

12. E. L. Muetterties, "Coordination Chemistry of Metal Surfaces," ACS Symp. Ser., "Reactivity of Metal-Metal Bonds" 155, 273 (1981).

†13. R. G. Teller, J. M. Williams, T. F. Koetzle, R. R. Burch, R. M. Gavin, and E. L. Muetterties, "The Crystal Structure of $\{HRh[P(O\text{-}i\text{-}C_3H_7)_3]_2\}_2$. A Neutron Diffraction Study," Inorg. Chem., 20, 1806 (1981).

†14. S. Slater and E. L. Muetterties, "Chemistry of the μ_2-Acetylene Ligand in $(\eta^5\text{-}C_5H_5)_2Ni_2(RC{\equiv}CR)$, Inorg. Chem., 20, 1604 (1981).

†15. M. Tachikawa, R. L. Geerts and E. L. Muetterties, "Metal Carbide Clusters Synthesis Systematics for Heteronuclear Species," J. Organomet. Chem., 213, 11 (1981).

†16. E. L. Muetterties, "Selective Reactions of Transition Metals and Their Complexes," Inorg. Chim. Acta, 50, 1 (1981).

†17. A. C. Sievert and E. L. Muetterties, "Arene Transition-Metal Chemistry 6. Hydride Reduction of η^6-Arene Iridium (I) Complexes," Inorg. Chem., 20, 2276 (1981).

18. R. M. Gavin, J. Reutt, and E. L. Muetterties, "Metal Hydrogen Bridge Bonding of Hydrocarbons on Metal Surface," Proc. Natl. Acad. Sci., USA, 78, 3981 (1981), (LBL-12868).

†19. H.-K. Wang, H. W. Choi, and E. L. Muetterties, "Catalytic Hydrogenation of Carbon Monoxide with $Ir_4(CO)_{12}$ and $AlCl_3$," Inorg. Chem., 20, 2661 (1981).

†20. H. W. Choi and E. L. Muetterties, "Catalytic Carbon Monoxide Hydrogenation with $Os_3(CO)_{12}$ and Boron Tribromide," Inorg. Chem., 20, 2664 (1981).

†21. R. R. Burch, E. L. Muetterties, A. J. Schultz, E. G. Gebert, and J. M. Williams, "Reaction of Carbon Monoxide with the Coordinately Unsaturated Metal Dimer $(\mu\text{-}H)_2Rh_2[P(O\text{-}i\text{-}C_3H_7)_3]_4$ with Retention of Dimeric Form. Crystal and Molecular Structure of $Rh_2(\mu\text{-}CO)_2\text{-}[P(O\text{-}i\text{-}C_3H_7)_3]_4$," J. Am. Chem. Soc., 103, 5517 (1981).

†22. R. A. Schunn, G. C. Demitras, H. W. Choi, and E. L. Muetterties, "Methane Formation in the Reaction of Carbon Monoxide and Hydrogen in the Presence of Iridium and Osmium Clusters," Inorg. Chem., 20, 4023 (1981).

†23. C. M. Friend, E. L. Muetterties, and J. Gland, "Vibrational Studies of CH_3CN and CH_3NC Adsorbed on Ni(111) and Ni(111)-C Surfaces," J. Phys. Chem. 85, 3256 (1918).

* * *

†Funded by a grant from the National Science Foundation under grant Nos. CHE 79-03933 and CHE 8000038.

Invited Talks

1. Edgar Fahs Smith Lecturer, University of Pennsylvania, March 1981.

2. Arthur D. Little Lecturer, Northeastern University, April 1981.

3. King Lecturer, Kansas State University, April 1981.

4. Lemieux Lecturer, University of Ottawa, Canada, May 1981.

5. Special Lecturer, University of California, Riverside, June 1981.

6. Plenary Lecturer, Xth Int'l. Conference on Organometallic Chemistry, Toronto, Canada, August, 1981.

7. Plenary Lecturer, Special Conference, University of Toronto, Canada, August 1981.

8. Distinguished Lecturer, Inorganic Chemistry Seminar Institut de Chimie Minerale et Analytique, Villars, Switzerland, September 1981.

9. Lecturer, Honor Lecture Series, Arizona State University, December 1981.

h. High-Energy Oxidizers and Delocalized-Electron Solids*

Neil Bartlett, Investigator

Introduction. This research group is concerned with the electron oxidation of aromatic molecules and other electron-delocalized materials. A major interest is graphite intercalation.[1] The factors that are important in bringing about intercalation are being assessed, as are the changes in the properties (particularly electrical conductivity) that accompany the intercalation. Since bands of the carbon-atom layers serve as the source (valence band) of electrons or the sink (conduction band) for electrons, and substantial electron-oxidation or reduction can occur without disruption of the graphite-sheet structure, graphite intercalation compounds offer the prospect of appreciable electrochemical oxidation (or reduction) without catastrophic structural change.

For a clear understanding of intercalation and its scope, it is essential to know the nature of the guest species (especially their charge), their concentration and, if possible, their disposition with respect to the carbon atoms of the infinite graphite sheet galleries within which they are contained. The mobility of the species within the graphite galleries is also of interest. Efforts are being made to determine how quickly and reversibly electrochemical oxidation and reduction of the graphite salts can be carried out. How far the graphite can be oxidized before structurally destructive and irreversible changes occur is also being investigated.

* * *

1. For recent review see LBL-13751.

1. GRAPHITE INTERCALATION BY FLUORINE AND HYDROGEN FLUORIDE†

Neil Bartlett and Tom Mallouk

Recent work in these laboratories has shown that graphite intercalation by AsF_5 in the presence of fluorine yields material of composition $C_xAsF_6{\cdot}F$, this extra fluorine (probably present as F^-) being available for oxidation. This intercalation of fluorine is in contrast to the frequently commented upon inability of fluorine alone to intercalate graphite. Indeed the extra fluorine cohabits with the AsF_6^-, and unoccupied galleries (of higher stages) do not take up fluorine. It was supposed that the inability of graphite to intercalate fluorine had its origin in the small F^- ion, which localizes charge on near-neighbor carbon atoms, thus producing a deep potential well. Therefore, it was decided that the intercalation of fluorine should be carried out in the presence of neutral molecules with which F^- can reversibly complex. The first choice was hydrogen fluoride.

In the presence of liquid hydrogen fluoride, fluorine is readily taken up by powdered graphite. Stoichiometric addition of fluorine gives the compound $C_{12}{}^+FHF^-$, which is hexagonal with $\underline{a} = 2.45$, $\underline{c} = 9.44$ Å. It is a good electrical conductor. The 00ℓ diffraction intensities indicate that this is a second stage intercalation compound with planar carbon layers at $\underline{z} = 0.181(5)$, $0.819(5)$ and fluorine at $\underline{z} = 0.48(4)$, $0.52(4)$. The shortest C-F contact is therefore ≥ 2.8 Å. When more fluorine is added, HF is displaced from the graphite and a first stage compound, C_xF, is formed ($4 \geq x \geq 2$), with $\underline{a} = 2.45 - 2.47$ and $\underline{c} = 5.2 - 6.2$ Å, the lattice parameters being dependent on x. The near identity of the $\underline{a}$ spacing in C_xF with that of pristine graphite indicates that the intercalation produces little or no structural change in the carbon network. The diffraction intensities from powder and single crystal samples again indicate planar carbon sheets at $\underline{z} = 0$ and fluorine at $\underline{z} \leq 0.25$ or ≥ 0.75 for the entire composition range. C_4F was prepared by Rüdorff,[1] who proposed a structure with covalent C-F bonds. We favor an ionic formulation $C_x{}^+F^-$, based on the ^{19}F - NMR chemical shift for $C_{2.0}F$ and on the fact that C_xF spontaneously intercalates GeF_4 to form compounds previously obtained from graphite, GeF_4, and fluorine.[2]

* * *

†Background is given in LBL-12211 and LBL-13815.

1. W. and G. Rüdorff, Chem. Ber., 80(5), 417 (1947).
2. E. M. McCarron, Y. J. Grannec, and N. Bartlett, J.C.S. Chem. Comm., 890 (1980), LBL-10228.

2. X-RAY DIFFRACTION AND VIBRATIONAL STUDIES OF $(GeF_5)_n{}^{n-}$ SALTS†

Tom Mallouk, Bernard Desbat and Neil Bartlett

Discovery in these laboratories of the intercalation of graphite by GeF_4 with fluorine present, and the existence of an equilibrium between the graphite salts, C_nGeF_6, and elemental fluorine, heightened interest in the fluorocomplexes of GeF_4. The fluoride-ion affinities of GeF_4 were pertinent to these properties. It also appeared possible that certain salts of GeF_5^- and GeF_6^{2-} (particularly where ion-tautomerism of the type $(XeF_5{}^+)_2GeF_6^{2-} \rightleftharpoons (Xe_2F_{11}{}^+, GeF_5^-$ could occur) could be good fluoride ion conductors. Both of these interests demanded structural studies.

Whenever possible the structural work has been based on single-crystal x-ray diffraction in combination with vibrational spectroscopy.

*This work was supported by the Director, Office of Energy Research, Office of Basic Energy Sciences, Chemical Sciences Division of the U. S. Department of Energy under Contract No. DE-AC03-76SF00098.

Last year we reported the structure of the salt $XeF_5^+GeF_5^-$, in which the anions were found to be infinite chains of GeF_6 octahedra which share trans vertices. The crystal structure of the new compound $ClO_2^+GeF_5^-$ (which should be compared with that of the XeF_5^+ salt) is given in Fig. 1. The anions again occur as polymeric chains of vertex-sharing octahedra, this time associating via cis fluorine bridges. On the basis of approximate point symmetries of O_{4h} (in XeF_5GeF_5) and C_{2v} (in ClO_2GeF_5) for the nonbridging F_4Ge units in the anion, the vibrations of these compounds have been correlated with their Raman and infrared spectra. Data are presented in Table 1. The higher symmetry of the $XeF_5^+GeF_5^-$ crystal permits a more detailed assignment of the anion bands than for $ClO_2^+GeF_5^-$.

The vibrational spectra of $AGeF_5$ salts (A = O_2, NO_2, NF_4, SF_3, Bu_4N) have been analyzed and from them we propose four structural types for GeF_5^- salts. Only in $XeF_5^+GeF_5^-$ is the anion trans bridged. In $O_2^+GeF_5^-$ and $ClO_2^+GeF_5^-$ we find an extended helix of cis-bridging octahedra, where the germanium atoms are nearly coplanar. $NO_2^+GeF_5^-$, $NF_4^+GeF_5^-$, and $SF_3^+GeF_5^-$ belong to a common structural type, which has yet to be elucidated; it is clear, however, that the anion must again involve linked GeF_6 units in rings or extended chains. Finally, in Bu_4NGeF_5 we find that the anion is monomeric and trigonal bipyramidal. Clearly the form of the GeF_5^- anion is determined by the subtleties of anion-cation packing in the crystal. The occurrence of one monomeric and several polymeric modifications indicates that all forms must be relatively close in energy.

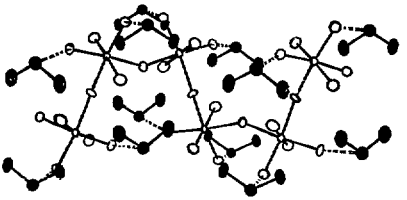

Fig. 1. The crystal structure of $ClO_2^+GeF_5^-$ (Small open circles are Ge atoms, large open circles and ellipses and F atoms, hatched ellipses are O atoms, filled circles are Cl atoms.) (XBL 821-7605)

* * *

†Brief version of LBL-13816.

Table 1. Vibrational spectra of $XeF_5^+FeF_5^-$ and $ClO_2^+FeF_5^-$.

Assignments						Assignments	
Raman	Infrared	$XeF_5^+(C_{4v})$	$(GeF_5)_n^{n-}(D_{4h})$	Raman	Infrared	ClO_2^+ (D_2)	$(GeF_5)_n^{n-}$
	700m		Square plane asym. stretch (ν_6)	1307 mw	1303 s	ν_3 (B_1,B_3)	
669 vs		$\nu_1(A_1)$			1086 m	ν_1 (A_1,B_2)	
	650-670	$\nu_7(E)$		1065 vs 1057 ms			
654 ms			Square plane sym. stretch in phase (ν_1)		1040 mw 1018 mw	2 x ν_2	
622 vs 602 vs		$\nu_4(B_2)$ $\nu_2(A_1)$		713 mw	695 vs		
	600 mw		chain stretching vibrations	657 vs	650 vs		stretching vibrations
526 w 518 w							
	500 m						chain vibrations
463w			Square plane sym. stretch out of phase (ν_4)	610 w 590 m 559 ms	595 ms		
417 m	415 w	$\nu_8(E)$					
381 mw	400 w		Square plane - chain angle deformation	520 m 512 s	518 s	ν_2 (A_1,B_2)	
354 m		$\nu_3(A_1)$	deformation of angles in the square plane	399 w	395 m		chain deformations
339 mw 331 mw				337 m			angle deformations of group
300 ms		$\nu_6(B_1)$		303 m 292 m	290 m		
263 vw		$\nu_5(B_2)$					
220 mw 208 w		$\nu_9(E)$		232 w 160 ms 138 s			chain torsions and rotations
184 w 122 m			chain rotation and torsion				

3. FLUORIDE-ION AFFINITIES AND ELECTRON AFFINITIES OF HIGH-OXIDATION-STATE FLUORIDES†

Tom Mallouk, Guy Rosenthal and Neil Bartlett

Evaluation of factors that determine the capability of graphite to intercalate fluorides has led to determination and redetermination of some fluoride ion affinities and electron affinities.

The enthalpy $MF_{x(g)}^- + F_{(g)} \rightarrow MF_{(n+1)(g)}^-$ has been evaluated from a Born-Haber cycle, for M = B, P and Ge. Fluoride-ion donors were either SF_4 or ClO_2F. Heats of reaction were determined calorimetrically or from dissociation pressure/temperature dependence data. The electrostatic part of the lattice enthalpy (ΔH_L) was evaluated from a Fourier summation described by Bertaut;[1] the repulsive, London, and covalent contributions to ΔH_L were calculated by standard methods. The following fluoride-ion affinities were obtained

Reaction	$-\Delta H^\circ$ (kcal mole^{-1})
$PF_{5(g)} + F_{(g)}^- \rightarrow PF_{6(g)}^-$	102 ± 8
$BF_{3(g)} + F_{(g)}^- \rightarrow BF_{4(g)}^-$	91 ± 8
$GeF_{4(g)} + F_{(g)}^- \rightarrow GeF_{5(g)}^-$	102 ± 8
$GeF_{4(g)} + 2F_{(g)}^- \rightarrow GeF_{6(g)}^-$	64 ± 10

Electron affinities have likewise been estimated, employing lattice energies derived using the Bertaut method and enthalpies for the reactions $A_{(g)} + MF_{6(g)} \rightarrow A^+MF_{6(c)}^-$ (A = O_2, M = Pt and NO, M = U). Hence we have:

Reaction	$-\Delta H^\circ$ (kcal mole^{-1})
$UF_{6(g)} + e^- \rightarrow UF_{6(g)}^-$	133 ± 8
$PtF_{6(g)} + e^- \rightarrow PtF_{6(g)}^-$	204 ± 12

This UF_6 electron affinity is approximately 20 kcal greater than the value given by Beauchamp[2] but in his derivation a fluoride-ion affinity for BF_3 of 71 kcal mole^{-1} was employed. Our work shows that is certainly in error. Employing a BF_3 fluoride ion affinity of 91 kcal mole^{-1}, with Beauchamp's ion-cyclotron measurements yields an electron affinity for UF_6 not significantly different from ours. These data support the earlier observation that an electron affinity in excess of 120 kcal mole^{-1} is required if a hexafluoroanion forming species is to intercalate into graphite.

* * *

†Brief version of LBL-13317.

1. F. Bertaut, J. Phys. Radium, 13, 499 (1952).
2. J. L. Beauchamp, J. Chem. Phys., 64, 929 (1976).

1981 PUBLICATIONS AND REPORTS

Refereed Journals

1. F. L. Tanzella and Neil Bartlett, "Quantitative Synthesis of $(C_6H_5)_2AsF_2^+AsF_6^-$ and $(C_6H_5)_2AsF_3$ via Interaction of Benzene with Arsenic Pentafluoride," Zeitschrift fur Naturforschung, Teil B, 346 (1981); LBL-12784.

2. T. E. Thompson, E. M. McCarron and Neil Bartlett, "The Electrical Conductivity of Graphite-AsF_5 Intercalation Compounds and Their Relationship to Other Graphite-MF_6 Salts," Synthetic Metals 3, 255 (1981); LBL-12211.

LBL Reports

1. Barry W. McQuillan, "The Synthesis and Characterization of Graphite-Metal Fluoride Intercalation Compounds," LBL-12228.

Other Publications

1. Neil Bartlett, Chapter 23 in Centenary Volume, Society of Chemical Industry, D. H. Sharp, Ed., Butterwork Press, England, Fall 1981; LBL-12475.

2. Neil Bartlett and B. W. McQuillan, "Graphite Chemistry," Chapter 2 in Intercalation Chemistry, Whittingham/Jacobson, Eds., Academic Press (1981); LBL-13751.

Invited Talks

1. Neil Bartlett, "Novel High-oxidation-state Species," The University of Leeds, England, March 10, 1981.

2. Neil Bartlett, "Noble Gas Chemistry, Its Discovery and Significance" a public lecture given at The University of Leeds, England, March 11, 1981.

3. Neil Bartlett, "Electron-oxidation of Benzene and Perfluoro-aromatic Molecules," The University of Leeds, England, March 13, 1981.

4. Neil Bartlett, "Synthetic Metals from Electron-oxidation of Graphite and Boron Nitride," The University of Leeds, England, March 17, 1981.

5. Neil Bartlett, "The Synthesis of Metals of High-oxidizing Potential," The University of Leeds, England, March 20, 1981.

6. Neil Bartlett, "Electron Oxidation of Aromatic Molecules, Layer Boron Nitrides and Graphite," Centenary Conference, Society of Chemical Industry, University of Cambridge, April 2, 1981.

7. Neil Bartlett, "Novel Electrical Conductors," Imperial Chemical Industries, Runcorn, England, May 10, 1981.

8. Neil Bartlett, "Some New 'Metallic' Graphite Salts of High Oxidizing Potential and Their Possible Use as Electrode Materials," Chemical

Engineering Colloquia, University of California, Berkeley, May 4, 1981.

9. Neil Bartlett, "Noble Gas Compounds, Their Discovery and Significance," The University of Newcastle-upon-Tyne, England, May 15, 1981.

10. Neil Bartlett, "Novel Synthetic Metals of High Oxidizing Potential Derived from Graphite," University of Chicago, May 18, 1981.

11. Neil Bartlett, "Some Chemistry of Graphite Intercalation," Fifteenth Biennial Conference on Carbon, University of Pennsylvania, June 23, 2981.

12. Neil Bartlett, "Electrical Conductivity of Intercalated Graphite Compounds," 182nd ACS National Meeting, New York, NY, August 25, 1981.

13. Neil Bartlett, "New Synthetic Metals Obtained by Intercalation of Graphite or Boron Nitride with Powerful Oxidizers." Mendeleev Congress on General and Applied Chemistry, Baku, USSR, September 24, 1981.

I. Transition Metal Catalyzed Conversion of CO, NO, H_2, and Organic Molecules to Fuels and Petrochemicals*

Robert G. Bergman, Investigator

Introduction. Small gaseous molecules (e.g., CO, NO, H_2) and volatile organic compounds (e.g., ethylene) are important chemical building blocks for a wide range of fuels and petrochemicals. Industry is making increasing use of these raw materials in homogeneous processes catalyzed by organotransition metal complexes, because homogeneous processes are capable of affording selectivities which often cannot be obtained in heterogeneous reactions. The goal of this project is to study the reactions of organotransition metal complexes with small molecules such as CO, H_2, NO, and ethylene, in order to develop new homogeneous processes and understand in detail how these processes operate. The work focuses on overall reactions which form new C-H, C-N, and C-C bonds. It concentrates on understanding the basic mechanistic steps which can be combined to carry out these overall reactions; the most critical of these involve formation and cleavage of metal-hydrogen, -nitrogen and -carbon bonds. In addition to providing direct information about homogeneous reactions catalyzed by complexes containing one metal, the research provides concepts and results applicable to related reactions involving catalysis by binuclear complexes, cluster complexes, and metal surfaces.

Most recently, work in this project has focused on the mechanisms by which metals induce the formation and cleavage of C-H bonds. In one set of studies, a new set of C-H bond forming processes involving two metals has been found. These reactions involve initial CO migratory insertion in a metal alkyl, and some attention has been directed toward understanding the role played by solvent in the section entitled, "Acyl- and Aldehyde-Forming Reactions of Metal Alkyl Complexes: Evidence for Solvent Coordination in the Migratory Insertion Step." The second part of the project is directed toward finding ways to activate C-H bonds in completely saturated hydrocarbons, which are normally very unreactive. This objective has been achieved this year; the first example of intermolecular oxidative addition of a metal into the C-H bonds of completely saturated hydrocarbons has been observed. This is reported in the second part of the report, entitled, "C-H Activation in Completely Saturated Hydrocarbons: Direct Observation of M + R-H ⇒ R-M-H."

*This work was supported by the Director, Office of Energy Research, Office of Basic Energy Sciences, Chemical Sciences Division of the U.S. Department of Energy under Contract No. DE-AC03-76SF00098.

1. ACYL- AND ALDEHYDE-FORMING REACTIONS OF METAL ALKYL COMPLEXES: EVIDENCE FOR SOLVENT COORDINATION IN THE MIGRATORY CO INSERTION STEP†

Michael J. Wax and Robert G. Bergman

The role of solvent in migratory CO insertion has been the object of considerable research, but until now has evaded complete elucidation. Because this reaction has great practical importance, occurring in hydroformylation, acetic acid synthesis, and possibly in Fischer-Tropsch synthesis, it seemed that further study would be of value. This project applies a novel approach to the problem, and provides evidence that CO insertion occurs via parallel solvent-catalyzed and uncatalyzed pathways.

Reaction of $CpMo(CO)_3CH_3$ (Complex 1, R=CH_3 in Scheme 1) with $PMePh_2$ was studied in a series of methyl-substituted tetrahydrofuran solvents varying in nucleophilicity but not in polarity, thus allowing separation of these effects. In tetrahydrofuran (THF), 3-methyl-, 2-methyl-, and 2,5-dimethyl-THF, disappearance of starting organometallic occurs in part according to second-order kinetics, with a rate constant which is independent of the medium (Table 1). Saturation kinetics, denoting a pathway involving an intermediate, accounts for the remainder of methyl complex consumption in this system. The fact that this intermediate is formed at a rate which increases with increasing solvent donicity suggests strongly that it is the solvated acyl, $CpMo(CO)_2(S)COCH_3$ (2, R=CH_3).

Additional proof of the nature of this intermediate arises from the expected first-order dependence of the rate of its formation on solvent. By using solutions of THF in the relatively nonnucleophilic 2,5-Me_2-THF, it is possible to vary THF concentration. The intermediate is produced at a rate which is a linear function of the concentration of this solvent over the entire mole fraction range, in accord with the above hypothesis.

The analogous aldehyde-producing reaction[1] of $CpMo(CO)_3H$ (Compound 4 in Scheme 1) with $CpMo(CO)_3R$ (1, R=CH_3, CH_2CH_3), a stoichiometric analog of hydroformylation, has also been investigated. The conclusion that solvent coordination, and not a generalized solvent effect, is involved in CO insertion bears directly upon consideration of the mechanism of this process. Reaction of 1 (R=CH_2CH_3) with 4 also occurs through parallel solvent catalyzed and uncatalyzed pathways. The rate constants presented in Table 2 indicate that attack of the hydride 4 upon both starting alkyl and intermediate acyl is slower than that of phosphine. The nature of this bimolecular step is not yet clear, but does not involve initial M-H bond breaking, as evidenced by the lack of a kinetic isotope effect when $CpMo(CO)_3D$ is used.

Scheme I

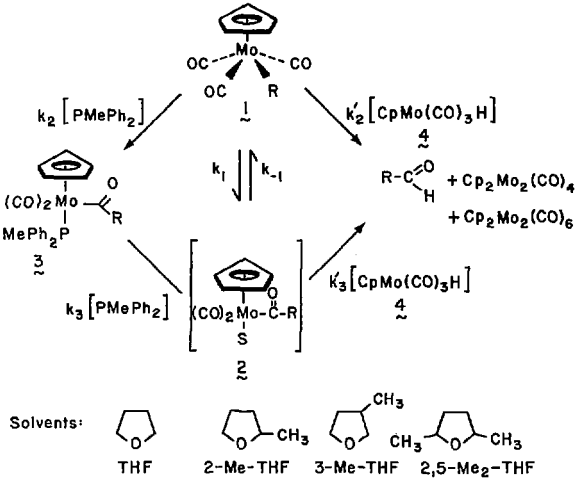

Table 1. Rate constants for the reaction of $Cp(CO)_3Mo(CH_3)$ with $PMePh_2$ at 59.9 ± 0.01°C.

Solvent	$10^4\ k_1(s^{-1})$	k_1/k_2 (M)	$10^4\ k_3(M^{-1}s^{-1})$
THF	7.78	0.0104	1.73
3-MeTHF	6.46	0.00821	1.86
2-MeTHF	1.48	< 0.001	1.95
2,5-Me_2THF	0.23	< 0.001	1.67

Table 2. Rate constants for the reaction of $Cp(CO)_3MoC_2H_5$ with various nucleophiles in 2.5-Me_2THF at 59.9 ± 0.1°C.

Nucleophile	$10^4\ k_1(s^{-1})$	k_{-1}/k_2 (M)	$10^9\ k_3(M^{-1}s^{-1})$
$CpMo(CO)_3H$	4.90	0.0505	1.48
$CpMo(CO)_3D$	4.63	0.0461	1.59
$PMePh_2$	5.29	< 0.001	69.1

* * *

†Brief version of J. Am. Chem. Soc. 103, 7028 (1981). (LBL-13401)

1. W. D. Jones and R. G. Bergman, J. Am. Chem. Soc. 101, 5447 (1979).

2. C-H ACTIVATION IN COMPLETELY SATURATED HYDROCARBONS: DIRECT OBSERVATION OF M + R-H ⇄ R-M-H

Andrew H. Janowicz and Robert G. Bergman

One of the most intriguing goals of homogeneous organotransition metal chemistry is to carry out selective chemical transformations on, or functionalize, very unreactive materials such as saturated hydrocarbons. The earliest examples of intermolecular C-H activation in saturated hydrocarbons are those involving soluble platinum salts at high temperature,[1] and more recently porphyrin complexes.[2] In none of these cases has the intermediate hydridoalkyl metal complex formed by direct oxidative addition to a C-H bond been detected. Reported here is the discovery of an organotransition metal system capable of intermolecular oxidative addition to C-H bonds in saturated hydrocarbons, leading to hydridoalkylmetal complexes in high yield at room temperature in homogeneous solution.

A novel dihydridoiridium complex $(Me_5C_5)IrPPh_3H_2$ (6), was prepared as shown in Scheme 2. Upon irradiation of 6 in benzene (λ max = 275 nm; high pressure Hg lamp, pyrex filter), there was a loss of hydrogen and the formation of two new complexes,

Scheme 2

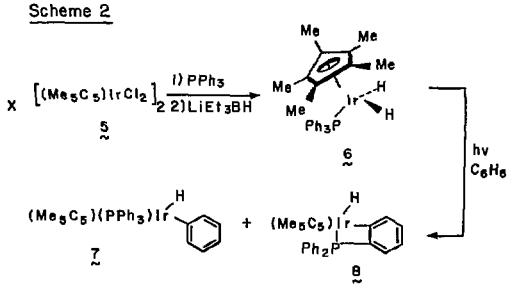

Scheme 3

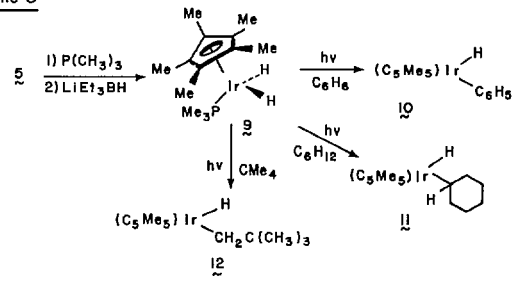

the hydridophenyl complex 7 and the orthometallated complex 8, presumably via the coordinatively unsaturated intermediate $(Me_5C_5)IrPPh_3$.

To make ortho-metallation less favorable, the analogous trimethylphosphine dihydride complex, 9, was prepared (Scheme 3). Irradiation of 9 in benzene yielded exclusively the hydridophenyl complex 10. However, when the irradiation was carried out in cyclohexane, a new material formed, $(Me_5C_5)IrPMe_3(H)C_6H_{11}$ (11), the result of oxidative addition to the C-H bond in cyclohexane.

The intermediate formed upon irradiation of 9 also reacts with neopentane to yield one new product, $(Me_5C_5)IrPMe_3(H)CH_2C(CH_3)_3$ (12). This indicates that oxidative addition to a primary C-H bond of a saturated alkane can also take place.

To further explore the mechanism of this reaction, a series of irradiations were carried out using deuterated and non-deuterated solvents. *First, irradiation of 9 in C_6D_{12} gave H_2 and 11-d_{12}.* Second, 9 was irradiated in a mixture of cyclohexane and neopentane forming products 11 and 12 in a 1.14 ratio. Lastly, 9 was irradiated in a mixture of cyclohexane-d_{12} and neopentane forming predominantly 11-d_{12} and 12. Thus the insertion proceeds with $\geq$ 90 percent intramolecularity.

* * *

1. Shilov, A. E., Pure Appl. Chem 50, 725 (1978).
2. (a) Groves, J. T., Adv. Inorg. Biochem. 1, 119 (1979); (b) Groves, J. T.; Nemo, T. E.; Myers, R. S., J. Am. Chem. Soc. 101, 1032 (1979); (c) Groves, J. T.; Van Der Puy, M., J. Am. Chem. Soc. 98, 5290 (1976); (*d*) Chang, C. K.; Kuo, M.-S., J. Am. Chem. Soc. 101, 3413 (1979); (e) Groves, J. T.; Kruper, W. J., Jr., J. Am. Chem. Soc. 101, 7613 (1979); (f) Hill, C. L.; Schardt, B. C., J. Am. Chem. Soc., 102, 6374 (1980).

3. WORK IN PROGRESS

Research during the coming year will focus on exploiting the discovery of homogeneous activation of C-H bonds in saturated molecules summarized in the second section of this report. Experiments will be carried out to determine the relative reactivities of a number of saturated molecules, and the effect of changing the structure of the iridium complex on its ability to activate C-H bonds. Reactivity of the complex with important functionalized organic molecules, such as methanol and ethylene, will also be carried out. Preliminary observations which indicate that analogous rhodium complexes also engage in C-H activation will be investigated more fully. Finally, experiments will be carried out aimed at incorporating the C-H activation reaction into cyclic mechanistic schemes, so that methods for catalytic functionalization of hydrocarbons can be developed.

1981 PUBLICATIONS AND REPORTS

Refereed Journals

†1. J. M. Huggins and R. G. Bergman, "Mechanism, Regiochemistry, and Stereochemistry of the Insertion Reaction of Alkynes with Methyl(2,4-Pentanedionato)(Triphenyl-phosphine)Nickel. A cis Insertion that Leads to trans Kinetic Products," J. M. Chem. Soc. 103, 3002 (1981).

2. A. H. Janowicz, H. E. Bryndza and R. G. Bergman, "Phosphine Substitution in η^5-Cyclopentadienyl-bis-Triphenylphosphinecobalt(I): Evidence for a Dissociative Mechanism," J. Am. Chem. Soc. 103, 1516 (1981); LBL-11160.

3. R. G. Bergman, "Physical Organic Studies of Organometallic Reactions," Pure and Applied Chemistry 53, 161 (1981); LBL-11827.

4. T. P. Lockhart and R. G. Bergman, "Evidence for the Reactive Spin State of 1,4-Dehydrobenzenes," J. Am. Chem. Soc., 103, 4091 (1981); LBL-11695.

5. T. P. Lockhart, P. B. Comita and R. G. Bergman," Kinetic Evidence for the Formation of Discrete 1,4-Dehydrobenzene Intermediates. Trapping by Intermolecular Hydrogen Atom Transfer and Observation of High-Temperature CIDNP," J. Am. Chem. Soc. 103, 4082 (1981); LBL-11696.

6. A. H. Janowicz and R. G. Bergman, "Methane-Producing Hydrogenolysis of (η^5-Cyclopentadienyl (triphenylphosphine)dimethylcobalt(III)). An Autocatalytic Mechanism Involving a Binuclear Metal Dihydride/Metal Dialkyl Reaction as a Critical Step," J. Am. Chem. Soc. 103, 2488 (1981); LBL-11932.

7. H. E. Bryndza and R. G. Bergman, "Reactions of η^5-cyclopentadienylcobalt(III) Alkyls with Cobalt(I) Phosphines and Iron Carbonyls. Evidence for Direct η^5-Cyclopentadienyl and Trimethylphosphine Group Transfer Between Metal Centers," Inorg. Chem. 20, 2988 (1981); LBL-11826.

8. W. D. Jones, J. M. Huggins and R. G. Bergman, "Comparative Reactivities of Two Isoelectronic Transition Metal Hydrides with Transition Metal Carbonyls and Alkyls," J. Am. Chem. Soc. 103, 4415 (1981); LBL-12273.

‡9. K. H. Theopold and R. G. Bergman, "Synthesis and Reactions of a Binuclear Cobalt Bridging Methylene (μ-CH_2) Complex. Conversion to μ-CH_2 Rh/Co and Rh/Rh Complexes, and Methylene Transfer to Ethylene Involving Activation by a Second Metal Complex," J. Am. Chem. Soc. 103, 2489 (1981).

†10. W. P. Weiner, M. A. White and R. G. Bergman, "Direct Observation of NO Migratory Insertion in an Organotransition Metal Complex," J. Am. Chem. Soc. 103, 3612 (1981).

‡11. W. H. Hersh and R. G. Bergman, "Synthesis and Reactions of a Dimetallacyclohexene. Thermal Conversion to an o-Xylylene Complex, and Phosphine-induced Conversion to Free o-Xylylene and a New Reactive Dinuclear Cobalt Complex," J. Am. Chem. Soc. 103, 6992 (1981).

12. M. J. Wax and R. G. Bergman, "Direct Evidence for Solvent Coordination in Migratory CO Insertion," J. Am. Chem. Soc. 103, 7028 (1981); LBL-13401.

LBL Reports

1. P. B. Comita, M. R. Berman, C. B. Moore and R. G. Bergman, "Laser-Powered Homogeneous Dissociation of Tetralin," LBL-12697.

2. A. H. Janowicz and R. G. Bergman, "C-H Activation in Completely Saturated Hydrocarbons: Direct Observation of M + R-H → M(R)(H)," LBL-13402.

Invited Talks

Robert G. Bergman presented talks on the general topic of "Activation of Organic Molecules Using Organotransition Metal Complexes" at the following places during 1981:

1. University of California, San Diego, January 28, 1981.

2. University of California, Santa Cruz, February 25, 1981.

3. California State University, Northridge, March 11, 1981.

4. University of California, Santa Barbara, March 16, 1981.

5. Pennsylvania State University, March 26, 1981.

6. University of Chicago, May 4, 1981.

7. Symposium on "Organic Transformations at Polynuclear Centers," National Meeting of the American Chemical Society, New York City, August 23-28.

8. College of Wooster, Wooster, Ohio, October 12-16, 1081.

9. Stanford University, November 25, 1981.

10. California Institute of Technology, December 16, 1981.

* * *

†Supported by the National Institutes of Health (Grant No. GM-25459).

‡Supported by the National Science Foundation (Grant No. CHE79-26291).

2. Analysis

a. Analysis of Transplutonium Elements in Dilute Solution*

Steven D. Brown, Investigator

1. RESOLUTION OF OVERLAPPED ELECTROCHEMICAL PEAKS WITH THE USE OF THE KALMAN FILTER†

T. F. Brown‡ and S. D. Brown‡

A major limitation in the use of electrochemical techniques for the quantitative analysis of mixtures is the difficulty of resolving overlapped peaks. The problem is further complicated by the low signal-to-noise ratios often encountered in trace analysis, and by the use of electrochemical techniques that produce broad, asymmetric waveforms.

We have applied a digital method known as the Kalman filter to perform multicomponent analysis of linear sweep voltammograms. This method extracts noise-free, separate peaks from noisy, overlapped responses. It also gives estimates of the error involved in the procedure.

Using the filter, peaks separated by as little as 2.5 mV could be quantitatively separated, and analyses of complex mixtures were possible.

* * *

†Brief version of Anal. Chem., 53, 1410 (1981); (LBL-11917).
‡Present address: Department of Chemistry, Washington State University, Pullman, WA 99164.

2. PEAK RESOLUTION BY SEMIDERIVATIVE VOLTAMMETRY†

J. J. Toman and S. D. Brown‡

In studies of metal complexation, indirect measurements of thermodynamic and kinetic parameters are required. However, appropriate transformation of the electrochemical data can be used to permit direct measurements of these physically significant parameters.

Convolution techniques can be applied to linear scan voltammograms to generate waveforms known as semiderivatives. These waveforms can be described analytically, so that kinetic and thermodynamic parameters may be obtained by numerical fitting of simple functions to the transformed data.

This technique has been applied to studies of overlapped peaks with varying degrees of electrochemical reversibility, in order to evaluate the limitations of the method. Separations were usually excellent unless peaks were severely overlapped.

* * *

†Brief version of Anal. Chem., 53, 1497 (1981); LBL-11738.
‡Present address: Department of Chemistry, Washington State University, Pullman, WA 99164.

3. SPECIATION OF METAL COMPLEX SYSTEMS USING THE KALMAN FILTER†

T. F. Brown,‡ D. M. Caster‡ and S. D. Brown‡

When metal-complex dissociation kinetics are slow, difficulties occur in attempts to measure stability constants using electrochemistry. If, in addition, the ligand is not present in excess, measurement of stability constants in this fashion is impossible.

Application of the Kalman filter to this problem allows the extraction of the free metal response, which can be followed as a function of ligand concentration. From this relationship, stability constants can be calculated by standard methods.

This approach was tested on Zn and Cd solutions with NTA ligands. The stability constants obtained for ZnNTA and CdNTA agreed well with previously reported values.

* * *

†Brief version of LBL-12625, May 1981.
‡Present address: Department of Chemistry, Washington State University, Pullman, WA 99164.

1981 PUBLICATIONS AND REPORTS

Refereed Journals

†1. J. J. Toman, R. M. Corn, and S. D. Brown, "Convolution Voltammetry of Metal Complexes," Anal. Chim. Acta., 123, 187 (1981); LBL-10820.

2. T. F. Brown and S. D. Brown, "Resolution of Overlapped Electrochemical Peaks with the Use of the Kalman Filter," Anal. Chem. 53, 1410 (1981); LBL-11917.

†3. J. J. Toman and S. D. Brown, "Peak Resolution by Semiderivative Voltammetry," Anal. Chem. 53, 1497 (1981); LBL-11738.

*This work was supported by the Director, Office of Energy Research, Office of Basic Energy Sciences, Chemical Sciences Division of the U.S. Department of Energy under Contract No. DE-AC03-76SF00098.

LBL Reports

†,‡1. J. J. Toman and S. D. Brown, "Application of Convolutive Voltammetric Curve Fitting Techniques to Non-Reversible Electrochemical Systems," LBL-13711.

Other Publications

1. T. F. Brown, D. M. Caster, and S. D. Brown, "Speciation of Labile and Quasi-Labile Metal Complex Systems Using the Kalman Filter," in Proceedings of the DOE/NBS Workshop on Environmental Speciation and Monitoring Needs for Trace Metal-Containing Substances, Gaithersburg, MD, May 18-20, 1981, NBS Spec. Pub. 681, November 1981, LBL-12625.

Invited Talks

1. S. D. Brown, "Chemical Speciation: Approaches Using Computer-Controlled Voltammetry," Dept. of Chemistry, University of California, Berkeley, January 1981.

2. S. D. Brown, "Chemical Speciation," Dept. of Chemistry, Oregon Graduate Center, Portland, OR, February 1981.

3. S. D. Brown, "Peak Deconvolution using the Kalman Filter," Dept. of Chemistry, Portland State University, Portland, OR, February 1981.

4. S. D. Brown, "Resolution of Overlapped Electrochemical Peaks using the Kalman Filter," 181st National Meeting of the American Chemical Society, Atlanta, GA, March 1981.

5. T. F. Brown, D. M. Caster and S. D. Brown, "Speciation of Labile and Quasi-Labile Metal Complex Systems Using the Kalman Filter," DOE/NBS Workshop on Environmental Monitoring needs for Trace Metal-Containing Substances, Gaithersburg, MD, May 1981.

6. S. D. Brown, "Speciation Using the Kalman Filter," General Chemistry Division, Argonne National Laboratory, Argonne, IL, May 1981.

7. S. D. Brown, "Computer-Controlled Electrochemistry: Examples Using Peak Deconvolution," Dept. of Chemistry, University of Idaho, Moscow, September 1981.

8. J. J. Toman, "Convolution Voltammetry," Dept. of Chemistry, University of the Pacific, Stockton, CA, December 1981.

* * *

†This work was supported, in part, by the Director, Office of Nuclear Waste Isolation, Basic Energy Sciences Division of the U.S. Department of Energy under Contract DE AC06-76R101830.

‡This work was supported, in part, by the Petroleum Research Fund, administered by the American Chemical Society.

3. Chemical Engineering Sciences

a. High-Pressure Phase Equilibria in Hydrocarbon-Water (Brine) Systems*

John M. Prausnitz, Investigator

Introduction. Geological studies[1] have indicated that there are large deposits of natural gas in deep, geopressured reservoirs in the coastal regions of Louisiana and Texas. These reservoirs contain natural gas (mostly methane) in contact with water or brine at pressures near 1000 bar and temperatures to 250°C. At present, it is not economic to mine these reservoirs, but, in view of the large deposits, there is much incentive to make such mining attractive. This project is concerned with obtaining some of the fundamental physicochemical information required to do so.

* * *

1. R. H. Wallace, Jr., T. F. Kraemer, R. E. Taylor, and J. B. Wesselman, "Assessment of Geopressured Resources in the Northern Gulf of Mexico Basin," in U.S. Geological Survey Circular 790, 1978.

1. EXPERIMENTAL HIGH-PRESSURE VAPOR-LIQUID-EQUILIBRIUM MEASUREMENTS

Eldon R. Larsen, Georg Roessling, Gabriele Di Giacamo, Wallace B. Whiting, and John M. Prausnitz

Few data are available for vapor-liquid equilibria of aqueous hydrocarbon systems at high pressure; very few are available for brine-hydrocarbon systems. Besides the direct need for these data for engineering applications, we need accurate measurements of fluid-phase equilibria at advanced temperatures and pressures to test theoretical models for mixtures of polar and nonpolar fluids.

Serious problems exist in performing such experimental work: both the strength and the corrosion resistance of the equilibrium cell must be extraordinary and accurate sampling techniques must be devised so that the samples are representative of the phases within the cell.

We have designed and built a high-pressure apparatus capable of operating at pressures to 2000 bar and to 400°C. The cell is fabricated of INCONEL (a high-strength, corrosion-resistant, nickel-chromium alloy); all other wetted components are cold-worked 316 stainless steel. Small samples (less than 0.1 ml each) are removed from the 165-ml cell under carefully controlled conditions to avoid changes in composition due to flashing. To ensure adequate mixing, we have constructed a nickel-plated, cylindrical mixing magnet that is periodically driven vertically through the cell contents by external electromagnets. We have measured methane-water equilibria at 105 and 220°C (95 and 155 bar) and found the results to agree with data from other laboratories.[1,2] In the first few months of 1982, we expect to obtain data for this system at higher pressures, where data are scarce. Then, we shall investigate brine-hydrocarbon systems.

* * *

1. Sultanov, R. G., V. G. Skripka, and A. Yu. Namiot, Gazov. Promysh., 16 (4), 6 (1971); Ibid. 17 (5), 6 (1972).
2. Welsch, H., Doctoral Dissertation, Universität Karlsruhe, 1973.

2. PURE-COMPONENT EQUATIONS OF STATE†

Wallace B. Whiting, Eldon R. Larsen, and John M. Prausnitz

For simple, nonpolar molecules (such as light hydrocarbons), simple, empirical equations (e.g., Redlich-Kwong and Peng-Robinson) correlate the vapor pressure and volumetric properties reasonably well. Polar fluids (notably water) cannot be so easily treated. To improve the fit for these substances, we use statistical mechanics to guide us in constructing simple, semi-theoretical equations of state. We also seek to develop more accurate equations of state for nonpolar fluids.

We have investigated two distinct methods for developing a better equation of state. In the first one, we note that for many polar fluids, the dipole-dipole interaction is the dominant polar contribution to the intermolecular potential. The effect of a point-dipole interaction on the angle-averaged potential between two molecules is the same as if the potential-well depth were temperature dependent. We have used the specific temperature dependence of this potential to modify the Perturbed-Hard-Chain Theory (PHCT)[1] for polar fluids. In addition, we have closed the truncated perturbation series of the PHCT by a method suggested by Barker and Henderson.[2] We have been successful in using this equation of state for strongly polar, pure fluids and for mixtures of polar and nonpolar fluids with the mixing rules described in the next section.

In the second method, we have modified the perturbation expansion of Alder[3] for square-well

*This work was supported by the Director, Office of Energy Research, Office of Basic Energy Sciences, Chemical Sciences Division of the U.S. Department of Energy under Contract No. DE-AC03-76SF00098.

molecules by determining empirically the coefficients in a temperature-density power series for the Helmholtz energy. We have correlated volumetric data for methane over a wide range of temperature and density. We are now trying to minimize the number of coefficients in the power series and to extend the equation to other fluids, especially to water.

* * *

†Brief version of LBL-12239.

1. Donohue, M. D. and J. M. Prausnitz, AIChE J., 24, 849 (1978).
2. Barker, J. A. and D. Henderson, Rev. Mod. Phys. 48, 587 (1976).
3. Alder, B. J., D. A. Young, and M. A. Mark, J. Chem. Phys., 56, 3013 (1972).

3. LOCAL-COMPOSITION MIXING RULES FOR EQUATIONS OF STATE†

Wallace B. Whiting and John M. Prausnitz

Nearly all of the mixing rules used for equations of state are modifications of van der Waals' one-fluid mixing rules.[1] The assumption of random mixing (no orientation effects) is implicit in these rules. Unfortunately, mixtures of molecules that differ appreciably in size or intermolecular potential are highly nonrandom and, therefore, require appropriate mixing rules. We have developed a new set of mixing rules that attempts to account for nonrandomness.

The most successful equations for liquid-state activity coefficients (e.g., Wilson, NRTL, and UNIQUAC equations) have used the concept of local compositions to account for nonrandomness. We extend the idea of local compositions to equations of state; we have succeeded in meeting necessary high- and low-density boundary conditions. We calculate the internal energy of a binary mixture using local compositions of two-fluid theory, in a manner similar to that suggested by Maurer and Prausnitz[2] and Kemeny and Rasmussen.[3]

Our local-composition theory can be applied to any equation of state of the van der Waals form to calculate fluid-phase equilibria for asymmetric mixtures. Good representation has been obtained for vapor-liquid equilibria for several asymmetric mixtures.[4] For example, we have shown that the new mixing rules, coupled with second-virial-coefficient data, can improve calculations of solubilities of methane in water by over two orders of magnitude.[5]

* * *

†Brief version of LBL-13568.

1. van der Waals, J. D., Z. Phys. Chem., 5, 133 (1890).
2. Maurer, G. and J. M. Prausnitz, Fluid Phase Equilibria, 2, 91 (1978).
3. Kemeny, S. and P. Rasmussen, Fluid Phase Equilibria, 7, 197 (1981).
4. Whiting, W. B. and J. M. Prausnitz, LBL-13568 (1981).
5. Whiting, W. B. and J. M. Prausnitz, LBL-12239 (1981).

1981 PUBLICATIONS AND REPORTS

Refereed Journals

†1. B. E. Poling, E. A. Grens II, and J. M. Prausnitz, "Thermodynamic Properties from a Cubic Equation of State: Avoiding Trivial Roots and Spurious Derivatives," Ind. Eng. Chem. Proc. Des. Develop. 20, 127 (1981).

‡2. D. Edwards, C. G. Van de Rostyne, J. Winnick, and J. M. Prausnitz, "Estimation of Vapor Pressures of High-Boiling Fractions in Liquefied Fossil Fuels Containing Heteroatoms Nitrogen or Sulfur," Ind. Eng. Chem. Proc. Des. Develop. 20, 138 (1981).

§3. P. J. Hicks, Jr., and J. M. Prausnitz, "Solubility of Acetone and Isopropyl Ether in Compressed Nitrogen, Methane, and Carbon Dioxide," J. Chem. Eng. Data 26, 74 (1981).

†4. A. I. El-Twaty and J. M. Prausnitz, "Generalized Van der Waals Partition Function for Fluids. Modification to Yield Better Second Virial Coefficients," Fluid Phase Equil. 5, 191 (1981).

†5. J. M. Prausnitz, "Calculation of Phase Equilibria for Separation Operations," Trans. Inst. Chem. Eng. 59, 3 (1981).

‡6. D. R. Edwards and J. M. Prausnitz, "Vapor Pressures of Some Sulfur-Containing, Coal-Related Compounds," J. Chem. Eng. Data 26, 121 (1981).

†7. G. Schulze and J. M. Prausnitz, "Solubilities of Gases in Water at High Temperatures," Ind. Eng. Chem. Fundam. 20, 175 (1981), LBL-12483.

‡8. D. R. Edwards and J. M. Prausnitz, "Estimation of Vapor Pressures of Heavy Hydrocarbons Containing Nitrogen or Sulfur by a Group-Contribution Method," Ind. Eng. Chem. Fundam. 20, 280 (1981).

†9. S. D. Schaffer and J. M. Prausnitz, "Correlation of Hydrogen Solubilities in Nonpolar Solvents Based on Scaled-Particle Theory," AIChE J. 27, 844 (1981).

Other Publications

†1. E. M. Pawlikowski, J. Newman, and J. M. Prausnitz, "Vapor-Liquid Equilibrium Calculations for Aqueous Mixtures of Volatile, Weak Electrolytes and Other Gases for Coal-Gasification Processes," Proceedings of the 2nd World Congress of Chemical Engineering, Montreal, October 4-9, 1981.

†2. E. M. Pawlikowski, "Vapor-Liquid Equilibria for Volatile, Weak Electrolytes in Aqueous Solutions," Ph.D. dissertation, Department of Chemical Engineering, University of California, Berkeley, December 1981.

LBL Reports

1. V. Brandani and J. M. Prausnitz, "Empirical

Corrections to the van der Waals Partition Function for Dense Fluids," LBL-12482.

Invited Talks

1. W. B. Whiting and J. M. Prausnitz, "Equations of State for Strongly Nonideal Fluid Mixtures. Application of the Local-Composition Concept." Spring National Meeting of the American Institute of Chemical Engineers, Houston, April 5-9, 1981; LBL-12239.

2. E. M. Pawlikowski, J. Newman, and J. M. Prausnitz, "Phase Equilibria for Aqueous Solutions of Ammonia and Carbon Dioxide. Effects of Salts in the Region 100-150°C." 80. Hauptversammlung der Deutschen Bunsen-Gesellschaft fuer Physikalische Chemie, Marburg, West Germany, May 28-30, 1981.

3. F. E. Anderson and J. M. Prausnitz, "Phase Equilibria for Inhibition of Hydrate Formation in Natural Gases. Effect of Water-soluble Fluids Like Methanol." 80. Hauptversammlung der Deutschen Bunsen-Gesellschaft fuer Physikalische Chemie, Marburg, West Germany, May 28-30, 1981.

4. E. R. Larsen, "High Pressure Vapor-Liquid Equilibria for Water/Methane," Department of Chemical Engineering, Arizona State University, Tempe, February 1981.

5. W. B. Whiting, "Calculation of High-Pressure Vapor-Liquid Equilibria for Asymmetric Mixtures," Department of Chemical Engineering; Illinois Institute of Technology, January 1981; Worcester Polytechnic Institute, January 1981; Polytechnic Institute of New York, Brooklyn, January 1981; West Virginia University, December 1981.

6. J. M. Prausnitz, "Molecular Thermodynamics for Chemical Process Design," Institute for Applied Chemistry, University of L'Aquila, Italy, April 1981; Department of Chemistry, Technische Hochschule, Darmstadt, West Germany, July 1981; Department of Chemical Engineering, Universtitaet Kaiserslautern, West Germany, July 1981; Department of Chemical Engineering, Technical University of Berlin, West Germany, May 1981; Department of Applied Chemistry, University of Lund, Sweden, June 1981.

‡7. G. L. Alexander and J. M. Prausnitz, "Phase-Equilibrium Calculations for Mixtures Containing Characterized Heavy-Fossil-Fuel Fractions," Annual Meeting of the American Institute of Chemical Engineers, New Orleans, November 8-12, 1981.

‡8. A. Monge, Jr., and J. M. Prausnitz, "An Experimental Method for Measuring Solubilities of Heavy Fossil-Fuel Mixtures in Compressed Gases to 100 Bar and 300°C," Annual Meeting of the American Institute of Chemical Engineers, New Orleans, November 8-12, 1981; LBL-13617.

9. W. B. Whiting and J. M. Prausnitz, "A Local-Composition Model for Equations of State for Mixtures," Annual Meeting of the American Institute of Chemical Engineers, New Orleans, November 8-12, 1981; LBL-13568.

* * *

†Work supported by the National Science Foundation.
‡Work supported by the Office of Energy Technology, Fossil Energy Program, U.S. Department of Energy.
§Work supported by the Petroleum Research Fund, administered by the American Chemical Society.

III Nuclear Sciences

A. Low-Energy Nuclear Sciences

1. Heavy Element Chemistry*

a. Actinide Chemistry*

Norman M. Edelstein, Richard A. Andersen, Neil Bartlett, John G. Conway, Kenneth N. Raymond, Glenn T. Seaborg, Andrew Streitwieser, Jr., David H. Templeton, and Alan Zalkin, Investigators

Introduction. The central purpose of the project in heavy element chemistry is to study lanthanide and actinide materials in order to provide the basic knowledge necessary for their safe and economic utilization in present and future technology. The work encompasses related problems of an applied nature in actinide chemistry.

The program includes the preparation of new gaseous, liquid, and solid phases and studies of their physical and chemical properties. Techniques for characterization include x-ray diffraction, optical and vibrational spectroscopy, magnetic resonance, and magnetic susceptibility. Equilibrium and kinetic data for complex formation are measured. From these complementary studies, new insights into the structural and chemical principles of actinide compounds are obtained with which to design new synthetic schemes to produce new materials.

Specific sequestering agents for the actinides continue to be developed and tested. A number of similarities in the coordination chemistry of Fe(III) and Pu(IV) have been noted previously. Based on the similarities in the chemical and the biological transport and distribution properties of Pu(IV) and Fe(III) and the observation that microbes produce specific sequestering agents for Fe(III) that incorporate chelating groups such as hydroxamic acids and catechol, a biomimetic approach has been used to design and synthesize a series of sulfonated catechoylamide sequestering agents that specifically complex plutonium(IV) and other actinide(IV) ions.

The fundamental chemistry of organoactinide, and related organolanthanide compounds, their reactions, structures and bonding, are being explored with the development of new materials, catalysts and reagents as the objective. Detailed spectroscopic studies are continuing on these new materials, on actinide ions diluted in host single crystals, and on the free atoms and free ions of the actinide series in order to understand their electronic structure and to compare the properties of the f transition series with the more thoroughly studied d transition series.

*This work was supported by the Director, Office of Energy Research, Office of Basic Energy Sciences, Chemical Sciences Division of the U.S. Department of Energy under Contract No. DE-AC03-76SF00098.

Specific Sequestering Agents for the Actinides

1. *SYNTHETIC ENTEROBACTIN ANALOGUES: CARBOXAMIDE-2,3-DIHYDROXY TEREPHTHALATE CONJUGATES OF SPERMINE AND SPERMIDINE*†‡

F. L. Weitl, K. N. Raymond and P. W. Durbin

Specific sequestering agents for the actinides continue to be developed and tested. We have noted a number of similarities in the coordination chemistry of Fe(III) and Pu(IV). Indeed, the great biological hazard of plutonium results because, once in the body, it is associated with the iron binding proteins transferrin and ferritin and is deposited essentially irreversibly in iron storage sites. Based on the similarities in the chemical and the biological transport and distribution properties of Pu(IV) and Fe(III) and the observation that microbes produce specific sequestering agents (siderophores) for Fe(III) that incorporate chelating groups such as hydroxamic acids and catechol, a biomimetic approach has been used to design and synthesize a series of sulfonated catechoylamide sequestering agents that specifically complex plutonium(IV) and other actinide(IV) ions.

Two examples of a new class of synthetic polycatecholate ligands, the carboxamido-2,3-dihydroxyterephthalate conjugates of spermine (8, Fig. 1) and of spermidine (10), have been synthesized via the generally useful synthon methyl-2-3-dimethoxyterephthaloyl chloride (6). Initial biological evaluation reveals tetrameric terephthalate (8) to be an extremely effective agent for sequestering and removing plutonium from mice; a single 25-μmol/kg (I.P.) dose of 8 removed 73 percent of the plutonium citrate previously injected (I.V., 1 h earlier). Under the same conditions, trimeric terephthalate (10) excreted only 49 percent of injected plutonium. In vitro kinetic experiments have shown that 10 rapidly and quantitatively removed Fe from human transferrin.

* * *

†This work was partially supported by the National Institutes of Health.

‡Abstract from J. Med. Chem. 24, 203 (1981); (LBL-11412)

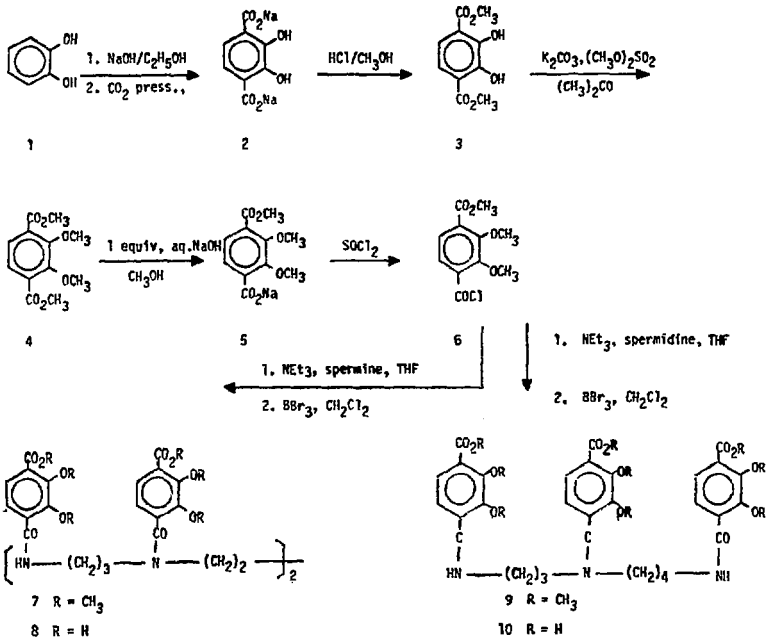

Fig. 1. Carboxamido-2,3,-dihydroxyterephthalate conjugages of spermine and spermidine. (XBL 812-8160)

2. SIDEROPHILIN METAL COORDINATION†‡§

W. R. Harris, C. J. Carrano, V. L. Pecoraro and K. N. Raymond

Since synthetic chelating agents must compete with biological ligands for plutonium, we are interested in the coordination chemistry of the plutonium-protein complexes. We therefore have begun a study on the binding of actinides by human serum transferrin (as a class these iron transport proteins are called siderophilins).

In order to probe the metal ion coordination site in transferrin, the complexation of a series of metal ions by the chelate analogue ethylene-bis(o-hydroxyphenylglycine) [EHPG] has been studied by difference uv spectroscopy. This technique has also been used to study the binding by human transferrin of the actinide ion Th^{4+}, a convenient model for Pu^{4+}.

The results obtained with EHPG taken with previously reported results for di(metallo) transferrin complexes show that two tyrosines are coordinated per metal ion for all the transition metals and the smaller lanthanides. Very large metal ions have difficulty fitting into one of the binding sites, and the number of coordinated metal ions decreases. This differential ability to coordinate large metal ions lends further support for non-equivalent complexation by the two metal binding regions of transferrin. The results obtained with di(thorium)transferrin were not only consistent with those cited above, but differences in Th^{+4} binding as a function of pH were used to deduce further details of metal ion coordination in the two transferrin binding sites.

* * *

†This work was partially supported by the National Institutes of Health.

‡Abstract from J. Am. Chem. Soc. 103, 2231 (1981). (LBL-11878).

§Abstract from Biochemistry, in press. (LBL-11657)

---

3. SYNTHETIC AND STRUCTURAL CHEMISTRY OF TETRAKIS(DIALKYLHYDROXAMATE)-THORIUM(IV) COMPLEXES†‡

W. L. Smith and K. N. Raymond

While hydroxamic acids have been used in quantitative analysis and solvent extraction of actinides, the complexes formed have not been structurally characterized. In order to characterize fully the formulation and coordination geometry of these compounds, as a prelude to the design of large chelating agents incorporating hydroxamate groups, the structures of tetrakis(N-isopropyl-3,3-dimethylbutano- and -2,2-dimethylpropanohydroxamato)thorium(IV) (Fig. 1) have been determined by single-crystal x-ray diffraction.

The complexes $Th[(CH_3)_2CHC(O)N(O)R]_4$ have been prepared from aqueous solutions of Th(IV) and the corresponding hydroxamic acid, for $R = C(CH_3)_3$ or $CH_2C(CH_3)_3$ (Fig. 1, compounds 1 and 2, respectively). Both complexes 1 and 2 are hydrocarbon soluble and remarkably volatile. The uranium(IV) analogue of 1 was also prepared, but the uranium(IV) hydroxamates undergo an internal redox reaction that involves oxygen atom transfer from the ligand to the metal to give a bis(hydroxamate)-uranyl complex and the amide of one hydroxamate ligand. The physical properties of the thorium hydroxamate complexes seem to primarily depend upon their hydrocarbon substituents, and the different steric constraints imposed by the C-substitutent tert-butyl and neopentyl groups of 1 and 2, respectively, give rise to dramatically different coordinate geometries. The t-butyl groups of 1 dominate the stereochemistry of the complex by assuming a tetrahedral disposition around the metal. The coordination polyhedron of 1, which has 4 (S_4) crystallographic symmetry, is nearly cubic. The sterically less constrained neopentyl derivative, 2, shows a more typical eight-coordinate geometry--the D_{2d} trigonal-faced (*mmm*) dodecahedron. Although there is no crystallographically imposed symmetry for 2, the polyhedron is close to the ideal dodecahedron.

†This work was partially supported by the National Institutes of Health.

‡Abstract from J. Am. Chem. Soc. 103, 3341 (1981). (LBL-12156)

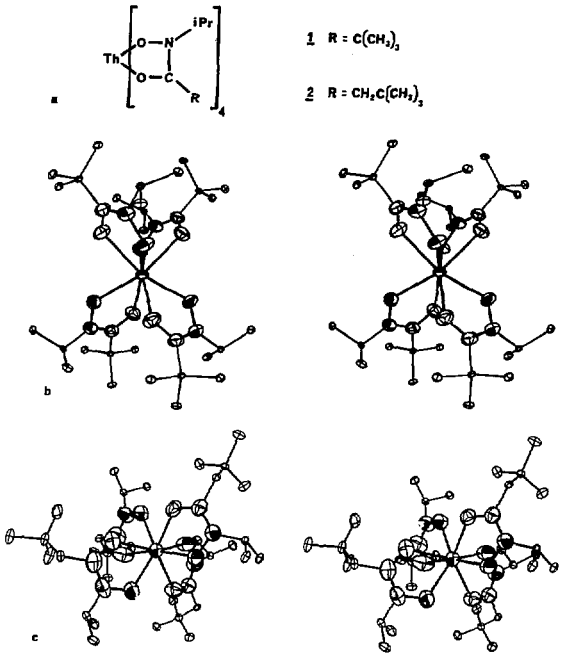

Fig. 1. a) Structural formulas of the thorium hydroxamate complexes.
b) Stereopair of Th[i-PrN(O)C(O)-t-Bu]$_4$ viewed down the dodecahedral mirror plane, perpendicular to c.
c) Stereopair of Th[i-PrN(O)C(O)neopentyl]$_4$ viewed down what would be the twofold axis of the D_{2d} dodecahedron.
(XBL 8112-13075)

4. TRICATECHOLAMIDE ANALOGS OF ENTEROBACTIN AS GALLIUM- AND INDIUM-BINDING RADIOPHARMACEUTICALS†‡

S. M. Moerlein, M. J. Welch, K. N. Raymond and F. L. Weitl

The siderophore enterobactin strongly complexes iron and facilitates its transport into microbial cells. However, it is a cyclic ester and readily hydrolyzes at physiological pH, and hence is not useful as a metal-complexing radiopharmaceutical. Development of 2,3-dihydroxybenzoylamide analogs of enterobactin has led to iron-binding ligands that are characterized by both high stability constants and resistance to solution hydrolysis. Nuclides of gallium and indium have found widespread use in nuclear medicine. Because these are group III B elements with charges and complexation characteristics similar to ferric ion, the applicability of synthetic tricatecholamide enterobactin analogs as gallium- and indium-binding radiopharmaceuticals has been investigated.

Stability constants for the tricatecholate ligands with gallium and indium were determined from competitive exchange experiments with EDTA. Biodistribution and clearance data were obtained using Sprague-Dawley rats.

Isopropyl N-substituted tricatecholamide analogs of enterobactin have been found to complex gallium and indium with very high stability constants and to exhibit in vivo characteristics significantly different from gallium- or indium-transferrin and EDTA. Relatively minor chemical changes altered the pharmacologic characteristics of the tricatecholamide complexes without attenuating the in vivo stability of metal binding. Sulfonation of the catechol rings caused the renal path of excretion to be followed, whereas absence of this functional group allowed for hepatic recognition and elimination into the bowel.

* * *

†This work was partially supported by the National Institutes of Health.

‡Abstract from J. Nucl. Med. 22, 710 (1981).

Synthetic and Structural Studies of Actinides and Other Compounds

1. TERTIARY PHOSPHINE DERIVATIVES OF THE f-BLOCK METALS; PREPARATION OF $X_4MMe_2PCH_2CH_2PMe_2)_2$ WHERE X IS HALIDE, METHYL, AND PHENOXO AND M IS THORIUM OR URANIUM. CRYSTAL STRUCTURE OF TETRA (PHENOXO)Bis[bis(1,2-DIMETHYLPHOSPHINO)ETHANE] *URANIUM(IV)*†

P. G. Edwards, R. A. Andersen, and A. Zalkin

A goal of synthetic chemistry is the creation of new molecules that have no precedent. The successful preparation of molecules that are not supposed to exist offers challenges to classical views of chemical bonding and reactivity and thus, changes the manner in which chemists think about the interaction of molecules. Simple phosphine complexes, R_3P, have not been described for the actinide metals. Indeed, conventional wisdom, based upon failed synthetic attempts, is that tertiary phosphines are very poor ligands to f-block metals. We have begun a study to challenge this concept.

Addition of bis(1,2-dimethylphosphino)ethane, dmpe, to uranium or thorium tetrachloride in dichloromethane gives $MCl_4(dmpe)_2$. These complexes react with four equivalents of methyllithium in diethylether to give the tetramethyl derivatives, $MMe_4(dmpe)_2$. The alkyls react with phenol to give the tetraphenoxides, $M(OPh)_4(dmpe)_2$.

The crystal structure of $U(OPh)_4(dmpe)_2$ has been solved by x-ray methods. The eight coordinate molecule has essentially D_{2d}-symmetry. The average U-O bond length is 2.17 ± 0.01 Å and the U-P bond length is 3.104 ± 0.006 Å.

* * *

†Brief version of LBL-13065.

2. CRYSTAL STRUCTURE OF BIS(PENTAMETHYLCYCLOPENTADIENYL)BIS(PYRIDINE) YTTERBIUM(II)†

T. D. Tilley, R. A. Andersen, B. Spencer, and A. Zalkin

The bonding of organometallic ligands to the f-block metals is thought to be primarily ionic. That is, there is essentially no mixing of metal electrons with ligand electrons, a feature that dominates the transition metal organometallic derivatives of the cyclopentadienyl complexes of these elements. Subtraction of the ionic radius from the crystallographically determined metal to carbon bond length will give the effective ionic radius of the cyclopentadienyl or substituted cyclopentadienyl group. If the bonding is predominantly ionic, the effective radius of the cyclopentadienyl or its substituted analogue should be constant for a wide variety of coordination numbers and geometries.

As part of a program to systematically explore the bonding in these molecules by use of structural methods, we have prepared $Yb(Me_5C_5)_2(py)_2$, as shown in the equation.

$$Yb(Me_5C_5)_2(OEt_2) + 2\ \text{pyridine} \rightarrow Yb(Me_5C_5)_2(py)_2$$

The most important feature of the structure is the average metal-carbon bond length of 2.742 ± 0.016 Å.

Using the ionic radii tabulated by Shannon[1] the effective ionic radius of the Me_5C_5 group in $(Me_5C_5)_2Yb$ complexes that have been structurally characterized can be estimated. These are recorded in Table 1. These radii are essentially constant and fall within the range (1.64 ± 0.04 Å) that has been suggested by Raymond[2] for predominantly ionic bonding of cyclopentadienyl groups in trivalent lanthanide complexes. Clearly the model is appropriate to the divalent derivatives also.

Table 1. Effective ionic radius (Å) of the Me_5C_5 group.

Compound	M-C bond length, Å	Metal ion radius, Å	Effective C_5Me_5- radius, Å	Reference
$Yb(C_5Me_5)_2(py)_2$	2.74(4)	1.14	1.60	this work
$Yb(C_5Me_5)_2(thf)$	2.66(2)	1.08	1.58	a
$Yb(C_5Me_5)_2(S_2CNEt_2)$	2.63(3)	0.985	1.64	b
$Yb(C_5Me_5)_2(thf)[Co(CO)_4]$	2.596(2)	0.985	1.61	c
$[Yb(C_5Me_5)_2]_2[Fe_3(CO)_{11}]$	2.57(1)	0.985	1.59	d
$[Li(OEt_2)_2][(C_5Me_5)_2YbCl_2]$	2.611(4)	0.985	1.63	e
$Yb(C_5Me_5)AlCl_4$	2.584(5)	0.985	1.60	e

a. Ref. 2
b. T. D. Tilley, R. A. Andersen, A. Zalkin, and D. H. Templeton, submitted.
c. T. D. Tilley and R. A. Andersen, J. Chem. Soc. Chem. Comm., in press.
d. T. D. Tilley and R. A. Andersen, submitted.
e. P. L. Watson, J. F. Whitney, and R. L. Harlow, Inorg. Chem., in press.

* * *

†Brief version of LBL-13380.

1. R. D. Shannon, Acta Cryst. A 32, 751 (1976).
2. K. N. Raymond and C. W. Eigenbrot, Acc. Chem. Res. 13, 276 (1980).

3. BIS(PENTAMETHYLCYCLOPENTADIENYL)CARBOXYLATO AND DITHIOCARBAMATO DERIVATIVES OF NEODYMIUM(III) AND YTTERBIUM(III). CRYSTAL STRUCTURE OF BIS(PENTAMETHYLCYCLOPENTADIENYL)DIETHYLDITHIO CARBAMATO YTTERBIUM†

T. D. Tilley, R. A. Andersen, A. Zalkin, and D. A. Templeton

One of our synthesis goals has been the preparation of base-free derivatives of the divalent lanthanide metals of the type $M(Me_5C_5)_2$. These molecules are of interest since they will be highly coordinatively unsaturated (a maximum coordination number of six is possible if the complexes are monomeric), a prerequisite for catalytic or stoichiometric synthesis at metal centers. Further, the large, divalent metal atoms can be oxidized to their trivalent oxidation state and fascile oxidation reactions are likely.

One approach to the synthesis of derivatives of this type is the reduction in non-basic solvents of molecules of the type $M(Me_5C_5)_2XY$ where XY are O_2CR or S_2CNR_2. The acetate and dithiocarbamate complexes were prepared as shown. Unfortunately, we have been unable to reduce these trivalent species.

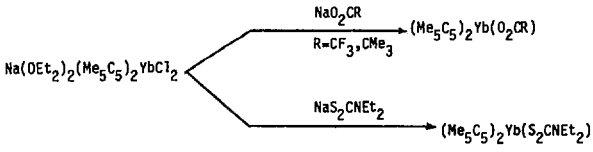

The dithiocarbamate complex is one of the few complexes in which sulfur is coordinated to a lanthanide metal. In order to determine the ytterbium to sulfur bond length (none have been determined) we have determined the crystal structure by x-ray methods. The Yb-S bond length is 2.70(1) Å. The average Yb-C bond length is 2.63 ± 0.03 Å.

* * *

†Brief version of LBL-13010.

4. PREPARATION AND CRYSTAL STRUCTURE OF BIS(PENTAMETHYLCYCLOPENTADIENYL) YTTERBIUM(III) TETRACARBONYL COBALTATE(TETRAHYDROFURAN); AN YTTERBIUM ISOCARBONYL(Yb-OC-Co) BOND†

T. O. Tilley and R. A. Andersen

The activation of CO by coordination to a transition metal, or transition metals, so that the carbon monoxide can be reduced by hydrogen is a challenging and useful reaction. Our strategy for exploring this chemistry is to use a divalent lanthanide metal complex, $Yb(Me_5C_5)_2$, to act as an oxidizing agent for transition metal carbonyls. Transfer of an electron into the lowest unoccupied molar orbital of a transition metal fragment will reduce the bond order of the CO and make it more susceptible for future reduction with hydrogen. Further, the oxidized lanthanide group will coordinate to the oxygen atom of the transition metal carbonyl group. This will cause a charge disparity in the $\underline{M}-\underline{C} \equiv \underline{O} - M'$ unit (where M is the transition metal and M' is a lanthanide metal) as shown. The charge disparity will greatly increase the tendency of the CO group to react with reducing agents.

This strategy was tested by allowing two molar equivalents of $(Me_5C_5)_2Yb(OEt_2)$ to react with $Co_2(CO)_8$, giving $(ME_5C_5)_2Yb\ Co(CO)_4$. Crystallization of this complex from tetrahydrofuran gives $(Me_5C_5)_2Yb\ Co(CO)_4(thf)$, whose structure was elucidated by x-ray methods. The most important feature to emerge from the structure is that the C(21)-O(1) bond length of 1.188(3) Å is significantly longer and therefore weaker than the average C(22,23,24)-O(2,3,4) bond length of 1.14 ± 0.02 Å, due to coordination of the former to the acidic lanthanide metal atom.

Thus, the strategy of using divalent lanthanide complexes to act as electron transfer reagents and Lewis acids towards transition metal carbonyls is a useful synthetic principle.

* * *

†Brief version of LBL-12844.

5. CONCERNING THE REACTION OF METALLOCENE DICHLORIDES OF TITANIUM(IV) AND ZIRCONIUM(IV) WITH LITHIUM BIS(TRIMETHYLSILYL)AMIDE†

S. J. Simpson and R. A. Andersen

In the 1980 annual report we described the preparation, reaction chemistry and mechanism of formation of the novel metallocycles, $[(Me_3Si)_2N]_2\overline{MCH_2SiMe_2NSiMe_3}$, where M is thorium or uranium. In order to probe the differences between the early transition metals (Ti and Zr) and the actinide metals we have begun a comparative study of the chemistry of these metals.

Initially our aim was to understand, in a mechanistic sense, the reaction of Cp_2TiCl_2 with $LiN(SiMe_3)_2$ to give $Cp_2\overline{TiCH_2SiMe_2N}(SiMe_3)$, since there is considerable confusion in the literature concerning its synthesis. Addition of one or two molar equivalents of $LiN(SiMe_3)_2$ to Cp_2TiCl_2 gives $Cp_2TiN(Si(Me_3)Cl$. Vacuum sublimation gives the metallocycle, $Cp_2\overline{TiCH_2SiMe_2NSiMe_3}$ and HCl. In contrast, reaction of Cp_2ZnCl_2 with two molar equivalents of $LiN(SiMe_3)_2$ gives $Cp_2Zr[N(SiMe_3)_2]_2$. The different reactivity of the metallocene dichlorides with $LiN(SiMe_3)_2$ can be most readily ascribed to the larger size of zirconium relative to titanium. Thus, the larger Zr atom can readily accommodate the two sterically large $(Me_3Si)_2N$ ligands without severe intramolecular repulsive interactions. A zirconium metallocycle, $Cp_2\overline{ZrCH_2SiMe_2NSiMe_3}$, can be prepared from Cp_2ZrHCl and $LiN(SiMe_3)_2$ by loss of hydrogen from $Cp_2ZrN(SiMe_3)_2H$ by a γ-elimination process.

* * *

†Brief version of LBL-12195.

6. SYNTHESES AND CHARACTERIZATION OF $(\eta^5-C_5H_5)_2U(NR_2)_2$ COMPOUNDS†

A. L. Arduini,‡ N. M. Edelstein, J. D. Jamerson,‡ J. G. Reynolds, K. Schmid,‡ and J. Takats‡

The synthesis of uranocene, $U(COT)_2$, has rekindled interest in the field of organoactinide chemistry in general and organouranium complexes in particular. Although a large variety of complexes have been synthesized, a review of the literature reveals a paucity of Cp_2UX_2- type complexes. The logical entry into this area of chemistry, "Cp_2UCl_2," appears to be a mixture of Cp_3UCl and $Cp_2UCl_2L_2$ (L=Lewis base). Only recently, by the clever use of the bulky pentamethylcyclopentadienyl ligand system, Marks et al. have succeeded in isolating $[C_5(CH_3)_5]_2UCl_2$ and utilized it as a versatile precursor to other $[C_5(CH_3)_5]_2UR_2$ complexes which have very rich chemistries of their own.

Our approach to the synthesis of Cp_2UX_2 complexes was based on the expectation that, given a suitable ligand, a stable and authentic Cp_2UY_2 complex could obtain. Furthermore, if Y happens to be an easily displaceable ligand as well, the material would provide an entry into the elusive area of Cp_2UX_2 (X=some functional group) type compounds.

The reaction of 2 equiv. of cyclopentadiene with $U(NPr_2)_4$ and the reaction of 1.5 equiv. of cyclopentadiene with $U(NEt_2)_4$, generated in situ, gives the corresponding $Cp_2U(NR_2)_2$ complexes in good yields. However, $U(N\text{-}i\text{-}Pr_2)_4$ does not react with cyclopentadiene at room temperature and

$U(NMe_2)_4$ gives mixture of $Cp_2U(NMe_2)_2$ and $CpU(NMe_2)$. Excess cyclopentadiene also reacts with $Cp_2U(NEt_2)_2$ to produce $Cp_3U(NEt_2)$. The transamination reaction of $Cp_2U(NEt_2)$ with pyrrole and 2,3-dimethylpyrrole gives mixtures of products; however, ethyl 3,4,5-trimethylpyrrole-2-carboxylate gives $Cp_2U[NC_4Me_3(COOEt)]_2$, and the reaction with 1 equiv. of diphenylamine yields $Cp_2U(NEt_2)((NPh_2)$. It is argued that the reactivity sequence and the stability of $Cp_2U(NR_2)_2$ compounds are best explained by steric effects. The spectral characteristics of the $Cp_2U(NR_2)_2$ complexes show that the compounds possess η^5-cyclopentadienyl moieties and monomeric solution behavior with no primary solvent interaction. In $Cp_2U[NC_4Me_3(COOEt)]_2$, additional interaction between uranium and oxygen of the carboxylate functionality is postulated.

* * *

†Brief version of LBL-13368.

‡Department of Chemistry, University of Alberta, Edmonton, Alberta, Canada T6G 2G2.

7. SYNTHESIS AND STRUCTURE OF DICYCLOPENTENOURANOCENE, $U[C_8H_6(CH_2)_3]_2$†

Allan Zalkin, David H. Templeton, Wayne D. Luke and Andrew Streitwieser, Jr.

As part of a continuing study of annulated derivatives[1,2] of uranocene[3] we report the synthesis and X-ray structure determination of bis-π-(cyclopenteno-[8]annulene)uranium(IV) (dicyclopentenouranocene). It was made by reaction of UCl_4 with dipotassium bicyclo[6.3.0]undeca-2,4,6-triene-1,8-diide. This compound was expected to involve a conformation sufficiently well defined to assist nmr interpretation. Also it is the first unstrained uranocene in which the ring-U axis is not a C_2 symmetry axis, and the position of the uranium is less restricted by symmetry than in previous examples.

The ^1H NMR (toulene-d_8) spectrum at 30°C showed six sharp well-resolved resonances upfield from TMS, -8.3 ppm (m, 2H), -18.8 ppm (m, 4H), -23.1 ppm (s, 4H), -32.6 ppm (m, 2H), -34.2 ppm (s, 4H), -41.2 ppm (s, 4H), and one resonance downfield from TMS, +24.4 ppm (m, 4H). The ^{13}C NMR spectrum (dioxane-d_8) at 39°C showed four broad peaks at 308.0, 296.9, 279.0, and 268.5 ppm downfield from TMS and two sharp peaks at 13.4 and -32.5 ppm.

The magnetic susceptibility was measured on the bulk solid from 2.4 to 95.6°K. Above 20°K the magnetic susceptibility follows the Curie-Weiss Law with $C = 0.743 \pm 0.005$ emu °K mol^{-1} $\mu = 2.4 \pm 0.1$ B.M. and $\theta = 16.6° \pm 0.5°$. Below 10°K the magnetic moment is independent of temperature with $\chi m = 2.56 \pm 0.03 \times 10^{-2}$ csu/mole. Using a diamagnetic correction of -187×10^{-6} emu mol^{-1} the corrected values are $C = 0.714 \pm 0.005$ emu °K mol^{-1}, $\mu = 2.4 \pm 0.1$ B.M. and $\theta = 16.1° \pm 0.5°$.[4]

The compound crystallizes in the orthorhombic space group Pbca with 8 molecules in the unit cell with dimensions $a = 17.393(8)$ Å, $b = 22.468(12)$ Å and $c = 8.931(4)$ Å. The structure was determined by single-crystal x-ray methods. The molecular structure (Fig. 1) has the uranium atom centrally sandwiched between the two 8-membered rings with a U-ring distance of 1.92 Å, in good agreement with

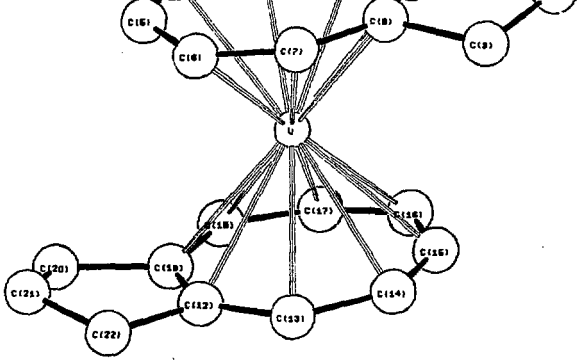

Fig. 1. ORTEP ball and spoke view of the molecule. (XBL 7811-12981)

the other uranocenes. The COT rings of the molecule are rotated about 8° from a staggered configuration. In other uranocenes both staggered and eclipsed configurations have been reported.

* * *

†Brief version of LBL-13216, August 1981.

1. A. Zalkin, D. H. Templeton, S. R. Berryhill, W. O. Luke, Inorg. Chem. 18, 2287 (1979).
2. W. D. Luke, S. R. Berryhill, A. Streitwieser, Jr., Inorg. Chem., in press.
3. A. Streitwieser, Jr., U. Muller-Westerhoff, G. Sonnischen, F. Mares, D. G. Morrell, K. O. Hodgson, C. A. Harmon, J. Am. Chem. Soc. 95, 8644 (1973).
4. D. Karraker, J. Stone, E. Jones, Jr., N. Edelstein, J. Am. Chem. Soc. 92, 4841 (1970).

8. SYNTHESIS AND STRUCTURE OF A URANYL COMPLEX WITH A DISULFIDE LIGAND†

Dale. L. Perry, Allan Zalkin, Helena Ruben, and David. H. Templeton

Bubbling carbonyl sulfide through a cold solution of di-n-propylamine in methanol, followed by the addition of $UO_2Cl_2 \cdot 3H_2O$ after one week produces dark olive-green crystals of $[n\text{-}C_3H_7)_2NH_2^+]_2[UO_2((n\text{-}C_3H_7)_2NCOS)_2(S_2)]^{-2}$. This complex crystallizes in the orthorhombic space group Pcan with cell dimensions a = 15.326(6) Å, b = 17.474(6) Å, c = 14.728(6) Å and four dimensions a = 15.326(6) Å, b = 17.474(6) Å, c = 14.728(6) Å and four molecules per unit cell.

The molecular structure was determined by single-crystal x-ray techniques (Fig. 1). A noteworthy feature of the complex is the disulfide ligand which is bonded in a "side-on" fashion to the central uranium atom. The uranium-sulfur bond distance involving the disulfide group is 2.714 Å, shorter than the 2.871-Å bond length between uranium and the sulfur atom in the monothiocarbamate ligand. The sulfur-sulfur distance is 2.05 Å.

This compound provides the first example of this type of disulfide bonding in an actinide element complex.

* * *

†Brief version of LBL-10654, May 1981.

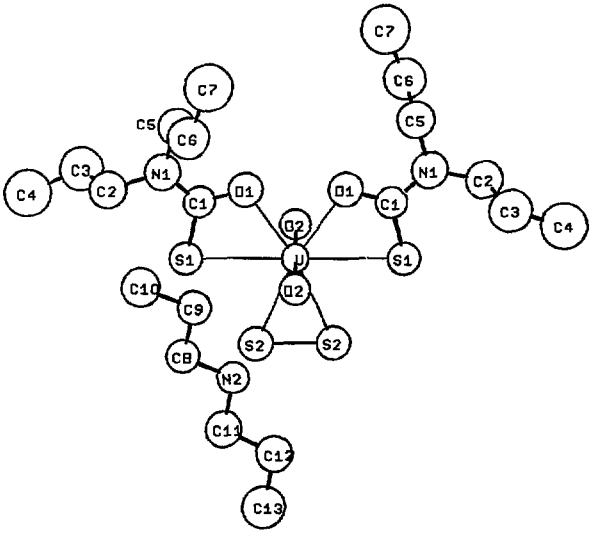

Fig. 1. ORTEP view of the structure. (XBL 784-8319)

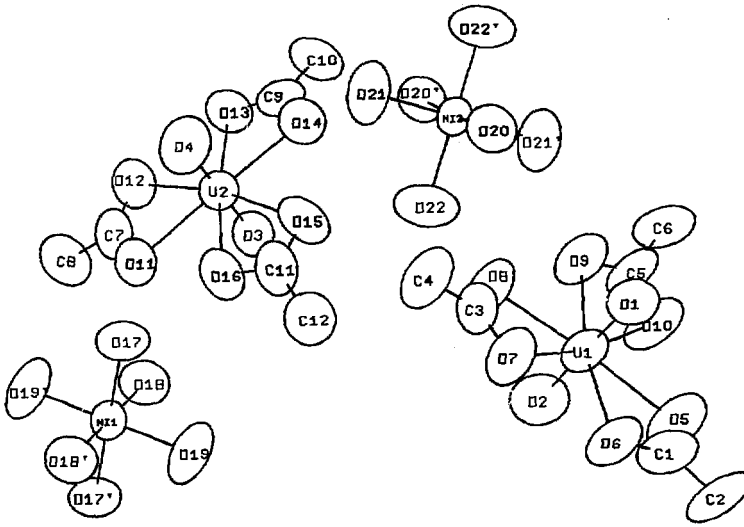

Fig. 1. ORTEP drawing of the nickel uranyl acetate structure.
(XBL 812-8221)

9. THE STRUCTURE OF NICKEL URANYL ACETATE HEXAHYDRATE†

Allan Zalkin, Helena Ruben, and David H. Templeton

As part of a study of uranium salts we prepared crystals of $Ni(H_2O)[UO_2(CH_3COO)_3]_2$ and determined its structure by single crystal x-ray methods. The material crystallizes in the monoclinic space group $P2_1/c$ with cell dimensions $\underline{a}$ = 13.387(3), $\underline{b}$ = 14.727(3), and $\underline{c}$ = 15.349(3) Å, β = 91.12 with $\overline{4}$ molecules in the unit cell.

The structure (Fig. 1) consists of packing of octahedral $Ni(H_2O)_6$ cations and hexagonal bipyramidyl $(CH_3COO)_3UO_2$ anions. Although there are two crystallographically different formula units in the asymmetric unit, their geometry is nearly the same. With some small shifts in the positional parameters, most of the structure could be described in the orthorhombic space group Pbca with only one formula unit per asymmetric unit; the monoclinic angle is only 1.12° from orthogonality. Only the water molecules deviate more than 0.3 Å from this orthorhombic symmetry.

All of the hydrogen atoms of the water molecules are involved in hydrogen bonds. This hydrogen bonding may explain why the structure deviates from the orthorhombic symmetry.

* * *

†Brief version of LBL-12551, April 1981.

10. THE SYNTHESIS AND CHARACTERIZATION OF $(UCp_3)_2$(PYRAZINE) and $[U(MeCp)_3]_2$(PYRAZINE): π-BRIDGED DIMERS OF U^{3+} †

C. W. Eigenbrot, Jr. and K. N. Raymond

In the organometallic chemistry of the lanthanide and actinide elements, a continuing question has been the role of f-electrons in the bonding. As part of a program to create, examine, and explain structural and magnetic probes of this bonding, we have sought the synthesis of appropriate dimeric species of uranium for detailed magnetic characterization.

The title compounds, formed by the reaction of $U(C_5H_5)_3(C_4H_8O)$ and $U(C_6H_7)_3(C_4H_8O)$ with pyrazine ($C_4H_4N_2$), have been characterized by elemental analysis, mass, infrared, ^1H nmr, and electronic spectra and by x-ray powder patterns. The $[U(C_6H_7)_3]_2(C_4H_4N_2)$ exhibits anomalous magnetic behavior that remains under investigation.

* * *

†Abstract from manuscript submitted to Polyhedron (LBL-13074).

11. SYNTHESIS AND CRYSTAL STRUCTURE OF $UCp_3(C_3H_3N_2)$. A NEW MODE OF PYRAZOLATE BONDING†

C. W. Eigenbrot, Jr., and K. N. Raymond

The title compound has been prepared by the reaction of tricyclopentadienyluranium chloride (UCp_3Cl) and sodium pyrazolate ($NaC_3H_3N_2$) in tetrahydrofuran (THF). The compound has been characterized by its infrared, visible-near-IR, ^1H NMR, and mass spectra and by single-crystal x-ray diffraction. The molecular structure consists of discrete $UCp_3(C_3H_3N_2)$ molecules in which the uranium(IV) ion is coordinated by three η^5-Cp rings in a nearly trigonal array similar to that of other lanthanide and actinide MCp_3X structures. However, unlike these other structures, the 11-coordinate geometry is achieved by having both of the adjacent nitrogen atoms of the pyrazolate ring coordinate to the metal ion so that the local twofold axis of the pyrazolate ring and the local threefold axis of the UCp_3 fragment coincide. This is the first example of this type of endobidentate η^2 coordination for the pyrazolate anion (see Fig. 1).

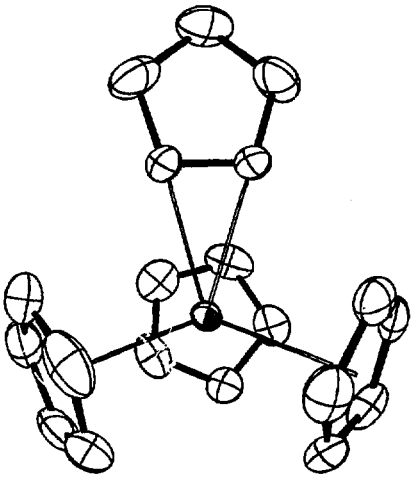

Fig. 1. Perspective drawing of $UCp_3(C_3H_3N_2)$. Thermal ellipsoids are drawn at the 50 percent probability level. The view is perpendicular to the pseudo-threefold axis. (XBL 804-9339)

* * *

†Abstract from *Inorg. Chem.* 20, 1553 (1981); LBL-11877.

12. CRYSTAL AND MOLECULAR STRUCTURE OF $[Nd(tren)_2(CH_3CN)](ClO_4)_3$ †

C. W. Eigenbrot, Jr. and K. N. Raymond

Lanthanide coordination chemistry is dominated by oxygen donor ligands, especially by chelate ligands such as β-diketonates or EDTA. However, recently several nitrogen-bonded complexes have been well characterized. As with oxygen donor ligands, amine complexes are generally more stable for chelating ligands. For example, pyridine complexes exist only in solution, while complexes with ethylenediamine or 1,10-phenanthroline can be isolated. We are interested in the structures of compounds of the type $Ln(tren)X_3$ [tren = $N(CH_2CH_2NH_2)_3$] and $Ln(tren)N_2X_3$ and their possible use as templates in macrocycle synthesis. There has been a continuing interest in the use of lanthanide ions as shift reagents in nmr spectroscopy. During the last decade, lanthanide shift reagents have been actively investigated and utilized in simplifying complex nmr spectra. The utility of these compounds has been hampered to some extent by the simplifying assumptions that must be made--including the geometries. It would be extremely interesting to have a substitutionally inert lanthanide complex formed by an amine macrocycle, such as might be produced from $Ln(tren)_2$. This report describes the structural characterization of $[Nd(tren)_2(CH_3Cn)](ClO_4)_3$, as the first step in this project.

The crystal and molecular structure of the title compound [tren = $N(CH_2CH_2NH_2)_3$] has been determined by single crystal x-ray diffraction. The structure consists of a three-dimensional hydrogen-bonding network of perchlorate anions and $[Nd(tren)_2(CH_3CN)]^{3+}$ cations at general positions in the unit cell. The coordination of the Nd^{3+} ion is by two tetradentate tren ligands and the nitrogen atom from an acetonitrile molecule, for a total coordination number of 9. The coordination polyhedron is a tri-capped trigonal prism. A similar complex of 1,5,9,13-tetraazacyclohexadine,

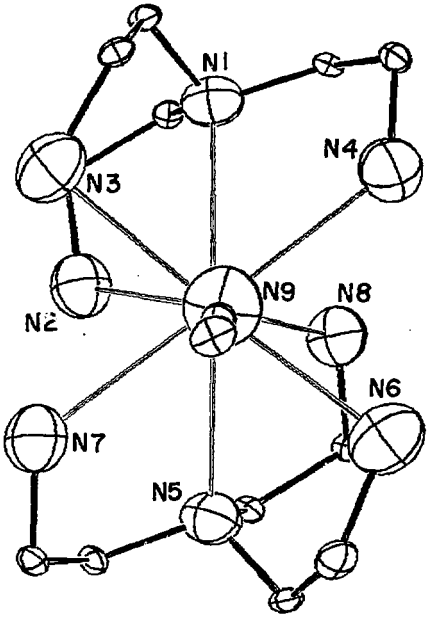

Fig. 1. ORTEP drawing of the molecular cation of $[Nd(tren)_2(CH_3CN)]-ClO_4)_3$ emphasizing the pseudo-twofold symmetry. The nitrogen atoms are drawn at the 50 percent contour. For clarity, the carbon atoms are drawn at the 10 percent contour.
(XBL 811-7792)

$[Nd([16]aneN_4)][ClO_4]_3$, has been prepared and its structure partially characterized (see Fig. 1).

* * *

†Abstract from manuscript submitted to Inorg. Chem; LBL-13075.

Physical and Spectroscopic Properties

1. ELECTRONIC STRUCTURE OF UCl_5: A REEXAMINATION†

E. Sonnie‡ and N. Edelstein

The optical and electron paramagnetic resonance (epr) spectra of UCl_6^-, an anion which has the $5f^1$ configuration outside closed electronic shells, have been studied extensively. The spectra are particularly easy to interpret because of the high symmetry (O_h) at the site of the U(V) ion, which results in an isotropic g value and an optical spectrum with at most four electronic transitions. The compound UCl_5, which is dimeric in the solid state, has a distorted octahedral symmetry at the site of the U(V) ion. Nevertheless, the optical spectrum is closely related to that for the octahedral UCl_6^- anion, and the epr spectrum of a UCl_5 powder has been reported to be a broad line centered about g = 1.18, like that of UCl_6^-. This apparent isotropy is anomalous in view of the distorted symmetry site of the uranium ion.

On the basis of the absorption spectrum of UCl_5 recorded at 4.2 K, Leung and Poon[1] attempted a determination of both the spin-orbit coupling constant and the crystal field parameters. Their parameters, however, led to a calculated g-tensor at variance with the position of the electron paramagnetic resonance line observed by Miyake et al.[2] From the absorption and EPR spectra, assuming the validity of the Newman superposition model, and taking the point symmetry group on each uranium of the $(UCl_5)_2$ dimer as C_{2v}, we obtain one and only one satisfactory solution, namely a set of parameters that reasonably reproduce the observed absorption peaks, and lead to the following principal values of the g-tensor:

g_x = 0.226 (unobservable);

g_y = 1.187;

g_z = 1.186

Therefore, the paradox stemming from the apparent isotropy of the EPR signal for a species of low point symmetry is resolved.

* * *

†Abstract from Physica 102B, 93 (1980).
‡Departement de Physico-Chimie, CEN-Saclay, B.P. No. 2, 91190 Gif-sur-Yvette, France.

2. OPTICAL SPECTRA AND ZEEMAN EFFECT FOR Pr^{3+} AND Nd^{3+} IN $LuPO_4$ AND YPO_4 †

T. Hayhurst, G. Shalimoff, J. G. Conway, N. Edelstein, L. A. Boatner,‡ and M. M. Abraham‡

The relatively long half-lives (10^3-10^5 yr) of many of the actinide isotopes produced as a by-product of nuclear reactors represent a severe constraint on the selection of a suitable substance for the primary isolation or containment of nuclear wastes. An examination of geological evidence has recently led to the suggestion[1,2] that synthetic analogs of the mineral monazite $[(La,Ce,Nd,Y,...)PO_4]$ have chemical and physical properties that make them attractive candidates as host materials for long-term storage of actinide wastes. Accordingly, the characterization of possible sites where actinide (and other) impurity ions can be incorporated in these materials and a determination of the oxidation states of these ions is pertinent to understanding the interrelationship between the chemical and physical properties of the lanthanide orthophosphate-impurity systems and the parameters appropriate to an acceptable stable waste form.

Absorption spectra of Pr^{3+} and Nd^{3+} diluted in $LuPO_4$ and YPO_4 crystals at a lanthanide ion site of D_{2d} symmetry, have been measured from 4,000 to 30,000 cm^{-1} at liquid He and N_2 temperatures. Fluorescence was observed for Pr^{3+} and Nd^{3+} in YPO_4, and Zeeman spectra were obtained in the visible region. The transitions were assigned and fit to a semi-empirical Hamiltonian with adjustable parameters via a least squares procedure. Satisfactory fits and reasonable agreement between calculated and measured g values were obtained.

Work is currently in progress on Ho^{3+}, Yb^{3+}, and Tm^{3+} in these same host materials to provide parameters from additional members of the lanthanide series and to establish trends for all the crystal field parameters. The analysis of a number of lanthanide ions in YPO_4 and $LuPO_4$ should make analysis of the spectra of the corresponding actinide ions easier. Crystals of U^{3+}:$LuPO_4$ are already available and preliminary investigations are in progress.

* * *

†Brief version of LBL-13388, submitted to J. Chem. Phys.

‡Solid State Division, Oak Ridge National Laboratory, Oak Ridge, TN 37380.

3. THE SYNTHESES AND ELECTRONIC STRUCTURES OF DECAMETHYLMETALLOCENES†

J. L. Robbins,‡ N. Edelstein, B. Spencer,§ and J. C. Smith‖

Since the discovery and structural characterization of ferrocene (η^5-$(C_5H_5)_2Fe$ or Cp_2Fe) in the early 1950s, at least one cyclopentadienyl derivative of every main group and transition metal, as well as most f-block metals, has been prepared and characterized. A large number of monoalkyl- and monoaryl-substituted cyclopentadienyl metal compounds have also been prepared, but extensive study of peralkylcyclopentadienyl metal compounds was not practical until the recent development of convenient and efficient synthetic routes to pentamethylcyclopentadiene and alkyltetramethylcyclopentadienes. A number of studies have now appeared demonstrating some dramatic differences between the structure and chemistry of cyclopentadienyl and pentaalkylcyclopentadienyl metal compounds. In general, these differences can be attributed to the relative steric bulk of the Me_5Cp^- ligand or to its lack of a reactive ring carbon-to-hydrogen bond. The latter feature has proven especially useful in studies of early transition metal cyclopentadienyl derivatives where a common mode of reactivity involves insertion of the metal into a C-H bond of C_5H_5.

The steric effects of complex ring alkylation have proven particularly influential in the structure and chemistry of uranium(IV) and thorium(IV) cyclopentadienyl derivatives. Complexes of these metals containing four Cp^- rings (Cp_4M; M=U,Th), three Cp^- rings (Cp_3MCl; M=U,Th), and one Cp^- ring ($CpUCl_3$(1,2-dimethoxyethane)) can be isolated, depending on reaction conditions and stoichiometry. The missing member of this series, Cp_2UCl_2, disproportionates to tris- and monocyclopentadienyl derivates in donor solvents and authentic Cp_2UCl_2 has not yet been isolated.

With pentamethylcyclopentadienide or ethyltetramethylcyclopentadienide ($EtMe_4Cp^-$), monomeric uranium(IV) and thorium(IV) compounds containing one peralkylated ring, ($(Me_5Cp)ThCl_3$; $(EtMe_4Cp)UCp_2Cl$) and two peralkylated rings ($(Me_5Cp)_2MCl_2$; M=Th,U; $(EtMe_4Cp)_2UCl_2$) have been prepared, but complexes containing three peralkylated rings have proven elusive.

A third possible consequence of complete alkylation of the Cp^- ring is a significant effect on the electron donor/acceptor properties of the ring and the electronic structures of the metal derivatives. Evidence for such an effect was described in our earlier studies of decamethylmanganocene. Magnetic studies of decamethylmanganocene showed that permethylation of the Cp^- ring results in an exclusively low-spin, $^2E_{2g}$ electronic configuration, in contrast to other manganocenes where high-spin, $^6A_{1g}$, states are thermally populated. In spite of the fact that Me_5Cp^- is a much bulkier ligand than Cp^-, the metal-to-ring carbon distances in $(Me_5Cp)_2Mn$ are about 0.3 Å shorter than those in high-spin manganocenes. Manganocenes with the low-spin configuration are inert towards ring displacement and hydrolysis. The permethylated complex does undergo reversible one-electron oxidation and reduction to give low-spin 16- and 18-electron derivatives for which no analogs exist in other manganocenes.

These results indicate that the ligand field strength of the Cp^- ring is significantly enhanced by the complete replacement of the hydrogens with electron-donating methyl groups. In this paper we describe studies that determine the nature, scope, and magnitude of such an effect via a systematic comparison of the chemistry and electronic structures of the metallocenes and the decamethylmetallocenes containing the first-transition series metals, V, Cr, Fe, Co, and Ni. Magnetic studies show the decamethylmetallocenes possess the same ground electronic configurations as their metallocene counterparts. Comparison of UV-visible spectra (and derived parameters) of the d^3, d^6, and d^8 metallocenes and decamethylmetallocenes is used to determine the effects of ring peralkylation on the ligand field splitting.

* * *

†Brief version of LBL-12258, to be published in J. Am. Chem. Soc.

‡Exxon Research and Engineering Co., P.O. Box 45, Linden, NJ 07036.

§Chemistry Department Beloit College, Beloit, WI 53511.

‖Solar Energy Research Institute, Golden, CO 80401.

4. SPECTRUM AND ENERGY LEVELS OF Nb^{4+}†

D. T. Kagan,‡ J. G. Conway, E. Meinders§

Nb^{4+} is isoelectronic with rubidium atom and has one active electron. The ground state is

$4p^6 4D$. Trawick[1] and Charles[2] derived 10 levels from 12 lines. The present analyses yield 30 levels derived from 84 lines.

The spectrum was excited in a vacuum sliding spark in an LRC circuit. The inductance and resistance were variable. Peak current pulses of 30 A and 1000 μsec top 1200 A and 50 μsec were possible. Data were recorded on spectrographs at Lawrence Berkeley Laboratory and the Zeeman Laboratory.

Isoelectronic data of various authors were treated by various methods such as curve fitting, quantum-defect extrapolation and core-polarization calculations to estimate the energy of new levels. The $4f^6$ ionization limit was calculated using the series-extrapolation formulas of Edlen.[3] The best value is most likely the one using 5g, 6g, 7g, 6h, 7h and 7i because these configurations interact very little with the core and thus are most hydrogen-like. The ionization limit of Nb^{4+} is 407897 ± 40 cm^{-1}. Further analysis of Nb^{4+} will require a study of the configurations of $4p^5 4d^2$, $4p^5 4d5s^{10}$ and $4p^5 5p^2$.

* * *

†Brief version of LBL-12404, published in J. Opt. Soc. Am. 71, 1193 (1981).

‡Physics Department, California State University, Chico, CA 95929.

§Zeeman-Laboratorium, Universiteit Van Amsterdam, Amsterdam, Netherlands.

1. M. W. Trawick, "The Spectra of Columbium V and Molybdenum VI," Phys. Rev. 46, 63 (1934).
2. G. W. Charles, "A Study of the Spectra of Columbium and Molybdenum in the Extreme Ultraviolet," Phys. Rev. 77, 120 (1950).
3. B. Edlen, "Atomic Spectra," Handb. Phys. 27, 80 (1964).

1981 PUBLICATIONS AND REPORTS

Refereed Journals

†1. F. L. Weitl, K. N. Raymond and P. W. Durbin, "Synthetic Enterobactin Analogues. Carboxamido-2,3-dihydroxyterephthalate Conjugates of Spermine and Spermidine," J. Med. Chem. 24, 203 (1981); LBL-11412.

†2. T. P. Tufano, V. L. Pecoraro and K. N. Raymond, "Ferric Ion Sequestering Agents. Kinetics of Iron Release from Ferritin to Catechoylamides," Biochim. Biophys. Acta 668, 420 (1981).

†3. V. L. Pecoraro, F. L. Weitl and K. N. Raymond, "Ferric Ion-Specific Sequestering Agents. 7. Synthesis, Iron-Exchange Kinetics, and Stability Constants of N-Substituted, Sulfonated Catechoylamide Analogues of Enterobactin," J. Am. Chem. Soc. 103, 5133 (1981); LBL-11807.

†4. W. R. Harris, K. N. Raymond and F. L. Weitl, "Ferric Ion Sequestering Agents. 6. The Spectrophotometric and Potentiometric Evaluation of Sulfonated Tricatecholate Ligands," J. Am. Chem. Soc. 103, 2667 (1981).

†5. W. R. Harris, C. J. Carrano, V. L. Pecoraro and K. N. Raymond, "Siderophilin Metal Coordination. 1. Complexation of Thorium by Transferrin: Structure-Function Implication," J. Am Chem. Soc. 103, 2231 (1981); LBL-11878.

†6. V. L. Pecoraro, W. R. Harris, C. J. Carrano, and K. N. Raymond, "Siderophilin Metal Coordination. 2. Difference Ultraviolet Spectroscopy of Di-, Tri-, and Tetravalent Metal Ions with Transferrin and Ethylene-bis(o-hydroxyphenylglycine)," Biochemistry, in press; LBL-11657.

†7. W. L. Smith and K. N. Raymond, "Specific Sequestering Agents for the Actinides. 6. Synthetic and Structural Chemistry of Tetrakis(N-Alkylalkane-hydroxamato)thorium(IV) Complexes," J. Am. Chem. Soc. 103, 3341 (1981); LBL-12156.

†8. S. M. Moerlein, M. J. Welch, K. N. Raymond and F. L. Weitl, "Tricatecholamide Analogs of Enterobactin as Gallium- and Indium-Binding Radiopharmaceuticals," J. Nucl. Med. 22, 710 (1981).

9. C. W. Eigenbrot, Jr. and K. N. Raymond, "Synthesis and Crystal Structure of $UCp_3(C_3H_3N_2)$. A New Mode of Pyrazolate Bonding," Inorg. Chem. 20, 1553 (1981); LBL-11877.

‡10. M. J. Miller, M. H. Lyttle and A. Streitwieser, Jr., "tert-Butyl-Substituted Cyclooctatetraenes," J. Org. Chem. 46, 1977 (1981), LBL-12138.

‡11. W. D. Luke and A. Streitwieser, Jr., "The Barriers to Ring Rotation in 1,1',4,4'-tetra-t-butyluranocene and 1,1',3,3'-tetra-t-butylferrocene," J. Am. Chem. soc. 103, 3241 (1981); LBL-11722.

‡12. M. H. Lyttle, A. Streitwieser, Jr. and R. Q. Kluttz, "The Unusual Equilibrium Between 1,4- and 1,6-Di-tert-butylcyclooctatetraenes," J. Am. Chem. Soc. 103, 3232 (1981); LBL-12196.

13. W. D. Luke, S. R. Berryhill, A. Streitwieser, Jr., "Bis-π-(cyclobutenocyclooctatetraene) uranium(IV)," Inorg. Chem. 20, 3086 (1981); LBL-12137.

14. R. A. Andersen, A. Zalkin, D. H. Templeton, "Crystal and Molecular Structure of Hydridotris[bis (trimethylsilyl)amido] Uranium(IV)," Inorg. Chem. 20, 622 (1981); LBL-10489.

15. T. D. Tilley, A. Zalkin, R. A. Andersen, D. H. Templeton, "Divalent Lanthanide Chemistry; Preparation of Some Four and Six Coordinate Bis(trimethylsilylamido) Complexes of Europium(II). The Crystal Structure of Bis(di(trimethylsilyl)amido)bis(1,2-dimethoxyethane) Europium(III)," Inorg. Chem. 20, 551 (1981); LBL-10858.

16. L. G. McCullough, H. W. Turner, R. A. Andersen, A. Zalkin, D. H. Templeton, "Preparation and Crystal Structure of the 1,2-dimethoxyethane Complex of Bis(di(trimethylsilyl)amido) dichlorouranium(IV)," Inorg. Chem. 20, 2869 (1981); LBL-11042.

17. D. T. Kagan, J. G. Conway, and E. Meinders, "Spectrum and Energy Levels of Nb^{4+}," J. Opt. Soc. Am. 71, 1193 (1981).

18. T. P Tufano and K. N. Raymond, "Coordination Chemistry of Microbial Iron Transport Compounds. 21. Kinetics and Mechanism of Iron Exchange in Hydroxamate Siderophore Complexes," J. Am. Chem. Soc. 103, 6617 (1981).

19. N. M. Edelstein, "Bonding in Metal Borohydride Complexes," Inorg. Chem. 20, 297 (1981).

20. T. Hayhurst, G. Shalimoff, N. Edelstein, L. A. Boatner, and M. M. Abraham, "Optical Spectra and Zeeman Effect for Er^{3+} in $LuPO_4$ and $HfSiO_4$," J. Chem. Phys. 74, 5449 (1981).

21. A. L. Arduini, N. M. Edelstein, J. D. Jamerson, J. G. Reynolds, K. Schmid, and J. Takats, "Syntheses and Characterization of $(\eta^5\text{-}C_5H_5)_2U(NR_2)_2$ Compounds," Inorg. Chem. 20, 2470 (1981).

22. B. Spencer and N. M. Edelstein, "Electron Paramagnetic Resonance Spectra of Erbium(III), Dysprosium(III), and Gadolinium(III) in Yttrium and Lanthanum Hydrides," Inorg. Chem. 20, 2736 (1981).

23. M. Baluka, N. Edelstein, and T. A. O'Donnell, "Electronic Solution Spectra for Uranium and Neptunium in Oxidation States III to VI in Anhydrous Hydrogen Fluoride," Inorg. Chem. 20, 3279 (1981).

24. S. J. Simpson and R. A. Andersen, "Actinide-Carbon Bonds: Insertion Reactions of Carbon Monoxide, tert-Butylisocyanide and tert-Butylcyanide into $[(Me_3Si)_2N]_2MCH_2Si(Me)_2NSiMe_3$," J. Am. Chem. Soc. 103, 4063 (1981).

25. S. J. Simpson, H. W. Turner, and R. A. Andersen, "Alkyl and Hydride $N(SiMe_3)_2$ Derivatives of Actinides Preparation and Hydrogen-Deuterium Exchange," Inorg. Chem. 20, 2991 (1981).

LBL Reports

1. C. W. Eigenbrot, Jr. and K. N. Raymond, "The Synthesis and Characterization of $(UCp_3)_2$(pyrazine) and $[U(MeCp)_3]_2$(pyrazine): π-Bridged Dimers of U^{3+}," submitted to Polyhedron, LBL-13074.

2. C. W. Eigenbrot, Jr. and K. N. Raymond, "Crystal and Molecular Structure of $[Nd(tren)_2(CH_3CN)](ClO_4)_3$," submitted to Inorg. Chem., LBL-13075.

3. A. Zalkin, D. H. Templeton, W. D. Luke and A. S. Streitwieser, Jr., "Synthesis of Dicyclopentenouranocene, $U(C_8H_6(CH_2)_3)_2$," in press, Organometallic Chemistry, LBL-13216.

4. D. L. Perry, D. H. Templeton, H. Ruben, A. Zalkin, "Synthesis, Characterization, and Structure of a Uranyl Complex with Disulfide Ligand, Bis(Di-n-propylammonium)disulfidobis (di-n-propylmonothiocarbamato) Dioxouranate(VI)," in press, Inorg. Chem., LBL-10654.

5. T. D. Tilley, R. A. Andersen, B. Spencer, A. Zalkin, "Crystal Structure of Bis(pentamethylcyclopentadienyl)bis(pyridine) Ytterbium(II)," in press, Inorg. Chem., LBL-13380.

6. A. Zalkin, H. Rubin, D. H. Templeton, "The Structure of Nickel Uranyl Acetate Hexahydrate," in press, Acta Cryst., LBL-12551.

7. J. A. Arenivar, V. V. Mainz, H. Ruben, R. A. Andersen, A. Zalkin, "Stereochemistry of Bis(carboxylato)bis(chloro)bis(tertiary phosphine) dimolybdenum Complexes; Crystal and Molecular Structure of Two Isomers of $(Me_3CCO_2)_2Cl_2(PEt_3)_2Mo_2$," in press, Inorg. Chem., LBL-13381.

8. T. D. Tilley, R. A. Andersen, A. Zalkin, D. H. Templeton, "Bis(pentamethylcyclopentadienyl) carboxylato and Dithiocarbamato Derivatives of Neodymium(III) and Ytterbium(III). Crystal Structures of Bis(pentmethylcyclopentadienyl) (diethyldithiocarbamato) Ytterbium(III)," in press, Inorg. Chem., LBL-13010.

9. P. G. Edwards, R. A. Andersen, A. Zalkin, "Tertiary Phosphine Derivatives of the f-Block Metals; Preparation of $X_4M(Me_2PLH_2CH_2PMe_2)_2$, where X is Halide, Methyl and Phenoxo and M is Thorium and Uranium. Crystal Structure of Tetra(Phenoxo)Bis(bis(1,2-dimethylphosphine)ethane) Uranium(IV)," in press, J. Am. Chem. Soc., LBL-13065.

†10. L. K. Templeton, D. H. Templeton, R. P. Phizackerley and K. O. Hodgson, "L_3-Edge Anomalous Scattering by Gadolinium and Samarium Measured at High Resolution with Synchrotron Radiation," in press, Acta Cryst. Sect. A, LBL-12825.

†11. D. H. Templeton and L. K. Templeton, "X-ray Dichroism and Polarized Anomalous Scattering of the Uranyl Ion," in press, Acta Cryst. Sect. A, LBL-12477.

12. D. T. Kagan, "The Spectrum of Four-Times Ionized Niobium, Including Zeeman Studies of Selected Lines and Laser Modification of the Population of Certain Levels in a Sliding Spark," Ph.D. Thesis, LBL-12858.

13. J. L. Robbins, N. Edelstein, B. Spencer, J. C. Smart, "The Syntheses and Electronic Structures of Decamethylmetallocenes," in press, J. Am. Chem Soc., LBL-12258.

14. J. L. Robbins, "The Syntheses and Electronic Structures of Decamethylmetallocenes," Ph.D. thesis, LBL-12556.

15. T. Hayhurst, G. Shalimoff, J. G. Conway, N. Edelstein, L. A. Boatner, and M. M. Abraham, "Optical Spectra and Zeeman Effect for Pr^{3+} and Nd^{3+} in $LuPO_4$ and YPO_4," submitted to J. Chem. Phys., LBL-13388.

Other Publications

1. N. M. Edelstein, Ed., "Actinides-1981 Abstracts," (LBL-12441).

2. K. N. Raymond, W. R. Harris, C. J. Carrano, and F. L. Weitl, "The Synthesis, Thermodynamic Behavior, and Biological Properties of Metal-Ion-Specific Sequestering Agents for Iron and the Actinides," reprinted from ACS Symposium Series, No. 140, Inorganic Chemistry in Biology and Medicine, Arthur E. Martell, Ed., American Chemical Society, Washington, D.C., 1980, p. 313-332; LBL-10466.

3. K. N. Raymond and W. L. Smith, "Actinide-Specific Sequestering Agents and Decontamination Applications," in Structure and Bonding, vol. 43, J. B. Goodenough, et al., Eds., Springer-Verlag Berlin, Heidelberg, 1981; LBL-11533.

4. K. N. Raymond and V. L. Pecoraro, "Coordination Chemistry," McGraw-Hill Yearbook of Science and Technology, 1981, p. 150-153.

5. K. N. Raymond, V. L. Pecoraro, and F. L. Weitl, "Design of New Chelating Agents," in Development of Iron Chelators for Clinical Use, A. E. Martell et al., Eds., Elsevier/North-Holland, New York, 1981, p. 165-187.

* * *

†Partially supported by the National Institutes of Health.

‡Partially supported by the National Science Foundation.

Invited Talks

1. A. Streitwieser, Jr., "Some Unusual Intramolecular Interactions," Chemistry Department, University of California, Berkeley, February 25, 1981.

2. A. Streitwieser, Jr., "Uranocenes with Aromatic Rings," 28th IUPAC Congress, Vancouver, B.C., Canada, August 17, 1981.

3. A. Streitwieser, Jr., "Chemistry of Uranocene," Hong Kong Chemical Society, August 28, 1981.

4. A. Streitwieser, Jr., "Chemistry of Uranocene," Nankai University, Tienjin, PRC, September 5, 1981.

5. A. Streitwieser, Jr., "Chemistry of Uranocene," Peking University, Peking, PRC, September 11, 1981.

6. A. Streitwieser, Jr., "New Developments in Uranocene Chemistry," Stanford University, November 10, 1981.

7. J. G. Conway, "Fourier Transform Spectroscopy in Heavy Elements," Berkeley, January 14, 1981.

8. D. H. Templeton, "Anomalous Dispersion," International Congress of International Union of Crystallography, Ottawa, Canada, August 16-25, 1981.

9. D. H. Templeton, "Diffraction and Anomalous Scattering of Synchrotron Radiation," Meeting of American Chemical Society, New York, NY, August 23-28, 1981.

10. K. N. Raymond, "Macrocyclic Ligands Specific for: A) Fe(III), B) Actinide(IV) Ions," Fourth Symposium on Macrocyclic Compounds, Provo, UT, August 11-13, 1980.

11. K. N. Raymond, "Design of New Chelating Agents," Second Symposium on Development of Iron Chelators for Clinical Use, San Francisco, CA, August 23-24, 1980.

12. K. N. Raymond, "Coordination Geometry and Iron Exchange Kinetics of Siderophores, Synthetic Analogues and Human Transferrin," COMO 10 Meeting, New Zealand, May 10-14, 1981.

13. K. N. Raymond, "New Actinide-Specific Sequestering Agents," Actinide Separations Workshop V, Argonne National Laboratory, Argonne, Illinois, June 11-12, 1981.

14. K. N. Raymond, V. L. Pecoraro, W. R. Harris, and C. J. Carrano, "Actinide Coordination and Discrimination by Human Transferrin," International Symposium on Migration in the Terrestrial Environment of Long-Lived Radionuclides from the Nuclear Fuel Cycle, Knoxville, TN, July 27-31, 1981.

15. K. N. Raymond, "Coordination Environments in Biochemical Iron Transport," Gordon Research Conference, New Hampton, NH, August 3-7, 1981.

16. K. N. Raymond, T. D. Chung, V. L. Pecoraro, and C. J. Carrano, "Iron Removal From Transferrin by Siderophores and Analogues, and Determination of the Number of Bound Tyrosines in Metal Transferrin Complexes," Fifth International Conference on Proteins of Iron Storage and Transport, La Jolla, CA, August 24-26, 1981.

17. K. N. Raymond, M. J. Palle, V. L. Pecoraro, W. R. Harris, C. J. Carrano, F. L. Weitl, and P. W. Durbin, "Specific Sequestering Agents for Actinide Ions," Actinides-1981, Pacific Grove, CA, September 10-15, 1981.

18. K. N. Raymond, "Specific Sequestering Agents for Iron III and Actinide IV Ions," at following: Series of five seminars—
Pasteur Institute, Strasbourg (France), January 8 to February 16, 1981.
Max-Planck Institute, Mülheim, West Germany, July 31, 1981.
University of Marburg, West Germany, February 2, 1981.
Leiden University, Leiden, Netherlands, February 9, 1981.
Erasmus University, Rotterdam, Netherlands, February 10, 1981.
Enschede Technical University, Enschede, Netherlands, February 11, 1981.
European Economic Commission, Brussels, Belgium, February 12, 1981.
University of Groningen, Groningen, Netherlands, February 13, 1981.
Institute for Radioactive Chemistry, Karlsruhe, West Germany, February 17, 1981.
College de France, Paris, February 20, 1981.
Munich University Nuclear Institute, Munich, West Germany, February 25, 1981.

French Center for Research, Rennes, March 12, 1981.
La Trobe University, Melbourne, Australia, May 18, 1981.
Australian National University, Canberra, May 20, 1981.
Sydney University, Sydney, Australia, May 22, 1981.

IV Fossil Energy

Fossil Energy

a. Electrode Surface Chemistry*

Phillip N. Ross, Investigator

Introduction. Commercialization of phosphoric acid fuel cell technology requires a capital cost reduction and an extension of power plant life compared to currently available technology. Significant capital cost reduction can be achieved if an oxygen reduction catalyst that is catalytically more active than platinum can be developed. The objective of the present research is to develop the physical and chemical understanding of the oxygen-platinum surface interactions necessary for the rational selection of alloying ligands that modify the basic catalytic properties of platinum. It is felt that the platinum-oxygen bond energy will be changed when ligands are bonded to the surface platinum atoms and that, by the use of appropriate ligands, an optimal bond energy will result in enhanced catalytic activity relative to the pure platinum surface.

Specific absorption of anions on the platinum surface in phosphoric acid interferes with the essential platinum-oxygen interaction. Perfluoroalkylsulfonic acids appear to have non-adsorbing anions and are being investigated to determine whether they would be superior to phosphoric acid as electrolytes for hydrogen-air fuel cells.

1. SURFACE PROPERTIES OF Pt-Zr AND Pt-Ti ALLOYS†

U. Bardi, P. N. Ross, and G. A. Somorjai

Many theoretical descriptions of catalytic reactions at metal surfaces attribute the remarkable catalytic properties of Pt to the unique d-electron configuration in this atom. The Engle-Brewer bonding rules suggest that the enormous thermodynamic stability of intermetallics like Pt_3Ti is due to strong metal-metal d-orbital bonding that is absent in the pure metals. The Engle-Brewer bonding picture for this class of intermetallics has not yet been confirmed by probes of the electronic structure. It is the objective of our study of Pt intermetallic surfaces to determine the effect on surface properties of alloying platinum with Group IVb metals (Zr and Ti) by use of the UHV techniques of Auger electron spectroscopy (AES), low energy electron diffraction (LEED), UV photoelectron spectroscopy (UPS), and thermal desorption spectroscopy (TDS). The surfaces were prepared by: a) evaporating in UHV one of the components of the alloy on an oriented single crystal of the other, and b) preparing the bulk compounds Pt_3X (X = Ti or Zr).

Metallic zirconium grows epitaxially on the Pt surface. For coverages under a monolayer it forms two dimensional islands, leaving part of the Pt surface free. Upon annealing, Zr dissolves into the Pt bulk. Partially-covered Pt surfaces do not show significant changes in the adsorptive properties of the single metals: oxygen is readily adsorbed on zirconium, forming a very stable oxide; CO is adsorbed dissociatively on the Zr layers, and non-dissociatively on the free Pt surface. CO is not adsorbed at all on an oxidized zirconium surface. The amount of CO detected in TDS experiments is proportional to the free Pt surface (as determined by AES).

Due to the difficulty of obtaining an oxygen-free Zr surface, Pt was deposited on Zr (0001) surfaces with constant and reproducible oxygen content obtained by exposure to 50 Langmuirs or more. Pt grows on this surface by the Volmer-Weber mechanism, i.e., forming three dimensional clusters on the surface. Annealing produces the dissolution of Pt into the metallic Zr substrate. Most importantly the chemisorptive properties of Pt did not appear to be changed by the substrate interaction, e.g., CO thermal desorption spectra were nearly identical to those observed for pure Pt surfaces.

UPS results on the intermetallic Pt_3Ti surface show a significant depletion in the density of states near the Fermi level in comparison to the pure Pt and Ti. This depletion is interpretable as due to the strong d-orbital interaction in the Ti-Pt bond, predicted by the Engel-Brewer theory, that produces electronic states which are shifted to lower energy. Examination of the intermetallic surface by scanning Auger microscopy shows titanium segregation at the grain boundaries. The titanium precipitated in the grain boundary regions is completely oxidized. No oxygen is observed by AES in the intermetallic region (the intergranular region) even after the sputter-cleaned surface is exposed to oxygen. Strong intermetallic bonding between Pt and Ti apparently stabilizes the metallic Ti state, as expected from the Engel-Brewer theory.

* * *

*This work was supported by the Assistant Secretary for Fossil Energy, Office of Fuel Cells, Advanced Concepts Division of the U.S. Department of Energy under Contract No. DE-AC03-76SF00098 through the Fuel Cell Project Office, NASA Lewis Research Center, Cleveland, OH.

†Joint program co-funded by the Director, Office of Energy Research, Office of Basic Energy Sciences, Chemical Sciences Division of U.S. Department of Energy under Contract DE-AC03-76SF00098.

2. INTERACTION OF OXYGEN WITH Pt SURFACES AT ELEVATED TEMPERATURE†

G. Derry and P. N. Ross

For certain hydrocarbon reactions, the pretreatment of Pt single crystal surfaces by oxygen at elevated temperatures produces an enhancement in catalysis. Correspondingly, smooth Pt electrodes subjected to an anodic pretreatment exhibit enhanced catalytic properties for oxygen reduction. However, supported Pt electrocatalysts do not exhibit this activated behavior. The activation effect may be associated with the creation of subsurface "oxide" that distorts the chemical environment of surface Pt atoms in such a way as to create new catalytic behavior. Supported Pt clusters have no subsurface region and thus perhaps cannot achieve the same activated state. To elucidate the state of activated Pt, we are studying the interaction of molecular oxygen with the [001] surface of Pt at elevated surface temperatures using thermal desorption spectroscopy (TDS), ultraviolet photoelectron spectroscopy (UPS), and x-ray photoelectron spectroscopy (XPS).

Thermal desorption showed interesting variations with surface temperature. Oxygen adsorption at near-ambient temperature resulted in a state which desorbs with second-order kinetics. The desorption energy of this state was calculated to be $E_d = 27 \pm 6$ kcal/mole. Quantitative determinations of absolute coverage were difficult; we estimate the saturation coverage to be $\theta_{sat} \approx 0.1$ monolayer. This value yields an Arrhenius pre-exponential of $k_2^{\circ} \approx 5 \times 10^{-8}$ cm^2/sec and an initial sticking coefficient of $S_0 \approx 2 \times 10^{-2}$. This latter value is much greater than previously reported sticking coefficients for oxygen on Pt [001]. We attribute this to the CO clean-off reaction, occurring in many of the other experiments, which has been minimized in our experiment. If the oxygen exposure is carried out at an elevated surface temperature (e.g., 300°C), then the thermal desorption is no longer characterized by a simple second-order process, as shown in Fig. 1. No linear combination of simple first or second order processes accounted for the O_2 and temperature dependences. A model that does give a good fit to the TDS data is the following: a mobile adsorbed oxygen state present in both temperature regimes coexistent with an immobile phase of nucleated islands growing in at elevated temperatures; desorption occurs when either two mobile atoms collide (and recombine) or when a mobile atom hits an island edge (and the two atoms recombine). XPS and UPS indicated that the surface phase formed at elevated temperature has the chemical state of the divalent Pt oxide (PtO). We have concluded that the higher surface temperature surmounts the activation barrier for charge transfer facilitating the initial growth of an oxide-like phase (the immobile phase) though still at submonolayer coverages. It may also be possible that oxygen is dissolved below the surface. In order to distinguish subsurface from surface oxygen, we are conducting angle-resolved XPS experiments on the same system. The degree of charge transfer in the Pt-O bond will be indicated by the chemical shifts of the core levels, and the angle-resolving spectrometer

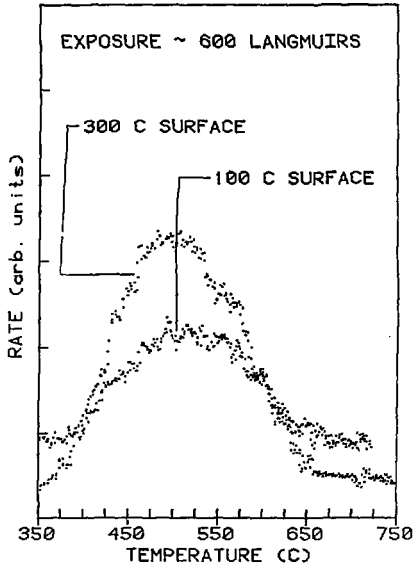

Fig. 1. Thermal desorption spectra of oxygen on the [001] surface of Pt for exposure at elevated temperatures. (XBL 821-7593)

will provide information on the location of oxygen atoms with respect to the surface plane.

3. OXYGEN REDUCTION ON Pt IN PERFLUOROALKYLSULFONIC ACID

P. Andricacos and P. N. Ross

Phosphoric acid is the electrolyte currently in use for commercial hydrogen-air fuel cells. It is a nonideal solution and a relatively weak acid, with pH = 1 at 0.7M H_3PO_4. Capacitance measurements have shown there is specific adsorption of phosphoric acid anions on Pt, and probably specific adsorption of neutral molecules as well. These adsorption processes are expected to interfere with the oxygen reduction reaction at Pt electrodes. Trifluoromethane sulfonic acid (TFMSA) is a very strong acid and dilute aqueous solutions are nearly ideal, with pH = 1 at 0.1M TFMSA. Anion adsorption on Pt in 0.1M TFMSA appears to be minimal as determined by capacitance measurements. Technologically, the problem with TFMSA as a fuel cell electrolyte is that in the concentrated form needed in practice the acid wets the polytetrafluoroethylene (PTFE) hydrophobic bonding agent

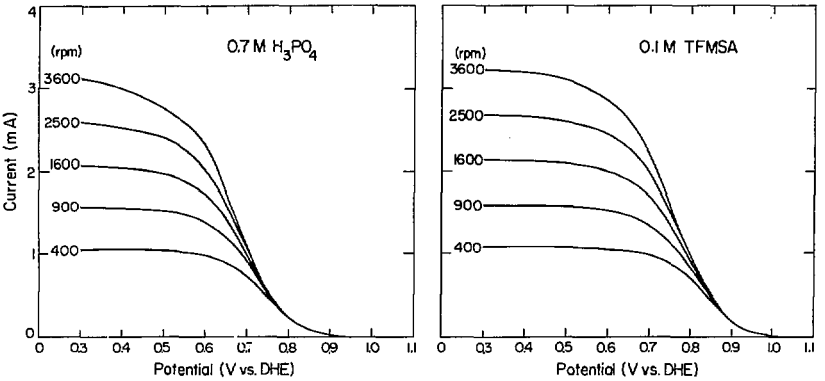

Fig. 1. Rotating disk current-potential curves for oxygen reduction on Pt at pH = 1, 25°C, and 10 mV/s.

(XBL 8011-2403)

used in gas diffusion electrodes causing a collapse of the three-phase interfacial structure. It is hypothesized that this wetting is due to the CF_3- functional group and that the higher homologs of this acid, e.g., tetrafluoroethane-1, 2-disulfonic acid (TFEDSA), would not wet PTFE. Recent work has shown that this is in fact the case; even very concentrated solutions (> 5M) of TFEDSA do not wet PTFE.

The kinetics of oxygen reduction on smooth Pt electrodes are being studied using the rotating ring-disk electrode (RRDE) technique in acid electrolytes at pH = 1. Oxygen reduction currents for the Pt rotating disk electrode in these electrolytes are shown in Fig. 1. At a given rotation rate, the current density in TFMSA is a factor of 4 to 5 larger than in H_3PO_4 of the same pH. The difference is not due to an increase in solubility or diffusivity, since the limiting currents in the two electrolytes are virtually identical. The ring currents indicated that less than 10 percent of the oxygen consumed produces peroxide intermediate. The differences represent much better kinetics in TFMSA than in H_3PO_4, probably as a result of minimal anion adsorption in TFMSA solutions. Oxygen reduction kinetics on Pt in TFEDSA at pH = 1 were about the same as in TFMSA; impurities in the TFEDSA, which is not available commercially and must be synthesized, prevent a quantitative comparison at present.

1981 PUBLICATIONS AND REPORTS

Refereed Journals

1. P. N. Ross, Jr., "Hydrogen Chemisorption on Pt Single Crystal Surfaces in Acidic Solutions," Surface Science, 102, 463 (1981).

2. P. N. Ross, Jr., "Voltage Losses in Fuel Cell Cathodes," J. Electrochem. Soc., 127, 2655 (1980).

LBL Reports

1. P. N. Ross, Jr., "Studies of Adsorption at Well-Ordered Electrode Surfaces Using Low Energy Electron Diffraction," to be published in Proceedings of the V International Summer Institute in Surface Science, Springer-Verlag, Berlin, 1982, LBL-13507.

Invited Talks

1. P. N. Ross, Jr., "Electrochemistry on Well-Ordered Metal Surfaces," Gordon Conference on Electrochemistry, Ventura, CA, January 18-23, 1981.

2. P. N. Ross, Jr., "Voltage Losses in Fuel Cell Electrodes," Texas Instruments Central Research Laboratories, Dallas, TX, January 5, 1981.

3. P. N. Ross, Jr., "Studies of Adsorption at Well-Ordered Electrode Surfaces Using Low Energy Electron Diffraction," V International Summer Institute in Surface Science, University of Wisconsin-Milwaukee, August 18-22, 1981.

b. Deuterium Analysis of Coal by NMR*

A. Pines, Investigator

Introduction. Solid materials of interest in energy research and catalysis are often not susceptible to classical analytical techniques. Such materials include coal, polymers and zeolites. Important questions about these materials concern the distribution of functional groups, changes during processing, active sites, bonding, motion, etc. New high resolution double quantum and magic angle spinning NMR techniques allow the study of ^{1}H, ^{2}D, ^{13}C, ^{27}Al and ^{29}Si which are important constituents of these materials, and are beginning to provide answers to some of the above questions.

1. HIGH RESOLUTION NMR OF DEUTERIUM IN ORGANIC SOLIDS†

R. Eckman, J. Millar, and A. Pines

Measurement of NMR chemical shifts of many nuclei in solids with spin I > 1/2 is often difficult due to the broadening of their spectra by the nuclear electric quadrupole interaction. Spectra of deuterium (I = 1), for instance in powders of amorphous materials that serve as models for coal, are often over 250 kHz in breadth, making the chemical shift unmeasurable. Observation of the chemical shift is an important tool for characterization of coal, coal conversion products, and many other noncrystalline materials.

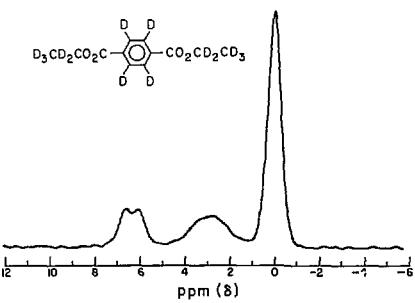

Fig. 1. Deuterium isotropic chemical shift spectrum of solid perdeuterated diethylterephthalate obtained by magic angle spinning with synchronous sampling. All chemical types are resolved and fine structure in the aromatic peak is due to crystallographic inequivalence of ring positions which does not appear in the liquid due to free rotation. (XBL 8111-12666)

We have recently demonstrated the measurement of deuterium isotropic chemical shifts in several labeled model compounds by precise magic angle sample rotation. Quadrupolar broadening is removed nearly completely by controlling the axis of sample rotation to within 0.0001°, and high power double resonance decoupling, is applied to remove broadening due to other nuclei.

Deuterium double quantum transitions have also been observed that reduce the stringent dependence of the experiments on spinner axis adjustment. Observation of such liquid-like chemical shift spectra for deuterium serves as an alternative approach to high resolution NMR of hydrogen types in solids. An example is shown in Fig. 1 in which all resonances of solid diethylterephthalate are resolved for the first time and fine structure in the aromatic peak due to crystallographic inequivalence is evident.

* * *

†Short version of LBL-13332.

2. RESOLVED ^{27}Al NMR IN ZEOLITES†

R. Eckman, J. Millar, Ye Chaohui, and A. Pines

The characterization of microscopic structure, distribution and function of zeolites is extremely important due to their use as catalysts. For example, the observation of resolved ^{29}Si and ^{27}Al NMR resonances in these materials can answer a host of questions not possible by x-ray or electron microscopy techniques. Using novel solid state NMR techniques, such resonances have been observed. Different types of Al sites and bonding can be distinguished. Some representative preliminary results on solid state ^{27}Al chemical shifts appear in Table 1. The zeolites were studied in collaboration with D. Whitehurst and K. Schmitt at Mobil Research Laboratory in Princeton.

* * *

†Brief version of LBL-14200.

*This work was supported by the Assistant Secretary for Fossil Energy, Office of Coal Research, Liquefaction Division of the U.S. Department of Energy under Contract No. DE-AC03-76SF00098 through the Pittsburgh Energy Center, Pittsburgh, PA.

Table 1. ^{27}Al in solids.

Compound	Frequency (MHz)	Static Width (Hz)	M.A.S Width (Hz)
$AlCL_3$(aqueous)	93,949,600	~ 500	-
$Al(OEt)_3$	93,949,900	-	1000[a]
$Al(acac)_3$	93,949,400	-	1000
$Al(ISO)_3$	93,950,300	-	2300
$Al_2(SO_4)_3 \cdot (H_2O)$	93,949,700	2400	750
$Al(NO_3)_3 \cdot (H_2O)$	93,949,500	2900[b] - 4600[c]	1200
Ruby (Ye)	93,950,800	~ 10,000[d]	1600[a]
Mobil Zeolite (~10% Al)	93,955,600	2500	720
Mobil Zeolite (~1% Al)	93,954,900	1800	720
Mixture of Zeolite (~10% Al)	Two lines at correct positions		
$Al_2(SO_4)_3 \cdot (H_2O)$			

[a]Strong sideband structure.

[b]With proton decoupling.

[c]No proton decoupling.

[d]Single crystal with quadrupolar satellites.

3. CARBON-13 NMR OF WHOLE AND PROCESSED COALS†

D. Wemmer,‡ D. D. Whitehurst,§ G. Drobny, and A. Pines

We have continued our studies of coal and coal processing by carbon-13 NMR, in collaboration with Mobil Research and Development. Four types of carbon (aliphatic, oxygen-bonded aliphatic, aromatic, and condensed aromatic) can be distinguished directly in the solid state. This has permitted a correlation of carbon type distribution with the source of coal, the type of coal, and with changes that occur during processing. As an example, the evolution of aromatic carbon content during solvent refining can be studied and shows a change only at ~ 80 percent conversion. The solvent refined coal (SRC) and the residue both exhibit an increase in aromatic carbon content. A number of our results are contrary to those obtained by indirect techniques, such as solution infrared spectroscopy, which until recently have not been able to study the solid samples directly.

* * *

†Based in part on LBL-10533; Phil. Trans. R. Soc. Lond. A300, 15-41 (1981).

‡Currently at Department of Chemistry, Stanford University, Stanford, CA.

§Mobil Research and Development

4. HIGH RESOLUTION PROTON NMR OF DILUTE SPINS IN SOLIDS†

R. Eckman, J. Millar, Ye Chachui, and A. Pines

Observation of proton chemical shift tensors in solids has long been difficult due to the large ^1H–^1H dipole–dipole broadening, which can be 50–100 kHz. Measurements have been made by combined multiple-pulse line narrowing with magic angle spinning, combined isotopic dilution of protons with deuterium double quantum decoupling, and single crystal studies; however, the residual dipolar or chemical shift anisotropy broadening is substantial. Increased resolution is necessary, especially when there are many possible resolvable proton chemical sites.

We have recently observed isotropic chemical shifts of dilute protons in a deuterated solid by magic angle spinning. Isotropic chemical shift spectra are obtained with greater resolution than all other methods to date without the technical difficulties of multiple rf pulses, synchronous data acquisition, or double resonance decoupling.

In Fig. 1 is shown the isotropic proton chemical shift spectrum of 93 percent deuterated lauric acid powder obtained from the Fourier transform of the fid after a single rf pulse with magic angle sample rotation of 2.25 kHz. Resonances of all chemical types are well resolved and individual methylene resonances are evident in the solid state that do not occur in solution due to free rotation of the molecule.

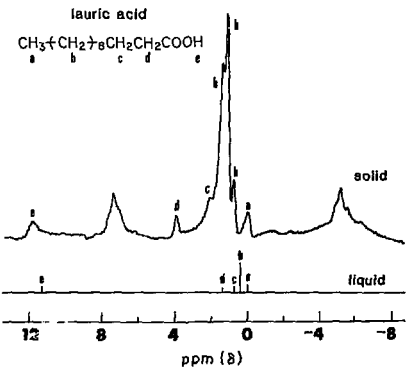

Fig. 2. Proton isotropic chemical shift spectrum of 95 percent-deuterated lauric acid solid obtained by magic angle spinning. All chemical types are well resolved and the methylene region (position b) is further resolved due to the rigid lattice of the solid in contrast to the liquid where the molecule rotates freely. Largely different shift are observed for the solid than the liquid also due to solid state effects. (XBL 8112-12910)

* * *

†Brief version of LBL-13332, J. Chem. Phys., in press.

5. CYLINDRICAL SAMPLE TURBINE FOR MAGIC ANGLE NMR†

R. Eckman and A. Pines

Measurement of isotropic chemical shift spectra in NMR in solids by magic angle sample spinning requires a high speed sample turbine, as is well known from recent novel studies of ^{13}C, ^2D and ^{27}Al in solids. For high resolution deuterium NMR in solids, these requirements are particularly stringent since a) the axis must be stable to within 0.001°, and b) the spectral bandwidth is limited to the spinner frequency due to the need for synchronous sampling. Mechanical design improvements in the sample turbine NMR probe now allow easily reproducible frequencies of rotation in excess of 300,000 rpm with previously used polymer turbines. Thus, the mechanical system exceeds the requirements for high resolution deuterium and ^{27}Al NMR in solids. A number of resolved ^2D and ^{27}Al spectra in solids have been obtained for the first time in this way. Construction of new sample turbines from boron nitride and glass ceramic materials has been achieved. These allow significantly higher frequencies of rotation which make isotropic spectra of carbon-13 at high field ($\omega_L(^{13}C)$ = 90 MHz readily available.

* * *

†Brief version of section of LBL-14200.

6. SYNTHESIS OF LABELED MODEL COMPOUNDS AND CRYSTALS

R. I. Goldberg and A. Pines

We are currently involved in three areas concerned with the synthesis of labeled compounds for use in magnetic resonance studies. The first of these is the synthesis of a large ring structure that includes a dibenzyl ketone moiety, the carbonyl carbon of which is enriched in carbon-13. The second area is the synthesis of benzene derivatives labeled with carbon-13 in two selected positions for solid state two-dimensional spectroscopy. Finally, we are involved in synthesizing selectively deuterated solid organic molecules to aid in investigating the potential for high resolution NMR in solids. The synthesis of 70% deuterated p-dimethoxybenzene has been completed, and ongoing is the partial deuteration of acetylsalicyclic acid (aspirin) and 2,6-dimethyl-benzoic acid, as well as the selective deuteration of lauric acid.

1981 PUBLICATIONS AND REPORTS

Refereed Journals

1. D. Wemmer, A. Pines and D. D. Whitehurst, "NMR Studies of Coal and Coal Extracts," Phil. Trans. R. Soc. Lond. A300, 15-41 (1981); LBL-10533.

2. D. E. Wemmer, and A. Pines, "Carbon-13 Chemical Shifts in Solid Metal Sandwich Compounds," J. Am. Chem. Soc., 103, 34 (1981); LBL-10864.

3. L. Müller, "Double Quantum Deuterium Echoes in Magic Angle Spinning Polycrystalline Solids," J. Mag. Res. 42, 324 (1981); LBL-11360.

4. L. Müller, "Proton-Deuterium Polarization Transfer in Magic Angle Spinning Polycrystalline Solids in the Rotating Frame," Chem. Phys., 61, 235 (1981); LBL-12314.

For further references, see section "Nuclear Magnetic Resonances," A. Pines, Investigator.

LBL Reports

1. R. Eckman, "High Resolution Proton NMR of Dilute Spins in Solids," submitted to J. Chem. Phys., LBL-13332.

Invited Talks

1. A. Pines, "NMR Determination of Coal Structure," Pittsburgh Energy Center, Contractors Conference on Coal Liquefaction Research, Pittsburgh, PA., October 6-7, 1981.

2. A. Pines, "Free Induction Decay - Where Does it Go?" Department of Chemistry, Harvard University, Cambridge, MA., October 28, 1981, seminar.

3. A. Pines, "NMR with Lots of Photons," The Guy Allen Lecture in Physical Chemistry, Yale University, New Haven, CT, October 30, 1981.

4. A. Pines, "Free Induction Decay - Where Does it Go?" Department of Chemistry, The University of Utah, Salt Lake City, UT., December 8, 1981, research seminar.

5. A. Pines, "Application of NMR to the Structure of Zeolites," Mobil Research and Development Corporation, Princeton, NJ, December 10, 1981, seminar.

6. R. Eckman, M. Alla, L. Müller and A. Pines, "Isotropic Deuterium NMR by Magic Angle Spinning," poster presentation, 22nd ENC Conference, Asilomar, CA, April 5-9, 1981.

c. Coal Liquefaction Alloy Test Program*

Alan V. Levy, Investigator

Introduction. The erosion behavior of steel alloys used to construct the slurry flow containment components of coal liquefaction systems is being investigated in this program. The effects on the erosion of steels of flow variables such as particle composition, size, and solids loading; temperature; flow passage geometry; the viscosity and lubricity of the carrier liquid and the velocity and angle of impingement of the particles were determined. The steel alloys selected for testing are those that are commonly used in chemical process plant piping systems. They include: A53 and A106 plain carbon piping steels; 2 1/4 Cr-1Mo, 5Cr 1/2 Mo, 9Cr-1Mo chromium bearing steels and types 410, 304, 310, 316, and 321 stainless steels. The particles that have been used in the slurries have been pulverized coal and SiC. The liquids tested include water, kerosene, creosote oil, hexadecane, and SRC process solvent.

1. EROSION BEHAVIOR OF ALLOYS IN COAL SLURRIES†

Greg Hickey and Alan Levy

The transport of coal using nonaqueous liquid carrier fluids in coal conversion and combustion systems causes erosion to occur on the containment walls of piping, pumps, valves and instrumentation probes. The purpose of this project was to determine the effect of flow variables on the erosion behavior of several steel alloys used in chemical process plant components. The relative performance of the steels tested was also determined.

A slurry pot tester was used in the tests performed. It rotates 3 mm diam by 5 cm long specimens held at the ends of arms on a central rotating shaft in a 3 liter tank of test slurry. Baffles on the tank's inside wall keep vortex flow patterns from occurring as the result of the stirring action. The tests were performed for 2 and 5 hours with periodic weight loss measurements of the test rods. The tester was filled with slurries of various liquids and varying coal content and size and operated at temperatures from 25°C to 175°C. Metallographic analysis of the eroded specimens was conducted after the test exposures to observe the mechanism of erosion.

The effect of particle size and solids loading on the erosion of A-53 mild steel and 304SS showed that more particles and larger size particles resulted in higher erosion rates, particularly at higher velocities. The velocity exponent was also greater for the larger particle size coal, 3 for -30 mesh coal compared to 2 for -200 mesh coal.

The effect of alloy composition, morphology, hardness, strength and ductility could not be related to the relative erosion rate of the nine steel alloys tested. The A53 mild steel and 304SS consistently eroded at higher rates than the other steels tested. Generally, increasing chromium content of the alloys resulted in lower erosion rates. The smaller grain size of the A106 mild steel caused a marked reduction in the erosion rate compared to the larger grain, same composition A53 mild steel. A variation of hardness of the steels from R_B 72 to R_B 97 could not be related to their erosion rates.

The effect of the temperature of the slurry on the erosion of several alloy steels is shown in Fig. 1. The higher erosion rates of the A53 mild steel and the 304SS compared to those of the other alloys tested was consistent for all variables tested, not just the temperature. The decrease in the erosion rate at the 94°C temperature compared to the 25°C tests is the result of the change in the nature of the slurry and the ductility of the

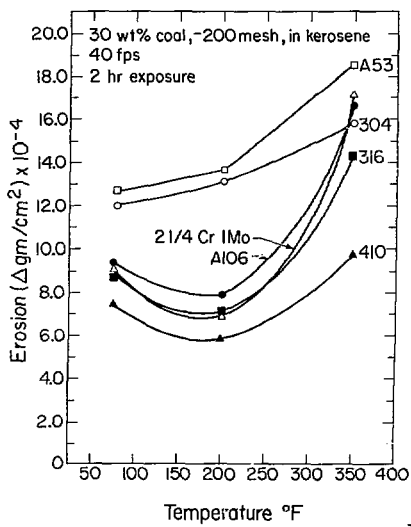

Fig. 1. Effect of test temperature on the erosion of alloys by a coal-kerosene slurry flow. (XBL 8110-7151A)

*This work was supported by the Assistant Secretary for Fossil Energy, Office of Coal Research, Materials Components Division of the U. S. Department of Energy under Contract No. DE-AC03-76SF00098 through the Fossil Energy Materials Programs, Oak Ridge National Laboratory, Oak Ridge, TN.

steels. The increase in erosion rate at the 177°C test temperature is primarily due to the decrease in the viscosity of the kerosene, which increases the erosivity of the slurry.

In other tests using hexadecane with and without hexadecanoic acid as the carrier liquid for the pulverized coal, it was determined that the lubricity of the liquid plays a major role in the erosivity of slurries. The liquid containing the 1/2 percent acid had a higher lubricity at the same viscosity, which resulted in a major reduction in the amount of erosion on the A53 mild steel and 304SS.

* * *

†Brief version of LBL-13804.

2. THE EROSION MECHANISM OF STEELS IN COAL-KEROSENE SLURRIES†

Phil Tom and Alan Levy

The mechanism of erosion of several alloy steels was investigated. An understanding of the active mechanism as it is affected by the test variables in a slurry environment is required for a predictive model of erosion. The selection and design of improved alloys for use in slurry-containing components of coal conversion and combustion system components also requires an understanding of the active mechanism of erosion. The knowledge of erosion mechanisms of ductile alloys which was developed in a complimentary gas-solid particle erosion study was used in this project.

A jet impingement tester capable of directing a stream of coal-kerosene at a flat test specimen was used. Eighteen gallons of slurry flowing at velocities ranging from 100 to 200 m/s were sufficient to produce reliable weight losses of the 2.5 x 3.5 cm test specimens at 25°C.

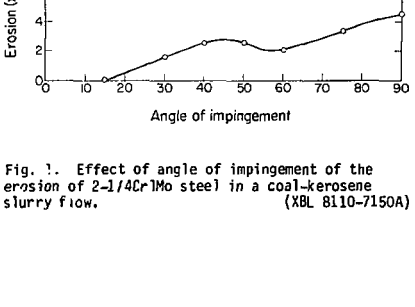

Fig. 1. Effect of angle of impingement of the erosion of 2-1/4Cr1Mo steel in a coal-kerosene slurry flow. (XBL 8110-7150A)

The effect of the impingement angle of the eroding stream on the erosion rate of an alloy steel, 2-1/4Cr1Mo, is shown in Fig. 1. An initial erosion peak occurs at an angle of 40°. A peak at 20° occurs in gas-solid particle erosion. The increased angle of the peak for the coal slurry is the result of the increased viscosity and lubricity of the slurry compared to a gas-solid particle stream. The amount of erosion in a gas-solid particle stream is roughly 4 orders of magnitude greater than that which occurs in a nonaqueous liquid-solid particle stream at the same particle velocity. The increase in erosion rate to the 90° impingement angle also differs from that in gas-solid particle streams, which cause lower erosion rates to occur after 20°. Lubricating liquids cause increased erosivity of the particles at steeper angles because the liquids carry particle kinetic energy to the eroding surface more effectively.

* * *

†Brief version of LBL-13805.

1981 PUBLICATIONS AND REPORTS

Refereed Journals

1. W. Tsai, J. Humphrey, I. Cornet and A. Levy, "Experimental Measurements of Accelerated Erosion in a Slurry Pot Tester," Wear 68-3, 305-332, May 1981.

2. S. Li, J. Humphrey, and A. Levy, "Erosive Wear of Ductile Metals by a Particle Laden High Velocity Liquid Jet," Wear 73-2, 295-310, November 1981.

LBL Reports

1. A. Levy and G. Hickey, "Surface Degradation of Metals in Simulated Synthetic Fuels Plant Environments," LBL-13804.

2. A. Levy and P. Tom, "The Mechanism of Erosion of Ductile Metals in Nonaqueous Slurry Flows," LBL-13805.

Papers Presented

1. A. Levy, "Erosion of Metals in Nonaqueous Coal Slurries," NACE, S.F. Chapter Meeting, Berkeley, CA, April 14, 1981.

2. A. Levy and G. Hickey, "Slurry Erosion Behavior of Alloy Steels at Elevated Temperatures," AIME-TMS Meeting, Louisville, KY, October 15, 1981.

3. A. Levy and P. Tom, "Jet Impingement Slurry Erosion of Alloy Steels," AIME-TMS Meeting, Louisville, KY, October 15, 1981.

d. Utilization of Metals in Oil Shale Retort Components*

Alan V. Levy, Investigator

Introduction. Work on the corrosion of low alloy steels and 300 series stainless steels in the high temperature oxidizing and sulfidizing environments of in-situ oil shale retorts was concluded and attention was turned to corrosion in above-ground retorts. An above-ground retort has the same corrosive sulfur and oxygen containing environment, but the lower operational temperatures do not impose such a severe corrosion environment on metals. Corrosion behavior of steels in retorted shale oil was also investigated.

1. HIGH TEMPERATURE CORROSION

Elliott Slamovich and Alan Levy†

The corrosion of low-alloy and stainless steels was determined in above-ground, simulated in-situ oil shale retorts by exposing 2.5 cm x 7.5 cm x 6 mm specimens in the 10-ton experimental retort at the Laramie Energy Technology Center (LETC). Further corrosion studies were conducted in a laboratory furnace crucible containing 15 grams of oil shale to determine the oxidation and sulfidation behavior of different alloys in a more controllable environment than occurs in the LETC retort. Sections of thermowell piping in underground in-situ retorts were also examined to study the effects of long term exposure to the retorting environment.

Test samples were run at LETC exposed to Moroccan "M" Zone high sulfur (4-5%) shale. The retorting run lasted only 30 hours and the temperature spiked at 1100°C, staying above 815°C for only six hours. Figure 1 shows the scales formed on 1018 plain carbon and 304 stainless steel. The difference in chromium content between the two steels, 0% and 18% respectively, was the main factor in the difference in the corrosion behavior observed. The 1018 steel has an outer layer of iron with deposits of iron oxide in it and an inner layer of iron oxide - iron sulfide directly attached to the remaining metal. The stainless steel has a thick layer of protective chromium

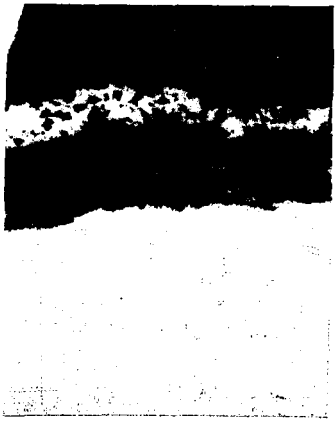

1018 Carbon Steel 25 μm

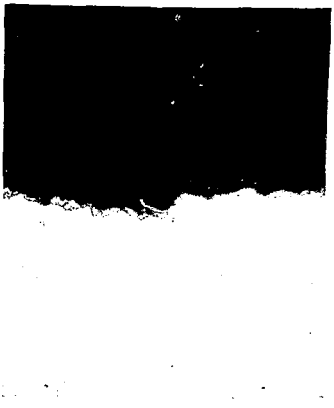

304 Stainless Steel 25 μm

Fig. 1. Corrosion scales on 1018 steel and 304SS.

(XBB 8112-11950)

*This work was supported by the Assistant Secretary for Fossil Energy, Office of Coal Research, Materials Components Division of the U. S. Department of Energy under Contract No. DE-AC03-76SF00098.

oxide on its surface with little or no attack down the grain boundaries. More extensive attack of both alloys would have occurred if the retorting operation had been longer.

De-emphasis of in-situ oil shale retort research has prevented LETC from testing the 2-1.4%, 5%, 9% and 12% chromium content steels. These alloys and various other low alloy and stainless steels are being tested in a laboratory crucible containing unreacted Anvil Pts. shale (1.7% S, 24 gal/ton) at 1000°C for 48 hours.

Figure 2 shows 304SS after a 48 hour exposure to shale. The outer scale is primarily chromium sulfide. A thin chromium oxide layer is between the outer scale and the metal. Internal sulfidation is found primarily along grain boundaries resulting from the inability of the chromium oxide layer to act as a diffusion barrier to sulfur. Diffusion of sulfur through the Cr_2O_3 protective scale duplicates the behavior of austenitic stainless steels in simulated in-situ retort exposures at LETC. The ability of the laboratory crucible to simulate the corrosion conditions that occur in large scale retorts was demonstrated. Analysis of exposures of other chromium containing steels showed a direct relation between corrosion resistance in an in-situ oil shale report and the chromium content of the alloy. Alloys with 12-18% Cr exhibited much higher corrosion resistance than alloys with 2 1/4%-9% Cr.

Analysis of a plain carbon steel pipe used as a thermowell protector in an actual underground in-situ retort (Fig. 3) shows a high level of corrosion with the formation of a porous layered scale on the base metal shown on the right side. X-ray maps show that there are three layers: a layer next to the base metal of iron oxide with a small amount of sulfur in it, a middle layer of iron sulfide, and an outer layer of iron oxide. At other locations along the 0.25-in. thick pipe, the metal was completely consumed, leaving layers of iron oxide and iron sulfide. The severe attack is typical of that of nonchromium containing alloys in in-situ oil shale retorts.

* * *

†Brief version of LBL-13809.

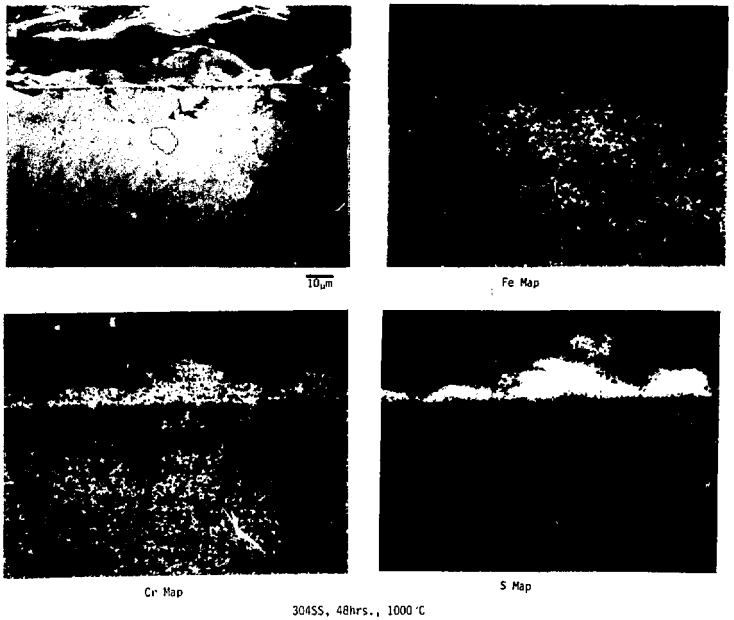

Fig. 2. Corrosion scale formed on 304SS in laboratory crucible test. (XBB 8112-11952)

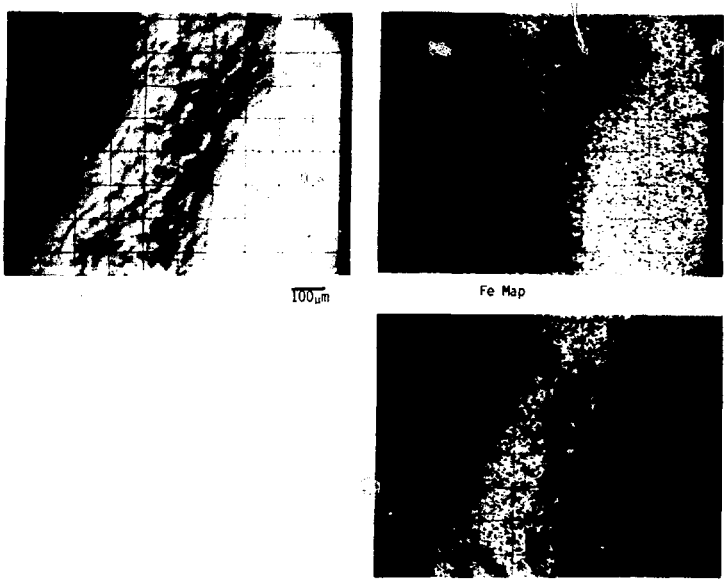

Fig. 3. Corrosion scale on a plain carbon steel pipe from an in-situ retort. (XBB 8112-11951)

2. LOW TEMPERATURE CORROSION

Elliott Slamovich, Jennifer Okano, and Alan Levy

As in the high temperature studies, tests were conducted in the field and laboratory. Samples 2.5 cm x 7.5 cm x 6 mm were exposed in a large scale, above ground retort in Colorado at temperatures to 500°C for 400 hours. Other exposures were made in LBL's 7.5-cm diam retort at 550°C for 48 hours. The effect of partial and total immersion in shale oil on the corrosion of steel was also studied at temperatures to 300°C.

Tests in the large scale, above ground retort showed mild corrosion only on the 1018 carbon steel. No corrosion was observed on the stainless steels exposed. Tests in the LBL 7.5-cm diam retort at 550°C showed mild attack only on the plain carbon 1018 steel. Exposure to shale oil at 300°C for 100 hours showed essentially no corrosion on stainless steels and only mild corrosion on 1018 steel. These results indicated that there will probably be little or no corrosion problems in above ground oil shale retort operations.

1981 PUBLICATIONS AND REPORTS

Other Publications

1. O. Whittle, M. El Dahshan, and A. Levy, "Corrosion of Materials in In-Situ Oil Shale Environments," Proc. 8th International Congress on Metallic Corrosion, ICC, Mainz, West Germany, September 6-11, 1981.

LBL Report

1. E. Slamovich, J. Okano, and A. Levy, "Corrosion of Metals in Oil Shale Retorting Environments," LBL-13809.

Presentations

1. A. Levy, W. Goward, and D. Boone, "High Temperature Corrosion of Metals and Coatings in Oil Shale Environments," 4th Annual Oil Shale Conversion Symposium, Denver, CO, March 25, 1981.

2. A. Levy and R. Bellman Jr., "Corrosion of Metals in Oil Shale Environments," NACE Corrosion 82, Toronto, Ont., April 6, 1981.

3. A. Levy, "Corrosion of Metals in Oil Shale Retorting Environments," ASM Spring Seminar, San Diego, CA, April 16, 1981.

e. Chemistry and Morphology of Coal Liquefaction*

Heinz Heinemann, Investigator, with Alexis T. Bell, R. G. Bergman, James W. Evans, Richard H. Fish, E. E. Petersen, A. V. Levy, G. A. Somorjai, and K. Peter C. Vollhardt, Investigators

Introduction. This program is concerned with a basic understanding of the chemistry and physics of coal liquefaction and with coal gasification as a preliminary step to liquefaction. It has brought together a team of organic, physical, and organometallic chemists, chemical engineers, and material scientists, some of whom have had extensive industrial experience. The advantages of an interdisciplinary approach have become apparent in regular meetings, numerous discussions, and suggestions, often coming from analogies in other areas. Accomplishments of the past year are briefly summarized below and then presented in somewhat greater detail, broken down into the six tasks involved.

(1) The carbon number distribution of C_2-C_{12} hydrocarbons produced via Fischer-Tropsch synthesis over an iron catalyst shows virtually no change as the conversion of CO is varied from 4 to 33, and only a small change in the olefin to paraffin ratio is detected. What is significant, though, is that the proportion of methane relative to C_{2+} hydrocarbons decreases with increasing conversion. Similar effects were observed using both fixed-bed and slurry reactors.

(2) Anatase has for the first time been identified by electron diffraction in a bituminous Kentucky coal. Since anatase had previously been found as a deposit on catalysts used for coal liquids hydrogenation and since it has not been found in coal ash, a question arises about the mechanism of its migration during coal liquefaction.

(3) The reaction of graphite with water has been investigated using alkali, alkali hydroxide, or carbonate catalysts. Methane and CO_2 were produced steadily at the surprisingly low temperature of 500 K using potassium on graphite. Lithium was the most active of the alkali catalysts.

(4) Work on the laser-powered homogeneous decomposition of tetralin, a compound that has frequently been used in model studies of hydrogen transfer processes occurring during coal liquefaction, was completed. Our results show that the primary homogeneous mode of decomposition involves carbon-carbon bond cleavage resulting in ethylene loss, rather than hydrogen loss as had been claimed earlier by other workers. We believe the hydrogen-loss pathway is primarily surface catalyzed. This work demonstrated the utility of the laser technique for insuring that one is examining truly homogeneous, rather than surface-catalyzed, processes.

(5) In work related to the laser studies mentioned in 4), we generated vibrationally excited tetralin by creating it in chemical reactions of varying exothermicity ("chemical activation"). These studies reinforced our conclusion that the major homogeneous decomposition pathway in tetralin involves loss of ethylene rather than H_2.

(6) Work on the generation and study of benzene-1,4-diyl diradicals ("1,4-dehydrobenzenes") uncovered one of the few examples of chemically induced dynamic nuclear polarization (CIDNP) arising from diradicals at high temperature, demonstrated conclusively that these diradicals exist as intermediates in the reactions of 1,2-diethynylethyenes, and obtained evidence that the diradicals react in the singlet state.

(7) A perusal of various first, second and third row transition metal carbonyl compounds, as homogeneous catalyst under water gas shift (WGS) conditions (CO, H_2O, base) with polynuclear aromatic hydrocarbons (PNA) reveals that only manganese and iron can effect reductions of these potential coal models to their partially reduced analogs in low yields (~ 10-30%). Dimanganese decacarbonyl ($Mn_2(CO)_{12}$) and various phosphine-substituted analogs react with PNA compounds, under synthesis gas (CO/H_2 1:1), to provide good yields of partially reduced PNA analogs (30-80%).

(8) Polynuclear heteroaromatic hydrocarbon compounds (PNHA, nitrogen as the heteroatom) are more reactive in homogeneous hydrogenation reactions under either WGS or syn gas conditions than their carbon analogs, e.g., acridine is more reactive than anthracene.

(9) The ruthenium cluster compound, $Ru_3(CO)_{12}$, is an extremely good catalyst (H_2 only) for the homogeneous hydrogenation of both PNA and PNHA compounds.

(10) The purported Fischer-Tropsch alkylation of benzene with $W(CO)_6$-$AlCl_3$ has been shown to be the result of Lewis acid catalyzed cracking of benzene.

---

*This work was jointly supported by the Director, Office of Energy Research, Office of Basic Energy Sciences, Chemical Sciences Division, and the Assistant Secretary for Fossil Energy, Office of Coal Research, Liquefaction Division of the U. S. Department of Energy under Contract No. DE-AC03-76SF00098 through the University Contracts Management Division of the Pittsburgh Energy Technology Center, Pittsburgh, PA.

Task 1: Selective Synthesis of Gasoline Range Components from Synthesis Gas

A. T. Bell, Investigator, with R. Dictor and J. Canella

The goal of these studies is to determine whether it is possible to obtain non-Schultz-Flory product distributions during the Fischer-Tropsch synthesis of hydrocarbons. Two approaches are being explored. The first involves the recycle of olefin products to interfere with the normal chain growth. The second approach is to use small pore zeolite supports or cocatalysts to limit the extent of chain growth or to reform the nascent products. Both a fixed-bed and a well-stirred slurry reactor are used. Products from these reactors are analyzed directly by gas chromatography, without the use of collecting traps, to avoid product fractionation.

Experiments conducted during the past year have focused on determining the effects of reaction conditions on product distribution before applying measures designed to modify the product distribution. All of this work has been conducted with a precipitated iron catalyst, promoted with copper and potassium.

Investigations with the fixed bed reactor were conducted at 10 atm and 300°C, using a 2:1 H_2/CO ratio in the feed gas. For syn-gas flow rates of 120 to 10 $cm^3/gm/min$, the CO conversion increased from 4 to 33. The distribution of C_2 through C_{12} products was unaltered over this range of conversions, but the formation of methane relative to other products was suppressed as the conversion increases. This effect was unexpected and at present no completely satisfactory explanation is available. In parallel with these effects, it was found that the olefin to paraffin ratio of the products decreased only slightly with increasing conversion. The change was most noticeable for products containing two and three carbon numbers but was virtually undetectable for products containing four or more carbon atoms. Storch/Anderson-Schultz/Flory (SA-SF) plots show that the data are in perfect agreement with a SA-SF distribution. The data for C_9+ paraffins follow the expected SA-SF distribution, the data for C_2 through C_8 paraffins fall below the line, and the point for methane lies well above the C_1 point on the line. This pattern is similar to that seen previously for synthesis over Ru. The effects of reaction conditions on the distribution of paraffins must be explored further before an explanation for the observed deviations from the SA-SF distribution can be given.

Preliminary results have been obtained using the slurry reactor. Working with a synthetic ammonia catalyst, it has been observed that at 10 atm and 300°C variations in the stirring speed from 800 to 1450 rpm have no effect on either the product distribution or the olefin to paraffin ratio. These results indicate the absence of mass-transfer effects under the chosen reaction conditions. Variations in the syn-gas feed rate produced effects virtually identical to those observed with the fixed bed reactor.

Task 2: Electron Microscope Studies of Coal During Hydrogenation†

J. W. Evans, Investigator, with D. Coates and M. L. Perez

Anatase has been identified by other workers as a deactivating deposit on cobalt-molybdena hydrodesulfurization catalysts used in coal liquefaction. Two hypotheses had been advanced to explain the origin of the anatase on the catalyst. One was that the titanium oxide originated from organically bonded titanium in the coal, which formed anatase during coal liquefaction. The second hypothesis was that the anatase was present in the coal as inorganic matter and found its way to the catalyst surface by physical processes. The second hypothesis was weakened by the fact that anatase had not been identified in coal.

Anatase has now been identified in a Kentucky bituminous coal, through electron diffraction (See Fig. 1). Deposits on catalyst particles used in liquefaction of the same coal also were found by electron diffraction to contain anatase. Furthermore, the particle size and morphology of the titanium containing mineral in the catalyst deposit and the coal were similar. The implication is that the second hypothesis advanced above may be true and that catalyst life might be extended if physical techniques can be developed to remove the anatase particles from the coal before liquefaction.

Another achievement this year has arisen from an examination of the oriented graphite being used in Task 3 of this project to study the catalysis of gasification by alkali metal compounds. Examination of the graphite before and after partial gasification in the presence of potassium hydroxide suggests that gasification takes place within pits on the graphite surface. The pits contain particles presumed to be potassium compounds, and if this is the case, the dispersion of the cata-

Fig. 1. Transmission electron micrograph of titanium containing particle in low temperature ashed coal with focused probe microdiffraction pattern identifying mineral as anatase.
(XBB 81B-7215)

lyst particles on the graphite surface will have a significant influence on catalysis.

* * *

†See LBL-13244 and LBL-11473.

Task 3: Catalyzed Low Temperature Hydrogenation of Coal†

G. A. Somorjai, Investigator, with H. Heinemann and A. Cabrera

Potassium carbonate and potassium hydroxide at present are among the best catalysts used for the gasification of coal with steam to carbon monoxide and hydrogen at high temperatures (in the range of 900-1000 K). In this temperature regime, hydrocarbons are unstable and their formation is not expected. There have been no reports of studies of the reaction of water vapor with carbon at lower temperatures where the conditions for the formation of hydrocarbons are more favorable. We have been exploring the possibility of catalyzed conversion of graphite directly to hydrocarbons using various gases as reactants, including H_2O, H_2, CO, and CO_2 near 1 atm and at low temperatures (300-700 K), and using potassium as a catalyst. We found no evidence for chemical reactions of the high-purity graphite samples with H_2, CO, or CO_2 in this temperature range. However, in the presence of water vapor, the potassium-covered graphite produced methane at a surprisingly low temperature (500 K) and this catalyzed methanation reaction continues for many hours without poisoning.

A pyrolytic graphite sample with a surface area of ~ 1 cm^2 was used in an ultrahigh vacuum system (< 10^{-9} torr). The sample surface was the subject of composition analysis by Auger electron spectroscopy (AES), ion sputter cleaning, and mass spectrometry. The system is also equipped with a high-pressure cell which isolates the sample and allows chemical reaction studies to be performed at high pressures (atmospheres). The product distribution obtained at high pressures was monitored by a gas chromatograph with a thermal conductivity detector. Half a monolayer of potassium was deposited on the graphite using a potassium-zeolite gun at the background pressure of 1 x 10^{-9} torr.

No chemical reaction between graphite and water vapor was detectable in the absence of the potassium catalyst. In the presence of potassium the concentrations of CH_4, CO_2, and CO were monitored as a function of time. The activation energy for production of CH_4 was estimated to be 10 ± 3 kcal/mole, from the rates of CH_4 production measured when the system is in steady state (after 60 min). The turnover frequency for the methane formation reaction is ~ 10^{-3} s^{-1} at 523 K, assuming that all the graphite surface atoms are active. In order to obtain carbon mass balance for the graphite-water reaction that produces methane, the CO_2 and CO produced by blank studies were subtracted from the total amount of CO_2 and CO detected under reaction conditions. After subtraction of the amount produced in the blank experiments, some CO_2 still remained. Therefore the reaction that produces CH_4 and CO_2 may be expressed as:

$$2H_2P + 2C\ (\text{graphite}) \xrightarrow{K} CH_4 + CO_2 (\text{at } 473\text{-}673\ K).$$

The highest fraction of conversion to CH_4 occurs at 523 K.

The production H_2 and CO_2 was enhanced when CO was added to water vapor. It appears that much of the H_2 and the excess CO_2 are produced by the potassium-catalyzed water-gas shift reaction:

$$H_2 + CO \xrightarrow{K} CO_2 + H_2.$$

When using mixtures of CO and H_2O, only H_2 and CO_2 formation could be detected indicating that the water-gas shift reaction was taking place efficiently and at the expense of the methanation reaction. In the presence of CO_2 and H_2O gas mixtures, no products of any kind were detected. Potassium appears to catalyze both the reduction of carbon to CH_4 and its oxidation to CO_2.

* * *

†LBL Preprint-12812: A. W. Cabrera, H. Heinemann, and G. A. Somorjai: "Methane Production from the Catalysed Reaction of Graphite and Water Vapor at Low Temperatures." In-press to Journal of Catalysis.

Task 4: Selective Hydrogenation, Hydrogenolysis, and Alkylation of Coal and Coal Related Liquids by Organometallic Systems†

K. P. C. Vollhardt, Investigator

The purpose of this work is to uncover novel ways by which coal and coal derived substances may be activated toward chemical reaction with small molecules such as hydrogen, carbon monoxide, ethylene, and others using transition metal catalysts and reagents. The approach is a synthetic-mechanistic one. New and novel structures are being synthesized, analyzed by spectroscopic means, and their reaction dynamics investigated.

1. THE REACTION OF BENZENE WITH ALUMINUM TRICHLORIDE†

Linda S. Benner, Yee-Hing Lai, and K. Peter C. Vollhardt

In 1979 it was reported[1] that certain transition metal carbonyls $M_m(CO)_n$ [M = W, Rh, Ru, Cr, Co] in the presence of $AlCl_3$ catalyzed the so-called Fischer-Tropsch alkylation of benzene. The reaction appeared of great significance since it was unprecedented and thought to be homogeneous.

It has been found that alkyl benzenes are formed under the reported conditions. However, use of D_2 does not give deuterated products and application of ^{13}CO does not result in incorporation of the label. Moreover, neither CO or H_2 nor the transition metal are necessary for formation of the observed products. Simply heating benzene and $AlCl_3$ in a glass pressure vessel furnishes alkyl benzenes in addition to a variety

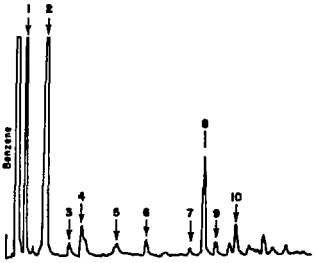

Fig. 1. A typical GC trace of the products from the reaction of benzene and $AlCl_3$ ([$AlCl_3$] = 0.7M, N_2 (1 atm), 160°C, 48 hr). 1 = toluene, 2 = ethylbenzene, 3 = isopropylbenzene, 4 = n-propylbenzene, 5 = butylbenzenes, 6 = tetralin, 7 = phenylcyclohexane, 8 = biphenyl, 9 = diphenylmethane, 10 = 1,2-diphenylethane. (XBL 812-13076)

of other products in rather similar proportions to those observed using literature[1] conditions (Fig. 1).

The major product of the reaction of benzene and $AlCl_3$ (0.18M) at reflux temperature is phenylcyclohexane, apparently a primary product which undergoes cracking reactions to the observed volatiles. At higher temperature the reaction is complicated by condensations, secondary cracking, and catalyst deactivation, most likely by π-complexation to higher benzenoids. The hydrogen necessary for alkylbenzene production is envisaged to arise via bi- and polyphenyl formation, as well as Scholl-type condensation reactions.[2]

Reaction of C_6D_6 gave completely labeled products. A 1:1 mixture of C_6H_6 and C_6D_6 gave complete scrambling. An equimolar mixture of C_6H_6 and $^{13}C_6H_6$ (90% enriched) was exposed to $AlCl_3$ [N_2 (1 atm), 169°C, 48 hr]. Surprisingly, ^{13}C-^{12}C exchange (~ 5%) was observed in recovered "unreacted" benzene and additional scrambling in all other volatile products. Nevertheless, the mass spectral peak patterns indicate substantially intact incorporation of alkyl chains derived from the original benzene ring. Thus, the connectivity of the initial carbon arrays is extensively preserved in the alkylaromatics formed. Processes such as those described here must play a significant role in any reaction that attempts to liquefy coal in the presence of Lewis acids.[3]

* * *

†Brief version of J. Am. Chem. Soc., 103, 3609 (1981). (LBL-12662)

1. G. Henrici-Olivé and S. Olivé, Angew. Chem., 91, 83, (1979); Angew. Chem., Int. Ed. Engl., 18, 77 (1979).
2. C. H. Thomas, "Anhydrous Aluminum Chloride in Organic Chemistry," Reinhold Publ. Corp., New York, NY, 1941.
3. N. D. Taylor and A. T. Bell, Fuel, 50, 499 (1980).

2. ON THE REVERSIBILITY OF η^4-CYCLOBUTADIENE METAL FORMATION FROM COMPLEXED ALKYNES†

Guy Ville, K. Peter C. Vollhardt, and Mark J. Winter

Vinylcarbon-carbon bond activation would be the prerequisite for the activation of aromatic and olefinic linkages in coal related structures. The feasibility of this process has been demonstrated in this work using transition metal complexed model compounds, which have also allowed the delineation of detailed mechanistic aspects.

Diastereomeric 1,2-bis(trimethylsilyl)-3-alkylcyclobutadiene cyclopentadienyl cobalt complexes 1 and 2 (see Scheme 1) in which the alkyl group contains a chiral center may be synthesized, separated, and equilibrated in the gas phase at 540-650° by flash pyrolysis or in solution in refluxing pristane (301°C). The process is unimolecular as shown by crossover experiments and kinetic analysis. Isomerization occurs by inversion at the four-ring, demonstrated by the pyrolysis of complexes enantiomerically enriched at the chiral carbon center and analysis of the products by optically active NMR shift reagents. *No other processes but diastereoisomerization are* observed in solution. In the gas phase increasing temperatures lead to increasing decomposition of starting complexes to cobalt metal and alkynes derived by retrocyclization of the cyclobutadiene ligand, in addition to positionally isomerized complexes. Such positional isomerization proceeding through B is also the mechanism of diastereoisomerization as shown by the pyrolysis of 1-triethylsilyl-2-trimethylsilyl substituted (1 ⇄ 2d); (1e ⇄ 2e) and ^{13}C-labeled complexes. The data strongly imply that the cyclization of alkynes to cyclobutadienes in the coordination sphere of cobalt is reversible. They do not necessitate the intermediacy of a metallacycle A, which, if present, would have to be configurationally stable (i.e., the η^5-C_5H_5 ligand has to remain on one face of the other π-ligand). This constitutes the first demonstration of reversible alkyne formation from cyclic π-systems in the coordination of sphere of metals and suggests experiments aimed at aromatic hydrocarbons activation.

* * *

†This work supported in part by NSF. Brief version of LBL-12943.

Scheme 1

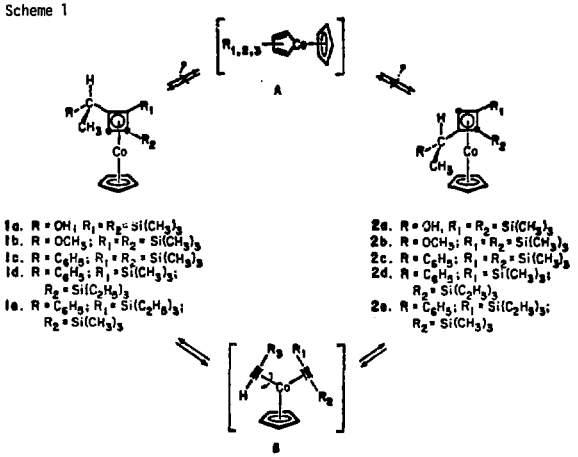

3. PREPARATIVE SEPARATION OF ORGANOMETALLIC COMPOUNDS BY HIGH PERFORMANCE LIQUID CHROMATOGRAPHY†

Joseph A. King, Jr. and K. Peter C. Vollhardt

Successful separations of complex mixtures of organometallic compounds by chromatography are rare. However, high performance reverse phase liquid chromatography (HPLC) of isomeric and structurally analogous complexes has been achieved. Although some of these compounds are moderately to strongly air-sensitive, quantitative isolation on a preparative scale is possible by using deoxygenated and argon saturated mobile phases. Among the organometallic complexes resolved are disastereomers and structural isomers; their separation demonstrates both the versatility and high resolving power of HPLC. All separations were accomplished using 10 x 250 mm ULTRASPHERE ODS columns (sample loop 1 ml). Initial gravity elution chromatography of these compounds gave inseparable mixtures.

* * *

†Brief version of J. Organometal. Chem., 208, 73 (1981); Altex Chromatogram, 3 (4), 2 (1980), LBL-11801.

4. WORK IN PROGRESS

The occurrence of hydrogen shifts has been well established in coal conversion reactions. However, the details of these processes which in many cases are catalyzed by the mineral matter present in coal, are not well understood. Moreover, aromatic and olefinic C-H bond activation could be an important step in approaches to coal liquefaction by lipophilization.

A very low activation energy process has been uncovered in which a vinyl-hydrogen is transferred from one end of a ligand bridging a binuclear metal system to the other. Kinetic and labeling experiments should provide important mechanistic information. The generality of this process is being investigated by ligand variation and changes in the metal. Two x-ray structural analyses have been completed which confirm structural assignments based on spectroscopic measurements.

Task 5 - Chemistry of Coal Solubilization and Liquefaction: Pyrolysis Studies.

(A) R. G. Bergman, Investigator

5. LASER-POWERED HOMOGENEOUS DISSOCIATION OF TETRALIN†

Paul B. Comita, Michael R. Berman, C. Bradley Moore, and Robert G. Bergman

In an effort to determine the products and mechanism of the truly homogeneous thermal dissociation of the aromatic hydrocarbon tetralin (compound 1 in Fig. 1), we have examined the products formed from this compound upon energization by infrared multiphoton excitation and SiF_4-sensitized infrared thermal activation. Six major products (Fig. 1) are formed in these reactions, three of

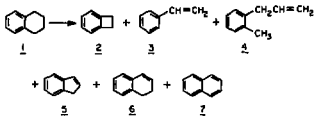

Fig. 1. Products formed on laser-powered decomposition of tetralin (1). (XBL 811-5038)

which appear to be primary dissociation products: these three are benzocyclobutene (2), o-allyltoluene (4), and 1,2-dihydronaphthalene (6). The lowest energy reaction channel is the ethylene-loss channel resulting in benzocyclobutene. The ring cleavage channel, giving rise to o-allyltoluene, has not not been previously observed. The dehydrogenation reaction, which forms 1,2-dihydronaphthalene, results primarily in loss of hydrogen from C1 and C2 and is predominantly a nonconcerted hydrogen elimination. We believe that in previous studies, where dehydrogenation was reported as the primary dissociation channel, the experiments were complicated by surface catalysis. In the laser-induced reactions, which are uncomplicated by problems due to surface catalysis, the true homogeneous decomposition takes place, and this involves primarily ethylene loss.

* * *

†This and additional work has been reported in detail in items 9-12 of the Refereed Journals listing at the end of this section.

(B) R. H. Fish and T. Vermeulen, Investigators, with G. A. Cremer and A. Thormodsen

6. HOMOGENEOUS CATALYTIC HYDROGENATION OF POLYNUCLEAR AROMATIC AND HETEROAROMATIC NITROGEN COMPOUNDS WITH TRANSITION METAL CARBONYLS†

The various synthetic fuel processes that involve coal liquefaction rely on large amounts of hydrogen in the upgrading or hydroprocessing of the liquid fuel products. Thus, it is extremely important to have a basic understanding of which polynuclear aromatic and polynuclear heteroaromatic compounds are hydrogenated in these complex fossil fuel matrices. It is particularly desirable to selectively hydrogenate the ring containing the heteroatom.

Several catalytic amounts of transition metal carbonyl compounds of Fe, Mn, Co, Ru, Rh, Re, Os, Cr, W and Mo, were reacted with model coal compounds under water gas shift (WGS) conditions (CO, H_2O, base). These included anthracene, phenanthrene, pyrene, acridine, quinoline, 5, 6, and 7, 8, benzoquinoline. Only Fe, Co, and Mn carbonyls react to any significant extent to produce partially hydrogenated analogs of the model coal compounds.

We have determined that carbon monoxide, in many cases, inhibits the reaction of the model coal substrate with catalytically generated transition metal carbonyl hydrides. Pertinent examples of CO inhibition that vividly make this point clear are those reactions with mononuclear and trinuclear ruthenium carbonyl compounds. In these two cases, the use of carbon monoxide completely inhibits substrate binding to a presumed coordinatively unsaturated ruthenium carbonyl intermediate. Interestingly, dimanganese decacarbonyl or cobalt octacarbonyl catalyzed reactions are not affected by the use of carbon monoxide. This observation establishes the mechanistic differences between Mn or Co and Ru carbonyls.

$Mn(CO)_8(PBu_3)_2$ reacts under either WGS (CO, H_2O, base) or Syn Gas [CO, H_2, 1:1] conditions with 9,10-dimethylanthracene to provide a mixture of cis and trans - 9,10-dimethyl- 9,10-dihydroanthracene compounds. This result is indicative of a free radical mechanism where both cis and trans 9,10-dimethyl- 9,10-dihydroanthracene would be expected to be produced.

The reactions of either $RuCl_2(CO)_2(\phi_3P)_2$ or $H_4Ru_4(CO)_{12}$ (as well as Bu_3P substituted analogs) under hydrogenation conditions, such as 350 psi H_2, sub/cat ~ 30, in THF for 2 hr, at 180°C, give excellent yields of partially reduced analogs of PNHA (nitrogen is the heteroatom) compounds. Coal models that were used included acridine, 5,6 and 7,8 benzoquinoline, quinoline and phenantridine.

* * *

†Brief version of LBL-13734 Preprint and LBL-13735 Preprint.

Task 6 - Coal Conversion Catalysts: Deactivation Studies

A. V. Levy and E. E. Petersen, Investigators

Sulfur compounds in petroleum residue and coal liquids are converted by reacting them with hydrogen over a Co-Mo-alumina catalyst to make hydrogen sulfide. These liquids also contain organically bound trace metals, typically vanadium, nickel, iron and titanium, which deposit on the catalyst as metal sulfides. These deposits block access to the surface and eventually render the catalyst useless.

We are investigating this metal deposition and catalyst deactivation behavior both experimentally and theoretically. We deposit a model metal compound, vanadyl naphthenate, dissolved in a high-sulfur gas oil onto a commercial hydrodesulfurization catalyst. The kinetics of demetallation and desulfurization are determined from the decline of metal and sulfur concentrations in the liquid and the metal sulfide concentration profiles in the catalyst measured with an electron microprobe. A model that predicts the shape of the metal deposit profile inside the catalyst has been developed and compared with published results. It has been experimentally determined that the local demetallation activity declines while the global demetalla-

tion and desulfurization activities are unchanged for the conditions used.

Our next objective is to apply a more sophisticated model to the results of demetallation and desulfurization experiments with a more realistic model metal compound, vanadyl tetraphenylporphyrin.

1981 PUBLICATIONS AND REPORTS

Refereed Journals

1. A. W. Cabrera, H. Heinemann, and G. A. Somorjai, "Potassium Catalysed Methane Production from Graphite at Low Temperatures," Chem. Physics Letters 81, 3, 402 (1981); LBL-12665.

2. A. W. Cabrera, Heinz Heinemann, and G. A. Somorjai, "Methane Production from the Catalysed Reaction of Graphite and Water Vapor at Low Temperatures," in press, Journal of Catalysis; LBL-12812.

3. L. S. Benner, Y. H. Lai, and K. P. C. Vollhardt, "On the Purported Fischer-Tropsch Alkylation of Benzene...," J. Am. Chem. Soc., 103, 3609 (1981); LBL-12662.

4. G. Ville, K. P. C. Vollhardt, and M. J. Winter, "On the Reversibility of η^4-Cyclobutadiene Metal Formation From Complexed Alkynes: Unimolecular Isomerization of Labelled Racemic and Enantiomerically Enriched η^5-Cyclopentadienyl-η^4-Cyclobutadiene Cobalt Complexes," J. Am. Chem. Soc., 103, 5267 (1981); LBL-12943.

5. J. M. Huggins, J. A. King, Jr., K. P. C. Vollhardt, and M. J. Winter, "Separation of Diastereomers, Structural Isomers, and Homologs of η^5-Cyclopentadienyl Cobalt and Dinuclear Molybdenum Complexes by Reverse Phase High Performance Liquid Chromatography Using Deoxygenated Solvents," J. Organomet. Chem., 208, 73 (1981); LBL-11801.

6. Y.-H. Lai, W. Tam, and K. P. C. Vollhardt, "Transition Metal Activation of η-Complexed Benzene: Double Nucleophilic Addition," J. Organometal. Chem., in press; LBL-12459.

7. J. A. Wittle, M. I. Perez and J. W. Evans, "Transmission Electron Microscopy Studies of Coal," LBL Preprint LBL-11473.

8. D. J. Coates, J. W. Evans, and S. S. Pollack, "Identification of the Origin of TiO_2 Deposits on a Hydrodesulfurization Catalyst," submitted to Fuel; LBL-13244.

9. T. P. Lockhart, P. B. Comita, and R. G. Bergman, "Kinetic Evidence for the Formation of Discrete 1,4-Dehydrobenzene Intermediates: Trapping by Inter- and Intramolecular Hydrogen Atom Transfer and Observation of High-Temperature CIDNP," J. Am. Chem. Soc., 103, 4082 (1981); LBL-11696.

10. T. P. Lockhart and R. G. Bergman, "Determination of the Reactive Spin State of 1,4-Dehydrobenzenes," J. Am. Chem. Soc., 103, 4091 (1981); LBL-11695.

11. Paul B. Comita, Michael R. Berman, C. Bradley Moore, and Robert G. Bergman, "Laser-Powered Homogeneous Dissociation of Tetralin," submitted to the Journal of Physical Chemistry; LBL-12697.

12. H. Heinemann, "A Brief History of Industrial Catalysis" in Catalysis, Science and Technology Vol. 1, Springer Verlag, 1981; LBL-10278.

13. H. Heinemann, "Technological Applications of Zeolites in Catalysis," Catal. Rev.-Sci. Eng. 23 (182), 315, (1981); LBL-11662.

LBL Reports

1. Richard H. Fish and Gregg A. Cremer, "Homogeneous Catalytic Hydrogenations: 1. Reductions of Polynuclear Aromatic and Heteroaromatic Nitrogen Compounds Utilizing Carbon Monoxide with Water or Hydrogen," LBL-13734.

2. Richard H. Fish and Gregg A. Cremer, "Homogeneous Catalytic Hydrogenations: 2. Regiospecific Reductions of Polynuclear Aromatic and Heteroaromatic Nitrogen Compounds Catalyzed by Ruthenium Carbonyl Hydrides," LBL-13735.

Invited Talks

G. A. Somorjai

"Graphite Gasification," DOE, BES, Chem. Sci. Meeting on Catalysis, May 1981.

"Surface Science Research," Welch Foundation Meeting, Houston, TX, Nov. 1981.

H. Heinemann

"Chemistry and Morphology of Coal Liquefaction," International Coal Science Congress, Düsseldorf, West Germany, Sept. 1981.

"Chemicals and Fuels from Coal," 2nd Mediterranean Chem. Eng. Congress, Barcelona, Spain, Nov. 1981.

"Catalytic Routes to 100 Octane Gasoline," Welch Foundation Meeting, Houston, TX, Nov. 1981.

R. H. Fish, T. Vermeulen and G. Cremer

"Utilization of Carbon Monoxide and Water as a Reducing Agent for Model Coal Compounds," 182nd National ACS Meeting, New York, Aug. 23-28, 1981, Abstract INOR 49; LBL-12518 Abstract.

G. A. Cremer, T. Vermeulen and R. H. Fish

Catalytic Hydrogenation of Model Coal Compounds by Soluble Transition Metal Hydrides," Pacific Conference on Chemistry and Spectroscopy, Anaheim, CA., Oct. 19-21, 1981, Abstract 188; LBL-1288 Abstract.

K. P. C. Vollhardt

"Transition Metal Mediated Carbon-Carbon Bond Making and Breaking Reactions," at University of Alberta, University of British Columbia,

Victoria University, and Simon Fraser University, Canada, January 1981.

K. P. C. Vollhardt

"The Transition Metal Mediated Conversion of Trimethylsilylalkynes to Complex Organic Molecules," Plenary Lecture, 181st ACS National Meeting, Symposium on Silicon in Organic Synthesis, Atlanta, GA, March 29-April 3, 1981.

"Transition Metal Mediated Carbon-Carbon Bond Formations," Plenary Lecture, 10th Conference on Coordination and Metallorganic Chemistry, Queenstown, New Zealand, May 10-15, 1981; also at University of Queensland, Australian National University, University of Adelaide, and Monash University, Australia, May 1981.

"Mechanistic Studies in Transition Metal Mediated Bond Breaking and Making Reactions," University of Missouri, St. Louis, November 1981.

"Remarkable Transformations in the Coordination Sphere of Cobalt," Australian National University, May 1981.

I. Solution Thermodynamics of Sulfites and Sulfite Oxidation Mechanisms*

Leo Brewer and Robert E. Connick, Investigators

Introduction. Burning of fossil fuels, particularly coal, introduces oxides of sulfur into the air. At sufficiently high pollution levels these chemicals are believed to cause health effects detrimental to humans. Heavy fall-out over certain terrains leads to severe destruction of fauna and flora through the phenomenon known as acid rain. The principal toxic compound of acid rain is sulfuric acid, formed by the oxidation of sulfur dioxide by oxygen, once the sulfur compound has been emitted into the atmosphere through combustion. The most prolific source of such sulfur dioxide is coal-burning power plants.

Processes have been developed for removing sulfur dioxide from the stack gases of power plants, but they are expensive and unreliable, in part because their complex chemistry is not fully understood. The research undertaken here is aimed at developing a better understanding of the chemistry of sulfur dioxide and related species in order that this information can be used to improve these processes. The work is fundamental to the understanding of the chemical fates of the sulfur dioxide once it escapes into the atmosphere.

1. THE RATE AND MECHANISM OF THE OXIDATION OF BISULFITE ION BY OXYGEN†

Thomas G. Braga‡ and Robert E. Connick

The reaction: $O_2 + 2HSO_3^- \rightarrow 2SO_4^{2-} + 2H^+$ occurs in flue gas desulfurization processes and probably in the atmospheric oxidation of SO_2 on the surface of particles suspended in air. The kinetics of this reaction has been the subject of many investigations, almost always at acidities at which SO_3^{2-} rather than HSO_3^- was the principal S(IV) species. Nearly every set of investigators finds a different rate and rate law, indicating that impurities play an important role. Since the reaction is known to go by a chain mechanism, such a result is not surprising. Attempts to purify the chemicals have given no clear indication that a system free of catalysis by impurities has ever been studied.

Because of the importance of the reaction to sulfur dioxide pollution, a fresh attempt has been made to investigate the rate and mechanism. Rather than try to purify chemicals more and more, the tack taken was to add deliberately substances that would control the three basic steps of the chain: initiation, propagation and termination. In this way it was hoped that the extreme irreproducibility of the rate could be controlled and rate laws and mechanisms determined. Once under control, the effect of a wide variety of catalysts and inhibitors could be tested and their roles in the mechanisms ascertained.

Ethanol, a well known inhibitor, was used to control the termination step. Manganous ion, an excellent catalyst, was tried as a propagator. Ultraviolet light was used as an initiator. The rate law was determined for the reaction with various combinations of these two catalysts and inhibitor present. All work was done at 25°C in a closed system with no gas space. The course of the reaction was followed by the decrease in the O_2 concentration using an oxygen meter. The pH ranged from ~ 3 to 5 so that HSO_3^-, which was in large excess compared to the O_2, was the principal S(IV) species. Under essentially all conditions the rate was zero order in oxygen concentration. With no alcohol present the chain termination appeared to be a bimolecular reaction between two chain carriers; with alcohol present it was first order in alcohol and first order in a chain carrier. The propagation step in the absence of Mn^{2+} was most simply interpreted as first order in HSO_3^- and first order in a chain carrier; with Mn^{2+} present it appeared to be first order in Mn^{2+} concentration. The initiation was most simply interpreted as first order in bisulfite concentration and inverse second order in hydrogen ion concentration, while with the ultraviolet light it became first order in bisulfite and zero order in hydrogen ion concentration. The above array of rate laws can in each case be interpreted in terms of more than one mechanism so that a mechanistic interpretation must await further information, although the results severely limit the possibilities. The experiments with ultraviolet light need to be extended with a more appropriate physical set-up so that the reproducibility of the experiments can be tested and the wavelength dependence of the initiation determined. Then it should be possible to study the role of a variety of catalysts and inhibitors in the reaction.

* * *

†Brief version of LBL-12342, pp. 118-138.

‡Present address: Petrolite Corporation, 369 Marshall Ave., St. Louis, MO.

2. SOLID-GAS EQUILIBRIA AND KINETICS OF THE $CaSO_3$-H_2O SYSTEM†

Bea-Jane Lin

The importance of the role played by calcium sulfite in the flue-gas desulfurization by lime-limestone scrubbers makes it desirable to characterize the thermodynamics and kinetics of the calcium sulfite-water system.

A thermogravimetric apparatus was used to study calcium sulfite hemihydrate and calcium sulfite anhydrite under a variety of temperatures and water pressures. Because of slow hydration and dehydration rates, equilibrium is reached very slowly and dynamic methods of determining equilibria were not effective.

*This work was supported by the Assistant Secretary for Fossil Energy, Office of Coal Research, Advanced Environmental Control Division of the U. S. Department of Energy under Contract No. DE-AC03-76SF00098 through the Morgantown Energy Technology Center, Morgantown, WV.

By combination of thermodynamic data available and use of predictive models, the kinetics and thermodynamics for dissociation of calcium sulfite hemihydrate was carefully examined and elaborated.

* * *

†Brief version of LBL-13466.

3. THERMODYNAMIC DATA FOR FLUE-GAS DESULFURIZATION PROCESSES†

Leo Brewer

The problem of extracting sulfur dioxide from flue gas has turned out to be more difficult to carry out at power-plant-scale operation than had been anticipated. The reactions involved in the oxidation of sulfur dioxide are quite complicated and adequate information is needed to design efficient extraction systems. There are two obstacles to obtaining the needed information. In many instances, the information is in the extensive literature going back over 100 years, but it is a difficult process to retrieve and evaluate this information and not much effort has been made in this direction. The other difficulty is that there are many aspects of the problem which have not been fully elucidated which require appropriate research to provide a fuller understanding.

In an effort to meet these needs, a review of the available thermodynamic data for sulfur compounds and related materials was carried out to provide the best set of internally consistent values obtainable from the literature and from current experiments. Although the main emphasis is on information needed for aqueous limestone or lime slurry treatment, the data could also be used for other processes covering a wider temperature range. Thus, whenever possible, thermodynamic data have been presented for the range from room temperature to at least 1000 K for pure systems and up to 500 K for aqueous solutes.

Altogether thermodynamic data have been tabulated for 84 gases, 90 solids and liquids, and 107 aqueous solutes. The extension of aqueous thermodynamic data to higher temperatures using various predictive models has provided thermodynamic data of practical accuracy for a wide range of aqueous solutions. It is expected that these compiled data will be of considerable use in improving and in working out adequate controls for limestone scrubbing processes.

* * *

†Brief version of LBL-11758 and paper 16 of CONF-801176.

4. ESTIMATION OF ACTIVITY COEFFICIENTS IN CONCENTRATED SULFITE-SULFATE SOLUTIONS†

G. M. Rosenblatt‡

The Pitzer theory was used to estimate geometric mean-ion activity coefficients in strong electrolyte solutions at 25-55°C. The ion-pair parameters make it possible to calculate activity coefficients to moderately high ionic strengths in aqueous mixtures containing the following ions:

Na^+, K^+, Mg^{2+}, Ca^{2+}, Cl^-, ClO_3^-, ClO_4^-, HCO_3^-,

HSO_3^-, CO_3^{2-}, SO_4^{2-}, SO_3^{2-}, and $S_2O_5^{2-}$.

* * *

†Brief version of AIChE Journal 27, 619-26 (1981).
‡Present address: Los Alamos National Laboratory, Los Alamos, NM 87545.

1981 PUBLICATIONS AND REPORTS

For a list of publications, reports, awards and invited talks, see section on "Formation of Oxy-Acids of Sulfur from SO_2" for R. E. Connick, and section on "High Temperature Thermodynamics" for L. Brewer.

g. Process Chemical Parameters in Aqueous Sulfur Dioxide Removal by Lime/Limestone Scrubbers*

Robert E. Connick, Investigator

Introduction. The purpose of this work is to elucidate the basic chemistry of aqueous sulfur-dioxide solutions. These solutions contain bisulfite, disulfite, and sulfur dioxide. They undergo slow auto-redox reactions in which the end product is elemental sulfur (S-0) and sulfate (S+VI). The reaction involves thiosulfate, polythionates, dithionate and other, as yet unidentified, metastable intermediates which form various soluble and insoluble products which may interfere with the scrubbing of flue gases with lime/limestone and other bases. The complex reactions are catalyzed by metal ions, elemental sulfur and thiosulfate. Intensive efforts of investigators over the last 150 years to analyze these systems (in order to develop a viable sulfur-dioxide scrubbing and recovery process) have failed, largely because the traditional analytical techniques are complex, cumbersome, interfere with the reaction, disturb the equilibria, and are not comprehensive. Our previous work has shown that laser Raman spectroscopy makes possible rapid, in situ analysis of the reactions.

Work on the thermodynamics of these systems conducted by L. Brewer and associates is described in the section "Solution Thermodynamics of Sulfites and Sulfite Oxidation Mechanisms." Kinetic studies conducted by R. E. Connick and associates are described in the same section.

1. DECOMPOSITION OF SULFUR DIOXIDE - AMMONIA SOLUTIONS†

C. B. Meyer, K. Koshlap and K. Ward‡

A computer-assisted laser Raman Spectrometer was used to record spectra of ammonia solutions saturated with sulfur dioxide sealed in evacuated glass tubes. The reaction was followed at 20°C, 35°C, 50°C, and 75°C, and the spectra were analyzed by comparison with standard solutions prepared from pure compounds. The reaction produces thiosulfate and dithionate as intermediates, and yields elemental sulfur and sulfate as end products. The half-life of the saturated solutions is about 48 hours at 70°C.

* * *

†Brief version of LBL-11969.

‡Permanent address: University of Washington, Seattle, WA.

*This work was supported by the Assistant Secretary for Fossil Energy, Office of Coal Research, Advanced Environmental Control Division of the U. S. Dept. of Energy under Contract No. DE-AC03-76SF00098 through the Morgantown Energy Technology Center, Morgantown, WV.

2. RAMAN SPECTROMETRIC DETERMINATION OF AQUEOUS SULFUR ANIONS

C. B. Meyer, M. Ospina,† A. Tini, K. Koshlap and K. Ward†

Standard spectra were prepared by recording four Raman scans each of 1M solutions of sulfate, bisulfate, sulfite, bisulfite, disulfite, dithionate, dithionite, trithionate, tetrathionate, pentathionate, thiosulfate, and elemental sulfur. Perchlorate and the internal water standard were verified by comparison with synthetic mixtures containing known concentration ratios of two or three of the above ions. These spectra have been used for the qualitative and semiquantitative analysis of the decomposition products of sulfur oxyacids and of sulfur scrubbing liquors.

* * *

†Permanent address: University of Washington, Seattle, WA.

3. CHEMISTRY OF OXYACIDS OF SULFUR†

C. B. Meyer, M. Ospina,‡ K. Ward,‡ M. Hinnawi‡

Thiosulfate, elemental sulfur, and metal ions are known catalysts for the decomposition of sulfite/bisulfite solutions. Work on copper, silver, and gold complexes of thiosulfate has shown that at least three different complexes exist with each metal ion in all of which the charge distribution within the thiosulfate is significantly changed, thus enhancing decomposition.

* * *

†Brief version of Ph.D. thesis, M. Hinnawi, University of Washington, Seattle, WA, 1981.

‡Permanent address: University of Washington, Seattle, WA.

4. THE STRUCTURE OF THE DITHIONITE ION†

B. Meyer and L. Peter‡

Raman Spectra of eight alkali and alkaline earth salts of dithionite have been compared with those of the corresponding solutions. The well established structure of sodium di-hydrate, C_{2v}, with a sulfur-sulfur bond distance of 2.389 Å is supported by the Raman spectra of the solid salts. However, in all solutions the aqueous ion is shown to have C_{2h} symmetry. This structure corresponds to that of P_2F_4, P_2Cl_4, P_2I_4, $P_2(CH_3)_4$ and $As_2(CH_3)_4$. It offers a far more favorable structure and charge distribution, and corresponds to a bond length of about 1.27 Å, which correlates far better with other oxyacid structures than the C_{2v} structure.

* * *

†Brief version of LBL-13783.
‡Current address: Seattle Pacific University, Seattle, WA.

5. THE SULFITE - FORMALDEHYDE REACTION†

B. Meyer, M. Rigdon,‡ R. Nunlist, and K. Koshlap

This reaction has been used for fifty years as a quantitative tool for determining both formaldehyde and sulfite, but this reaction is not well understood. C-13 NMR and Raman spectra show that the sulfite causes step-wise degradation of aqueous formaldehyde polymers and is reversible. Isotope work shows that the compound contains a C-S bond. This work has led to studies of formaldehyde measurements in indoor air and formaldehyde release from consumer products in support of regulatory activities of the U.S. Consumer Product Safety Commission and the U.S. Department of Housing and Urban Development.

* * *

†Brief version of LBL-12452. Work supported in part by the U.S. Consumer Product Safety Commission via the Analytical Chemistry and Environmental Health Division of Oak Ridge National Laboratory.
‡Current address: University of Washington, Seattle, WA.

6. WORK IN PROGRESS

More than four hundred spectra from a dozen experiments with trithionate and tetrathionate at 20°C, 35°C, 50°C, and 70°C have been recorded and are being evaluated to identify all intermediates and estimate the concentration of all components as a function of time so that a mass balance can be calculated, in order to derive the reaction mechanisms, and to determine the kinetics in these systems.

The ammonia-sulfur dioxide system is being evaluated in the presence of elemental sulfur and selenium as catalysts. The effect of thiosulfate is studied in order to elucidate the reason for the induction period observed in this reaction.

A study of the thermal auto-redox decomposition of dithionite is under way to determine the intermediates in the oxidation state (S+2) and to elucidate the kinetics.

1981 PUBLICATIONS AND REPORTS

Refereed Journals

1. B. Meyer and R. Nunlist, "C-13 NMR Identification of Urea-Formaldehyde Resins," in Symposium on Aqueous Polymers, L. J. Guilbault, ed., Polymer Reprints 24, 112 (1981); LBL-11762.

LBL Reports

1. B. Meyer, K. Koshlap, M. Rigdon, M. Ospina, and K. Ward, "Thermal Decomposition of Sulfite, Disulfite and Bisulfite," February 1981, LBL-11969.

2. B. Meyer and M. Rigdon, "C-13 NMR and Raman Spectroscopic Study of the Sulfite-Formaldehyde Reaction," May 1981, LBL-12452.

3. B. Meyer and L. Peter, "The Structure of the Dithionite Ion," December 1981, LBL-13783.

Other Publications

1. B. Meyer, K. Koshlap and M. Ridgon, "Thermal Decomposition of Ammonium Disulfite," Proc. Symp. on Flue Gas Desulfurization, G. Rochelle and M. Hudson, eds., Am. Chem. Soc. Symp. Proceedings, 1981.

2. B. Meyer, M. Rigdon, T. Burner, K. Koshlap, M. Ospina, and K. Ward, "Thermal Decomposition of Sulfur Oxyacids," Proc. Flue Gas Desulfurization Conf., Morgantown, WV, November 6-7, 1980, L. Brewer, ed., Conf-801176, LBL-12342.

3. M. Hinnawi, "Thiosulfate Complexes of Copper, Silver, and Gold," Ph.D. thesis, University of Washington, Seattle, WA, 1981.

Invited Talks

1. B. Meyer, K. Koshlap, K. Ward, and M. Ospina, "Thermal Decomposition of Bisulfite, Disulfite, and Aqueous Sulfur Dioxide," Symposium on Flue Gas Desulfurization, National ACS Meeting, Atlanta, GA, March 31, 1981 (based on LBL-11969).

2. B. Meyer, "Air Analysis and the Formaldehyde-Sulfite Reaction: Formaldehyde Emission from Consumer Products," University of Dortmund, West Germany, Polymer Science and Chemistry Department, Feb. 24, 1981 (based on LBL-12570). Same presentation given Feb. 26, 1981 at Heidelberg University Medical School.

3. B. Meyer and R. Nunlist, "The C-13 Analysis of Urea-Formaldehyde Resins," in Symposium on Aqueous Polymer Systems, ACS National Meeting, April 2, 1981, Atlanta, GA (based on LBL-11762).

4. B. Meyer and K. Koshlap, "Analysis of Formaldehyde-Sulfite Solutions," HUD-Workshop on Advanced Notice of Proposed Regulation for Formaldehyde Emission Measurements and Indoor Air Standards for Mobile Homes, Washington, DC, April 20, 1981 (based on LBL-12570). Same talk also presented in Washington DC on July 6 and Aug. 10, 1981, at CPSC Workshops on voluntary formaldehyde release standards.

5. B. Meyer, "Indoor Air Analysis and Analysis of Formaldehyde by Sulfite Sampling," Richmond, BC, Canada, School District No. 38 Board Meeting and Public Hearing, Vancouver, BC, October 12, 1981.

6. B. Meyer, "The Role of Sulfur in Polymer Chemistry," International Rubber Research Hall of Sciences Symposium, Akron, Ohio, November 20, 1981.

h. Materials Characterization in Fossil Fuel Combustion Products*

Donald H. Boone, David P. Whittle, and Alan V. Levy, Investigators

Introduction. The durability of directly fired heat engines operated on coal-derived liquids, shale oil, coal slurries, and other minimally processed alternate fuels is dependent on the surface stability of combustion zone components. Some type of protective coating system will be mandatory if the potential advantages of lower fuel costs and more efficient combustion are to be fully realized.

The DOE Combustion Zone Durability Program is involved in the development and evaluation and the materials technology necessary for the successful use of these fuels.

The LBL portion of this effort is focused on developing a better understanding of the structure of the various types and forms of ceramic thermal barrier coatings and their behavior in a variety of testing and engine environments. Additional LBL functions in this effort include the coordination and documentation of test specimen production, testing and analysis for the entire program, and participation on the Combustion Zone Durability Steering Panel.

1. PLASMA SPRAYED THERMAL BARRIER COATINGS†

Donald H. Boone

Ceramic coatings are currently being evaluated for a number of thermal barrier applications because the coatings provide both insulation, allowing hotter gas temperatures, and an inert barrier to isolate the metallic components from the corrosive environment. Plasma sprayed ZrO_2 is a prime candidate, and this study is concentrating on determining the effects of stabilizing MgO or Y_2O_3 additions in modifying the protective properties of the coating.

The initial plasma sprayed ZrO_2 studies involve structures prepared by the Central Institute of Industrial Research (CIIR), Oslo, Norway. These ceramic coatings are undergoing tests in slow speed ship diesel engines. Preliminary results show a benefit of the MgO-stabilized ZrO_2 over the Y_2O_3-stabilized ceramic (YSZ). Similar structures prepared by CIIR and tested in a Transamerica Delaval diesel on exhaust valves showed an apparent reversal of these results after a 4000 hour exposure. In other test programs, it has been found that the MgO-stabilized ZrO_2 is more resistant to vanadium-induced attack. The cleaner fuels used by Delaval in their tests may reflect a measure of resistance to thermally induced stresses rather than to chemical attack.

* * *

†Brief version of LBL-13777.

2. THERMAL BARRIER COATINGS APPLIED BY PHYSICAL VAPOR DEPOSITION†

Donald H. Boone

Efforts to improve the thermal fatigue resistance of ceramic thermal barrier coatings by structural modification include segmentation by chemical and mechanical means. A promising approach is the use of the characteristically columnar oriented growth structure produced by physical vapor deposition (PVD) such as electron beam evaporation and sputtering. This study, in collaboration with Airco-Temescal, is concentrating on the effects of the deposition variables on the structure and adherence of electron beam PVD applied Y_2O_3-ZrO_2.

The oriented growth structure of the PVD-deposited ceramic ensures a low effective modulus in a direction perpendicular to the columnar grains and, thus, any thermally induced strains are only weakly transmitted to the ceramic-metal interface, resulting in improved thermal fatigue behavior. Processing variables such as deposition temperature and rate, initial surface condition and geometry all affect the development of the columnar structure. Figure 1 shows a fracture section through a PVD fully stabilized ZrO_2 coating deposited at about 800°C. The high length/diameter ratio of the columnar grains and the sensitivity of the ceramic-metal interface to adherence (lower figure) are clearly seen. Increase in the deposition temperature of 600°C to 1100°C resulted in an increase in average columnar diameter. Surface temperature cycling with rotation during deposition resulted in detrimental renucleation

*This work was supported by the Assistant Secretary for Fossil Energy, Office of Coal Research, Heat Engines and Heat Recovery Division of the U.S. Department of Energy under Contract No. DE-AC03-76SF00098 through the Battelle Memorial Institute, Pacific Northwest Laboratories, Richland, WA.

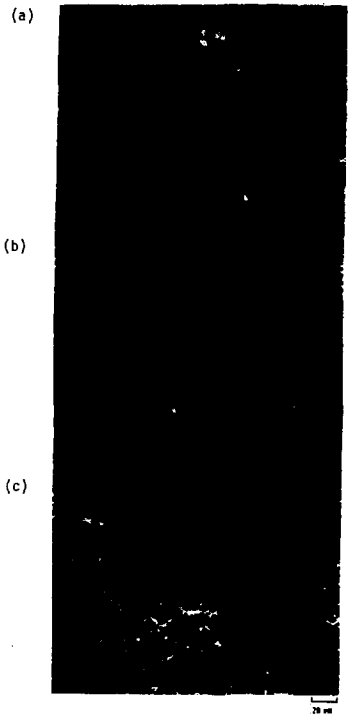

Fig. 1. Microstructure of an electron beam physical vapor deposited Y_2O_3-stabilized ZrO_2 coating: (a) surface, (b) fracture cross-section, and (c) interface surface between deposited ZrO_2 and metallic interlayer.

(XBB 817-5936)

and interrupted column growth.

Future studies will concentrate on ceramic-metal or ceramic-oxide-metal coating systems since the substrate surface is often a pre-oxidized interface.

* * *

†Brief version of LBL-13721.

3. INTERACTIONS BETWEEN COATINGS AND SUBSTRATES AT ELEVATED TEMPERATURES†

Donald H. Boone and David P. Whittle

Three principal types of coatings have been developed: diffusion aluminides, overlay coatings, and ceramic or thermal barrier coatings. This order of development also represents what might at first be anticipated to be an increasing independence of the substrate. However, it is slowly being realized that this is certainly not the case for aluminide and overlay coatings, and is probably not even true for ceramic coatings.

An important question is which are the beneficial and detrimental substrate elements incorporated into the coating and to what extent do they interact with protective oxide formation on the coating. W, Mo, and Ta may contribute toward acid fluxing of the oxide in service conditions involv-

ing sulfate contamination; Ti, Hf and Zr may contribute to scale adhesion or compete with Al for protective oxide formation. Calculations have shown that at temperatures above about 1000°C, substrate elements can diffuse rapidly through a nominally 150 μm thick coating. However, at lower temperatures, effects of the substrate elements were still present in the coatings, even at short exposure times, which strongly suggests that some elements are able to diffuse rapidly during the coating deposition process itself. This hinders the coating from developing a truly protective Al_2O_3 film.

* * *

†Brief version of LBL-13350.

1981 PUBLICATIONS AND REPORTS

Refereed Journals

1. J. Maasberg, D. H. Boone, D. P. Whittle, and A. V. Levy, "Erosion Resistance of CoCrAl Coatings Containing Active Element Additions," Thin Solid Films 84, 315-322 (1981); LBL-12016.

2. D. H. Boone, D. A. Crane, and D. P. Whittle, "The Structure and Interdiffusional Degradation of Aluminide Coatings on Oxide Dispersion Strengthened Alloys," Thin Solid Films 84 (1981).

Other Publications

1. D. P. Whittle and D. H. Boone, "Oxidation Characteristics of CoCrAl Type Protective Coatings," Proc. 8th Int. Congress on Metallic Corrosion, Vol. I, Frankfurt, 1981; publ. by DECHEMA (1981) 718-723.

2. D. H. Boone and M. E. Browning, "The Advancing Deposition Process," Proc. of 68th Annual AES Meeting, Boston, MA. (1981).

3. D. P. Whittle and D. H. Boone, "Interactions Between Coatings and Substrates at Elevated Temperatures," Proc. of the DOE-EPRI Second Conf. on Advanced Materials for Alternative-Fuel Capable Heat Engines, Monterey, CA. (Aug. 1981); LBL-13350.

LBL Reports

1. E. Demeray, J. W. Fairbanks, and D. H. Boone, "Physical Vapor Deposition of Ceramic Coatings for Gas Turbine Engines," LBL-13721.

2. D. A. Crane, R. Lambertson and D. H. Boone, "The Protective Oxide Characterization of Mn Modified Electrophoretically Applied Aluminide Coatings," LBL-13776.

3. D. A. Crane, R. Lambertson and D. H. Boone, "Characterization of Plasma Spray Applied Ceramic Coated Diesel Engine Exhaust Valves. Part I As-coated Condition and Part II Engine Tested," LBL-13777.

Invited Talks

1. D. H. Boone, "Mechanical Property Effects of Protective Coatings for Energy Conversion Systems," Golden Gate Metals and Welding Conf., San Francisco, CA., January 1981.

2. D. P. Whittle, D. H. Boone and S. Shaffer, "Oxidation Properties of CrAl-based Coatings," AIME Annual Meeting, Chicago, IL., February 1981.

3. D. H. Boone, D. P. Whittle and D. A. Crane, "The Structure and Interdiffusional Degradation of Aluminide Coatings on Oxide Dispersion Strengthened Alloys," AIME Annual Meeting, Chicago, IL., February 1981.

4. D. H. Boone, W. D. Goward and P. G. Moore, "Structure of Laser Treated MCrAlY Coatings," Int. Conf. on Metallurgical Coatings, San Francisco, CA., April 1981.

5. D. H. Boone, D. A. Crane and D. P. Whittle, "Oxide Structure on Aluminide Coatings," Int. Conf. on Metallurgical Coatings," San Francisco, CA., April 1981.

6. D. P. Whittle, S. Shaffer and D. H. Boone, "Relationships Between Oxide Morphology and Coating Structure," Int. Conf. on Metallurgical Coatings, San Francisco, CA., April 1981.

7. D. H. Boone, "Films and Coatings for Technology," Continuing Education Institute Short Course, Los Angeles, CA., May 1981.

8. D. H. Boone, "Selection and Processing of High Temperature Coatings, Deposition Technologies and Applications Short Course, Linkoping University, Sweden, June 1981.

9. D. H. Boone, "Coatings for Gas Turbines," IPAT-81 (Ion Plating Assisted Technologies), Amsterdam, Netherlands, June 1981.

10. D. H. Boone, "Recent Advances In Coating Deposition Techniques," Linkoping University, Sweden, November 1981.

11. D. H. Boone, "Substrate Effects on Coating Protective Oxide Formation," Brown, Boveri and Cie, Central Research Institute, Heidelberg, West Germany, November 1981.

12. D. H. Boone, "The Science of Protective Coatings," MTU Moteren und Turbinen-Union, Munchen, West Germany, November 1981.

I. Coal Liquefaction Research*

Heinz Heinemann, Investigator

Introduction. The synthesis of hydrocarbons from CO and H_2 is usually carried out in fixed or fluid bed reactors. More than 30 years ago H. Kölbel proposed a slurry reactor and published considerable data on its operation. He found that among other advantages, the slurry reactor could tolerate higher CO/H_2 ratios that other reactors. This finding has recently become of renewed interest, because newer coal gasifiers produce high CO/H_2 ratio gas. It was the major purpose of this project in 1981 to investigate the possibility that mass transfer effects could explain this difference between slurry and fixed bed reactors. The findings of this year's studies complement the investigation of the effects of greater isothermicity in slurry reactors reported last year.

1. MASS TRANSFER EFFECTS IN SLURRY BED FISCHER-TROPSCH REACTORS†

D. Stern, A. T. Bell, and Heinz Heinemann

The influence of mass transfer on the H_2/CO ratio in the liquid phase of a slurry reactor used for Fischer-Tropsch synthesis has been analyzed theoretically. It is determined that even under circumstances where the gas-liquid mass-transfer resistance is a small fraction of the overall resistance, differences in the solubilities and diffusivities of H_2 and CO can give rise to liquid-phase H_2/CO ratios that differ substantially from that of the gas fed to the reactor. The direction and magnitude of the change in the liquid-phase H_2/CO ratio is dependent on the H_2-CO consumption ratio, the interfacial area for mass transfer from the bubble phase, the Damkohler number, and the space velocity of the feed gas.

It has been demonstrated that the influence of mass-transfer effects on the liquid-phase H_2/CO ratio can be large even under circumstances where the gas-liquid mass-transfer resistance is a relatively small fraction of the overall reaction resistance. Since the liquid-phase H_2/CO ratio influences the average molecular weight of the products formed, the olefin to paraffin ratio of the products and the formation of free carbon, knowledge of the dependence of the H_2/CO ratio on reaction conditions should be taken into account in the design of slurry columns used for Fischer-Tropsch synthesis.

Figure 1 presents one of many curves developed for the H_2/CO ratio in the liquid-phase $\left(\frac{C_{L,H_2}}{C_{L,CO}}\right)$

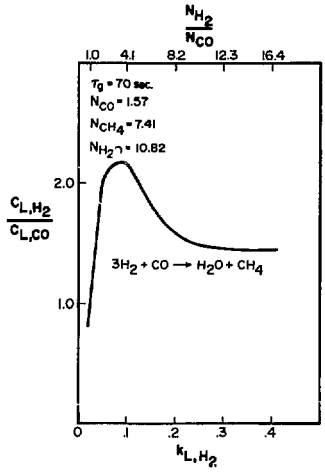

Fig. 1. (XBL 818-1720)

as a function of the Stanton numbers (NH_2/N_{CO}) and of the liquid-phase mass transfer coefficient for hydrogen (K_L, H_2) for a gas space time of 70 seconds and a liquid space time of 700 seconds.

* * *

†Brief version of LBL-13238.

*This work was supported by the Assistant Secretary for Fossil Energy, Office of Coal Research, Liquefaction Division of the U. S. Department of Energy under Contract No. DE-AC03-76SF00098 through the Pittsburgh Energy Technology Center, Pittsburgh, PA.

1981 PUBLICATIONS AND REPORTS

LBL Reports

1. Heinz Heinemann, "Coal Liquefaction Research," LBL-13238.

Invited Talks

1. Heinz Heinemann, "Coal Liquefaction Research," DOE Meeting of Recipients of Distinguished Scientist/Engineer Awards, Washington, DC, June 1981.

2. A. T. Bell, Contractors Meeting, DOE Fossil Energy, Coal Liquefaction, Pittsburgh, PA, June 1981.

V

Advanced Isotope Separation Technology

Advanced Isotope Separation Technology

a. Isotope Separation by Laser Photochemistry*

C. Bradley Moore, Investigator

Introduction. In most practical schemes of laser isotope separation, isotope-selective photoexcitation is followed by molecular dissociation and separation of the chemically different dissociation products. Therefore, an understanding of the nature of the energy levels produced, the quantitative heights of dissociation barriers and thresholds, and the mechanism of dissociation is important in devising and practicing schemes of laser isotope separation.

1. FORMALDEHYDE FLUORESCENCE LIFETIMES: A PROBE OF GROUND LEVEL STRUCTURE

Douglas J. Bamford and C. Bradley Moore

The variation of fluorescence lifetimes with rotational state and dc electric field demonstrates that the highly vibrationally excited levels of ground electronic state formaldehyde near 28,000 cm^{-1} form a structural "lumpy continuum."[1] Tunneling through a barrier to molecular dissociation, $H_2CO(S_0)^{\ddagger} \rightarrow H_2 + CO$, at approximately the same energy provides a good semi-quantitative explanation for the existence of such a lumpy continuum.[2] The molecular beam experiment (see article 2 below) proves that dissociation in fact occurs. As total energy increases dissociation rates should increase, the continuum should be smoothed out (dissociation rate becomes large compared to level spacing) and the lifetime fluctuations damped.

Lifetime measurements were made in a cooled supersonic beam near 28,000 cm^{-1} to check the validity of the gas cell data,[1] to study lifetime fluctuations vs total energy and to prepare for the molecular beam photofragment experiment (see article 2 below). The observed lifetime ranges do in fact decrease as total energy increases (Table 1). Data will allow testing of nonradiative transition rate theories.

* * *

1. J. C. Weisshaar and C. B. Moore, J. Chem. Phys. 72, 5415 (1980).
2. W. H. Miller, Y. Yamaguchi, and H. F. Schaefer, J. Am. Chem. Soc. 103, 1900 (1981).

Table 1.

S_1 level	Energy(cm^{-1})	Lifetime range (nsec)
4^0	28,188	66 - 4200
4^1	28,313	20 - 3100
$2^1 4^1$	29,495	12 - 114
5^1	31,156	30 - 64

2. IR MULTIPHOTON DISSOCIATION OF D_2CO: DETERMINATION OF THE DISSOCIATION BARRIER HEIGHT†

Michael R. Berman and C. Bradley Moore

There are two dissociation channels open for formaldehyde

$$H_2CO^{\ddagger} \rightarrow H_2 + CO \quad \text{(molecular)}$$
$$\rightarrow H + HCO \quad \text{(radical)},$$

as illustrated in Figs. 1 and 2. The radical threshold is known to be 86 ± 2 kcal/mole. For molecules with more than this amount of energy the branching between radical and molecular products is a sensitive function of the energy difference between radical and molecular thresholds.

Multiphoton IR excitation of D_2CO by a focused CO_2 TEA laser has been used to pump D_2CO past the dissociation thresholds (Fig. 1). The relative

*This work was supported by the Assistant Secretary for Nuclear Energy, Office of Advanced Isotope Separation Technology, Advanced Isotope Separation Division of the U. S. Department of Energy under Contract No. DE-AC03-76SF00098.

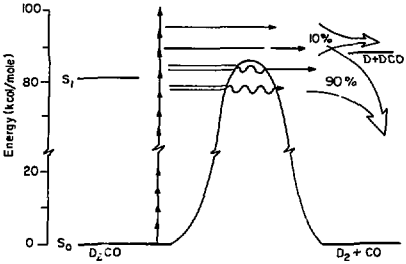

Fig. 1. Energy diagram for competitive dissociation of D_2CO to radical and molecular products during IR multiphoton excitation. Wavy arrows indicate tunneling through the molecular barrier. (XBL 811-5056)

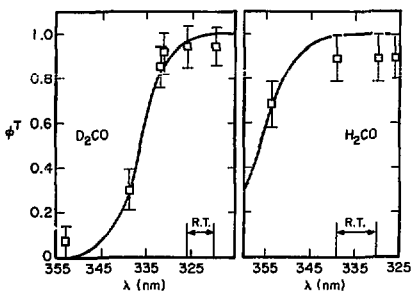

Fig. 2. Experimental quantum yield for UV photolysis (□) compared to yields calculated (—) from rate equations used to analyze IRMPD data. (XBL 811-7502)

amounts of radical and molecular products at known laser fluence were measured as 10/90. A knowledge of the order of magnitude of IR excitation rates, collisional relaxation rate, and dissociation rates with tunneling included, allows the molecular barrier energy to be fixed as 84 ± 3 kcal/mole. The same rates and energies give calculated UV photochemical dissociation yields (vs collisional deactivation) as a function of wavelength in excellent agreement with experiment (Fig. 2).

These experiments are now being combined with the highest level of molecular quantum mechanical calculations in the groups of H. F. Schaefer and W. A. Lester, Jr., along with complete dynamical calculations in the group of W. H. Miller, to yield a complete picture of the dissociation of formaldehyde molecules.

(See also the report, "Photofragmentation of Formaldehyde in a Molecular Beam" in the Advanced Isotope section of this annual report.)

* * *

†Brief version of LBL-12213.

1981 PUBLICATIONS AND REPORTS

Refereed Journals

†1. J. C. Weisshaar, D. J. Bamford, E. Specht, and C. B. Moore, "Quenching Electronic Energy Transfer and Rotational Relaxation of S_1 Formaldehyde," J. Chem. Phys. 74, 226 (1981); LBL-11453.

‡2. P. B. Comita, M. R. Berman, C. B. Moore, and R. G. Bergman, "Laser-Powered Homogeneous Dissociation of Tetralin," J. Phys. Chem. 85, 3266, (1981); LBL-12697.

LBL Reports

†1. P. Ho, D. J. Bamford, R. J. Buss, Y. T. Lee, and C. B. Moore, "Photodissociation of Formaldehyde in a Molecular Beam," LBL-13438.

Ph.D. Theses

‡1. Michael Robert Berman, "Competing Reaction Channels in IR Laser-Induced Unimolecular Reactions," LBL-12213.

2. Hai-Lung Dai, "Multiphoton Dissociation and Thermal Unimolecular Reactions Induced by Infrared Lasers," LBL-12626.

3. Pauline Ho, "Formaldehyde Photodissociation: Molecular Beam, Product Appearance Rate, and Carbon-14 Isotopic Enrichment Studies," LBL-13869.

Invited Talks

1. C. Bradley Moore, "High Resolution Photochemistry of Formaldehyde," Physical Chemistry Seminar, University of California, Berkeley, Department of Chemistry, May 12, 1981.

2. C. Bradley Moore, "Selectivity in Laser Photochemistry," Kansas State University, Manhattan, Department of Chemistry Colloquium, October 15, 1981.

3. C. Bradley Moore, "Selectivity in Laser Photochemistry," University of Kansas, Lawrence, Department of Chemistry Colloquium, October 16, 1981.

4. C. Bradley Moore, "High Resolution Photochemistry - Formaldehyde," Columbia University, New York, NY, Department of Chemistry Colloquium, November 19, 1981.

5. C. Bradley Moore, "Sorting Things Out - Selective Molecular Excitation and Laser Isotope Separation," Swarthmore College, Swarthmore, PA, Department of Chemistry. Lecture part of "Chemistry Along a Laser Beam," The Dreyfus Lecture Series, December 1, 1981.

6. C. Bradley Moore, "High Resolution Photochemistry - Formaldehyde," Swarthmore College, Swarthmore, PA, Department of Chemistry. Lecture part of "Chemistry Along a Laser Beam," The Dreyfus Lecture Series, December 3, 1981.

* * *

†Partially supported by the National Science Foundation.

‡Partially supported by the Director, Office of Energy Research, Office of Basic Energy Sciences, Chemical Sciences Division of the U.S. Department of Energy under Contract No. DE-AC03-76SF00098.

b. Molecular Beam Laser Isotope Separation*

Yuan T. Lee and Y. Ron Shen, Investigators

1. VIBRATIONAL PREDISSOCIATION SPECTRA OF $(HF)_n$, n = 2 to 6†

James M. Lisy, Andrzej Tramer, Matthew F. Vernon, and Y. T. Lee

Hydrogen bonding is an interestin[illegible] and important interaction in chemical and biochemical systems. Detailed molecular beam studies of $(H_2O)_2$ (Ref. 1) and $(HF)_2$ (Ref. 2) have established the vibrationally averaged ground state structures and provided information on the potential energy surface near the minimum. Infrared absorption studies of small hydrogen-bonded clusters have been hindered by uncertainty in assigning features to a specific cluster. Here we report on molecular beam studies of the vibrational predissociation spectra of $(HF)_n$, n = 2 to 6, in the 3000 to 4000 cm^{-1} range, associated primarily with the intramolecular stretching motion, using a tunable infrared laser.

The assignment of spectra to specific clusters was done through a series of experiments by varying the source pressure, carrier gas and seeding ratio. The mass spectrometer was essential in confirming the assignments by comparing spectra at different m/e settings. For example, the $(HF)_3$ bands are observed only at m/e = 41, while $(HF)_4$ bands can be found at both m/e = 41 and 61 (see Fig. 1).

The $(HF)_n$ n = 3 to 6 clusters exhibit a larger frequency shift from the HF fundamental than was observed for the dimer. No absorption was observed above 3500 cm^{-1}, indicating the absence of a terminal ----H-F or ---F-H group. Therefore, we conclude $(HF)_n$, n = 3 to 6, to have cyclic structures with each HF as both a proton donor and acceptor, in agreement with previous molecular beam deflection[2] results. The $(HF)_n$, n = 3 to 6 spectra have a similar structure fit by $\nu_n = \nu_n' + m\nu_n''$ (m = 0,1,2), where ν_n' decreases and ν_n'' increases with cluster size, n. It seems likely that those progressions are combination bands involving coupled H-F (ν_n') and F-H----F (ν_n'') modes. The frequency variations with n are in accord with the strengthening of the intermolecular interactions and weakening of the intramolecular bands in progressively larger clusters.

Further experiments involving $(DF)_n$ and $(DF)_n(HF)_m$ are planned, inducing predissociation by excitation of the fundamental and overtone bands. This information will be used to understand the intermolecular potentials, binding energies and structures of HF clusters.

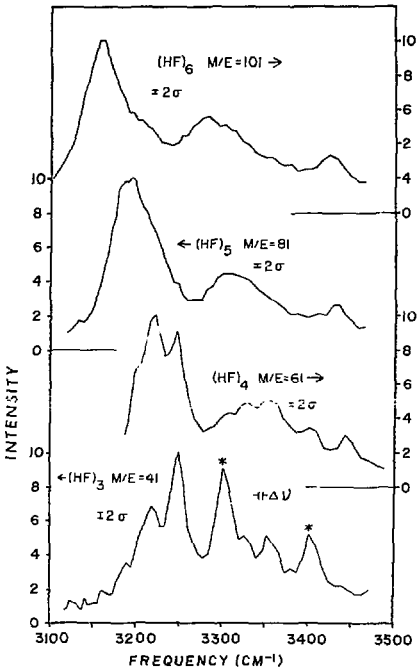

Fig. 1. Vibrational predissociation spectra of $(HF)_n$, n = 3-6, corrected and normalized for photon number. The peaks marked with asterisks in the m/e = 41 spectrum are from $(HF)_3$, the other peaks are due to larger clusters.

(XBL 816-10400)

* * *

*This work was supported by the Assistant Secretary for Nuclear Energy, Office of Advanced Isotope Separation Technology, Advanced Isotope Separation Division of the U. S. Department of Energy under Contract No. DE-AC03-76SF00098.

†Brief version of LBL-13037, July 1981.

1. T. R. Dyke, K. M. Mack, J. S. Muenter, J. Chem. Phys. 66, 498 (1977).
2. T. R. Dyke, B. J. Howard, W. Klemperer, J. Chem. Phys. 56, 2442 (1972).

2. PHOTOFRAGMENTATION OF FORMALDEHYDE IN A MOLECULAR BEAM

D. J. Bamford, R. J. Buss, P. Ho, Y. T. Lee, and C. B. Moore

The photodissociation of CH_2O has been the subject of much experimental and theoretical work aimed at understanding the reaction dynamics. A large variation of fluorescence decay times with excitation to different rotational states near the S_1 origin has been explained with a sequential coupling model[1] that predicts that decay to CO + H_2 will occur in the absence of collisions. Collisionless decay had not been observed, and the major objective of this project was to examine the effect of laser excitation on CH_2O under collision-free conditions.

A supersonic beam of CH_2O was produced by expansion of 10% CH_2O in helium carrier gas from a nozzle and was excited by a laser beam after three stages of differential pumping. Experiments included excitation in two energy regimes; tunable uv, 338-354 nm was used to excite CH_2O near the S_1 origin, and frequency doubling the dye laser output to produce 283 nm photons gave excitation higher in the S_1 manifold, above the threshold for production of radicals H + CHO. For excitation in the 2^14^1 vibrational state of CH_2O, velocity distributions of the product CO + H_2 were obtained at four laboratory angles. From these data, the product translational energy distribution, P(E), shown in the figure was obtained. Upon excitation with 283 nm laser light, only radical products were detected; it is concluded that molecular products CO + H_2 are less than 10% of the total dissociation events at this excitation, 15 kcal/mole above the radical threshold.

The major finding is that CH_2O excited near the S_1 origin does dissociate to give CO + H_2 product in the absence of collisions, lending strong support to the sequential coupling model. The product translational energy is found to be high, averaging 66% of the available energy. Application of an impulse model to this system using the theoretical transition state structure and the measured P(E), suggests that the CO is formed with high rotational excitation. The radical product formed at the higher energy was found to have low translational energy averaging less than 20% of the available energy.

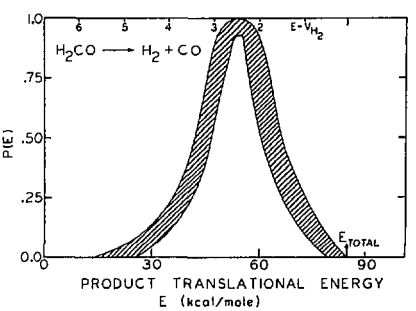

Fig. 1. Product translational energy for $CH_2O \rightarrow CO + H_2$ from excitation in the 2^14^1 vibrational band of the S_1 state.

(XBL 818-11416)

* * *

1. J. C. Weisshaar, D. J. Bamford, E. Specht, and C. B. Moore, J. Chem. Phys. 74, 226 (1981).

1981 PUBLICATIONS AND REPORTS

Refereed Journals

1. Yuan T. Lee and Y. Ron Shen, "Studies with Crossed Laser and Molecular Beams," Physics Today, 33, 52 (1980).

2. M. W. Sigrist, D. J. Krajnovich, F. Huisken, Z. J. Zhang, Y. T. Lee and Y. R. Shen, "Laser-Induced Dissociation of Monomers and Dimers of Bromine," Helv. Phys. Acta 53, 289 (1980).

LBL Reports

1. M. F. Vernon, J. M. Lisy, H. S. Kwok, D. J. Krajnovich, A. Tramer, Y. R. Shen, and Y. T. Lee, "Vibrational Predissociation of Benzene Dimers and Trimers by the Crossed Laser-Molecular Beam Technique," submitted to J. Phys. Chem. June 1981, LBL-12985.

2. D. Krajnovich, Z. Zhang, F. Huisken, Y. R. Shen, and Y. T. Lee, "The Effects of Reagent Translational and Vibrational Energy on the Dynamics of Endothermic Reactions," invited paper presented at the XII IPEAC 1981: International Conference on the Physics of Electronics and Atomic Collisions, Gatlinburg, TN, July 15-22, 1981, LBL-12982.

3. James M. Lisy, Matthew F. Vernon, Andrzej Tramer, Hoi-Sing Kwok, Douglas J. Krajnovich, Y. R. Shen, and Y. T. Lee, "Infrared Vibrational Predissociation Spectroscopy of Small Molecular Clusters," invited paper presented at the Fifth International Conference on Laser Spectroscopy, Jasper Park Lodge, Alberta, Canada, June 29-July 3, 1981, LBL-12981.

4. Pauline Ho, Douglas J. Bamford, Richard J. Buss, Yuan T. Lee, and C. Bradley Moore, "Photodissociation of Formaldehyde in a Molecular Beam," submitted to J. Chem. Phys. October 1981, LBL-13438.

5. M. F. Vernon, D. J. Krajnovich, H. S. Kwok, J. M. Lisy, Y. R. Shen, and Y. T. Lee, "Infrared Vibrational Predissociation Spectroscopy of Water Clusters by the Crossed Laser - Molecular Beam Technique," submitted to J. Chem. Phys. November 1981, LBL-11970.

Invited Lectures

1. Y. T. Lee, "Dynamics of Infrared Multiphoton

Dissociation of Polyatomic Molecules," Lawrence Livermore National Laboratory, March 10, 1981.

2. D. J. Krajnovich, "Effect of Reagent Translational and Vibrational Energy on the Dynamics of Endothermic Reactions," XII International Conference on the Physics of Electronic and Atomic Collisions, Gatlinburg, Tennessee, July 15-21, 1981.

VI Energy Storage

Energy Storage

A. Electrochemical Energy Storage

The overall aim of this program is to improve the energy efficiency, lower the capital cost, and increase the materials yield of electrochemical processes employed in the conversion and storage of energy in electrolytic and galvanic cells.

a. Surface Morphology of Metals in Electrodeposition*

Charles W. Tobias, Investigator

Introduction. The objective of this project is to develop a pragmatic understanding of the partial processes governing the macrocrystallization of metals. This understanding is necessary for the design and optimization of metal deposition processes, including those in rechargeable galvanic cells. Current projects include: (a) The effect of hydrodynamic flow on the surface morphology of copper and of zinc, and (b) dynamic modeling of surface profiles in electrodeposition and dissolution.

1. THE INFLUENCE OF LEAD IONS ON THE MACROMORPHOLOGY OF ELECTRODEPOSITED ZINC†

Tetsuaki Tsuda and Charles W. Tobias

The morphology of zinc as it is electrodeposited from acid solutions demonstrates a remarkable imprint of electrolyte flow conditions. The development of macromorphology of zinc deposits has been investigated under galvanostatic conditions on a rotating platinum disk electrode by use of photomacrography, scanning electron microscopy (SEM), electron probe microanalysis and Auger microprobe analysis. Logarithmic spiral markings, which reflect the hydrodynamic flow on a rotating disk, appear in a certain region of current density well below the limiting current density (Fig. 1). Morphological observations revealed the major influence of trace lead ions on the amplification of surface roughness through coalescence and preferred growth of initial protrusions. Results obtained from ultra-pure electrolyte suggest preferred crystal growth towards well-mixed regions of the concentration field caused by slight differences in crystallization overpotential.

The spiral striations form by the sequence (Fig. 2): 1) nucleation and growth of nuclei, 2) coalescence of nuclei into larger protrusions,

Fig. 1. The dotted line is an Archimedes spiral described by $\theta-\theta_0 = 0.0304\ (r - r_0)$. The fine solid curve is a logarithmic spiral described by $\theta - \theta_0 = 1.25 \ln r/r_0$. Note that the Archimedes spiral deviates greatly from the striation. (XBB 817-6215A)

3) preferential growth of larger protrusions, and 4) successive coalescence, and consumption of smaller protrusions by larger ones.

The concentration field is disturbed by these protrusions acting as distributed roughness elements. Eventually well established secondary flows occur. Local eddy mixing is originated by protrusions, the heights of which reach a certain portion of the thickness of the diffusion boundary layer. Slight differences in zinc concentration results in slight differences in crystallization over-potential, causing enhanced crystal growth in well mixed locations. Thus, connection of protrusions along spiral lines occur. Secondary flow

*This work was supported by the Assistant Secretary for Conservation and Renewable Energy, Office of Energy Systems Research, Energy Storage Division of the U. S. Department of Energy under Contract No. DE-ACD3-76SF00098.

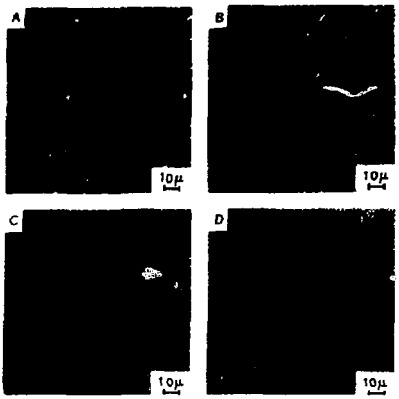

Fig. 2. Effect of current density on the numbers and size of initial protrusions. (a) 10 mA/cm^2 x 1.5 min, (b) 30 mA/cm^2 x 0.5 min, (c) 60 mA/cm^2 x 15 sec, (d) 120 mA/cm^2 x 5 sec. 1M $ZnCl_2$ with 4.8 x 10^{-5} M Pb at 800 rpm.

(XBB 817-6791A)

occurs as connection of protrusions proceeds. Spiral ridges become more pronounced owing to mass transfer onto ridges rather than into recesses.

The role of minor species (lead or hydrogen ions) may be summarized as follows: they 1) decrease the number of initial nucleation sites for zinc, 2) poison the platinum surface for hydrogen evolution; hence, the whole surface can be covered by a thin layer of zinc-platinum alloy from the very beginning of deposition, 3) enhance successive coalescence and preferential growth of protrusions, and 4) deform the crystalline structure to a rounded shape.

H^+ ions seem not to affect either the initial nucleation or successive coalescence of protrusions, but change the crystalline structure to a rounded shape with decreasing pH values.

* * *

†Brief version of LBL-13057.

2. THE MORPHOLOGY OF ELECTRODEPOSITED COPPER†

Andrew Kindler and Charles W. Tobias

When a metal is electrodeposited, the developing surface morphology determines surface properties such as brightness, smoothness and hardness, and, indirectly, compactness, strength and ductility. This investigation deals with the surface morphology of copper produced under well defined conditions of mass transfer and uniform current distribution in the absence of inhibitors.

Morphology was investigated with SEM after electrodeposition from an aqueous $CuSO_4$-H_2SO_4 solution in a flow cell with plane parallel electrode. Uniform current distribution and well defined mass transfer conditions present during turbulent forced convection made investigation of three regimes possible: 1) dc deposition at the limiting current, 2) dc deposition below the limiting current, and 3) pulsed current deposition below the limiting current.

In Regime 1 nodular powder deposits are due to transformation from a dendritic structure to a coherent one when the mass transfer boundary layer at the growing dendrite tip thins out. The coherent portion of the structure caps the dendrite, giving it a mushroom-like appearance in photomicrographs of the deposit cross section. In Regime 2 the roughness generated during electrodeposition results from the growth of a few large protruding crystals embedded in a very fine flat polycrystalline deposit resembling sand. These large crystals originate mostly near the electrode/deposit interface. After their growth ends, coverage by the "sandy" deposit gives the crystals a deceptively nodular and amorphous appearance (Fig. 1). The number of large crystals

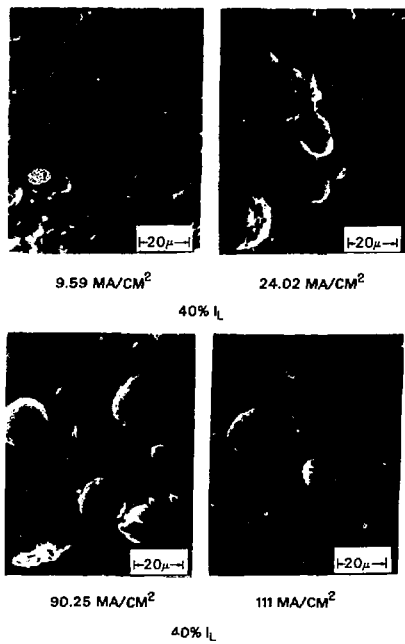

Fig. 1. Grain size of fine structure decreases with increasing current. (XBB 812-1783)

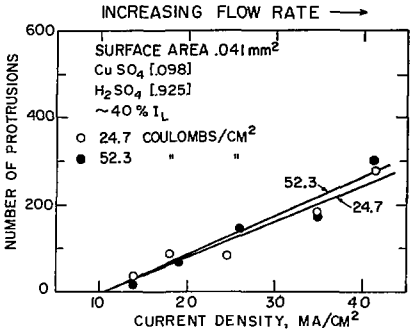

Fig. 2. Effect of current density on the number of protrusions. (XBL 805-5131)

decreased with increasing interfacial $CuSO_4$ concentration and decreasing current density. Average crystal size decreases as the number of crystals, and/or the interfacial concentration increases. The number of smaller crystals in the fine structure depends on current density (Fig. 2) and concentration similarly; the average size is inversely related to the number density.

Further observations demonstrate that: 1) the electrode preparation influences the number of crystals (large and small) because the energy of the surface is linked to its pretreatment, and 2) increased roughness found in thicker deposits is generated by preferential deposition of fine structure on the large crystals. In Regime 3 the growth of the large crystals can be inhibited with pulsed current instead of with organic inhibitors. The off-time between the pulses is demonstrated to be the cause of this phenomenon. It is proposed that during this period, passivation of crystal growth sites occurs.

* * *

†Brief version of LBL-12838.

3. WORK IN PROGRESS

The effects of current density, time of metal deposition, hydrodynamic conditions, and substrate conditions on the zinc electrodeposition process are being studied in a channel flow cell with planar electrodes. The morphology of zinc deposited under galvanostatic conditions from 1M $ZnCl_2$ acidified solution is evaluated well below the limiting current.

A finite element model is under development for modeling electrodes which exhibit passivity. In particular we focus on the coexistence of active and passive regions on the same surface. The finite element technique, relatively new to current-distribution modeling, is generally regarded as superior to the finite difference method for accomodating singularities and irregular geometries. To evaluate the validity of the assumptions made in setting up the model, the current distribution and the location of the "boundary" corresponding to active-passive transition will be measured on a rotating cylinder experiment using a segmented nickel anode.

The thickness and chemical nature of surface films on lithium in propylene carbonate electrolytes are under study. This project is carried out under the direction of Dr. R.H. Muller as part of efforts devoted to the identification of novel solvent-electrode combinations of potential interest for use in electrolysis and in batteries.

The use of a benzophenone-alkali-metal ketal as either an effective drying agent of non-aqueous electrolytes, or in combination with an inert electron collector, as an alkali metal electrode, is being investigated.

1981 PUBLICATIONS AND REPORTS†

Refereed Journals

1. C. W. Tobias, "The Coming of Age of Electrochemical Engineering," AIChE Symposium Series, 204, 77 (1981).

2. C. W. Tobias and H. H. Law, "The Morphology of Potassium Deposited from Propylene Carbonate Electrolyte," Proceedings of the Symposium on Electrocrystallization, Rolf Weil, Ed. Proceedings vol 81-6, The Electrochemical Society, June, 1981.

LBL Reports

1. G. A. Prentice, "Modeling of Changing Electrode Profiles," Ph.D. dissertation, University of California, Berkeley, December 1980, LBL-11694.

2. G. A. Prentice and C. W. Tobias, "A Survey of Numerical Methods and Solutions of Current Distribution Problems," accepted for publication in the Journal of the Electrochemical Society, January 1981, LBL-12191.

3. G. A. Prentice and C. W. Tobias, "Finite Difference Calculation of Current Distributions at Polarized Electrodes," accepted for publication in the AIChE Journal, LBL-11058.

4. G. A. Prentice and C. W. Tobias, "Deposition and Dissolution on Sinusoidal Electrode," accepted for publication in the Journal of the Electrochemical Society, January 1981, LBL-12167.

5. G. A. Prentice and C. W. Tobias, "Simulation of Changing Electron Profiles," accepted for publication in the Journal of the Electrochemical Society, January 1981, LBL-12192.

6. A. Kindler (with C. W. Tobias), "The Morphology of Electrodeposited Copper," Ph.D. dissertation,

University of California, Berkeley (1981), LBL-12838.

7. T. Tsuda and C. W. Tobias, "The Influence of Lead Ions on the Macromorphology of Electrodeposited Zinc," M. S. thesis, University of California, Berkeley (1981), LBL-13057.

Other Publications

H. Gerischer and C. W. Tobias, editors, Advances in Electrochemistry and Electrochemical Engineering, Wiley-Interscience, New York, Vol. 12, November 1981.

Invited Talks

1. R. T. Atanasoski, H. H. Law, and C. W. Tobias, "Determination of Water in Propylene Carbonate Electrolytes by Cyclic Voltammetry," Meeting of the Electrochemical Society, Minneapolis, MN, May 10-15, 1981; Extended Abstracts, vol. 81-1, no. 392, p. 985-986, (based on LBL-11847).

2. C. W. Tobias, "Electrochemical Engineering of Batteries," invited lecture, Short Course, Continuing Education Institute, Cherry Hill, NJ, June 22-26, 1981.

3. C. W. Tobias, "Prospects of the Electrochemical Technology," invited lecture, W. R. Grace Research Center, Columbia, MD, September 18, 1981.

4. H. H. Law and C. W. Tobias, "The Cathodic Overpotential of Potassium in KAlCl-Propylene Carbonate Electrolyte," contributed paper, Meeting of the Electrochemical Society, Denver, CO, October 11-16, 1981; Extended Abstracts, vol. 81-2, no. 585, p. 1403 (based on LBL-11487).

* * *

†A complete listing of publications, reports, and papers presented by Charles W. Tobias and his associates is provided under "Electrochemical Processes" in the Materials Sciences section of this Annual Report.

b. Surface Layers on Battery Materials*

Rolf H. Muller, Investigator

Introduction. The purpose of this work is to provide direct experimental information about formation and properties of surface layers on battery-electrode materials. A more broadly based, fundamental research program, supported by the Division of Materials Sciences, Office of Basic Energy Sciences, is described under "Electrochemical Phase Boundaries," R. H. Muller, Investigator, and "Electrochemical Processes," C. W. Tobias, Investigator.

1. ELECTROCHEMICAL STUDIES OF THE FILM FORMATION ON LITHIUM IN PROPYLENE CARBONATE SOLUTIONS UNDER OPEN CIRCUIT CONDITIONS†

Y. Geronov, F. Schwager, and R. H. Muller

Lithium is thermodynamically unstable in contact with most nonaqueous battery electrolytes and can be used only because of the formation of protective surface layers on the metal. The properties of these layers are important for the current delivery, the shelf-life, and the rechargeability of lithium electrodes. The aim of this study is to determine the mode of formation and properties of films that spontaneously form on lithium in propylene carbonate solutions of $LiClO_4$ and $LiAsF_6$ in order to identify means to improve electrode performance.

Film-formation under open circuit conditions was followed by use of galvanostatic pulse polarization techniques. For the measurement of electrode capacitance, pulses of typically 0.1 mA/cm^2 amplitude and 5 μs duration were employed. For polarization measurements, pulse amplitude was 1-20 mA/cm^2 and duration 10 ms.

The kinetic behavior of the Li electrodes is found to be controlled by the field-assisted ion conduction through an insulating surface layer. The thickness of this layer, as derived from capacitance measurements, increases with time according to a parabolic rate law, with the rate increasing with water content of the solution. The exchange current density of 5.5 mA/cm^2 determined here on a smooth surface at the beginning of immersion in 1M $LiClO_4$, when the surface layer is only about 20 Å thick, agrees with the value of 12 mA/cm^2 reported for an anodically cleaned rough electrode. The results are consistent with the fast formation of a compact protective film by reaction with residual water. This layer acts as a solid ionic conductor. Li_2O is the thermodynamically favored reaction product. Capacitance measurements are sensitive to this layer which faces the electrode. A nonprotective porous overlayer, which faces the solution and is formed by electrode corrosion or solvent decomposition, has little electrical effect. It is visible in scanning electron micrographs and found by ellipsometry. Future efforts will be directed toward increasing the ionic conductivity of the compact surface layer.

* * *

†Brief version of LBL-12102, Rev. 2.

2. ELLIPSOMETRIC STUDIES OF SURFACE LAYERS ON LITHIUM†

F. Schwager, Y. Geronov, and R. H. Muller

Protective surface layers are necessary for the use of lithium in batteries with nonaqueous solvents but have been implicated in the poor rechargeability of lithium electrodes. The purpose of this study, which was conducted in parallel with electrochemical measurements reported in the preceding section, was to provide independent optical data on the thickness, structure and composition of surface layers formed on lithium in $LiClO_4$ and $LiAsF_6$ solutions in propylene carbonate solvent. Ellipsometry is particularly well suited for the in situ observation of electrochemical film formation because of its great sensitivity and minimum disturbance to the surface.

Ellipsometric and electrochemical measurements were conducted in a hermetically sealed polypropylene cell consisting of an electrode compartment with two strain-free quartz windows arranged for 75° angle of incidence of the light beam, and a solution compartment located above the electrode compartment and connected with it by internal valves. This configuration enables one to take measurements very soon after the electrode is brought in contact with the solution. The ellipsometer used was of the self-compensating type in the polarizer/quarter-wave plate/sample analyzer configuration.[1] A mercury lamp for the wavelength of 5461 Å and an argon-ion laser at a wavelength of 5145 Å were used as light sources. The cell was assembled in an inert atmosphere box with recirculatng helium (< 0.5 ppm O_2, H_2O, 5 ppm N_2). After the experiment, the working electrode was washed with pure propylene carbonate, dried and transferred to vacuum for scanning electron microscopy, Auger spectroscopy or ellipsometry of the dry film.

This work has shown that the growth of surface layers on lithium in propylene carbonate solutions can be followed by ellipsometry, although the refractive indices of many potential film materials are close to those of the electrolyte. Film thicknesses calculated from ellipsometer measurements increase linearly over periods of several days at open circuit; thicknesses are several times larger than those derived from galvonostatic

*This work was supported by the Assistant Secretary for Conservation and Renewable Energy, Office of Energy Systems Research, Energy Storage Division of the U. S. Department of Energy under Contract No. DE-AC03-76SF00098.

pulse measurements. Films are found to be inhomogeneous with properties varying as a linear function of thickness; compact regions are located adjacent to the metal and porous regions adjacent to the solution. The compact region is responsible for the electrode capacitance and can also be generated by reaction with water in the vapor phase. The porous region is primarily responsible for the ellipsometer measurements. It may be formed by the precipitation of decomposition products of the solution.

* * *

†Brief version of LBL-13657.

1. H. J. Mathieu, D. E. McClure, and R. H. Muller, Rev. Sci. Instrum. 45, 798 (1974).

3. WORK IN PROGRESS

Electrical impedance measurements are conducted to further characterize surface layers on lithium in propylene carbonate solutions and to determine the effect of anodic and cathodic electrode polarization.

1981 PUBLICATIONS AND REPORTS

LBL Reports

1. Y. Geronov, F. Schwager, and R. H. Muller, "Electrochemical Studies of the Film Formation on Lithium in Propylene Carbonate Solutions under Open Circuit Conditions," LBL-12102, Rev., and Rev. 2.

2. Felix Schwager, "Operation of Inert Atmosphere Glove Box," LBL-13774.

3. Felix Schwager, "Operating Procedure for Combined Auger- and UHV System," LBL-13609.

Invited Talks

1. Rolf H. Muller, "Highlights of In-House Research Programs, Development of Electrochemical Synthesis and Energy Storage," Annual Program Managers Meeting, Division of Energy Storage, DOE, Washington, DC, October 6, 1981.

c. Analysis and Simulation of Electrochemical Systems*

John Newman, Investigator

Introduction. This program includes the investigation of efficient and economical methods for electrical energy conversion and storage, development of mathematical models to predict the behavior of electrochemical systems and to identify important process parameters. Experiments are used to verify the completeness and accuracy of the models. Specific projects include analysis of flow-through porous electrodes for metal-ion removal from waste streams and for energy storage, and development of an electrochemical impregnation method of preparing porous Ni electrodes for high-energy battery applications.

1. WORK IN PROGRESS

An alternating voltage impedance method will be used to study the anodic behavior of zinc in an acidic aqueous medium. This work will have practical applications ranging from the study of corrosion of underground and underwater pipelines to the prevention of battery discharge due to the formation of pits within the electrodes. In this investigation, impedance measurements will be performed on both rotating disk and rotating hemispherical zinc electrodes. The advantage of using a rotating hemispherical electrode is that the metal dissolution does not interfere with the fluid flow, as it would with a rotating disk electrode.

Theoretical work has begun on the frequency response of current and potential to high-frequency sinusoidal speed modulation on a rotating-disk electrode. The unsteady state Navier-Stokes equations, coupled with the convective diffusion equation were solved numerically to give velocity and concentration profiles at high modulation frequencies. This work is useful for studying the mass transfer characteristics of corrosion processes because accurate diffusion coefficients can be obtained by combining the theoretical predictions with experimental impedance measurements. Excellent agreement between the theory and experiment has been found with the $Fe(CN)_6^{3-}/Fe(CN)_6^{4-}$ system at the half-wave potential in galvanostatic regulation.

Theoretical work examining the feasibility of several proposed battery systems will begin. Among these, the polyacetylene battery recently appearing in the literature will be examined. Emphasis will be on developing general design criteria for such prospective battery systems.

Many electrochemical systems use channel flow between two plane parallel electrodes. For example, this configuration can be used in Fe^0-Fe^{2+}-Fe^{3+} energy storage cells or in electroorganic synthesis. A mathematical model, useful in the design of such systems, is being developed to calculate the concentration, potential and current distribution in a thin-gap flow cell. While previous models have assumed that the interelectrode gap is much larger than the diffusion boundary layer thickness, the present model allows the gap to be thin enough for the diffusion boundary layers to interact. The model also can take into account multiple reactions at the electrodes.

An electrochemical impregnation method of preparing porous Ni electrodes for high-energy battery applications is being investigated. The method used currently involves electroprecipitation of $Ni(OH)_2$. An understanding of the electroprecipitation is necessary to develop an improved preparation process for producing Ni battery electrodes. Preliminary experiments have shown that the $Ni(OH)_2$ deposit becomes less adherent as the temperature of the acidic nickel nitrate bath decreases.

Molten sodium sulfide and sodium polysulfides are involved in a number of practical engineering applications. In particular, the use of sulfur and associated sodium polysulfides as the cathode in a sodium-sulfur secondary cell seems especially promising. Sodium-sulfur batteries are expected to possess a high specific energy greater than 150 W-hr/kg and a cycle life greater than 1000 cycles. These characteristics, combined with the abundant availability and the low price of sulfur make the sulfur electrode and the sodium-sulfur battery attractive for both vehicle propulsion and utility load leveling applications. It has been determined that the rate limiting process occurring at the sulfur cathode is the diffusion of charged species within the polysulfide melt. Since the performance of sodium-sulfur cells is strongly influenced by the diffusion of anions and cations through the melt, optimal design of sulfur electrodes will depend upon the availability and accuracy of diffusion coefficient data for polysulfide melts. An experimental apparatus has been designed to measure the diffusion coefficient of sodium ions in melts of sodium polysulfides, using the method of restricted diffusion. The advantage of this method is that the current densities will be low enough to eliminate the problem of electrode blockage by insoluble polysulfide or sulfur phases.

In many practical electrochemical applications, the formation and growth of dendrites can be critical to the operation and performance of the system. In zinc batteries the metal deposition and subsequent dendritic growth can pierce separators and cause internal shorting. In plating operations, the formation of dendrites can give a rough, unattractive finish to the final product. Presently, the physics of initiation and growth of dendrites is not well understood. A theoretical stability analysis will be undertaken to examine

*This work was supported by the Assistant Secretary for Conservation and Renewable Energy, Office of Energy Systems Research, Energy Storage Division of the U. S. Department of Energy under Contract No. DE-AC03-76SF00098.

the effects of plating additives, current density, flow hydrodynamics, and electrode materials on dendrite initiation.

The effects of process variables on the removal of lead from dilute sulfuric waste streams is being investigated in a high pressure electrochemical reactor. In particular, the effect of pressure on the current efficiency of the process is being determined through current-potential measurements and effluent analysis. Higher reactor pressures thermodynamically reduce the amount of hydrogen discharged, and further inhibit hydrogen nucleation, which would increase the ohmic potential drop through the reactor.

1981 PUBLICATIONS AND REPORTS

Refereed Journals

1. R. Pollard and J. S. Newman, "Mathematical Modeling of the Lithium-Aluminum, Iron Sulfide Battery. I. Galvanostatic Discharge Behavior," J. Electrochem. Soc., 128, 491-502 (1981).

2. R. Pollard and J. S. Newman, "Mathematical Modeling of the Lithium-Aluminum, Iron Sulfide Battery. II. The Influence of Relaxation Time on the Charging Characteristics," J. Electrochem. Soc., 128, 503-507 (1981).

3. J. A. Trainham and J. S. Newman, "A Comparison between Flow-through and Flow-by Porous Electrodes for Redox Energy Storage," Electrochim. Acta, 26, 455-469 (1981).

LBL Reports

1. P. S. Fedkiw and J. S. Newman, "Mass-Transfer Coefficients in Packed Beds at Very Low Reynolds Numbers," LBL-12497.

Papers Presented

1. J. S. Newman, "Thermodynamics and Cell Potential, Mass Transfer, and Mathematical Modeling of Battery Systems," Three lectures for Electrochemical Engineering of Batteries, a national short course, Cherry Hill, NJ, June 22-26, 1981.

2. W. Tiedemann and J. S. Newman, "Simulation of Electric Vehicle Driving Profiles Based on Mathematical Models of the Lead-Acid Battery System." Detroit Meeting of the American Institute of Chemical Engineers, August 16-19, 1981.

d. Electrode Kinetics and Electrocatalysis*

Philip N. Ross, Investigator

Introduction. Complex electrochemical reactions in which chemical bonds are broken and/or formed are invariably catalytic, with electrode kinetics varying by many orders of magnitude for different electrode materials. Catalytic electrode materials are essential to technologies like fuel cells, metal-air batteries, electrolyzers, and electro-organic synthesis. Air electrodes constitute a major technology in themselves. In addition to being integral parts of fuel cells, air batteries, and water electrolyzers, air electrodes are being used increasingly in metal electro-refining and in air depolarized electrolytic cells. Alkaline fuel cells (e.g., Zn-air, Al-air and H_2-air) are receiving renewed attention for use in transportation applications and for on-site plant electricity generation from waste hydrogen. Interest in electrochemical processes for synthesis of organics has been increasing in recent years due to new classes of catalysts, e.g., alloys and organometallics.

1. CHARACTERISTICS OF AN NH_3-AIR ALKALINE FUEL CELL IN A VEHICLE APPLICATION†

P. N. Ross and V. Kopytov‡

The use of hydrogen-air alkaline fuel cells in a consumer vehicle application was examined. Liquid anhydrous ammonia was found to be an excellent storage medium for hydrogen, even though the endothermicity of the NH_3 cracking reaction results in some efficiency penalty. In the system developed here, hydrogen is supplied to a fuel cell by the catalytic cracking of liquid anhydrous ammonia, making the total system an indirect NH_3-air fuel cell. The advantages of the alkaline fuel cell relative to any acid fuel cell are higher power density (factor of 2-3) and lower cost (factor of 2) resulting in significantly lower total cost (factor of 4-6).

Laboratory scale examinations were made of the ammonia cracking reaction and the power characteristics of an alkaline fuel cell running on cracked ammonia and air. Single cell testing indicated system thermal efficiencies of 34-44 percent (based on H.H.V. of NH_3) can be achieved at power densities of 2600-1000 W/m^2 using currently known electrode technology that does not require the use of precious metal (e.g., Pt) catalyst. Computer simulations of vehicle characteristics were developed in cooperation with the LLNL electric and hybrid vehicle program. The vehicle chosen was a fuel cell-Zn/NiOOH battery hybrid, with the fuel cell sized for sustained cruising at 55 mph and the battery providing all peak power requirements. The fuel consumptions for the simulated SAE J227a "D" driving cycle with different power plant configurations are summarized in Table 1. Diesel ICE equivalent (33 W/kg) vehicle performance can be achieved in a fuel cell-battery hybrid vehicle that yields an NH_3 consumption rate of 10-20 km/l (2 seater urban car to 5 seater Volkswagen Rabbit type). A full performance ICE equivalent (49 W/kg) vehicle could be achieved with only a small penalty in fuel efficiency. For NH_3 produced from coal, the energy yield is slightly lower than for methanol from coal but the ammonia fuel cell powered vehicle is more than twice as efficient as the methanol ICE powered vehicle for the same performance. The result is a primary energy consumption one-half that for the ICE powered vehicle.

* * *

†Brief version of LBL-12754.

‡Lawrence Livermore National Laboratory.

*This work was supported by the Assistant Secretary for Conservation and Renewable Energy, Office of Energy Systems Research, Energy Storage Division of the U. S. Department of Energy under Contract No. DE-AC03-76SF00098.

Table 1. NH_3 consumption rates for fuel cell-battery powered hybrid vehicles of varying performance and cost (current density).

Design option	Curb wt.	Fuel cell	Ni-Zn bat	Full tank	Fuel consumed* km/l
	----------component masses [kg]----------				
INTERMEDIATE PERFORMANCE (Power-to-mass ratio: 33 W/kg, Range: 240 km):					
2 seater vehicle:					
(0.40 A/cm^2)	332	46	20	13.3	18.2
(0.15 A/cm^2)	372	81	22	9.9	20.6
5 seater vehicle:					
(0.40 A/cm^2)	893	71	52	24.2	10.0
(0.15 A/cm^2)	976	127	58	21.4	11.3
EQUIVALENT PERFORMANCE (Power-to-mass ratio: 49 W/kg, Range: 400 km):					
2 seater vehicle:					
(0.40 A/cm^2)	401	48	44	24.0	16.8
(0.15 A/cm^2)	464	85	50	21.5	18.8
5 seater vehicle:					
(0.40 A/cm^2)	1057	76	110	44.7	9.0
(0.15 A/cm^2)	1153	136	120	39.6	10.2

[a] Divide into 9.606 to obtain primary energy in kWh/km.

2. METAL OXIDE DOPED ACTIVE CARBONS AS OXYGEN REDUCTION CATALYSTS IN ALKALINE ELECTROLYTE†

P. N. Ross

It is well known that activated carbon blacks and certain transition metal oxides are catalysts for oxygen reduction. These two materials are felt to have very different catalytic action. Carbon blacks appear to catalyze oxygen reduction via a peroxide sequence,

$$O_2 + 2H_2O + 2e^- \rightleftharpoons HO_2^- + 2OH^- \quad \text{(fast)}$$

$$HO_2^- + H_2O + 2e^- \rightleftharpoons 3OH^- \quad \text{(slow)}$$

with the peroxide elimination step rate limiting. This type of catalytic action limits the potential that can be achieved in air electrodes to about -0.25V (vs Hg/HgO). Transition metal oxides appear to catalyze via a four electron sequence not involving an HO_2^- species in solution. In addition, some transition metal oxides are very effective HO_2^- reduction catalysts. It is therefore of considerable interest to consider whether the combination of a transition metal oxide with an activated carbon support would give rise to a synergistic effect between the two. The metal oxide is dispersed into carbons of variable activity. A synergistic effect would appear as an increase in the specific activity relative to that of the oxide on an inert substrate.

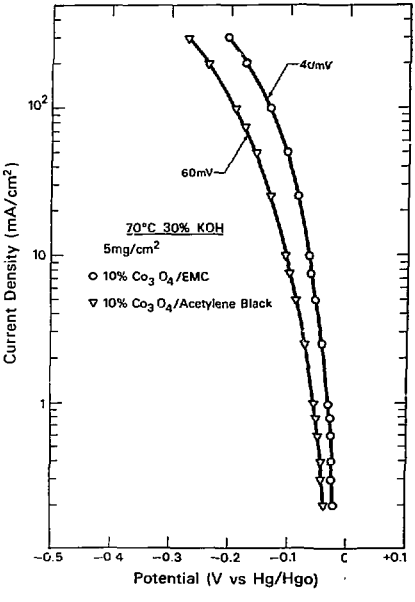

Fig. 1. Polarization curve for the reduction of pure O_2 with gas diffusion electrodes using Co_3O_4 impregnated black. (XBL 821-48)

An example of this analysis is shown in Fig. 1 for carbon black impregnated with Co_3O_4. In our study, Co_3O_4 was the most active non-Pt group transition metal oxide for oxygen reduction in alkali. Shawinigan acetylene black is a nearly inert substrate, having an activity level two orders of magnitude below that for the most active carbon investigated, designated EMC in Fig. 1. Co_3O_4/EMC carbon had 5 times the activity of Co_3O_4/acetylene black in the potential region above -0.1 V (vs Hg/HgO), or about 3 times the specific activity of unsupported oxide of the same nominal surface area. The explanation of this synergistic effect we favor at present is a "peroxide spillover" mechanism in which HO_2^- formed on the carbon surface migrates via surface diffusion to the Co_3O_4 where reduction occurs to OH^-. In addition, O_2 is reduced directly to OH^- on the Co_3O_4 clusters as if the carbon were not present.

* * *

†Brief version of LBL-11891.

3. BIFUNCTIONAL AIR ELECTRODE STUDIES†

P. N. Ross and L. R. Johnson

These studies provide supporting research in air-electrode technology for DOE metal-air battery projects. Metal-air systems have in principle the highest energy density and the highest power density (> 100 Wh/kg, > 100 W/kg) of all ambient temperature systems because of the electroactive species (oxygen) need not be contained within the battery. However, practical development of this technology has been slow due to problems in developing suitable air electrode materials. In electrically rechargeable metal-air batteries, the positive electrode must be bifunctional, both evolving and consuming oxygen. Few materials are stable at the potentials required for oxygen evolution; of these, fewer still are catalytically active for oxygen reduction and evolution. A number of metals and/or metal oxides have been examined for their stability and catalytic activity. With virtually every material examined, the polarization was greater in one direction than the other. Qualitatively the results were:

Unstable (dissolution): Ag, Pd, Fe_3O_4, MnO_2

Reduction activity: Pt > Ru > Co_3O_4 ≈ Rh ≈ Ir > NiO

Evolution activity: Ir ≈ Ru > Co_3O_4 > NiO > Pt

Co_3O_4 was the most cost effective catalyst of those studied so far and was very stable in the potential range of interest for air electrodes (+ 0.6V to -0.2V vs. Hg/HgO) e.g., less than 2 ppm Co detected in solution after 100 cycles. We have therefore concentrated on bifunctional electrodes based on Co_3O_4 as the catalytic material.

In order to prepare Co_3O_4 of the highest possible surface area, the oxide was impregnated into a carbon black support material and carefully heat treated to produce the Co_3O_4 phase. Analysis by x-ray diffraction and electron microscopy indicated that the characteristic size of oxide particles was 100-200 Å (equivalent to about 50 m^2/gm) when the carbon black used was Shawinigan acetylene black. This material is used by Westinghouse in their developmental air electrode. To determine the stability of the carbon phase, we have developed a ^{14}C tracer method that produces in situ determination of carbon loss from the electrode. The characteristic cycling behavior of an Fe-air battery using a standard Westinghouse 100 mAh/cm^2 iron electrode and an air electrode fabricated from the Co_3O_4 catalyst is summarized in Fig. 1. Carbon loss was appreciable and after 15% carbon loss the gas pores in the catalyst layer became progressively filled with electrolyte, resulting in rapidly increasing polarization. Analysis of the electrolyte and of the electrode revealed no loss of cobalt from the electrode. The failure of the electrode was attributed directly to the carbon corrosion.

Corrosion of acetylene black in the potential region for oxygen evolution was studied using the ^{14}C tracer method. The results are summarized in Fig. 2. The corrosion rate showed a strong dependence on both potential and temperature, 140 mV per decade and 23 kcal/gmol, respectively. The

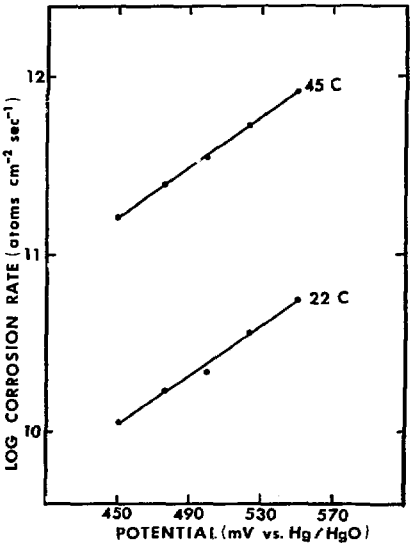

Fig. 2. Tafel plots for acetylene black corrosion at oxygen evolution potentials.

(XBL 822-7826)

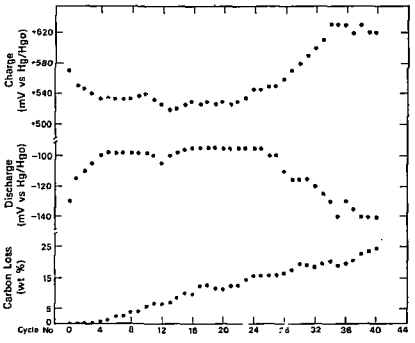

Fig. 1. Cycling behavior of a Co_3O_4 impregnated acetylene black air electrode. Galvanostatic at I = 10 mA/cm^2, 25 mg/cm^2, 45°C, 10^{-4} Hz.

(XBL 821-[illegible])

corrosion current was calculated from the mass rate of carbon loss assuming $6e^-$ per atom, equivalent to oxidation to CO_3^{2-}. Chemical analysis of the electrolyte has, however, indicated that the principal corrosion product is not CO_3^{2-}. These corrosion rates indicate that at 23°C a charging potential of +500 mV vs Hg/HgO would extend the cycle life relative to the test conditions by a factor of 30 (to about 900 cycles). To reduce the charging potential to +500 mV will require a substantial improvement in oxygen evolution catalysis relative to that achieved with Co_3O_4.

* * *

†Brief version of LBL-11891.

1981 PUBLICATIONS AND REPORTS

LBL Reports

1. P. N. Ross, "Characteristics of an NH_3-Air Fuel Cell for Vehicle Applications, LBL-12754.

2. P. N. Ross, "Oxygen Reduction with Carbon Supported Metallic Cluster Catalysts in Alkaline Electrolyte," LBL-11891.

Other Publications

1. P. N. Ross, "Characteristics of an NH_3-Air Fuel Cell for Vehicle Applications," Proceedings of the 16th I.E.C.E.C., Volume 1, pg. 726-733 (1981).

2. P. N. Ross, F. Will, and W. O'Grady (editors), Proceedings of the Symposium on Electrocatalysis, The Electrochemical Society Proceedings, Volume PV81-6, 1981.

Invited Talks

1. P. N. Ross, "Oxygen Reduction with Carbon Supported Metallic Cluster Catalysts in Alkaline Electrolyte," Occidental Research, Irvine, CA, February 1981.

2. P. N. Ross, "Oxygen Reduction with Carbon Supported Metallic Cluster Catalysts in Alkaline Electrolyte," Diamond Shamrock, Cleveland, OH, March 1981.

3. P. N. Ross, "Characteristics of an NH_3-Air Fuel Cell for Vehicle Applications," General Motors Research Center, Warren, MI, June 1981.

4. P. N. Ross, "Oxygen Reduction with Carbon Supported Metallic Cluster Catalysts in Alkaline Electrolyte," The Electrochemical Society Meeting, Minneapolis, MN, May 10-15, 1981.

5. P. N. Ross, "Characteristics of an NH_3-Air Fuel Cell for Vehicle Applications," 16th I.E.C.E.C., Atlanta, GA, August 15-18, 1981.

e. Electrochemical Properties of Nasicon*

Lutgard C. De Jonghe, Investigator

1. CHEMICAL STABILITY OF NASICON†

H. Schmid, L. C. De Jonghe, and C. Cameron

Nasicons, $Na_{1+x}Si_xZr_2P_{3-x}O_{12}$, were identified by Hong et al.[1] as possible alternatives to sodium-β and β" solid electrolytes. One important requirement of these ceramic electrolytes is that they be chemically stable toward the battery electrodes. It has been noted that while ionic resistivities of a few ohm-cm can be readily achieved, many Nasicons appear to degrade and crack rapidly when in contact with molten sodium at temperatures around 300°C. The rate at which the degradation occurs depends both on the chemical composition of the Nasicon and the presence of impurities. Since there appears to be some question as to whether Nasicons are chemically stable in contact with sodium, some other Nasicon applications were explored as well.

Nasicon powders with x = 2 and with the recently proposed new composition[2] of $Na_{3.1}Zr_{1.55}Si_{2.3}P_{0.7}O_{11}$ were fabricated by a sol-gel method and sintered for 24 hours at 1220°C in air. Densities of around 95% theoretical were achieved. The specimens were then immersed in sodium at 300°C for a period of up to two weeks. Analysis with x-rays showed that the lattices of both electrolytes had undergone changes as a result of chemical reaction with the sodium. The x-ray diffractograms from as prepared and immersed material could be fitted to a monoclinic and a rhombohedral unit cell. The comparison of the diffractograms as prepared (A) and immersed (B) electrolytes is shown in Fig. 1, illustrating the shifts in the lattice parameters. The data indicated that the samples were actually a mixture of rhombohedral and monoclinic phases. The data also indicated that the reaction with metallic sodium increased the sodium content of the Nasicon electrolytes. The lattice parameter changes were sufficiently large to produce stresses that fractured the electrolytes.

Minor alumina contamination was found to lead to the formation of a sodium alumino-silicate intergranular phase that was rapidly attacked by the sodium. Elimination of contamination by alumina dramatically increased the resistance to chemical degradation of the electrolytes. Nevertheless, after about 10 weeks of immersion at 300°C, the electrolytes again showed the same type of degradation that was observed in the more rapidly degrading electrolytes containing some alumina. Experiments are continuing to explore the dependence of the susceptiblity to chemical attack by sodium for electrolytes of different composition.

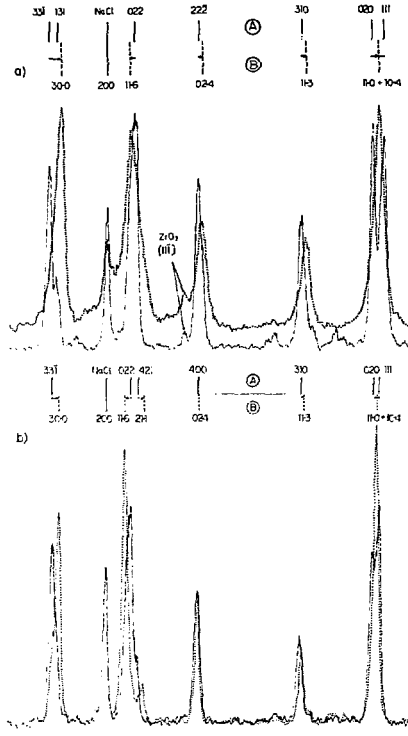

Fig. 1. Comparison of as prepared (A) and sodium immersed (B) electrolyte diffraction patterns. NaCl was used as a standard. (a) $Na_3Si_2Zr_2PO_{12}$. (b) $Na_{3.1}Zr_{1.55}Si_{2.3}P_{0.7}O_{11}$. Solid lines: as prepared; dotted lines: after immersion in Na, for 16 days at 300°C. (XBL 813-8555A).

Indications are that Nasicons containing less phosphorous have increased stability towards sodium at higher temperatures. Nasicons are currently being tested for application in different environments. A potentially important application makes

*This work was supported by the Assistant Secretary for Conservation and Renewable Energy, Office of Energy Systems Research, Energy Storage Division of the U. S. Department of Energy under Contract No. DE-AC03-76SF00098.

use of thin Nasicon membranes in chloralkali cells. Nasicons have been found to be far more resistant to degradation by water than the sodium-beta aluminas, making Nasicon potentially suitable for applications involving aqueous electrolytes. In preliminary tests, Nasicon membranes were subjected to current densities of up to 1 A/cm^2 for about 2 hours in a chloralkali cell, at 80°C. Static tests showed that the Nasicons were stable in saturated sodium chloride solutions and in sodium hydroxide solutions containing more than 30 wt% of sodium hydroxide.

* * *

†Short version of LBL-12460

1. H. Y-P Hong, Math. Res. Bull. 11, 173, (1976); and M. B. Goodenough, H. Y-P. Hong, and J. A. Kafalas, Mat. Res. Bull. 11, 203, (1976).
2. U. Von Alpen, M. F. Bell, and W. Wichelhouse, Mat. Res. Bull. 14, 1317 (1979).

1981 PUBLICATIONS AND REPORTS

LBL Reports

1. H. Schmid, L. C. De Jonghe, and C. Cameron, "Chemical Stability of Nasicon," May 1981, LBL-12460.

†2. L. C. De Jonghe, "Transport Number Gradients in Solid Electrolyte Degradation," May 1981, LBL-12070, Rev.

†3. L. C. De Jonghe, L. Feldman, and A. Buechele, "Failure Modes of Sodium Beta Alumina," April 1981, LBL-12445.

†4. L. Feldman and L. C. De Jonghe, "Initiation of Mode I Degradation in Sodium Beta Alumina Electrolytes," April 1981, LBL-12194.

†5. L. C. De Jonghe, A. Buechele, "Chemical Coloration of Sodium Beta Alumina," March 1981, LBL-12251.

Other Reports

†1. L. C. De Jonghe, "Performance of Sodium Beta Alumina Solid Electrolytes in Na/S Cells," Proceedings 16th Intersociety Energy Conversion Engineering Conference, Volume I, American Society of Mechanical Engineers, 1981, pg. 826.

Invited Talks

†1. L. C. De Jonghe, "Factors Affecting the Performance of Solid Electrolytes," 4th US-DOE Battery and Electrochemical Contractors Conference, June 2-4, 1981, Washington DC.

†2. L. C. De Jonghe, "Solid Electrolyte Batteries," American Ceramics Society, August 1981, Berkeley, CA.

* * *

†With support from the Electric Power Research Institute.

f. Improvements in Efficiency of Aluminum Reduction Cells*

James W. Evans, Investigator

Introduction. The purpose of this investigation is to reduce the energy consumed in the electrolytic production of aluminum. Approximately 11 GW per year of electrical energy are consumed in the U.S. for aluminum production, and there is, therefore, considerable incentive for the development of new technology that will minimize such energy consumption. The work described in this report is the development of a mathematical model that will predict the performance of the electrolytic cell that produces the aluminum based on the design of the cell and operating parameters under the control of the cell user. By means of the model, rapid screening of alternative cell designs or operating practices can be carried out, promoting the development of cells consuming less electrical energy.

1. DEVELOPMENT AND TESTING OF THE MATHEMATICAL MODEL FOR THE HALL-HÉROULT CELL†

Steve Lympany, Huai-Chuan Lee, and James W. Evans

The major consumer of energy in the production of aluminum is the Hall-Héroult cell wherein electrical energy is used to electrolytically reduce aluminum oxide to metal. A mathematical model for the cell has been under development for some years, and has now reached the point of testing and refinement. Two performance parameters of interest from an energy consumption viewpoint are the current efficiency of the cell and the flatness of the interface between the two liquid layers in the cell (molten aluminum and the molten salt electrolyte). The former has an obvious connection with energy consumed per unit mass of product; the latter variable is important because "bowing" of this interface prevents the shortening of the anode-interface distance (shortening this distance reduces energy consumption by reducing resistive losses in the electrolyte).

Both the current efficiency and flatness of the interface are primarily dependent on electromagnetic forces that rise within the cell from the interaction of cell currents with magnetic fields. The magnetic fields arise from the currents flowing within the cell, surrounding conductors ("bus bars") and surrounding cells. The current efficiency is less than 100 percent because the aluminum product has a slight solubility in the electrolyte, and this dissolved aluminum is transported to the anode where it re-oxidizes. This transport of aluminum is due to turbulent convection in the electrolyte, and is, therefore, a function of the electrolyte flow, a flow which is driven by the electromagnetic forces. The model computes the current distribution in the cell, the magnetic field, the electromagnetic stirring forces, the velocity field of the electrolyte and aluminum, the bowing of the interface, and the current efficiency.

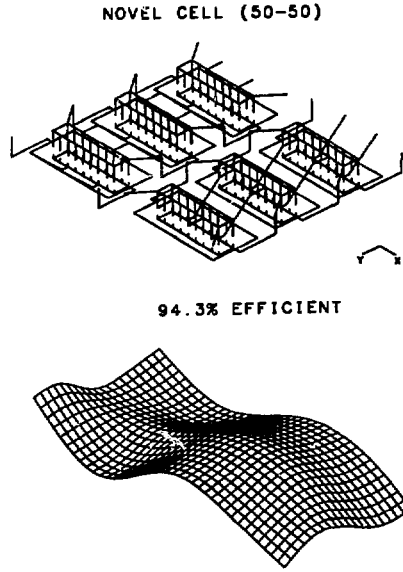

Fig. 1. A novel conductor arrangement for six Hall-Héroult cells and the current efficiency for such an arrangement. The lower half of the figure depicts the computed shape of the interface between molten metal and salt (vertical scale exaggerated for effect).

(XBL 823-8492)

Figure 1 is typical of results recently generated by the model. It depicts the conductors for six cells (the cell of interest, plus two adjacent cells in the same line of cells, plus the three closest cells in an adjacent line). The cell is different from the usual Hall-Héroult cell in that

*This work was supported by the Assistant Secretary for Conservation and Renewable Energy, Office of Energy Systems Research, Energy Storage Division of the U. S. Department of Energy under Contract No. DE-AC03-76SF00098.

the current is taken out of the cell by conductors ("collector bars") passing out through the bottom of the cell; the usual cell has conductors passing out through the side. The computed current efficiency is 93.1 percent versus a best computed current efficiency of 91.7 for a comparable cell of conventional design. The aluminum-electrolyte for the novel cell is depicted in the lower half of Fig. 1. and is flatter than that of a comparable conventional cell (4.6 cm trough to peak distance versus 7.0 cm. for the conventional cell).

* * *

†Brief version of LBL-11675 (Oct. 1980) now published in Metallurgical Transactions, vol. 12B, p. 353, 1^81 (Evans, Zundelevich, and Sharma, authors), plus more recent unpublished material.

2. WORK IN PROGRESS

The refinement of the mathematical model is continuing. An example of such refinement would be incorporation of vertical electromagnetic forces into the model. These forces are of less importance than the horizontal forces that are presently included in the model. A second refinement that is being attempted is the incorporation of the effect of gas bubbles. These bubbles, generated at the anode, are thought to affect the circulation of electrolyte and, thereby, current efficiency. An attempt is also being made to compare the predictions of the model with experimental measurements. Measurements on actual cells are not available, either because of the difficulty of making them in the cell environment (960°C with molten aluminum and salt present) or because information is retained by cell operators on proprietary grounds. A "cold" physical model of the cell is, therefore, being built. The model, approximately one-tenth the scale of a real cell, is to contain a low melting point alloy. Measurements of the velocity of the metal in the cold model can then be compared with computer predictions for the model.

1981 PUBLICATIONS AND REPORTS

Refereed Journals

1. J. W. Evans, Y. Zundelevich, and D. Sharma, "A Mathematical Model for Prediction of Currents, Magnetic Fields, Melt Velocities, Melt Topography and Current Efficiency in Hall-Heroult Cells," Metallurgical Transactions, 12B, 353 (1981); LBL-11675.

†2. D. P. Ziegler, M. Dubrovsky, and J. W. Evans, "A Preliminary Investigation of Some Anodes for Use in Fluidized Bed Electrodeposition of Metals," J. Appl. Electrochem., 11, 625 (1981).

LBL Reports

1. D. J. Coates, J. W. Evans, and S. S. Pollack, "Identification of the Origin of TiO_2 Deposits on Hydrodesulfurizaton Catalysts," LBL-13244.

2. D. J. Coates, J. W. Evans, and K. H. Westmacott, "Defects in Antiferromagnetic Nickel Oxide," LBL-13704.

Other Publications

‡1. M. Dubrovsky and J. W. Evans, "Fluidized Bed Electrowinning of Cobalt" in Processes and Fundamental Considerations of Selected Hydrometallurgical Systems, M. C. Kuhn (ed.), AIME, New York, 1981.

2. J. W. Evans, S. Lympany, and D. Sharma, "A Mathematical Model of the Hall-Héroult Cell and Calculations for Some Improved Cell Designs," Proceedings of the 2nd World Congress of Chemical Engineering, Montreal, Canada, 6, 211 (1981).

†‡3. M. Dubrovsky, D. P. Ziegler, I. F. Masterson, and J. W. Evans, "Electrowinning of Copper and Cobalt Using Fluidized Bed Cathodes," Proceedings of Extraction Metallurgy '81, London, England, Inst. Min. and Met., London, 1981.

Papers Presented at Meetings

§1. J. W. Evans and M. H. Abbasi, "Diffusion and Radiant Heat Transport in Porous Solids or Packed Beds," AIME Annual Meeting, Chicago, February, 1981.

§2. J. W. Evans and M. Dubrovsky, "The Use of a Fluidized Bed Cathode for Selective Deposition of Metals from Aqueous Solutions," AIME Annual Meeting, Chicago, February, 1981.

---

†Supported by the Office of Surface Mining, Department of the Interior.

‡Supported by National Science Foundation.

§Supported by intramural funds, University of California.

B. Engineering Analysis

a. Engineering Analysis of Gas Evolution in Electrolysis*

Charles W. Tobias, Investigator

Introduction. Gas evolution by electrolysis is one of the most common reaction types in electrosynthesis. Electrically rechargeable batteries are now under development that also develop gases on charge. This project is directed toward the physical description and correlation of the behavior of electrochemically generated gas-electrolyte emulsions, including the effect bubble streams have on mass transport at electrode surfaces. Liberation of hydrogen, oxygen or chlorine from various substrates situated in a flow channel, is observed under intense illumination over broad ranges of current densities and flow rates. The ohmic component of overpotential is measured and correlated to process conditions. Understanding the behavior of bubble streams should lead to improvements in the energy efficiency of gas-generating processes.

1. BUBBLE DYNAMICS AT ELECTRODE SURFACES

Philippe Cettou and Charles W. Tobias

Gas evolution is usually accompanied by two effects brought on by the bubbles: an increase in mass transfer rate and a rise in ohmic losses. With the rising cost of energy, the latter has received growing attention. In a gas-evolving cell the bubbles responsible for the losses can be classified into two categories: bubbles in the bulk, which do not interact with the electrode surface, and bubbles in the vicinity of the surface, referred to as the bubble layer. Practical improvements of cell and electrode design have largely eliminated the resistance caused by bubbles in the bulk, but the bubble layer, with its characteristics not well known, remains a problem. The aim of this work is to advance the fundamental understanding of this bubble layer to stimulate improvements in cell performance.

We have chosen to study the first generation of bubbles at the electrode, which evolves just after the current is turned on. During this initial period of gas evolution, there are no bubbles in the bulk, and the events occurring at the electrode surface are easily observed. Also during this period, we can measure the contribution of the bubble layer to the total cell resistance.[1]

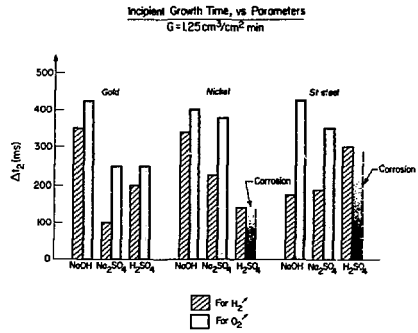

Fig. 1. Bubble residence times at the electrode surface. 1.25 $cm^3/cm^2/min$.

(XBL 819-1314)

The evolution of hydrogen and oxygen was observed on three different electrode materials (gold, nickel, and stainless steel) and with three electrolytes (sodium hyroxide, sodium sulfate, and sulfuric acid). The influence of current density is also considered. The events associated with gas evolution--nucleation, growth by diffusion and by coalescence, and departure from the electrode--occur rapidly and on a small scale. To reveal details of these events, high speed cinematography through a microscope is required.

The results of the motion picture studies are qualitative in nature, but they reveal striking differences in nucleation density, residence time and surface coverage from case to case, depending on conditions. For example, the residence time of bubbles at the electrode surface is always higher for oxygen than for hydrogen (Fig. 1). The average size of the bubbles depends strongly on the frequency of coalescence, which is in turn very sensitive to the nature of the electrolyte (Fig. 2). We have experimentally determined the dependence of electrical resistance upon electrode coverage; this compared favorably with predictions from established theoretical models. To minimize the resistance of a gas evolving cell, both the electrode coverage and the bubble layer thickness should be lowered. Our studies show that strong coalescence achieves both of these desired effects. This leads to the conclusion that it is advantageous to operate under conditions under which coalescence readily occurs, as in our experiments

*This work was supported by the Assistant Secretary for Conservation and Renewable Energy, Office of Energy Systems Research, Energy Storage Division of the U.S. Department of Energy under Contract No. DE-AC03-76SF00098 through the Chicago Operations Office, Technical Management Division of the Argonne National Laboratory, Argonne, IL.

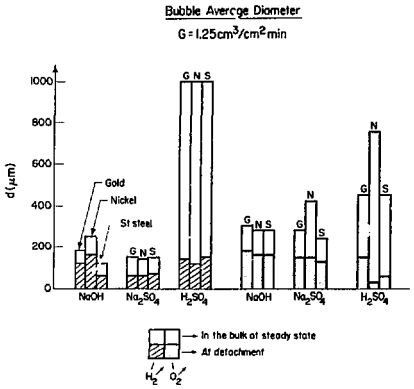

Fig. 2. Average bubble diameters at detachment and at steady state. G = 1.25 $cm^3/cm^2/min$. (XBL 819-1313)

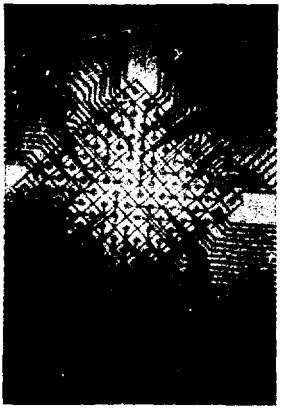

Fig. 1. 10 x 10 matrix of electrically isolated platinum coated segments on 100 micron centers; produced on a silicon wafer in collaboration with Hewlett-Packard. (CBB 809-11046)

in sulfuric acid. In the light of this fact, it appears worthwhile to conduct further studies on bubble dynamics, particularly on coalescence phenomena.

* * *

1. Philippe Cettou and Charles W. Tobias, "Bubble Dynamics at Electrode Surfaces," LBL-13632.

2. WORK IN PROGRESS

Studies of Bubble Dynamics on a Mosaic Electrode

Dennis Dees and Charles W. Tobias

Electrochemically generated gas bubbles have a significant effect on mass transport at electrode surfaces. This effect is a result of the convection generated by bubble phenomena occurring at the electrode, which include growth, coalescence, disengagement, and ascension of the bubbles. Previous work[1] done in this laboratory has demonstrated that each of these phenomena can be produced separately and their effect on the mass transport measured. To obtain quantitative measurements of the change in mass transport, a novel mosaic electrode has been produced jointly by this laboratory and Hewlett-Packard Co. The electrode has been prepared on a silicon chip by integrated circuit technology. It consists of a 10 by 10 matrix of square platinum segments on 100 micron centers which are electrically isolated from each other (Fig. 1). The matrix is surrounded by 12 specially positioned segments and a relatively large buffer segment, all coated with platinum. The matrix simulates a continuous surface, while at the same time, one is able to control and measure the current and/or potential for each segment.

Changes in mass transfer rates as a result of a single bubble disengagement were studied with the mosaic electrode. All of the electrode segments were polarized cathodically in the mass transfer limiting region to reduce ferric- to ferrous-ion, just above the potential for hydrogen evolution. By reducing the potential of an individual segment approximately 300 mV below the other segments, a single bubble could be nucleated and grown. The change in mass transfer when the bubble disengaged was measured by monitoring the current at a segment where only the redox couple reaction was occurring. A typical plot is given in Fig. 2.

The rise time of the current is on the order of tenths of seconds. The initial rise is due to the collapse of the bubble contact area. There is a decrease in the current after the maximum below the base line current. Theoretical results indicate that the decrease is caused by the convection generated by the ascension of the bubble from the horizontal plane.

* * *

1. Dennis Dees and Charles W. Tobias, "Mass Transfer Studies with a Micro-Segmented Electrode," MMRD Annual Report 1980, LBL-12000.

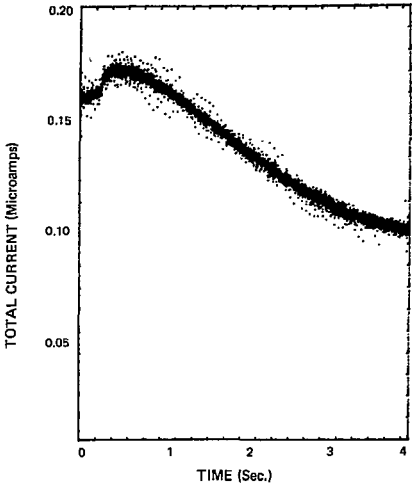

Fig. 2. Current to a segment 400 microns from the center of a disengaging 1485 micron diameter bubble. (XBL 823-8143)

1981 PUBLICATIONS AND REPORTS†

Refereed Journals

1. C. W. Tobias, "The Coming of Age of Electrochemical Engineering," AIChE Symposium Series, 204, 77 (1981).

‡2. P. C. Foller and C. W. Tobias, "The Effect of Electrolyte Anion Adsorption on Current Efficiencies for the Evolution of Ozone," J. Phys. Chem., 85, 3238 (1981). [Joel H. Hildebrand Centennial Issue].

LBL Reports

§1. P. J. Sides (with C. W. Tobias), "Bubble Dynamics at Gas Evolving Electrodes," Ph.D. dissertation, University of California, Berkeley, LBL-11849.

§2. C. W. Tobias and P. J. Sides," Resistance of a Planar Array of Spheres; Gas Bubbles on an Electrode," submitted to the Journal of the Electrochemical Society, LBL-13468.

3. P. Cettou and C. W. Tobias, "Bubble Dynamics at Electrode Surfaces," December 1981, LBL-13632.

Other Publications

Book Edited: H. Gerischer and C. W. Tobias, Advances in Electrochemistry and Electrochemical Engineering, Wiley-Interscience, New York, Vol. 12, November 1981.

Invited Talks

§1. P. J. Sides and C. W. Tobias, "A Close View of Gas Evolution," invited paper, Meeting of the Electrochemical Society, Minneapolis, Minn., May 10-15, 1981; Extended Abstracts, Vol. 81-1, No. 392, P. 985-986 (based on LBL 11849].

‡2. P. C. Foller and C. W. Tobias, "The Effect of Electrolyte Anion Adsorption on Current Efficiencies for the Evolution of Ozone," invited paper, Meeting of the Electrochemical Society, Minneapolis, Minn., May 10-15, 1981; Extended Abstracts, vol. 81-1, No. 478, p. 1182-83.

3. C. W. Tobias, "Electrochemical Engineering of Batteries," invited lecture, Short Course, Continuing Education Institute, Cherry Hill, NJ, June 22-26, 1981.

4. C. W. Tobias, "Prospects of the Electrochemical Technology," invited lecture, W. R. Grace Research Center, Columbia, MD, September 18, 1981.

5. Philippe Cettou and C. W. Tobias, "The First Generation of Bubbles on Gas-Evolving Electrodes," contributed paper, Meeting of the Electrochemical Society, Denver, CO., October 11-16, 1981; Extended Abstracts, vol. 81-2, no. 584, p. 1401 (based on LBL-13632).

6. C. W. Tobias, "On the Nature of Electrolytic Gas Evolution," invited lecture, Department of Chemical Engineering, University of Houston, TX, November 6, 1981.

* * *

†A complete listing of publications, reports and papers presented by Charles W. Tobias and his associates is provided under "Electrochemical Processes" in the Materials Sciences section of this Annual Report.

‡Supported entirely from University funds.

§Supported by the Division of Materials Sciences, Office of Basic Energy Sciences, U.S. Department of Energy.

VII Magnetic Fusion Energy

Magnetic Fusion Energy

a. Structural Materials and Weldments for High Field Superconducting Magnets*

J. W. Morris, Jr., Investigator

Introduction. The choice of materials for the structures of the high field superconducting magnets that are essential to the successful development of fusion power poses particular materials problems. The magnet case must sustain the high structural loads imposed by the magnet winding, must successfully withstand these loads at the temperature (4.2 K) of the helium used to cool the magnet winding, and must do so in the presence of a high magnetic field. The combined requirements of high structural strength, high fracture toughness, and fatigue resistance in the superconducting magnet environment make it probable that new classes of structural materials will be required before commercial fusion energy devices can be constructed. The present project is intended to contribute to the development of these new materials by clarifying the behavior of structural materials in the magnet environment and by designing, identifying, and testing new alloys and weldments that promise superior structural properties.

1. DESIGN AND CONSTRUCTION OF THE CRYOGENIC TESTING FACILITY

B. Fultz

A mechanical testing device was designed and constructed to permit tensile, fracture toughness, or fatigue testing at temperatures as low as 4.2 K. The testing device is attached to a hydraulic testing machine with an overhead actuator. The device consists of two concentric cylindrical columns of structural steel configured so that appropriate testing grips can be attached to the ends of the columns and mechanical tests conducted by displacing the inner cylinder with respect to the fixed outer cylinder. The double column fixture is lowered into a cryostat or helium dewar for mechanical testing. In its present form the device can apply mechanical loads in excess of 20,000 lb on a sample immersed in liquid helium, and, by applying the hydraulic testing machine, can conduct the full range of appropriate mechanical property tests. The machine has been used for tensile, fracture toughness, and fatigue testing at 4.2 K, and has proven to be frugal in helium consumption.

2. THE INFLUENCE OF HIGH MAGNETIC FIELDS ON CRYOGENIC MECHANICAL PROPERTIES

B. Fultz and G. M. Chang

While the structural materials of high field superconducting magnets operate in an intense magnetic field, there is very little data on the influence of high magnetic fields on the mechanical properties of structural materials. During the past year a pulsed magnet was used to do exploratory investigations on two classes of cryogenic materials. In the first series of tests, a ferritic cryogenic steel which was toughened by the addition of precipitated austenite in the ferrite matrix was subjected to pulse magnetic fields up to 16 T at 77 K. The pulsed magnetic field led to partial transformation of the precipitated austenite within the steel matrix, and caused a measurable decrease in the upper shelf impact toughness of the material with a concomitant rise in the ductile-to-brittle transition temperature. In a second set of experiments metastable 304 austenitic steel was subjected to repeated magnetic pulses of up to 16 T while under load in a bolt loading device. The results of these tests showed that the martensitic transformation in the steel was promoted by the pulse magnetic field when the specimen was loaded into the plastic region. The measurable elongation of the specimen was associated with the martensitic transformation. These preliminary tests demonstrate the influence of high magnetic fields on the mechanical properties of structural steels through its promotion of the martensitic transformation.

3. FERRITIC STRUCTURAL STEELS AND WELDMENTS

H. J. Kim and H. L. Lin

Previous research in this laboratory has shown that it is possible to achieve reasonable toughnesses in ferritic steels at 4.2 K if these steels have high nickel content (9-12Ni) and if they are given thermal cycling treatments that impart a fine grain structure. Further research had shown that multi-pass gas tungsten arc welding can be used to weld Ni steel with ferritic metal so that reasonably toughness is preserved at 4.2 K in both the weld metal and the heat-affected zone. Research during the past year concentrated on improving the reliability and reproducibility of the grain refining treatment for Fe-Ni ferritic cryogenic steels, and on establishing the weldability of the commercial 9Ni grades. The reproducibility problem in grain-refined Fe-Ni cryogenic steels is evidenced by a substantial sample to sample variation in toughness at 4.2 K. Microstructural studies carried out over the past year suggest that these variations arise from variations in the effective

*This work was supported by the Director, Office of Energy Research, Office of Fusion Energy, Development and Technology Division of the U. S. Department of Energy under Contract No. DE-AC03-76SF00098.

packet size of the heat treated materials. The effective packet size is influenced by both small changes in the composition of the steel and by changes in the specific heat treatment schedule. While the superficial changes in microstructure resulting from minor variations in compositions or heat treatment are subtle, they have consequences for the ductile-to-brittle transition temperature within the processed alloy. Research is under way to clarify these effects so that reliable heat treatments can be developed. Research on the multi-pass GTAW welding of 9Ni cryogenic steel has shown that it is possible to weld this material with ferritic filler metal so that good cryogenic structural properties are obtained in both the weldment and heat-affected zone. The surprising result of this research was the recognition that the welding process virtually eliminates precipitated austenite from both the weldment and the regions of the heat-affected zone in the immediate proximity to the weldment. While it has generally been assumed that a fine distribution of precipitated austenite must be present in 9Ni steels to establish low temperature toughness, the present investigation shows that rapidly cycled material is tough at low temperature even in the absence of precipitated austenite. The source of these good properties appears to lie in the mechanism of transformation of precipitated austenite during rapid thermal cycling, which leads to an effective grain refinement of the rapidly cycled material.

4. AUSTENITIC FE-MN CRYOGENIC STEELS

R. Ogawa

Research in a number of laboratories has suggested that austenitic steels based on the Fe-Mn system may offer a particularly attractive combination of cryogenic strength, toughness, and economics for use in magnetic structures. The metallurgy of these steels is, however, not well understood, and the low temperature properties of these steels occasionally show anomalous features, such as a consistent loss in fracture toughness as the testing temperature is lowered. To clarify these phenomena a variety of austenitic Fe-Mn steels have been tested over a range of temperatures. The results suggest that alloy strength is the principal determinant of toughness irrespective of the testing temperature; but microstructural influences are also apparent. In particular, the precipitation of carbides or carbo-nitrides within the steel causes a consistent deterioration in the cryogenic toughness. The stability of the austenite phase is also important, but the influence of phase transformation is not yet clear, and is under continued investigation.

1981 PUBLICATIONS AND REPORTS

LBL Reports

1. H. J. Kim, C. K. Syn, and J. W. Morris, Jr., "Ferritic Weldment of Ferritic Ni Steels for Liquid Helium Use," LBL-13017.

2. H. J. Kim and J. W. Morris, Jr., "The Development of a Ferritic Consumable for Welding Grain-Refined Fe-12Ni-0.25Ti to Retain Toughness at 4.2 K," LBL-13046.

Other Publications

1. B. Fultz and J. W. Morris, Jr., "A Mössbauer Study of Microstructural and Chemical Changes in Fe-9Ni Steel during Two-Phase Tempering," in Nuclear and Electron Resonance Spectroscopies Applied to Materials Science, eds., Kaufmann and Shenoy, Elsevier North Holland, 1981.

Invited Talks

1. J. W. Morris, Jr., "Advances in Cryogenic Steels," Paton Institute, Kiev, USSR, March 18, 1981.

VIII Nuclear Waste Management

Nuclear Waste Management

a. Thermodynamic Properties of Chemical Species in Nuclear Waste*

Norman M. Edelstein, Investigator

Introduction. The purpose of this program is to investigate the thermodynamic properties of anticipated actinide and fission product ions and the compounds they may form in geologic environments, so that their chemical behavior and potential migration in a nuclear waste setting can be assessed with improved capability.

A number of laboratory studies are being undertaken to obtain data concerning species, oxidation states, effect of complexing ligands, and other related information. Such data will contribute to a better understanding of the chemical systems that may be involved in various geologic media and will furnish more reliable parameters for radionuclide migration modeling studies.

1. STUDIES ON TRIVALENT AND TETRAVALENT NEPTUNIUM AND PLUTONIUM WITH COMPUTER CONTROLLED VOLTAMMETRY†

H. Nitsche, S. D. Brown,‡ and N. M. Edelstein

Thermodynamic data for aqueous actinide systems in trace and ultratrace concentrations are needed as input parameters for chemical modeling of nuclear waste in geologic repositories.[1] Computer controlled voltammetry is a relatively new analytical technique that can be used at these levels for the determination of stability constants[2-4] of tri- and tetravalent neptunium and plutonium systems.

Preliminary studies have been carried out on the performance of various electrodes (dropping mercury, hanging mercury drop, mercury film rotating disk, glassy carbon, gold film rotating disk, platinum rotating disk) with the application of different waveforms (linear scan, differential pulse, differential pulse anodic stripping voltammetry). The detection limits were determined for various conditions.

Np(IV,III) in acidic solutions gave reproducible responses on stationary Hg electrodes. The Np(IV)/Np(III) couple can be considered as quasi-reversible with the transport of the electroactive neptunium species to and from the electrode surface controlled by a diffusion-limited adsorption or desorption process. No electrochemical response was observed with Np(IV) carbonate solutions with Hg electrodes, which suggests the reduction potentials are more negative than −1.9V, requiring fairly large stability constant(s) for the complex(es) of Np(IV) with carbonate ions.

Pu(III) and Pu(IV) solutions in 1M HCl did not produce any response on a glassy carbon electrode with linear sweep voltammetry contrary to a previous report.[5] In addition, no response was obtained with the application of a square wave to a platinum disk electrode in a solution of 9.5 x 10^{-5} M Pu(IV) in 1M HCl.[6] Differential pulse and differential pulse anodic stripping voltammetry gave excellent response and precision on the platinum disk electrode with peak potentials in agreement with values obtained by coulometry.[7] The Pu(IV)/Pu(III) couple appears to be electrochemically reversible in 1M HCl. The mode of transport, as with Np(IV)/Np(III), is a diffusion-limited adsorption process.

Pu(IV) in 1M carbonate solutions gave good signals using differential pulse polarography at the hanging mercury drop electrode. Peak potentials are in excellent agreement with oscillopolarographic data.[8] Lowering the carbonate concentration by use of 1M $NaHCO_3$ shifted the Pu(IV) peak to a distinctly less cathodic potential than in 1M Na_2CO_3 (see Fig. 1). Standard addition curves for Pu(IV) in 1M Na_2CO_3 and 1M $NaHCO_3$ are shown in Fig. 2. Differential pulse polarography at a platinum disk electrode, applied to solutions of Pu(IV) in 1M Na_2CO_3, showed well-formed peaks for the Pu(IV)/Pu(III) charge transfer. Again, sensitivity appears to be limited by a diffusion-controlled adsorption process.

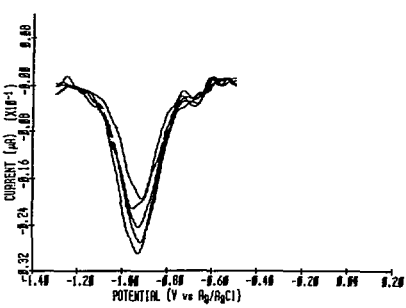

Fig. 1. Differential pulse voltammetry of Pu(IV) at different concentrations in 1M $NaHCO_3$ at a hanging mercury drop electrode. (XBL 818-1759)

*This work was supported by the Assistant Secretary of Nuclear Energy, Office of Commercial Nuclear Waste Management, Commercial Waste Management Program Division of the U. S. Department of Energy under Contract No. DE-AC03-76SF00098 through the Battelle Memorial Institute, Office of Nuclear Waste Isolation (ONWI), Columbus, Ohio, under MPO No. E511-05100.

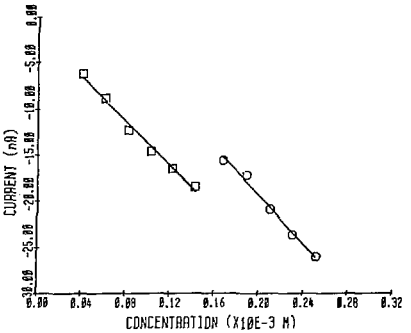

Fig. 2. Standard addition curves of Pu(IV) in 1M Na_2CO_3 (squares) and in 1M $NaHCO_3$ (octagons). (XBL 818-1760)

Complexation studies of Pu(III)(IV) carbonate systems are currently under investigation.

* * *

†Summary of a paper presented at "Actinides-1981" Asilomar, CA, September 10-15, 1981, LBL-12441.

‡*Present address:* Department of Chemistry, Washington State University, Pullman, WA 99164.

1. J. M. Cleveland, in Chemical Modeling in Aqueous Systems, ed. E. A. Jenne (ACS Symposium Series 93, Washington, DC, 1979) p. 16.
2. S. D. Brown and B. R. Kowalski, Anal. Chim. Acta 107, 13 (1979).
3. S. D. Brown and B. R. Kowalski, Anal. Chem. 51, 2133 (1979).
4. J. J. Toman, R. M. Corn, and S. D. Brown, Anal. Chim. Acta 123, 187 (1981).
5. C. E. Plock, Anal. Chim. Acta 49, 83 (1970).
6. K. Koyma, Anal. Chem. 32, 523 (1960).
7. W. D. Shults, Talanta 10, 833 (1963).
8. S. Casadio and F. Orlandini, J. Electroanal. Chem. 26, 91 (1970).

2. APPLICATION OF CONVOLUTIVE VOLTAMMETRIC CURVE FITTING TECHNIQUES TO NON-REVERSIBLE ELECTROCHEMICAL SYSTEMS†

J. J. Toman and S. D. Brown

The application of convolutive potential sweep voltammetric (c.p.s.v.) and, in particular, semidifferential voltammetric curve fitting techniques has been shown to be useful in the peak resolution of overlapped waves of reversible systems.[1] This technique is superior to other electrochemical curve fitting techniques in that linear sweep voltammetric (l.s.v.) waves are transformed numerically into shapes that are describable by simple analytic functions. In addition, all peaks are defined completely by three parameters that are related directly to peak potential, height, and width, and no single peak parameters need be assumed to resolve systems of several overlapped peaks. This work extends the application of convolutive potential sweep voltammetric curve fitting techniques to some nonreversible electrochemical systems of environmental interest, namely systems with quasi- or irreversible charge transfer kinetics or nonlabile homogeneous kinetics preceding charge transfer.

The c.p.s.v. technique is tested by application to synthetic l.s.v. data files created by finite difference digital simulation or, in the case of fast homogeneous kinetics, by the numerical integration method of Nicholson and Shain.[2] Effectiveness of the curve fitting techniques was judged by the application of theoretical expressions relating dimensionless charge transfer and homogeneous kinetic rate constants to parameters obtained from the fitting process, such as peak potential and width.

A semiderivative of a quasi-reversible charge transfer with the corresponding fit, a hyperbolic secant squared function, is shown in Fig. 1. The $sech^2$ fitting function is found to be excellent in the curve fitting of semiderivatives of both quasi- and irreversible charge transfer kinetic systems. Coefficients of determination for all fits are close to 1, indicating goodness of fit, and all expressions relating returned parameters to rate constants are obeyed closely.

Curve fitting of $sech^2$ functions to semiderivatives of systems with nonlabile homogeneous kinetics preceding charge transfer was found to work in the limiting cases of diffusion controlled behavior as described by Saveant and Vianello.[3] As shown in Fig. 2, for systems not in these limits there is a tail to the semiderivative that the $sech^2$ function does not fit well.

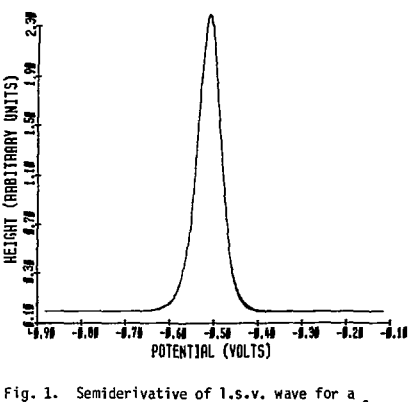

Fig. 1. Semiderivative of l.s.v. wave for a quasi-reversible charge transfer and the $sech^2$ fit to the semiderivative. (XBL 8112-13073)

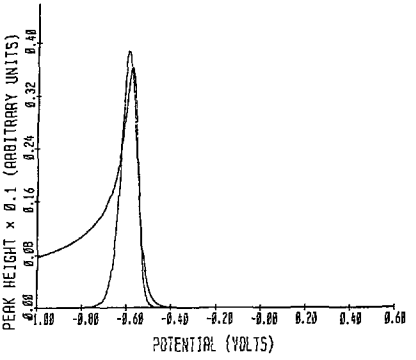

Fig. 2. Semiderivative of l.s.v. wave for a system with homogeneous kinetics not in the limiting case of diffusion controlled behavior and the $sech^2$ fit to the semiderivative.
(XBL 8112-13074)

For the limiting case of pure kinetic behavior (i.e., for a case of balancing diffusion and kinetic effects such that a constant flow of depolarizer is maintained to the electrode) curve fitting of a $sech^2$ function to the function

$$f(E) = \frac{m^2(E)(i_L - i(E))^2}{[m^2(E)+(i_L - i(E))^2]^2}$$

where m(E) is the semiintegral, i(E) is the current, and i_L is the limiting current at large negative potentials, works well, as shown by coefficients of determination near 1 for fits and by close agreement between returned fit parameters and parameters derived from theory.

* * *

†Brief version of LBL-13711, paper submitted to Anal. Chem.
‡Department of Chemistry, Washington State University, Pullman, WA 99164.

1. J. J. Toman and S. D. Brown, Anal. Chem. 53, 1497 (1981).
2. R. S. Nicholson and I. Shain, Anal. Chem. 36, 706 (1964).
3. J. M. Saveant and E. Vianello, Electrochim. Acta 8, 905 (1963).

1981 PUBLICATIONS AND REPORTS

Refereed Journals

1. J. J. Toman, R. M. Corn, and S. D. Brown, "Convolution Voltammetry of Metal Complexes," Anal. Chim. Acta 123, 187 (1981); LBL-10820.
2. J. J. Toman and S. D. Brown, "Peak Resolution by Semiderivative Voltammetry," Anal. Chem. 53, 1497 (1981); LBL-11738.

LBL Report

1. J. J. Toman and S. D. Brown, "Application of Convolutive Voltammetric Curve Fitting Techniques to Non-Reversible Electrochemical System," submitted to Anal. Chem., LBL-13711.

IX Work for Others

Work for Others

a. Phase Equilibria for Fixed Bed Gasification Products, Byproducts, and Water*

John M. Prausnitz, Investigator

Introduction. Many modern coal-gasification processes include a quench step where the hot effluent gases from the gasifier are cooled quickly by water. This quench step is necessary to strip heavy tar components and entrained ash from the gases prior to further processing. Current designs for quench steps operate at temperatures near or below 250°C. Either three or four phases may be present in the quench vessel; these include a vapor phase, a light hydrocarbon or oil phase, an aqueous liquid phase, and a heavy hydrocarbon or tar phase. The oil and tar phases may combine under some conditions. To design the quench operation and subsequent coal tar-water separation, phase equilibria must be available. These equilibria must be presented in a correlated form; they must also be integrated into a computer model so that limited mutual solubility data may be extrapolated to other pressures and temperatures.

The contents of the quench vessel are a complicated mixture of both light and heavy components. Light components include hydrogen, methane, carbon monoxide, carbon dioxide, hydrogen sulfide, and ammonia. Heavy components include a wide variety of aromatic hydrocarbons, phenolics, furans, pyridines, thiophenes, and other organic heteroatomic compounds. These components are present in coal tar in a diverse molecular-weight range. The presence of entrained ash complicates mixture properties through inorganic salts that can affect phase equilibria.

At equilibrium, the fugacity of each component is the same in all phases. Given a suitable molecular-thermodynamic model, we can calculate the fugacity of each component in each phase as a function of temperature, pressure, and composition.

Molecular-thermodynamic models, capable of representing complex phase equilibria, must contain parameters that are related to the potential energies of interaction and to the sizes of the various molecular species present in the mixture. These parameters must be obtained by fitting the model to vapor-liquid-liquid or mutual solubility data. A literature search for such data has been completed; we have found that very few essential data have been published. For this reason, we have initiated an experimental program to obtain such data. Due to the complexity of coal tar, we are forced to simplify our experimental program; we measure phase equilibria for several well chosen model compounds with water.

*This work was supported by the Electric Power Research Institute (EPRI) under Contract No. RP 1901-1 through an agreement with the Director, Office of Energy Research, U. S. Department of Energy under Contract No. DE-AC03-76SF00098.

1. MEASUREMENT OF PHASE EQUILIBRIA†

Frank E. Anderson and John M. Prausnitz

To measure vapor-liquid-liquid equilibria for binary, three-phase, model compound water systems, we have constructed an equilibrium cell. We withdraw a sample of each phase in the cell and determine its composition.

The equilibrium cell is in a constant-temperature air bath. Since it is advantageous to see the contents of the cell at any time during a run, the walls of the equilibrium cell are of optical-quality quartz glass. A window in the air bath allows viewing the cell contents. Each end of this quartz tube is clamped to a Monel flange. Equilibration of the contents of the cell is facilitated by a mechanical agitator. The temperature and pressure of the cell are measured respectively with resistance temperature detectors and a pressure transducer.

The sampling portion of the apparatus permits withdrawal of samples of each liquid phase and then flashing to form a vapor phase. A sample of the vapor phase from the cell is also expanded to produce a vapor phase of about the same pressure. The vaporized samples are then analyzed with a gas chromatograph.

* * *

†Brief version of "Phase Equilibria for Coal Tar-Water Systems," presented at the First Annual EPRI Contractors' Conference on Coal Gasification, Palo Alto, CA, October 27-29, 1981.

2. THEORETICAL METHODS FOR CORRELATION OF PHASE EQUILIBRIA†

Frank E. Anderson and John M. Prausnitz

There are two thermodynamic procedures for the correlation of phase equilibrium data. The first uses liquid-phase activity coefficients. In this procedure, we calculate vapor and liquid phase fugacities by two different models. For the vapor phase, we calculate the fugacity coefficient using a modified version of the Redlich-Kwong equation of state suitable for the vapor phase alone. For the liquid phases, we can calculate activity coefficients by some liquid-mixture model such as UNIFAC.

In the UNIFAC method, we divide the molecules in the liquid phase into functional groups and relate the activity coefficient to the sum of the functional-group interactions. We account for the

size of the functional groups through group-volume parameters. The activity coefficient calculated by the UNIFAC method depends on composition and temperature. UNIFAC surface-area and volume parameters are available from crystallographic measurements. These properties have been tabulated for essentially all groups of interest here. The UNIFAC interaction-energy parameters, however, must be obtained by fitting the UNIFAC model to experimental data. We have found that if we fit UNIFAC to liquid-liquid equilibria, we can do a reasonable job of correlation, provided that we are well removed from the critical-solution temperature, and provided that the temperature range is relatively narrow, on the order of 30°C. For a general correlation of coal tar-water phase equilibria, we would like to correlate our data with a model that is applicable to a wide range of temperature.

The second procedure calculates fugacity coefficients for each of the three (or four) phases present in the mixture. These fugacity coefficients can be calculated by a modified version of the Redlich-Kwong equation of state suitable for vapor and liquid phases. To calculate mixture properties from the pure-component Redlich-Kwong constants a(T) and b, we must have a set of mixing rules that relate pure-component parameters to parameters for the mixture. These mixing rules should reflect the nonrandom, partially-ordered structure of the liquid phases. Here, we have combined the local-composition theory (used to derive the UNIFAC model) with the equation of state.

* * *

†Brief version of LBL-12329.

3. CHARACTERIZATION†

Michael M. Gibson and John M. Prausnitz

To calculate phase equilibria for mixtures of coal tar and water, we must relate the properties of the coal tar to constants in our molecular-thermodynamic models. For the UNIFAC method, this extension is straightforward. Group interaction parameters are fit from our model-compound-water binary data; these parameters are then used to calculate coal-tar-water phase equilibria. We must, however, know the relative amounts of the groups in the tar. We obtain this information from our tar-characterization procedure. Similarly, to obtain Redlich-Kwong constants, we relate equation-of-state constants a(T) and b to our four characterization variables for each tar fraction: number average molecular weight, fraction aromaticity (or hydrogen-to-carbon ratio), heteroatomicity (or functional-group analysis), and one vapor-pressure datum for each tar fraction.

We obtain the vapor-pressure data for the tar by distilling the entire tar into narrow-boiling fractions in a spinning-band column at high reflux. For each fraction, we measure the boiling-point range. We then measure the number-average molecular weight of each tar fraction by freezing-point depression. An elemental analysis is performed on each tar fraction. This gives us the percentage of carbon, hydrogen, oxygen, nitrogen, and sulfur in the tar fraction. The elemental analysis is used in combination with Nuclear Magnetic Resonance Spectroscopy (NMR) and Infrared Spectroscopy (IR) to arrive at values for the aromaticity and heteroatomicity, respectively, for each tar fraction. The IR data also help us to distinguish between ether and alcohol oxygen atoms and between nitrogen atoms in a ring and nitrogen atoms in an amine.

* * *

†Brief version of "Phase Equilibria for Coal Tar-Water Systems", presented at the First Annual EPRI Contractors' Conference on Coal Gasification, Palo Alto, CA, October 27-29, 1981.

1981 PUBLICATIONS AND REPORTS

Refereed Journals

†1. B. E. Poling, E. A. Grens, II, and J. M. Prausnitz, "Thermodynamic Properties from a Cubic Equation of State: Avoiding Trivial Roots and Spurious Derivatives," Ind. Eng. Chem. Proc. Des. Develop. 20, 127 (1981).

‡2. D. Edwards, C. G. Van de Rostyne, J. Winnick, and J. M. Prausnitz, "Estimation of Vapor Pressures of High-Boiling Fractions in Liquefied Fossils Fuels Containing Heteroatoms Nitrogen or Sulfur," Ind. Eng. Chem. Proc. Des. Develop. 20, 138 (1981).

§3. P. J. Hicks, Jr., and J. M. Prausnitz, "Solubility of Acetone and Isopropyl Ether in Compressed Nitrogen, Methane, and Carbon Dioxide," J. Chem. Eng. Data 26, 74 (1981).

†4. A. I. El-Twaty and J. M. Prausnitz, "Generalized Van der Waals Partition Function for Fluids. Modification to Yield Better Second Virial Coefficients." Fluid Phase Equil. 5, 191 (1981).

†5. J. M. Prausnitz, "Calculation of Phase Equilibria for Separation Operations," Trans. Inst. Chem. Eng. 59, 3 (1981).

‡6. D. R. Edwards and J. M. Prausnitz, "Vapor Pressures of Some Sulfur-Containing, Coal-Related Compounds," J. Chem. Eng. Data 26, 121 (1981).

†7. G. Schulze and J. M. Prausnitz, "Solubilities of Gases in Water at High Temperatures," Ind. Eng. Chem. Fundam. 20, 175 (1981), LBL-12483.

‡8. D. R. Edwards and J. M. Prausnitz, "Estimation of Vapor Pressures of Heavy Liquid Hydrocarbons Containing Nitrogen or Sulfur by a Group-Contribution Method," Ind. Eng. Chem. Fundam. 20, 280 (1981).

†9. S. D. Schaffer and J. M. Prausnitz, "Correlation of Hydrogen Solubilities in Nonpolar Solvents Based on Scaled-Particle Theory," AIChE J. 27, 844 (1981).

Other Publications

†1. E. M. Pawlikowski, J. Newman, and J. M. Prausnitz, "Vapor-Liquid Equilibrium Calculations for Aqueous Mixtures of Volatile, Weak Electrolytes and Other Gases for Coal-Gasification Processes," Proceedings of the 2nd World Congress of Chemical Engineering, Montreal, October 4-9, 1981.

2. E. M. Pawlikowski, "Vapor-Liquid Equilibria for Volatile, Weak Electrolytes in Aqueous Solutions," Ph.D. dissertation, Department of Chemical Engineering, University of California, Berkeley, December 1981.

LBL Reports

1. V. Brandani and J. M. Prausnitz, "Empirical Corrections to the van der Waals Partition Function for Dense Fluids," LBL-12482.

Invited Talks

1. W. B. Whiting and J. M. Prausnitz, "Equations of State for Strongly Nonideal Fluid Mixtures. Application of the Local-Composition Concept." Spring National Meeting of the American Institute of Chemical Engineers, Houston, April 5-9, 1981; LBL-12239.

†2. E. M. Pawlikowski, J. Newman, and J. M. Prausnitz, "Phase Equilibria for Aqueous Solutions of Ammonia and Carbon Dioxide. Effects of Salts in the Region 100-150°C." 80. Hauptversammlung der Deutschen Bunsen-Gesellschaft fuer Physikalische Chemie, Marburg, West Germany, May 28-30, 1981.

3. F. E. Anderson, and J. M. Prausnitz, "Phase Equilibria for Inhibition of Hydrate Formation in Natural Gases. Effect of Water-soluble Fluids Like Methanol." 80. Hauptversammlung der Deutschen Bunsen-Gesellschaft fuer Physikalische Chemie, Marburg, West Germany, May 28-30, 1981.

4. E. R. Larsen, "High-Pressure Vapor-Liquid Equilibria for Water/Methane," Department of Chemical Engineering, Arizonia State University, Tempe, February 1981.

5. W. B. Whiting, "Calculation of High-Pressure Vapor-Liquid Equilibria for Asymmetric Mixtures," Departments of Chemical Engineering; Illinois Institute of Technology, January 1981; Worcester Polytechnic Institute, January 1981; Polytechnic Institute of New York, Brooklyn, January 1981; West Virginia University, December 1981.

6. J. M. Prausnitz, "Molecular Thermodynamics for Chemical Process Design," Institute for Applied Chemistry, University of L'Aquila, Italy, April 1981; Department of Chemistry, Technische Hochschule, Darmstadt, West Germany, July 1981; Department of Chemical Engineering, Universitaet Kaiserslautern, West Germany, July 1981; Department of Chemical Engineering, Technical University of Berlin, West Germany, May 1981; Department of Applied Chemistry, University of Lund, Sweden, June 1981.

‡7. G. L. Alexander and J. M. Prausnitz, "Phase-Equilibrium Calculations for Mixtures Containing Characterized Heavy-Fossil-Fuel Fractions," Annual Meeting of the American Institute of Chemical Engineers, New Orleans, November 8-12, 1981.

‡8. A. Monge, Jr., and J. M. Prausnitz, "An Experimental Method for Measuring Solubilities of Heavy Fossil-Fuel Mixtures in Compressed Gases to 100 Bar and 300°C," Annual Meeting of the American Institute of Chemical Engineers, New Orleans, November 8-12, 1981; LBL-13617.

9. W. B. Whiting and J. M. Prausnitz, "A Local-Composition Model for Equations of State for Mixtures," Annual Meeting of the American Institute of Chemical Engineers, New Orleans, November 8-12, 1981; LBL-13568.

‖10. F. E. Anderson and J. M. Prausnitz, "Phase Equilibria for Coal Tar-Water Systems," First Annual EPRI Contractors' Conference on Coal Gasification, Palo Alto, California, October 27-29, 1981.

* * *

†Work supported by the National Science Foundation.
‡Work supported by the Office of Energy Technology, Fossil Energy Program, U. S. Department of Energy.
§Work supported by the Petroleum Research Fund, administered by the American Chemical Society.
‖Work supported by the Electric Power Research Institute under Contract No. RP1901-1.

b. Improved Beta-Alumina Electrolytes for Advanced Storage Batteries*

Lutgard C. De Jonghe, Investigator

Introduction. Beta batteries using a sodium-beta alumina solid electrolyte membrane to separate molten sodium and sodium polysulfide electrodes are an attractive method for load leveling or electric vehicle propulsion. While the technical feasibility of the battery has been proven, a key factor impeding immediate large scale adoption of this high energy-density battery has remained in question. This factor is the ultimate lifetime of the solid electrolyte in the aggressive battery environment. Although the required operating lifetime of five years appears to be almost within reach, it has not yet been achieved. It is, therefore, important to find if any electrolyte degradation mechanisms exist that cannot possibly be suppressed for a long time.

We find that a number of interrelated phenomena must cooperate to bring about electrolyte failure. The alteration of electronic properties of the electrolyte as a consequence of contact with molten sodium appears to play a central role in all forms of degradation. Our considerations lead us to conclude that the electrolyte degradation can be suppressed if limits on a number of cell operating parameters are observed. These include controlling the charging over-voltages and operating the cell to avoid the development of polarization layers on the electrolyte/sulfur electrode interface.

1. CHEMICAL COLORATION†

L. C. De Jonghe and A. Buechele

When sodium-beta alumina electrolytes are in prolonged contact with molten sodium, a grey-brown discoloration develops from the contact interface, even without ionic charge transfer. Our experiments on single- and polycrystals have indicated that this coloration is due to reduction of the electrolyte by the metallic sodium. The oxygen removal from the electrolyte was found to occur mainly through the spinel blocks,[1] leading to isotropic coloration of single crystals. Bleaching in air was found to be highly anisotropic, indicating that the reoxidation involved mainly oxygen transport through the conduction planes. Heating single crystals chemically colored by prolonged immersion in molten sodium in a very low oxygen partial pressure did not result in bleaching. These three observations demonstrate that the chemical coloration involves reduction of the solid electrolyte, leading to oxygen vacancy formation. The oxygen vacancies would be charge compensated by electrons. This conclusion can be deduced from the appearance of the broad optical absorption band, and the observation of some electronic conductivity at high temperatures.[2] The absence of a narrow optical absorption band indicates that the electron-oxygen vacancy binding is weak, possibly on the order of 0.1 eV. Introduction of oxygen vacancies, which appear to behave as shallow donors, would tend to raise the Fermi level to close to the conduction band edge of the solid electrolyte. It may thus be expected that electron injection from the sodium/electrolyte interface would not be rate limiting for electron conduction through the electrolyte. The gradient in electronic conductivity that is produced for the electrolyte thus causes a gradient in the electronic/ionic transport number ratio. Charge transfer through such a transport number inhomogeneity could lead to internal formation of Na metal, as discussed below.

* * *

†Short version of Ref. 1.

1. L. C. De Jonghe and A. Buechele, LBL-12440, April 1980.
2. N. Weber, Energy Conversion, 14, 1 (1974).

2. TRANSPORT IN AN INHOMOGENEOUS ELECTROLYTE†

Lutgard C. De Jonghe

Charge transfer through an electrolyte containing a gradient in electronic/ionic transport number ratio was recently considered by De Jonghe.[1] The chemical action of the sodium metal on the negative electrode/electrolyte interface produces a slowly evolving gradient in the transport number ratio. If this gradient is in a first approximation considered immobile during charge transfer then it can be shown that the chemical potential of the sodium in an electrolyte containing a linear gradient of the transport number ratio, can be approximated as

$$\eta_{Na} \simeq \frac{x}{l}\,(\Delta\eta^{\circ}/FV_T) + FV_T\, f(p^x)$$

l = electrolyte thickness
x = distance from the negative interface
F = Faraday's constant
V_T = Applied voltage over the electrolyte
$\Delta\eta^{\circ}/F$ = cell counter-EMF over the electrolyte
$f(p^x)$ = function describing the spatial dependence of the transport number ratio p^x.

Thus, it may be considered possible that internal electrolysis could take place, causing the electrolyte to behave similarly to a distributed electrode.[2] At sufficiently high V_T and with a negative electrode consisting of sodium metal, internal formation of sodium under pressure might result in electrolyte fracture.

This response of an inhomogeneous electrolyte

*This work was supported by the Electric Power Research Institute (EPRI) under Contract No. RP 252-3 through an agreement with the Assistant Secretary for Conservation and Renewable Energy, U. S. Department of Energy under Contract No. DE-AC03-76SF0009B.

subjected to charge transfer permits the interpretation of a variety of degradation phenomena that have been observed so far. The phenomena that it can explain include the low current density at which the Mode I degradation is initiated, and the observation of a Mode II degradation in beta battery electrolytes that had been subjected to charging voltages above 5 volts.

* * *

†Short version of Ref. 1.

1. L. C. De Jonghe, LBL-12070, February, 1981.
2. P. Fabry and M. Kleitz, in "Electrode Processes in Solid State Ionics," M. Kleitz and J. Dupuy, Eds., D. Reidel Publ. Co., Dordrecht, Holland, 1976, pg. 331.

3. MODE I FAILURE: ELECTRO-MECHANICAL FRACTURE†

Les Feldman and Lutgard C. De Jonghe

Electromechanical failure of solid electrolytes was first treated by Armstrong et al.[1] They described the main features of metal dendrite and associated crack propagation from the metal electrode/electrolyte interface during electrolysis. Cathodic plating of Na in a small crack and the associated current focusing on it causes crack extension by the generated Poiseuille pressure. The electrolyte then fails by propagation of such a surface crack. A number of observations have well documented this type of fracture,[2-4] and a variety of treatments have refined the original argument. Disturbing in these treatments, however, is that further refinements lead to calculated microscopic current densities necessary to initiate the Mode I failure that are a factor of 10^5 too high, compared with the actual observations. In our treatment,[5] the critical current density is found to be:

$$j_{crit} = K_{IC}^4 \, E'^{-3} \, ne/(3.32\tau l),$$

where

j_{crit} = the critical macroscopic current density to initiate Mode I
K_{IC} = mechanical stress intensity factor
E' = Young's modulus
n = the atomic number density of sodium
e = charge of sodium ion
l = the crack length
τ = the viscosity of sodium.

We believe that the discrepancy lies in the assumption of the models that the mechanical stress intensity factor is identical to the electromechanical one during cell charging. The effects described in the previous section should bring into play a voltage as well as a current effect. From the sharp crack tips, involved in Mode I initiation, local electron injection should be possible. The injection of electrons should be facilitated by the raising of the Fermi level close to the conduction band edge as a consequence of electrolyte reduction. This would cause internal sodium metal deposition just ahead of the crack tip, leading to an actual stress intensity factor at the flaw tip that is significantly higher than the mechanical one. Qualitatively, these considerations are in agreement with the observation of critical current density thresholds of at most a few amperes/cm^2 on fresh electrolytes, and the rapid decrease of j_{crit} as the temperature is lowered (applied voltage must increase to maintain the same current density). Qualitatively, it could also be predicted that if the electrolyte ionic resistance went up, e.g., as a result of contamination by impurities, the actual stress intensity factor would be unfavorably affected since the local electric field gradient would increase.

* * *

†Short version of Ref. 5.

1. R. D. Armstrong, T. Dickinson, and J. Turner, Electrochim. Acta., 19, 187 (1974).
2. R. N. Richman, and G. J. Tennenhouse, J. Amer. Ceram. Soc., 58, 63 (1975).
3. D. K. Shetty, A. V. Virkar, and R. S. Gordon in "Fracture Mechanics of Ceramics," Vol. 4, R. L. Bradt and D. P. H. Hasselman, Eds., Plenum Press, New York, 1978, pg. 651.
4. M. P. J. Brennan, Electrochim Acta., 25, 621 (1980).
5. L. Feldman and L. C. De Jonghe, accepted J. Mat. Sci., LBL-12194 (1981).

4. MODE II DEGRADATION: INTERNAL SODIUM DEPOSITION†

Lutgard C. De Jonghe, Les Feldman, and Andrew Buechele

Our recent observations on electrolytes from beta batteries[1] indicated that internal sodium deposition with associated electrolyte microfracture could occur. It is quite possible that a Mode II degradation evolved into a Mode I fracture through microfracture growth, or coalescence. Mode I, however, can also be induced without any demonstrable Mode II degradation. The initiation of Mode II degradation is made possible by the gradient in electron-ion transport number ratio, $\nabla(p^x)$, caused by the chemical coloration. This gradient makes the electrolyte nonhomogeneous, permitting the effect discussed before to operate above a critical applied voltage. To find the critical applied voltage V_T at which this Mode II might occur requires knowledge of $\Delta\mu^\circ/F$ and of the electrolyte internal fracture strength. In general, if $\Delta\mu^\circ/F$ and the mechanical strength of the electrolytes are low, then V_T would be low. Under the reasonable assumption that $\Delta\mu^\circ F = 2$ V and that the electrolyte fracture strength would be about 400 MPa (60,000 psi), a charging voltage of about 3 V would have to be exceeded before the Mode II internal degradation would occur. Although this is not much above the charging voltages used for current Na/NaS_x cells, it still permits indefinite inhibition of this mechanism if the sulfur electrode polarization and contamination of the Na electrode can be kept low during cell operation.

The considerations concerning the Mode II degradation led to identifying the following factors as contributing adversely to the electrolyte performance when the cell is operated in a current controlled mode:

1. High charging current densities requiring a charging voltage, V_T, over 3 volts.
2. Increased electrolyte thickness (increased V_T)
3. Increased electrolyte resistance (increased V_T)
4. Polarization layers at the sulfur electrode/electrolyte interface (decreased $\Delta n^{\circ}/F$).

* * *

†Short version of Ref. 1.

1. L. C. De Jonghe, L. Feldman, and A. Buechele, J. Mat. Sci., in Press, March, 1981.

1981 PUBLICATIONS AND REPORTS

Refereed Journals

1. L. C. De Jonghe, L. Feldman, and A. Buechele, "Slow Degradation and Electron Conduction in Sodium-Beta Aluminas," J. Mat. Sci., 16, 780 (1981).

LBL Reports

1. L. C. De Jonghe, "Transport Number Gradients and Solid Electrolyte Degradation," LBL-12070R, accepted J. Electrochem. Soc.

2. L. C. De Jonghe, L. Feldman and A. Buechele, "Failure Modes of Na-Beta Alumina," LBL-12445.

3. L. C. De Jonghe, "Performance of Na-Beta Alumina in Na/S Cells," LBL-12617.

4. L. C. De Jonghe and A. Buechele, "Chemical Coloration in Sodium-beta Alumina Electrolytes," LBL-12194, accepted J. Mat. Sci.

5. L. Feldman and L. C. De Jonghe, "Initiation of Mode I Degradation in Sodium-Beta Alumina Electrolytes," LBL-12194, accepted J. Mat. Sci.

Invited Talks

1. L. C. De Jonghe, "Degradation in Solid Electrolytes," Internat. Workshop, Solid Electrolytes, Heidelberg, West Germany, October 9, 1980.

2. L. C. De Jonghe, "Properties of Electrolytes for Na/S Cells," Max-Planck Institut, Stuttgart, West Germany, October 15, 1980.

X Appendices

Appendix A

Materials and Molecular Research Division Personnel

Scientific Staff

Investigators	Postdoctoral and Other Scientists	Graduate Students
Neil Bartlett	B. Desbat F. Dove R. Hoppe C. Platte T. Richardson W. Totsch	T. Mallouk B. McQuillan F. Okino G. Rosenthal S. Yeh
Alexis Bell	W. Cant *A. Daneshrad	J. Baker W. Canella R. Dictor T. Frederick R. Hicks C. Kellner M. Reichmann J. Rieck D. Stern P. Winslow
Robert Bergman	W. Hersh M. Matturro E. Petersen	P. Becker J. Bonfiglio H. Bryndza C. Carriere P. Comita A. Janowicz M. Seidler P. Seidler K. Theopold R. Ugolick M. Wax S. Webb W. Weiner G. Yang
Robert Bragg	O. Adewoye	D. Baker L. Henry J. Hoyt J. Johnson B. Mehrotra A. Pearson
Leo Brewer	D. Davis K. Krushwitz C-B. Meyer G. Rosenblatt	D. Davis J. Gibson B. Lin
Steven Brown	T. Brown	D. Castor

Investigators	Postdoctoral and Other Scientists	Graduate Students
John Clark	P. Clark D. Guthals W. Hopewell T. Richardson H. Sokol	D. Anthon M. Chastain D. Le H. Nathel L. Phillips J. Stephens M. Tolbert S. Walsh
John Clarke	C. Adkins T. Lemberger D. Van Harlingen	C. Hilbert R. Koch R. Lee H. Mamin J. Martinis P. Maxton R. Miracky D. Seligson
Marvin Cohen	S. Froyen S. Louie D. Vanderbilt	C.T. Chan M-Y. Chou P. Lam Z. Levine J. Northrup M. Yin
Robert Connick	T. Braga K. Krushwitz M. Ospina A. Tini	D. Horner
Lutgard De Jonghe	H. Schmid K-H. Yoon	A. Buechele C. Cameron M. Chang J-C. Chen M. Herrara D. Hitchcock S-C. Hu R. McClelland G. Raj S. Wu
Didier de Fontaine	W. Teitler	H-M. Jang K. Krishnan H-C. Tsai
Norman Edelstein N. Bartlett S. Brown J. Conway K. Raymond G. Seaborg A. Streitwieser D. Templeton A. Zalkin	K. Abu-Dari R. Andersen J. Bucher S. Davis P. Edwards E. Gamp T. Hayhurst S. Hubert R. Klutz J.C. Krupa	J. Arenivar S. Barclay P. Becker J. Boncella J. Brennan C. Carriere D. Caster M. Derzon C. Eigenbrot G. Freeman

Investigators	Postdoctoral and Other Scientists	Graduate Students
Edelstein (cont'd)	H. Nische W. Muller C. Orvig H. Ruben G. Shalimoff L. Templeton H-K. Wang F. Weitl D. White G. Wong Y-T. Wu D. Zhu	B. Gilbert G. Girolami M. Halpern D. Kagan M. Kappel S. Kinsley M. Lyttle V. Mainz V. Pecoraro R. Planalp B. Raine S. Rutan R. Shinomoto K. Smith T. Tilley J. Toman S. Un
Anthony Evans	W. Kriven J. Lamon D. Marshall M. Nisenholz J. Porter H. Ruf T. Uchiyama	W. Blumenthal S. Chiang G. Crumley K. Faber Y. Fu C-H. Hsueh M. Huang S. Johnson J. Maasberg J. Marion C. Ostertag A. Rana C. Rossington M. Sakarcan M. Spears M. Thouless
James Evans	D. Coates S. Lympany Y. Nakano	M. Abbasi H-C. Lee C. Palmer M. Rau
Leo Falicov		R. Osario DeCerqueira J. Tersoff
Iain Finnie		S. Chavez
Andreas Glaeser		J-C. Chen
Ron Gronsky	J. Penisson P. Rez J. Steeds L. Tanner	L. Andersen P. DeRoo J. Briceno-Valero S. Cheruvu J. Howe E. Kamenetsky R. Kilaas J. Mazur J. Rose G. Tamayo E. Thomann

Investigators	Postdoctoral and Other Scientists	Graduate Students
Charles Harris	H. Robota	M. Berg C. Berman G. Erdheim S. George G. Goncher A. Harris S. Marks H. Robota P. Whitmore
Heinz Heinemann		
Dennis Hess		C. Blair A. Wakita L. Williams
Carson Jeffries	J. Furneaux	J. Culbertson B. Furman G. Held E. Pakulis J. Perez J. Testa
Harold Johnston	R. Carlson	M. Kowalczyk W. Marinelli J. Podolske S. Solomon D. Swanson
William Jolly	K. Bomben C. Eyermann A. Gin	M. Ajmani A. Bakke
Yuan Lee	J-P. Briad R. Buss O. Dutuit G. He J. Hepburn F. Houle J. Lisy J. O'Brien A. Tramer Z-J. Zhang	S. Anderson R. Baseman R. Brudzynski S. Bustamente C. Hayden S. Huang C. Kahler D. Krajnovich T. Minton D. Neumark M. Okumura R. Page J. Reutt P. Schulz M. Vernon P. Weiss A. Wodtke
William Lester	K. Jolls P. Reynolds	L. Johnson

Investigators	Postdoctoral and Other Scientists	Graduate Students
Alan Levy	D. Boone W. Coons I. Cornet I. Finnie J. Flores T. Foley R. Glardon M. Holt J. Humphrey A. Modavi H. Nguyen J. Sabnis R. Varma W. Worrell A. Yaniv	M. Arnal P-K. Chen T. Foley H. Frank M. Khatibloo I. Kliafas S. Li F. Pourahmadi M. Smith P. Turi K. Weddle M. West R-J. Yang W. Yeung
Steven Louie		
Bruce Mahan		A. O'Keefe T. Turner
Richard Marrus	J-P. Briad P. Bucksbaum A. Chetioui E. Commins H. Gould J. Leavitt M. Mittleman M. Prior H. Shugart	P. Drell L. Hunter C. Munger
William Miller	C. Cerjan G. Herling L. Hubbard S. Shi	D. Ali P. Dardi S. Gray S. Schwartz B. Waite
C. Bradley Moore	C. Chi-Ke M. Diegelmann J. Jasinski A. Kung	A. Abbate D. Bamford M. Berman H-L. Dai J. Frisoli P. Ho F. Hovis A. Langford W. Natzle H. Petek E. Specht J. Wong L. Young
John W. Morris, Jr.	M. Hong G-X. Hu J. Kim R. Ogawa	G-M. Chang D. Dietderich D. Fior-Zurlo B. Fultz

Investigators	Postdoctoral and Other Scientists	Graduate Students
Morris, Jr. (cont'd)	D. Powell J.M. Sanchez M-C. Shin C. Syn	M. Hong H. Kim H-J. Kim Y-H. Kim E. Kostlan H. Lee H-L. Lin T. Mohri K. Sakai J. Sanchez Y-C. Shih H-K. Shin M. Strum L. Summers D. Wedge I-W. Wu
Earl Muetterties	R. Feltham J. Kouba J. Stein M. Tachikawa	J. Bleeke R. Burch H. Choi W. Cwirla C. Friend T. Gentle G. Schmidt K. Shanahan S. Slater M. Tsai R. Wexler
Rolf Muller	W. Giba T. Hryniewicz W. Plieth D. Rajhenbah F. Schwager	C. Coughanowr J. Farmer R. Gyory J. Stoughton
John Newman	R. Pollard	D. Bernardi V. Edwards A. Hauser N. Matlosz M. Orazem P. Pierini T. Risch G. Trost
Donald Olander	M. Balooch T. Green R. Kohli A. Machiels S. Zhou	D. Dooley M. Farnaam K. Kim G. Mitchem S. Shann D. Sherman F. Tehranian C. Tsai S. Yagnik R. Yang
Joseph Pask	P. Spencer A. Tomsia F. Zhang	P. Flaitz S. Johnson K. Wada

Investigators	Postdoctoral and Other Scientists	Graduate Students
Norman Phillips	G. Brodale J. Lasjaunias K. Matho	J. Boyer W. Fogle M. Mayberry J. Van Buren
Alexander Pines	R. Goldberg U. Nitsan	J. Baum G. Drobny R. Eckman J. Garbow J. Millar J. Murdoch S. Sinton L. Sterna J. Tang R. Tycko D. Weitekamp Y-S. Yen G. Wolf D. Zax
Kenneth Pitzer	P. Christiansen K. Balasubramanian	J. Simonson
John Prausnitz		F. Anderson M. Gibson E. Larsen W. Whiting
Paul Richards	H. Levinson A. Smith H. Van Kempen	J. Bonomo W. Challener S. Chiang M. Hueschen S. McBride W. McGrath G. Tobin
Robert Ritchie	S. Suresh	J-L. Tzou
Philip Ross	P. Andricacos U. Bardi G. Derry F. Wagner	F. Wagner
H. Fritz Schaefer	J. Goddard R. Pitzer A. Schier M. Vincent Y. Yamaguchi Y. Yoshioka	D. Fox J. Gaw M. Hoffman K. Kim W. Laidig G. Pittman G. Raine P. Saxe

Investigators	Postdoctoral and Other Scientists	Graduate Students
Alan Searcy	D. Beruto A. Buchler D. Chung D. Meschi Z. Munir	T. Dai J. Farnsworth A. Hegedus N. Jacobson M.G. Kim T. Reis S. Roche
Y. Ron Shen	S. Arakeline C. Chen D. Ricard S. Shen H. Zhu	G. Boyd S. Durbin T. Heinz H. Hsiung J. Hunt R. Page R. Pecyner H. Tom
David Shirley	U. Becker P. Dabbousi W. Heppler Z. Hussain D. Trevor E. Umbach	A. Baca C. Bahr J. Barton R. Davis T. Ferrett L. Klebanoff P. Kobrin D. Lindle C. Parks J. Pollard S. Robey D. Rosenblatt S. Southworth J. Tobin C. Truesdale
Gabor Somorjai	M. Asscher A. Cabrera R. Casanova P. Davies G. Ertl S. Ferrer M. Langell C. Leygraf R-F. Lin J. Maj W. McLean C. Minot J. Sachtler M. Salmeron N. Spencer M. Van Hove P. Watson	A. Alivisatos E. Benjamin R. Carr J. Crowell S. Davis C. Galik E. Garfunkel W. Guthrie M. Karplus B. Koel R. Koestner T. Lin D. Ogletree M. Quinlan F. Zaera
Gareth Thomas	R. Hoel N. Kim J. Koo C. Kung R. Mishra J. Rayment J. Steeds M. von Heimendahl	C. Ahn J. Ahn R-S. Caron L. Chan T. Dinger J-S. Gau A. Jhingan N. Kim

Investigators	Postdoctoral and Other Scientists	Graduate Students
Thomas (cont'd)	A-J. Yang	K. Krishnan C. Kwok I-N. Lin A. Nakagawa S. Ong L. Rabenberg W. Salesky M. Sarikaya T. Shaw M. Sung H. Tokushige J. Wasynczuk X-F. Wu Y-S. Yoon
Charles Tobias	P. Cettou D. Doh T. Hryniewicz P. Sides	D. Dees J. Dukovic J. Faltemier D. Fischl K. Hanson W. Hui R. Hyman P. Johnson A. Kindler G. Prentice D. Roha P. Sides T. Tsuda G. Whitney
K. Peter Vollhardt	Y-H. Lai D. Van Horn	D. Clabo R. Colborn J. Drage J. King W. Tam J. Tane M. Tilset E. Walborsky T. Weidman
Jack Washburn	R. Hagstrom G. Hirsch C. Lampert D. Sadana	P. Ling W-L. Lo T. Mowles T. Sands D. Sipes T-H. Wei N-R. Wu T. Zee
Kenneth Westmacott	D. Banks R. Conlan U. Dahmen J. Davey M. Hall T. Harvey J. Leteurtre G. Monks R. Schonbucher G. Szaloky	R. Kilaas J-M. Lang A. Pelton S. Puranikmath L.K. Wu

Investigators	Postdoctoral and Other Scientists	Graduate Students
David Whittle	H. Hindam H. Schmid S. Smith M. Yee	H. Akuezue S. Berggren S-H. Choi P. Hou J-Y. Lee A. Misra R. Pendse P. Risse F. Yang
John Winn	M. Maier	J. Goble B. Hale W. Hollingsworth D. Horak H. Luftman S. Sherrow
Peter Yu	N. Caswell	C. Collins J. Weiner

Support Staff

Division Administrative Staff

C. Peterson - Assistant Head, Administration
K. McArthur - Assistant Division Administrator

Administration
M. Janzen
L. Irvin
M. Bowman
I. Rochell
S. Shirey

Personnel
S. Quarello
P. Paladini
I. Pelletreau

Purchasing
S. Stewart
C. Sterling

Technical Editing
J. Kright

Special Projects
E. Skrydlinski

Administrative/Secretarial Staff

L. Allen
M. Atkinson
K. Becky
M. Besser
K. Brusse
G. Brazil
B. Burt
B. Carter
J. Denney
S. Ewing
V. Farr
L. Franson
S. Ganwer
P. Gassler
C. Gliebe
C. Hacker
A. Harrington
S. Harris
H. Johnson
R. Jones
S. Macahilig
D. Merrill
M. Moore
B. Moriguchi
V. Narasimhan
M. Noyd
A. Ozturkmen
M. Rector
J. Shull
J. Smith
A. Weightman
C. Yoder
S. Young

Technical Staff

W. Toutolmin - Technical Coordinator

D. Ackland
G. Baum
T. Bakker
J. Barrett
D. Bazell
E. Benjamine
H. Bowman, Jr.
H. Brendel
M. Brown
R. Brusasco
E. Carter
S. Carter
C. Carvalho
B. Chandler
P. Chik
M. Cima
M. Clement
C. Coulman
J. Cox
D. Crane
M. Des Jardin
D. Dietderich
E. Fong
K. Frank
R. Friedman
L. Galovich
K. Gaugler
W. Giba
C. Gibson
J. Glanville
A. Gronsky
W. Goward
H. Harrell
C. Hickey
G. Hirsch
J. Holthuis
H-Y. Hu
R. Indig
J. Jacobsen
M. Jayko
L. Johnson
M. Johnson
D. Jurica
K. Koshlap
E. Kostlan
D. Krieger
M. Kujala
C. Lam
W. Lau
M. Lutz
J. Lince
D. MacDonald
R. Mackey
V. Manty
C. Markley
J. Martinis
L. McCullough
C. Morley
M. Mulvehill
W. Murrell
B. Neilson
Q. Nguyen
A. Pentecost
M. Perez
J. Peterson
H. Riebe
M. Rigdon
D. Rosenberg
P. Ruegg
K. Sakai
E. Scherr
C. Scolari
S. Shaffer
J. Severns
L. Sindelar
M. Snow
H. Sokol
B. Steakley
V. Stumpf
C. Thom
P. Tom
M. Trask
P. Trevor
P. Turi
K. Wada
J. Wafer
R. Wagner
J. Wallace
H. Weeks
W. Wong
N. Yates
M. Yee
C. Yu

Appendix B

MMRD Committees

DIVISIONAL COUNCIL

M. Cohen
N. Edelstein
H. Heinemann
H. Johnston*
J. Morris, Jr.

BUILDING AND SPACE COMMITTEE
(Includes Buildings 62, 70A, 72 and the Chemical and Materials Sciences Laboratory)

R. Gronsky
D. Meschi
R. Muller*
A. Zalkin

DIVISIONAL RESEARCH STAFF COMMITTEE

N. Edelstein
L. Falicov
R. Muller*
K. Westmacott

ELECTRON MICROSCOPE USERS COMMITTEE

R. Gronsky
J. Morris, Jr.
P. Ross*
K. Westmacott

EQUIPMENT REVIEW COMMITTEE

J. Clarke
A. Evans
C. B. Moore
R. Muller*

SAFETY AND LABORATORY STANDARDS COMMITTEE

D. Ackland
G. Baum
T. Britt
D. Davis
B. Fultz
T. Gentle
W. Giba
W. Hemphill
H. Hindam
J. Holthuis
L. Irvin
L. Johnston
D. Krieger
K. McArthur
D. Meschi*
R. Muller
C. Peterson
J. Severns
W. Toutolmin
W. Wong

TECHNICAL STAFF AND SHARED FACILITIES COMMITTEE

L. De Jonghe*
R. Gronsky
J. Morris, Jr.
P. Ross
G. Somorjai
D. Whittle

MMRD Building 62 Building Manager: D. Meschi
(Alternate: C. Peterson)

MMRD Building 72 Building Manager: K. Westmacott
(Alternate: D. Ackland)

---

*Chairman

Appendix C

List of Seminars

Surface Science and Catalysis Science

Date	Speaker and Affiliation	Seminar Title
1-7-81	Prof. B. J. Anderson Oklahoma State University	Structure of Sheared Colloidal Suspensions
1-21-81	Prof. M. Prutton University of York York, England	Electron Scattering Studies of the Cubic Faces of Divalent Metal Oxides
1-28-81	Prof. K. A. R. Mitchell University of British Columbia	Surface Structures and Bond Lengths from LEED Crystallography
2-4-81	Dr. H. D. Shih Stanford/NASA Joint Institute	Adsorbate Induced Surface Reconstruction: $Fe(110)_p$ (2 x 2)-S
2-11-81	Prof. H. H. Kung Northwestern University	Towards Fundamental Understanding in Catalysis by Transient Metal Oxides
*2-13-81	Prof. J. Oudar University of Paris	Adsorption of Sulfur on Metal Surfaces
2-17-81	Dr. F. Netzer National Bureau of Standards	Interaction of Oxygen, Water and Hydrogen with Rare Earth Metal Surfaces: Er - UPS, XPS, ELS, AES, $\nabla\phi$
2-18-81	Dr. D. G. Levine Exxon Research and Engineering Company, Linden, NJ	Physics and Chemistry of Coal
2-19-82	Dr. P. H. Citrin Bell Laboratories	Recent Progress in Surface EXAFS
2-25-82	Dr. D. J. Swyer Exxon Research and Engineering Company	Inorganic Chemistry of Fischer-Tropsch Catalysts
3-4-81	Dr. D. D. Whitehurst Mobil Research and Development Corporation, Princeton, NJ	Criticalities of Solvent Composition in Coal Liquefaction
3-11-81	Prof. G. Haller Yale University	Hydrogenation-Hydrogenolysis Selectivity and Support Effects on Rhodium Bimetallic Catalysts
3-17-81	Prof. M. Simonetta University of Milan	Force Field Calculations for Organic Molecules and Crystals
*4-2-81	Prof. J. M. Blakely Cornell University	Morphology and Phase Transitions on Nickel Surfaces
4-8-81	Dr. L. E. Firment Du Pont Company	Reactivity of Rutile TiO_2 Surfaces
4-15-81	Dr. R. Sullivan Chevron Research Company	Catalytic Upgrading of Coal Liquids
*4-21-81	Prof. J. M. White University of Texas	Coadsorption of CO/H_2 and CO/H_2O on Group VIII Metals

Surface Science and Catalysis Science (continued)

Date	Speaker and Affiliation	Seminar Title
4-22-81	Prof. F. Hanson University of Utah	The Production and Characterization of the Hydrocarbon Liquid Obtained from a Bitumen Impregnated Sandstone by a Fluidized Bed Pyrolysis Technique
4-29-81	Mr. C. D. Chang Mobil Research and Development	Shape Selective Reactions of Some Simple Oxygen Compounds over Zeolites
*4-30-81	Dr. J. R. Anderson CSIRD/University of Melbourne	Nature of Metallic Catalysts and Skeletal Reactions of Hydrocarbons.
5-8-81	Dr. M. L. Poutsma Oak Ridge National Laboratory	Thermolysis of Model Structures for Coal
5-13-81	Dr. D. R. Voorhoeve Celanese Research Corporation	Defect Oxides in Catalytic Reactions
5-20-81	Dr. B. Granoff Sandia National Laboratory	The Role of Catalysts in Direct Coal Liquefaction
5-27-81	Prof. M. B. Webb University of Wisconsin	Noble Gas Adsorption on Metals
*5-29-81	Prof. Thor Rhodin Cornell University	Recent Photoelectron Diffraction Structure and Reactivity Studies of Molecular Adsorbates on Nickel and Iron
6-3-81	Dr. L. L. Kesmodel University of Indiana	Chemisorption Studies with High Resolution Electron Energy Loss Spectroscopy
*6-30-81	Prof. V. Ponec University of Leiden, Netherlands	Carbon Monoxide Adsorption and Reactions: A Comparison of Metals
*7-23-81	Dr. M. Drechsler CNRS - France	The Study of Surface Self-diffusion by Mass Transfer on Field Emitters
*7-24-81	Dr. J. Suzanne University of Marseille, France	Orientational Epitaxy of an Incommensurate Neon Monolayer Adsorbed on Graphite: Another Verification of Novaco-McTague's Theory
*8-6-81	Dr. J. H. Block Max Planck Gesellschaft Berlin-Dahlen (Germany)	Surface Reactions Studied by Field Desorption and Photon-induced Field Desorption
*8-28-81	Dr. W. Mönch Walter Schottky Visiting Professor of Materials Science	Chemisorption and Defects at III-V Semiconductor Surfaces
*9-1-81	Prof. L. Kihlborg University of Stockholm	Recent Electron Microscopy Studies of Binary and Ternary Tungsten Oxides
10-1-81	Prof. G. Ertl University of Munich	Reactive Scattering at Surfaces
*10-7-81	Dr. A. W. Klein IBM, San Jose	Rotational Energy Transfer in Direct Inelastic Surfaces Scattering of NO from the Ag(111) Surface
10-8-81	Dr. A. J. Jacobson Exxon Research, Linden, NJ	Intercalation Chemistry and Reactions in Layered Compounds
10-15-81	Prof. T. F. Yen University of Southern California	Applications of Asphaltene Chemistry: Surface and Catalytic Effects

Surface Science and Catalysis Science (continued)

Date	Speaker and Affiliation	Seminar Title
*10-16-81	Prof. D. L. Mills UC Irvine	Electron Loss Spectroscopy of Adsorbed Atoms
10-22-81	Dr. S. W. Polichnowski Tennessee Eastman Company	Industrial Chemicals from Coal via Coal Gasification
10-29-81	Dr. C. D. Prater Mobil Research	Disguised Kinetics in Catalysis and Reaction Engineering
*11-3-81	Dr. W. C. Baird Exxon Research	Paraffin Aromatization with New Polymetallic Catalysts
*11-4-81	Dr. T. P. Wilson Union Carbide	Effects of Additives and Supports on Rhodium-based Catalysts for the Conversion of Synthesis Gas
11-5-81	Dr. R. Van Nordstrand Chevron Research	Zeolite Modifications
11-12-18	Dr. M. Cardillo Bell Laboratories	He Diffraction from Semiconductor Surfaces: A Quantitative Structural Probe
11-19-81	Prof. G. S. Louie UC Berkeley, Dept. of Physics	Electronic Structure of Clean and Adsorbate Covered Transition Metal Surfaces
12-3-81	Dr. H. Poppa NASA/Ames Research Center	Catalytic Model Experiment with UHV-Deposited Metal Particles
*12-4-81	Prof. T. Engel University of Washington	Surface Structural Determination Using Helium Diffraction
Reaction Dynamics		
2-11-81	Dr. W. Jackson Howard University Department of Chemistry Washington, DC	Laser Investigations of Photodissociation Dynamics
2-23-81	Prof. J. O. Hirschfelder University of Wisconsin Department of Chemistry Madison, WI	Multiple Moments and Long Range Intermolecular Forces of Rotating, Vibrating Molecules
3-25-81	Prof. W. Hase Wayne State University Department of Chemistry Detroit, MI	Classical Trajectory Studies of Molecular Beam Reactions Which Proceed Through Reaction Complexes
4-29-81	Dr. P. L. Jones FB Physik der Univ.-KL 0750 Kaiserslautern West Germany	Scattering of Rate Gas Atoms with Na_2
6-3-81	Prof. R. Gilbert University of Sydney Department of Theoretical Chemistry, Australia	Dynamics of Unimolecular Decomposition
*6-23-81	Prof. Z. Y. Hua Fudan University Shanghai, China	The Resonant Photoelectron Appearance Potential Spectroscopy and Its Applications
7-8-81	Prof. Dr. I. Hertel Freie Universität Berlin Berlin, West Germany	Recent Studies of Electronic To Vibrational, Rotational and Translational Energy Transfer

Reaction Dynamics (continued)

Date	Speaker and Affiliation	Seminar Title
7-10-81	Dr. H. Schmidt Institute of Molecular Physics, University of Berlin Berlin, West Germany	Ion-Atom Scattering on Laser State Prepared Sodium
7-13-81	Dr. H. C. W. Beijerinck Eindhoven University of Technology Department of Physics; Eindhoven, The Netherlands	Accurate Measurements of Total Scattering Cross Sections for Rare Gas Systems
9-21-81	Dr. D. Auerbach IBM Research Laboratory San Jose, CA	Molecular Beam Scattering From Surfaces
10-5-81	Dr. A. Kline IBM Research Laboratory San Jose, CA	Sub-picosecond Experiments on Molecular Vibration
10-26-81	Mr. S. L. Anderson Lawrence Berkeley Laboratory Materials and Molecular Research Division	Vibrationally State Selected Ion-Molecule Reactions

Electron Microscopy of Materials

1-22-81	Dr. S. Roberts University of Bristol, England	Design and Construction of a Cathodoluminescence System for a Philips Electron Microscope 400 With Some Preliminary Results on II-VI Compounds
1-23-81	Dr. B. Jouffrey Laboratoire d'Optique Electonique Centre National de la Recherche Scientifique	On Some Aspects of High Resolution Studies In Electron Microscopy and Some Recent Results in Energy Loss Studies As A Function of Accelerating Voltage
2-13-81	Prof. P. R. Howell University of Cambridge Department of Metallurgy and Materials Sciences, England	The Isothermal Decomposition of Austenite In Steels and Iron-Base Alloys
4-10-81	Dr. A. S. Rao Argonne National Laboratory SAREF Project, Argonne, IL	The Structure of Graphite Resulting From Light Ion Injection
5-26-81	Dr. T. Malis Research and Development Center Aluminum Company of Canada Kingston, Ontario	Grain Boundary Segregation in Aluminum-Magnesium Alloys
7-22-81	Dr. S. Barnard Metallurgy-Materials Science Department, Oxford University	Applications of Atom Probe Spectroscopy in Materials Science
7-28-81	Dr. R. Portier University of Paris	Use of High Resolution Electron Microscopy for Imaging the Structure of Incommensurate Phases in Metallic Alloys
8-24-81	Prof. S. Ranganathan Indian Institute of Science Bangalore	Ordering in Ni-base Alloys
8-28-81	Dr. O. Terasaki Tohoku University, Department of Physics, Sendai, Japan	Structure Imaging of Two-Dimensionally Ordered Alloys by High Voltage Electron Microscopy
10-30-81	Prof. N. Uyeda Kyoto University, Japan	High Resolution Electron Microscopy

Electron Microscopy of Materials (continued)

Date	Speaker and Affiliation	Seminar Title
11-30-81	Dr. P. Mazaisz REMAG, Oak Ridge National Laboratory	Progress in Alloy Development in Fusion Materials Program
Other Seminars Hosted		
6-5-81	Prof. Dr. R. Hoppe Justus-Liebig-Universität Giessen, West Germany	Small Anionic Entities in Metal Oxides (Host, N. Bartlett)
7-28-81	Dr. R. Portier CECM/CNRS, Ecole Nationale Supérieure de Chemie Paris, France	Study of Long-Period Superstructures by High-Resolution Electron Microscopy (Host, D. de Fontaine)
8-4-81	Dr. K. Ross Department of Physics University of Birmingham, U. K.	The Use of Monte Carlo Simulations in the Study of a Real Lattice Gas (Host, D. de Fontaine)
9-28-81	Dr. B. L. Gyorffy H. H. Wills Physics Laboratory University of Bristol, U. K.	Concentration Waves and the Fermi Surface in Ramdom Metallic Alloys (Host, D. de Fontaine)
9-16-81	Dr. R. M. Canon MIT, Cambridge, MA	Microstructure Evolution During Sintering (Host, A. Evans)
11-6-81	Dr. K. Okazaki National Defense Academy, Japan	The Mechanical Properties of Piezoelectric Ceramics (Host, A. Evans)
2-2-81	Prof. D. B. Williams Department of Metallurgy and Materials Engineering Lehigh University Bethlehem, PA	Al-Li-X: The Next Generation of Aerospace Alloys (Host, R. Gronsky)
7-8-81	Dr. S. Stucki Brown Boveri Research Center Baden, Switzerland	Solid Polymer Electrolyte Water Electrolysis (Host, R. Muller)
1-31-81	Dr. S. Vega Weizmann Institute of Science	Multiphoton NMR Using Amplitude Modulation (Host, A. Pines)
3-3-81	Dr. J. Bargon IBM Research Laboratory San Jose, CA	Chemically Induced Magnetic Polarization (Host, A. Pines)
4-10-81	Dr. J. Schaffer Monsanto Research Laboratory St. Louis, MO	Solid Carbon and Nitrogen NMR Studies of Plant Metabolism (Host, A. Pines)
4-15-81	Prof. D. Ziessow Technical University of Berlin Berlin, West Germany	Two-Dimensional Correlation Spectroscopy (Host, A. Pines)
6-5-81	Prof. R. Gilbert University of Sydney Sydney, Australia	Theories of Dilute Polymers (Host, A. Pines)
6-8-81	Prof. M. Mehring University of Dortmund	Phase Transitions in One- and Two-Dimensional Conductors (Host, A. Pines)
10-2-81	Prof. J. Waugh MIT, Cambridge, MA	Wideband Proton Decoupling (Host, A. Pines)
10-2-81	Prof. D. Stehlik Free University of Berlin Berlin, West Germany	Optical Nuclear Polarization in Organic Crystals (Host, A. Pines)

Other Seminars Hosted (continued)

Date	Speaker and Affiliation	Seminar Title
7-17-81	Dr. S. Skjold-Jorgensen Instituttet for Kemiteknik Danmarks Tekniske Hojskole Lyngby	Excess Gibbs Energy Models Equations of State and the Local Composition Concept (Host, J. Prausnitz)
1-26-81	Dr. G. Kaindl Free University of Berlin Berlin, West Germany	Layer-Dependent Core-Level Shifts of Adsorbates on Metals (Host, D. Shirley)
1-29-81	Prof. F. R. McFeely MIT, Cambridge, MA	Angle-Resolved Photoemission of Molecular Solids (Host, D. Shirley)
8-13-81	Prof. J. Maier University of Basel Basel, Switzerland	Molecular Ion Optical and Photoelectron Spectroscopy (Host, J. Winn)

Appendix D

Index of Investigators

Andersen, Richard A. 221

Bartlett, Neil 204, 221
Bell, Alexis T. 190, 254
Bergman, Robert G. 208, 254
Boone, Donald H. 266
Bragg, Robert H. 57
Brewer, Leo 108, 262
Brown, Steven D. 213

Clarke, John 92
Cohen, Marvin L. 98
Connick, Robert E. 189, 262, 264
Conway, John G. 221

de Fontaine, Didier 25
De Johnghe, Lutgard C. 55, 67, 294, 316

Edelstein, Norman M. 221, 307
Evans, A. G. 39, 68
Evans, James W. 24, 254, 296

Falicov, L. M. 96
Finnie, Iain 72
Fish, Richard H. 254

Glaeser, Andreas M. 70
Gronsky, Ronald 5, 20

Harris, Charles B. 143
Heineman, Heinz 254, 269
Hess, Dennis W. 116

Jeffries, Carson D. 87
Jolly, William L. 197
Johnston, Harold S. 139

Lee, Yuan T. 159, 175, 276
Levy, Alan V. 74, 248, 250 254, 266

Mahan, Bruce H. 159
Marrus, R. 186
Miller, William H. 161
Moore, C. Bradley 151, 273
Morris, J. W., Jr. 28, 303
Muetterties, Earl L. 202
Muller, Rolf H. 118, 285

Newman, John 287

Olander, Donald R. 111

Pask, Joseph A. 49
Petersen, E. E. 254
Phillips, Norman E. 101
Pines, A. 130, 244
Pitzer, Kenneth S. 154
Prausnitz, John M. 215, 313

Raymond, Kenneth N. 221
Richards, Paul L. 80
Ritchie, R. O. 46
Ross, Phillip N. 241, 289

Schaefer, Henry F., III 181
Seaborg, Glenn T. 221
Searcy, Alan W. 51
Shen, Y. Ron 83, 276

Shirley, David A. 163
Somorjai, Gabor A. 121, 137, 190, 254

Streitwieser, Andrew, Jr. 221

Templeton, David H. 221
Thomas, Gareth 8, 20
Tobias, Charles W. 104, 281, 298

Vermeulen, T. 254
Vollhardt, K. Peter C. 194, 254

Washburn, Jack 33
Westmacott, Kenneth H. 17, 20, 24
Whittle, David P. 59, 69, 266
Winn, John S. 149, 159

Yu, Peter Y. 90

Zalkin, Alan 221

GPO 587-122/2